

AD-A032 634

AIRESEARCH MFG CO OF CALIFORNIA TORRANCE
HIGH POWER STUDY--CONVENTIONAL GENERATORS, SUPERCONDUCTING GENE--ETC(U)
JUL 76 L SCHIPPER
76-12446

F/G 10/2

F33615-75-C-2071

NL

UNCLASSIFIED

AFAPL-TR-76-39

1 OF 5
AD
A032634



AD A032634

AFAPL-TR-76-39

✓ (12)

**HIGH POWER STUDY
CONVENTIONAL GENERATORS SUPERCONDUCTING
GENERATORS NON-AIR-BREATHING TURBINES**

*AIRESEARCH MANUFACTURING COMPANY OF CALIFORNIA
A DIVISION OF THE GARRETT CORPORATION
2525 W. 190th STREET, TORRANCE, CALIF. 90509*

JULY 1976

TECHNICAL REPORT AFAPL-TR-76-39
FINAL REPORT FOR PERIOD 2 JUNE 1975 to 31 DECEMBER 1975

Approved for public release; distribution unlimited

AIR FORCE AERO PROPULSION LABORATORY
AIR FORCE WRIGHT AERONAUTICAL LABORATORIES
AIR FORCE SYSTEMS COMMAND
WRIGHT-PATTERSON AIR FORCE BASE, OHIO 45433

DDC
RECEIVED
NOV 29 1976
B

NOTICE

When Government drawings, specifications, or other data are used for any purpose other than in connection with a definitely related Government procurement operation, the United States Government thereby incurs no responsibility nor any obligation whatsoever; and the fact that the government may have formulated, furnished, or in any way supplied the said drawings, specifications or other data, is not to be regarded by implication or otherwise as in any manner licensing the holder or any other person or corporation, or conveying any rights or permission to manufacture, use, or sell any patented invention that may in any way be related thereto.

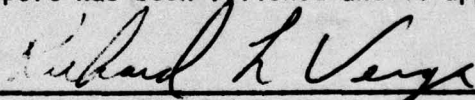
This final report was submitted by AiResearch Manufacturing Company of California, a division of The Garrett Corporation, under Contract 33615-75-C-2071. The effort was sponsored by the Air Force Aero Propulsion Laboratory, Air Force Systems Command, Wright-Patterson AFB, Ohio under Project 3145, Task 32 and Work Unit 35 with Mr. Richard L. Verga as Project Engineer. Mr. Leon Schipper of AiResearch was technically responsible for the work.

The study described in this report required the assistance of numerous individuals throughout the AiResearch Manufacturing Company of California. The author wishes to acknowledge the unique contributions of R. Smisek in the areas of generator design trade and overall system evaluation; of F. McCarty in the area of generator modeling and computer coding; and of M. Hsia in the area of computer program coding. Appreciation also is extended to the following individuals whose contributions made this report possible:

T. E. Brown	K. Ikeda
A. R. Druzba	E. G. Koltz
F. E. Faulkner	P. F. Snider
B. Foster	S. Tepper

This report has been reviewed by the Information Office (ASD/OIP), and is releasable to the National Technical Information Service (NTIS). At NTIS, it will be available to the general public including foreign nations.

This technical report has been reviewed and is approved for publication.



Richard L. Verga,
Project Engineer



Philip E. Stover,
Chief, High Power Branch

Copies of this report should not be returned unless return is required by security considerations, contractual obligations, or notice on a specific document.

UNCLASSIFIED

SECURITY CLASSIFICATION OF THIS PAGE (When Data Entered)

19 REPORT DOCUMENTATION PAGE		READ INSTRUCTIONS BEFORE COMPLETING FORM	
1. REPORT NUMBER	2. GOVT ACCESSION NO.	3. RECIPIENT'S CATALOG NUMBER	
18 AFAPL-TR-76-39			
4. TITLE (and Subtitle)		5. TYPE OF REPORT & PERIOD COVERED	
6 HIGH POWER STUDY--CONVENTIONAL GENERATORS, SUPERCONDUCTING GENERATORS, NON-AIR-BREATHING TURBINES.		Final report 6/75 through 12/75	
7. AUTHOR(s)		6. PERFORMING ORG. REPORT NUMBER	
10 Leon Schipper		14 76-12446	
9. PERFORMING ORGANIZATION NAME AND ADDRESS		8. CONTRACT OR GRANT NUMBER(s)	
AirResearch Manufacturing Co. of California, A Division of The Garrett Corp. 2525 W. 190th St., Torrance, Calif. 90509		15 F33615-75-C-2071 new	
11. CONTROLLING OFFICE NAME AND ADDRESS		10. PROGRAM ELEMENT, PROJECT, TASK AREA & WORK UNIT NUMBERS	
U.S. Air Force, Air Force Systems Command Aeronautical Systems Division/PPMNB Wright-Patterson AFB, Ohio 45433		Project: 3145 Task: 32 Work Unit: 35	
14. MONITORING AGENCY NAME & ADDRESS (if different from Controlling Office)		12. REPORT DATE	
16 3145		11 22 Jul 76	
17 32		13. NUMBER OF PAGES	
		362	
		15. SECURITY CLASS. (of this report)	
		Unclassified	
		15a. DECLASSIFICATION/DOWNGRADING SCHEDULE	
		N/A	
16. DISTRIBUTION STATEMENT (of this Report)			
Approved for public release; distribution unlimited.			
9 Final rept. Jan - Dec 75,			
17. DISTRIBUTION STATEMENT (of the abstract entered in Block 20, if different from Report)			
12 383 p.			
18. SUPPLEMENTARY NOTES			
19. KEY WORDS (Continue on reverse side if necessary and identify by block number)			
High-power conventional generators High-power superconducting generators High-power non-air-breathing turbines			
ABSTRACT (Continue on reverse side if necessary and identify by block number)			
In this study, parametric data and key computer codes were developed and point designs evaluated on the subject of conventional generators, superconducting generators, and non-air-breathing turbines for high-power airborne application. In addition, a set of development and technology programs was developed as a means to enhance rapid development or reduce the technical risk of the various components.			

DD FORM 1 JAN 73 1473

EDITION OF 1 NOV 65 IS OBSOLETE

Unclassified

SECURITY CLASSIFICATION OF THIS PAGE (When Data Entered)

387 343 mt

AFAPL-TR-76-39

CONTENTS

<u>Section</u>		<u>Page</u>
1	INTRODUCTION	1
2	SUMMARY	2
	Applications Syntheses	2
	Computer Coding Development	5
	Point Designs Evaluation	6
	Development and Technology Programs	12
	Algorithms	12
3	PRELIMINARY DESIGNS	14
	Introduction and Requirements	14
	Medium-Power Application, Conventional Generator	16
	Medium-Power Application, Superconducting Generator	36
	Medium-Power Application, Turbine	44
	Medium-Power Application, Turbogenerator Power System	52
	Medium-Power Application, Design Points 3, 4, and 5	57
	Low-Power Application, Design Points 1 and 2	66
	High-Power Application, Design Points 7 and 8	80
	Fast Startup Operation	91
4	OPERATIONAL SUITABILITY	93
	Introduction	93
	Summary	93
	Safety	95
	Automatic Sequencing and Controls	98
	Reliability and Availability	98
	Restartability	99
	Power Source Protection	102
	IR Signature	102
	Startup Time	103

CONTENTS (Continued)

<u>Section</u>		<u>Page</u>
	Turnaround Time	103
	Performance Degradation With Time	103
	Maintenance	103
	Logistical Support	104
5	DEVELOPMENT AND TECHNOLOGY PROGRAMS	106
	Introduction	106
	Generator Development Programs	109
	Turbine/Combustor Development Program	118
	High-Power System Development Program	121
	Generator Technology Plans	122
	Combustor Technology Program	128
6	CONVENTIONAL GENERATOR DESIGN CONSIDERATIONS AND TRADE STUDY	131
	Introduction	131
	Summary	131
	Selection of Machine Type	132
	Configuration Selection	134
	Computer Program	141
	Parametric and Sensitivity Studies	144
	Thermal Design and Cooling System	165
	Mechanical and Structural Design	179
7	SUPERCONDUCTING GENERATOR DESIGN CONSIDERATIONS AND TRADE STUDY	192
	Introduction	192
	Summary	192
	Design Considerations	193
	Superconducting Generator Description	205
	Computer Program	212
	Parametric Studies	216
	Cooling System	222

CONTENTS (Continued)

<u>Section</u>		<u>Page</u>
8	TURBINE DESIGN CONSIDERATIONS AND TRADE STUDY	227
	Introduction	227
	Summary	227
	Aerodynamic Turbine Design Considerations and Characteristics	228
	Fast Startup Design Considerations and Characteristics	246
	Structural Design Considerations and Characteristics	251
9	TURBODRIVE SUBSYSTEM	266
	Propellants	266
	Propellant Storage and Delivery Assembly	270
	Gas Generator Assembly	272
	Control Assembly	290
 <u>Appendix</u>		
A	POTENTIAL APPLICATION OF AIR CUSHIONED RESEARCH VEHICLE GENERATOR	297
B	GENERATOR PARAMETRIC CRITICAL SPEED EVALUATION	316
C	FIRST-STAGE TURBINE DISC STRESS ANALYSIS	338
D	SECOND-STAGE TURBINE VIBRATION AND STRESS EVALUATION	348

ACCESSION for	
HTIS	White Section <input checked="" type="checkbox"/>
DOC	Buff Section <input type="checkbox"/>
UNANNOUNCED <input type="checkbox"/>	
JUSTIFICATION	
BY	
DISTRIBUTION/AVAILABILITY CODES	
Dist.	AVAIL. and/or SPECIAL
A	

ILLUSTRATIONS

<u>Figure</u>		<u>Page</u>
1	Fast Startup, Monopropellant Application	17
2	Fast Startup, Bipropellant Application	17
3	Effect of Duty Cycle and Cooling Method on Conventional Generator Weight Characteristics	19
4	Generator Transient Temperature Distribution	34
5	Cooling System Schematic Diagram	34
6	Idling Operation, Monopropellant Application	36
7	Airborne Liquid Helium Supply Schematic	44
8	Off-Design Turbine Performance, Fixed Design, Variable Speed, Variable Propellant	48
9	Off-Design Turbine Performance, Fixed Speed, Variable Inlet-Exit Pressures	48
10	First-Stage Temperature Distribution	50
11	Second-Stage Temperature Distribution	50
12	Second-Stage Turbine Disc Stress Review	53
13	Second-Stage Turbine Blade Vibration--Interference Diagram	53
14	Generator Weight vs Coolant Pressure Drop	56
15	Rotor L/D vs Coolant Pressure Drop	56
16	Pilot-Thermal Gas Generator Characteristics	92
17	Conventional Generator Application Turbogenerator Startup Characteristics	92
18	Fluid-Cooled Generator Program Plan and Schedule	113
19	Thermal-Lag Generator Program Plan and Schedule	113
20	TLRV Synchronous Condenser	115

ILLUSTRATIONS (Continued)

<u>Figure</u>		<u>Page</u>
21	Near-Term Demonstrator and Test Bed Program, Fluid-Cooled Generator	117
22	Near-Term Demonstrator and Test Bed Program, Uncooled Generator	117
23	Combustor Development Program Plan and Schedule	119
24	Turbine Development Program Plan and Schedule	121
25	High-Power Airborne Power Unit Development Plan and Schedule	123
26	Rotor Technology Program Plan and Schedule	125
27	Winding Technique Technology Program Plan and Schedule	127
28	Effective Fluid Cooling Concept Program Plan and Schedule	128
29	Schematic Diagram of Combustor Based on Hypergolic Ignition and Monopropellant Sustained Operation	129
30	Combustor Technology Program Plan and Schedule	130
31	Wound-Field, Synchronous Generator, Solid Core, Distributed Nonsalient-Pole Field Coil, Round-Rotor	133
32	Lundell Generator, Salient Pole, Composite Rotor and Stationary Field Coil	133
33	Homopolar Inductor, Generator, Solid-Core, Salient-Pole, Stationary Field Coil	133
34	Influence of Cooling Method on Generator Weight	135
35	Conduction-Cooled Round Rotor	137
36	Alternator with Flow-Cooled Rotor	137
37	Hollow-Conductor-Cooled Rotor Configuration	138
38	Water-Cooled, Hollow-Conductor Rotor for 10-MVA TACRV Machine	138
39	Flow-Cooled Stator Configuration	140

ILLUSTRATIONS (Continued)

<u>Figure</u>		<u>Page</u>
40	Water-Cooled, Hollow-Conductor, 10-MVA Stator	140
41	Flow-Cooled Stator Configuration	142
42	Flow-Cooled Stator with Bore Seal	142
43	Round-Rotor Alternator Design Program Flow Chart	143
44	Sample Printout, Short Form	146
45	Generator Weight vs Dc Voltage for Different Power Loads	148
46	Generator Weight vs Rotational Speed for Different Dc Voltages	149
47	Generator Weight vs Rotational Speed for Different Power Levels	151
48	Thermal-Lag Generator Weight, Diameter, and Length vs Rotational Speed for Specific SOW Design Points	152
49	Effect of Duty Cycle and Cooling Method on Weight	154
50	Duty Cycle Sensitivity of Thermal Lag Conventional Generators	155
51	Weight Sensitivity of Conventional Generator to Number of Poles, Insulation Stress, and Tip Speed	156
52	Generator Weight Sensitivity to Insulation Working Stress at High Voltage	158
53	Weight Sensitivity of Generator with Load Type and Commutation Reactance	158
54	Apparent Power Factor and other Parameters for a 3-Phase, F-W Rectifier Supplied by an Alternator	159
55	Generator Weight Sensitivity to Materials and Stator Peak Core Density	161
56	Generator Weight Sensitivity to Initial and Final Copper Temperature	161
57	Rotor L/D vs Coolant Effectiveness	162
58	Generator Weight vs Coolant Pressure Drop	162

ILLUSTRATIONS (Continued)

<u>Figure</u>		<u>Page</u>
59	Relationship of Generator Rotor Polar Moment of Inertia to Coolant Pressure Drop and Rotational Speed	163
60	Hydraulic Power Dissipated in Cooling the Generator	163
61	Simplified Flow Chart of Subroutine COND	168
62	Radial View of 25-MW Generator Thermal Model	169
63	Axial View of 25-MW Generator Thermal Model	170
64	Coolant Oil Flow Paths	170
65	Generator Transient Temperatures	173
66	Cooling System Schematic Diagram	177
67	Cooling System Weight vs Generator Power Level, Efficiency, and Operating Duration	177
68	Power, Weight and Flow Rate of Coolant Pump and Motor as a Function of Generator Power Level	178
69	Typical Superconductor Wire Characteristics	198
70	Helium Temperature Rise in Centrifugal Field	198
71	Superconducting Generator Design Concepts	202
72	Superconducting Field Rotor Configuration	206
73	Stator Configuration	206
74	Superconducting Generator Cross Section and Geometric Nomenclature	207
75	Superconducting Generator Design Program Flow Chart	213
76	Sample Printout, Short Form	218
77	Superconducting Generator Weight as a Function of Rotational Speed and Dc Voltage	220
78	Superconducting Generator Weight as a Function of Rotational Speed and Power Level	221

ILLUSTRATIONS (Continued)

<u>Figure</u>		<u>Page</u>
79	Superconducting Generator Diameter and Length-to-Diameter Ratio as a Function of Rotational Speed and Power Level	222
80	Representation of the Liquid Helium Storage Vessel	223
81	Weight and Volume of Expendable Liquid Helium Storage System	225
82	Weight, Volume, and Power Requirements for Closed-Cycle Helium Liquefaction System	226
83	Turbine Performance Evaluation Procedure and Technique	231
84	Zeus Turbine Off-Design Computer Program Performance Correlation	233
85	Effect of Turbine Stage, Rotational Speed, and Pitch Velocity	234
86	Rotational Speed Selection	
87	Optimal Turbine Rotational Speed	237
88	First-Stage Blade Height Optimization	238
89	Stage Pressure Ratio Split	239
90	Optimized Turbine Weight and Inertia	240
91	Turbine Altitude Design Trade	241
92	Off-Design Performance Trade	242
93	Propellant Performance Comparison	244
94	Turbine Algorithm	245
95	Fast-Startup System Program Model System Schematic	250
96	Pilot-Thermal Gas Generator Characteristics	252
97	Startup Times	252
98	Turbine Assembly Modal Model	256
99	Cycle A Thermal Distribution	256

ILLUSTRATIONS (Continued)

<u>Figure</u>		<u>Page</u>
100	First-Stage Temperature Distribution	257
101	Second-Stage Temperature Distribution	257
102	First-Stage Turbine Disc Stress Review	259
103	Second-Stage Turbine Disc Stress Review	261
104	Second-Stage Turbine Blade Vibration-Interference Diagram	262
105	Block Diagram of Typical Turbogenerator Subsystem	266
106	Propellant Storage and Delivery Design Considerations	271
107	Pressurant Gas Storage Characteristics, Startup	273
108	Pressurant Gas Storage Characteristics Nominal Operation	274
109	Propellant Start Tank Storage Characteristics	275
110	Propellant Start Tank Storage Characteristics	276
111	Propellant Main Storage Tank Characteristics	277
112	Decomposition Chamber Operation Options	279
113	All Catalytic Combustor Chamber Characteristics	281
114	Pilot Thermal Combustor Chamber Characteristics	282
115	JP-4, 10 Percent H_2O , 90 Percent H_2O_2 Combustion	285
116	Double-Reduction Four-Branch Assembly	287
117	Gearbox Specific Weight	288
118	Lubrication Assembly Schematic Diagram	290
119	Control Operational Modes and Implementation Techniques	291
120	Bipropellant Control Systems	294

TABLES

<u>Table</u>		<u>Page</u>
1	Turbogenerator Assembly Weight and Size Summary	7
2	Turbogenerator Power Supply Assembly 25-MW Output With Rectified Load, Mission: 3 Pulses, 21 Sec On, 300 Sec Off	7
3	Rating Matrix	8
4	25-MW Power System Candidate Comparisons	9
5	Design Point Algorithms	13
6	SOW Design Requirement Identification	14
7	Conventional Generator, Thermal Lag, Point Design 6	23
8	Conventional Generator - Thermal Lag, Material Part List	25
9	Conventional Generator - Thermal Lag, Critical Stress Review	25
10	Conventional Generator - Thermal Lag Preliminary Critical Speed Review	26
11	Conventional Generator, Fluid-Cooled, Point Design 6	28
12	Conventional Generator, Fluid-Cooled, Materials List	31
13	Conventional Generator, Fluid-Cooled, Critical Stress Review	32
14	Conventional Generator, Fluid-Cooled, Preliminary Critical Speed Review	32
15	Conventional Generator, Fluid-Cooled Cooling Sub- system Characteristics	35
16	Superconducting Generator; Point Design 6; Low-Speed, Low-Voltage Design	39
17	Superconducting Generator; Point Design 6; High-Speed, Low-Voltage Design	40

TABLES (Continued)

<u>Table</u>		<u>Page</u>
18	Superconducting Generator; Point Design 6; Low-Speed, High-Voltage Design	41
19	Superconducting Generator Cooling Subsystem Characteristics	45
20	Point Design 6 Turbine Design Characteristics	46
21	First Stage Turbine Disc Stress Summary	51
22	Turbogenerator Power Supply Assembly Point Design 6 Requirements (25 MW/3 Pulses, 21 Sec On, 300 Sec Off)	54
23	Conventional Generator, Thermal Lag, Point Design 3	59
24	Conventional Generator, Thermal Lag, Point Design 5	60
25	Conventional Generator, Thermal Lag, Point Design 4	62
26	Conventional Generator, Thermal Lag Preliminary Critical Speed Evaluations of Point Designs 3, 4, and 5	63
27	Conventional Generator, Fluid Cooled, Point Designs 3, 4, 5, And 6	65
28	Conventional Generator, Thermal Lag, Point Design 1	71
29	Conventional Generator, Thermal Lag, Point Design 2	72
30	Conventional Generator, Thermal Lag Preliminary Critical Speed Evaluations of Point Designs 1 and 2	73
31	Conventional Generator, Fluid Cooled, Point Designs 1 and 2	75
32	Conventional Generator, Fluid Cooled Preliminary Critical Speed Evaluations of Point Designs 1 and 2	76
33	Superconducting Generator, Point Designs 1 and 2	79
34	Conventional Generator, Thermal Lag, Point Design 7	82
35	Conventional Generator, Thermal Lag, Point Design 8	83

TABLES (Continued)

<u>Table</u>		<u>Page</u>
36	Conventional Generator, Thermal Lag Preliminary Critical Speed Evaluations of Point Designs 7 and 8	84
37	Conventional Generator, Fluid Cooled Point Designs 7 and 8	86
38	Conventional Generator, Fluid Cooled Preliminary Critical Speed Evaluations of Point Designs 7 and 8	87
39	Superconducting Generator, Point Designs 7 and 8	90
40	Recommended Reliability Goals By Subsystems [25-MW Thermal-Lag System Used As Baseline]	100
41	Comparison of Reliability and Availability of Candidate Turbogenerator Systems	101
42	Summary of Recommended Conventional Generator Development Programs	107
43	Summary of Recommended Turbine/Combustor and Turbogenerator Power System Development Programs	108
44	Generator Development Programs Estimated Probability of Success	110
45	User-Defined Inputs	145
46	Optional Inputs	145
47	Stator and Rotor Materials	146
48	Baseline Values of Study Parameters	147
49	Summary of Results Obtained from Thermal Analyzer Program H0298	172
50	Basic Properties of Candidate Coolants	175
51	Water Boiler Design Summary	179
52	Representative Materials for High-Power Alternator Study	183

TABLES (Continued)

<u>Table</u>		<u>Page</u>
53	Materials Parts List 25-MW Output; 3 Pulses; 21 Sec On; 300 Sec Off	184
54	Structural Analysis Summary 25-MW Output; 3 Pulses; 21 Sec On; 300 Sec Off	184
55	Critical Speed Summary High-Power Conventional Generators	188
56	Thermal-Lag Conventional Generator Algorithms	190
57	Fluid-Cooled Conventional Generator Algorithms	191
58	Superconducting Generator Design Program User-Defined Inputs	214
59	Superconducting Generator Design Program	215
60	Superconducting Generator Design Program Stator Materials	216
61	Superconducting Generator Design Program Nb-Ti Superconductor at 4.2 K	216
62	Baseline Values of Study Parameters	219
63	Liquid Helium Storage System Summary	224
64	Fast Startup Concepts Review	248
65	First-Stage Turbine Disc Stress Summary	260
66	Key Characteristics of Candidate Propellants	268
67	Chemical Equilibrium Compositions Occurring as a Result of Combustion of JP Fuel and Oxygen	286
68	Valve Design Parameters	295
69	Valve Selection Comparison	296

SECTION 1

INTRODUCTION

This report describes the results of a study program conducted by the AiResearch Manufacturing Company of California, a Division of The Garrett Corporation, on the characterization of the size, weight, and performance of conventional generators, superconducting generators, and non-air-breathing turbines of high-power-output capability. These component studies were conducted to present the data necessary for the Air Force to select the appropriate power generation system for an airborne high-power application.

A substantial amount of the material accumulated during this seven-month study program is described in this report. The summary of the study program is presented in Section 2. Section 3 details the various point designs of interest with respect to individual component and power generating system applications. Section 4 reviews the airborne operational suitability of the various concepts reviewed. Recommended development and technology programs are described in Section 5. Sections 6, 7, and 8 describe the design considerations and trade studies conducted on the three generic components of interest, i.e., conventional generator, superconducting generator, and non-air-breathing turbines. Section 9 describes the various assemblies encompassed in a non-air-breathing turbogenerator power system. Where appropriate, each section features a summary of the various salient items covered in it.

SECTION 2

SUMMARY

A study program was conducted to provide to the Air Force the means of selecting the appropriate power source conversion for specific high-power airborne applications. Parallel studies, of variable emphasis, were conducted for the component design evaluation of conventional generators, superconducting generators, and non-air-breathing turbines. Contractual requirements called for the design evaluation of identified key components. It was, felt, however, that restricting the study to component evaluation, per se, may lead to erroneous assessment of the capability and requirements of the components in the particular system application specified. Accordingly, the procedure adopted was to conduct sufficient system study such that the individual component operating characteristics clearly reflect its ability within the intended system application. Parametric data were generated, key computer codes developed, and point designs of the components of interest were evaluated at the specific operating conditions described in Section 3. In addition, a set of development and technology programs recommended as means to enhance rapid development or reduce the technical risk and/or weight and volume of the components of interest is described.

APPLICATIONS SYNTHESIS

The following observations pertain to the application of a conventional generator, a superconducting generator, and non-air-breathing turbines as independent components or in a combined turbogenerator in the present intended application.

Turbogenerator Rotational Speed

The selection of rotational speed is governed by power level. At the low-power spectrum (10 MW), the use of a gear-driven concept is indicated because, at this power level, optimum component speed selection predominates. At the medium-power range of interest (25 MW), component rotational speed compromises can be tolerated, and the direct-driven multicomponent approach is indicated. At the high-power level of interest (50MW), selection of assembly rotating speed is primarily dictated by turbine structural design considerations such that direct drive is imposed.

Low-Voltage Output Operation

Low-voltage generator output requiring the use of a transformer is recommended. In the conventional generator application, this approach results in the lowest weight design, low development risk, and desired design flexibility. In the superconducting generator application, a weight penalty results, while still maintaining desired low risk and flexibility.

Rectified Load Application

For generators feeding a rectified load, the power factor and commutation reactance are related. Minimum generator weight is obtained with a commutation reactance of 0.27, which gives a power factor of 0.88 lagging. This allows sufficient reactance for a lightweight transformer (low voltage-to-high voltage) design to be made that is compatible with the rectifier.

Conventional Generator, Thermal-Lag

The thermal-lag conventional generator offers operational simplicity. The weight of the generator is highly dependent on the operating duty cycle. In the medium-power range of interest (25 MW), for integrated mission ON times below 45 sec, the thermal-lag design approach is competitive with or lighter than its fluid-cooled counterpart design approach.

Conventional Generator, Fluid-Cooled

The use of an effective fluid-cooled conventional generator design concept reduces assembly weight and introduces considerable flexibility to the mission duty cycle capability. Its weight variation for a particular duty cycle is primarily a function of the integrated ON time, which determines the amount of evaporative coolant heat sink (and associated tankage) that must be carried for mission completion. The OFF time duty cycle has only a minor effect on fluid-cooled generator capability, because it primarily affects coolant flow rate required and aircraft interface power and associated equipment weight.

Generator Weight Reduction

As the quest for generator weight reduction is pursued, the simultaneous imposition of high peripheral and rotational speeds will result in a high length-to-diameter ratio design. This necessitates traversing one or two operating critical speed modes. Fortunately, by varying the combinations of

bearing stiffness and mount resilience, the effective spring rate of the complete dynamic system (rotor, stub shaft, bearing, and bearing mount) can be modulated over a wide range such to ensure that rotor critical speeds do not occur near the component operating speed.

Superconducting Generator

The selected superconducting generator concept consists of a rotating dewar containing the superconducting field with a stationary external armature. This concept was selected due to the compatibility of the present state of development with the time frame of the present application. The use of this concept results in minimum assembly weight. The low weight achievement is made possible through the use of a complex concept and logistics considerations.

The superconducting generator concept, preferred from the technical suitability standpoint, consists of a stationary dewar containing the superconducting field with a rotating external armature. This concept, however, is not compatible with the time frame of the present application.

Turbines

Supersonic operation should be selected in all stages of a multiple-stage turbine design. The prime consideration leading to this design approach is that the majority of the anticipated missions occur at altitude with a reduced, variable back pressure. The availability of latter-stage supersonic blade contour will reduce fuel consumption or increase mission duration for a fixed fuel quantity.

Conventional Generator, APU

Fast startup on the order of 1.5 to 2.0 sec is possible for all power levels of interest without introducing unusual power system operational complexity. This fast startup operation is achievable with the use of either thermal-lag or fluid-cooled conventional generator design concepts.

Superconducting Generator, APU

The operating characteristics of the superconducting generator are such as to exclude fast-startup capability. APU idling operation (generator assembly rotating, turbine assembly stationary) is required with appropriate complete assembly engagement and disengagement upon demand.

COMPUTER CODING DEVELOPMENT

Three major computer design codes were developed in the study program, namely, (1) a conventional round-rotor generator design program, (2) a superconducting field in a rotating dewar, stationary armature generator design program, and (3) a turbine design program combining aerodynamic, structural, and thermal design aspects into a single computational procedure.

Generator Design Programs

The generator programs allow optimization of weight, volume, efficiency, and other significant parameters as a function of input variables such as power level, voltage, rotational speed, and duty cycle. As few as nine input data items suffice to produce a generator design; however, up to 22 input data for the conventional and 27 input data for the superconducting items may be used for specific design points or parametric studies.

A significant feature of both generator programs is the incorporation of a thermal subroutine to minimize alternator size and weight. This subroutine determines the maximum current density permissible for a given duty cycle without exceeding the specified maximum temperature limit. Two operating modes can be used: (1) thermal lag, in which the heat generated in the machine is absorbed by the thermal capacitance of the machine materials, and (2) active cooling, in which a fluid is circulated through the copper windings to absorb the heat generated and reject it to an external heat sink.

The generator programs also include a mathematical model of a three-phase full-wave rectifier that defines the power factor seen by the generator as a function of the generator commutation reactance. The subroutine is used for generator optimization because consideration must be given to the interaction of the generator and output rectifier necessary to supply the dc load.

Turbine Assembly Program

With respect to the turbine design program, the adopted integral procedure allows assessment of complete turbine assembly characteristics. Considerations reviewed include turbine aerodynamic design and iterative evaluation to ensure satisfactory supersonic operation. Structural elements of the assembly also interact, in an iterative fashion, with evaluated time- and position-determined thermal distribution to arrive at a satisfactory design concept.

POINT DESIGNS EVALUATION

The component assembly, inclusive of required ancillary equipment, shows a substantial variation in performance characteristics and operational suitability. To assist in the selection procedure, the merits of each concept were reviewed in terms of (1) performance characteristics as a turbogenerator assembly, (2) performance characteristics as a power supply system, and (3) preparation of rating matrixes covering the application of the various concepts to help identify components or groups of components that either have inherently high technical risk, system criticality, operational suitability considerations, or high weights and volumes associated with them. The eight turbogenerator point designs of interest are summarized in terms of associated weight and size in Table 1.

The performance summarized in Table 1 refers to the potential use of the conventional generator (thermal-lag, fluid-cooled) or superconducting generator in a turbogenerator. The performance characteristics shown are for a turbogenerator assembly encompassing combustor, turbine, generator, and associated required cooling equipment. Table 2 describes the performance characteristics associated with a power system satisfying point design 6 requirements. The weights shown refer to the application of conventional generators (thermal-lag, fluid-cooled) and superconductor generators (direct turbine drive at 10,000 rpm, and gear drive of generator at 8000 rpm, and turbine speed at 14,000 rpm). Characteristics shown are exclusive of APU control and structural support.

As shown in Table 2, in terms of a power system application, the weight differentials of the various concepts are rather small; therefore, the selection procedure must heavily consider other remaining factors. Among the remaining factors that must be appraised in the application of a high-power generating system for in-service airborne use is the suitability of the unit in the operating environment. To assist in this test, the rating matrix of Table 3 was established.

The applications of the three generic concepts at design point 6 requirements are compared in Table 4.

TABLE 1

TURBOGENERATOR ASSEMBLY WEIGHT AND SIZE SUMMARY

Design Point	1	2	3	4	5	6	7	8
Output Power, MW	10	10	25	25	25	25	50	50
Number of Pulses/ON Time/ OFF Time	3/21/30	3/21/300	16/4/4	1/120/N/A	3/21/30	3/21/300	3/25/N/A	10/12/78
CONVENTIONAL THERMAL LAG								
Max. length, in.	134.3	132.1	168.2	160.0	168.8	161.1	197.0	211.0
Max. height, in.	32.0	32.0	39.5	37.0	39.5	39.5	48.8	48.8
Max. width, in.	37.0	37.0	39.5	49.0	39.5	39.5	48.8	48.8
Wet weight, lb	2794	2714	6219	8333	6192	5778	11,660	13,049
Specific weight, lb/kW	0.279	0.271	0.249	0.333	0.248	0.231	0.233	0.261
CONVENTIONAL FLUID COOLED								
Max. length, in.	128.0	128.0	151.0	151.0	151.0	151.0	234.0	234.0
Max. height, in.	36.0	36.0	41.0	41.0	41.0	41.0	48.5	48.5
Max. width, in.	48.0	48.0	56.0	56.0	56.0	56.0	74.0	74.0
Wet weight, lb	2423	2423	5136	5377	5136	5136	10,690	11,016
Specific weight, lb/kW	0.242	0.242	0.205	0.215	0.205	0.205	0.214	0.220
SUPERCONDUCTING								
Max. length, in.	148.0	148.0	157.5	157.5	157.5	157.5	167.0	167.0
Max. height, in.	49.0	49.0	45.1	45.1	45.1	45.1	58.0	58.0
Max. width, in.	50.0	50.0	63.5	63.5	63.5	63.5	61.5	61.5
Wet weight, lb	2160	2160	4704	4966	4704	4704	8519	8771
Specific weight, lb/kW	0.216	0.216	0.188	0.199	0.188	0.188	0.170	0.175

TABLE 2

TURBOGENERATOR POWER SUPPLY ASSEMBLY
 25-MW OUTPUT WITH RECTIFIED LOAD,
 MISSION: 3 PULSES, 21 SEC ON, 300 SEC OFF

Assembly	Conventional		Superconducting	
	Thermal Lag	Fluid Cooled	Direct Drive	Gear Drive
Generator Assembly				
Rotational speed, rpm	12,500	12,500	10,000	8000
Generator, lb	4271	2948	1475	1585
Cooling system, dry, lb	-	383	390	546
Fluids:				
Coolant, lb	-	51	15	15
Water, lb	-	247	207	270
Helium, lb	-	-	85	85
Subtotal	4271	3629	2172	2501
Specific weight, lb/kW	0.171	0.145	0.087	0.100
Gearbox/clutch/lube assembly, lb	35	35	390	1077
Turbocompressor assembly, lb	1472	1476	2436	1126
Propellant assembly, lb	3506	3574	3046	3122
Turbogenerator assembly, lb	9284	8714	8044	7826
Turbogenerator specific weight, lb/kW	0.371	0.349	0.322	0.313
Relative weight factor	1.0	0.94	0.87	0.84

TABLE 3
RATING MATRIX

Considerations	Relative Weighting Factor, Percent	Remarks
Weight	10	Include total system encompassing all ancillary equipment.
Volume	5	Package volume in lieu of displacement volume
Operational suitability	15	Include restartability, turnaround time, startup time, off-design operation, performance degradation with time, component/system maintainability, ground checkout problems, signature, and reliability.
Aircraft interface	5	Include problems with exhausting gases, requirements for aircraft power, heat rejection or thermal problems, EMI, vibration, and structural mounting problems.
Cost of development prototype	5	Cost of presently defined three-year program including test stand costs.
Cost of production	15	Cost for 20 systems/year for three years.
Operational costs	5	Does not include production cost but must include fuel, maintenance, consumables, servicing requirements, and component replacement frequency.
Safety	10	Must include both ground and in-flight hazards of combustion, explosion, toxicity, and electrical shock.
Ground support	10	Equipment and personnel requirements
Contribution to technology	3	Advance in the state of the art and of future applicability.
Probability of success	15	Impacts of cost, development time, and technology.
Power conditioning	2	Usage applicability.
Total	100	

TABLE 4
25-MW POWER SYSTEM CANDIDATE COMPARISONS

Considerations	Relative Weighting Factor, Percent	Conventional Turbogenerator Type			Superconducting		
		Thermal Lag	Rating	Fluid Cooled	Fluid Cooled	Rating	Rating
Weight	10	15 percent heavier	6	8 percent heavier	Lightest	8	10
Volume	5	Smallest	5	38 percent larger	43 percent larger	4	4
Operational suitability	15	Cooldown period restricted	13	Coolant supply	Coolant and helium supply	15	8
Aircraft interface	5	Mission restricted		Mission independence	Mission independence		
		Hot exhaust	5	Hot exhaust	Hot exhaust	4	3
		Self-energized		Aircraft power	High aircraft power		
Prototype cost	5	Lowest	5	3.6 percent higher	22 percent higher	4	3
Production cost	15	Lowest	15	11 percent higher	60 percent higher	13	10
Operational cost	5	Lowest	5	4 percent higher	27 percent higher	4	2
Safety	10		10		Highest complexity	10	8
Ground support	10	Minimal	10	Simple	Complex	9	6
Contribution to technology	3	High power/fast start	1	High power/fast start	High power-efficiency	2	3
Probability of success	15	Low specific wt		Low specific wt	Lowest specific wt		
		90 to 100 percent	15	75 to 85 percent	60 to 70 percent	12	10
Power conditioning	2	Transformer rectifier	2	Transformer rectifier	Transformer rectifier	2	2
Rating, Total	100		92			87	69

The conclusions reached with respect to applicability are as follows:

- The thermal lag conventional generator is heaviest in weight and offers the smallest packaging volume. The use of this system poses the fewest real or latent problems connected with service deployment, operational use, and ground support. It presents the fewest problems to the systems integrator, and has the highest probability for success. An especially significant feature is its similarity, except for power rating and size, to an analogous program presently being conducted by AiResearch for the Air Force. Feedback and spinoff from this other program are quite relevant, and the two programs complement each other. For the condition where a mission duty cycle can be timely specifically defined, the selection of this concept is recommended.
- The fluid-cooled conventional generator provides a slight decrease in weight and increase in packaging volume at the expense of mission independency. The unit is not quite as reliable as the thermal-lag generator because of additional components required and fluid connections, but it is deemed to be nearly as suitable for service deployment. The requirement for resupplying a few hundred pounds of water following each mission increases the resupply ground crew workload only minimally, and there is no anticipated complexity of control in flight or ground checkout. The problem of reliable fluid connections can be resolved because AiResearch has previously employed such a concept in an experimental liquid-cooled electric propulsion system. The probability for success for this approach is considered to be quite high, but not as high as for the thermal-lag approach. For the condition where a mission duty cycle cannot timely be clarified the use of this concept is recommended.
- From an operational suitability point of view, the superconducting approach for the present application is deemed to be highly questionable. This design concept is experimental in nature, development risk is considered high, there are unknowns that are difficult to evaluate, and it poses some unique problems in support at the operational level (replenishment and storage of cryogenics, and the need for prolonged

chill-down). It is not a flexible approach, and, in addition, is considered to be the least reliable. The unit is restricted to idling operation with subsequent power engagement cycles, thus encompassing increase in operational complexity and the need to satisfactorily demonstrate such a capability.

- The selection of low-voltage generator designs with transformers employed to attain the desired high-voltage supply provides increased reliability and flexibility in the present application. Protection of the alternators and of the load is straightforward and well within the state of the art, and electrical shock hazards lend themselves to ready analysis and suitable safeguards.
- As long as the recommendations, procedures, safeguards, and hazard controls of the Air Force report on hydrazine safety are observed, carrying hydrazine in large quantities onboard a military aircraft is feasible and safe.
- Ground and inflight safety dictates that an automatic sequencing and control subsystem be incorporated in the high-power system. The sequencing and control subsystem will be energized prior to takeoff and will be used to monitor all salient operational parameters continuously to flight termination and display critical parameters continuously on a supervisory control console. Such equipment is mandatory for operational safety and suitability of the proposed airborne equipment, and also is included in a current USAF-AiResearch contract for a much smaller but analogous prototype system. The subsystem permits safe starts, safe aborts, and safe electrical isolation of faults. It monitors pressures, temperatures, speeds, voltages, currents, vibration levels, and imbalance, and can sense and act upon developing faults before they can damage equipment or create a hazardous condition to the aircraft. This electronic subsystem incorporates a programmable digital computer and can be readily modified for a new system with different valued parameters. The current input is 30 separate parameters.

DEVELOPMENT AND TECHNOLOGY PROGRAMS

Six potential development programs have been identified to provide for the eventual development of a high-power system. They are:

- Prototype conventional generator, fluid-cooled
- Prototype conventional generator, thermal-lag
- Near-term demonstrator and test bed conventional generator, fluid-cooled
- Near-term demonstrator and test bed conventional generator, thermal-lag
- Prototype turbine/combustor
- Prototype turbogenerator power system

The first four programs, relating to the electric generator, provide a list of options available in charting the future course of the high-power generator program. All recommended development plans, whether at the component level or full high-power system level, are consistent with the availability of a lightweight system in the 1978-1979 time frame.

In addition, four technology programs have been identified that could provide significant improvements in the present state of the art within the time-frame of the high-power system program. They are:

- Advanced structural rotor design concepts
- Novel generator winding techniques
- Generator size and weight reduction by effective use of coolant fluids
- Combustor hypergolic ignition with sustained monopropellant operation

ALGORITHMS

Simplified algorithms shown in Table 5, based on the design studies conducted, have been established for the conventional generator (thermal-lag, fluid-cooled), for the generator cooling subsystem, and for the turbine assembly.

TABLE 5
DESIGN POINT ALGORITHMS

Parameter	Conventional Generator	
	Thermal Lag	Fluid-Cooled
WA, generator weight, lb	$WA = (-33.43 + 63.90 \ln \tau) P^{0.961}$	$WA = 78.20 P^{1.116}$
DA, generator diameter, in.	$DA = 13.27 \exp (0.010 P)$	$DA = 11.27 \exp (0.010 P)$
LA, generator length, in.	$LA = (-0.612 + 27.69 \ln \tau) (-0.218 + 0.355 \ln P)$	$LA = -59.86 + 47.06 \ln P$
WX, exciter weight, lb	$WX = 22.47 + 5.248 P$	$WX = 78.00 + 7.682 P$
DX, exciter diameter, in.	$DX = 8.600 \exp (0.010 P)$	$DX = 7.435 \exp (0.010 P)$
LX, exciter length, in.	$LX = 2.454 + 3.884 \ln P$	$LX = 5.05 + 5.01 \ln P$
N, rotational speed, rpm	$N = 15,209 - 113.3 P$	$N = 15,209 - 113.3 P$
Vdc, dc voltage, V	$Vdc = (1700 + 519 \ln \tau) (0.665 + 0.0184 P)$	$Vdc = 1793 + 55.54 P$
η , efficiency, percent	$\eta = 100 - (1.0794 + 1.0583 \ln P) \exp (0.0043 \tau)$	$\eta = 89.28 + 1.153 \ln P$
I_p , rotor inertia, in.-lb-sec ²	$I_p = (-3.845 + 7.248 \ln \tau) \exp (0.0576 P)$	$I_p = 8.594 \exp (0.065 P)$
W_c , cooling system weight, lb	N/A	$W_c = 130 P^{0.375} + 2.36 \left(\frac{100 - \eta}{\eta} \right) n \dot{u}_{on}$

$$\tau = \left\{ \frac{n \dot{u}_{on}}{1 + \frac{(n-1) \dot{u}_{off}}{n \dot{u}_{on} + (n-1) \dot{u}_{off}}} \right\} = \text{effective ON time, sec}$$

P = generator output, MW

n = number of pulses

\dot{u}_{on} = duration of each pulse, sec

\dot{u}_{off} = time between pulses, sec

Parameter	Turbine Characteristics
D_T , turbine tip diameter, in.	$D_T = (3.89 \times 10^{-5}) N^{-1}$
W_T , turbine assembly weight, lb	$W_T = 0.3455 D_T^{2.362}$
I_{PT} , rotor inertia, in.-lb-sec ²	$I_{PT} = (1.967 \times 10^{-5}) D_T^{4.614}$

N = turbine rotational speed, rpm

SECTION 3

PRELIMINARY DESIGNS

INTRODUCTION AND REQUIREMENTS

Parallel studies, of variable emphasis per contractual requirements, were conducted for conventional generators, superconducting generators, and non-air-breathing turbines to generate tradeoff analyses to assist the Air Force in selecting the appropriate concepts for high-power application. The procedures followed in the study program encompass the generation of parametric data and the development of key computer codes, with subsequent point design evaluation of the components of interest at the specified operating conditions (Table 6).

TABLE 6

SOW DESIGN REQUIREMENT IDENTIFICATION

Parameter	Range	Point Design Number							
		1	2	3	4	5	6	7	8
Power, MWe	10 to 50	10	10	25	25	25	25	50	50
Voltage, kV	20 to 250	60	60	60	60	60	60	200	200
Duty cycle, sec									
On time	1 to 120	21	21	4	120	21	21	25	12
Off time	2 to 300	30	300	4	N/A	30	300	N/A	78
No. of cycles/mission		3	3	16	1	3	3	3	10
Total run time, sec	30 to 120	63	63	64	120	63	63	75	120
Startup time, sec		1	1	1	1	1	1	1	1
Idle time, min	5 to 120	0	0	0	0	0	0	0	0

- Notes: (1) The subsystem shall be designed for a 100-mission life (total life = 100 x number of cycles above).
- (2) Electrical sources shall be designed to produce 60 kV, if possible. If the source cannot achieve 60 kV directly, design for minimum weight and volume regardless of voltage.
- (3) The subsystem shall be designed for 1-sec startup time, if possible. If 1-sec startup is not possible, design for minimum startup time. If startup time is greater than 3 sec, provide for 10-min idle.

Contractual requirements called for the design evaluation of identified key components. It was felt, however, that restricting the study to component evaluation, per se, may lead to erroneous assessment of the capability and requirements of the particular component under evaluation. Furthermore, very often a component characteristic is described without including ancillary equipment. The procedure adopted, therefore, was to conduct sufficient system study such that the individual component operating characteristics clearly reflect its requirements within the intended application. For example, the selection of rotational speed is greatly influenced by overall power system considerations. At the low power range of interest (approx. 10 MWe), the individual component characteristics of the turbine and generator indicate the selection of optimum speed for the individual components with the use of an interconnecting gearbox. At the medium power level of interest (25 MWe), for the majority of the cases, power system considerations indicate the desirability of rotational speed compromise between the driver (turbine) and the driven component (generator) by using a direct-drive power assembly. At the high power level of interest (50 MWe), selection of rotational speed of the power drive assembly is dictated by structural considerations for the turbine, so a direct-drive assembly is used.

Many of the various technical disciplines associated with preliminary component and system analyses were not conducted in this study program. Typical examples encompass evaluation of component and system controls, critical speed and detail stress evaluation of the superconducting generator, ancillary component detail designs (lubrication pumps and recirculating pumps), etc. Providing the selected operating characteristics reflect previously established designs, these technical disciplines merely refine the specific component operating characteristics and, as such, add little in the initial component conceptual design identification. For ease of presentation, the design description initially concentrates on the medium power range of interest: 25 MW electrical output at three bursts of 21 sec on with 300 sec off (point design 6). Many of the independent detailed analyses were carried out for point design 6 to verify the validity of models used in the design techniques. Examples of such backup analyses include a detailed review of turbine blade vibration and stress. This medium power range description is followed by descriptions of the remaining point designs

encompassing design characterization of conventional generators (thermal-lag and fluid-cooled), superconducting generators, and turbines as individual components and turbogenerators. Design characteristics of complete power systems and fast startup capability also are described.

MEDIUM-POWER APPLICATION, CONVENTIONAL GENERATOR

The conventional generator, whether of thermal-lag or actively fluid-cooled design concept, naturally lends itself to fast startup operation. It is equally adaptable to either monopropellant or bipropellant turbogenerator power systems. Schematics of such turbogenerator power system concepts are shown in Figures 1 and 2. Figure 1 refers to a monopropellant application; Figure 2 refers to a bipropellant application. For clarity, required electronic control package and supervisory control console are not shown.

System simplicity, the use of a single feed and control subsystem, and minimum weight lead to the selection of a monopropellant-energized turbogenerator design concept; however, propellant cost associated with concept development and operation and, to a lesser degree, monopropellant combustor development, may lead to the desirability of a bipropellant turbogenerator concept even with its additional weight penalty and increased operational complexity. Detail considerations are described in Sections 4, 5, 8, and 9. For illustrative purposes, the subsequent description refers to the application of a monopropellant turbogenerator power system. The majority of component operational characteristics and various comments are, however, equally applicable, whether monopropellant or bipropellant turbogenerator power system use is eventually selected.

Operational Sequence

The following sequential operational procedures are used to promote fast startup in a conventional generator turbogenerator power system (refer to Figure 1). Upon start signal, the nitrogen pressurization vessel shutoff valve is opened to pressurize the propellant stored in the start tank; subsequently, the fuel shutoff and fuel control valves are actuated to the fully open position to allow flow from the start storage to provide high-pressure, high-flow energy to the turbine for fast startup. The startup control mode is pressure regulated (ratio dependent upon startup time sought); thus, during

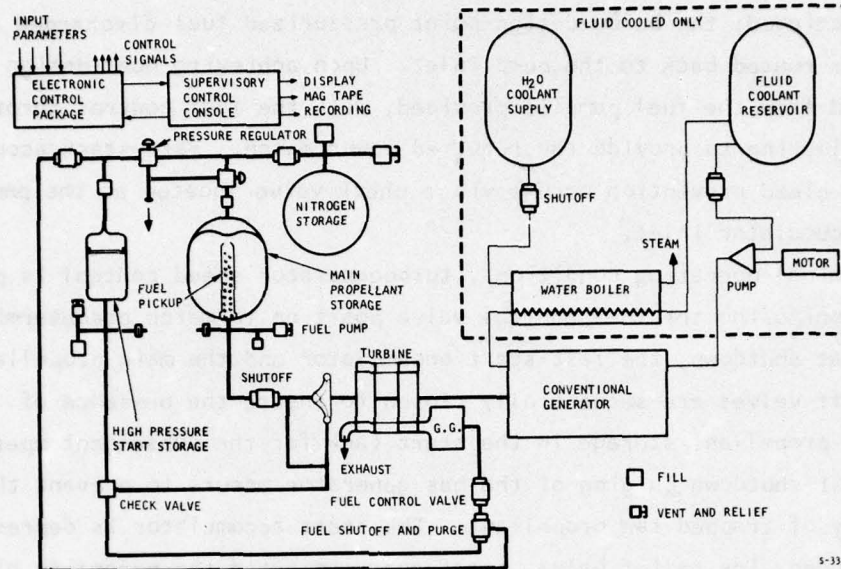


Figure 1. Fast Startup, Monopropellant Application

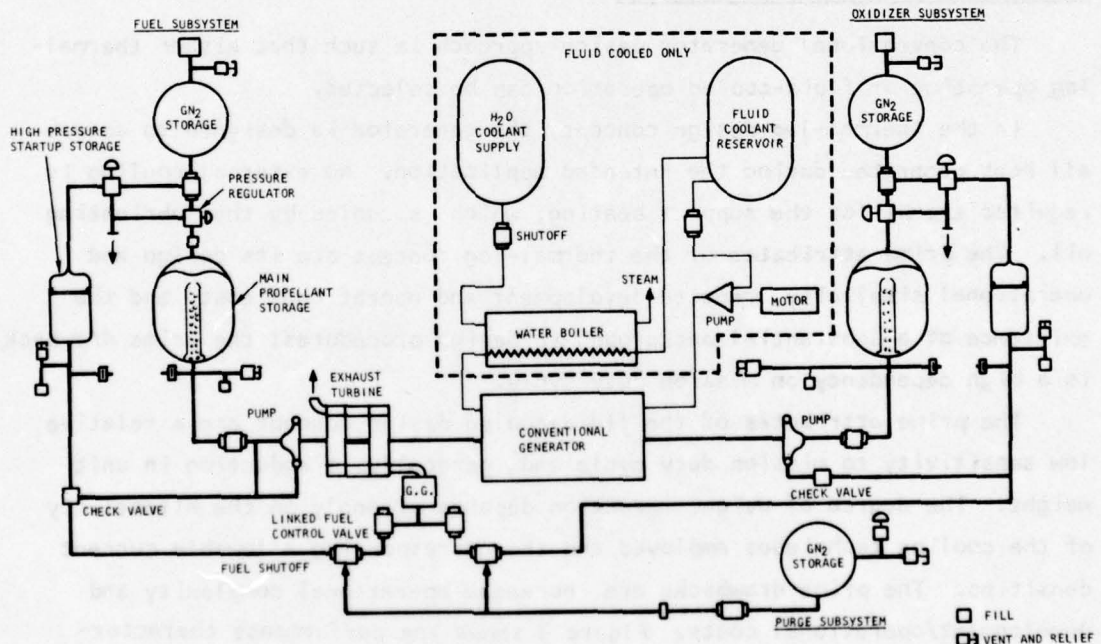


Figure 2. Fast Startup, Bipropellant Application

this operating sequence, the fuel control valve is in a wide-open position to provide maximum flow to the turbine. Until satisfactory operating speed range is achieved, the below-design-point pressurized fuel discharged from the pump is routed back to the pump inlet. Upon achieving near-design speed, direct feed from the fuel pump is provided, with the fuel control throttle valve readjusting to provide the required power match. Fast-start accumulator fillup and bleed prevention occurs via a check valve located at the pump exit and the accumulator inlet.

At nominal operating conditions, turbogenerator speed control is provided by monitoring the fuel control valve position to match predetermined torques. At shutdown, the fast-start accumulator and the main propellant fuel shutoff valves are sequentially closed to ensure the presence of sufficient propellant storage in the start tank for the subsequent operating cycle. Post-shutdown purging of the gas generator occurs to prevent the possibility of trapped raw propellant. The start accumulator is depressurized via a nitrogen-side relief valve, a safeguard to avoid the necessity of long-term, high-pressure, airborne hydrazine storage.

Thermal-Lag vs Fluid-Cooled Design

The conventional generator design approach is such that either thermal-lag operation or fluid-cooled operation can be selected.

In the thermal-lag design concept, the generator is designed to absorb all heat generated during the intended application. No external cooling is required except for the support bearing, which is cooled by the lubricating oil. The prime attributes of the thermal-lag concept are its design and operational simplicity, reduced development and operational cost, and the existence of a substantial background in design procedures; the prime drawback is a high dependency on mission duty cycle.

The prime attributes of the fluid-cooled design concept are a relative low sensitivity to mission duty cycle and, generally, a reduction in unit weight. The degree of weight reduction depends strongly on the effectivity of the cooling techniques employed and the corresponding allowable current densities. The prime drawbacks are increased operational complexity and development/operational costs. Figure 3 shows the performance characteristics of conventional thermal-lag and fluid-cooled designs at the medium

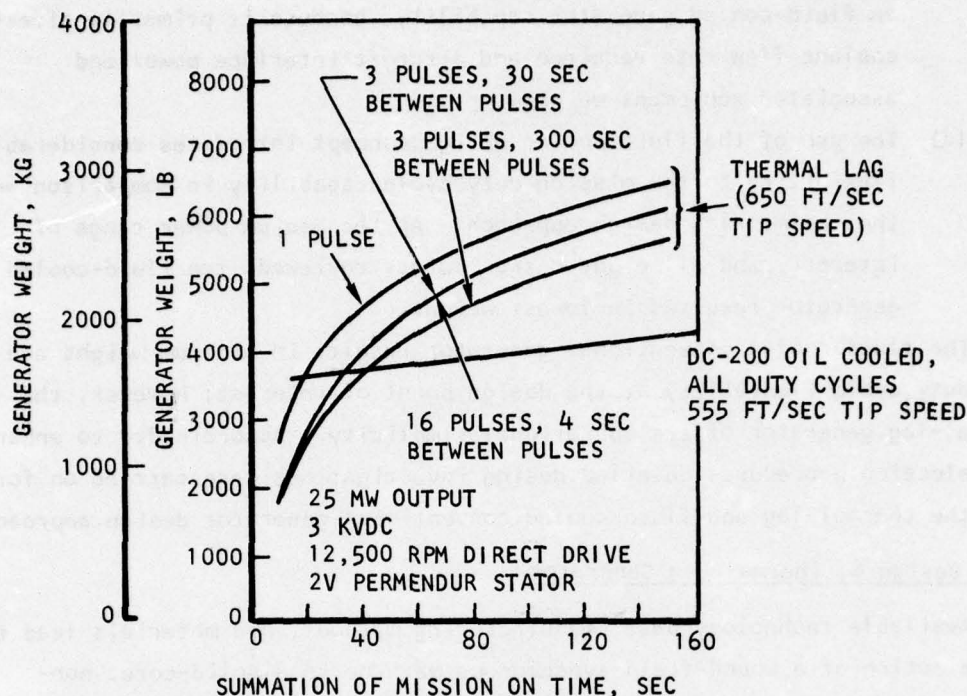


Figure 3. Effect of Duty Cycle and Cooling Method on Conventional Generator Weight Characteristics

power range of interest, as a function of integrated mission time, with duty cycle as a parameter. The following comments apply:

- As expected, the weight of the thermal-lag generator is highly dependent on the operating duty cycle. Variation in the number of pulses, pulse duration, and OFF times between active pulses significantly affects the weight of the thermal-lag generator design.
- In the medium power range of interest, for integrated mission ON times below 45 sec, the thermal-lag design approach is competitive with or lighter than its fluid-cooled counterpart design approach.
- The fluid-cooled generator is relatively independent of the mission duty cycle. Its weight variation is primarily a function of the integrated ON time, which determines the amount of evaporative coolant heat sink (and associated tankage) that must be carried for mission completion. The OFF time duty cycle has only a minor effect

on fluid-cooled generator capability, because it primarily affects coolant flow rate required and aircraft interface power and associated equipment weight.

- (d) The use of the fluid-cooled design concept introduces considerable flexibility to the mission duty cycle capability in comparison with the thermal-lag design approach. At the medium power range of interest, and all eight design points reviewed, the fluid-cooled generator resulted in lowest weight.

The fluid-cooled conventional generator results in minimum weight and high duty cycle flexibility at the design point of interest; however, the thermal-lag generator offers operational simplicity. Accordingly, to enhance the selection procedure, detailed design investigations were carried on for both the thermal-lag and fluid-cooled conventional generator design approaches.

Point Design 6, Thermal Lag Generator

Available technology base, manufacturing methods, and materials lead to the selection of a wound-field synchronous machine in a solid-core, non-salient-pole (round-rotor) configuration as the optimum choice. The use of this concept has shown to be significantly superior in weight and performance to either the Lundell or homopolar inductor types in applications requiring generator output dc rectification. Drawing L2016296 is a preliminary conceptual layout of a conventional thermal-lag generator satisfying the point design 6 requirements. Generator design details are summarized in Table 7.

Optimal generator design configuration favors the use of low rotational speed with associated low length-to-diameter (L/D) ratio in view of the relatively low sensitivity of weight variation as a function of speed; however, turbogenerator application considerations indicate the desirability of a rotational speed compromise between the driver (turbine) and the driven component (generator) such that direct drive power assembly results. Involved component weight, structural, and critical speed considerations established selection of 12,500 rpm as the design rotational speed.

With respect to the generator, a low-voltage design approach is selected requiring the use of a transformer. This design approach results in the minimum weight design, low development risk, and desired design flexibility.

AFAPL-TR-76-39

D

C

B

A

12

11

10

21

12

11

10

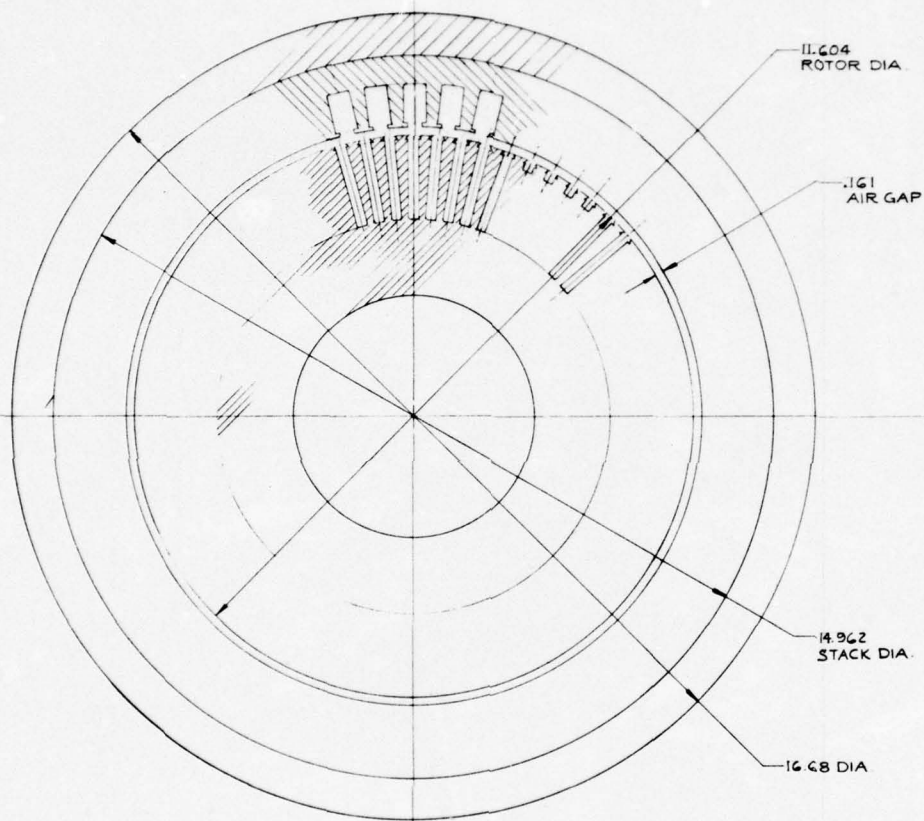
11.604
ROTOR DIA.

.161
AIR GAP

14.962
STACK DIA.

16.68 DIA

SECTION A-A



2

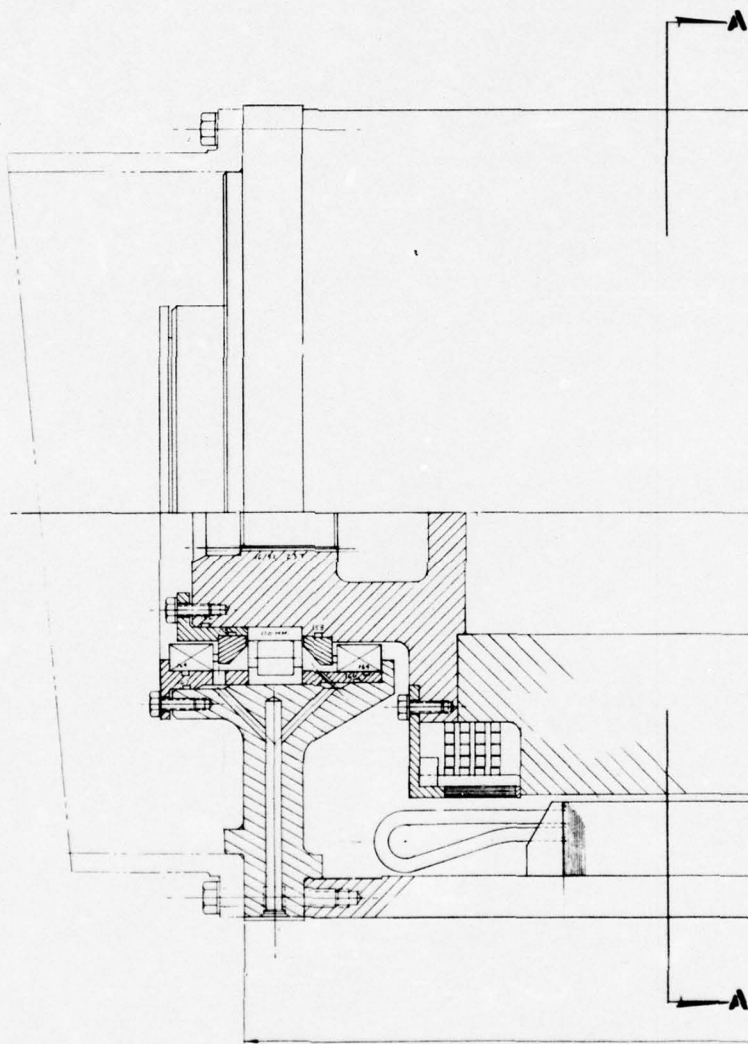
10

1

9

8

1



120.25

10

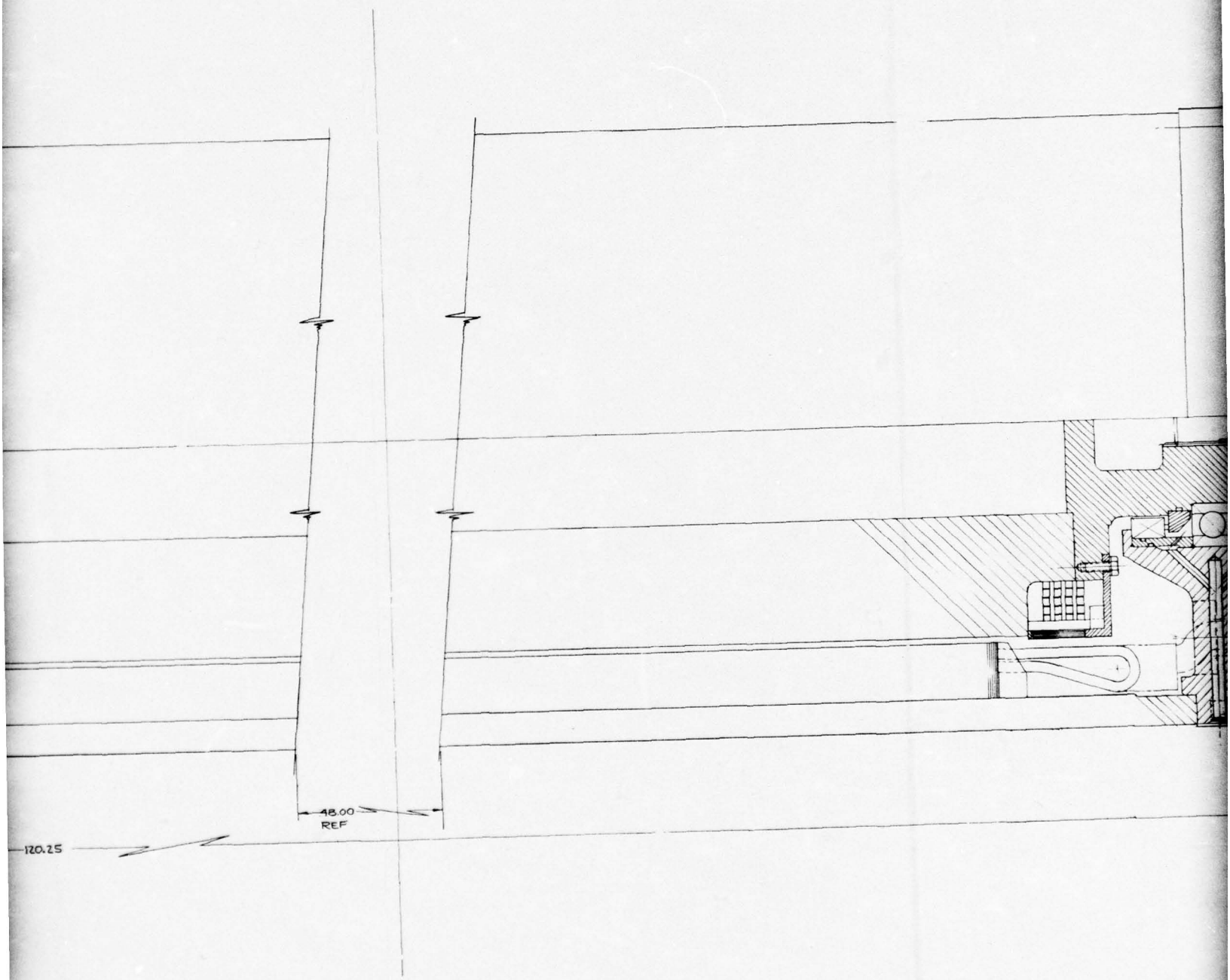
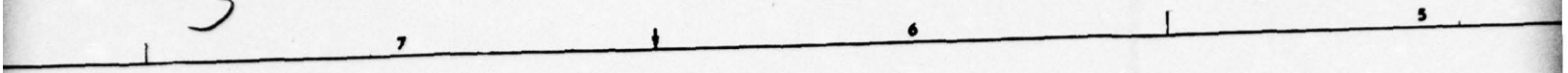
1

9

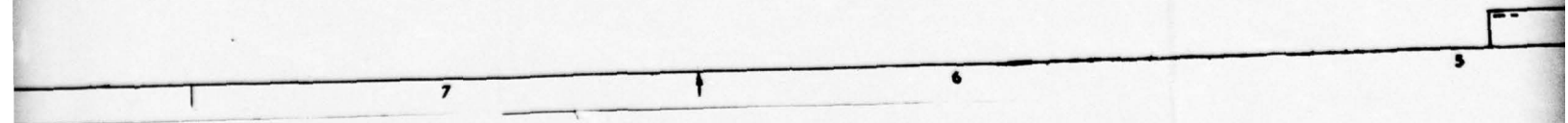
8

1

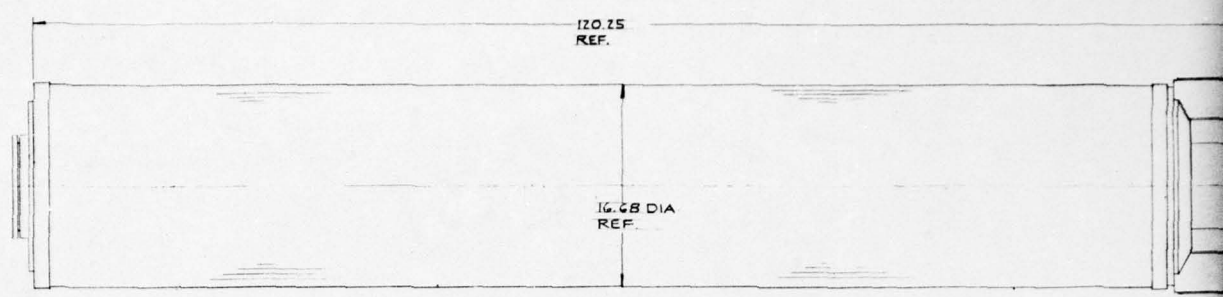
3'



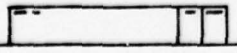
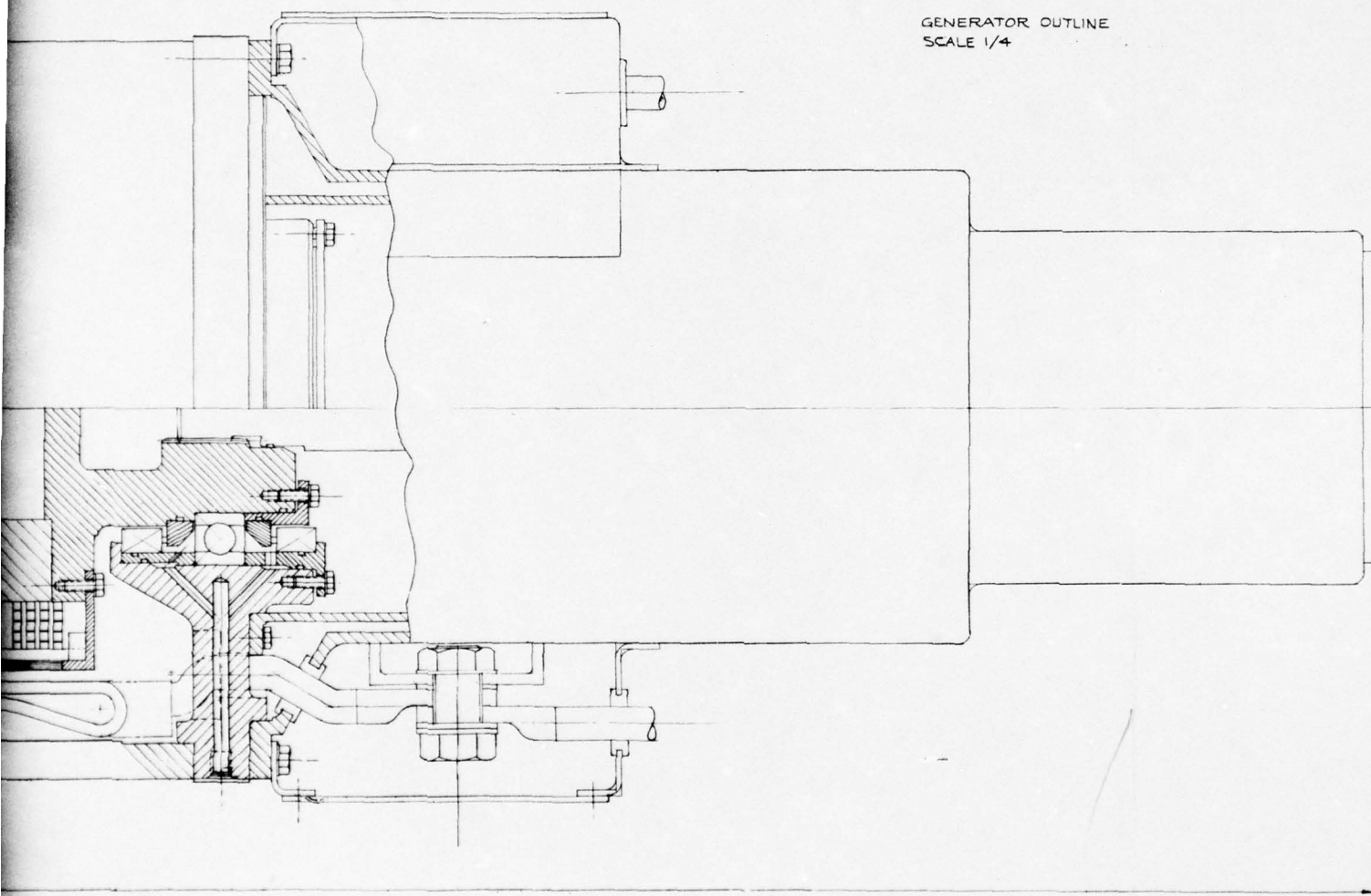
120.25



4

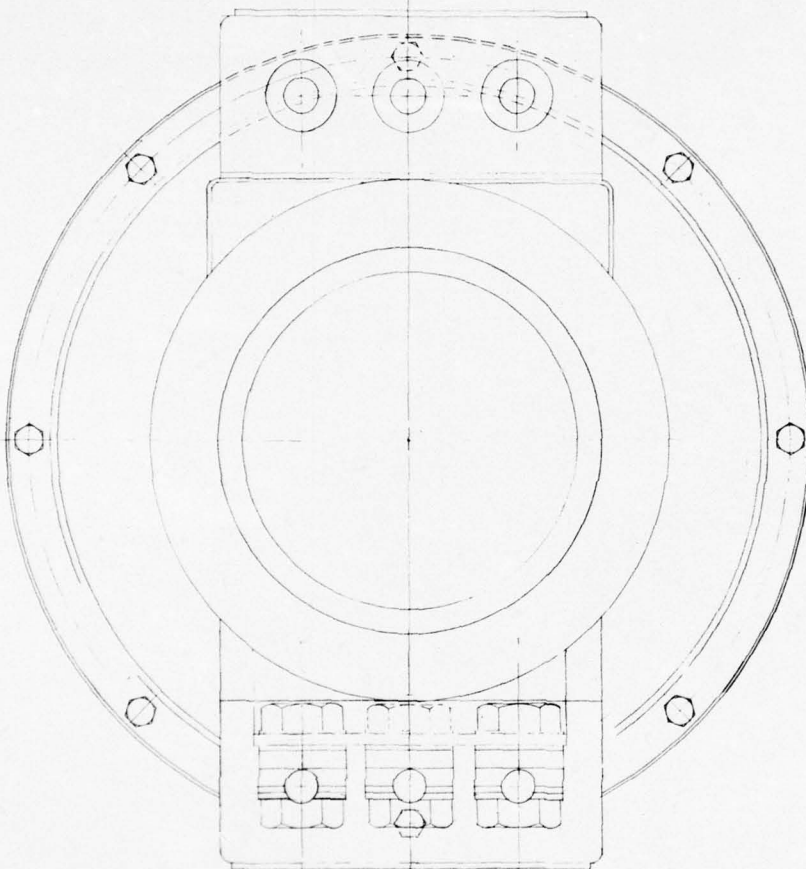
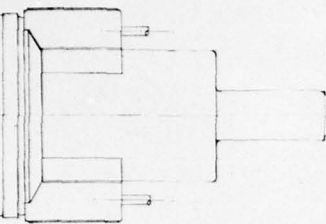


GENERATOR OUTLINE
SCALE 1/4



NOTES: UNLESS OTHERWISE SPECIFIED

1



REVISIONS				
ZONE	LYR	DESCRIPTION	DATE	APPROV

[illegible]

NOTES: UNLESS OTHERWISE SPECIFIED

1

10

1

1

1

AFAPL-TR-76-39

TABLE 7
CONVENTIONAL GENERATOR, THERMAL LAG, POINT DESIGN 6

Power level, MW	<u>25</u>	Cooling system weight	
Type of load	<u>Rectified</u>	(including fluids), lb	<u>N/A</u>
Cooling method	<u>Thermal lag</u>	Total weight of generator	
Coolant	<u>None</u>	and cooling system, lb	<u>N/A</u>
Coolant flow rate, gpm	<u>N/A</u>	Specific weight, lb/kW	<u>0.171</u>
Coolant pressure drop, psi	<u>N/A</u>	Duty cycle:	
		Number of pulses	<u>3</u>
Voltage, L-N, V	<u>1737</u>	ON time per pulse, sec	<u>21</u>
Stator current density, A/sq in.	<u>14,529</u>	OFF time per pulse, sec	<u>300</u>
Field current density, A/sq in.	<u>14,655</u>	Initial copper temp, F	<u>130</u>
Stator material	<u>2V Permendur 0.010</u>	Final copper temp, F	<u>450</u>
Rotor material	<u>HP 9-4-20</u>	Number of phases	<u>3</u>
Rotor rotational speed, rpm	<u>12,500</u>	Power factor	<u>0.879 lagging</u>
Rotor peripheral speed, ft/sec	<u>650</u>	Number of poles	<u>6</u>
Rotor outside dia., in.	<u>11.60</u>	Frequency, Hz	<u>625</u>
Rotor magnetic length, in.	<u>83.07</u>		
Main generator dia.		Rotor length/dia.	<u>7.16</u>
(excluding flanges), in.	<u>16.67</u>	Exciter dia, in.	<u>10.75</u>
Main generator length, in.	<u>96.36</u>	Exciter length, in.	<u>14.56</u>
Main generator volume, cu in.	<u>21,032</u>	Exciter volume, cu in.	<u>1320</u>
Main generator weight, lb	<u>4,120</u>	Exciter weight, lb	<u>151</u>
		Field power, kW	<u>223.5</u>
Total generator volume, cu in.	<u>22,352</u>	Total losses, kW	<u>1,385</u>
Total generator weight, lb	<u>4,271</u>	Overall efficiency	<u>0.9471</u>
Rotor inertia, in.-lb-sec ²	<u>103.8</u>		
Motor-pump input power, kW	<u>N/A</u>		

Assembly specific weight = 0.171 lb/kW

Minimum generator assembly weight is established because the combined weight of the low-voltage generator (0.17 lb/kW) and the transformer (0.06 lb/kW) is lower than with the use of direct required voltage output generator design (0.42 lb/kW). The use of a stationary transformer to obtain high voltage output from the low-voltage generator reduces associated development risk. Furthermore, in the final application, several output voltage levels (not firmly established) will be required. Thus, the present design using a low-voltage generator with transformer adds to system flexibility.

Because a rectified type of load is used, the apparent power factor is uniquely related to the commutation reactance. The value of the apparent power factor corresponding to the optimum-weight generator is 0.879 lagging.

1. Structural Evaluation

As shown in Drawing L2016296, the generator assembly is a dual-bearing horizontal-flange-mount configuration with a maximum outside diameter of 16.68 in. and a maximum length of 120.75 in. including the self-energized permanent magnet (PM) exciter, the main exciter, and the generator.

In the conceptual design evaluation, careful consideration was given to selection of materials that will result in an acceptable low-weight generator design. Materials selected for the various key elements of the generator are summarized in Table 8.

All materials listed have been used in previous AiResearch designs and have been characterized in such areas as optimum heat treatment, weldability, and machinability. This includes the advanced composite material used in the rotor end rings. Table 9 summarizes the various stress evaluations conducted at critical generator locations to ensure the viability of the proposed design.

As shown in Table 9, the stress evaluation at critical elements of the generator provides the required and desired margin of safety.

TABLE 8

CONVENTIONAL GENERATOR - THERMAL LAG

MATERIAL PART LIST

Machine Element	Material
Stator lamination	2V - Permendur
Stator housing	6061 Al
End bells	A356 Al
Stator conductor	Cu, CDA 102
Stator conductor insulation	Class H, Epoxy-mica
Rotor core	HP9-4-20 Steel
Rotor conductor	Cu, CDA 102
Rotor end rings	Fiber-epoxy
Rotor insulation	Hard mica splitting
Coil blocking/bracing	Epoxy
Stator stack retainer	6061 Al

TABLE 9

CONVENTIONAL GENERATOR - THERMAL LAG

CRITICAL STRESS REVIEW

Part Name	Characteristic Stress, Psi	Allowable Stress, Psi
Coil retaining wedge	93,849 (compressive)	150,000
Slot	30,950 (cyclic)	94,000
Field conductor	8,838 (contact)	10,000
End rings	114,210 (hoop)	203,000

2. Critical Speed Evaluation

The unusually high L/D imposed by the desirability of achieving high power and low generator weight requires the evaluation of component critical speed. By necessity, a simplified model was used. By varying the combinations of bearing stiffness and resilience, the effective spring rate of the complete dynamic system (rotor, stub shaft, bearing, and bearing mount) can be modulated over a wide range such to ensure that rotor critical speeds do not occur near the component operating speed. Table 10 presents the critical speed summary for variable bearing stiffness and bearing mount resilience of the conventional thermal-lag generator, point design 6.

Referring to Table 10, the use of medium bearing stiffness in a stiff resilient mount must be avoided because the second flexural mode provides only 6 percent safety margin. The medium stiffness bearing in a soft resilient mount provides the largest spread in the critical speeds about the nominal operating speed; however, three critical speeds must be traversed to reach the operating speed. A stiff bearing in a rigid mount provides a slightly smaller spread of critical speeds about the operating speeds, but requires that only two critical speeds be traversed. Accordingly, the latter provides the best choice. Notice that rigid mount implies stiff in comparison with the bearing, not necessarily infinitely stiff. A bearing mount of high stiffness can be conveniently achieved by making the bearing housing an integral part of the generator support structure.

TABLE 10
CONVENTIONAL GENERATOR - THERMAL LAG PRELIMINARY CRITICAL SPEED REVIEW

Bearing Stiffness	Bearing Mount	NCR, Generator Rotor Critical Speeds, rpm			
		First Rigid Body and First Flexural	Second Rigid Body	Second Flexural	First Freebody
Medium	Soft resilient	1852	3368	7,406	17,883
Medium	Stiff resilient	2936	5449	11,745	17,883
Soft	Rigid	3872	7379	15,486	17,883
Stiff	Rigid	4806	8642	19,222	17,883
NOTES: Rotor dia = 11.60 in., rotor length = 83.07 in., L/D = 7.16, operating speed = 12,500 rpm					

It must be realized that traversing several critical speeds is inherent in the design of a generator where minimum component weight is achieved by the simultaneous selection of high peripheral and rotational speeds. As the quest for component weight reduction is pursued, increasingly sophisticated design of rotating assemblies is implied. For example, provisions may have to be made for hydraulic damping around the bearings to limit shaft deflections and bearing loads. The analysis of critical speed problems, mode shape, and response characteristics (startup, shutdown, etc.) requires the use of rather elaborate analytical techniques. These tools are well established and available, but their application is beyond the scope of the present study program. The critical speed evaluation carried is preliminary in nature; however, the multiplicity of possible design approaches indicates that a low-weight, high L/D generator is indeed a viable concept.

Point Design 6, Fluid-Cooled Generator

Drawing L2016297 is a preliminary conceptual layout of a conventional fluid cooled generator satisfying the point design No. 6 requirements. Generator design details are summarized in Table 11.

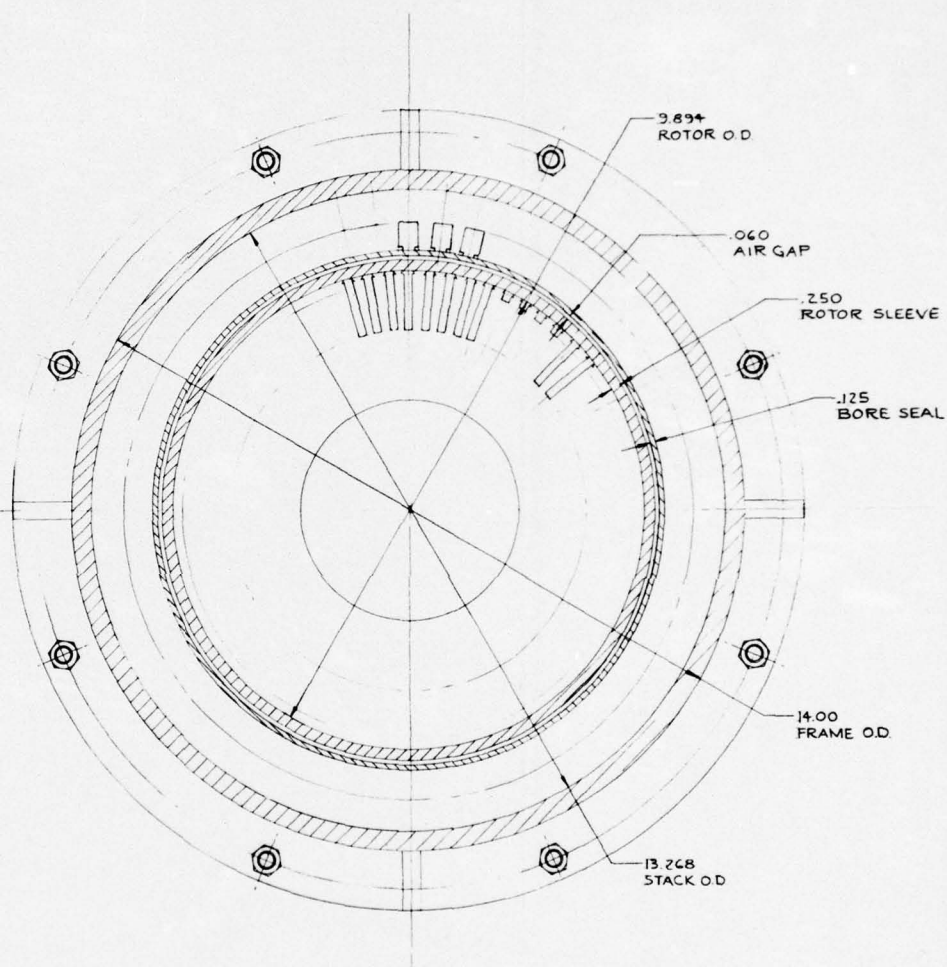
The generator is a wound-field, solid-core, nonsalient-pole (round-rotor) configuration. The selected cooling method uses hollow conductors in the rotor and the stator in conjunction with a bore seal in the stator. The use of this highly effective cooling technique allows the use of increased current densities, so the generator is lighter than its conventional thermal-lag counterpart design. The potential of continuous duty cycle operation is obtained at the expense of a relatively minor weight penalty, namely, required coolant and storage tank weight, which is a function of mission time. Rotational speed and output voltage selection considerations previously described for the thermal-lag design version are equally applicable.

TABLE 11
CONVENTIONAL GENERATOR, FLUID-COOLED, POINT DESIGN 6

Power level, MW	<u>25</u>	Cooling system weight	
Type of load	<u>Rectified</u>	(including fluids), lb	<u>716</u>
Cooling method	<u>Fluid</u>	Total weight of generator	
Coolant	<u>DC-200</u>	and cooling system, lb	<u>3,664</u>
Coolant flow rate, gpm	<u>228.3</u>	Specific weight, lb/kW	<u>0.147</u>
Coolant pressure drop, psi	<u>120</u>	Duty cycle	<u>Continuous duty</u>
Voltage, L-N, V	<u>1617</u>	Number of pulses	<u>N/A</u>
Stator current density, A/sq in.	<u>38,142</u>	ON time per pulse, sec	<u>N/A</u>
Field current density, A/sq in.	<u>37,366</u>	OFF time per pulse, sec	<u>N/A</u>
Stator material	<u>2V Permendur 0.010</u>	Initial copper temp, F	<u>230</u>
		Final copper temp, F	<u>400</u>
Rotor material	<u>HP 9-4-20</u>	Number of phases	<u>3</u>
Rotor rotational speed, rpm	<u>12,500</u>	Power factor	<u>0.876 lagging</u>
Rotor peripheral speed, ft/sec	<u>555</u>	Number of poles	<u>6</u>
Rotor outside dia., in.	<u>9.89</u>	Frequency, Hz	<u>625</u>
Rotor magnetic length, in.	<u>78.27</u>	Rotor length/dia.	<u>7.91</u>
Main generator dia.		Exciter dia, in.	<u>9.27</u>
(excluding flanges), in.	<u>14.19</u>	Exciter length, in.	<u>20.93</u>
Main generator length, in.	<u>89.83</u>	Exciter volume, cu in.	<u>1411</u>
Main generator volume, cu in.	<u>14,189</u>	Exciter weight, lb	<u>257</u>
Main generator weight, lb	<u>2,691</u>	Field power, kW	<u>581</u>
Total generator volume, cu in.	<u>15,600</u>	Total losses, kW	<u>1,873</u>
Total generator weight, lb	<u>2,948</u>	Overall efficiency	<u>0.9296</u>
Rotor inertia, in.-lb-sec ²	<u>49.92</u>		
Motor-pump input power, kW	<u>30.3</u>		

Assembly specific weight = 0.147 lb/kW

AFAPL-TR-76-39



SECTION A-A

2'

10

9

8

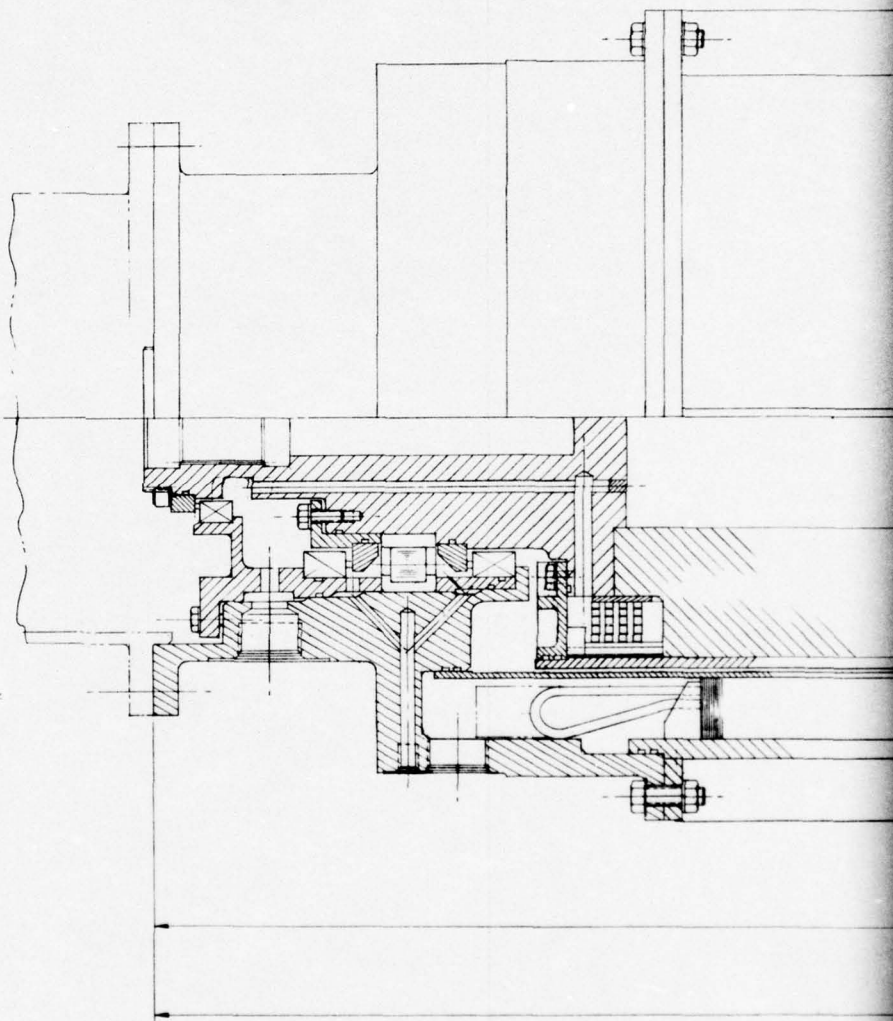
00

060
AIR GAP

250
ROTOR SLEEVE

125
BORE SEAL

14.00
FRAME O.D.



10

9

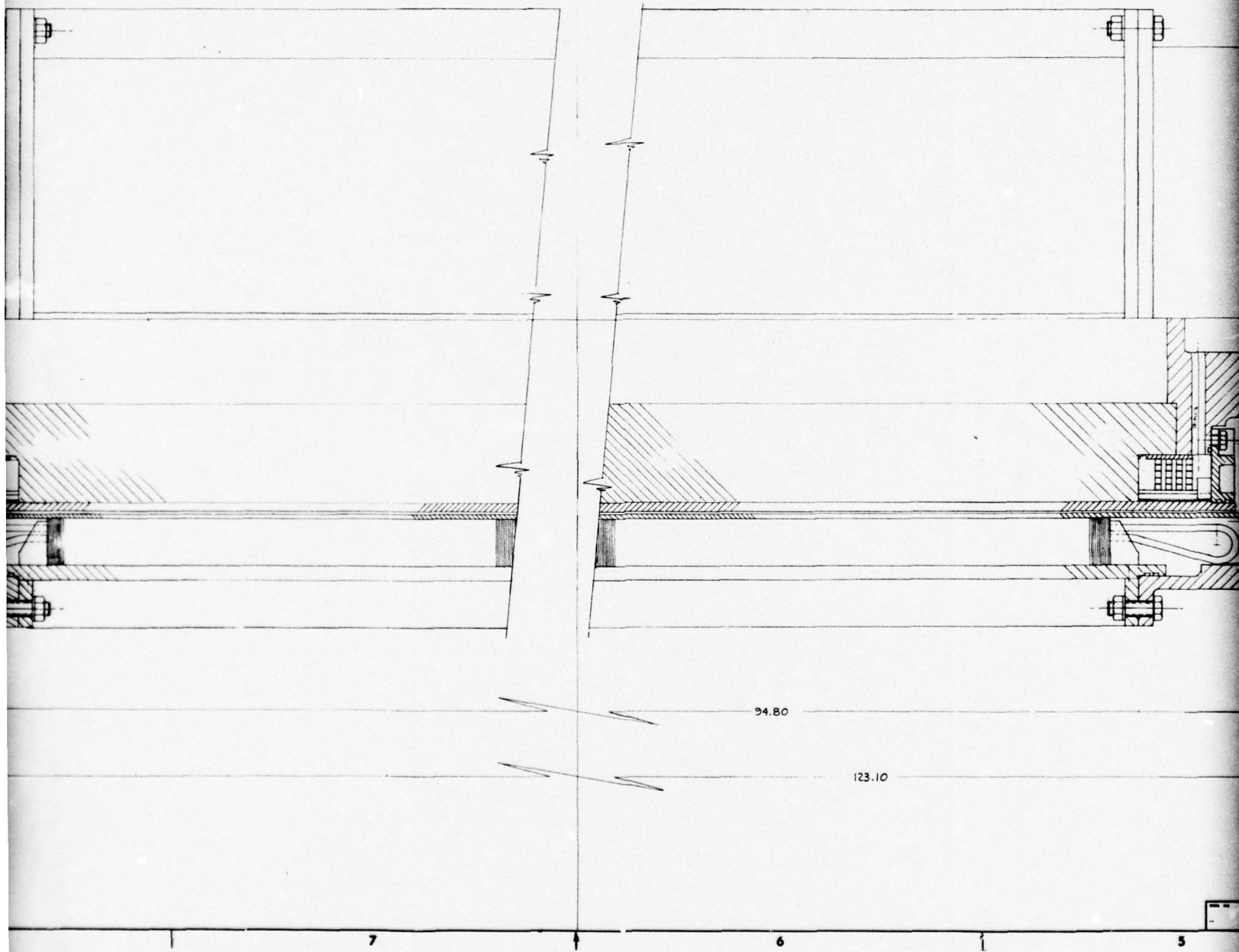
8

3

7

6

5



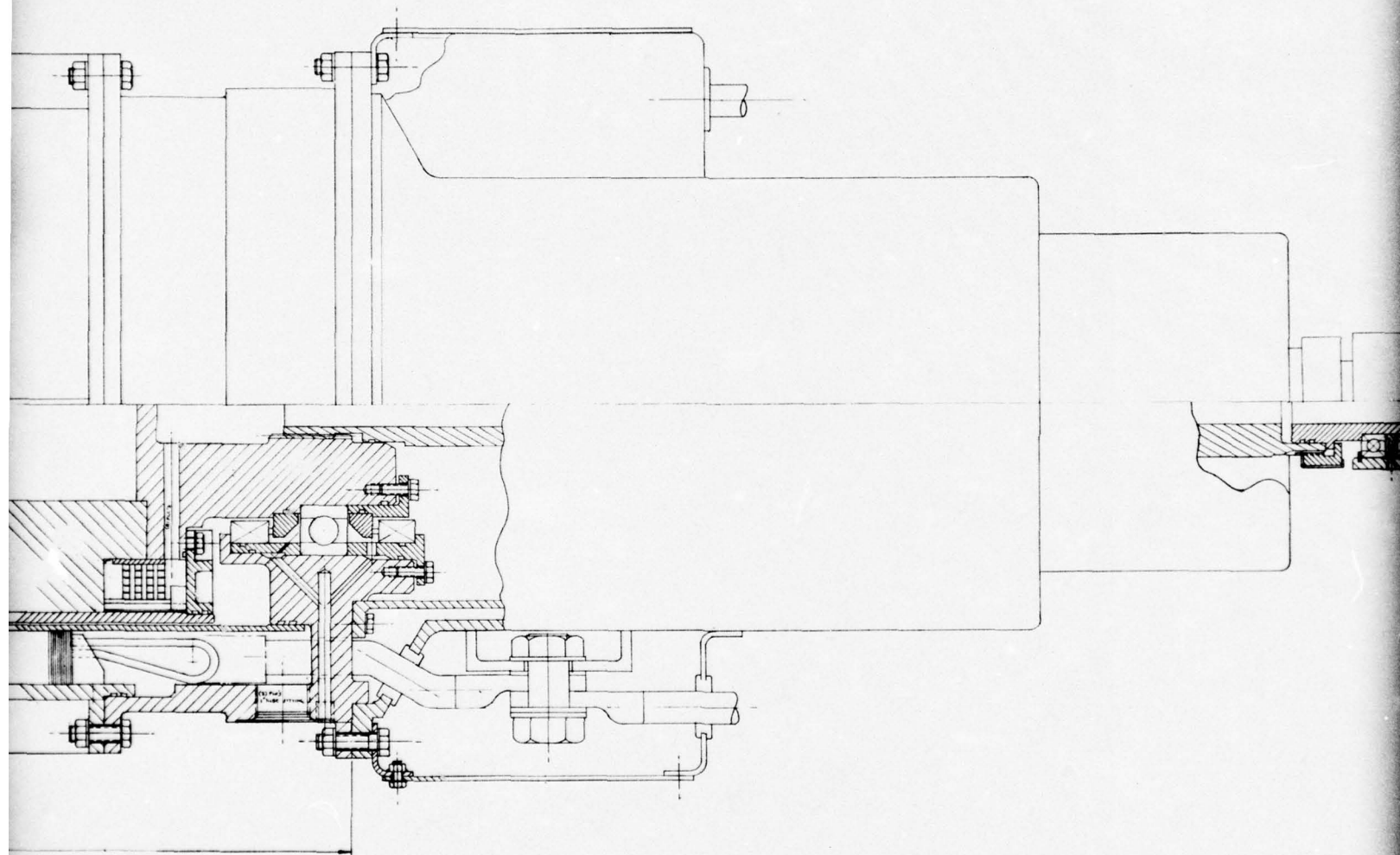
4

5

4

3

2



5

4

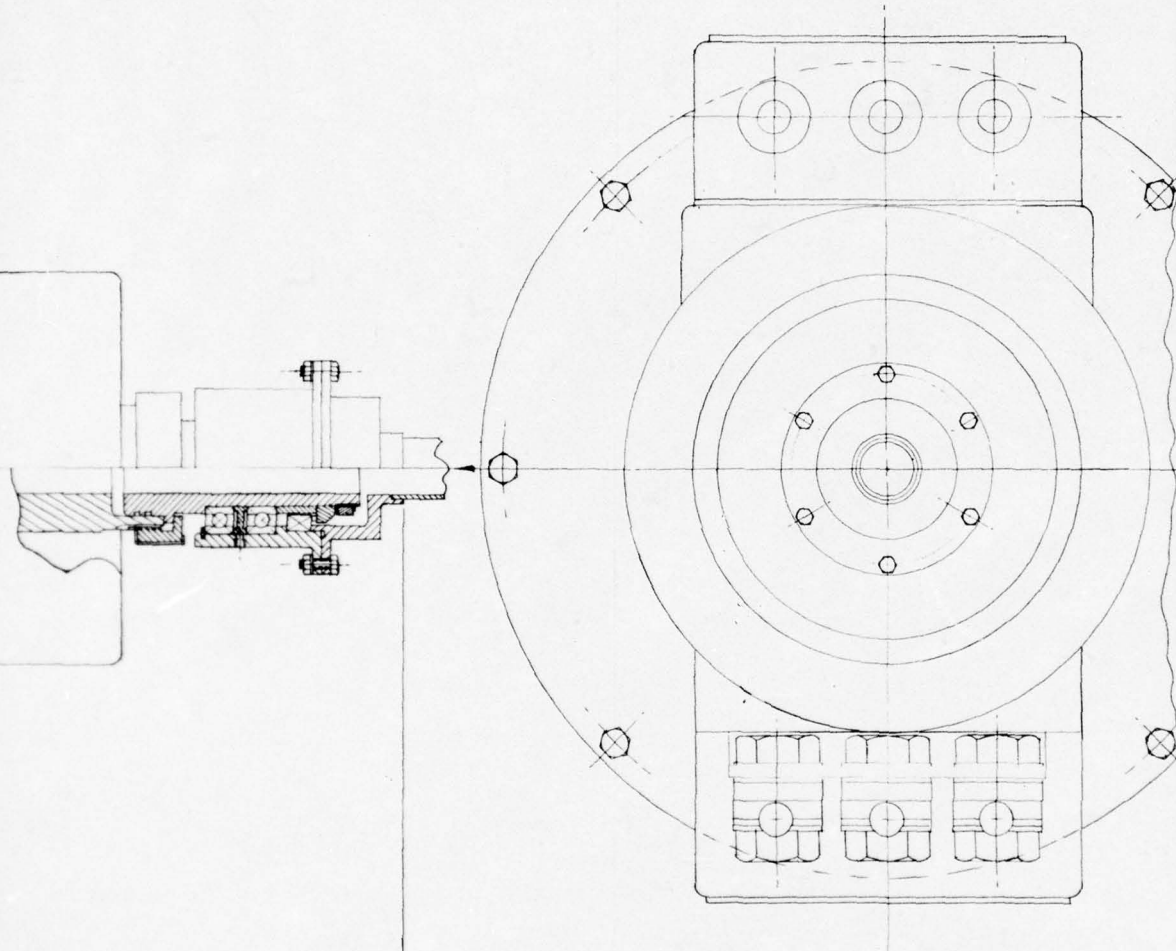
3

NOTES UNLESS OTHERWISE

5

1. This drawing is for the purpose of showing the general arrangement of the parts and is not to be used for manufacturing purposes. It is not to be used for the purpose of showing the details of the parts or the method of construction.

REVISIONS			
NO.	DATE	DESCRIPTION	BY
1			



NOTES: UNLESS OTHERWISE SPECIFIED

QTY REQD	ITEM NO	CODE NO	PART OR IDENTIFYING NO	NOMENCLATURE OR DESCRIPTION	SYM	ZONE
PARTS LIST				AMERICAN MANUFACTURING COMPANY OF CALIFORNIA A DIVISION OF THE BARRETT CORPORATION THERMANS, CALIFORNIA		
UNLESS OTHERWISE SPECIFIED: BASE CONTROL PER IDENTIFICATION MARKING PER STD INTERPRETATIONS PER PWS				11-7-77		
HEAT TREATMENT PROCESS PER PWS				GENERATOR 25MW OIL COOLED		
APPLICATION				J 70210 L2016297		
SCALE				SHEET OF		

L2016297

AFAPL-TR-76-39

1. Structural and Critical Speed Evaluation

Materials selected for the various key elements of the generator are summarized in Table 12.

TABLE 12

CONVENTIONAL GENERATOR, FLUID-COOLED, MATERIALS LIST

Machine Element	Material
Stator lamination	2V - Permendur
Stator housing	6061 Al
End bells	A356 Al
Stator conductor	Cu, CDA 102
Stator conductor insulation	Class H, Epoxy-mica
Rotor core	HP9-4-20 Steel
Rotor conductor	Cu, CDA 102
Rotor end rings	Inconel 718
Rotor insulation	Hard mica splitting
Coil blocking/bracing	Epoxy
Stator stack retainer	6061 Al

Table 13 summarizes the various stress evaluations carried out at critical generator locations. Table 14 summarizes variable bearing stiffness and bearing mount resilience. Although identical component rotational speed selection is indicated (in reference to the thermal-lag design), the additional complexity associated with a fluid-cooled generator is reflected in the necessity of reduction in peripheral speed. Structural considerations indicate the selection of a nominal rotor peripheral speed of 555 ft/sec.

Referring to Table 14, the selection of a soft or stiff bearing in a rigid mount provides an adequate spread of critical speeds while traversing two critical speed modes.

2. Thermal Performance Verification

The path to lightweight conventional generator design is through the use of high current densities in the conductors. This, however, increases the resistance losses in the copper and, consequently, the heat that must be removed or absorbed. Although a substantial number of elements of the gener-

TABLE 13

CONVENTIONAL GENERATOR, FLUID-COOLED,
CRITICAL STRESS REVIEW

Part Name	Characteristic Stress, psi	Allowable Stress, psi
Coil retaining wedge	71,331 (compressive)	150,000
Slot	12,597 (cyclic)	94,000
Field conductor	3,412 (contact)	10,000
End rings	117,340 (hoop)	150,000

TABLE 14

CONVENTIONAL GENERATOR, FLUID-COOLED,
PRELIMINARY CRITICAL SPEED REVIEW

Bearing Stiffness	Bearing Mount	N _{CR} , Generator Critical Speeds, rpm			
		First Rigid Body and First Flexural	Second Rigid Body	Second Flexural	First Free Body
Medium	Soft resilient	2,118	3,835	8,470	17,216
Medium	Stiff resilient	3,344	5,896	13,377	17,216
Soft	Rigid	4,333	7,792	17,332	17,216
Stiff	Rigid	4,953	8,860	19,812	17,216
Notes:					
Rotor diameter = 9.89 in.		L/D = 7.91			
Rotor length = 78.27		Operating speed = 12,500 rpm			

ator must be maintained at temperatures that do not produce adverse effects, the thrust of the thermal emphasis is associated with appropriate conductor cooling and heat sink capacity necessary to achieve the desired high operational current densities at acceptable operating temperatures. Successful thermal achievement also introduces the important attribute of low sensitivity to mission duty cycle variations.

The round-rotor generator design computer programs (for thermal-lag and fluid-cooled configurations), delivered to the Air Force under this study program, incorporate new subroutines that determine maximum current density, hence, minimum weight, permissible for a given duty cycle without exceeding the specified maximum temperature limit. To verify the validity of the new round-rotor generator design program incorporating the thermal routines, a detailed transient thermal analysis was conducted. Available detailed AiResearch Thermal Analyzer Computer Program H-0298 was used to assess temperatures and temperature distribution within the fluid-cooled 25-MW generator satisfying the specified requirements of point design 6.

Figure 4 summarizes a typical generator element temperature-time distribution, obtained by the independent, more detailed thermal analysis. Details of the model used and associated operating temperatures are described in Section 6. The results of the evaluation indicate that after three cycles of operation consisting of three power-on periods and two power-off periods, the maximum winding temperature is 398 F in lieu of the design value of 400 F. This temperature level prevails at the conductor rotor end section at the coolant outlet end of the generator. This independent thermal analysis compares most favorably with predicted values, thus verifying the accuracy of the delivered design computer program.

3. Cooling Subsystem Design

To make a valid comparison of the thermal-lag and fluid-cooled conventional generator design characteristics, it is necessary to define the characteristics of the coolant system. The selected coolant system, schematically shown in Figure 5, is of the recirculation type using water as an evaporative heat sink. Coolant is recirculated in a closed loop by an electric-motor-driven pump. The heat absorbed by the coolant in the generator is transferred to the water by vaporization in the boiler. The steam thus generated in the

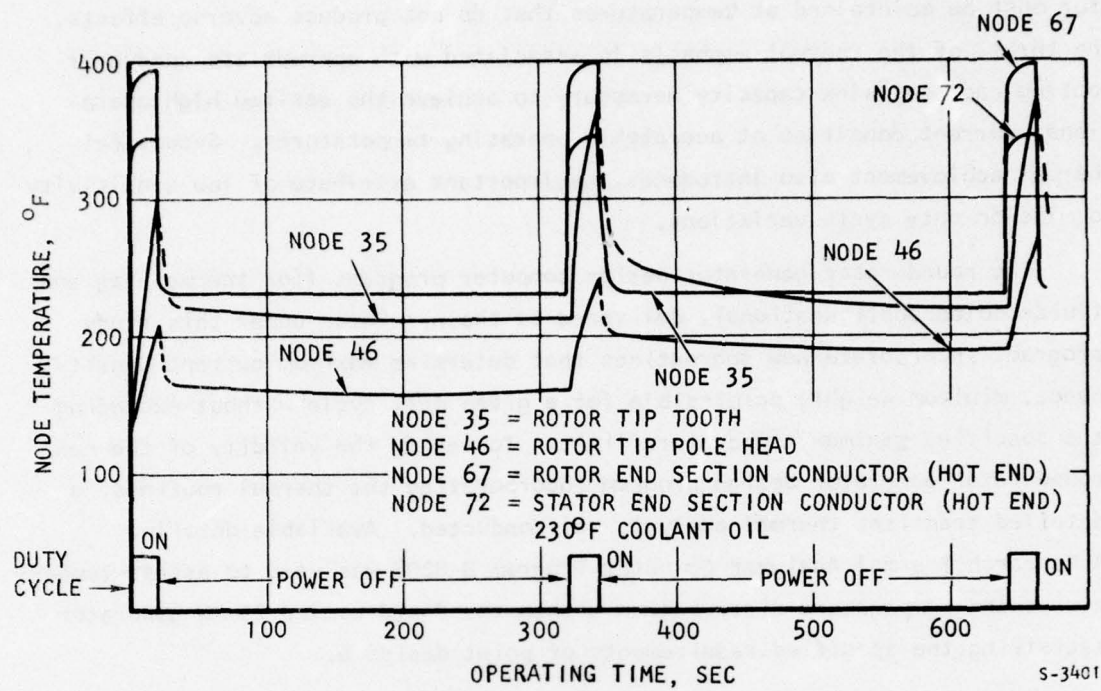


Figure 4. Generator Transient Temperature Distribution

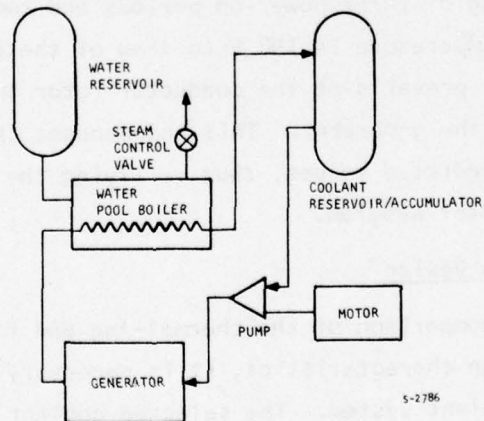


Figure 5. Cooling System Schematic Diagram

boiler is dumped overboard through a control valve that regulates the boiling pressure, hence, operating temperature. For design flexibility a boiling pressure slightly above sea level is used (sea level application). A water blowdown reservoir is used to maintain the required water level in the evaporative pool boiler. The use of the evaporative water coolant concept provides the desired aircraft-independent operation. For a particular mission duty cycle variant, all that is required is an accordingly appropriate selection of water coolant supply. Table 15 summarizes the cooling system characteristics for the point design 6 requirement.

TABLE 15

CONVENTIONAL GENERATOR, FLUID-COOLED
COOLING SUBSYSTEM CHARACTERISTICS

Coolant Subsystem Characteristics	
Heat load, Kw	1873
Coolant type	DC-200
Coolant flow rate, gpm	228.3
Water flow rate, gpm	15.5
Coolant Subsystem Weight	
Subsystem dry weight, lb	383
Lubrication assembly weight, lb	35
Coolant weight, lb	51
Water weight, lb	247
Subsystem wet weight, lb	716
Water-Coolant Heat Exchanger Design Characteristics	
Coolant flow length, in.	32
Water flow length, in.	7.8
No-flow length, in.	12.5

MEDIUM-POWER APPLICATION, SUPERCONDUCTING GENERATOR

Fast startup operation imposes the necessity of achieving full field winding excitation within the short specified acceleration period. Selection of this operational procedure is not recommended for the superconducting airborne generator. The considerations that negate this approach encompass: (1) the need to cool down to a superconducting state the various elements of the generator, (2) the heating in the field windings due to the temperature rise associated with the use of a rotating field, and (3) the possible heating due to encountered friction associated with the potential motions of the superconducting wire. Cool down of the critical elements of the superconducting stage can be achieved via the use of ground support equipment with follow-on airborne limited liquid helium cooling for temperature control purposes; however, the heating associated with rotating field operation and wire motion are such to dictate idle operational mode. The schematic of such a typical airborne superconducting turbogenerator power system is shown in Figure 6. Figure 6 refers to a monopropellant application, the superconducting turbogenerator is equally applicable to the use of bipropellant energized systems with all the design considerations previously described in reference to the merits of either monopropellant or bipropellant use.

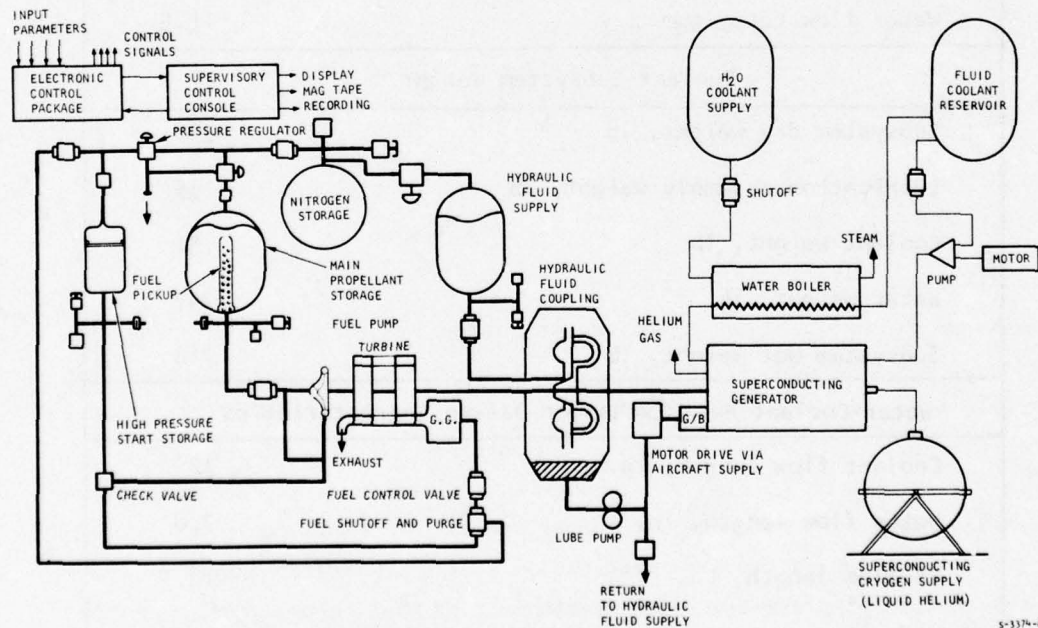


Figure 6. Idling Operation, Monopropellant Application

Operational Sequence

Referring to Figure 6, during the quiescent operating periods, the generator is decoupled from the turbine assembly and idles near design speed in the full excitation mode. The separately driven generator startup acceleration and idling operating mode are provided via the use of aircraft power. This power train can either be in the form of an independent auxiliary motor drive, as shown in Figure 6, or in the form of a hydraulic motor and fluid supply from the aircraft hydraulic subsystem. Regardless of the idling drive concept, the power required is relatively low; basically to overcome supply generator no-load losses, involved operating parasitic losses, and acceleration to the idling design condition in an unexcited operational sequence.

Prior to or upon power demand, the turbine assembly is accelerated in the manner previously described for the conventional turbogenerator power system. The turbine assembly is engaged with the generator assembly with the use of a hydraulic clutch. A hydraulic clutch is preferred to friction and electromagnetic clutches, based upon achieving a superior ability to cushion associated shock and torsional shaft windup with steep load transients.

At power startup operating sequence, the hydraulic clutch is engaged simultaneously with ignition of the gas generator by opening a solenoid valve, thus forcing fluid into the impeller torus from the pressurized fluid supply. A pump is used to return the fluid to the fluid supply through a check valve. In the fluid return circuit, lubrication and cooling of the auxiliary idle drive unit is provided.

Point Design 6, Superconducting Generator

The superconducting generator design is an alternating current machine consisting of a rotating dewar in which the liquid-helium-cooled superconducting coils are located, and a stationary stator that utilizes copper windings at normal temperatures. Three superconducting generator detail designs were established to satisfy the point design 6 requirements. The first two concepts are of low-voltage design output with rotational speeds of 8,000 and 10,000 rpm, respectively. The low-rotational-speed design nearly duplicates the rotor L/D of the design concept presently under development at Westinghouse. In a turbo-generator application, this unit, however, requires the use of an intermediate

gearbox. The high-speed low-voltage operating speed design is such that direct turbodrives is possible. The high-voltage design concept is of interest because it eliminates the use of a transformer; this design approach is, however, of considerably higher risk. Generator design details are shown in Tables 16, 17, and 18. Table 16 refers to the characteristics of the low-speed, low-voltage design approach, Table 17 refers to the high-speed, low-voltage design approach, and Table 18 refers to the low-speed, high-voltage design approach.

For all design concepts, the rotor is excited through slip rings, with 4.2 K liquid helium provided to the superconducting field in the rotor through a dynamic seal located at the center axis of the rotor. The helium is circulated through the rotor windings, boiled off in an electrothermal damper shield, and exhausted back over the inlet feed. All units are of ironless stator design, with a laminated core behind the stator windings to increase rotor-stator magnetic coupling and to provide magnetic shielding. Design details of the superconducting generator are as follows:

1. Stator

The ironless stator is electromagnetically similar to a conventional three-phase multipole stator winding with no iron teeth between the coils. Omission of the iron teeth requires the use of nonmetallic wedges between coils to transfer torque to the generator frame and necessitates the use of many fine, insulated, transposed strands and transposed conductors to reduce eddy currents that would otherwise be excited by the strong, high-gradient field resulting from the ironless construction.

2. Stator Core (Back-Iron)

The coupling of the rotor field into the stator is enhanced by the use of a laminated core behind the stator coils. The stator core also provides a low-reluctance magnetic shield to prevent high magnetic induction in the space around the installation.

3. Rotor

The rotor incorporates superconducting field coils analogous to the coil of a salient-pole conventional machine. The coils are radially arrayed about a nonmagnetic hub and constrained to this hub by the use of a hoop of high strength, nonmetallic fiber.

TABLE 16

SUPERCONDUCTING GENERATOR; POINT DESIGN 6; LOW-SPEED, LOW-VOLTAGE DESIGN

Power level, MW	<u>25</u>	Cooling system weight	
Type of load	<u>Rectified</u>	(including fluids), lb	<u>1006</u>
		Total weight of generator	
Stator cooling method	<u>Fluid cooled</u>	and cooling system, lb	<u>2511</u>
Coolant, stator	<u>MIL-L-23699</u>	Specific weight, lb/kW	<u>0.100</u>
Coolant flow rate, gpm	<u>197.4</u>		
Coolant pressure drop, psi	<u>20</u>	Duty cycle:	<u>Continuous duty</u>
		Number of pulses	<u>N/A</u>
Voltage, L-N, V	<u>2000</u>	ON time per pulse, sec	<u>N/A</u>
Stator current density, A/sq in.	<u>24,513</u>	OFF time per pulse, sec	<u>N/A</u>
Field current density, A/sq in.	<u>370,700</u>	Initial copper temp, F	<u>230</u>
Stator material	<u>2 V Permendur</u>	Final copper temp, F	<u>400</u>
Rotor material	<u>Superconductor</u>	Number of phases	<u>3</u>
Rotor rotational speed, rpm	<u>8,000</u>	Power factor	<u>0.88 lagging</u>
Rotor peripheral speed, ft/sec	<u>500</u>	Number of poles	<u>6</u>
Rotor outside dia., in.	<u>14.33</u>	Frequency, Hz	<u>400</u>
Rotor magnetic length, in.	<u>26.81</u>		
		Rotor length/dia.	<u>1.87</u>
Main generator dia.		Exciter dia, in.	<u>N/A</u>
(excluding flanges), in.	<u>26.16</u>	Exciter length, in.	<u>N/A</u>
Main generator length, in.	<u>32.81</u>	Exciter volume, cu in.	<u>N/A</u>
Main generator volume, cu in.	<u>N/A</u>	Exciter weight, lb	<u>N/A</u>
Main generator weight, lb	<u>N/A</u>		
		Field power, kW	<u>N/A</u>
Total generator volume, cu in.	<u>17,640</u>	Total losses, kW	<u>412.1</u>
Total generator weight, lb	<u>1,505</u>	Overall efficiency	<u>0.9838</u>
Rotor inertia, in.-lb-sec ²	<u>26.34</u>		
Motor-pump input power, kW	<u>5.5</u>		

Assembly specific weight = 0.10 lb/kW

TABLE 17

SUPERCONDUCTING GENERATOR; POINT DESIGN 6; HIGH-SPEED, LOW-VOLTAGE DESIGN

Power level, MW	<u>25</u>	Cooling system weight	
Type of load	<u>Rectified</u>	(including fluids), lb	<u>752</u>
Stator		Total weight of generator	
Cooling method	<u>Fluid cooled</u>	and cooling system, lb	<u>2147</u>
Coolant stator	<u>MIL-L-23699</u>	Specific weight, lb/kW	<u>0.086</u>
Coolant flow rate, gpm	<u>136.3</u>		
Coolant pressure drop, psi	<u>20</u>	Duty cycle:	<u>Continuous duty</u>
		Number of pulses	<u>N/A</u>
Voltage, L-N, V	<u>2000</u>	ON time per pulse, sec	<u>N/A</u>
Stator current density, A/sq in.	<u>22.178</u>	OFF time per pulse, sec	<u>N/A</u>
Field current density, A/sq in.	<u>438,000</u>	Initial copper temp, F	<u>230</u>
Stator material	<u>2 V Permendur</u>	Final copper temp, F	<u>400</u>
Rotor material	<u>Superconductor</u>	Number of phases	<u>3</u>
Rotor rotational speed, rpm	<u>10,000</u>	Power factor	<u>0.88 lagging</u>
Rotor peripheral speed, ft/sec	<u>500</u>	Number of poles	<u>6</u>
Rotor outside dia., in.	<u>11.47</u>	Frequency, Hz	<u>500</u>
Rotor magnetic length, in.	<u>42.12</u>		
Main generator dia.		Rotor length/dia.	<u>N/A</u>
(excluding flanges), in.	<u>22.64</u>	Exciter dia, in.	<u>N/A</u>
Main generator length, in.	<u>48.12</u>	Exciter length, in.	<u>N/A</u>
Main generator volume, cu in.	<u>N/A</u>	Exciter volume, cu in.	<u>N/A</u>
Main generator weight, lb	<u>N/A</u>	Exciter weight, lb	<u>N/A</u>
		Field power, kW	<u>N/A</u>
Total generator volume, cu in.	<u>19,360</u>	Total losses, kW	<u>430.5</u>
Total generator weight, lb	<u>1,395</u>	Overall efficiency	<u>0.9831</u>
Rotor inertia, in.-lb-sec ²	<u>13.5</u>		
Motor-pump input power, kW	<u>3.8</u>		

Assembly specific weight = 0.086 lb/kW

TABLE 18

SUPERCONDUCTING GENERATOR; POINT DESIGN 6; LOW-SPEED, HIGH-VOLTAGE DESIGN

Power level, MW	<u>25</u>	Cooling system weight	
Type of load	<u>Rectified</u>	(including fluids), lb	<u>1006</u>
Cooling method	<u>Fluid cooled</u>	Total weight of generator	
Coolant, stator	<u>MIL-L-23699</u>	and cooling system, lb	<u>3426</u>
Coolant flow rate, gpm	<u>91.5</u>	Specific weight, lb/kW	<u>0.137</u>
Coolant pressure drop, psi	<u>20</u>	Duty cycle	<u>Continuous duty</u>
Voltage, L-N, V	<u>30,000</u>	Number of pulses	<u>N/A</u>
Stator current density, A/sq in.	<u>17,630</u>	ON time per pulse, sec	<u>N/A</u>
Field current density, A/sq in.	<u>381,900</u>	OFF time per pulse, sec	<u>N/A</u>
Stator material	<u>2 V Permendur</u>	Initial copper temp, F	<u>230</u>
		Final copper temp, F	<u>400</u>
Rotor material	<u>Superconductor</u>	Number of phases	<u>3</u>
Rotor rotational speed, rpm	<u>8,000</u>	Power factor	<u>0.88 lagging</u>
Rotor peripheral speed, ft/sec	<u>500</u>	Number of poles	<u>6</u>
Rotor outside dia., in.	<u>14.33</u>	Frequency, Hz	<u>400</u>
Rotor magnetic length, in.	<u>52.52</u>	Rotor length/dia.	<u>3.67</u>
Main generator dia.		Exciter dia, in.	<u>N/A</u>
(excluding flanges), in.	<u>28.97</u>	Exciter length, in.	<u>N/A</u>
Main generator length, in.	<u>58.52</u>	Exciter volume, cu in.	<u>N/A</u>
Main generator volume, cu in.	<u>N/A</u>	Exciter weight, lb	<u>N/A</u>
Main generator weight, lb	<u>N/A</u>	Field power, kW	<u>N/A</u>
Total generator volume, cu in.	<u>38,570</u>	Total losses, kW	<u>378.4</u>
Total generator weight, lb	<u>2420</u>	Overall efficiency	<u>0.9851</u>
Rotor inertia, in.-lb-sec ²	<u>49.08</u>		
Motor-pump input power, kW	<u>2.6</u>		

Assembly specific weight = 0.137 lb/kW

4. Rotor Conductor

The rotor conductor is a niobium-titanium multitwisted-filament conductor in a copper matrix operated at 65 percent capacity of 4.2 K short sample data. This provides operating margin from potential losses under load and field changing and/or temperature rise due to heating of the cryogen helium under vibration, shock, acceleration from the shaft center to the rotor coils due to centrifugal head, and variable rotational speeds.

5. Rotor Coil Protection

The rotor coils and excitation circuit are designed to permit nondestructive quenching of the superconducting coils. To provide the required control voltage during a quench, the connection design is such to prevent excessive deflection of the rotor and rubbing of the stator due to the presence of unbalanced magnetic forces.

6. Electrothermal Shield

A damper is provided between the rotor fields and the stator to prevent excessive variation in the mutual field that may quench the superconductor. The damper design is a shield of pure copper incorporated inside the rotating dewar and cooled to the cryogenic state by boil-off of the liquid helium discharged from the field coils.

7. Dewar

The incorporated dewar excludes ambient heat from the field coils. The wall thickness of the vacuum jacket is essentially constant. Transporting helium from the storage supply into the generator dewar, and absorbing heat conducted from ambient along the field connection leads account for an important part of the refrigerated load.

8. Fault Protection

The superconducting field tends to be a constant flux source; flux is only slightly altered when the load current changes, whereas the stator winding has relatively low impedance due to the ironless stator construction. Consequently, unusually high short-circuit and fault currents can be generated. Heating, torque, and magnetic forces on the stator conductors, field coils, and damper shield present difficult problems under fault and abnormal load conditions.

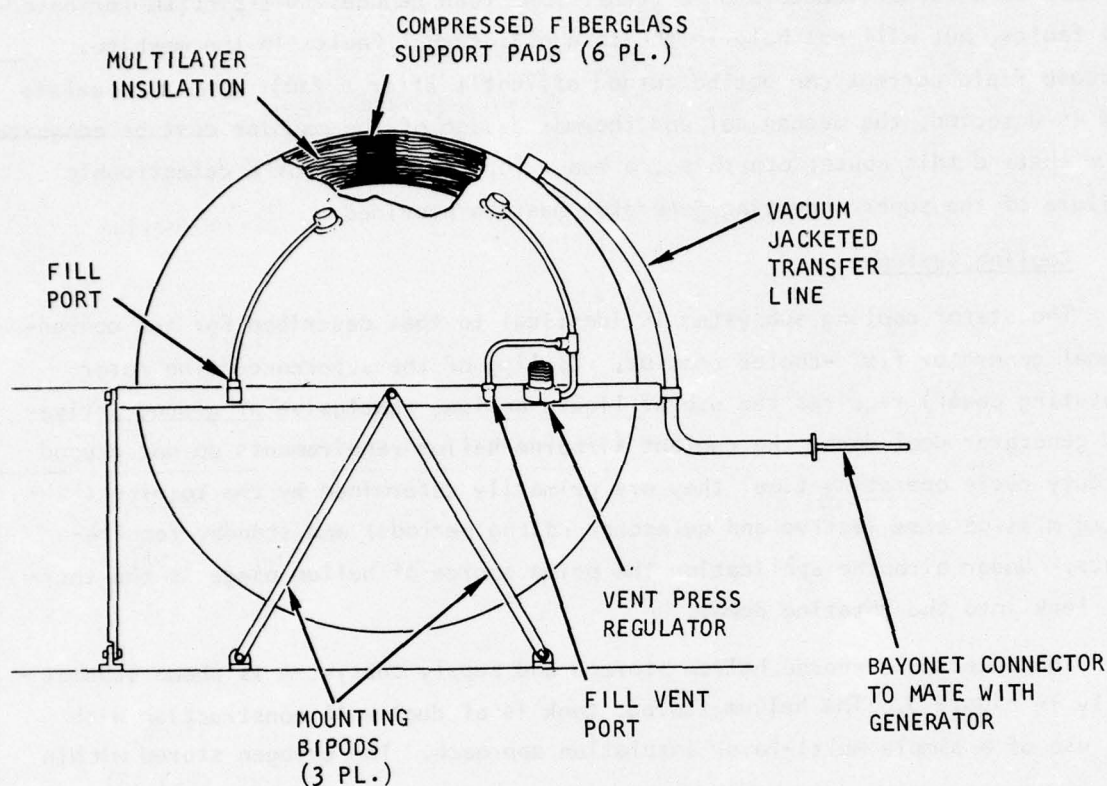
The use of external reactors or a transformer load reduces this problem for external faults, but will not help in the case of internal faults in the machine. Because field current can not be turned off until after a fault condition exists and is detected, the mechanical and thermal design of the machine must be adequate to withstand this abuse; otherwise, a means for containment of a catastrophic failure of the superconducting generator must be provided.

9. Cooling System

The stator cooling subsystem is identical to that described for the conventional generator fluid-cooled concept. Cooling of the superconducting rotor (rotating dewar) requires the use of liquid helium. Exclusive of ground activated generator cool down, the coolant airborne helium requirements do not depend on duty cycle operating time; they are primarily determined by the total anticipated mission time (active and quiescent idling periods) and standby requirements. Under airborne application the prime source of helium usage is the thermal leak into the rotating dewar.

The selected airborne helium storage and supply subsystem is shown schematically in Figure 7. The helium storage tank is of dual wall construction with the use of a simple multi-layer insulation approach. The cryogen stored within the pressure vessel provides helium supply to the generator via a regulator valve at 14.7 psia. The selected materials, Ti-5 Al-2.5 Sn alloy for the pressure vessel, 2219 Al alloy for the vacuum jacket, and evacuated crinkled aluminized Mylar, provide reasonable weight without the need for vapor-cooled shield. Required thermal insulation between the pressure vessel, vacuum jacket, and supports, is provided by the use of 6 compressed fiberglass support pads. In the absence of specific envelope constraints, spherical tank configuration is used. In sizing the helium storage supply subsystem, a vented standby period of 24 hr is provided with required delivery rate based on a 10-hr operating period.

The cooling system performance characteristics, satisfying the requirements of point design 6 superconducting generator approach, are summarized in Table 19.



S-3255

Figure 7. Airborne Liquid Helium Supply Schematic

MEDIUM-POWER APPLICATION, TURBINE

Shaft power for generator drive is provided by a two-stage, axial-flow, pressure-compounded turbine. Turbine attachment is provided by off-centerline bolts with curvic couplings. Torque provided by the turbine is transmitted to the generator and remaining rotating elements via a spline attachment. Pertinent design details of the turbine assembly are shown in Table 20.

Altitude operation introduces two unusual design considerations in the intended application: (1) the selection of turbine overall pressure ratio, and

TABLE 19

SUPERCONDUCTING GENERATOR COOLING SUBSYSTEM CHARACTERISTICS

Coolant Subsystem Characteristics (Low-speed, low-voltage, 8000 rpm)	
Coolant load, kw	378.4
Coolant type	DC-200/helium
Coolant flow rate	
DC-200, gpm	1.5
Helium, liter/hr	20.3
Coolant Subsystem Weight	
Subsystem dry weight, lb (kg)	546 (248.2)
Lubrication assembly, lb (kg)	90 (40.91)
Coolant weight, lb (kg)	15 (6.82)
Water weight, lb (kg)	270 (122.73)
Helium weight, lb (kg)	85 (38.64)
Subsystem wet weight, lb (kg)	1006 (457.28)
Helium Storage Supply Design Characteristics	
Tank assembly dry weight, lb (kg)	139 (63.18)
Tank assembly wet weight, lb (kg)	224 (101.82)
Lines and mounting pads, lb (kg)	10 (4.55)
Total weight, lb (kg)	234 (106.36)
Outer shell diameter, in. (m)	41.49 (1.05)
Girth ring diameter, in. (m)	45.04 (1.14)

TABLE 20

POINT DESIGN 6 TURBINE DESIGN CHARACTERISTICS

Propellant	Combustion products of neat hydrazine
Nozzle inlet	2110 R(1172.2 K)/850 psia (5.86 MPa)
Overall pressure ratio	42.5
Rotational speed	12,500 rpm
Number of stages	2
Shaft power	36,300 hp
Turbine flow rate	41.2 lb/sec (18.73 kg/sec)
Overall efficiency	76.1 percent
Weight	1,200 lb (545.5 kg)
<u>First Stage</u>	
Inlet temperature	2,110 R (1172.2 K)
Flow rate	41.2 lb/sec (18.7 kg/sec)
Blade height	0.91 in. (0.023 m)
Pitch velocity	1,650 ft/sec (502.9 m/sec)
Disc weight	358 lb (162.7 kg)
<u>Second Stage</u>	
Inlet temperature	1,619 R (899.4 K)
Flow rate	40.4 lb/sec (18.4 kg/sec)
Blade height	3.06 in. (0.078 m)
Pitch velocity	1,532 ft/sec (467 m/sec)
Disc weight	326 lb (148.2 kg)

(2) for an overall pressure ratio, the selection of optimum stage pressure ratio split. Altitude operation affects turbine performance in several ways. With respect to aerodynamic considerations, for a fixed nozzle inlet condition, higher altitude operation increases propellant potential energy and reduces the parasitic losses associated with turbine performance. The higher pressure ratio operation, however, causes a reduction in turbine efficiency, high Mach number operation, and lower chord Reynolds number operation. Thus, aerodynamic considerations with respect to selection of an overall turbine pressure ratio call for an evaluation of the available expansion head and associated efficiency capability. Structural, weight, and development test demonstration considerations substantially negate the potential benefits associated with an altitude operation turbine design. At the power level of interest, fuel consumption reduction achieved by altitude operation design results in an increase in volumetric flow (reduced density) and requires a speed reduction imposed by blade stress and blade vibrational considerations. Increased blade height and reduction in rotational speed lead to increased turbine weight, which must be matched to fuel consumption decrease. Furthermore, the additional considerations of simplified ground development demonstration desirability and off-design performance behavior lead to the selection of a back pressure of 20 psia.

For an established overall pressure ratio of 42.5, available stage pressure ratio splits are such that selection of either supersonic/subsonic or all supersonic multistage design operation is feasible. Supersonic-subsonic multistage pressure split tends to give a very slight improvement in turbine performance at fixed design operating conditions; however, in the present application, off-design operation (variable back pressure associated with variable altitude) predominates. This consideration leads to the design selection of multistage supersonic operation pressure split (approximately equal stage pressure ratio). This design approach, results in minimal fuel consumption under airborne operating conditions. Multistage supersonic operation at low relative Mach numbers has been successfully demonstrated in the Hydrogen-Oxygen multistage APU turbine recently built by AiResearch for NASA.

Off-design, variable-rotational-speed turbine performance characteristics are shown in Figure 8. As previously stated, the application of multipropellants for a variety of reasons merits consideration. Figure 8 also illustrates

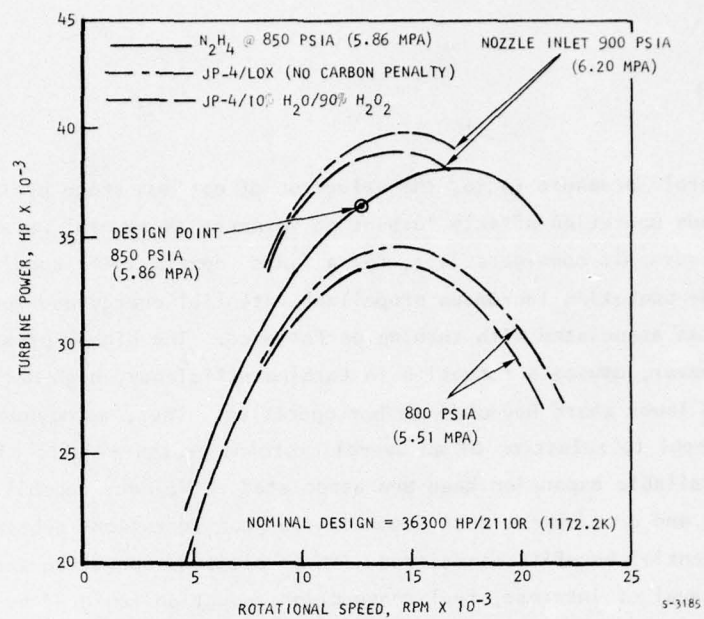


Figure 8. Off-Design Turbine Performance, Fixed Design, Variable Speed, Variable Propellant

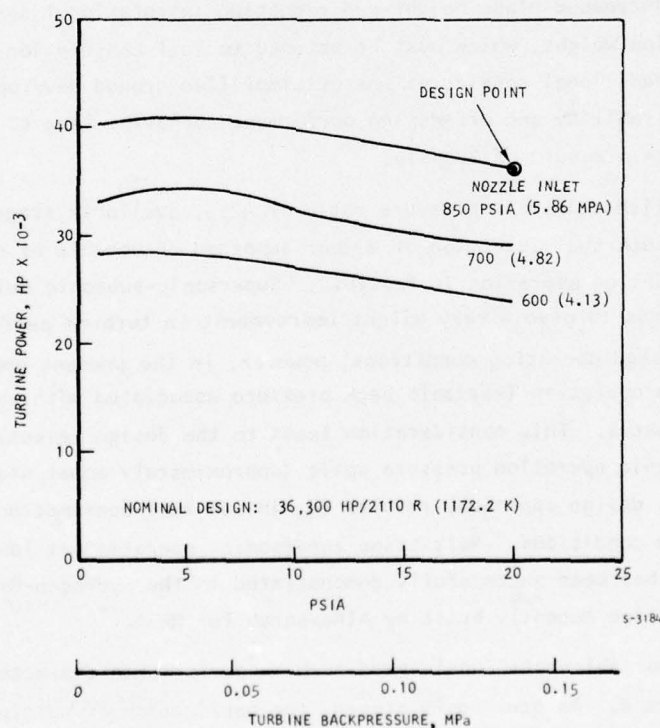


Figure 9. Off-Design Turbine Performance, Variable Inlet/Exit Pressures, Fixed Speed

the effects of variable propellant use on a turbine initially designed for neat hydrazine use. Substituting the use of either JP-4/LOX or JP-4/10 percent H_2O - 90 percent H_2O_2 requires basically a slight increase in operational pressure. Off-design, variable inlet and exit pressure turbine performance characteristics with neat hydrazine operation are shown in Figure 9.

Structural Design Evaluation

A multiplicity of structural design efforts must be conducted to establish the validity of the selected turbine design concept. The structural design evaluation encompasses thermal performance evaluation under transient and steady-state operation, turbine disc transient and steady-state operation, and turbine blade stress and vibrational evaluation. In the final analysis, turbine design involves an appropriate balance between aerodynamic and structural considerations.

1. Thermal Performance Evaluation

Thermal evaluation must be performed and coordinated with other design activities to establish realistic designs geared to achieve desired performance and reliability of the turbine assembly. Accordingly, detailed, independent thermal evaluations on both turbine stages were carried out. Results of these evaluations are shown in Figures 10 (first stage) and 11 (second stage). The thermal history thus obtained is used to determine applicable turbine structural limits in terms of permissible peripheral speeds, rotational speeds, and generalized operating characteristics of the turbine.

2. Turbine Disc Stress, Blade Stress, and Blade Vibration Evaluation

The design procedure generally followed in this study was to combine into a single evaluation procedure the turbine aerodynamic, thermal, and structural considerations; e.g., use of developed computer program TAPE. By necessity, however, this procedure introduces simplifications in the evaluation procedure. Accordingly, more detailed design analyses were conducted to ensure that the imposed simplifications are indeed acceptable. With respect to the turbine, the follow-on analyses encompassed a thorough review of the turbine disc and blade stresses in addition to blade vibration examinations.

With respect to the first stage under the steady-state condition, the resulting stresses are below the yield stress for the material, at the indicated temperatures; however, under transient conditions, stresses at the rim

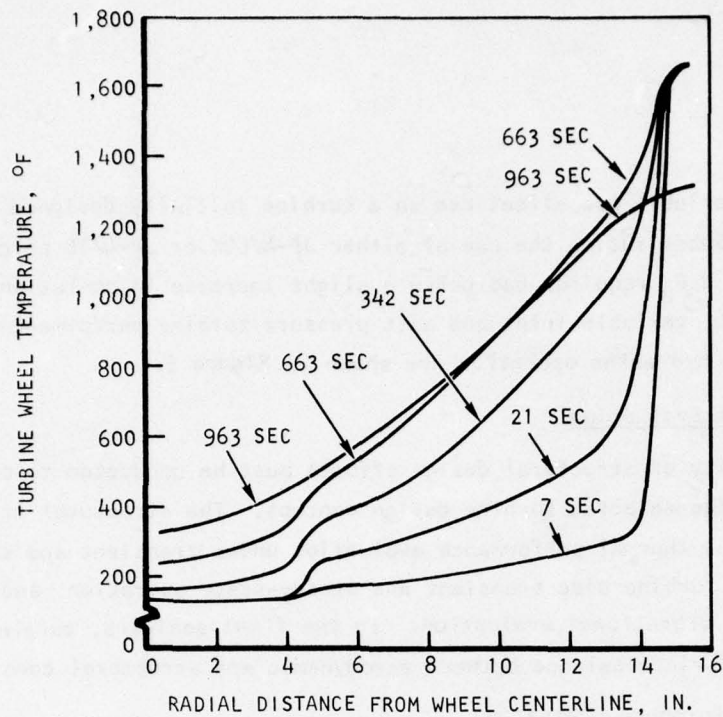


Figure 10. First-Stage Temperature Distribution

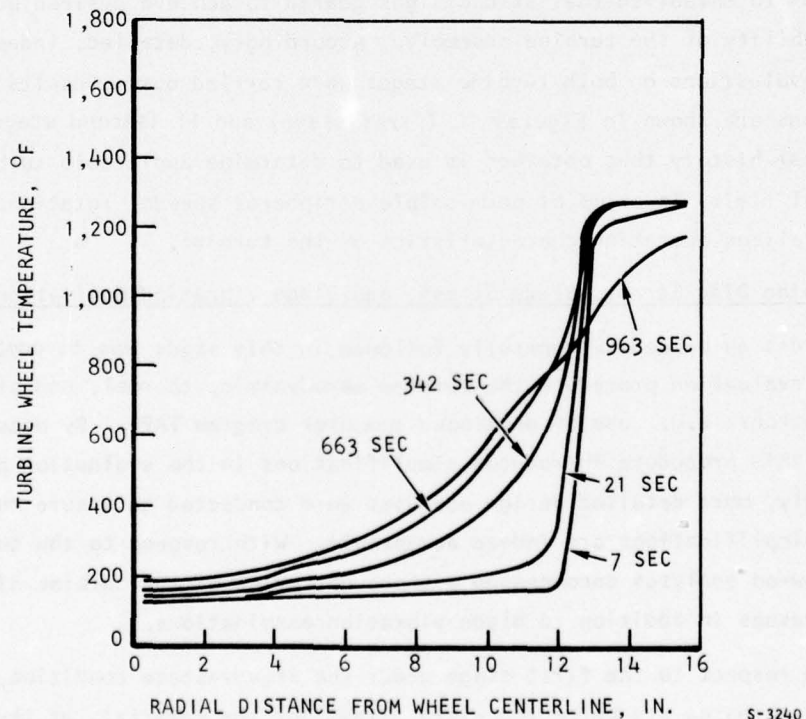


Figure 11. Second-Stage Temperature Distribution

exceeded allowable yield strength. The adopted solution involves the use of a slotted disc to avoid the high negative tangential (hoop) stresses. The use of a slotted disc is an acceptable approach to relieve the encountered stresses in the first-stage turbine. Alternative acceptable concepts involve the use of cast blades with fir trees. Table 21 summarizes the detailed operational stresses of the first stage under steady-state and transient thermal distribution. This structural evaluation indicates satisfactory stress and burst margin under both steady-state and transient operation.

The resultant turbine disc profile based upon the detailed stress evaluation showed close correlation to the one determined by Program TAPE subroutine. Transient thermal distribution considerations imposed an increase in the turbine hub thickness of the second stage; however, because this information is an input to the program, subsequent turbine structural evaluation, per TAPE,

TABLE 21
FIRST STAGE TURBINE DISC STRESS SUMMARY

Condition 13,125 rpm	Position	Radius, in.	Temp, F	Material Properties		Max. Effective Stress, ksi
				Yield, ksi	Ultimate, ksi	
Steady- state	Center	0	1200	126	163	96.3
	Middle	6.25	1396	118	145	72.1
	Live rim	12.50	1592	80	83	48.7
	Blade root	14.67	1660	58	61	20.1
	Average tangential stress					57.65
663-sec transient	Center	0	200	139	183	110.5
	Middle	6.25	500	135	179	85.4
	Live rim	12.50	1069	128	169	72.9
	Blade root	14.67	1660	58	61	20.1
	Average tangential stress					47.25

incorporated an increase in hub width. Second-stage detailed evaluation turbine finite element model use, and resultant transient/steady-state thermal distribution effective stresses are shown in Figure 12.

The second-stage turbine blades are tapered and cored to reduce centrifugal loading and bring blade root stress to an acceptable level. Coring the blades reduces thermal gradients through the blade cross section. Centrifugal stress analysis of the second-stage turbine blade was performed using AiResearch finite element computer program BOSS 1. The resulting stresses were found in agreement with the values calculated by the incorporated subroutines in TAPE. Blade vibration analysis was conducted for the second-stage blade to investigate the possibility of blade structural resonance with aerodynamic excitation frequencies. The natural frequencies were determined using AiResearch computer program VIBE 1 and are plotted in the interference diagram, Figure 13.

The first five vibration modes were investigated at 0 rpm, 13,125 rpm (105 percent of maximum operating speed), and 8,125 rpm (65 percent of maximum operating speed) for the use of either hollow or solid blades. The interference diagram shown in Figure 13 indicates that the 1-per-revolution excitation is well below the maximum operating speed and that the 83 values possible excitation line intersects the first five modes below 6,000 rpm. The use of hollow blades with an area taper ratio of 1.5 is quite acceptable (low stresses, non-critical natural frequencies, and lower weight).

The stress and blade vibration analyses conducted primarily with highly sophisticated tools indicate that the selected rotational speed, blade height, and peripheral speed are acceptable.

MEDIUM-POWER APPLICATION, TURBOGENERATOR POWER SYSTEM

The component assembly, inclusive of required ancillary equipment, shows a substantial variation in performance characteristics and operational suitability. To assist in the selection procedure, potential system study application was carried on to more truly reflect the merits of the various component concepts within the intended application. Results of this study phase, with respect to point design 6 requirements are summarized in Table 22.

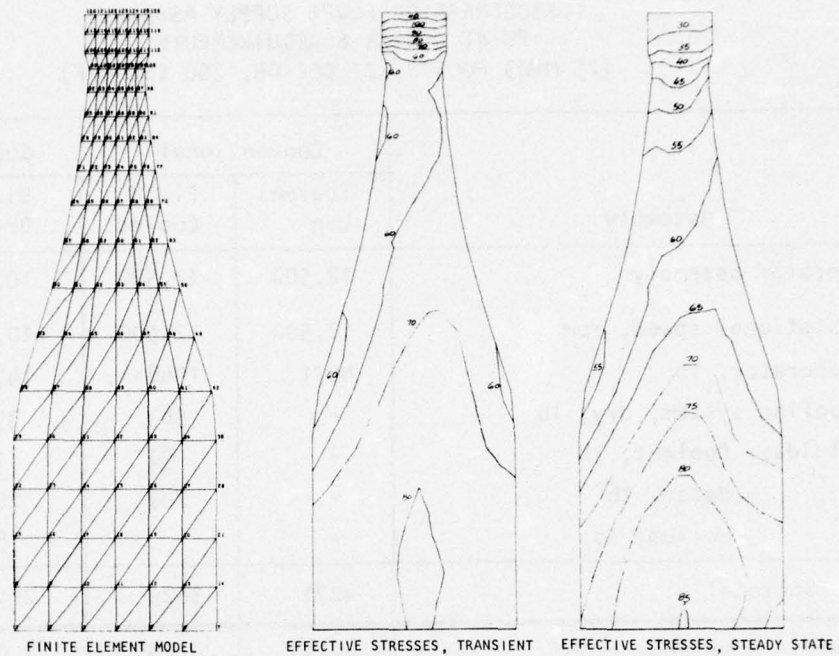


Figure 12. Second-Stage Turbine Disc Stress Review

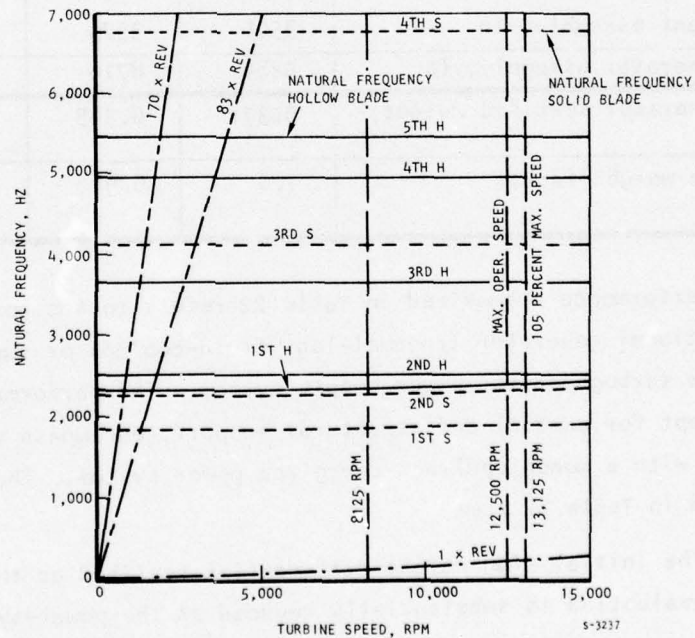


Figure 13. Second-Stage Turbine Blade Vibration--Interference Diagram

TABLE 22

TURBOGENERATOR POWER SUPPLY ASSEMBLY
POINT DESIGN 6 REQUIREMENTS
(25 MW/3 PULSES, 21 SEC ON, 300 SEC OFF)

Assembly	Conventional		Superconducting	
	Thermal Lag	Fluid Cooled	Direct Drive	Gear Drive
Generator assembly	12,500	12,500	10,000	8000
Rotational speed, rpm	12,500	12,500	10,000	8000
Generator, lb	4271	1948	1475	1585
Cooling system, dry, lb	-	383	390	546
Fluids: Coolant, lb	-	51	15	15
Water, lb	-	247	207	207
Helium, lb	-	-	85	85
Subtotal	4271	3629	2172	2501
Specific weight, lb/kW	0.171	0.145	0.087	0.100
Gearbox/clutch/lube assembly, lb	35	35	390	1077
Turbocombustor assembly, lb	1472	1476	2436	1126
Propellant assembly, lb	3506	3574	3046	3122
Turbogenerator assembly, lb	9284	8714	8044	7826
Turbogenerator specific weight, lb/kW	0.371	0.349	0.322	0.313
Relative weight factor	1.0	0.94	0.87	0.84

The performance summarized in Table 22 refers to the potential use of the conventional generator (thermal-lag, fluid-cooled) or superconducting generator in a turbogenerator power supply system. The performance characteristics shown, except for control and structural support, encompass all elements associated with a monopropellant-energized power system. The salient features illustrated in Table 22 are:

- (a) The initial high weight differential realized at the component-level evaluation is substantially reduced at the power-system level.

- (b) The small system weight differential comparison realized seriously questions the desirability of selecting a superconducting generator for electrical power delivery in the present application. Considerations of importance include operational suitability and complexity. Both considerations involve assessment of the need for ground support cooldown to the cryogenic state, the use of cryogen supply airborne assembly, and the need for idling operation with associated use of clutching.
- (c) With respect to superconducting generator application, use of the low-rotational-speed design concept results in minimum weight. This unit requires the use of a gearbox, but results in a substantial weight saving associated with the use of an optimized rotational speed design turbine. The direct-drive approach results in a high weight penalty associated with the use of a low-rotational-speed turbine.

Conventional Generator Rotational Speed Selection Criteria

The conventional generator design characteristics described in the previous pages produce minimum weight components within the operational constraints of the intended application. For a given permissible peripheral speed, low component weight and inertia for the fluid-cooled conventional generator is achieved at a high rotational speed and high coolant pressure differential through the generator. The high rotational speed results in high L/D unit design. The high pressure drop (high coolant flow rate) increases operational complexity. It is, therefore, of interest to establish the effects of these operating characteristics on generator performance potential. Results of the effects of variation in rotational speed and coolant pressure differential on a 25-MW conventional fluid-cooled generator are shown in Figures 14 and 15. Reduction in rotational speed results in a substantial lowering of the unit L/D at the expense of unit weight. This weight differential, however, is sensitive to the selected coolant pressure differential, which is primarily determined by allowed operational complexity.

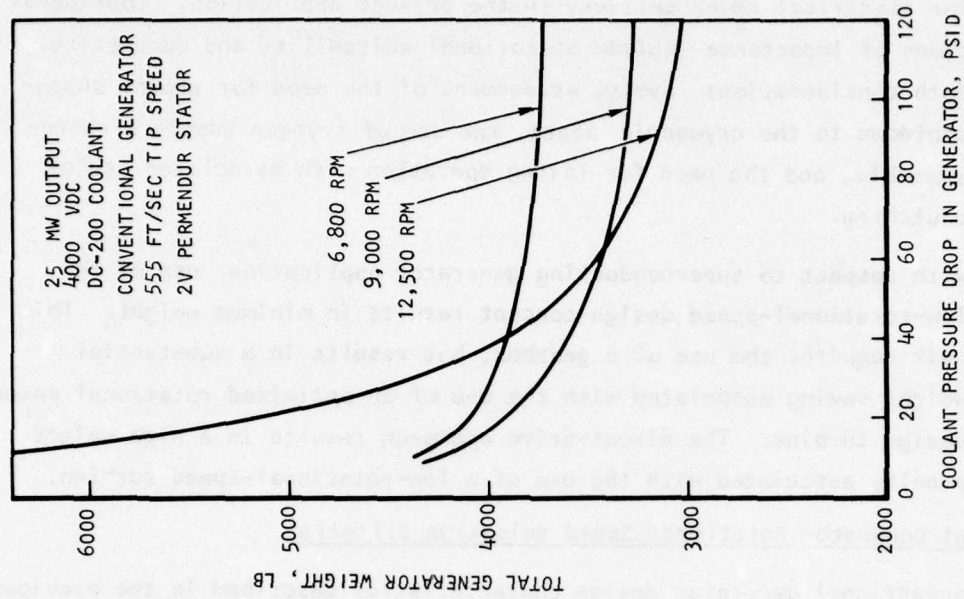


Figure 14. Generator Weight vs Coolant Pressure Drop

S-3204

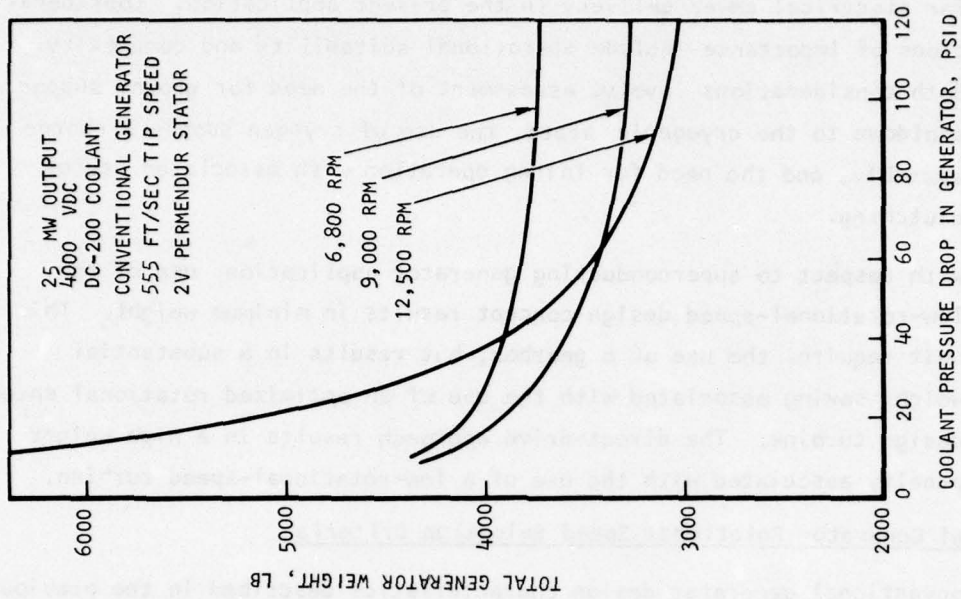


Figure 15. Rotor L/D vs Coolant Pressure Drop

S-3205

MEDIUM POWER APPLICATION, DESIGN POINTS 3, 4, AND 5

Conventional Generator, Thermal-Lag

Drawing PA113337 is a preliminary package outline of the conventional thermal-lag turbogenerator designs satisfying the requirements of point designs 3 and 5 (also applicable to point design 6). The outline drawing encompasses all the auxiliary equipment exclusive of pressurant gas, the propellant system, controls, and structural support. The outline of the system is such that either internal-aircraft or under-aircraft fuselage packaging can be conveniently achieved. Typical mounting pads for aircraft fuselage packaging approach are shown in the drawing. Generator design details for point design 3 are shown in Table 23. Table 24 summarizes the generator design details for point design 5. Drawing PA113337 also gives the various turbogenerator subsystem weights exclusive of the propellant assembly, controls, and structure.

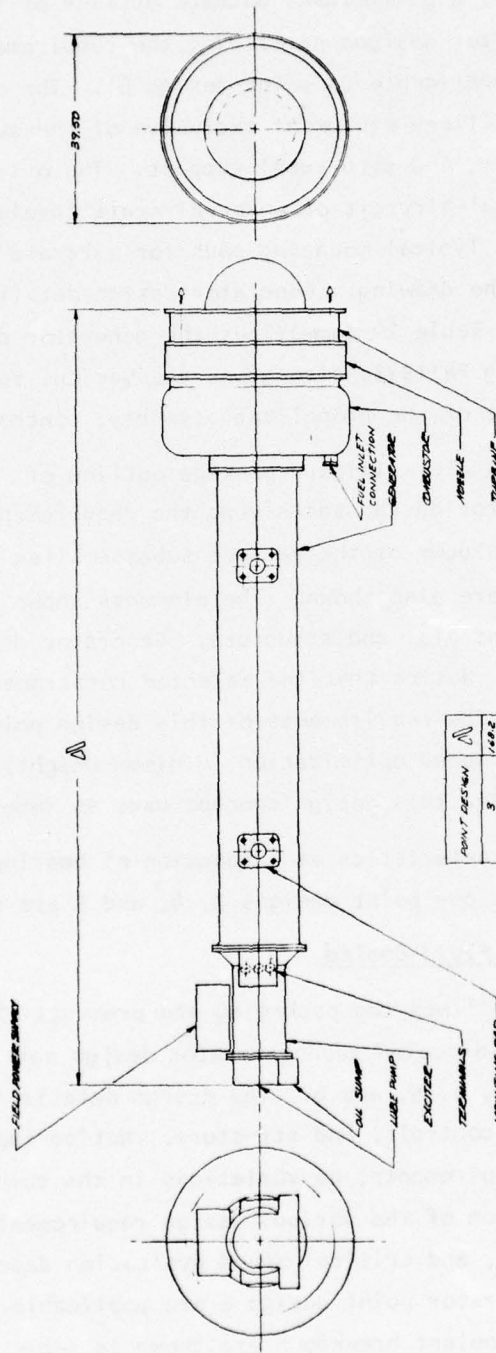
Drawing PA113339 is a preliminary package outline of the conventional thermal-lag turbogenerator design satisfying the requirements of point design 4. A weight breakdown of the various subassemblies in the turbogenerator power system are also shown. The elements shown are exclusive of propellant assembly, controls, and structure. Generator design details are summarized in Table 25. Notice that the selected rotational speed of the generator is 8500 rpm. The requirements of this design point (single ON time of 120 sec) dictate the speed optimization (minimum weight) of the generator and turbine. Accordingly, this design concept uses an intermediary gearbox.

Critical speed characteristics as a function of bearing stiffness and bearing mount resilience per point designs 3, 4, and 5 are shown in Table 26.

Conventional Generator, Fluid-Cooled

Drawing PA113338 outlines the packaging and presents the weight breakdown of the conventional fluid-cooled turbogenerator design satisfying the requirements of point designs 3, 4, 5, and 6. The design details are exclusive of propellant assembly, controls, and structure. Notice that, except for variation in coolant requirements, no variations in the turbogenerator assembly are realized as a function of the various design requirements. Turbine performance characteristics, and critical speed evaluation described for conventional fluid-cooled generator point design 6 are applicable. Generator design details, including the coolant breakdown are shown in Table 27.

11/3337



POINT DESIGN	1	2	3	4	5	6
	1482	1482	1482	1482	1482	1482

POINT	1	2	3	4	5	6
DESIGN	1482	1482	1482	1482	1482	1482

POINT	1	2	3	4	5	6
DESIGN	1482	1482	1482	1482	1482	1482

TURBOGENERATOR OUTLINE	
CONVENTIONAL DESIGN, 3500 RPM, 1000 KW	
D 70210 24/5337	
SCALE	

TABLE 23
CONVENTIONAL GENERATOR, THERMAL LAG, POINT DESIGN 3

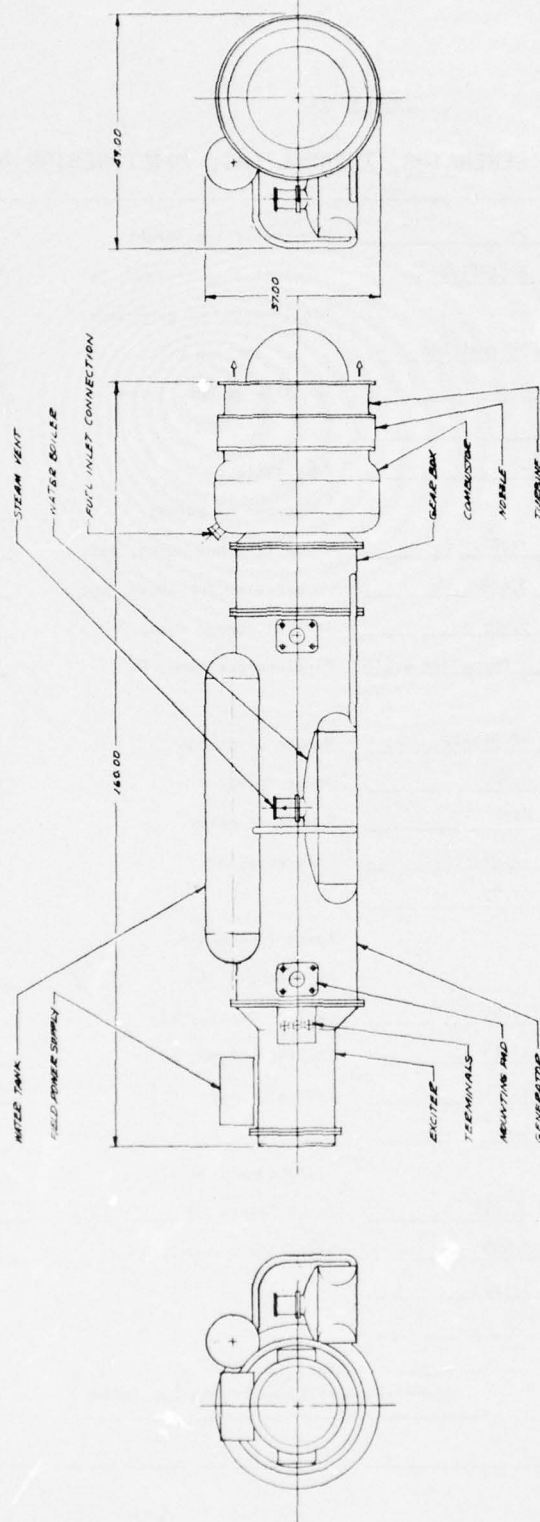
Power level, MW	25	Cooling system weight	
Type of load	Rectified	(including fluids), lb	N/A
		Total weight of generator	
Cooling method	Thermal lag	and cooling system, lb	N/A
Coolant	N/A	Specific weight, lb/kW	0.188
Coolant flow rate, gpm	N/A		
Coolant pressure drop, psi	N/A	Duty cycle:	
		Number of pulses	16
Voltage, L-N, V	1845	ON time per pulse, sec	4
Stator current density, A/sq in.	13,228	OFF time per pulse, sec	4
Field current density, A/sq in.	13,068	Initial copper temp, F	130
Stator material	2 V Permendur 0.0100	Final copper temp, F	450
Rotor material	HP 9-4-20	Number of phases	3
Rotor rotational speed, rpm	12,500	Power factor	0.877 lagging
Rotor peripheral speed, ft/sec	650	Number of poles	6
Rotor outside dia., in.	11.62	Frequency, Hz	625
Rotor magnetic length, in.	90.37		
		Rotor length/dia.	7.78
Main generator dia.		Exciter dia, in.	10.75
(excluding flanges), in.	16.70	Exciter length, in.	14.45
Main generator length, in.	103.56	Exciter volume, cu in.	1311
Main generator volume, cu in.	22,672	Exciter weight, lb	147
Main generator weight, lb	4,565		
		Field power, kW	207.6
Total generator volume, cu in.	23,983	Total losses, kW	1397
Total generator weight, lb	4,712	Overall efficiency	0.9466
Rotor inertia, in.-lb-sec ²	114.4		
Motor-pump input power, kW	N/A		

Assembly specific weight = 0.188 lb/kw

TABLE 24
CONVENTIONAL GENERATOR, THERMAL LAG, POINT DESIGN 5

Power level, MW	<u>25</u>	Cooling system weight	
Type of load	<u>Rectified</u>	(including fluids), lb	<u>N/A</u>
Cooling method	<u>Thermal lag</u>	Total weight of generator	
Coolant	<u>N/A</u>	and cooling system, lb	<u>N/A</u>
Coolant flow rate, gpm	<u>N/A</u>	Specific weight, lb/kW	<u>0.187</u>
Coolant pressure drop, psi	<u>N/A</u>	Duty cycle:	
		Number of pulses	<u>3</u>
Voltage, L-N, V	<u>1830</u>	ON time per pulse, sec	<u>21</u>
Stator current density, A/sq in.	<u>13,329</u>	OFF time per pulse, sec	<u>30</u>
Field current density, A/sq in.	<u>13,187</u>	Initial copper temp, F	<u>130</u>
Stator material	<u>1 V Permendur 0.010</u>	Final copper temp, F	<u>450</u>
Rotor material	<u>HP 9-4-20</u>	Number of phases	<u>3</u>
Rotor rotational speed, rpm	<u>12,500</u>	Power factor	<u>0.877 lagging</u>
Rotor peripheral speed, ft/sec	<u>650</u>	Number of poles	<u>6</u>
Rotor outside dia., in.	<u>11.62</u>	Frequency, Hz	<u>625</u>
Rotor magnetic length, in.	<u>89.86</u>	Rotor length/dia.	<u>7.73</u>
Main generator dia.		Exciter dia, in.	<u>10.74</u>
(excluding flanges), in.	<u>16.70</u>	Exciter length, in.	<u>14.56</u>
Main generator length, in.	<u>103.04</u>	Exciter volume, cu in.	<u>1317</u>
Main generator volume, cu in.	<u>22,555</u>	Exciter weight, lb	<u>146</u>
Main generator weight, lb	<u>4,539</u>	Field power, kW	<u>209.5</u>
Total generator volume, cu in.	<u>23,872</u>	Total losses, kW	<u>1,385</u>
Total generator weight, lb	<u>4,685</u>	Overall efficiency	<u>0.9470</u>
Rotor inertia, in.-lb-sec ²	<u>113.8</u>		
Motor-pump input power, kW	<u>N/A</u>		

Assembly specific weight = 0.187 lb/kw



RETATIONAL SPEEDS TURBINE 1400 RPM
GENERATOR 1800 RPM
EXCITER 1800 RPM
FIELD POWER SUPPLY 1800 RPM
SECOND FIELD BOBY 1800 RPM

UNIT	WATER	STEAM	EXCITER	GENERATOR	TURBINE
1	110	130	140	150	160

PARTS LIST		NOMINATURE OF DESCRIPTION	
QTY	UNIT	QTY	UNIT
1	1	1	1
TUBES GENERATOR OUTLINE		CONVENTIONAL THERMAL LAB	
25 MM. POINT-255N		D 70210	
D 70210		F413339	

TABLE 25

CONVENTIONAL GENERATOR, THERMAL LAG, POINT DESIGN 4

Power level, MW	<u>25</u>	Cooling system weight	
Type of load	<u>Rectified</u>	(including fluids), lb	<u>N/A</u>
		Total weight of generator	
Cooling method	<u>Thermal lag</u>	and cooling system, lb	<u>N/A</u>
Coolant	<u>None</u>	Specific weight, lb/kW	<u>0.234</u>
Coolant flow rate, gpm	<u>-</u>		
Coolant pressure drop, psi	<u>-</u>	Duty cycle:	
		Number of pulses	<u>1</u>
Voltage, L-N, V	<u>1508</u>	ON time per pulse, sec	<u>120</u>
Stator current density, A/sq in.	<u>9,649</u>	OFF time per pulse, sec	<u>0</u>
Field current density, A/sq in.	<u>9,795</u>	Initial copper temp, F	<u>130</u>
Stator material	<u>2 V Permendur 0,010</u>	Final copper temp, F	<u>450</u>
Rotor material	<u>HP 9-4-20</u>	Number of phases	<u>3</u>
Rotor rotational speed, rpm	<u>8,500</u>	Power factor	<u>0.876 lagging</u>
Rotor peripheral speed, ft/sec	<u>650</u>	Number of poles	<u>6</u>
Rotor outside dia., in.	<u>17.27</u>	Frequency, Hz	<u>425</u>
Rotor magnetic length, in.	<u>51.72</u>		
		Rotor length/dia.	<u>2.99</u>
Main generator dia.		Exciter dia., in.	<u>15.87</u>
(excluding flanges), in.	<u>24.41</u>	Exciter length, in.	<u>16.52</u>
Main generator length, in.	<u>71.14</u>	Exciter volume, cu in.	<u>3267</u>
Main generator volume, cu in.	<u>33,284</u>	Exciter weight, lb	<u>232</u>
Main generator weight, lb	<u>5,608</u>		
		Field power, kW	<u>153.2</u>
Total generator volume, cu in.	<u>36,551</u>	Total losses, kW	<u>1201</u>
Total generator weight, lb	<u>5,840</u>	Overall efficiency	<u>0.9537</u>
Rotor inertia, in.-lb-sec ²	<u>322.6</u>		
Motor-pump input power, kW	<u>N/A</u>		

Assembly specific weight = 0.234 lb/kw

TABLE 26
CONVENTIONAL GENERATOR, THERMAL LAG
PRELIMINARY CRITICAL SPEED EVALUATIONS OF POINT DESIGNS 3, 4, AND 5

Point Design	Bearing Stiffness	Bearing Mount	Generator Rotor Critical Speeds, RPM				Operating Speed, rpm	Selected Bearing and Mount Combination
			First Rigid Body and First Flexural Modes	Second Rigid Body Mode	Second Flexural Mode	First Free Body Mode		
3	Medium	Soft resilient	1,758	3,155	7,031	15,146	12,500	Stiff bearing in a rigid mount
	Medium	Stiff resilient	2,774	5,078	11,096	15,146		
	Soft	Rigid	3,646	6,822	14,584	15,146		
	Stiff	Rigid	4,452	7,951	17,809	15,146		
4	Medium	Soft resilient	1,610	3,077	6,439	68,998	8,500	Stiff bearing in a rigid mount
	Medium	Stiff resilient	2,857	5,493	11,427	68,998		
	Soft	Rigid	4,300	8,195	17,200	68,998		
	Stiff	Rigid	5,432	10,442	21,730	68,998		
5	Medium	Soft resilient	1,765	3,171	7,060	15,343	12,500	Stiff bearing in a rigid mount
	Medium	Stiff resilient	2,787	5,106	11,147	15,343		
	Soft	Rigid	3,664	6,865	14,654	15,343		
	Stiff	Rigid	4,480	8,005	17,918	15,343		

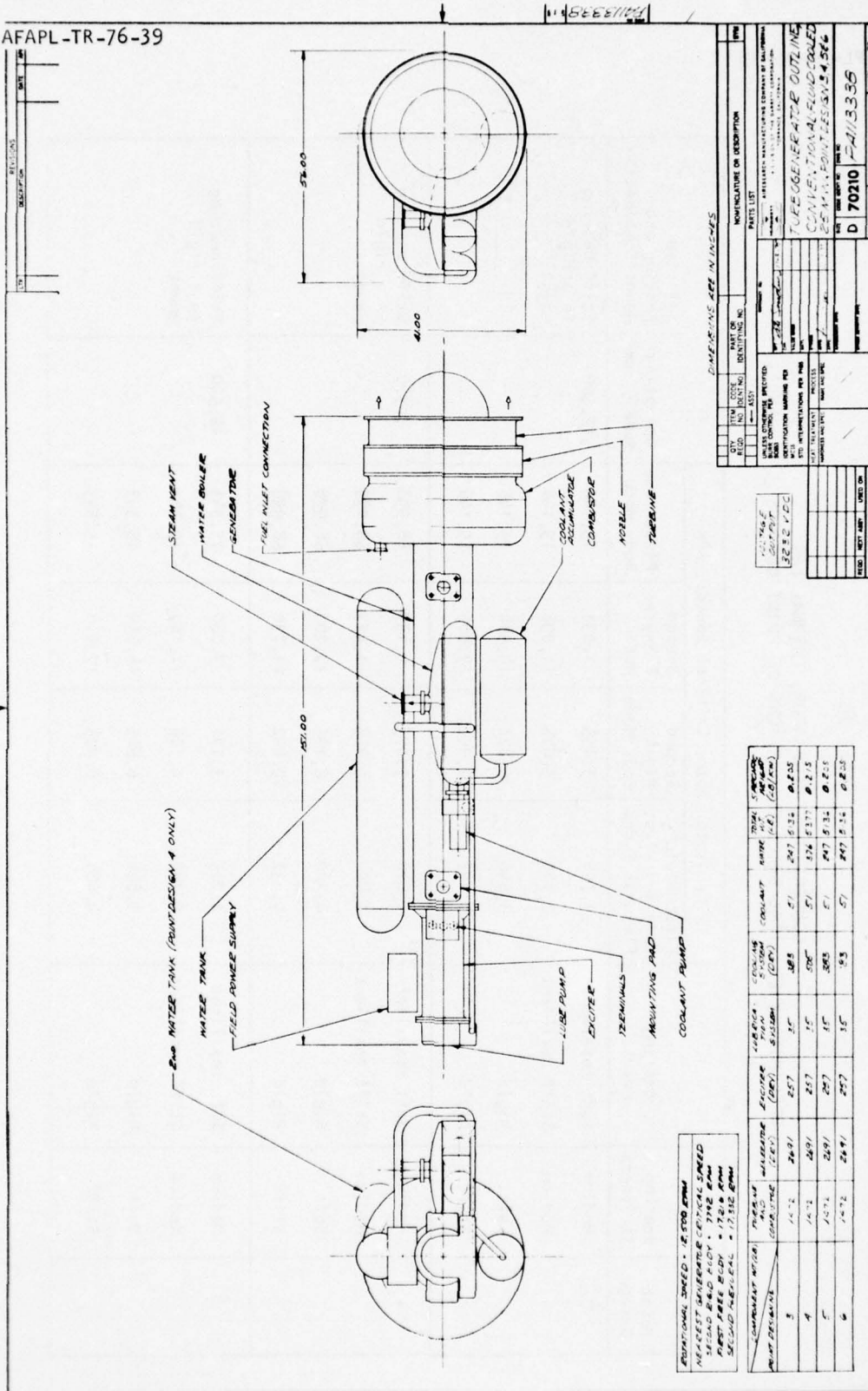


TABLE 27
CONVENTIONAL GENERATOR, FLUID COOLED, POINT DESIGNS 3, 4, 5, AND 6

Power level, MW	<u>25</u>	Cooling system weight		
Type of load	<u>Rectified</u>	(including fluids), lb	<u>716</u>	} Point Designs 3, 5, & 6
Cooling method	<u>Fluid</u>	Total weight of generator and cooling system, lb	<u>3,664</u>	
Coolant	<u>DC-200</u>	Specific weight, lb/kW	<u>0.147</u>	
Coolant flow rate, gpm	<u>228.3</u>			
Coolant pressure drop, psi	<u>120</u>	Duty cycle	Continuous duty	
		Number of pulses	<u>N/A</u>	
Voltage, L-N, V	<u>1617</u>	ON time per pulse, sec	<u>N/A</u>	
Stator current density, A/sq in.	<u>38,142</u>	OFF time per pulse, sec	<u>N/A</u>	
Field current density, A/sq in.	<u>37,366</u>	Initial copper temp, F	<u>230</u>	
Stator material	<u>1 V Permendur 0.010</u>	Final copper temp, F	<u>400</u>	
Rotor material	<u>HP 9-4-20</u>	Number of phases	<u>3</u>	
Rotor rotational speed, rpm	<u>12,500</u>	Power factor	<u>0.876 lagging</u>	
Rotor peripheral speed, ft/sec	<u>555</u>	Number of poles	<u>6</u>	
Rotor outside dia., in.	<u>9.89</u>	Frequency, Hz	<u>625</u>	
Rotor magnetic length, in.	<u>78.27</u>			
Main generator dia.		Rotor length/dia.	<u>7.91</u>	
(excluding flanges), in.	<u>14.19</u>	Exciter dia, in.	<u>9.27</u>	
Main generator length, in.	<u>89.83</u>	Exciter length, in.	<u>20.93</u>	
Main generator volume, cu in.	<u>14,189</u>	Exciter volume, cu in.	<u>1411</u>	
Main generator weight, lb	<u>2,948</u>	Exciter weight, lb	<u>257</u>	
		Field power, kW	<u>581</u>	
Total generator volume, cu in.	<u>15,600</u>	Total losses, kW	<u>1,873</u>	
Total generator weight, lb	<u>2,948</u>	Overall efficiency	<u>0.9296</u>	
Rotor inertia, in.-lb-sec ²	<u>49.92</u>	Cooling system weight (including fluids), lb	<u>971</u>	} Point Design 4
Motor-pump input power, kW	<u>30.3</u>	Total weight of generator/ cooling system, lb	<u>3,919</u>	
		Specific weight, lb/kW	<u>0.157</u>	

Assembly specific weight, point designs 3, 5, and 6 = 0.147 lb/kw

Assembly specific weight, point design 4 = 0.157 lb/kw

Superconducting Generator

Drawing PA113346 outlines the packaging and presents the weight breakdown of the superconducting turbogenerator assembly design satisfying point designs 3, 4, 5, and 6 requirements. The design shown in Drawing PA113346 is a low-voltage, low-rotational-speed design and, accordingly, requires the use of a gearbox. Drawing PA113344 is a low-voltage, high-speed design and thus a direct-drive turbogenerator is used. Drawing PA113345 is a high-voltage low-speed design with an intermediary gearbox. The design details and weight breakdown shown in the drawing, pertain to the use of a turbogenerator system exclusive of propellant assembly, controls, and gearbox. Generator design details are identical to those previously described in the superconductor generator point design 6 description.

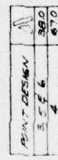
LOW-POWER APPLICATION, DESIGN POINTS 1 AND 2

Conventional Generator, Thermal-Lag

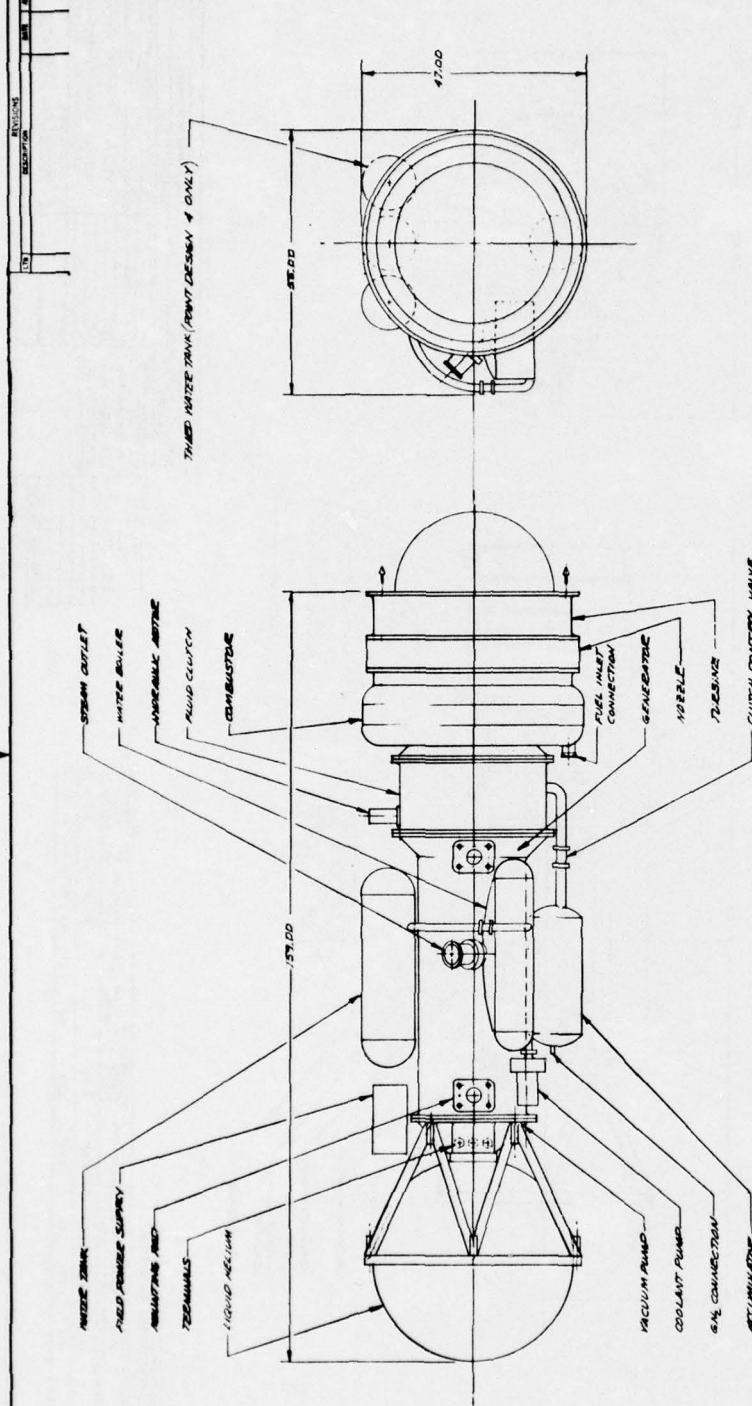
Drawing PA113340 presents the package outline and weight breakdown of a conventional thermal-lag turbogenerator assembly satisfying point designs 1 and 2 requirements. The elements shown in the drawing are for a power system exclusive of the propellant assembly, controls, and structure. The electrical output power required dictates optimum speed selection for the turbine and generator with the use of an intermediate gear drive. Generator design details of point design 1 requirements are described in Table 28. Table 29 describes the generator design details pertaining to point design 2 requirements. Critical speed characteristics for the two design points are shown in Table 30.

Conventional Generator, Fluid-Cooled

Drawing PA11341 presents package outline and weight breakdown of a conventional fluid-cooled turbogenerator assembly satisfying point designs 1 and 2 requirements. The elements shown in the drawing are for a power system exclusive of the propellant assembly, controls, and structure. Generator design details, applicable to point designs 1 and 2 are summarized in Table 31. Critical speed characteristics are shown in Table 32.

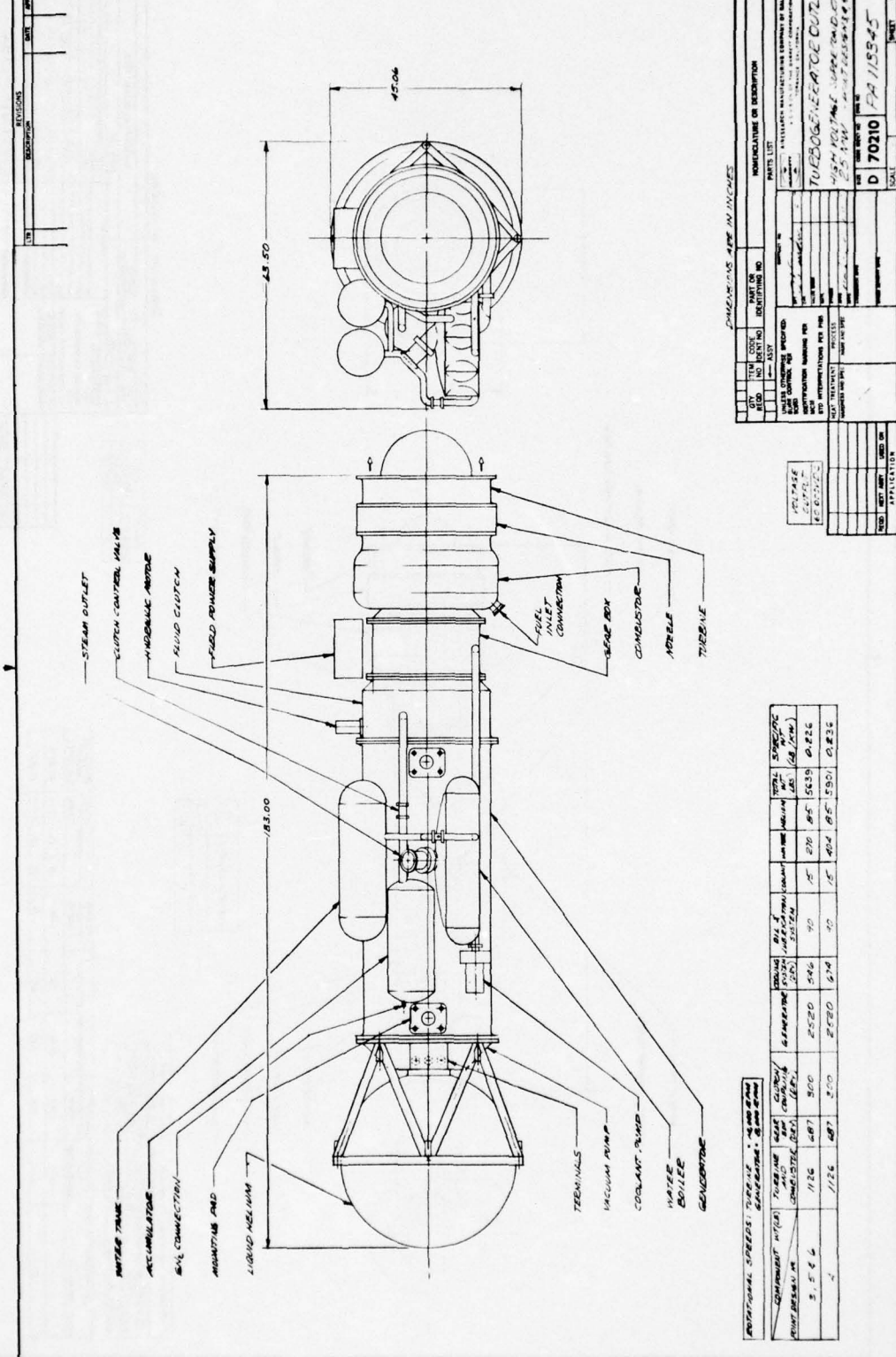


Son's Noddy *Stercorarius*



PART OR IDENTIFICATION NO.		NOMENCLATURE OR DESCRIPTION	
QTY	UNIT	QTY	UNIT
1	EA	1	EA
PARTS LIST		PARTS LIST	
TUBOGENERATOR OUTLINE		TUBOGENERATOR OUTLINE	
SUPERCONDUCTING DIRECT DRIVE		SUPERCONDUCTING DIRECT DRIVE	
D 70210 PA113344		D 70210 PA113344	
SCALE 1/2"		SCALE 1/2"	

COMPONENT	THICKNESS	LENGTH	WIDTH	HEIGHT	WEIGHT	VOLUME	AREA	PERIMETER	DIAMETER	THICKNESS	LENGTH	WIDTH	HEIGHT	WEIGHT	VOLUME	AREA	PERIMETER	DIAMETER
1	0.005	1.000	0.500	0.500	0.000	0.000	0.250	1.500	0.500	0.005	1.000	0.500	0.500	0.000	0.000	0.250	1.500	0.500
2	0.005	1.000	0.500	0.500	0.000	0.000	0.250	1.500	0.500	0.005	1.000	0.500	0.500	0.000	0.000	0.250	1.500	0.500
3	0.005	1.000	0.500	0.500	0.000	0.000	0.250	1.500	0.500	0.005	1.000	0.500	0.500	0.000	0.000	0.250	1.500	0.500
4	0.005	1.000	0.500	0.500	0.000	0.000	0.250	1.500	0.500	0.005	1.000	0.500	0.500	0.000	0.000	0.250	1.500	0.500
5	0.005	1.000	0.500	0.500	0.000	0.000	0.250	1.500	0.500	0.005	1.000	0.500	0.500	0.000	0.000	0.250	1.500	0.500
6	0.005	1.000	0.500	0.500	0.000	0.000	0.250	1.500	0.500	0.005	1.000	0.500	0.500	0.000	0.000	0.250	1.500	0.500
7	0.005	1.000	0.500	0.500	0.000	0.000	0.250	1.500	0.500	0.005	1.000	0.500	0.500	0.000	0.000	0.250	1.500	0.500
8	0.005	1.000	0.500	0.500	0.000	0.000	0.250	1.500	0.500	0.005	1.000	0.500	0.500	0.000	0.000	0.250	1.500	0.500
9	0.005	1.000	0.500	0.500	0.000	0.000	0.250	1.500	0.500	0.005	1.000	0.500	0.500	0.000	0.000	0.250	1.500	0.500
10	0.005	1.000	0.500	0.500	0.000	0.000	0.250	1.500	0.500	0.005	1.000	0.500	0.500	0.000	0.000	0.250	1.500	0.500



ENGINEERING AND DESIGN

DATE: 11/25/76

DESIGNER: D. 70210

PROJECT: TURBOGENERATOR ENGINE

REVISION: 1

APPROVED: 11/25/76

1. TURBOGENERATOR ENGINE

2. TURBOGENERATOR ENGINE

3. TURBOGENERATOR ENGINE

4. TURBOGENERATOR ENGINE

5. TURBOGENERATOR ENGINE

6. TURBOGENERATOR ENGINE

7. TURBOGENERATOR ENGINE

8. TURBOGENERATOR ENGINE

9. TURBOGENERATOR ENGINE

10. TURBOGENERATOR ENGINE

11. TURBOGENERATOR ENGINE

12. TURBOGENERATOR ENGINE

13. TURBOGENERATOR ENGINE

14. TURBOGENERATOR ENGINE

15. TURBOGENERATOR ENGINE

16. TURBOGENERATOR ENGINE

17. TURBOGENERATOR ENGINE

18. TURBOGENERATOR ENGINE

19. TURBOGENERATOR ENGINE

20. TURBOGENERATOR ENGINE

21. TURBOGENERATOR ENGINE

22. TURBOGENERATOR ENGINE

23. TURBOGENERATOR ENGINE

24. TURBOGENERATOR ENGINE

25. TURBOGENERATOR ENGINE

26. TURBOGENERATOR ENGINE

27. TURBOGENERATOR ENGINE

28. TURBOGENERATOR ENGINE

29. TURBOGENERATOR ENGINE

30. TURBOGENERATOR ENGINE

31. TURBOGENERATOR ENGINE

32. TURBOGENERATOR ENGINE

33. TURBOGENERATOR ENGINE

34. TURBOGENERATOR ENGINE

35. TURBOGENERATOR ENGINE

36. TURBOGENERATOR ENGINE

37. TURBOGENERATOR ENGINE

38. TURBOGENERATOR ENGINE

39. TURBOGENERATOR ENGINE

40. TURBOGENERATOR ENGINE

41. TURBOGENERATOR ENGINE

42. TURBOGENERATOR ENGINE

43. TURBOGENERATOR ENGINE

44. TURBOGENERATOR ENGINE

45. TURBOGENERATOR ENGINE

46. TURBOGENERATOR ENGINE

47. TURBOGENERATOR ENGINE

48. TURBOGENERATOR ENGINE

49. TURBOGENERATOR ENGINE

50. TURBOGENERATOR ENGINE

51. TURBOGENERATOR ENGINE

52. TURBOGENERATOR ENGINE

53. TURBOGENERATOR ENGINE

54. TURBOGENERATOR ENGINE

55. TURBOGENERATOR ENGINE

56. TURBOGENERATOR ENGINE

57. TURBOGENERATOR ENGINE

58. TURBOGENERATOR ENGINE

59. TURBOGENERATOR ENGINE

60. TURBOGENERATOR ENGINE

61. TURBOGENERATOR ENGINE

62. TURBOGENERATOR ENGINE

63. TURBOGENERATOR ENGINE

64. TURBOGENERATOR ENGINE

65. TURBOGENERATOR ENGINE

66. TURBOGENERATOR ENGINE

67. TURBOGENERATOR ENGINE

68. TURBOGENERATOR ENGINE

69. TURBOGENERATOR ENGINE

70. TURBOGENERATOR ENGINE

71. TURBOGENERATOR ENGINE

72. TURBOGENERATOR ENGINE

73. TURBOGENERATOR ENGINE

74. TURBOGENERATOR ENGINE

75. TURBOGENERATOR ENGINE

76. TURBOGENERATOR ENGINE

77. TURBOGENERATOR ENGINE

78. TURBOGENERATOR ENGINE

79. TURBOGENERATOR ENGINE

80. TURBOGENERATOR ENGINE

81. TURBOGENERATOR ENGINE

82. TURBOGENERATOR ENGINE

83. TURBOGENERATOR ENGINE

84. TURBOGENERATOR ENGINE

85. TURBOGENERATOR ENGINE

86. TURBOGENERATOR ENGINE

87. TURBOGENERATOR ENGINE

88. TURBOGENERATOR ENGINE

89. TURBOGENERATOR ENGINE

90. TURBOGENERATOR ENGINE

91. TURBOGENERATOR ENGINE

92. TURBOGENERATOR ENGINE

93. TURBOGENERATOR ENGINE

94. TURBOGENERATOR ENGINE

95. TURBOGENERATOR ENGINE

96. TURBOGENERATOR ENGINE

97. TURBOGENERATOR ENGINE

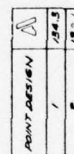
98. TURBOGENERATOR ENGINE

99. TURBOGENERATOR ENGINE

100. TURBOGENERATOR ENGINE

REV	DATE	DESCRIPTION
1	11/25/76	INITIAL DESIGN
2	11/25/76	REVISION 1
3	11/25/76	REVISION 2
4	11/25/76	REVISION 3
5	11/25/76	REVISION 4
6	11/25/76	REVISION 5
7	11/25/76	REVISION 6
8	11/25/76	REVISION 7
9	11/25/76	REVISION 8
10	11/25/76	REVISION 9
11	11/25/76	REVISION 10
12	11/25/76	REVISION 11
13	11/25/76	REVISION 12
14	11/25/76	REVISION 13
15	11/25/76	REVISION 14
16	11/25/76	REVISION 15
17	11/25/76	REVISION 16
18	11/25/76	REVISION 17
19	11/25/76	REVISION 18
20	11/25/76	REVISION 19
21	11/25/76	REVISION 20
22	11/25/76	REVISION 21
23	11/25/76	REVISION 22
24	11/25/76	REVISION 23
25	11/25/76	REVISION 24
26	11/25/76	REVISION 25
27	11/25/76	REVISION 26
28	11/25/76	REVISION 27
29	11/25/76	REVISION 28
30	11/25/76	REVISION 29
31	11/25/76	REVISION 30
32	11/25/76	REVISION 31
33	11/25/76	REVISION 32
34	11/25/76	REVISION 33
35	11/25/76	REVISION 34
36	11/25/76	REVISION 35
37	11/25/76	REVISION 36
38	11/25/76	REVISION 37
39	11/25/76	REVISION 38
40	11/25/76	REVISION 39
41	11/25/76	REVISION 40
42	11/25/76	REVISION 41
43	11/25/76	REVISION 42
44	11/25/76	REVISION 43
45	11/25/76	REVISION 44
46	11/25/76	REVISION 45
47	11/25/76	REVISION 46
48	11/25/76	REVISION 47
49	11/25/76	REVISION 48
50	11/25/76	REVISION 49
51	11/25/76	REVISION 50
52	11/25/76	REVISION 51
53	11/25/76	REVISION 52
54	11/25/76	REVISION 53
55	11/25/76	REVISION 54
56	11/25/76	REVISION 55
57	11/25/76	REVISION 56
58	11/25/76	REVISION 57
59	11/25/76	REVISION 58
60	11/25/76	REVISION 59
61	11/25/76	REVISION 60
62	11/25/76	REVISION 61
63	11/25/76	REVISION 62
64	11/25/76	REVISION 63
65	11/25/76	REVISION 64
66	11/25/76	REVISION 65
67	11/25/76	REVISION 66
68	11/25/76	REVISION 67
69	11/25/76	REVISION 68
70	11/25/76	REVISION 69
71	11/25/76	REVISION 70
72	11/25/76	REVISION 71
73	11/25/76	REVISION 72
74	11/25/76	REVISION 73
75	11/25/76	REVISION 74
76	11/25/76	REVISION 75
77	11/25/76	REVISION 76
78	11/25/76	REVISION 77
79	11/25/76	REVISION 78
80	11/25/76	REVISION 79
81	11/25/76	REVISION 80
82	11/25/76	REVISION 81
83	11/25/76	REVISION 82
84	11/25/76	REVISION 83
85	11/25/76	REVISION 84
86	11/25/76	REVISION 85
87	11/25/76	REVISION 86
88	11/25/76	REVISION 87
89	11/25/76	REVISION 88
90	11/25/76	REVISION 89
91	11/25/76	REVISION 90
92	11/25/76	REVISION 91
93	11/25/76	REVISION 92
94	11/25/76	REVISION 93
95	11/25/76	REVISION 94
96	11/25/76	REVISION 95
97	11/25/76	REVISION 96
98	11/25/76	REVISION 97
99	11/25/76	REVISION 98
100	11/25/76	REVISION 99

REV	DATE	DESCRIPTION
1	11/25/76	INITIAL DESIGN
2	11/25/76	REVISION 1
3	11/25/76	REVISION 2
4	11/25/76	REVISION 3
5	11/25/76	REVISION 4
6	11/25/76	REVISION 5
7	11/25/76	REVISION 6
8	11/25/76	REVISION 7
9	11/25/76	REVISION 8
10	11/25/76	REVISION 9
11	11/25/76	REVISION 10
12	11/25/76	REVISION 11
13	11/25/76	REVISION 12
14	11/25/76	REVISION 13
15	11/25/76	REVISION 14
16	11/25/76	REVISION 15
17	11/25/76	REVISION 16
18	11/25/76	REVISION 17
19	11/25/76	REVISION 18
20	11/25/76	REVISION 19
21	11/25/76	REVISION 20
22	11/25/76	REVISION 21
23	11/25/76	REVISION 22
24	11/25/76	REVISION 23
25	11/25/76	REVISION 24
26	11/25/76	REVISION 25
27	11/25/76	REVISION 26
28	11/25/76	REVISION 27
29	11/25/76	REVISION 28
30	11/25/76	REVISION 29
31	11/25/76	REVISION 30
32	11/25/76	REVISION 31
33	11/25/76	REVISION 32
34	11/25/76	REVISION 33
35	11/25/76	REVISION 34
36	11/25/76	REVISION 35
37	11/25/76	REVISION 36
38	11/25/76	REVISION 37
39	11/25/76	REVISION 38
40	11/25/76	REVISION 39
41	11/25/76	REVISION 40
42	11/25/76	REVISION 41
43	11/25/76	REVISION 42
44	11/25/76	REVISION 43
45	11/25/76	REVISION 44
46	11/25/76	REVISION 45
47	11/25/76	REVISION 46
48	11/25/76	REVISION 47
49	11/25/76	REVISION 48
50	11/25/76	REVISION 49
51	11/25/76	REVISION 50
52	11/25/76	REVISION 51
53	11/25/76	REVISION 52
54	11/25/76	REVISION 53
55	11/25/76	REVISION 54
56	11/25/76	REVISION 55
57	11/25/76	REVISION 56
58	11/25/76	REVISION 57
59	11/25/76	REVISION 58
60	11/25/76	REVISION 59
61	11/25/76	REVISION 60
62	11/25/76	REVISION 61
63	11/25/76	REVISION 62
64	11/25/76	REVISION 63
65	11/25/76	REVISION 64
66	11/25/76	REVISION 65
67	11/25/76	REVISION 66
68	11/25/76	REVISION 67
69	11/25/76	REVISION 68
70	11/25/76	REVISION 69
71	11/25/76	REVISION 70
72	11/25/76	REVISION 71
73	11/25/76	REVISION 72
74	11/25/76	REVISION 73
75	11/25/76	REVISION 74
76	11/25/76	REVISION 75
77	11/25/76	REVISION 76
78	11/25/76	REVISION 77
79	11/25/76	REVISION 78
80	11/25/76	REVISION 79
81	11/25/76	REVISION 80
82	11/25/76	REVISION 81
83	11/25/76	REVISION 82
84	11/25/76	REVISION 83
85	11/25/76	REVISION 84
86	11/25/76	REVISION 85
87	11/25/76	REVISION 86
88	11/25/76	REVISION 87
89	11/25/76	REVISION 88
90	11/25/76	REVISION 89
91	11/25/76	REVISION 90
92	11/25/76	REVISION 91
93	11/25/76	REVISION 92
94	11/25/76	REVISION 93
95	11/25/76	REVISION 94
96	11/25/76	REVISION 95
97	11/25/76	REVISION 96
98	11/25/76	REVISION 97
99	11/25/76	REVISION 98
100	11/25/76	REVISION 99



INDEPENDENT VARIATES	% OF TOTAL AND CONCENTRATION	DEPENDENT VARIABLES	RELATIONSHIP (CORR.)	COEFFICIENT OF DETERMINATION (R ²)	P-VALUE (P)	TOTAL SAMPLE SIZE (N)
PERCENT BROWN IN SOIL	1	# 2	.98	.96	.71	2,754
						0.275

POINT DESIGN	DC WEBSITE
1	5430

[illegible]

TABLE 28
CONVENTIONAL GENERATOR, THERMAL LAG, POINT DESIGN 1

Power level, MW	10	Cooling system weight	
Type of load	Rectified	(including fluids), lb	N/A
Cooling method	Thermal lag	Total weight of generator and cooling system, lb	N/A
Coolant	None	Specific weight, lb/kW	0.194
Coolant flow rate, gpm	-		
Coolant pressure drop, psi	-	Duty cycle:	
		Number of pulses	3
Voltage, L-N, V	1815	ON time per pulse, sec	21
Stator current density, A/sq in.	13.329	OFF time per pulse, sec	30
Field current density, A/sq in.	13.279	Initial copper temp, F	130
Stator material	1 V Permendur 0.010	Final copper temp, F	450
Rotor material	HP 9-4-20	Number of phases	3
Rotor rotational speed, rpm	14,000	Power factor	0.878 lagging
Rotor peripheral speed, ft/sec	650	Number of poles	6
Rotor outside dia., in.	10.39	Frequency, Hz	700
Rotor magnetic length, in.	45.71		
Main generator dia.		Rotor length/dia.	4.40
(excluding flanges), in.	14.97	Exciter dia, in.	9.58
Main generator length, in.	51.60	Exciter length, in.	11.50
Main generator volume, cu in.	10,136	Exciter volume, cu in.	828
Main generator weight, lb	1.864	Exciter weight, lb	76
		Field power, kW	89.7
Total generator volume, cu in.	10,964	Total losses, kW	423
Total generator weight, lb	1,940	Overall efficiency	0.9591
Rotor inertia, in.-lb-sec ²	37.25		
Motor-pump input power, kW	N/A		

Assembly specific weight = 0.194 lb/kw

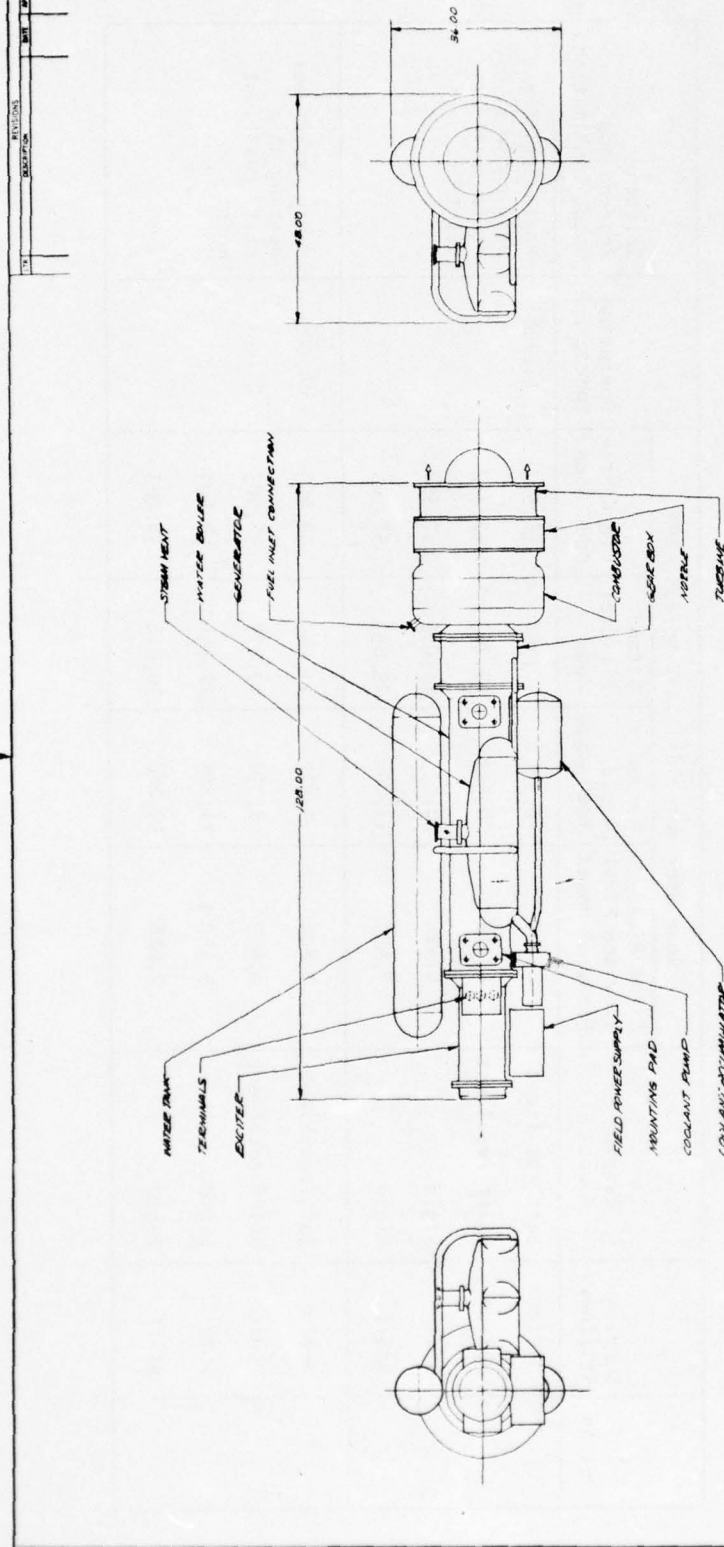
TABLE 29
CONVENTIONAL GENERATOR, THERMAL LAG, POINT DESIGN 2

Power level, MW	<u>10</u>	Cooling system weight	
Type of load	<u>Rectified</u>	(including fluids), lb	<u>N/A</u>
Cooling method	<u>Thermal lag</u>	Total weight of generator	
Coolant	<u>None</u>	and cooling system, lb	<u>N/A</u>
Coolant flow rate, gpm	<u>-</u>	Specific weight, lb/kW	<u>0.186</u>
Coolant pressure drop, psi	<u>-</u>	Duty cycle:	
Voltage, L-N, V	<u>1785</u>	Number of pulses	<u>3</u>
Stator current density, A/sq in.	<u>14,529</u>	ON time per pulse, sec	<u>21</u>
Field current density, A/sq in.	<u>14,593</u>	OFF time per pulse, sec	<u>300</u>
Stator material	<u>2 V Permendur 0,010</u>	Initial copper temp, F	<u>130</u>
		Final copper temp, F	<u>450</u>
Rotor material	<u>HP 9-4-20</u>	Number of phases	<u>3</u>
Rotor rotational speed, rpm	<u>14,000</u>	Power factor	<u>0.875 lagging</u>
Rotor peripheral speed, ft/sec	<u>650</u>	Number of poles	<u>6</u>
Rotor outside dia., in.	<u>10.38</u>	Frequency, Hz	<u>700</u>
Rotor magnetic length, in.	<u>43.47</u>		
Main generator dia.		Rotor length/dia.	<u>4.19</u>
(excluding flanges), in.	<u>14.94</u>	Exciter dia, in.	<u>9.60</u>
Main generator length, in.	<u>55.29</u>	Exciter length, in.	<u>11.63</u>
Main generator volume, cu in.	<u>9,683</u>	Exciter volume, cu in.	<u>842</u>
Main generator weight, lb	<u>1,778</u>	Exciter weight, lb	<u>81</u>
		Field power, kW	<u>102.3</u>
Total generator volume, cu in.	<u>10,525</u>	Total losses, kW	<u>431</u>
Total generator weight, lb	<u>1,859</u>	Overall efficiency	<u>0.9582</u>
Rotor inertia, in.-lb-sec ²	<u>35.56</u>		
Motor-pump input power, kW	<u>N/A</u>		

Assembly specific weight = 0.186 lb/kw

TABLE 30
CONVENTIONAL GENERATOR, THERMAL LAG
PRELIMINARY CRITICAL SPEED EVALUATIONS OF POINT DESIGNS 1 AND 2

Point Design	Bearing Stiffness	Bearing Mount	Generator Rotor Critical Speeds, RPM				Operating Speed, rpm	Selected Bearing and Mount Combination
			First Rigid Body and First Flexural Modes	Second Rigid Body Mode	Second Flexural Mode	First Free Body Mode		
1	Medium	Soft resilient	2,741	5,374	10,966	52,962	14,000	Medium stiffness bearing in a stiff resilient mount
	Medium	Stiff resilient	4,316	8,511	17,263	52,962		
	Soft	Rigid	5,524	10,825	22,095	52,962		
	Stiff	Rigid	7,407	13,846	29,630	52,962		
2	Medium	Soft resilient	2,804	5,522	11,215	58,403	14,000	Medium stiffness bearing in a stiff resilient mount
	Medium	Stiff resilient	4,419	8,751	17,675	58,403		
	Soft	Rigid	5,659 1	11,133	22,634	58,403		
	Stiff	Rigid	7,628	14,288	30,512	58,403		



DIMENSIONS ARE IN INCHES				INFORMATION OF DESCRIPTION	
ITEM	ITEM	ITEM	ITEM	ITEM	ITEM
NO.	NO.	NO.	NO.	NO.	NO.
1	2	3	4	5	6
7	8	9	10	11	12
13	14	15	16	17	18
19	20	21	22	23	24
25	26	27	28	29	30
31	32	33	34	35	36
37	38	39	40	41	42
43	44	45	46	47	48
49	50	51	52	53	54
55	56	57	58	59	60
61	62	63	64	65	66
67	68	69	70	71	72
73	74	75	76	77	78
79	80	81	82	83	84
85	86	87	88	89	90
91	92	93	94	95	96
97	98	99	100	101	102
103	104	105	106	107	108
109	110	111	112	113	114
115	116	117	118	119	120
121	122	123	124	125	126
127	128	129	130	131	132
133	134	135	136	137	138
139	140	141	142	143	144
145	146	147	148	149	150
151	152	153	154	155	156
157	158	159	160	161	162
163	164	165	166	167	168
169	170	171	172	173	174
175	176	177	178	179	180
181	182	183	184	185	186
187	188	189	190	191	192
193	194	195	196	197	198
199	200	201	202	203	204
205	206	207	208	209	210
211	212	213	214	215	216
217	218	219	220	221	222
223	224	225	226	227	228
229	230	231	232	233	234
235	236	237	238	239	240
241	242	243	244	245	246
247	248	249	250	251	252
253	254	255	256	257	258
259	260	261	262	263	264
265	266	267	268	269	270
271	272	273	274	275	276
277	278	279	280	281	282
283	284	285	286	287	288
289	290	291	292	293	294
295	296	297	298	299	300
301	302	303	304	305	306
307	308	309	310	311	312
313	314	315	316	317	318
319	320	321	322	323	324
325	326	327	328	329	330
331	332	333	334	335	336
337	338	339	340	341	342
343	344	345	346	347	348
349	350	351	352	353	354
355	356	357	358	359	360
361	362	363	364	365	366
367	368	369	370	371	372
373	374	375	376	377	378
379	380	381	382	383	384
385	386	387	388	389	390
391	392	393	394	395	396
397	398	399	400	401	402
403	404	405	406	407	408
409	410	411	412	413	414
415	416	417	418	419	420
421	422	423	424	425	426
427	428	429	430	431	432
433	434	435	436	437	438
439	440	441	442	443	444
445	446	447	448	449	450
451	452	453	454	455	456
457	458	459	460	461	462
463	464	465	466	467	468
469	470	471	472	473	474
475	476	477	478	479	480
481	482	483	484	485	486
487	488	489	490	491	492
493	494	495	496	497	498
499	500	501	502	503	504
505	506	507	508	509	510
511	512	513	514	515	516
517	518	519	520	521	522
523	524	525	526	527	528
529	530	531	532	533	534
535	536	537	538	539	540
541	542	543	544	545	546
547	548	549	550	551	552
553	554	555	556	557	558
559	560	561	562	563	564
565	566	567	568	569	570
571	572	573	574	575	576
577	578	579	580	581	582
583	584	585	586	587	588
589	590	591	592	593	594
595	596	597	598	599	600
601	602	603	604	605	606
607	608	609	610	611	612
613	614	615	616	617	618
619	620	621	622	623	624
625	626	627	628	629	630
631	632	633	634	635	636
637	638	639	640	641	642
643	644	645	646	647	648
649	650	651	652	653	654
655	656	657	658	659	660
661	662	663	664	665	666
667	668	669	670	671	672
673	674	675	676	677	678
679	680	681	682	683	684
685	686	687	688	689	690
691	692	693	694	695	696
697	698	699	700	701	702
703	704	705	706	707	708
709	710	711	712	713	714
715	716	717	718	719	720
721	722	723	724	725	726
727	728	729	730	731	732
733	734	735	736	737	738
739	740	741	742	743	744
745	746	747	748	749	750
751	752	753	754	755	756
757	758	759	760	761	762
763	764	765	766	767	768
769	770	771	772	773	774
775	776	777	778	779	780
781	782	783	784	785	786
787	788	789	790	791	792
793	794	795	796	797	798
799	800	801	802	803	804
805	806	807	808	809	810
811	812	813	814	815	816
817	818	819	820	821	822
823	824	825	826	827	828
829	830	831	832	833	834
835	836	837	838	839	840
841	842	843	844	845	846
847	848	849	850	851	852
853	854	855	856	857	858
859	860	861	862	863	864
865	866	867	868	869	870
871	872	873	874	875	876
877	878	879	880	881	882
883	884	885	886	887	888
889	890	891	892	893	894
895	896	897	898	899	900
901	902	903	904	905	906
907	908	909	910	911	912
913	914	915	916	917	918
919	920	921	922	923	924
925	926	927	928	929	930
931	932	933	934	935	936
937	938	939	940	941	942
943	944	945	946	947	948
949	950	951	952	953	954
955	956	957	958	959	960
961	962	963	964	965	966
967	968	969	970	971	972
973	974	975	976	977	978
979	980	981	982	983	984
985	986	987	988	989	990
991	992	993	994	995	996
997	998	999	1000	1001	1002
1003	1004	1005	1006	1007	1008
1009	1010	1011	1012	1013	1014
1015	1016	1017	1018	1019	1020
1021	1022	1023	1024	1025	1026
1027	1028	1029	1030	1031	1032
1033	1034	1035	1036	1037	1038
1039	1040	1041	1042	1043	1044
1045	1046	1047	1048	1049	1050
1051	1052	1053	1054	1055	1056
1057	1058	1059	1060	1061	1062
1063	1064	1065	1066	1067	1068
1069	1070	1071	1072	1073	1074
1075	1076	1077	1078	1079	1080
1081	1082	1083	1084	1085	1086
1087	1088	1089	1090	1091	1092
1093	1094	1095	1096	1097	1098
1099	1100	1101	1102	1103	1104
1105	1106	1107	1108	1109	1110
1111	1112	1113	1114	1115	1116
1117	1118	1119	1120	1121	1122
1123	1124	1125	1126	1127	1128
1129	1130	1131	1132	1133	1134
1135	1136	1137	1138	1139	1140
1141	1142	1143	1144	1145	1146
1147	1148	1149	1150	1151	1152
1153	1154	1155	1156	1157	1158
1159	1160	1161	1162	1163	1164
1165	1166	1167	1168	1169	1170
1171	1172				

AD-A032 634

AIRESEARCH MFG CO OF CALIFORNIA TORRANCE
HIGH POWER STUDY--CONVENTIONAL GENERATORS, SUPERCONDUCTING GENE--ETC(U)
JUL 76 L SCHIPPER

F/G 10/2

F33615-75-C-2071

UNCLASSIFIED

76-12446

AFAPL-TR-76-39

NL

2 OF 5
AD
A032634



TABLE 31

CONVENTIONAL GENERATOR, FLUID COOLED, POINT DESIGNS 1 AND 2

Power level, MW	10	Cooling system weight	
Type of load	Rectified	(including fluids), lb	438
		Total weight of generator	
Cooling method	Fluid	and cooling system, lb	1,647
Coolant	DC-200	Specific weight, lb/kW	0.165
Coolant flow rate, gpm	147.7		
Coolant pressure drop, psi	120	Duty cycle	Continuous duty
		Number of pulses	N/A
Voltage, L-N, V	1154	ON time per pulse, sec	N/A
Stator current density, A/sq in.	52,522	OFF time per pulse, sec	N/A
Field current density, A/sq in.	52,538	Initial copper temp, F	230
Stator material	2 V Permendur 0.016	Final copper temp, F	400
Rotor material	HP 9-4-20	Number of phases	3
Rotor rotational speed, rpm	14,000	Power factor	0.880 lagging
Rotor peripheral speed, ft/sec	555	Number of poles	6
Rotor outside dia., in.	8.70	Frequency, Hz	700
Rotor magnetic length, in.	39.05		
		Rotor length/dia.	4.49
Main generator dia.		Exciter dia, in.	8.29
(excluding flanges), in.	12.56	Exciter length, in.	16.70
Main generator length, in.	49.32	Exciter volume, cu in.	900
Main generator volume, cu in.	6,105	Exciter weight, lb	163
Main generator weight, lb	1,046		
		Field power, kW	408
Total generator volume, cu in.	7,005	Total losses, kW	870
Total generator weight, lb	1,209	Overall efficiency	0.9195
Rotor inertia, in.-lb-sec ²	15.03		
Motor-pump input power, kW	20.4		

Assembly specific weight = 0.165 lb/kw

TABLE 32
CONVENTIONAL GENERATOR, FLUID COOLED
PRELIMINARY CRITICAL SPEED EVALUATIONS OF POINT DESIGNS 1 AND 2

Point Design	Bearing Stiffness	Bearing Mount	Generator Rotor Critical Speeds, RPM				Operating Speed, rpm	Selected Bearing and Mount Combination
			First Rigid Body and First Flexural Modes	Second Rigid Body Mode	Second Flexural Mode	First Free Body Mode		
1 and 2	Medium	Soft resilient	3,308	6,566	13,232	60,738	14,000	Medium stiffness bearing in a stiff resilient mount
	Medium	Stiff resilient	4,887	9,729	19,548	60,738		
	Soft	Rigid	7,040	13,542	28,162	60,738		
	Stiff	Rigid	7,959	15,027	31,837	60,738		

Shaft power for generator drive via a gearbox is provided by a two-stage axial-flow, pressure-compound turbine rotating at 21,500 rpm. Pertinent design details of the turbine are:

Propellant	Combustion product of neat hydrazine
Nozzle outlet	2110 R (1172.2 K)/850 psia (5.86 MPa)
Overall pressure ratio	425
Rotational speed	21,500 rpm
Number of stages	2
Shaft power	15,220 hp
Turbine flow rate	17.58 lb/sec (7.94 kg/sec)
Overall efficiency	74.8 percent

First Stage

Inlet temperature	2110 R (1172.2 K)
Flow rate	17.58 lb/sec (7.99 kg/sec)
Blade height	0.528 in. (0.0134 m)
Pitch velocity	1650 ft/sec (502.9 M/sec)

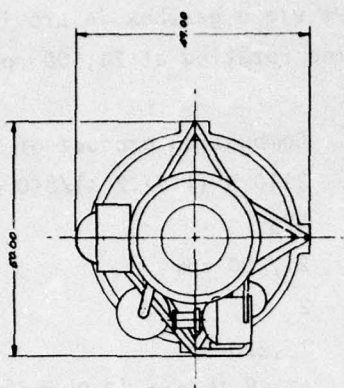
Second Stage

Inlet temperature	1625 R (902.8 K)
Flow rate	17.02 lb/sec (7.74 kg/sec)
Blade height	2.33 in. (0.0592 m)
Pitch velocity	1480 ft/sec (451.1 m/sec)

Superconducting Generator

Drawing PA113349 shows the package outline and weight breakdown of a superconducting turbogenerator assembly satisfying point designs 1 and 2 requirements. The elements shown in the drawing are for a power system exclusive of the required propellant assembly, controls, and structure. Generator design details applicable to both point designs are summarized in Table 33. Helium airborne supply details are as follows:

Power	10 MW
Helium flow rate	18.3 liter/hr
Heat leak	6.7 Btu/hr



OUTLET	100000
RECEIVE	100000
100000	100000

[illegible]

TABLE 33
SUPERCONDUCTING GENERATOR, POINT DESIGNS 1 AND 2

Power level, MW	<u>10</u>	Cooling system weight	
Type of load	<u>Rectified</u>	(including fluids), lb	<u>625</u>
Stator		Total weight of generator	
Cooling method	<u>Fluid cooled</u>	and cooling system, lb	<u>1265</u>
Coolant, stator	<u>MIL-L-23699</u>	Specific weight, lb/kW	<u>0.127</u>
Coolant flow rate, gpm	<u>80.5</u>		
Coolant pressure drop, psi	<u>20</u>	Duty cycle: continuous duty	
		Number of pulses	<u>N/A</u>
Voltage, L-N, V	<u>2000</u>	ON time per pulse, sec	<u>N/A</u>
Stator current density, A/sq in.	<u>30,917</u>	OFF time per pulse, sec	<u>N/A</u>
Field current density, A/sq in.	<u>435,100</u>	Initial copper temp, F	<u>N/A</u>
Stator material	<u>2 V Permendur</u>	Final copper temp, F	<u>N/A</u>
Rotor material	<u>Superconductor</u>	Number of phases	<u>3</u>
Rotor rotational speed, rpm	<u>10,000</u>	Power factor	<u>0.88 lagging</u>
Rotor peripheral speed, ft/sec	<u>500</u>	Number of poles	<u>6</u>
Rotor outside dia., in.	<u>11.47</u>	Frequency, Hz	<u>500</u>
Rotor magnetic length, in.	<u>22.05</u>		
Main generator dia.		Rotor length/dia.	<u>1.92</u>
(excluding flanges), in.	<u>22.44</u>	Exciter dia, in.	<u>N/A</u>
Main generator length, in.	<u>28.05</u>	Exciter length, in.	<u>N/A</u>
Main generator volume, cu in.	<u>N/A</u>	Exciter volume, cu in.	<u>N/A</u>
Main generator weight, lb	<u>N/A</u>	Exciter weight, lb	<u>N/A</u>
		Field power, kW	<u>N/A</u>
Total generator volume, cu in.	<u>11,090</u>	Total losses, kW	<u>162.3</u>
Total generator weight, lb	<u>640</u>	Overall efficiency	<u>0.9840</u>
Rotor inertia, in.-lb-sec ²	<u>7.33</u>		
Motor-pump input power, kW	<u>2.3</u>		

Assembly specific weight = 0.127 lb/kw

Tank assembly	
Dry weight	127.1 lb
Wet weight	206.6 lb
Lines, mounting, etc.	10.0 lb
Total system weight	216.6 lb (98.45 kg)
Outer shell diameter	40.47 in. (1.03 m)
Girth ring diameter	44.07 in. (1.12 m)

HIGH-POWER APPLICATION, DESIGN POINTS 7 AND 8

Conventional Generator, Thermal-Lag

Drawing PA113342 shows the package outline and weight breakdown of a conventional thermal-lag design approach turbogenerator assembly satisfying point designs 7 and 8 requirements. The elements shown in the drawing are exclusive of the propellant assembly, controls, and structural supports. Turbine structural considerations dictate the design rotational speed of 9500 rpm in a direct turbogenerator drive system. Generator design details applicable to point designs 7 and 8 are shown in Tables 34 and 35, respectively.

Critical speed characteristics for the two design points are shown in Table 36.

Conventional Generator, Fluid-Cooled

Drawing PA113343 shows the package outline and weight breakdown of a conventional fluid-cooled turbogenerator assembly satisfying point designs 7 and 8 requirements. The elements shown are for a power system exclusive of the propellant assembly, controls, and structure. Generator design details applicable to both operating conditions of interest are shown in Table 37.

Critical speed characteristics are shown in Table 38.

AFAPL-TR-76-39

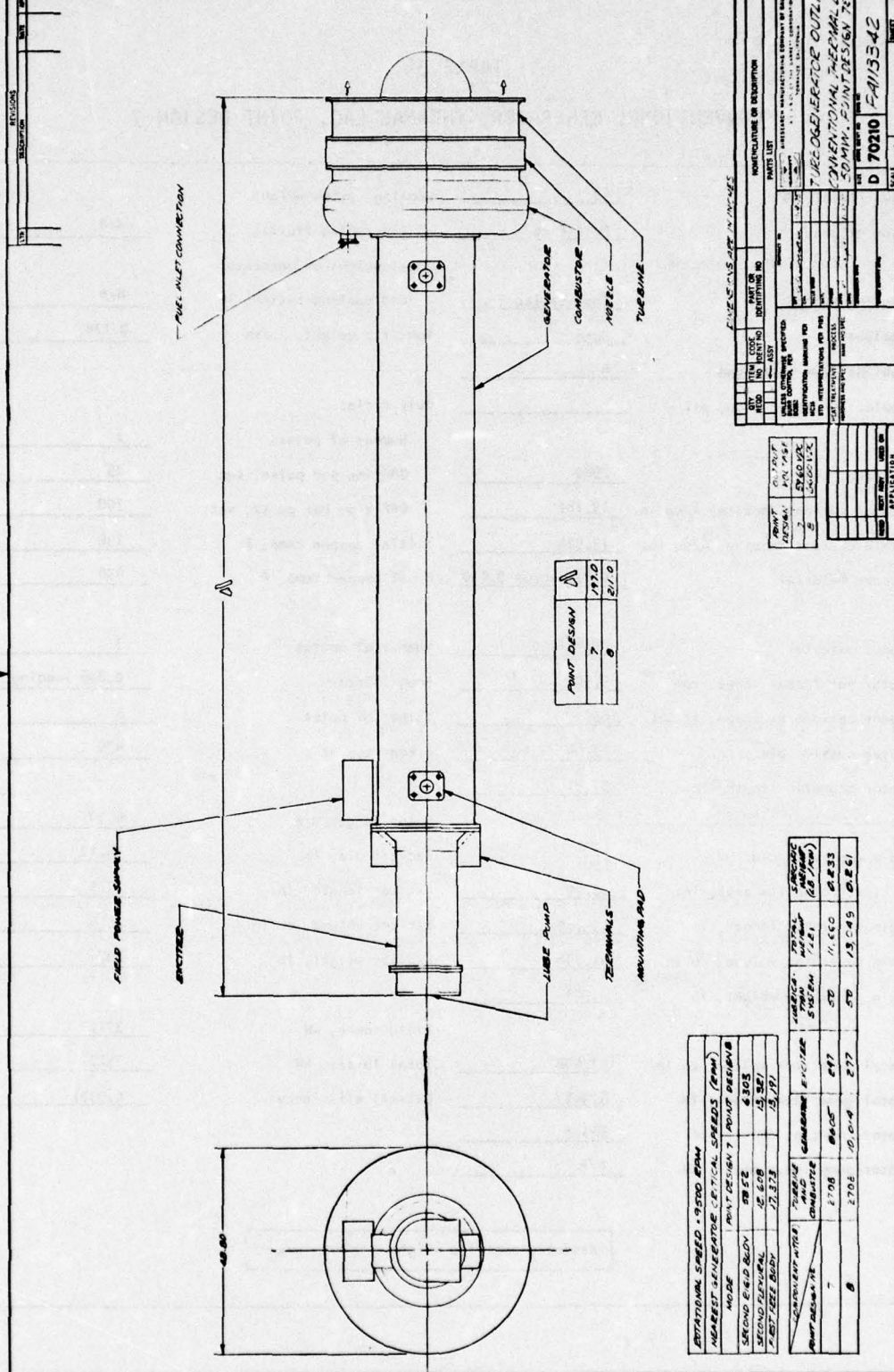


TABLE 34
CONVENTIONAL GENERATOR, THERMAL LAG, POINT DESIGN 7

Power level, MW	<u>50</u>	Cooling system weight	
Type of load	<u>Rectified</u>	(including fluids), lb	<u>N/A</u>
		Total weight of generator	
Cooling method	<u>Thermal lag</u>	and cooling system, lb	<u>N/A</u>
Coolant	<u>None</u>	Specific weight, lb/kW	<u>0.178</u>
Coolant flow rate, gpm	<u>-</u>		
Coolant pressure drop, psi	<u>-</u>	Duty cycle:	
		Number of pulses	<u>3</u>
Voltage, L-N, V	<u>2980</u>	ON time per pulse, sec	<u>25</u>
Stator current density, A/sq in.	<u>13,182</u>	OFF time per pulse, sec	<u>300</u>
Field current density, A/sq in.	<u>13,524</u>	Initial copper temp, F	<u>130</u>
Stator material	<u>2 V Permendur 0,010</u>	Final copper temp, F	<u>450</u>
Rotor material	<u>HP 9-4-20</u>	Number of phases	<u>3</u>
Rotor rotational speed, rpm	<u>9,500</u>	Power factor	<u>0.876 lagging</u>
Rotor peripheral speed, ft/sec	<u>650</u>	Number of poles	<u>6</u>
Rotor outside dia., in.	<u>15.44</u>	Frequency, Hz	<u>475</u>
Rotor magnetic length, in.	<u>97.31</u>		
		Rotor length/dia.	<u>6.30</u>
Main generator dia.		Exciter dia, in.	<u>14.12</u>
(excluding flanges), in.	<u>22.29</u>	Exciter length, in.	<u>17.97</u>
Main generator length, in.	<u>114.69</u>	Exciter volume, cu in.	<u>2814</u>
Main generator volume, cu in.	<u>44,734</u>	Exciter weight, lb	<u>297</u>
Main generator weight, lb	<u>8,903</u>		
		Field power, kW	<u>371.2</u>
Total generator volume, cu in.	<u>47,548</u>	Total losses, kW	<u>3322</u>
Total generator weight, lb	<u>8,903</u>	Overall efficiency	<u>0.9371</u>
Rotor inertia, in.-lb-sec ²	<u>383.3</u>		
Motor-pump input power, kW	<u>N/A</u>		

Assembly specific weight = 0.178 lb/kw

TABLE 35
CONVENTIONAL GENERATOR, THERMAL LAG, POINT DESIGN 8

Power level, MW	50	Cooling system weight	
Type of load	Rectified	(including fluids), lb	N/A
Cooling method	Thermal lag	Total weight of generator	
Coolant	None	and cooling system, lb	N/A
Coolant flow rate, gpm	-	Specific weight, lb/kW	0.210
Coolant pressure drop, psi	-	Duty cycle:	
Voltage, L-N, V	3300	Number of pulses	10
Stator current density, A/sq in.	10,384	ON time per pulse, sec	12
Field current density, A/sq in.	10,938	OFF time per pulse, sec	78
Stator material	1 V Permendur 0.010	Initial copper temp, F	130
		Final copper temp, F	450
Rotor material	HP 9-4-20	Number of phases	3
Rotor rotational speed, rpm	9,500	Power factor	0.877 lagging
Rotor peripheral speed, ft/sec	650	Number of poles	6
Rotor outside dia., in.	15.46	Frequency, Hz	475
Rotor magnetic length, in.	111.78		
Main generator dia.		Rotor length/dia.	7.23
(excluding flanges), in.	22.46	Exciter dia, in.	14.12
Main generator length, in.	129.03	Exciter length, in.	17.69
Main generator volume, cu in.	51.072	Exciter volume, cu in.	2770
Main generator weight, lb	10,245	Exciter weight, lb	277
		Field power, kW	308.1
Total generator volume, cu in.	53,842	Total losses, kW	3608
Total generator weight, lb	10,522	Overall efficiency	0.9321
Rotor inertia, in.-lb-sec ²	446.9		
Motor-pump input power, kW	N/A		

Assembly specific weight = 0.210 lb/kw

TABLE 36
CONVENTIONAL GENERATOR, THERMAL LAG
PRELIMINARY CRITICAL SPEED EVALUATIONS OF POINT DESIGNS 7 AND 8

Point Design	Bearing Stiffness	Bearing Mount	Generator Rotor Critical Speeds, RPM				Operating Speed, rpm	Selected Bearing and Mount Combination
			First Rigid Body and First Flexural Modes	Second Rigid Body Mode	Second Flexural Mode	First Free Body Mode		
7	Medium	Soft resilient	1,326	2,437	5,304	17,373	9,500	Soft bearing in a rigid mount
	Medium	Stiff resilient	2,228	4,118	8,912	17,373		
	Soft	Rigid	3,152	5,852	12,608	17,373		
	Stiff	Rigid	3,691	7,140	14,764	17,373		
8	Medium	Soft resilient	1,224	2,210	4,895	13,191	9,500	Stiff bearing in a rigid mount
	Medium	Stiff resilient	2,031	3,698	8,122	13,191		
	Soft	Rigid	2,843	5,199	11,371	13,191		
	Stiff	Rigid	3,330	6,303	13,321	13,191		

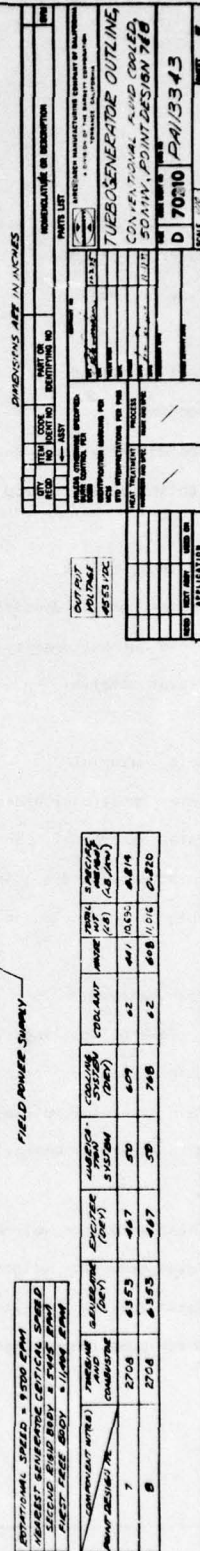


TABLE 37
CONVENTIONAL GENERATOR, FLUID COOLED
POINT DESIGNS 7 AND 8

Power level, MW	<u>50</u>	Cooling system weight	
Type of load	<u>Rectified</u>	(including fluids), lb	<u>1148</u>
		Total weight of generator	
Cooling method	<u>Fluid</u>	and cooling system, lb	<u>7968</u>
Coolant	<u>DC-200</u>	Specific weight, lb/kW	<u>0.159</u>
Coolant flow rate, gpm	<u>378.6</u>		
Coolant pressure drop, psi	<u>120</u>	Duty cycle:	<u>Continuous operation</u>
		Number of pulses	<u>N/A</u>
Voltage, L-N, V	<u>2280</u>	ON time per pulse, sec	<u>N/A</u>
Stator current density, A/sq in.	<u>31,579</u>	OFF time per pulse, sec	<u>N/A</u>
Field current density, A/sq in.	<u>31,488</u>	Initial copper temp, F	<u>230</u>
Stator material	<u>2V Permendur 0.010</u>	Final copper temp, F	<u>400</u>
Rotor material	<u>HP 9-4-20</u>	Number of phases	<u>3</u>
Rotor rotational speed, rpm	<u>9500</u>	Power factor	<u>0.876 lagging</u>
Rotor peripheral speed, ft/sec	<u>555</u>	Number of poles	<u>6</u>
Rotor outside dia., in.	<u>12.99</u>	Frequency, Hz	<u>475</u>
Rotor magnetic length, in.	<u>110.22</u>		
		Rotor length/dia.	<u>8.48</u>
Main generator dia.		Exciter dia, in.	<u>12.22</u>
(excluding flanges), in.	<u>18.66</u>	Exciter length, in.	<u>24.75</u>
Main generator length, in.	<u>125.25</u>	Exciter volume, cu in.	<u>2899</u>
Main generator volume, cu in.	<u>34,253</u>	Exciter weight, lb	<u>467</u>
Main generator weight, lb	<u>6353</u>		
		Field power, kW	<u>937</u>
Total generator volume, cu in.	<u>37,152</u>	Total losses, kW	<u>3262</u>
Total generator weight, lb	<u>6820</u>	Overall efficiency	<u>0.9381</u>
Rotor inertia, in.-lb-sec ²	<u>206.3</u>		
Motor-pump input power, kW	<u>48.2</u>	Point design 7	<u>1498</u>
			<u>8318</u>
			<u>0.166</u>

Assembly specific weight = 0.159 lb/kw

Point
Design
8

TABLE 38
 CONVENTIONAL GENERATOR, FLUID COOLED
 PRELIMINARY CRITICAL SPEED EVALUATIONS OF POINT DESIGNS 7 AND 8

Point Design	Bearing Stiffness	Bearing Mount	Generator Rotor Critical Speeds, RPM				Operating Speed,	Selected Bearing and Mount Combination
			First Rigid Body and First Flexural Modes	Second Rigid Body Mode	Second Flexural Mode	First Free Body Mode		
7 and 8	Medium	Soft resilient	1,430	2,518	5,720	11,404	9,500	Soft bearing in a rigid mount
	Medium	Stiff resilient	2,280	4,030	9,121	11,404		
	Soft	Rigid	3,150	5,445	12,599	11,404		
	Stiff	Rigid	3,691	6,501	14,765	11,404		

Shaft power for direct drive generator is provided by two stage axial-flow, pressure-compounded turbine rotating at 9500 rpm. Pertinent design details are as follows:

Propellant	Combustion products of neat hydrazine
Nozzle inlet	7110 R (1172.2 K)/850 psia (5.86 MPa)
Overall pressure ratio	42.5
Rotational speed	9500 rpm
Number of stages	2
Shaft power	72000 hp
Turbine flow rate	81.66 lb/sec (37.12 kg/sec)
Overall efficiency	76.19 percent

First Stage

Inlet temperature	2110 R (1172.2 K)
Flow rate	81.66 lb/sec (37.12 kg/sec)
Blade height	1.19 in. (0.03 m)
Pitch velocity	1650 ft/sec (502.9 m/sec)

Second Stage

Inlet temperature	1618 R (898.9 K)
Flow rate	80.52 lb/sec (36.6 kg/sec)
Blade height	4.80 in. (0.122 m)
Pitch velocity	1500 ft/sec (457.2 m/sec)

Superconducting Generator

Drawing PA113350 presents the package outline and weight breakdown of a superconducting turbogenerator application satisfying the requirements of point designs 1 and 2. Elements in the drawing are for a power system exclusive of the required propellant assembly, controls, and structural support. Generator design details for both operating conditions are shown in Table 39.

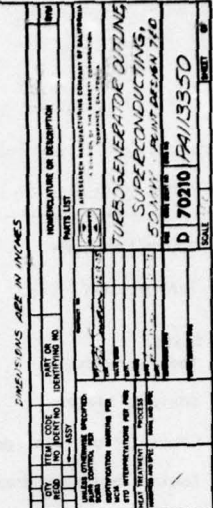
[illegible]

TABLE 39
SUPERCONDUCTING GENERATOR, POINT DESIGNS 7 AND 8

Power level, MW	<u>50</u>	Cooling system weight		
Type of load	<u>Rectified</u>	(including fluids), lb	<u>1123</u>	
Stator		Total weight of generator		Point Design 7
Cooling method	<u>Fluid cooled</u>	and cooling system, lb	<u>3836</u>	
Coolant, stator	<u>MIL-L-23699</u>	Specific weight, lb/kW	<u>0.077</u>	
Coolant flow rate, gpm	<u>196.8</u>			
Coolant pressure drop, psi	<u>20</u>	Duty cycle:	<u>Continuous Duty</u>	
		Number of pulses	<u>N/A</u>	
Voltage, L-N, V	<u>2000</u>	ON time per pulse, sec	<u>N/A</u>	
Stator current density, A/sq in.	<u>18,863</u>	OFF time per pulse, sec	<u>N/A</u>	
Field current density, A/sq in.	<u>373,600</u>	Initial copper temp, F	<u>N/A</u>	
Stator material	<u>2V Permendur</u>	Final copper temp, F	<u>N/A</u>	
Rotor material	<u>Super conductor</u>	Number of phases	<u>3</u>	
Rotor rotational speed, rpm	<u>8000</u>	Power factor	<u>0.88 lagging</u>	
Rotor peripheral speed, ft/sec	<u>500</u>	Number of poles	<u>6</u>	
Rotor outside dia., in.	<u>14.33</u>	Frequency, Hz	<u>400</u>	
Rotor magnetic length, in.	<u>43.68</u>			
		Rotor length/dia.	<u>3.05</u>	
Main generator dia.				
(excluding flanges), in.	<u>26.34</u>			
Main generator length, in.	<u>49.68</u>			
Total generator volume, cu in.	<u>27,070</u>	Total losses, kW	<u>909.9</u>	
Total generator weight, lb	<u>2713</u>	Overall efficiency	<u>0.9821</u>	
Rotor inertia, in.-lb-sec ²	<u>41.40</u>	Cooling system weight		
Motor-pump input power, kW	<u>8.3</u>	(including fluids), lb	<u>1375</u>	Point Design 8
		Total weight of generator	<u>4088</u>	
		and cooling system, lb		
		Specific weight, lb/kW	<u>0.082</u>	

Assembly specific weight, point design 7 = 0.077 lb/kW
 Assembly specific weight, point design 8 = 0.082 lb/kW

Helium airborne supply subsystem details are as follows:

Power	50 MW
Helium flow rate	23.3 liter/hr
Heat leak	7.8 Btu/hr
Tank assembly	
Dry weight	152.2 lb
Wet weight	248.3 lb
Line, mounting, etc.	10.0 lb
Total system weight	258.3 lb (117.4 Kg)
Outer shell diameter	42.89 in. (1.09 m)
Girth ring diameter	46.4 in. (1.18 m)

FAST STARTUP OPERATION

One of the major operational requirements is multiple-cycle fast starting capability. At present, fast startup is restricted to the use of conventional generator, whether of thermal-lag or fluid-cooled design concept. In the fast startup evaluation conducted, gas generator characteristics as shown in Figure 16, were used for all in addition to remaining associated propellant lead system time constants.

The resultant startup times for the various conventional generator design points of interest shown in Figure 17. For the conventional generator, whether of thermal-lag or fluid-cooled design, startup times of 1.0 to 1.8 sec are possible, depending only upon the selection of excess nozzle inlet pressure during the starting phase. Furthermore, for a stated output, i.e., 25 MW, the use of fluid-cooled, in lieu of thermal-lag design approach, substantially reduces startup times or excess drive energy required.

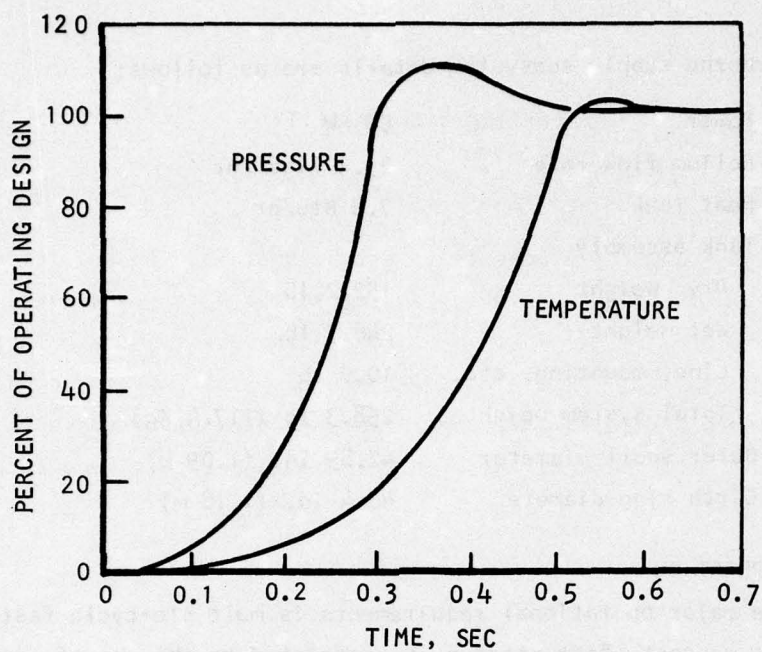
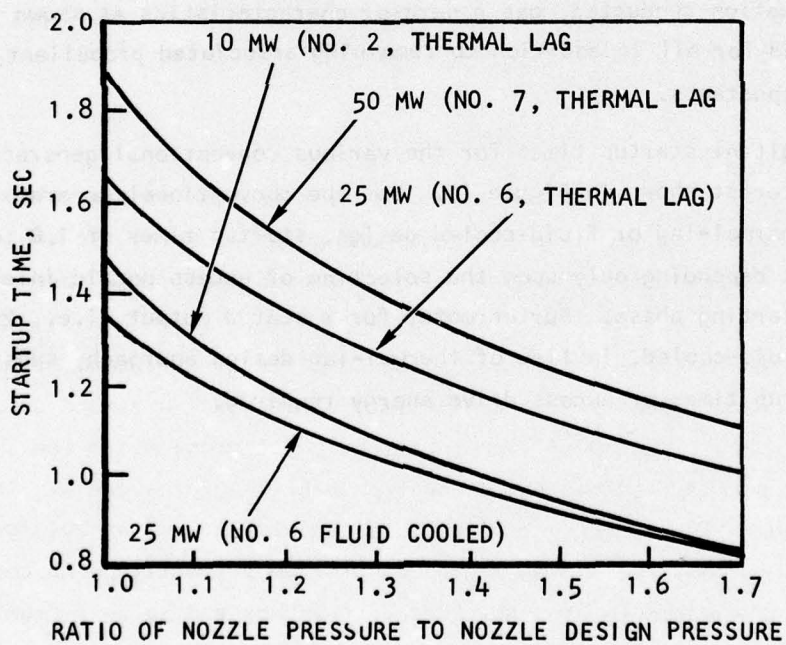


Figure 16. Pilot-Thermal Gas Generator Characteristics



S-3186

Figure 17. Conventional Generator Application Turbogenerator Startup Characteristics

SECTION 4

OPERATIONAL SUITABILITY

INTRODUCTION

Among the many considerations that must be appraised in the future development of a high-power generating system suitable for in-service airborne use is the suitability of the unit in its operating environment. This section discusses this subject as it relates to the three turbogenerator concepts studied during this program; i.e., the turbogenerators using conventional thermal-lag generators, conventional fluid-cooled generators, and superconducting generators.

The following topics are discussed.

Safety	Startup time
Sequencing and controls	Turnaround time
Reliability and availability	Performance degradation
Restartability	Maintenance
Power source protection	Logistical support
IR signature	

SUMMARY

The conclusions reached with respect to all aspects of operational readiness, flexibility, development risk, and general overall suitability of the high-power generator system for the intended application are as follows:

- (a) The thermal-lag system poses the fewest real or latent problems connected with service deployment, operational use, and ground support. It also will present the fewest problems to the systems integrator, and has the highest probability for success. An especially significant feature is its similarity, except for power rating and size, to an analogous program presently being conducted by AiResearch for the Air Force. Feedback and spinoff from this other program are quite relevant, and the two programs complement each other.

- (b) The fluid-cooled conventional generator is not quite as reliable as the thermal-lag generator because of additional components required and fluid connections, but it is deemed to be nearly as suitable for service deployment. The requirement for resupplying a few hundred pounds of water following each mission increases the resupply ground crew workload only minimally, and there is no anticipated complexity of control in flight or ground checkout. The problem of reliable fluid connections can be resolved because AiResearch has previously employed such a concept in an experimental liquid-cooled electric propulsion system. The probability for success for this approach is considered to be quite high, but not as high as for the thermal-lag approach.
- (c) From an operational suitability point of view, the superconducting approach for the present application is deemed to be highly questionable. This design concept is experimental in nature, development risk is considered high, there are unknowns that are difficult to evaluate, and it poses some unique problems in support at the operational level (replenishment and storage of cryogenics, and the need for prolonged chill-down). It is not a flexible approach, and, in addition, is considered to be the least reliable. The unit is restricted to idling operation with subsequent power engagement cycles, thus encompassing increase in operational complexity and the need to satisfactorily demonstrate such a capability.
- (d) The selection of low-voltage generator designs with transformers employed to attain the desired high-voltage supply provides increased reliability and flexibility in the present application.
- (e) Protection of the alternators and of the load is straightforward and well within the state of the art, and electrical shock hazards lend themselves to ready analysis and suitable safeguards.
- (f) As long as the recommendations, procedures, safeguards, and hazard controls of the Air Force report on hydrazine safety (Ref. 1)*

* Ref. 1: Hydrazine Safety Report, Air Force Report AFWL-TR-73-50, Air Force Weapons Laboratory (LRL) Air Force System Command, Kirtland Air Force Base, New Mexico, July 1973.

are observed, carrying hydrazine in large quantities onboard a military aircraft is feasible and safe. Appendix II to the Air Force report covers the subject of safe jettisoning of hydrazine from an aircraft in flight. The report, by using dispersion estimates, concludes that as much as 2300 lb of hydrazine can safely be dumped in flight under appropriate conditions.

- (g) Ground and inflight safety dictates that an automatic sequencing and control subsystem be incorporated in the high-power system. The sequencing and control subsystem will be energized prior to takeoff and will be used to monitor all salient operational parameters continuously to flight termination and display critical parameters continuously on a supervisory control console. Such equipment is mandatory for operational safety and suitability of the proposed airborne equipment, and also is included in a current USAF-AiResearch contract for a much smaller but analogous prototype system. The subsystem permits safe starts, safe aborts, and safe electrical isolation of faults. It monitors pressures, temperatures, speeds, voltages, currents, vibration levels, and imbalance, and can sense and act upon developing faults before they can damage equipment or create a hazardous condition to the aircraft. This electronic subsystem incorporates a programmable digital computer and can be readily modified for a new system with different valued parameters. The current input is 30 separate parameters.

SAFETY

Safety is the most important parameter when considering the operational suitability of the high-power system. The real or latent hazards that have been considered in terms of safety are discussed in the following paragraphs.

Toxicity

Hydrazine fuel is toxic and constitutes a latent hazard for uninitiated personnel and the environment of both the aircraft and operating base. Fuel leakage and evaporation, fuel handling and spillage, exposure to fumes, and undecomposed fuel in the turbine exhaust must all be considered in the safe design and operating procedures of the high-power system.

All hydrazine fuel lines, materials, and construction must be of Air Force recognized suitability. Ground spills and leakage must be directed toward sumps or accumulators provided specifically for this purpose. All hydrazine tanks, lines, and related hardware must be color coded, and quick disconnects, if any, must be capable of being satisfied. Ground personnel must comply with existing hydrazine safety handling manual procedures. With reasonable precautions, trained personnel, and adequate procedures, the proper handling of hydrazine should present no serious hazards. Only trained and certificated personnel should be permitted access to this subsystem. Fuel system pressure relief and bypass is mandatory. All pressure relief devices must be made redundant so that no overpressure is possible. Undecomposed hydrazine in the exhaust system must be assumed to be present at all times, and purging operation is indicated. Any scheme of emissions control probably would involve some kind of afterburner.

Inflight Fire

The entire hydrazine installation must incorporate emergency jettisoning capability of hydrazine from the aircraft commander's position. Automatic hydrazine fuel system shutoff must be backed up by manual emergency shutoff. According to Ref. 1, Hydrazine may be safely dumped from aircraft, but see Appendix II of Ref. 1.

Explosion

Decomposition chambers, combustors, and afterburners must either vent directly to air or incorporate large-area burst discs for explosion proofing. Stress analysis in design is needed to ensure that burst discs open without overstressing the main components being protected. The location of burst discs is dictated by the proximity of aircraft structure. Where analysis indicates inadequacy of burst disc areas to pressure-relieve quickly, analysis must provide identification of the probable direction of explosion and levels of energy anticipated.

Machinery Rupture

The turbogenerator must have redundant speed controls. The backup control, often called the speed topping control, must be entirely independent

and have no common mode of failure with the primary speed control. It should be set slightly higher than the top calibration of the primary mode control. The speed topping system, to ensure its independence, must not share any common electrical power source, control, or computer loop employed by the primary control, nor can it be allowed to use the same means of quick shut-down, but must trigger an entirely different loop and valve provided for this sole purpose. In addition, high-speed turbomachinery intended for aircraft installation is usually required to incorporate a containment ring. This is desirable, but due to the associated weight penalty, may not prove attractive for this installation. Orientation to the aircraft and proximity to the aircraft main propulsion engines may dictate a containment ring. In any case, such a ring is ineffective in protecting the explosive system, and the main propulsion engines do not incorporate containment rings.

Electric Shock

Provisions are required to isolate causes of faults causing overcurrent devices to open when equipment is bonded to the aircraft structure. All electrical connectors are to be safe-tied. Lightning protection is required for airborne units. A complete electrical shock hazard analysis must be conducted on the complete installed system. Electrical interlocks are required for all access doors, and provision is required for shorting high-voltage capacitors with approved shorting rods.

Overpressurization

Prevention of overpressurization of all fluid lines and storage tanks requires foolproof automatic and redundant pressure relief provisions incorporated into the design; this includes not only the hydrazine gas generator, but coolant, oil, and water boiler lines and tanks. The calibration points and ranges should be made with due regard to the proof and burst levels to be specified in procurement documents. Fuel pressure relief should receive particular safety attention.

Overtemperature

Overtemperature of any critical point in the system requires sensing and input to the main sequencing and control computer, and backup quick

shutdown sensors and controls that are independent of the primary control loop. The difference in calibration point is important to preclude unnecessary shutdown.

Loss-of-Cooling Accidents

Loss-of-cooling accidents could result in serious damage to explosive machinery. Loss of cooling flow should be sensed directly and not be an analog such as overtemperature. Loss of cooling must be detectable during a very brief ground functional inspection and checkout, and before serious temperature soak-back damage can result.

AUTOMATIC SEQUENCING AND CONTROLS

The salient item of safety is the known, but unemphasized, need for a very complete, fully computerized automatic sequencing and control system, which also performs all monitoring functions required, including emergency quick shutdown. Such a device feeds certain salient information to the supervisory control console. It is important to recognize how crucial to success and safety such a scheme is. There are about 30 parameters or inputs required to operate any of the turbogenerators studied, including safe startup and shutdown. The design and development of such equipment must keep pace with that for the turbine and generator. The many functions that must be sequenced, synchronized, monitored, and controlled require split-second timing if a fast startup time is to be safely achieved. The feasibility of the whole concept stands or falls on the realization of the absolute necessity for such automatic equipment.

RELIABILITY AND AVAILABILITY

Design or inherent availability has been defined (by MIL-STD-778 and other sources) as up-time divided by the sum of up-time and down-time. The mean time between failures (MTBF) can be used as an approximation of up-time, while mean time to repair (MTTR) is a reasonable estimate of down-time. Thus, availability, A, is given by

$$A = \frac{MTBF}{MTBF + MTTR}$$

In the following discussion, repair means remove and replace with a servicable unit. Only with this maintenance concept can the availability be estimated at this time, and this concept yields the greatest values of availability. The results of the study of these parameters are summarized in Tables 40 and 41. The values in the tables are not predictions in any sense; they are deemed to be values the Air Force could require in technical specifications and are sufficiently reasonable for prospective offerers to accept as design goals and possibly as firm requirements. It is considered that these values are minimums for a practical system worthy of procurement and deployment. The mean times to repair (by removal and replacement), and availabilities and unavailabilities (U)* are included for comparison of competing candidate systems at the 25-MW rating. In theory, inherent availability is under some control of the system and component designers. This study indicates the necessity of furthering a module concept of assembly and disassembly with a clear need to make hardware interfaces as simple as possible.

The differences between reliability and availability of the three candidate high-power systems, as shown in Table 41, are related to the additional hardware associated with the fluid cooling and cryogenic helium subsystems as well as basic differences in generator construction. The additional hardware is deemed significant, as it embraces such additional items as storage tanks, pumps, valves, fluid lines, and fluid connections. This is the reason the thermal-lag system of Table 40 has a higher value of MTBF assigned.

The units employed for MTBF and failure rate were dictated by both common Air Force practice and the fact that the control system will be energized for all of the flight. This is made necessary by the need to monitor various parameters continuously in order to be sure of such things as starting capability. It is considered imperative that the status of the system at all times be a known quantity, readily observed from the supervisory control console.

RESTARTABILITY

The state of the high-pressure (approx. 1000 psi) storage tank used for starting will be monitored continuously, and its state displayed on the

*Unavailability is defined as 1-A.

TABLE 40

RECOMMENDED RELIABILITY GOALS BY SUBSYSTEMS
[25-MW THERMAL-LAG SYSTEM USED AS BASELINE]

Subsystem Description	MTBF, Flight-Hours	Production Failure Rate Per Million Flight-Hours
Auto sequencing, monitoring, and control subsystem (including digital computer, supervisory console, power supply, interconnecting electrical cables, and equipment sensors). This subsystem is ON during the entire mission and is energized prior to takeoff.	1428	700
Power turbine (including speed reduction gearbox, turbine fuel pump, gas generator, emissions control, but not IR suppressor).	1500	667
Thermal-lag alternator (including exciter)	2500	400
Transformer/rectifier power conditioning subsystem	2500	400
Hydrazine storage, distribution, and starting subsystem	3000	333
System total	400	2500

Note: Conforms to duty cycle of point design 6 of SOW.

TABLE 41

COMPARISON OF RELIABILITY AND AVAILABILITY
OF CANDIDATE TURBOGENERATOR SYSTEMS

Turbogenerator System	MTTR*	Service MTBF, Flight-hours	A**	U	In-Service Failure Rate per 10 ⁶ Flight-hours
Baseline thermal-lag, 25-MW	12	400	0.971	0.029	2500
Conventional fluid- cooled, 25-MW	13	333	0.9625	0.0375	3000
Superconducting, 25-MW	20	250	0.926	0.074	4000

*Note: The average repair times shown are preliminary estimates only, and MTTR means restoration of the subsystem to serviceability; it does not mean actual repair of the removed item. In detail design, provision must be made for furthering the concepts of modularity, so that major items can be hoisted away and replaced as modules. Successful design would be the ability to repair the system by replacement of a module. It is generally believed that repair times of subsystems and system are lag-normally distributed. An in-depth maintenance study is required once a decision is reached to procure production systems. No such in-depth analysis has been attempted during this study.

**A = inherent or design availability.

the supervisory control console. Whenever the system has been started and has attained design speed, the starting loop is automatically recharged for the next command to start. There is enough capability designed into the tank to tolerate one abortive start, but design speed must be achieved on the second attempt to start. Once design speed is reached, the starting system is always returned to its initial condition of possessing two full starts, thus again having a tolerance for one abortive start.

POWER SOURCE PROTECTION

The primary provision for system safety, including protection, is the continuously monitored status of all salient electrical outputs. This automatic monitoring and quick shutdown is a function of the automatic sequencing and control subsystem. Classical methods of protection must be augmented by the simultaneous shutdown of the turbine whenever the load requires disconnecting due to a fault. Even faster control is required for the superconducting alternator should it quench. Thirty or so parameters are monitored continuously, including alternator and rectified voltage. For the superconducting alternator, voltage monitoring may provide the earliest warning of quenching. Because quenching can be a reversible transient phenomenon about which no action need be initiated, some appropriate voltage ratio and magnitude of rise needs to be established and sensed to trigger a quick disconnect of load and simultaneous cutoff of hydrazine fuel to the turbine. Pressure relief of generated helium gases must also be incorporated to avoid overpressure damage to the superconducting coil compartments. Some of this work currently is in progress at AiResearch in connection with a USN contract for superconducting ships propulsion.

IR SIGNATURE

The problem of IR signature (not addressed in the SOW) was not studied; however, it would appear that the turbine exhaust from the turbogenerator in the high-power system should possess an IR signature on the same order of magnitude as the aircrafts' main propulsion engines.

STARTUP TIME

The study has revealed the fact that startup time for the thermal-lag generator approach will be on the order of 1.5 sec, with the fluid-cooled system somewhat faster due to a lower moment of inertia of the rotating assemblies. The startup time of the superconducting scheme will be appreciably greater, and continuous idle is contemplated for that approach.

TURNAROUND TIME

Turnaround time for future systems is strongly influenced by the speed of refilling onboard aircraft tankage and the fill accessibility, thus the aircraft systems integrator will determine how fast a turnaround is achievable. The systems integrator must provide the required accessibility for refill. Since turnaround time is of critical importance to the Air Force, it is presumed that any future specification will stipulate the requirement. The components studied, other than the resupply of expendables, do not determine turnaround time in any sense. The thermal-lag system, requiring only refueling, may have a very slight edge over the fluid-cooled system, which also will require a few hundred pounds of water for the boiler if the system was used on the previous flight. The quantity of hydrazine is significant and the hydrazine tanker trucks currently in Air Force inventory may have pumping rates which are less than optimum. The same may apply to the cryogenic dewars already in Air Force inventory for IR open-cycle systems.

PERFORMANCE DEGRADATION WITH TIME

There should be relatively little degradation with time of any of the three generator approaches. Only the combustor and fluid filter will require replacement or cleaning during the less than 3-1/2 hr (100 missions x 120 sec/mission) of hot-gas operation. Prototype test results should be used to determine any schedule of replacement. There is little applicable experience to allow more conclusive findings at this time.

MAINTENANCE

Considering the size and weight of some of the components of the high-power systems studied, a modular approach to design, with machine interfaces kept as simple as possible, is desirable. Very little is known about optimum

procedures for such massive equipment, and the system integrator maintenance philosophy appears to be remove and replace, with the implication of spares for turbines and alternators, as well as smaller parts. The automatic sequencing and control subsystem consists of fairly standard electronic parts, but a form of module functional design is desirable to improve both troubleshooting and speed of removal and replacement. The same philosophy applies to the diodes or SCR's that would be used in the rectifier section.

LOGISTICAL SUPPORT

All three turbogenerator concepts have very nearly the same propellant requirements, regardless of the propellant finally selected. Any facility from which the high-power system operates will require propellant storage and refueling capability. Obviously, selection of a common propellant for the turbogenerator will minimize any special logistical support requirements necessary solely for operation of the high-power system. Because several thousand pounds of propellant are required for each mission, use of exotic fuels, which are not presently available at most of the operational facilities, will pose a significant logistical problem, at least initially. The main point to be recognized is that all turbogenerator concepts will have the same logistical support problem in relation to propellant requirements; however, the various concepts differ greatly in terms of logistical support requirements for their cooling subsystems.

The conventional thermal-lag generator has no logistical support requirements for its cooling needs except for bearing requirements. The conventional fluid-cooled generator requires several hundred pounds of water per mission for heat sink. Although the water used must be specially processed to minimize corrosion and scale buildup in the water boiler, this is already standard operating procedure for many systems presently onboard a variety of military aircraft. Therefore, the logistical support requirements specifically needed for cooling of the conventional generators are minimal.

The superconducting generator approach requires the logistical support requirements of the conventional fluid-cooled generator in addition to logistical support to supply liquid helium to the high-power system on a more-or-less continual basis. Because cool-down of the superconducting machine requires

extensive time, to maintain operational readiness requires that the liquid helium temperature be maintained in the superconducting coil. This means continuous resupply of liquid helium to maintain the ready state as well as sufficient onboard capacity of liquid helium to last the duration of the mission.

Because liquid helium is not a commonly used commodity in military systems, a completely new logistical system will be required to handle it. Although this is of minimal technical difficulty, it will be an appreciable expense that is not shared by the conventional generator approaches.

SECTION 5

DEVELOPMENT AND TECHNOLOGY PROGRAMS

INTRODUCTION

This section presents the recommended development and technology programs resulting from the present study. These programs are recommended as reasonable means to minimize size, weight, and technical risk during the development of high-power APU's for airborne applications.

SUMMARY

Six development programs have been identified as significant steps in the eventual development of a high-power system for airborne applications.

They are:

- (a) Prototype generator, conventional fluid cooled
- (b) Prototype generator, conventional thermal lag
- (c) Near-term demonstrator and test bed generator, conventional fluid cooled
- (d) Near-term demonstrator and test bed generator, conventional thermal lag
- (e) Prototype turbine/combustor
- (f) Prototype turbogenerator system

These six recommended development programs are summarized in Table 42 and 43. The first four programs, relating to the electric generator, provide a list of options available in charting the future course of the high-power generator program. All recommended development plans, whether at the component level or full high-power system level, are consistent with the availability of a flightweight system in the 1978-1979 time frame.

In addition, four technology programs have been identified that could provide significant improvements in the present state of the art within the time frame of the high-power system program. They are:

- (a) Advanced structural rotor design concepts
- (b) Novel generator winding techniques
- (c) Generator size and weight reduction by effective use of coolant fluids
- (d) Combustor hypergolic ignition with sustained monopropellant operation.

TABLE 42
SUMMARY OF RECOMMENDED CONVENTIONAL GENERATOR DEVELOPMENT PROGRAMS

Consideration	Prototype Generator Development Programs		Demonstrator and Test Bed Generator Programs	
	High-Power, Flightweight, Fluid-Cooled Design	High-Power, Flightweight, Thermal-Lag Design	Near-Term, High-Power, Fluid-Cooled, TLRV SC Modification	Near-Term, High-Power, Thermal-Lag, TLRV SC Modification
Objective	Reliable, moderate risk, moderate lead time, flightweight, high-power generator demonstration	Reliable, moderate risk, moderate lead time, flightweight, high-power generator demonstration	Reliable, low-risk, low-cost, short-lead-time, ground-based, high-power generator demonstrator and test bed	Reliable, low-risk, low-cost, short-lead-time, ground-based, high-power generator demonstrator and test bed
Capability	25-MW power level Continuous duty	25-MW power level 43-sec continuous operation 3 pulses, 21 sec on, 30 sec (or longer) off 16 pulses, 4 sec on, 4 sec (or longer) off	10 MW/20 MW with double existing length Continuous-duty operation	10 MW/20 MW with double existing length 15 sec continuous operation, no cooling 3 pulses, 21 sec on, 180 sec (or longer) off, air cooling
High-power program contribution	High-power size, weight, performance demonstration	High-power size, weight, performance demonstration	High-power size, weight, performance demonstration	High-power size, weight, performance demonstration
AF test program	High-power system demonstration Load investigations (design abnormal) Steady-state/transient electrical system performance PCE test and evaluation contributions Control requirements and fast startup	High-power system demonstration Load investigations (design abnormal) Steady-state/transient electrical system performance PCE test and evaluation contributions Control requirements and fast startup	High-power system demonstration Load investigations (design abnormal) Steady-state/transient electrical system performance PCE test and evaluation contributions Control requirements and fast startup	High-power system demonstration Load investigations (design abnormal) Steady-state/transient electrical system performance PCE test and evaluation contributions Control requirements and fast startup
Schedule	24 months to delivery of hardware	21 months to delivery of hardware	15 months to delivery of hardware	12 months to delivery of hardware

TABLE 43
SUMMARY OF RECOMMENDED TURBINE/COMBUSTOR AND TURBOGENERATOR
POWER SYSTEM DEVELOPMENT PROGRAMS

Consideration	High-Power, Flightweight Prototype Turbine/Combustor Development Program	Flightweight Prototype High-Power Turbogenerator System Development Program
Objective	Development of a new high-power turbine/combustor to overcome long-lead item and establish satisfactory size, weight, performance, and life capability	Development of a total high-power APU to integrate fuel storage, fuel delivery, turbine, combustor, generator, and controls
Capability	25-MW power level Long life Fast startup	25-MW power level Long life Fast startup
High-power program contribution	High-power turbocompressor size, weight, performance, and life demonstration	High-power APU size, weight, performance, and life demonstration
AF test program	High-power system demonstration Fast startup Steady-state/transient performance Control requirements	High-power APU demonstration Fast startup Steady-state/transient performance Control performance
Schedule	27 months to delivery of hardware	36 months to delivery of hardware

GENERATOR DEVELOPMENT PROGRAMS

In pursuing the further development of high-power generators, a relatively conservative low-risk approach can be used or a venturesome, higher risk approach can be taken with the incentive being significant technical gains. The low-risk approach emphasizes the following factors:

- Design based on demonstrated hardware
- Application of proven materials
- Established construction techniques
- Minimal extension of operating factors and margins

The factors stressed in following the higher risk approach are:

- Design based on new concepts
- Extended application of
 - Materials/construction techniques
 - Operating characteristics

In terms of the generator designs considered in the study conducted, the conventional thermal-lag generator is deemed to be the low-risk approach, while utilizing effective cooling methods in a conventional machine results in a somewhat higher risk. The high-voltage superconducting generator represents the greatest risk, with a low-voltage design reducing the risk substantially. Comparison of the various high-power generator approaches with estimates of the probability of success in the time frame considered is presented in Table 44. It is to be acknowledged, that upon satisfactory prototype demonstration, the production probability of success shown in Table 44 will increase.

Fluid-Cooled Conventional Generator Development

This development program is intended to result in a high-power, flight-weight, fluid-cooled conventional generator prototype unit capable of continuous-duty operation. The unit would be designed, built, and tested to the requirements of the high-power system application.

1. Objectives

The objectives of this development program are to design and build a flightweight, high-power generator demonstrator that is reliable, has moderate

TABLE 44
GENERATOR DEVELOPMENT PROGRAMS
ESTIMATED PROBABILITY OF SUCCESS

Baseline Concepts	Demo (1976)	Prototype		Production	Weight/ Cost	Remarks
		(1979)	(1980)			
Conventional generator Modification of existing hardware (synchronous condenser)	100%	-	-	-	High/low	Power, fast start, life, control demonstration.
Low-risk approach (thermal-lag)	-	90%	100%	90-100%	Moderate/ low	Excellent candidate.
High-risk approach (fluid-cooled)	-	75%	85%	60%	Moderate/ high	Improve performance, weight, with reason- able development.
Superconducting generator	-	60%	70%	40%	Low/high	Excellent weight, performance. High development risk. Logistic consider- ations.
Low-risk approach (low-voltage)	-	40%	50%	20%	Low/high	Lowest weight, highest develop- ment risk.

risk associated with its development, and can be available with a moderate lead time. This unit will be used for two purposes: (1) to demonstrate the adequacy of design and manufacture of the generator and (2) to provide a test bed for high-power system and component testing.

2. Capability

A power level of 25 MW is suggested for this unit to fully demonstrate the ability to design and build reliable high-power generators. Being in the medium range of power levels of interest in the high-power system application, the 25-MW level minimizes the risk involved in direct scale-up or scale-down of the design evolved.

The fluid-cooled generator possesses continuous-duty operational capability as long as heat sink for the coolant is available. The continuous-duty capability provides considerable flexibility in generator usage.

3. Design Demonstration

The prototype high-power generator developed in this recommended program would demonstrate:

- (a) Acceptable operating performance
- (b) Acceptable life capability under the operating conditions
- (c) Satisfactory electromechanical design and manufacture for the intended application
- (d) Material compatibility with the coolant fluid
- (e) Flightweight/volume demonstration

4. High-Power System Test Bed

The prototype high-power generator developed in this recommended program could be used as a test bed to conduct:

- (a) High-power system demonstration tests
- (b) Load investigations (design and abnormal)
- (c) Steady-state and transient electrical system performance
- (d) Power conditioning equipment test and evaluation
- (e) System control and fast startup investigations

5. Program Plan and Schedule

A two-phase program has been formulated to ensure satisfactory generator development. Phase I covers the generator detail design, the tooling design, the ordering of long lead item material, and the start of the manufacturing drawings. The second phase covers manufacture, assembly, and test of the unit.

The program plan and schedule is shown in Figure 18. The program yields a fully tested and characterized generator 24 months after program start.

Thermal-Lag Conventional Generator Development

The thermal-lag conventional generator development program is an alternative to the fluid-cooled conventional generator development program just described. This alternative program is a lower risk approach that can be accomplished in a shorter time at lower cost; however, this is accomplished at the expense of capability and flexibility. The thermal-lag generator is designed for a specific duty cycle, and significant cool-down times are required before the unit can be operated at the specified duty cycle. The suggested design capability of the generator is at the 25-MW power level with the following equivalent duty cycles: (1) 43-sec continuous operation, or (2) 3 pulses of 21 sec with 30 sec (or longer) between pulses, or (3) 16 pulses of 4 sec with 4 sec (or longer) between pulses.

The thermal-lag conventional generator development program is identical in concept to the fluid-cooled generator program just described. The objectives are the same in addition to the ability to use the unit as a design demonstration unit and/or high-power system test bed. The program plan and schedule are shown in Figure 19. A tested and fully characterized alternator will be available 21 months after program start.

Near-Term Fluid-Cooled Demonstrator and Test Bed

This program is intended to produce a *workhorse* high-power generator in the near future. It would be a ground-based unit having low development risk and short lead time. This will be accomplished by modifying the existing TLRV synchronous condenser, which is a fluid-cooled machine with coolant flowing through hollow conductors.

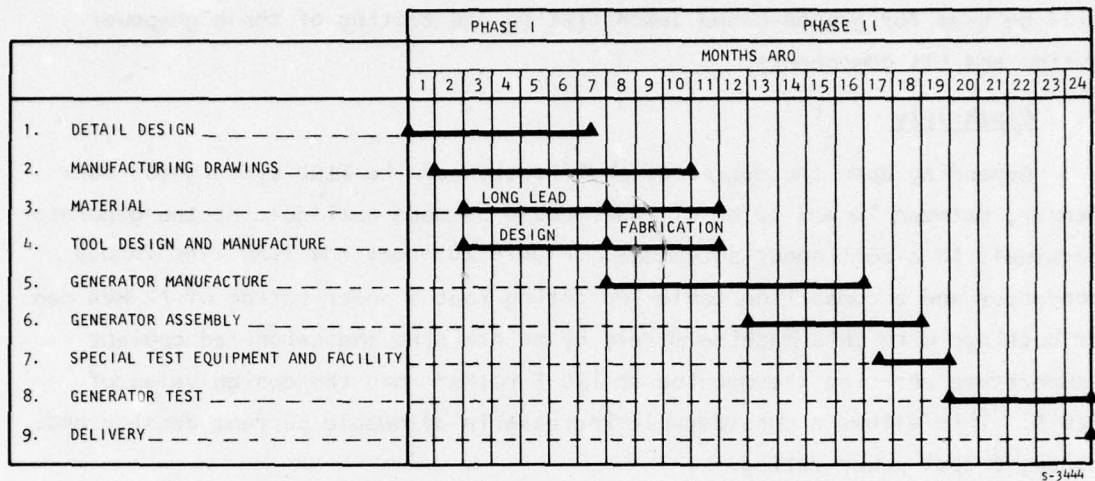


Figure 18. Fluid-Cooled Generator Program Plan and Schedule

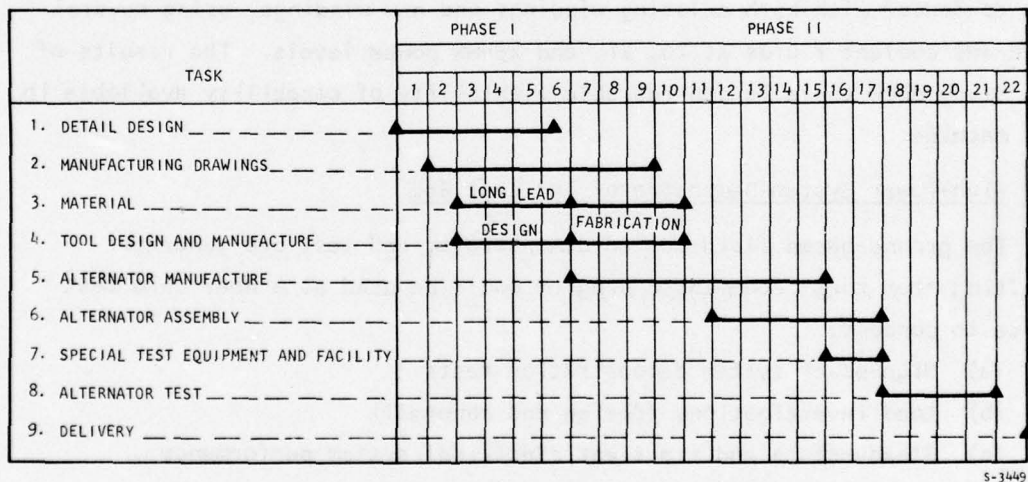


Figure 19. Thermal-Lag Generator Program Plan and Schedule

1. Objective

The objective of this program is to provide the Air Force with a reliable high-power test-bed generator as soon as possible with low risk. This unit will be used for ground-based demonstration and testing of the high-power system and its components.

2. Capability

Depending upon the degree of modification of the TLRV synchronous condenser, between 10 and 20 MW of power could be made available at the generator terminals in a continuous-duty mode. Figure 20 shows the TLRV synchronous condenser and a comparison table indicating that a power rating of 12 MVA can be obtained with this machine merely by maintaining the deionized coolant temperature entering the machine at 130 F rather than the design value of 220 F. This allows a considerable increase in allowable current density and, hence, output power rating.

Double the machine rating can be obtained by doubling the existing length. This would be accomplished by using two existing rotors rather than a new single rotor.

Appendix A presents the results of a study conducted on the TLRV synchronous condenser with both existing windings and new windings, using several different coolant fluids at 10, 21, and 25-MW power levels. The results of this study show there is considerable flexibility of capability available in this machine.

3. High-Power System Demonstrator and Test Bed

The ground-based fluid-cooled demonstrator and test bed generator resulting from this recommended program could be used as a near-term test device to conduct:

- (a) High-power system demonstration tests
- (b) Load investigations (design and abnormal)
- (c) Steady-state and transient electrical system performance
- (d) Power conditioning equipment test and evaluation
- (e) System controls studies



PARAMETERS	NOMINAL DESIGN	GENERATOR USING REDUCED TEMPERATURE
RATING, MVA	7	12
POWER FACTOR	0	1.0
VOLTAGE, VRMS	4130/7150	4130/7150
CURRENT DENSITY, AMP/IN. ²	18,700	32,000
SPEED, RPM	4950	4950
COOLANT	DEIONIZED WATER	DEIONIZED WATER
COOLANT TEMP, °F	220 INLET	130 INLET
AVERAGE WINDING TEMP, °F	360	360
DUTY	CONTINUOUS	CONTINUOUS
WEIGHT	4202	4202

F-22891

Figure 20. TLRV Synchronous Condenser

This generator could continue to be used, even after delivery of a flightweight unit designed specifically for the high-power system application, for numerous component and subsystem tests where size, weight, and rotating inertia are unimportant. Early evaluation of the electrical system in terms of control problem investigation, generator-load interactions, and fault conditions will help define the problems and solutions associated with high-power systems of this type and usage.

4. Program Plan and Schedule

A 15-month program to modify, fabricate, and test the existing TLRV synchronous condenser is shown in Figure 21.

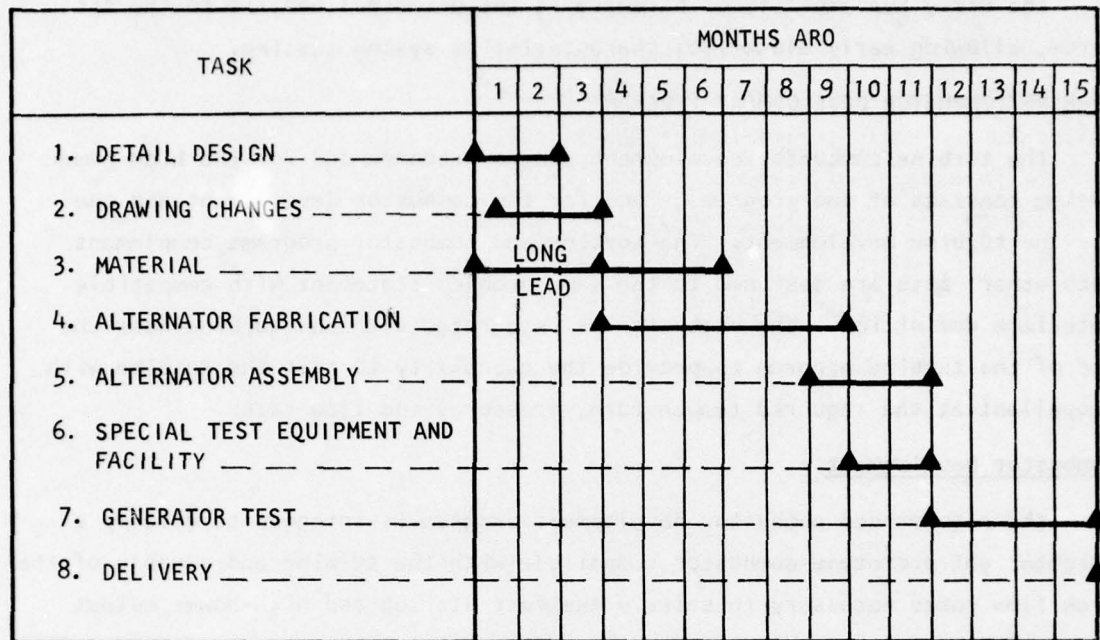
Near-Term Thermal-Lag Demonstrator and Test Bed

The near-term thermal-lag demonstrator and test bed program is an alternative to the fluid-cooled program just described. This alternative program is a lower risk approach that can be accomplished in a shorter time at lower cost; however, this is accomplished at the expense of capability and flexibility. The thermal-lag generator is capable of specific duty cycles only, and significant cooldown times are required before the unit can be used for the next operating cycle.

The study described in Appendix A shows the capability of the TLRV synchronous condenser with no cooling or air cooling, as well as its fluid-cooled capability. At the 10-MW power level, the existing TLRV synchronous condenser has the following operational capability: (1) 15-sec continuous operation without any cooling, or (2) 3 pulses of 21 sec with 180 sec (or longer) between pulses.

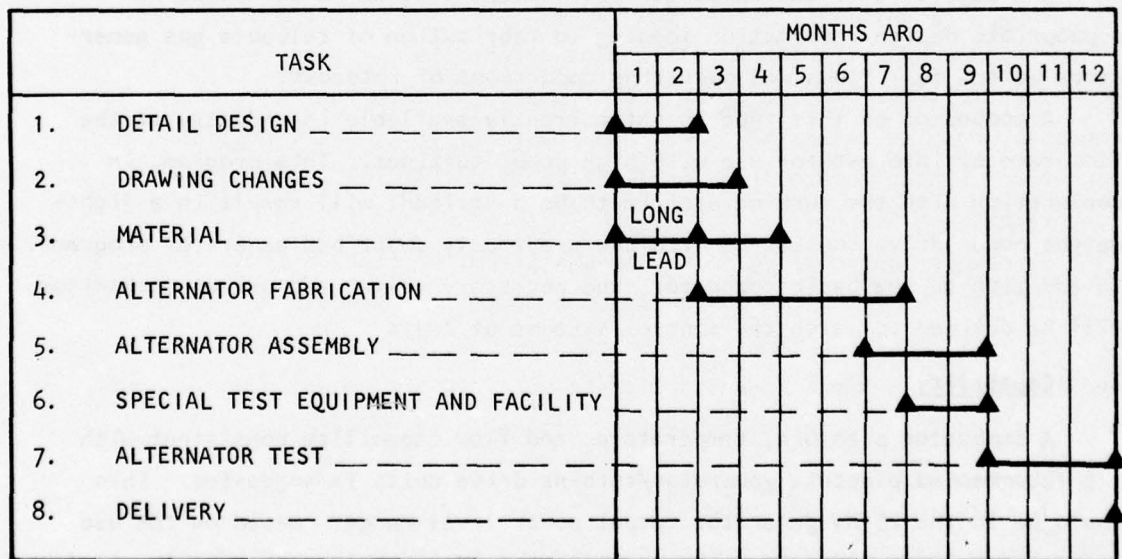
Except for the cooling method, this alternative program is identical in concept with the fluid-cooled generator program just described. It is based on modification of the same existing machine (the TLRV synchronous condenser) and it offers the Air Force an option to obtain a high-power demonstrator and test bed for electrical subsystem testing in the shortest possible time (12 months).

The program plan and schedule are shown in Figure 22. The allotted design and drawing change times are minimal, leading to rapid fabrication and assembly on existing tooling. A fully tested generator would be available one year after program start.



S-3442

Figure 21. Near-Term Demonstrator and Test Bed Program, Fluid-Cooled Generator



S-3443

Figure 22. Near-Term Demonstrator and Test Bed Program, Uncooled Generator

The early availability of hardware is the principal benefit to the Air Force, allowing early electrical characteristics system testing.

TURBINE/COMBUSTOR DEVELOPMENT PROGRAM

The turbine/combustor development program recommended for the high-power system consists of two programs: one for the combustor development and one for the turbine development. The turbine and combustor programs complement each other; both are designed to the same problem statement with compatible interface definition. The combustor is integrated with the turbine near the end of the turbine program to provide the capability to test the turbine with propellant at the required temperature, pressure, and flow rate.

Combustor Development

The recommended combustor development program is intended to develop a lightweight prototype combustor compatible with the turbine and capable of the high flow rates necessary to satisfy the fast startup and high-power output requirements of the total system. In addition, it must possess safe and reliable fast restart capability to accommodate the high-power system duty cycles.

1. Objective

The objective of the combustor development program is to determine appropriate design information leading to fabrication of reliable gas generators at the fuel flows and operating conditions of interest.

A combustor of this type is not currently available in industry at the flow rate of interest for use with high-power turbines. This program, in conjunction with the turbine program to be described, will result in a lightweight power drive consistent with the previously described generator programs. In addition to the basic combustor, the necessary valves and driver mechanisms will be defined to match the control systems of APU's

2. Capability

A combustor pressure, temperature, and flow capability consistent with the recommended electric generator/turbine drive units is suggested. This would be in the 25-MW generator output power level range. Based on the use of monopropellant hydrazine, the combustor would require a pressure level of

approximately 850 psia with an output flow of 41.5 lb/sec at 1650 F. To be compatible with fast startup capability for the high-power system, ignition delay must be minimized. With pulsed duty cycles, restart capability must be reliable as well as safe.

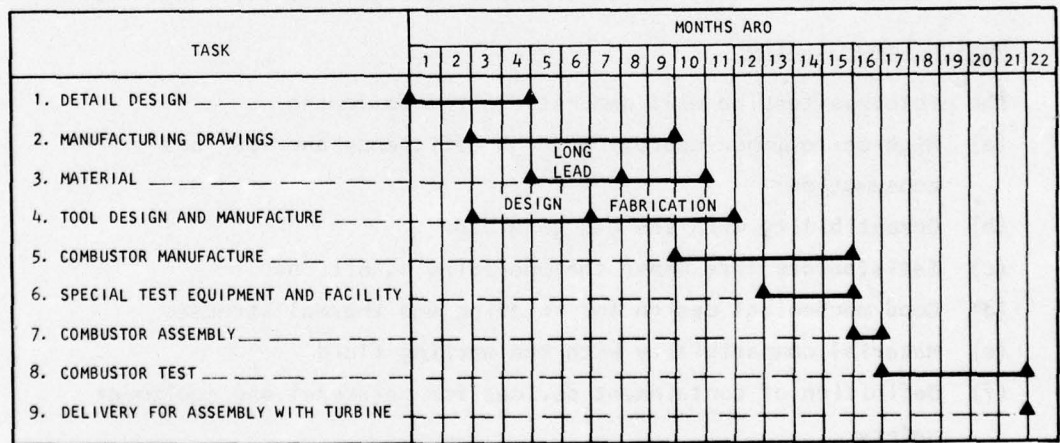
3. Design Demonstration

The prototype combustor design will demonstrate the following:

- (a) Applicability of design techniques for combustors at the required flow rates
- (b) Ignition reliability and repeatability
- (c) Determination of ignition times and times to full pressure and temperature (fast start and restart capability)
- (d) Demonstration of satisfactory combustor life
- (e) Flightweight/volume demonstration
- (f) Materials compatibility with the propellant and products of combustion

4. Program Plan and Schedule

Figure 23 shows the proposed program plan and schedule. A gas generator, tested and characterized, will be available for use in the turbine programs 21 months after program start.



S-3450

Figure 23. Combustor Development Program Plan and Schedule

Turbine Development

This recommended program is intended to develop a flightweight prototype turbine capable of the high-power output necessary to satisfy the generator drive requirements. In addition, it must have a satisfactory life and be capable of fast startup.

1. Objective

The objective of the turbine development program is to determine appropriate mechanical design information leading to solutions to the requirement for fast startup capability, efficient operation, and long life.

The benefit to the Air Force of funding this program is the availability of a high-power supersonic turbine consistent with airborne use, having long life, good performance, and capable of fast-starting high-power generators.

2. Capability

Turbine power output and fast startup capability consistent with other development programs previously described are recommended; i.e., generator output power level of approximately 25 MW. The turbine must be designed to be compatible with the gas generator, both in mechanical interfaces and gas characteristics. Based on the use of monopropellant hydrazine, gas inlet conditions to the turbine will be approximately 850 psia and 1650 F. Flow requirements will be approximately 41.5 lb/sec. In addition to high performance and fast startup capability, the turbine must be designed for long life.

3. Design Demonstration

The prototype turbine will demonstrate the following:

- (a) High-performance operation (high efficiency and low fuel consumption)
- (b) Compatibility with the gas generator
- (c) Satisfactory life under the operating conditions
- (d) Good mechanical design for rotating and thermal stresses
- (e) Material compatibility with the working fluid
- (f) Definition of containment devices for personnel and equipment safety

4. Program Plan and Schedule

Figure 24 shows the turbine development program plan and schedule. As can be seen, a thoroughly tested turbine will be available 27 months after program start.

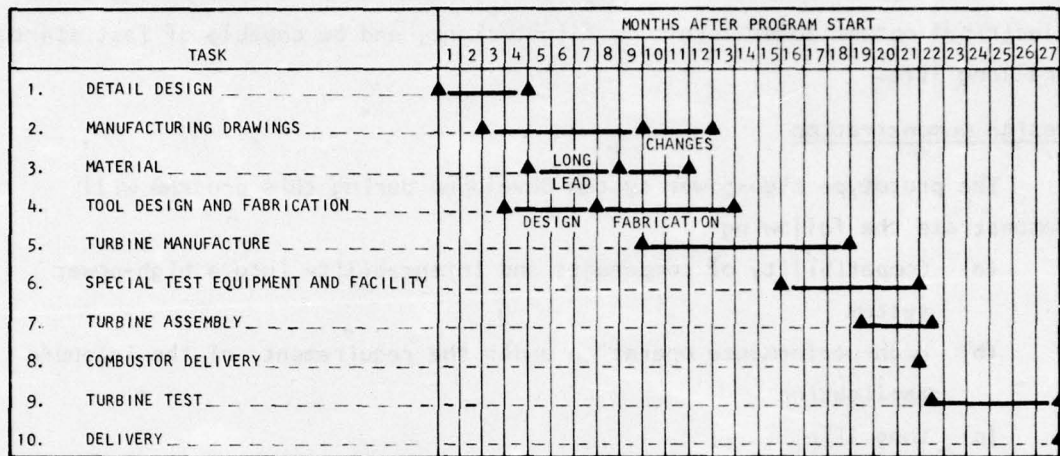


Figure 24. Turbine Development Program Plan and Schedule

HIGH-POWER SYSTEM DEVELOPMENT PROGRAM

The recommended high-power system development program is an extension of the previously described generator and turbine/combustor development programs. It includes the system controls and the fuel storage and delivery subsystem in addition to the generator, turbine, and combustor. The result will be a completely integrated, flightweight prototype high-power APU, of required life capability, and with performance characteristics based on today's state-of-the-art design techniques.

Objective

The intent of this recommended program is to develop a complete high-power APU integrating fuel storage, fuel delivery, turbine, combustor, generator, and controls. The prototype high-power system will be flightweight and capable of performing to the application requirements. It will provide:

- (a) Definition of key component characteristic requirements
- (b) Optimum integration of a multiplicity of components into a power system

- (c) Development of necessary controls and determination of control characteristics
- (d) Flyable test-bed high-power system

Capability

It is recommended that the high-power system be developed at the 25-MW electrical output power level, be flightweight, and be capable of fast startup and long life.

Design Demonstration

The prototype high-power system developed during this program will demonstrate the following:

- (a) Compatibility of components and integrability into a high-power system
- (b) High-performance operation under the requirements of the intended application
- (c) Long life
- (d) High reliability
- (e) Weight/volume characteristics
- (f) Satisfactory control characteristics

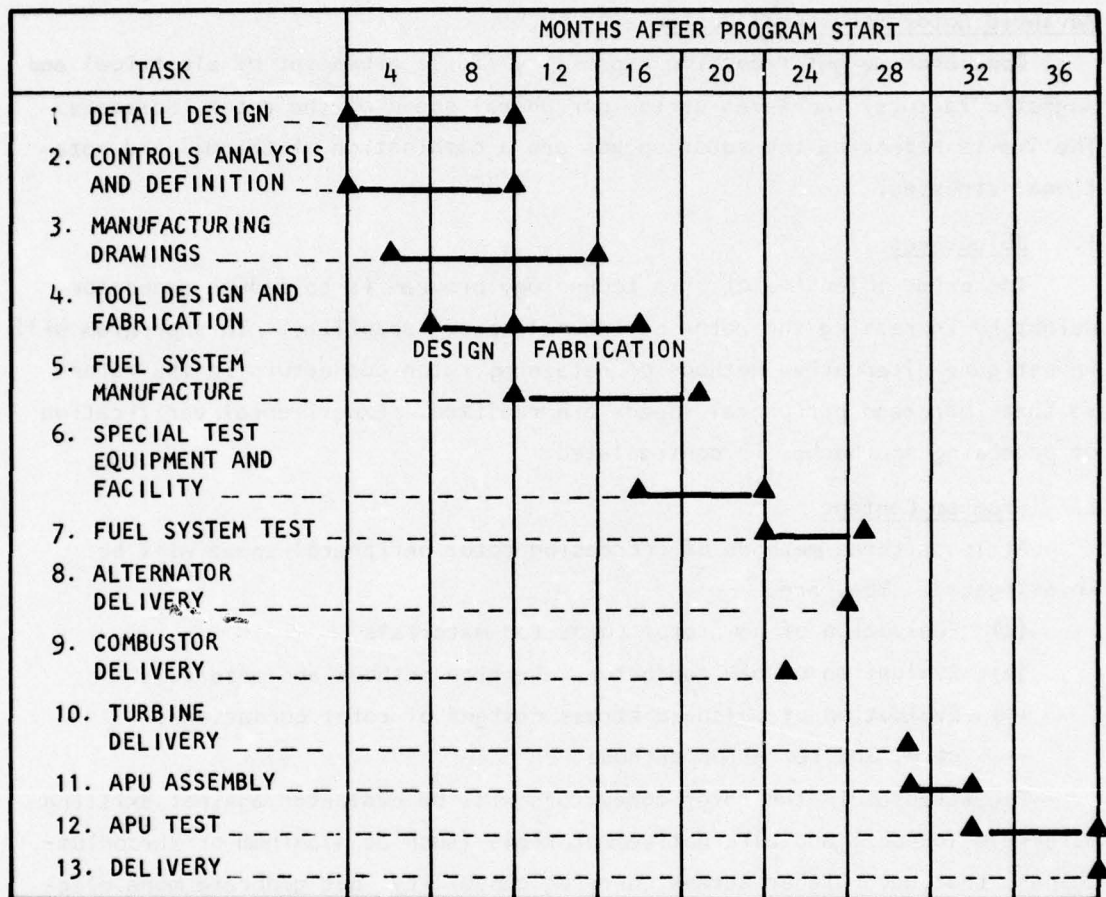
As a result of this program completion, the Air Force will have a high-power APU, designed to be compatible with flight use, capable of supplying electrical power over long periods with demonstrated life and reliability, and capable of fast starts. The system controls will have been demonstrated, and the APU will serve as a prototype for complete user systems requiring this type of power.

Program Plan Schedule

Figure 25 shows the recommended program plan and schedule. It is estimated that a prototype high-power APU can be delivered to the Air Force 36 months after program start.

GENERATOR TECHNOLOGY PLANS

Three areas of technology improvement potential exist in conventional generator design which, if properly explored, could lead to significant reductions in overall generator weight and volume and an increase in device efficiency. These three areas are:



S-3446

Figure 25. High-Power Airborne Power Unit Development Plan and Schedule

- (a) Advanced rotor structural design concepts
- (b) Novel generator winding techniques
- (c) Effective fluid-cooling concepts

The following technology plans describe each program's objectives, content, and schedule.

Advanced Rotor Structural Design

Generator weight reduction capability (for a given set of electrical and magnetic factors) increases as the peripheral speed of the rotor increases. The limits affecting the rotor speeds are a combination of thermal and rotational stresses.

1. Objectives

The prime objective of this technology program is to reduce generator weight by increasing the rotor peripheral speed capability. This program will investigate alternative methods of retaining rotor conductors in the rotors so that increased peripheral speeds are realized. Experimental verification of promising approaches is contemplated.

2. Program Content

At least three methods of increasing rotor peripheral speed will be investigated. They are:

- (a) Evaluation of new rotor conductor materials
- (b) Evaluation of new conductor retention methods and materials
- (c) Evaluation of balanced stress designs of rotor conductors, core, and retention methods

The stresses in the rotor conductors will be evaluated against existing materials (copper) and alternative materials (such as aluminum or zirconium-copper) that have higher stress carrying capability, but generate more electrical losses. Trade studies will be performed to identify the optimum material resulting in the highest peripheral speed. With respect to the end rings, materials such as filamentary-resin combinations will be evaluated against the more commonly used Inconel to determine the benefits of their use.

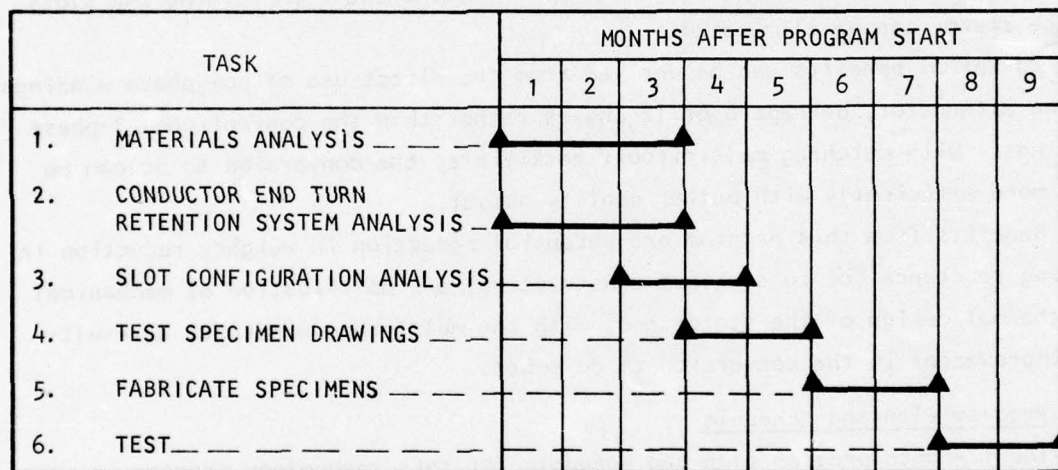
In parallel with the investigations of conductor and end-ring materials, a reassessment of the current rotor slot configurations will be performed to evaluate the stresses in the conductors, conductor retainers, and rotor core of new configurations and to determine potential benefits.

Subsequent to the preceding analyses, an experimental demonstration of optimum configurations will be run to verify the concepts.

The benefits from this program are potential weight reduction in generators, improved form factors of generators, i.e., lower length/diameter ratios, both of which factors will be applicable to all classes of generators.

3. Program Plan and Schedule

The proposed nine-month program schedule is shown in Figure 26.



S-3431

Figure 26. Rotor Technology Program Plan and Schedule

Novel Generator Winding Techniques

This recommended technology program will investigate improvements in generator design, weight, and performance attainable by novel winding techniques.

1. Objective

The objective of this program is to find special winding techniques that are suitable for the intended application and will result in improved generator performance. An experimental program will be conducted to verify promising concepts.

2. Program Content

At least two winding concepts will be investigated in detail: (1) using airgap windings in the stator to reduce stator iron requirements and (2) use of polyphase windings in the generator matched to multicircuit rectifier circuits for increased ac to dc conversion.

Because a large portion of the conventional generator weight is in the stator iron, airgap winding techniques that significantly reduce iron requirements are of interest. Current conventional generator designs have stator windings carried in slots in the stator iron and require elaborate insulation schemes to prevent wire-to-wire shorting and wire-to-ground shorting. The conceptual approach in the airgap winding scheme is to mount the stator conductors essentially in the airgap between the rotor and the back iron. In this way, the insulation requirements will be simplified, and the iron forming the slots in the stator can be eliminated.

Potential benefits can be derived from the direct use of polyphase windings in the alternator, perhaps 6 or 12 phases rather than the conventional 3-phase windings. With matching multicircuit rectifiers, the conversion to dc can be made more efficiently with better quality output.

Benefits from this program are potential reduction in weight, reduction in winding reactance due to slotless construction, a simplification of mechanical and thermal design of the stator and, with the multiphase windings, a resulting improvement in the conversion to dc power.

3. Program Plan and Schedule

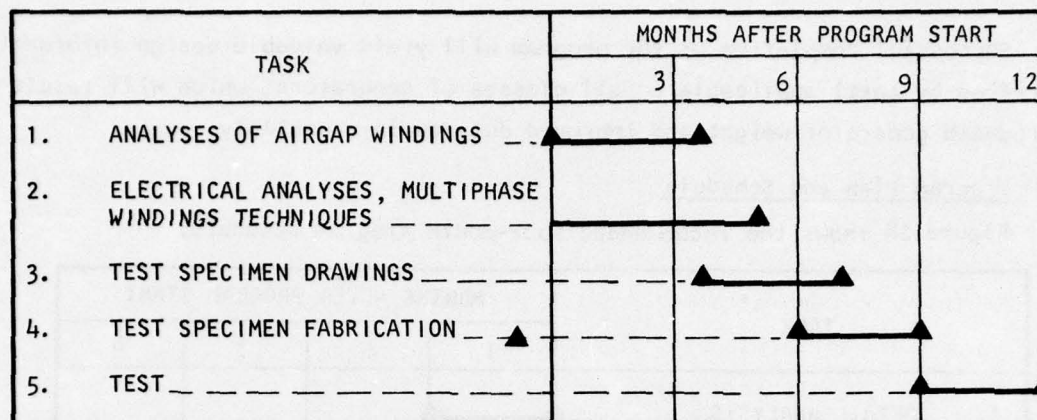
The 12-month program plan and schedule for this technology program is presented in Figure 27.

Effective Fluid Cooling

Generator weight depends to a significant extent on the allowable current densities in the rotor and stator conductors. The higher the allowable current density, the smaller the conductor cross section required for a given rating; hence, less copper is required as the allowable current density is increased. This results in lower machine weight.

1. Objective

The prime objective of this recommended program is to establish the most effective method of cooling conductors in electric generators so higher



S-3439

Figure 27. Winding Technique Technology Program Plan and Schedule

allowable current densities can be achieved to produce reductions in specific generator weight.

2. Program Content

The recommended program is an analytical study combined with a simplified test program of promising approaches identified in the study. A comprehensive study will be conducted on the required coolant operating characteristics necessary to achieve high current densities in the conductors. Among the parameters to be investigated will be the following:

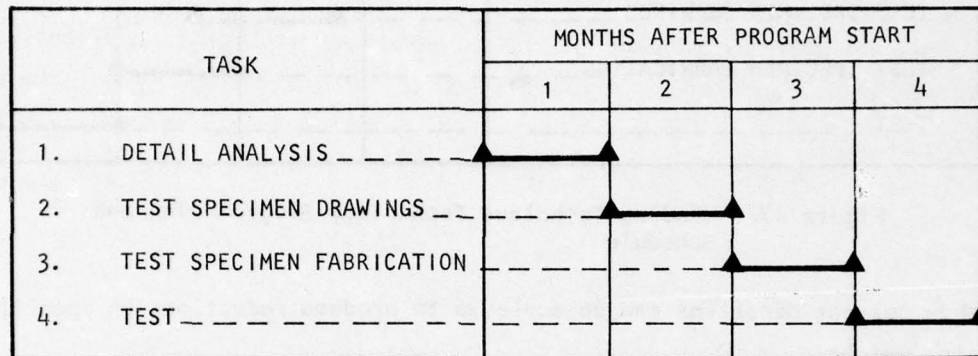
- (a) Type of coolant fluid
- (b) Flow area/conductor area
- (c) Flow cross-sectional geometry
- (d) Flow rate
- (e) Pressure drop
- (f) Temperature rise

The use of hollow conductors in which fluid flowing in the conductor removes heat at the source of generation (I^2R losses) is well established in the commercial power generator industry. Cooled conductors have been used in the electrical propulsion system for the Tracked Levitated Research Vehicle (TLRV) where weight of equipment was important. In very lightweight airborne alternators, data are required on the interrelationships of the preceding parameters to obtain optimum weight machines. These data will be estimated by analytical study and confirmed on single-coil test specimens mounted in a test rotor.

Successful completion of the program will yield valuable design information (verified by test) applicable to all classes of generators, which will result in reduced generator weight and improved duty-cycle capability.

3. Program Plan and Schedule

Figure 28 shows the recommended four-month program schedule.



S-3430

Figure 28. Effective Fluid Cooling Concept Program Plan and Schedule

COMBUSTOR TECHNOLOGY PROGRAM

Among the most important components in the high-power system that requires an advance in the state of present-day technology is the combustor. To take advantage of the operational simplicity and reduction in specific propellant consumption attainable with the use of monopropellant hydrazine, it is necessary to have a combustor that is capable of fast startup, can be reliably and safely restarted many times and has long life (preferably with a minimum of refurbishment). To be assured of reliable starts, design of such a unit with present-day technology results in the use of: (1) a very expensive catalyst (Shell 405), (2) a thermal glow coil that consumes large amounts of electrical power, and (3) combinations of the above.

The Shell 405 catalyst (approximately \$5000/lb) is fragile and requires replenishment due to lost mass resulting from shattering and breakage during operation. Thus, rather frequent maintenance and refurbishment are required.

Use of the thermal glow coil requires continuous use of electric power during the mission. Thus, the energy drain of such a device is considerable and should be avoided if possible. In addition, there is a substantial time

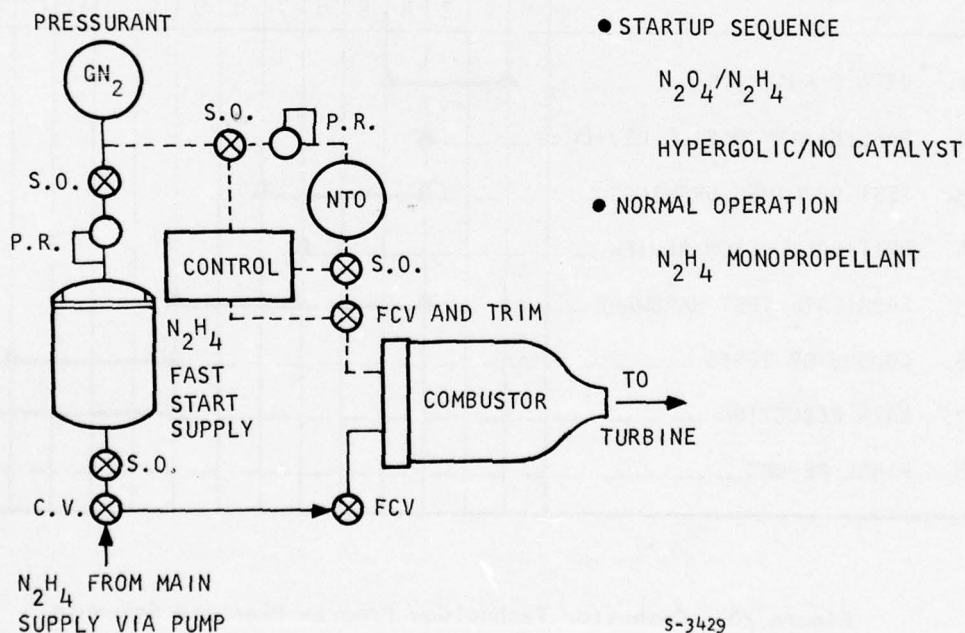
lag involved in bringing a cold chamber up to temperature. The combined use of a catalytic bed and heater is generally dictated in an attempt to minimize required catalyst and electric power, while achieving fast startup requirements.

Objectives

The technology program recommended is intended to produce an advance in the state of present-day technology in the design and operation of hydrazine combustors. An experimental program will be conducted to produce a prototype combustor that can be safely and reliably started and restarted without the use of catalyst or electric heaters. In addition, goals of this program will be to achieve fast startup capability, possess long life with minimal or no maintenance, and achieve significant reductions in weight, volume, and cost in comparison with present-day units of similar capability.

Program Content

The recommended combustor technology program consists of a combination analytical and experimental program based on initiation of the hydrazine decomposition process by hypergolic ignition such as that illustrated in Figure 29.

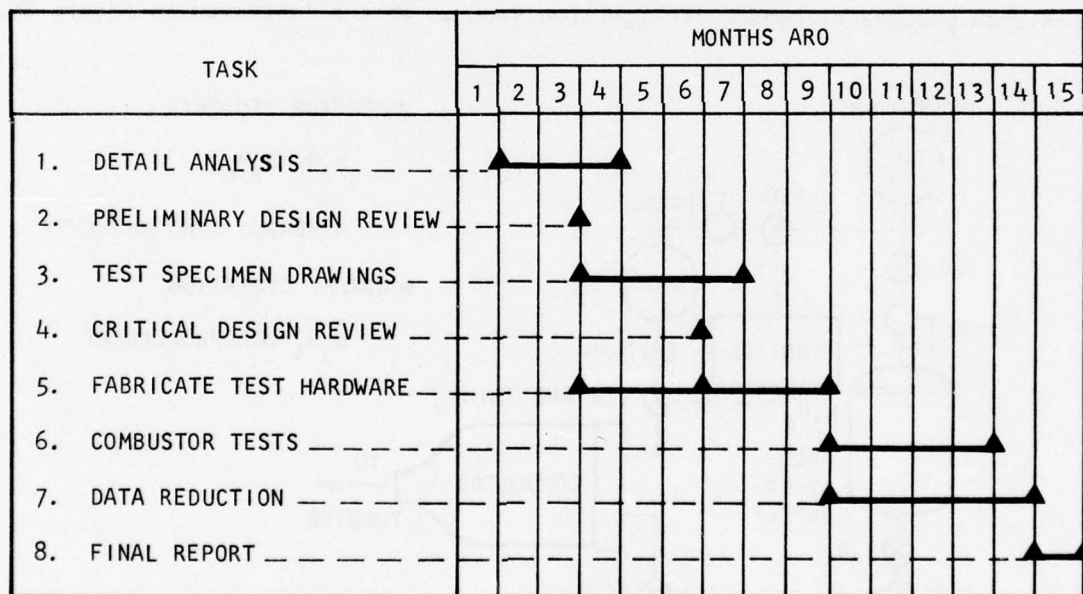


Numerous possibilities exist as to hypergolic agents that can be used with hydrazine, the particular combustor configuration, use of pilot startup chambers and mode of operation (hypergolic startup only vs continuous bipropellant operation).

All possibilities conceived will be investigated, with the most promising receiving very close analytical scrutiny. These will then be evaluated and a single most promising approach recommended for further investigation by experimentation. A prototype combustor will be built and tested to verify the analytical results. Determination of startup time, startup reliability and safety, life capability, maintenance requirements, weight, volume, and cost will be made.

Program Plan and Schedule

Figure 30 presents the recommended program plan and schedule. As can be seen, it is divided into analytical and experimental tasks and will require 15 months to complete.



S-3428

Figure 30. Combustor Technology Program Plan and Schedule

SECTION 6

CONVENTIONAL GENERATOR DESIGN CONSIDERATIONS AND TRADE STUDY

INTRODUCTION

This section describes the various design considerations involved in determining the optimum design of a high-power, lightweight conventional electric generator. It also presents the results of the parametric and sensitivity studies conducted to obtain optimum generator designs for both thermal-lag and fluid-cooled machines. For convenience, this section is subdivided as follows:

- Selection of machine type
- Configuration selection
- Computer program
- Parametric and sensitivity studies
- Thermal design and cooling system
- Mechanical and structural design
- Algorithms

SUMMARY

The trade studies conducted and machine design layout drawings prepared establish the following with respect to high-power conventional generators:

- (a) The wound-field synchronous alternator in a solid-core nonsalient-pole (round-rotor) configuration is the most suitable generator type.
- (b) The fluid-cooled generator configuration selected uses hollow conductors and a bore seal.
- (c) A round-rotor alternator design computer program incorporating a thermal subroutine to maximize allowable current densities and, hence, minimize weight was prepared and provided to the Air Force.
- (d) Optimum weight designs are obtained at voltages in the range of 2000 to 6000 Vdc. Weight penalties become excessive as the voltage increases above 10,000 Vdc.
- (e) There is an optimum rotational speed to obtain minimum weight at each power output and voltage level.
- (f) Considerable savings in weight can be obtained by cooling the conductors with a coolant fluid.
- (g) The thermal-lag generator weights are sensitive to duty cycle. The fluid-cooled designs are independent of duty cycle.

- (h) For generators feeding a rectified load, the power factor and commutation reactance are related. Minimum generator weight is obtained with a commutation reactance of 0.27, which gives a power factor of 0.88 lagging. This provides the reactance required to make a light-weight transformer (low voltage-to-high voltage) design that is compatible with the rectifier.
- (i) The fluid-cooled generator designs are sensitive to coolant pressure drop through the generator. This sensitivity increases with rotational speed.
- (j) The cooling system required for the fluid-cooled machines weighs much less than the weight difference between the thermal-lag and fluid-cooled generators; however, the coolant pumping power required is appreciable and should be supplied from an aircraft source.
- (k) The generator designs have high length-to-diameter ratios (roughly from 4 to 8). This requires the rotor to traverse one or two critical speeds during startup and shutdown.
- (l) Simple algorithms were developed for the generator, exciter, and cooling system involving only power level and duty cycle.

SELECTION OF MACHINE TYPE

In approaching the SOW requirements, AiResearch initially gave consideration to the wound-field synchronous (Figure 31), Lundell (Figure 32), and homopolar inductor (Figure 33) machines each in a number of configuration variants that included differences in rotor construction and/or rotor and stator magnetic circuit arrangements and cooling methods. The wound-field synchronous machine in a solid-core nonsalient-pole (round-rotor) configuration was selected as the type most suitable for the application based on the reasons given below.

In normal construction using rotating coils of high-conductivity copper and solid-core nonsalient-pole construction as in Figure 31, the wound-field synchronous machine with its useful range of peripheral velocity (i.e., up to 750 ft/sec) can be shown to be significantly superior in weight and performance to either the Lundell or homopolar inductor machines. In general, this advantage is due to the relative magnetic circuit arrangements; the wound-field synchronous machine has inherently lower magnetic leakage, reactances, and weight.

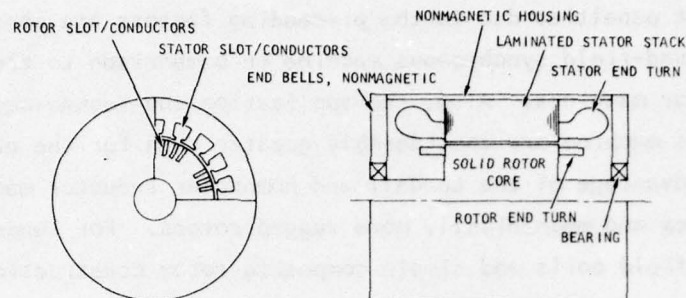


Figure 31. Wound-Field, Synchronous Generator, Solid Core, Distributed Nonsalient-Pole Field Coil, Round-Rotor

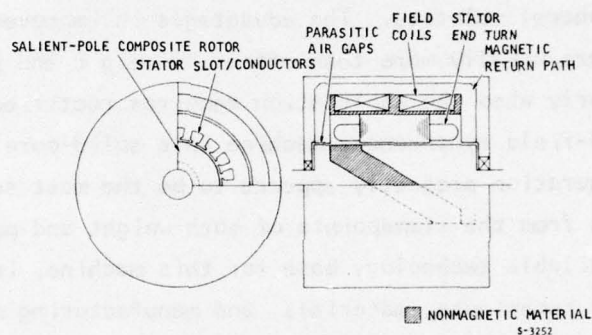


Figure 32. Lundell Generator, Salient Pole, Composite Rotor and Stationary Field Coil

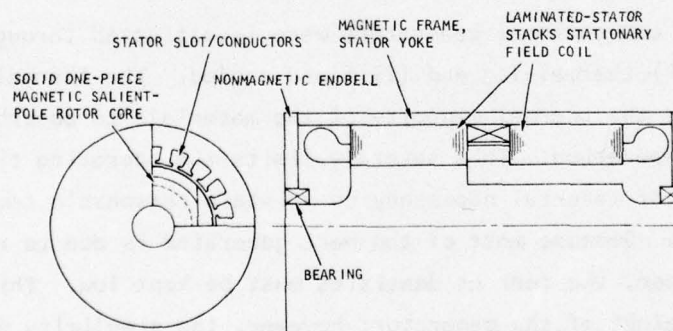


Figure 33. Homopolar Inductor, Generator, Solid-Core, Salient-Pole, Stationary Field Coil

In applications requiring a generator output rectified to dc, machine rating and weight penalties due to the preceeding factors are considerably lower for the wound-field synchronous machine in comparison to the Lundell and homopolar inductor machines. Also, the application and technology of the wound-field synchronous machine are considerably greater than for the other two types.

The major advantage of the Lundell and homopolar inductor machines is their less complex and mechanically more rugged rotors. For Lundell machines with stationary field coils and simple composite rotor construction consisting of solid magnetic and nonmagnetic material only, as shown in Figure 32, this normally allows operation at up to 1100 ft/sec peripheral velocity. In contrast, the homopolar inductor machine with a stationary field coil and a solid single-magnetic-material rotor, as shown in Figure 33, may be operated at up to 1600 ft/sec peripheral velocity. The advantages in improved peripheral velocity, however, are usually more than offset by weight and performance penalties, particularly when the application requires rectified output.

Thus, the wound-field synchronous machine in a solid-core nonsalient-pole (round-rotor) configuration presently appears to be the most suitable choice for this application from the standpoints of both weight and performance. Furthermore, the available technology base for this machine, including development history, design techniques, materials, and manufacturing methods, greatly favors its selection.

CONFIGURATION SELECTION

Two types of conventional generators were investigated throughout this study program: (1) thermal-lag and (2) fluid-cooled. The thermal-lag machine configuration uses the thermal capacity of the materials to absorb the heat generated during operation. This severely limits the operating time available before the weight of material necessary to maintain reasonable temperatures becomes excessive. Because most of the heat generated is due to resistive losses in the copper, the current densities must be kept low. This also tends to increase the weight of the generator; however, the simplicity of the thermal-lag generator compared to the fluid-cooled machines makes it an attractive candidate for the present application. Consequently, this configuration has been studied in parallel with the fluid-cooled configuration throughout the program.

Figure 34 illustrates the weight reduction potential available by using fluid-cooled designs, which allow the use of much higher current densities. As shown, there are two possible methods of producing fluid-cooled machines: (1) conductive cooling and (2) hollow cooled conductors. Each of the two methods is described in the following paragraphs. The hollow cooled conductor approach was chosen in order to obtain the maximum benefit in weight reduction and maximum flexibility in duty cycle/operating duration.

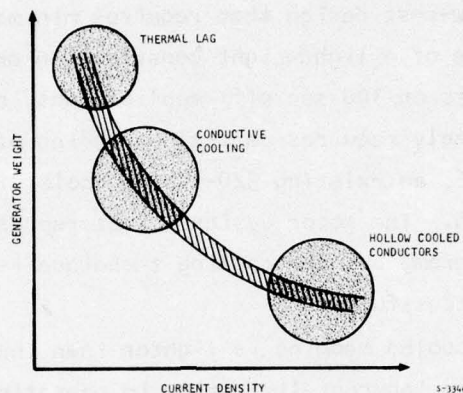


Figure 34. Influence of Cooling Method on Generator Weight

Rotor Configurations

Proper rotor design is the key to designing a compact alternator. Operation at the highest possible tip speed is desirable; but speed is limited by stress considerations for the structure and coil insulation, and by requirements for optimizing magnetic geometry for the specified power rating. Vibration (critical speed) and frequency constraints also usually affect rotor optimization. Frequency constraints are probably not critical for the present application in which the alternator output is rectified, because the power rectifier will probably be capable of operating efficiently at frequencies considerably higher than optimum for the generator.

The following paragraphs illustrate typical rotor design concepts investigated in this program and show machines that have been built using these concepts. Each approach is discussed briefly.

1. Conduction-Cooled Round Rotor

Figure 35 shows the simplest approach to fluid-cooled rotor construction, a conduction-cooled round-rotor configuration. Heat generated in the rotor is transferred through the rotor by conduction and to a coolant passing through an axial heat exchanger in the rotor yoke.

This approach requires no hoses or elastomer seals in the rotor; coolant selection is simple, and the coolant is at a relatively low pressure. It leads to a rugged, reliable, low-cost design that requires minimal development. It would, however, permit use of a lightweight construction only in short-duty-cycle (approximately 30 sec on/300 sec off) applications, because it has a low cooling rate. Also, assembly requires partial unwinding of each coil. The machine shown in Figure 36, an existing 520-kVa homopolar inductor alternator, uses this cooling approach. The rotor design is not representative of those to be considered on this program, but the cooling technique is similar and has thus been demonstrated successfully.

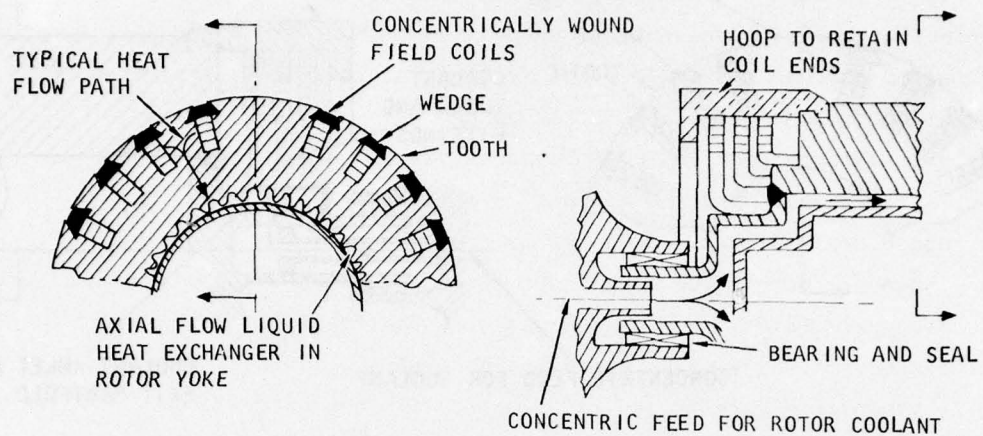
Although this fluid-cooled machine is lighter than the thermal-lag generator, it still has the same inherent limitation in operating duration; it does not have continuous-duty capability.

2. Hollow-Conductor-Cooled Round Rotor

Efficient conductor cooling is achieved by flowing coolant through holes in the individual conductors (Figures 37 and 38). This allows a very significant increase in current density and, consequently, reduced weight. In addition, effective cooling of the conductors in this manner makes the generator applicable to continuous operation. This results in duty cycle insensitivity.

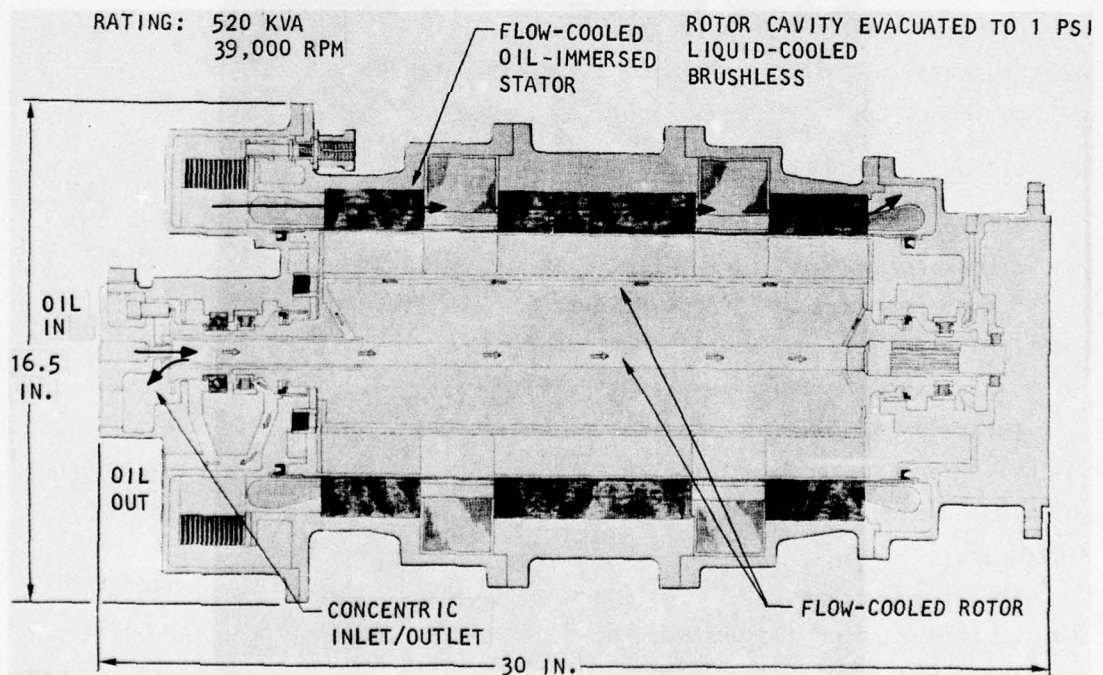
This type of construction with each conductor cooled individually is used on the 10-MVA Tracked Levitated Research Vehicle (TLRV) water-cooled alternator, which has a specific weight of 0.42 lb/kVA. The TLRV rotor is shown in Figure 38.

The disadvantages of the hollow-conductor-cooled round rotor are: (1) complex construction (because of the many joints, coolant tubes, and fittings used); (2) high coolant pressure (required to eliminate hot spots and generated by centrifugal force); (3) high coolant pressure drop (because coolant flows through the total length of each conductor); (4) low conductor space factor



5-75859

Figure 35. Conduction-Cooled Round Rotor



F-22844

Figure 36. Alternator with Flow-Cooled Rotor

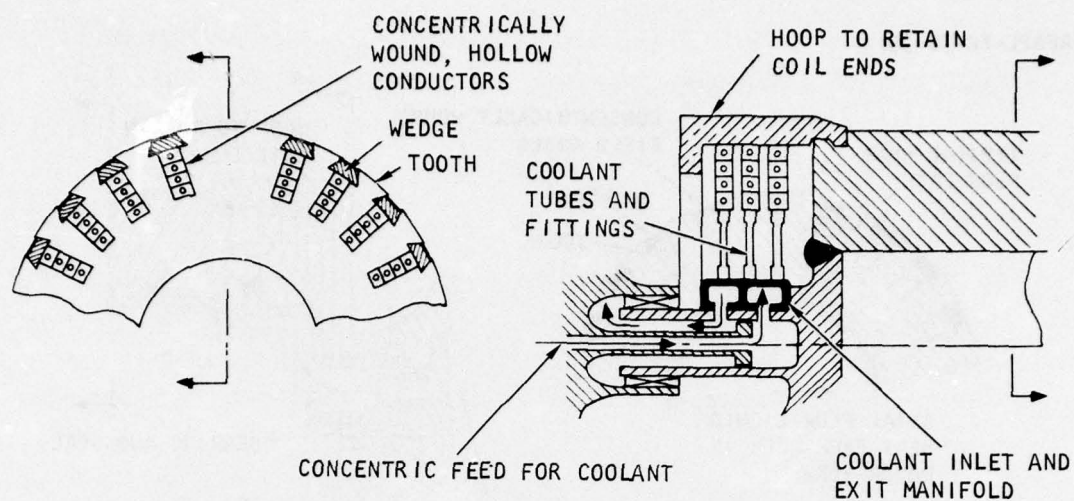
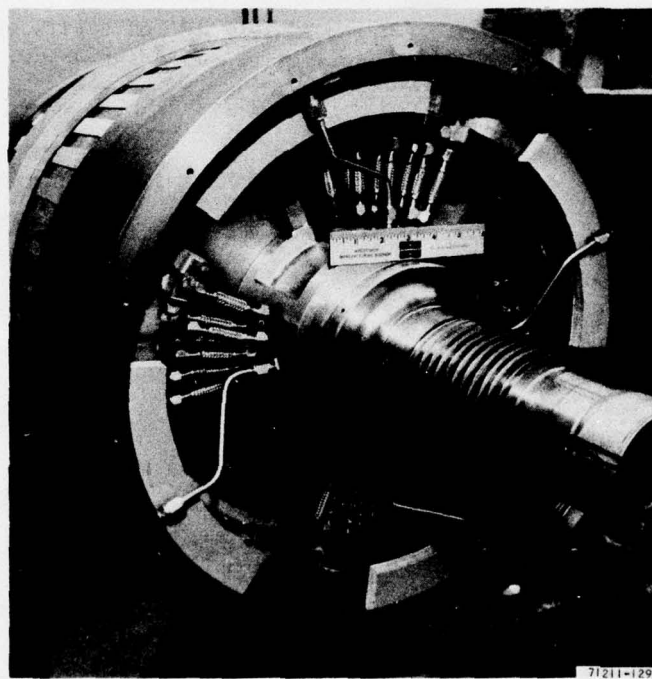


Figure 37. Hollow-Conductor-Cooled Rotor Configuration



F-22841

Figure 38. Water-Cooled, Hollow-Conductor Rotor for 10-MVA TACRV Machine

(because the conductor is hollow); and (5) assembly requires partial coil unwinding. These disadvantages, however, are more than offset by the lower generator weight and the ability to achieve continuous-duty operation (duty cycle independence).

Stator Configurations

The requirements for magnetic circuit compactness, high conductor current density, and high insulation voltage stress are major considerations for the stator in this application. The choice of coolant and cooling technique are particularly important because reliable operation at relatively high voltage is required.

For intermittent operation with low ON times, it might be possible to use the thermal capacity of the conductors for heat absorption or to use conductive cooling with a low cooling rate. For continuous duty or duty with a large ratio of ON to OFF time, direct conductor cooling will be required. The following paragraphs describe typical stator arrangements studied during this program. The flow-cooled stator with bore seal using hollow conductors was chosen to obtain maximum benefit of the cooling supplied to minimize weight and make the generator duty cycle independent.

1. Flow-Cooled Stator Without Bore Seal

Figures 39 and 40 show a stator configuration similar to that used on the TLRV alternator. Hollow conductors are used, and each conductor is cooled individually. Deionized water is used as coolant for the TLRV application, for which current densities of 27,000 A/sq in. have been achieved. Electrolytic corrosion at fittings is a potential problem with this arrangement, and long flexible lines will be required for dielectric considerations.

The major thermal advantage of this approach is the ability to use the most efficient coolant: water; however, as shown in Figure 40, this arrangement involves complex plumbing.

2. Flow-Cooled Stator With Bore Seal

A desirable approach to stator designs is to immerse the stator in a dielectric fluid and provide cooling by flowing the fluid through the coils

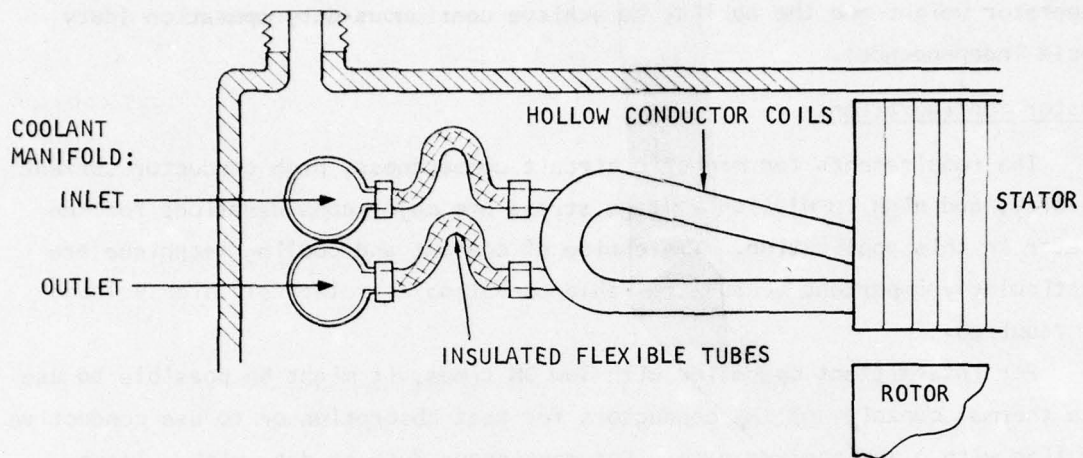
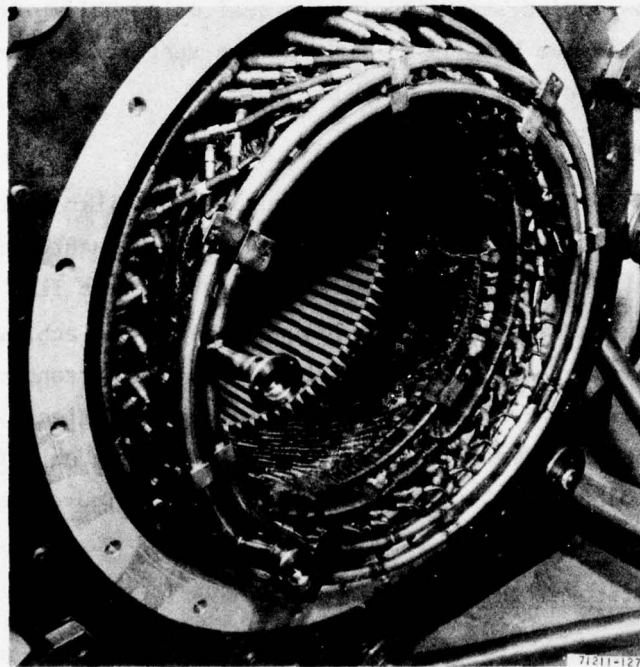


Figure 39. Flow-Cooled Stator Configuration



F-22842

Figure 40. Water-Cooled, Hollow-Conductor, 10-MVA Stator

and the stator core, as shown in Figure 41. Reliable insulation operation is possible because the dielectric fluid helps to avoid regions of high voltage stress, which typically cause corona and insulation deterioration.

Figure 42 shows a stator arrangement using this approach. As indicated, a thin bore seal (a ceramic tube or sleeve of Al_2O_3) is used for fluid containment. The seal must be nonconductive and nonmagnetic and must have high strength to withstand fluid pressure.

AiResearch has developed two lightweight military alternators using bore seals: the 520-kVA, 39,000-rpm machine previously shown in Figure 36 and 587-kVA, 24,000-rpm machine. This success was due to the technique developed for supporting a thin tube resiliently.

The arrangement shown in Figure 42 offers the advantage of proven construction for high-pressure, military vehicle usage, enhanced insulation reliability, and uniform cooling of iron and copper. Plumbing is simplified because coolant can be admitted to the interior of the conductors through holes properly located in the coil wraps and allowed to flow axially through the stator. It has the disadvantages of high bore seal cost and the requirement for complete exclusion of moisture from the dielectric fluid (to prevent hydrolysis of the insulation). Thus, the most efficient coolant (water) cannot be used.

COMPUTER PROGRAM

To perform the parametric studies and point designs required under the contract, AiResearch used its round-rotor alternator design program. This digital computer program is capable of computing conventional three-phase alternator machine designs over a wide range of ratings with a minimum of input data. It provides a comprehensive tool for the study of high-power generators and can be used for specific generator designs or for parametric studies of both thermal-lag and fluid-cooled designs.

This conventional generator program allows optimization of weight, volume, efficiency, and other significant parameters as a function of input variables such as power level, voltage, rotational speed, and duty cycle. As few as nine input data items suffice to produce a three-phase generator design; however, up to 22 input data items may be used for specific design points or parametric studies.

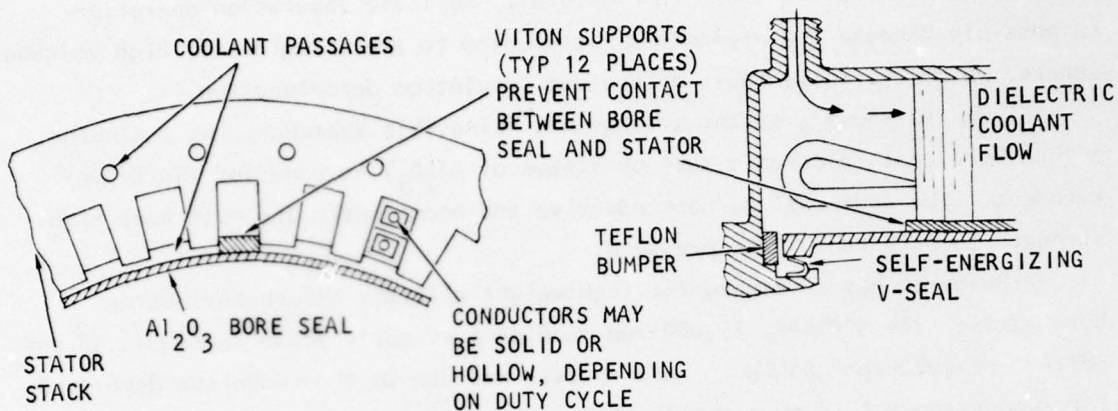
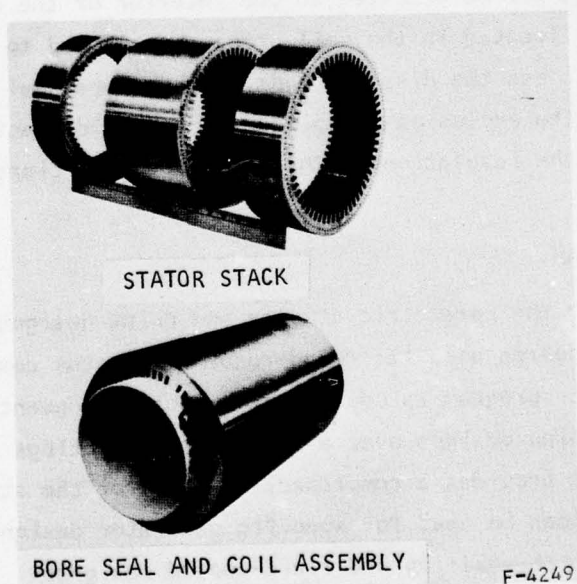


Figure 41. Flow-Cooled Stator Configuration



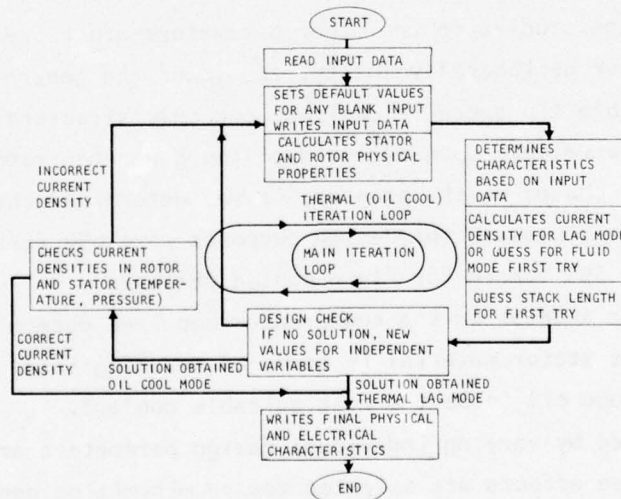
F-22843

Figure 42. Flow-Cooled Stator with Bore Seal

A significant feature of this alternator program is the incorporation of a thermal subroutine to minimize alternator size and weight. This subroutine allows operation at the maximum current density permissible for a given duty cycle without exceeding the specified maximum temperature limit. Two operating modes can be used: (1) thermal lag, in which the heat generated in the machine is absorbed by the thermal capacitance of the machine materials, and (2) active cooling, in which a fluid is circulated through the copper windings to absorb the heat generated and reject it to an external heat sink. In the fluid-cooled mode, the machine design is relatively insensitive to duty cycle because steady-state operation is attained in a matter of a few seconds.

The round-rotor alternator design program also includes a mathematical model of a three-phase full-wave rectifier that defines the power factor seen by the generator as a function of the generator commutation reactance. The subroutine is used for generator optimization because consideration must be given to the interaction of the generator and output rectifier necessary to supply the dc load.

Figure 43 is a flow chart of the program showing the main iteration and thermal loops. This chart represents the fundamental logic employed in designing a round-rotor alternator using this program.



S-3256

Figure 43. Round-Rotor Alternator Design Program Flow Chart

Table 45 defines the nine variables that must be input by the user. Table 46 lists the optional inputs together with the default values used by the program if these optional variables are not specified by the user. Table 47 lists the stator and rotor materials available for use in the program.

The program prints two different types of output--short format or long format--as specified by the user. The short format is generally sufficient for most purposes and is self-explanatory. A sample of the short format is given in Figure 44. The long format has two additional pages specifying internal dimensions and parameters defining the detail design.

PARAMETRIC AND SENSITIVITY STUDIES

The round-rotor computer program was used to conduct an extensive parametric and sensitivity study to determine the effect of individual parameters on the conventional generator design. These parameters were individually optimized in an effort to obtain a minimum-weight generator. Table 48 presents a list of the baseline values of the parameters used in the parametric and sensitivity studies.

The initial studies arbitrarily used a rotor peripheral velocity of 600 ft/sec with a M-15 HR silicon steel stator. The initial fluid-cooled designs used MIL-L-23699 lubricating oil for the cooling fluid. Although this peripheral velocity, stator material, and cooling fluid are not the optimum choice, the trends of the machine studies on the other parameters are representative.

The higher the rotor peripheral velocity, the lower the generator weight. Thus, the highest possible tip speed is desired, and only structural considerations limit the useable value. Upon analysis of the generator rotor designs obtained in the initial phases of the program, it was determined that the allowable rotor tip speeds useable for design purposes were 650 ft/sec for thermal-lag designs and 555 ft/sec for fluid-cooled designs.

Subsequent computer studies on the round-rotor machines determined 2V Permendur to be the best stator material in terms of reducing total generator weight and DC-200 silicone oil to be the most suitable coolant.

The effects produced by varying individual design parameters are listed below. In general, these effects are oriented toward minimizing generator weight.

TABLE 45
USER-DEFINED INPUTS

Variable	Description
1. KW	Output power rating, kw
2. VLN	Line-neutral voltage rating of machine, volts
3. PF	Power factor of the load (-lagging, +leading)
4. POLES	Number of poles
5. RPM	Rotor speed, rpm
6. TON	Duration of a single load pulse, sec
7. TOFF	Off-time between pulses, sec
8. PULSES	Number of load pulses or input 0. for continuous repetitions
9. TSTART	The initial copper temperature, °F

TABLE 46
OPTIONAL INPUTS

Variable	Description	If Input = 0., Defaults to:
10. VPMIL	Dielectric strength of stator insulation, V/mil	80.
11. FTPSEC	Rotor tip speed at the stator bore diameter, ft/sec	500.
12. X2	Per unit negative sequence reactance	0.375
13. BETAC	Peak stator core flux density, kilolines/sq in.	100.
14. BHS1	Stator material code number	1.
15. TBI	Thickness of stator lamination, in.	0.01
16. BHRI	Rotor material code number	11.
17. CWIDT	Negative ratio of stator tooth flux density to gap flux density	-2.36
18. CURDNS	Current density in the rotor, A/sq in.	Program determined
19. CURDNF	Current density in the rotor, A/sq in.	Program determined
20. RECMOD	1. = rectified, 0. = linear load	0.
21. TMAX	Maximum allowable stator and rotor temperature, °F	400.
22. COOL	Type of cooling employed. Input 0. for thermal lag. Input fraction of gross conductor section that carries current; e.g., 0.65 to 0.85 for fluid cooling	0.
23. XIPRT	Print switch to control amount of output detail. 0. = min. print, 1.0 = max. print	0.

TABLE 47
STATOR AND ROTOR MATERIALS

Code	Material	Thickness
1.	M-15 HR	0.014 in.
2.	M-19 HR	0.014 in.
3.	Trancor "T"	0.007 in.
4.	Trancor "T"	0.005 in.
5.	2V Permendur	0.010 in.
6.	HP-9-4-20 ingot	Solid
7.	4340 ingot	Solid
8.	Al 4750 at 1600 cps	0.006 in.
9.	Monimax at 2000 cps	0.004 in.
10.	1010 annealed	Solid
11.	HP-9-4-20 at 500°F	Solid
12.	HIPERCO 27	0.008 in.

CONVENTIONAL GENERATOR

SAMPLE CASE 1, DC-200 COOLED CONVENTIONAL GENERATOR

DATE = 02 DEC 75

TIME = 09:59:32

USER DEFINED INPUTS

K _a	24757.11	VOLTS, L-N	1617.00
PF	-0.877	POLES	6.0
RPW	12500.	LOAD PULSE DURATION, SEC	21.0
TIME BETWEEN PULSES, SEC	300.0	**NO. OF LOAD PULSES	3.0
INITIAL COPPER TEMP, DEG F	230.0		

OPTIONAL INPUTS

DEFAULT- IF INPUT = 0.0

VOLTS/MIL	100.0	80.0	V/MIL
TIP SPEED AT BORE DIA	555.00	500.00	FT/SEC
X2	0.2692	0.3750	PU
STATOR CORE DENSITY (PEAR) 150.		100.0	KL/50. IN.
STATOR MAT'L 2V PERMENDUR.01		.014	SILICON STEEL
STATOR LAM THICKNESS 0.0100		.01	IN.
ROTOR MAT'L HP 9-4-20 5000F		HP 9-4-20	
(-I)RATIO, BETAT/BETAG -3.150		-2.36	
CURRENT DENSITY, STATOR 40086.		PROGRAM ITERATES TO OBTAIN SPECIFIED TEMP	
CURRENT DENSITY, FIELD 37662.		PROGRAM ITERATES TO OBTAIN SPECIFIED TEMP	
RECTIFIED OR LINEAR LOAD 1.		LINEAR	
MAX COPPER TEMPERATURE 400.0 STATOR	400.0 ROTOR	400.0	DEG F
COOLING METHOD, FLUID 0.000		THERMAL LAG	
*** DC200 COOLING FLUID USED ***			

OUTPUTS

TOTAL WEIGHT, LB, KG	2964.340	1344.505	ALTERNATOR FRAME DIAMETER, IN, CM	14.153	35.949
SPECIFIC WEIGHT, LB/MM, KG/MM	0.120	0.054	TOTAL LENGTH, IN, CM	129.076	327.853
WEIGHT OF ACTIVE MATERIALS, LB, KG	2047.781	928.853	ALTERNATOR VOLUME, CU IN, CU CM	14129.	231526.
ALTERNATOR HEIGHT, LB, KG	2062.113	1207.508	EXCITER VOLUME, CU IN, CU CM	3022.	49526.
EXCITER WEIGHT, LB, KG	302.227	137.087	TOTAL VOLUME, CU IN, CU CM	17151.	281052.
ROTOR INCHES, IN-LB-SEC2, NEWTON-M2	49.760	0.502	FIELD POWER, KW, KW	579.534	579.534
EFFICIENCY, PERCENT, PERCENT	93.987	93.987	TOTAL LOSSES, KW, KW	1583.766	1583.766
ROTOR LENGTH/DIAMETER RATIO	8.363		ROTOR TOTAL LENGTH, IN, CM	82.747	210.178
			ROTOR DIAMETER, IN, CM	4.894	25.131
COOLANT FLOW RATE, STATOR, GPM, LPM	125.579	475.355	COOLANT FLOW RATE, ROTOR, GPM, LPM	71.498	270.642
COOLANT DELTA-P, STATOR, PSID, MEGAPASCAL	119.087	0.821	COOLANT DELTA-P, ROTOR, PSID, MEGAPASCAL	119.121	0.821
COOLANT DELTA-T, STATOR, DEG-F, DEG-C	89.005	49.892	COOLANT DELTA-T, ROTOR, DEG-F, DEG-C	139.378	77.432
STACK LENGTH, IN, CM	76.743	194.927	ALTERNATOR STACK DIAMETER, IN, CM	12.687	32.226
STATOR SLOT HEIGHT, IN, CM	0.580	1.494	BORE DIAMETER, IN, CM	10.183	25.866
END COIL EXTENSION, IN, CM	2.440	6.199	ROTOR SLOT DEPTH, IN, CM	1.163	2.955

* FOR FLUID COOLING, INPUT=(NET/GROSS) FOR THE HOLLOW CONDUCTOR.
IF CURRENT DENSITY IS INPUT, THE CORRESPONDING TEMPERATURE IS CALCULATED. OTHERWISE, DENSITY TO YIELD MAX TEMPERATURE IS CALCULATED.
**FOR CONTINUOUS REPETITIVE PULSES, INPUT NO. PULSES = 0. IN CONTINUOUS LAG MODE, THERMAL ROUTINES ARE BYPASSED. CURRENT DENSITIES MUST BE SPECIFIED IN BYPASS MODE.

Figure 44. Sample Printout, Short Form

TABLE 48
BASELINE VALUES OF STUDY PARAMETERS

Parameter	Value
Number of poles	6
Type of load	Rectified
Apparent power factor	0.88 lagging
Commutation reactance (per unit)	0.27
Insulation stress (volts per mil)	100
Stator core density, peak, Kilolines per sq in.	100 (M-15 HR silicon steel) 150 (2V Permendur)
Rotor material	HP 9-4-20 steel
Initial copper temperature, °F	230 (oil cooled) 130 (thermal lag)
Maximum copper temperature, °F	400 (oil cooled) 450 (thermal lag)
Coolant pressure drop, psi	120 (through generator) 220 (for total cooling system)
Oil flow area (percent of conductor)	20

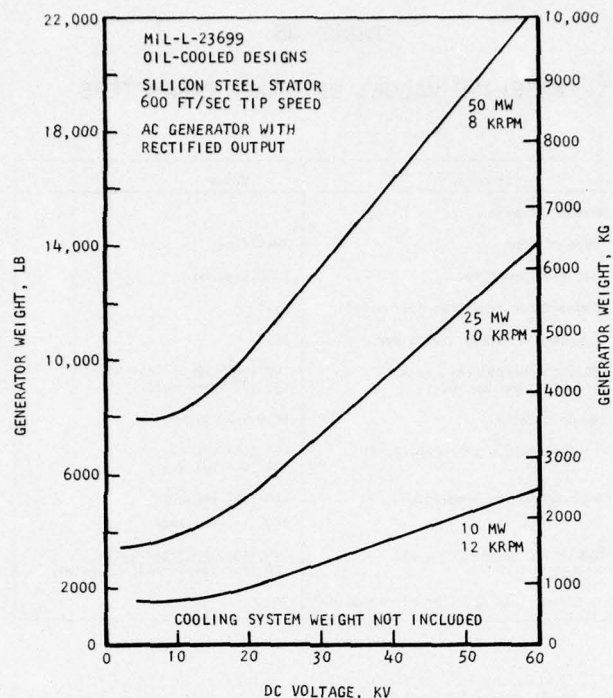
The parametric and sensitivity studies conducted include the effects produced by the following parameters:

- | | |
|----------------------|--|
| (a) Voltage | (h) Insulation working stress |
| (b) Rotational speed | (i) Type of load |
| (c) Power level | (j) Commutation reactance/power factor |
| (d) Cooling method | (k) Stator material/core density |
| (e) Duty cycle | (l) Copper temperature limits |
| (f) Number of poles | (m) Coolant pressure drop |
| (g) Tip speed | |

Voltage Effects

The trend of oil-cooled generator weight with output voltage at various constant power levels of interest is shown in Figure 45. As shown, the generator weight is highly sensitive to both output voltage and power level, increasing significantly with both parameters. The important conclusions to be drawn from this figure are:

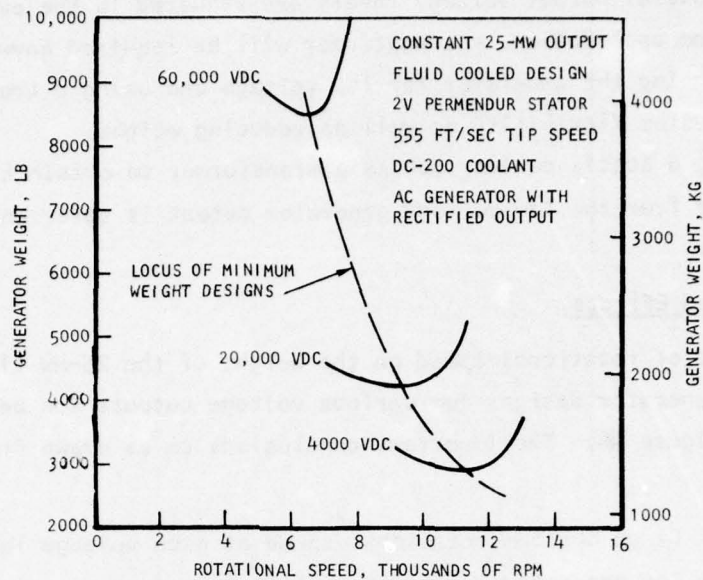
- (a) Weight variation of the generator with voltage is minimal below approximately 10,000 Vdc.
- (b) Generator weight increases rapidly with increasing output voltage above 10,000 Vdc.



S-2790

Figure 45. Generator Weight vs Dc Voltage for Different Power Loads

Although Figure 45 trend results are correct, they are somewhat misleading as to the severity of weight penalty imposed by using high-output-voltage designs. This is because the curves in the figure are for constant rotational speed at each power level and are optimum only near 4000 Vdc. A more accurate picture of the voltage effects is obtained when the rotational speed is optimized at each output voltage as shown in Figure 46, which shows the fluid-cooled 25-MW generator weight as a function of rotational speed for several voltage levels. Although Figure 46 shows a significant reduction in the weights of the high-voltage machine designs from those of Figure 45, the basic conclusion is the same; i.e., the weight penalty incurred in the generator design becomes increasingly severe as the voltage level increases.



5-2792

Figure 46. Generator Weight vs Rotational Speed for Different Dc Voltages

AIResearch has elected to design the high-power generator at the low voltages, which produce near optimum generator weights. This requires the use of a transformer to convert the resulting low output voltage from the generator to the desired high-voltage output necessary from the high-power system. Although this approach results in an additional component, the use of a transformer presents several additional significant advantages to the overall high power system. They are:

- (a) A net overall weight saving is obtained in the system because the transformer weight is less than the added weight when the generator is designed for high voltage. A short study on thermal-lag transformers was conducted for design point 6, which resulted in a transformer weight of 0.06 lb/kW compared to the generator specific weight of 0.17 lb/kW (thermal lag).
- (b) The transformer weight is relatively independent of primary-to-secondary voltage ratio at the levels and duty cycles of interest. This allows the final power system output voltage to be changed by altering the transformer, rather than the generator, with very little weight change to the system.

- (c) If several output voltage levels are required in the eventual power system application, a transformer will be required anyway. Thus, designing the generator for low voltage and using a transformer adds to system flexibility as well as reducing weight.
- (d) Using a static device such as a transformer to obtain high-voltage power from the low-voltage generator output is safer and more reliable.

Rotational Speed Effects

The effect of rotational speed on the weight of the 25-MW fluid-cooled conventional generator designs for various voltage outputs can be seen by referring to Figure 46. The important conclusions to be drawn from this figure are:

- (a) There is an optimum rotational speed at each voltage level for which the generator weight is a minimum.
- (b) The optimum rotational speed shifts to lower values as the generator design output voltage increases.
- (c) The speed range at each voltage level at which the generator weight is near the optimum value is quite narrow. Weight increases very rapidly as the design rotational speed shifts away from the optimum, especially in the increasing speed direction.

Figure 47 presents data similar to that in Figure 46 except that it is for low voltage generator designs at various power levels rather than several voltage levels at a constant power level. In addition, at the 25-MW power level, Figure 47 shows both thermal-lag and oil-cooled designs to indicate the magnitude of weight reduction that can be obtained by using effective cooling techniques. The significant features illustrated by Figure 47 are:

- (a) There is an optimum rotational speed at each power level for which the generator weight is a minimum.
- (b) The optimum rotational speed shifts to lower values as the generator design power output increases.

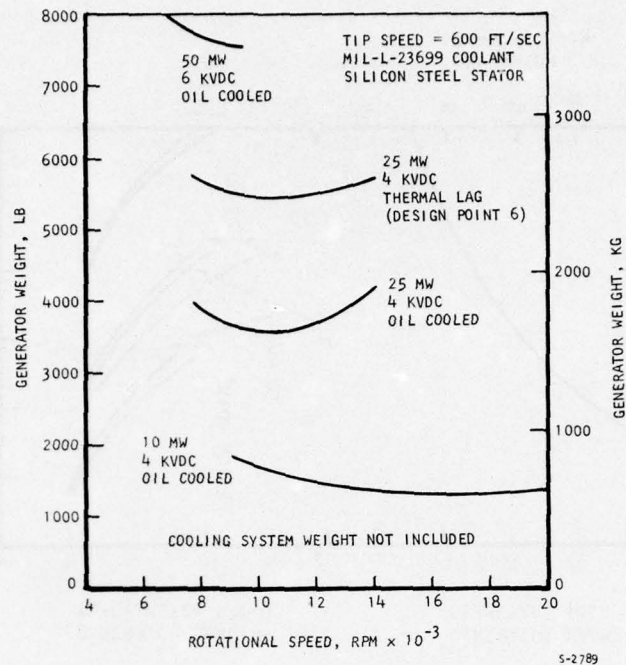


Figure 47. Generator Weight vs Rotational Speed for Different Power Levels

- (c) The speed range at each power level at which the generator weight is near the optimum value is quite broad. The lower the power level the broader the range of acceptable speeds.
- (d) The optimum speed to obtain minimum weight generator designs is approximately the same for thermal-lag machines as for oil-cooled machines.

A weight and volume summary of thermal-lag conventional generator designs for all eight SOW design points is presented in Figure 48 as a function of design rotational speed. The weight trends are similar to those shown in Figure 47; however, the geometric trends of the generator are new. The significant features in machine geometry affected by rotational speed as shown in Figure 48 are:

- (a) The frame diameter of the generator varies inversely with rotational speed and is independent of output power level.

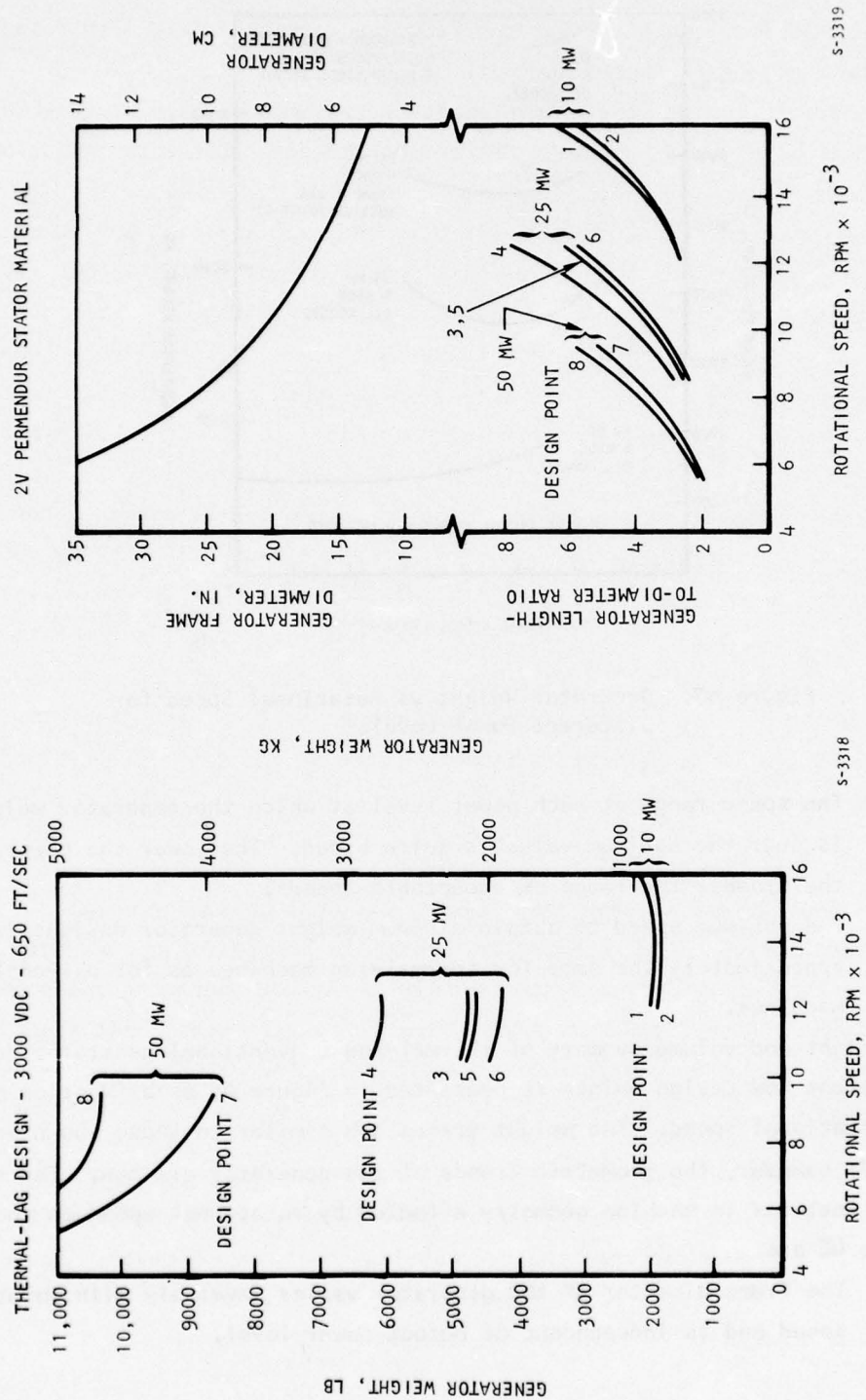


Figure 48. Thermal-Lag Generator Weight, Diameter, and Length vs Rotational Speed for Specific SOW Design Points

- (b) The machine length-to-diameter ratio increases rapidly with rotational speed at constant power output.
- (c) Constant machine length-to-diameter ratios can be maintained with increasing power levels by decreasing the generator rotor rotational speed.

Selection of the actual design value of rotational speed at any power level is not always determined by the generator alone. Optimum system weight may not occur at the optimum generator weight when the generator is driven directly by a turbine. In addition, other factors may influence the final rotational speed selection such as (1) critical speeds or (2) whether or not the use of a gearbox between the generator and drive turbine can be eliminated by compromising the design rotational speeds of the two individual units.

The rotational speeds selected for many of the conventional generator designs were in fact determined by compromise. The direct-driven 50-MW generator rotational speed is determined by the turbine, while the direct-driven 25-MW unit is a compromise between the optimum rotational speeds of the generator and turbine. The 10-MW units require a gearbox between the generator and turbine because of the large disparity between the optimum speeds of the generator and turbine. Thus, the 10-MW generators were designed at the optimum rotational speed for minimum weight.

Power Level Effects

Figures 45, 47, and 48 show that the conventional generator weight increases approximately in direct proportion to the increase in power output capability of the machine for the same type of generator operating under the same conditions. These figures also show that the design rotational speed decreases with increasing power level, while the machine diameter increases with power level.

Cooling Method Effects

An effect that would appear to be intuitively obvious is that the fluid-cooled generator is lighter than the thermal-lag generator; however, Figure 49 shows that if the duty cycle is short enough, the thermal-lag machine can be lighter than its fluid-cooled counterpart.

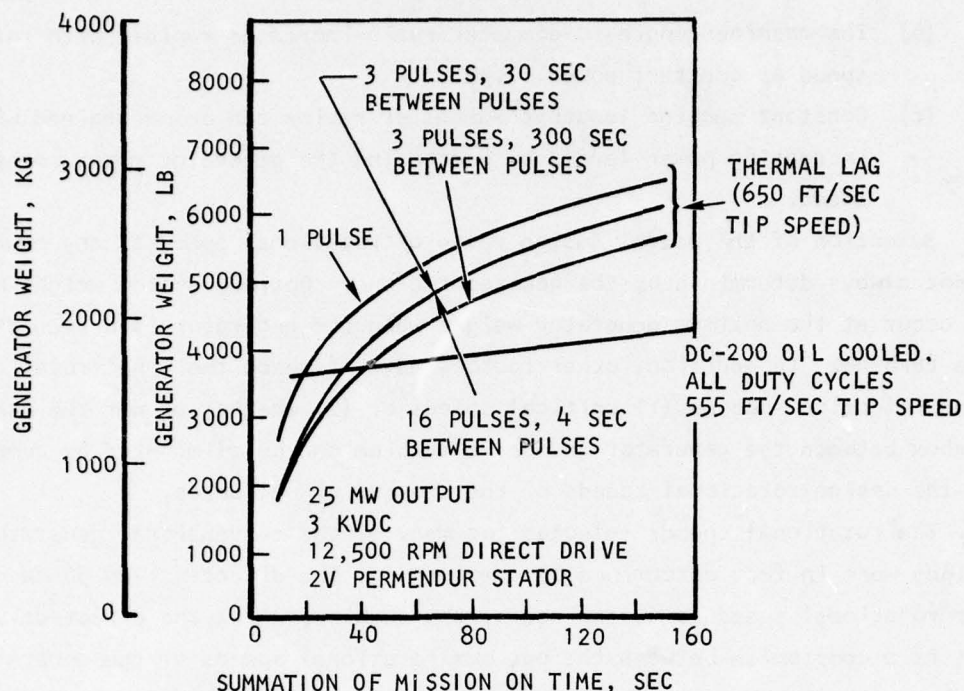


Figure 49. Effect of Duty Cycle and Cooling Method on Weight

For the eight design points considered in this study, the operating duration is long enough at each point to show a significant weight advantage for the fluid-cooled generator in comparison to the thermal-lag machine.

Duty Cycle Effects

Figures 48, 49, and 50 show the effect on conventional generator weight produced by variation in the design point duty cycle. Thermal-lag generator weights are shown in Figure 48 for all eight 50W design points, and the effect of varying the number of pulses, pulse duration, and time between pulses (one at a time) is investigated in Figure 50. Both thermal-lag and fluid-cooled generators including cooling systems are shown in Figure 50 at the 25-MW power level. The prime points illustrated by these figures are:

- (a) The weight of a thermal-lag generator is very much dependent on the operating duty cycle for which it is designed. The thermal-lag generator weight depends on number of pulses, pulse duration, and time between pulses. Variation of any of these parameters significantly affects the weight of the thermal-lag generator design.

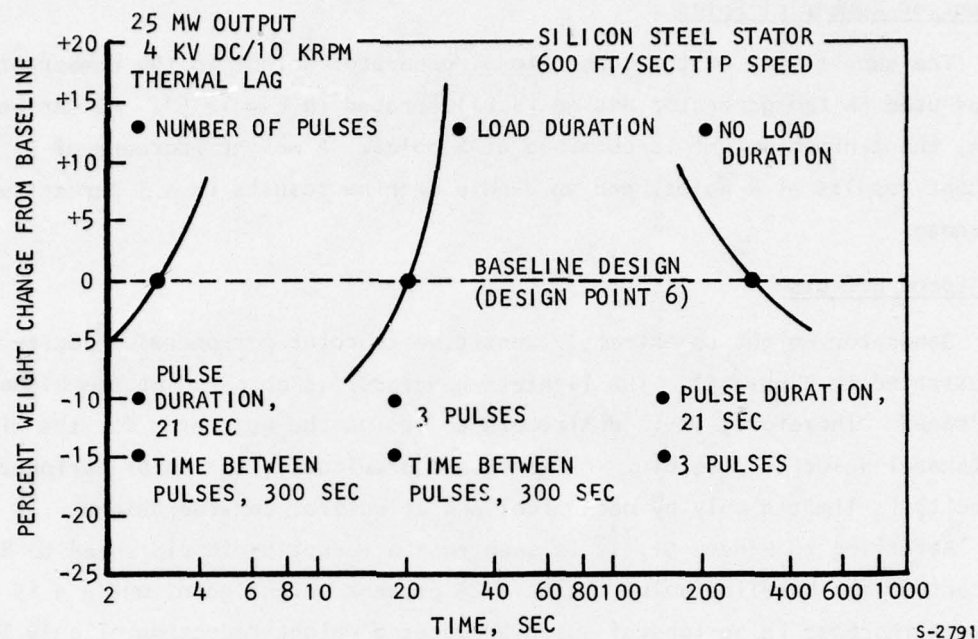


Figure 50. Duty Cycle Sensitivity of Thermal Lag Conventional Generators

- (b) The fluid-cooled generator is relatively independent of the mission duty cycle. Its weight variation depends only on the total ON time during the mission, which determines the amount of evaporative coolant heat sink (and associated tankage) that must be carried for mission completion. This lends considerable flexibility to the mission duty cycle selection in comparison to the thermal-lag machine.
- (c) The fluid-cooled generator is always lighter than the thermal-lag generator for the eight SOW design points investigated during this study.
- (d) For total mission ON times below approximately 45 sec, the thermal-lag generator is competitive with or lighter than the fluid-cooled machine.

Effect of Number of Poles

The sensitivity of the conventional generator weight to the number of poles used in the generator design is illustrated in Figure 51. As can be seen, the minimum weight is obtained at 6 poles. A weight increase of 7 percent results at 4 poles, and an 8-pole machine results in a 3 percent weight increase.

Tip Speed Effects

Generator weight is extremely sensitive to rotor peripheral velocity as illustrated in Figure 51. The lightest generator is obtained at the highest tip speed. Therefore, it is desirable to design the generator for the highest peripheral velocity possible. As mentioned previously, the rotor peripheral velocity is limited only by mechanical and structural considerations.

Referring to Figure 51, it is seen that a reduction in tip speed to 85 percent of the baseline value causes a 25 percent weight gain, while a 15 percent increase in peripheral speed produces a weight reduction of only 10

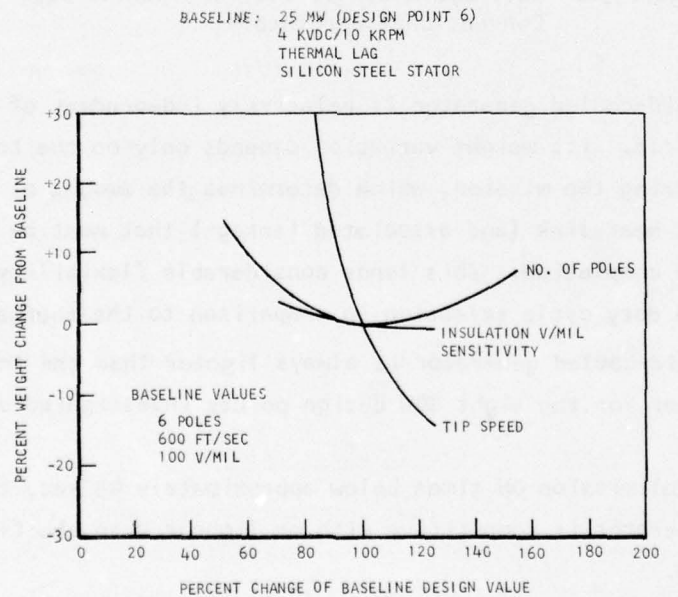


Figure 51. Weight Sensitivity of Conventional Generator to Number of Poles, Insulation Stress, and Tip Speed

percent. The law of diminishing returns is in effect here; you lose much more by reducing tip speed than you gain by a similar increase in tip speed.

The conclusion reached remains unchanged; the lightest generator is obtained by operating at the highest peripheral speed structurally permissible.

Effect of Insulation Working Stress

The weight change in the conventional generator produced by a 20 percent change in the baseline insulation working stress is almost imperceptible. This was graphically illustrated in Figure 51.

The baseline insulation working stress of 100 V/mil results in small insulation thickness at the low voltages selected for the conventional generator designs. This undoubtedly leads to the insensitivity of generator weight with insulation working stress at these low voltage levels; however, at high voltages, the generator weight sensitivity to insulation working stress would be expected to be high. This is illustrated in Figure 52.

Effect of Load Type

The variation in generator weight with commutation reactance is shown in Figure 53 for both rectified and linear loads. As can be seen, the generator feeding a linear load is considerably lighter than the generator designed to feed a rectified load. This result is of academic interest only, because the actual generator must be designed to feed a rectified load.

Figure 54 presents general rectifier data required to define generator voltage, current, and apparent power factor, PF. The data presented are based on Fourier analysis of the generator current wave when the overlap angle varies from 0 to 60 deg, which corresponds to a variation of commutation reactance, X_{COM} , from 0 to 0.48 per unit. All required relationships are defined in Figure 54.

Effect of Commutation Reactance/Apparent Power Factor

Figure 53 also shows the effect that commutation reactance and apparent power factor have on generator weight. For a rectified load, the apparent power factor is determined by the commutation reactance as shown in the figure. The important conclusions drawn are:

- (a) There is an optimum value of commutation reactance for which the generator weight is a minimum. This value is approximately 0.27 per unit.

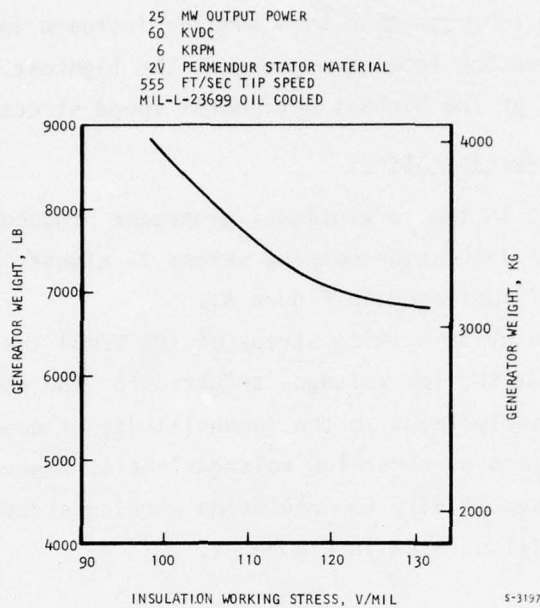


Figure 52. Generator Weight Sensitivity to Insulation Working Stress at High Voltage

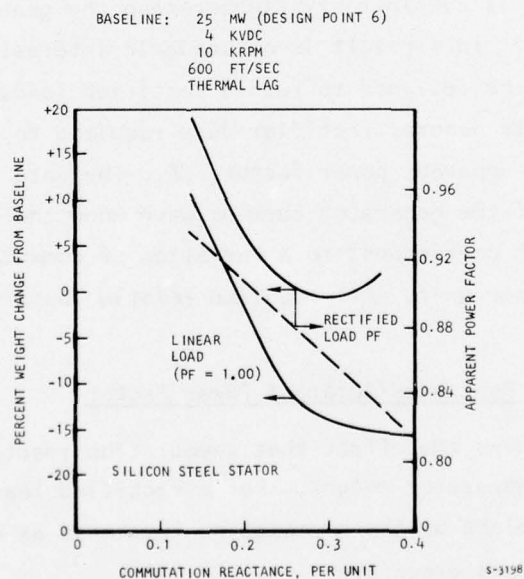
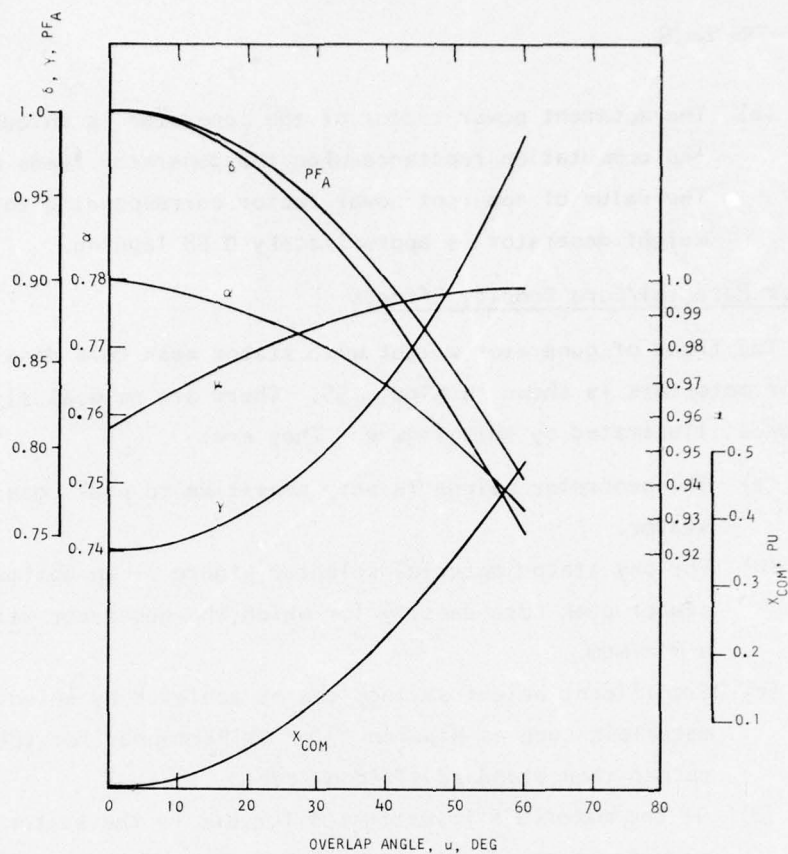


Figure 53. Weight Sensitivity of Generator with Load Type and Commutation Reactance



NOTES

$$PFA = \text{APPARENT POWER FACTOR} = \frac{W_{DC}}{\sqrt{3} V_{LL1} I_1}$$

W_{DC} = DC POWER, W

I_1 = FUNDAMENTAL COMPONENT OF AC CURRENT, A

X_{COM} = PER UNIT COMMUTATION REACTANCE

$$\alpha = \text{CURRENT FACTOR} = \frac{I_1}{I_{DC}}$$

I_{DC} = DC CURRENT, A

$$\gamma = \text{VOLTAGE RATIO} = \frac{V_{LL1}}{V_{DC}} = \frac{\pi}{3\sqrt{2} \delta}$$

V_{LL1} = FUNDAMENTAL VOLTAGE LINE-TO-LINE,

V_{DC} = DC LOAD VOLTAGE, V

$$\delta = \text{DC VOLTAGE REGULATION FACTOR} = \frac{V_{DC @ \text{FULL LOAD}}}{V_{DC @ \text{NO-LOAD}}} = \cos^2 u/2$$

$$\mu = \text{CURRENT DISTORTION FACTOR} = \frac{I_1}{I_{RMS}}$$

S-7267

Figure 54. Apparent Power Factor and other Parameters for a 3-Phase, F-W Rectifier Supplied by an Alternator

- (b) The apparent power factor of the generator is uniquely related to the commutation reactance when the generator feeds a rectified load. The value of apparent power factor corresponding to the optimum weight generator is approximately 0.88 lagging.

Stator Material/Core Density Effects

The trend of generator weight with stator peak core density for several stator materials is shown in Figure 55. There are several significant features illustrated by this figure. They are:

- (a) The generator weight is very sensitive to peak core density in the stator.
- (b) For any stator material selected, there is an optimum value of stator peak core density for which the generator weight will be a minimum.
- (c) Significant weight savings can be achieved by selecting more expensive materials such as Hiperco 27 or 2V Permendur for the stator material rather than standard silicon steel.
- (d) Of the materials investigated for use in the stator, 2V Permendur results in the lightest weight design. This is achieved at a stator peak core density of approximately 150 kilolines/sq in.

Effect of Copper Temperature Limits

Figure 56 presents the sensitivity of generator weight to initial and final copper temperature. The main conclusions to be drawn are:

- (a) Reducing the initial copper temperature from 130°F to 40°F results in a weight saving of only 5 percent.
- (b) Changing the final copper temperature of 450°F by $\pm 50^\circ\text{F}$ results in a weight change of the generator of ± 4 percent.

Coolant Pressure Drop Effects

Figures 57 through 60 show coolant pressure drop effects. Cooling of the fluid-cooled generators is accomplished by transporting the coolant fluid through hollow conductors. The coolant passages are configured in parallel so that the coolant flows from one end of the machine to the other in a single pass. This arrangement of flow paths (single-pass, multiple parallel-flow

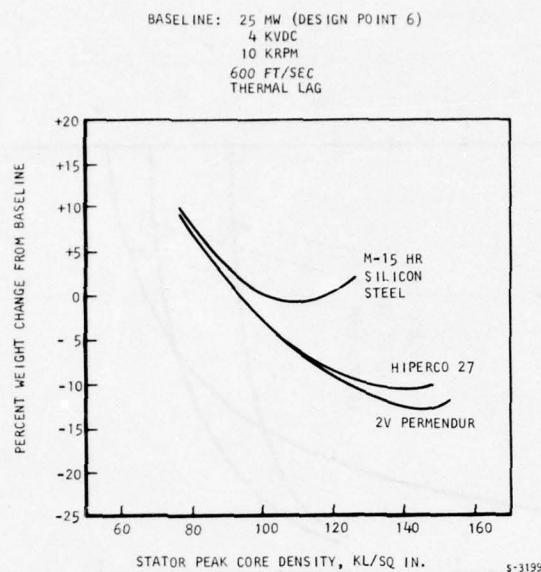


Figure 55. Generator Weight Sensitivity to Materials and Stator Peak Core Density

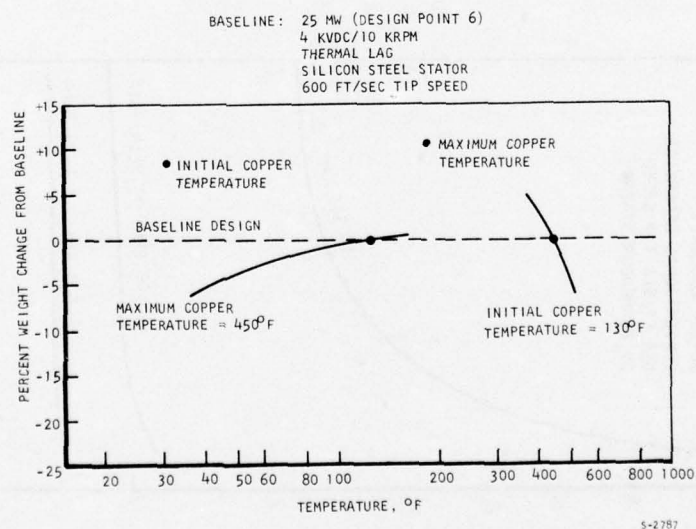
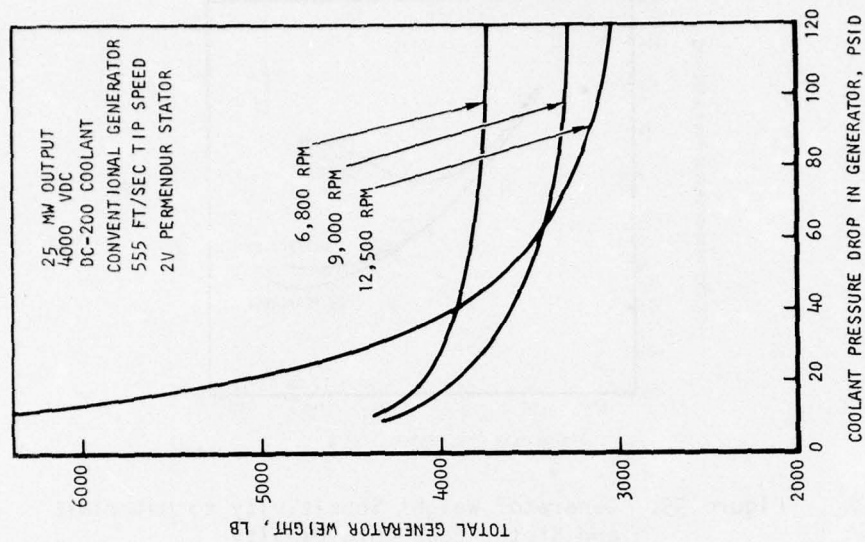
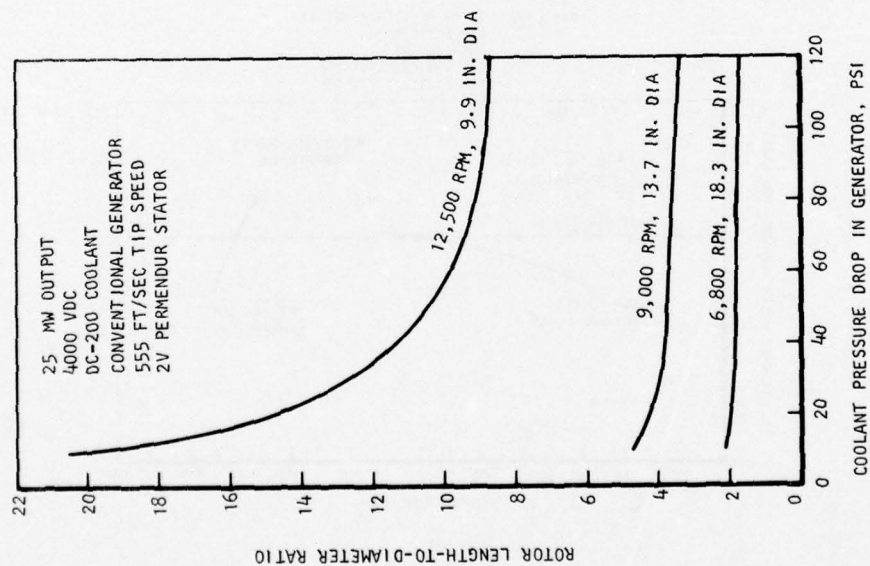


Figure 56. Generator Weight Sensitivity to Initial and Final Copper Temperatures



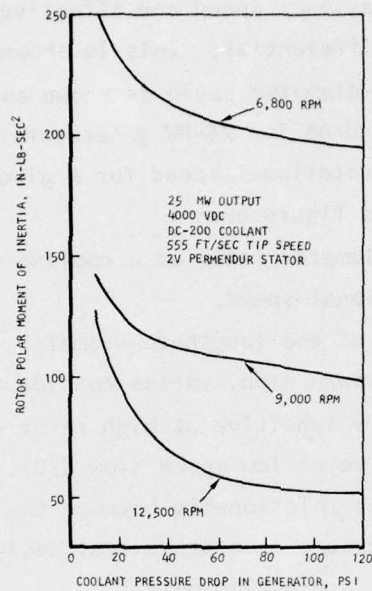
S-3205

Figure 58. Generator Weight vs Coolant Pressure Drop



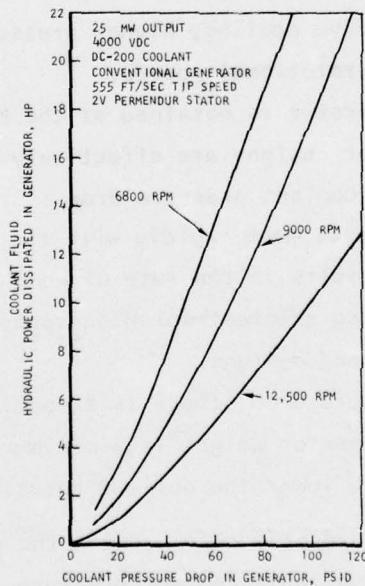
S-3204

Figure 57. Rotor L/D vs Coolant Effectiveness



S-3195

Figure 59. Relationship of Generator Rotor Polar Moment of Inertia to Coolant Pressure Drop and Rotational Speed



S-3196

Figure 60. Hydraulic Power Dissipated in Cooling the Generator

passages) makes the generator design sensitive to resulting length-to-diameter ratio for a specified rotational speed and effectiveness of coolant as expressed by operational pressure differential. This is shown graphically in Figure 57 where the rotor length-to-diameter ratio is shown as a function of coolant effectiveness or pressure drop for 25-MW generators of three different sizes (diameters determined by rotational speed for a given tip speed). The important points illustrated by this figure are:

- (a) The length-to-diameter ratio at a cooling capability is sensitive to design rotational speed.
- (b) The sensitivity of the length-to-diameter ratio to coolant effectiveness, hence pressure drop, varies considerably with design rotational speed, being very sensitive at high rotor speeds (high L/D) and rather insensitive at low speed (low L/D).

Figure 58 presents the relationship between the fluid-cooled generator weight and the coolant pressure drop at several design rotational speeds. This illustrates the following interesting points.

- (a) The fluid-cooled generator weight is sensitive to coolant pressure drop through the generator. The higher the design rotational speed, the greater the sensitivity.
- (b) To achieve effective cooling, higher pressure drops must be available at higher design rotational speeds.
- (c) The lightest generator is obtained at the highest rotational speed when all generator designs are effectively cooled.
- (d) As the available coolant pressure drop is reduced, the effectivity of cooling decreases most rapidly with the higher speed generator designs. This results in the rate of weight increase due to reduced pressure drop being greatest for high-speed generator designs and lowest for low-speed designs.
- (e) For a fixed pressure drop, there is an optimum design rotational speed for which the generator weight is a minimum. The lower the available pressure drop, the lower the optimum rotational speed and vice versa.

Figure 59 presents the relationship between the generator rotor polar moment of inertia and the available coolant pressure drop at several design rotational speeds. The following observations were noted.

- (a) The rotor polar moment of inertia is extremely sensitive to design rotational speed. The higher the rotational speed the lower the inertia.
- (b) The rotor polar moment of inertia also is sensitive to coolant pressure drop, the lower the available pressure drop, the faster the inertia increases.

The hydraulic power dissipated by the coolant fluid as it passes through the generator is presented in Figure 60 for several design rotational speeds as a function of pressure drop. A recirculation pump must be provided in the coolant circuit to furnish the motive power necessary to recirculate the coolant fluid. The pumping power required is equal to the sum of (1) the hydraulic power dissipated in the generator as given in Figure 60, (2) the hydraulic power losses in the remainder of the cooling circuit, and (3) the inefficiency of the coolant pump. The main conclusions are:

- (a) The hydraulic power dissipated in the generator is very sensitive to pressure drop, increasing rapidly as the available pressure drop increases.
- (b) For a given pressure drop, the higher speed machine designs dissipate less hydraulic power. This is because the higher L/D of high-speed generators produces a reduced coolant flow rate for a given pressure drop.
- (c) The pumping power required for the coolant circuit is of consideration for any generator designed to be effectively cooled.

THERMAL DESIGN AND COOLING SYSTEM

One of the most important tasks in the design of a lightweight, high-power electric generator is the thermal design. To build any machine that will operate successfully, the various component parts must be maintained at temperatures that do not produce adverse effects.

In normal electric generator designs, the principal areas where cooling is required are on the bearings and the electrical insulation on the windings. Cooling also may be required to maintain the strength of materials in the rotor that are subjected to large centrifugal stress loads and to maintain shrink fits between the various parts of the machine. Repeated large temperature changes

produce problems of differential thermal expansion between the windings and the iron. The repeated expansion and contraction can produce cracks in the insulation unless the insulation is ductile and the generator is designed to accommodate this thermal expansion process.

For the generators designed in this study, the preceding factors are important, but the prime emphasis is on the conductors. The path to light-weight generator designs is through the use of high current densities in the conductors. This, however, increases the resistance losses in the copper and, consequently, the heat that must be removed or absorbed. Thus, the main thermal emphasis thrust in this study is associated with the conductor cooling and heat sink capacity that is necessary to achieve high current densities and low generator weights.

Accordingly, the thermal analyses conducted during this study have been concentrated in three key areas: (1) incorporation of the thermal model into the round-rotor generator program and verifying the results with the thermal analyzer computer program, (2) selection of the coolant to be used in the fluid-cooled generator designs and (3) design of the cooling system required for the fluid-cooled generator designs.

Generator Thermal Model

A significant improvement was made in the existing AiResearch round-rotor alternator design computer program by incorporating two new thermal subroutines: (1) CURDNZ for thermal-lag generators and (2) COND for fluid-cooled machines (hollow conductors). These subroutines allow meaningful reductions in generator size and weight to be obtained by operation at the maximum current density permissible for a given duty cycle without exceeding the specified maximum temperature limit. Two operating modes can be used: (1) thermal lag, in which the heat generated in the machine is absorbed by the thermal capacitance of the machine materials, and (2) active cooling, in which a fluid is circulated through the copper windings to absorb the heat generated for rejection to an external heat sink. In the fluid-cooled mode, the machine design is relatively insensitive to duty cycle because steady-state operation is attained in a matter of a few seconds.

These thermal subroutines calculate either the peak and time average conductor currents corresponding to the selected maximum conductor temperature, or the maximum conductor temperature corresponding to the selected input peak current. Three basic current waveshape characteristics can be examined: (1) repeating on-off square wave current on infinite cycles, (2) square wave current of selected number of cycles, and (3) constant current.

The computer subroutine COND calculates the heat transfer and fluid characteristics in internally cooled conductors used in square-wave power or constant-power applications. Figure 61 shows a simplified flowchart of COND. Basically the program first finds the fluid flow rate that satisfies the pressure drop requirement. Next the conductor temperature is compared with the requirement specified in the program input. An option is provided in the program for the selection of different coolant fluids. The conductor data are supplied to the subroutines through the common statements.

Verification of Generator Thermal Model

A detailed transient thermal analysis was conducted on a 25-MW fluid-cooled generator design to verify the results produced by the new round-rotor alternator design program incorporating the new thermal subroutines. This analysis verified the accuracy of the new generator thermal model.

AiResearch thermal analyzer computer program H0298 was used to predict the temperatures within the fluid-cooled 25-MW generator as a function of time when operated in accordance with the design point 6 duty cycle (3 pulses of 21 sec duration with 300 sec between pulses). The thermal models used in the analysis are shown in Figures 62, 63, and 64. Figure 62 shows the solid nodes in the radial view of the stator and rotor sections, which include the conductors, rotor pole head, teeth, and cores. In Figure 63 are the nodes in the axial view of the rotor, stator, and housing. Figure 64 presents the coolant flow paths. No forced air cooling of the conductor is employed, and the housing is cooled by radiation and free convection to an ambient of 130 F and 14.7 psia. Prior to operation, the generator interior temperatures are initially at 130 F. Once operation is commenced, coolant is supplied at 230 F to the rotor and stator. The coolant is continuously supplied at the same rate during the entire duty cycle to prevent excessive soakback temperatures during the power-off period. A maximum conductor temperature of 400 F is allowed.

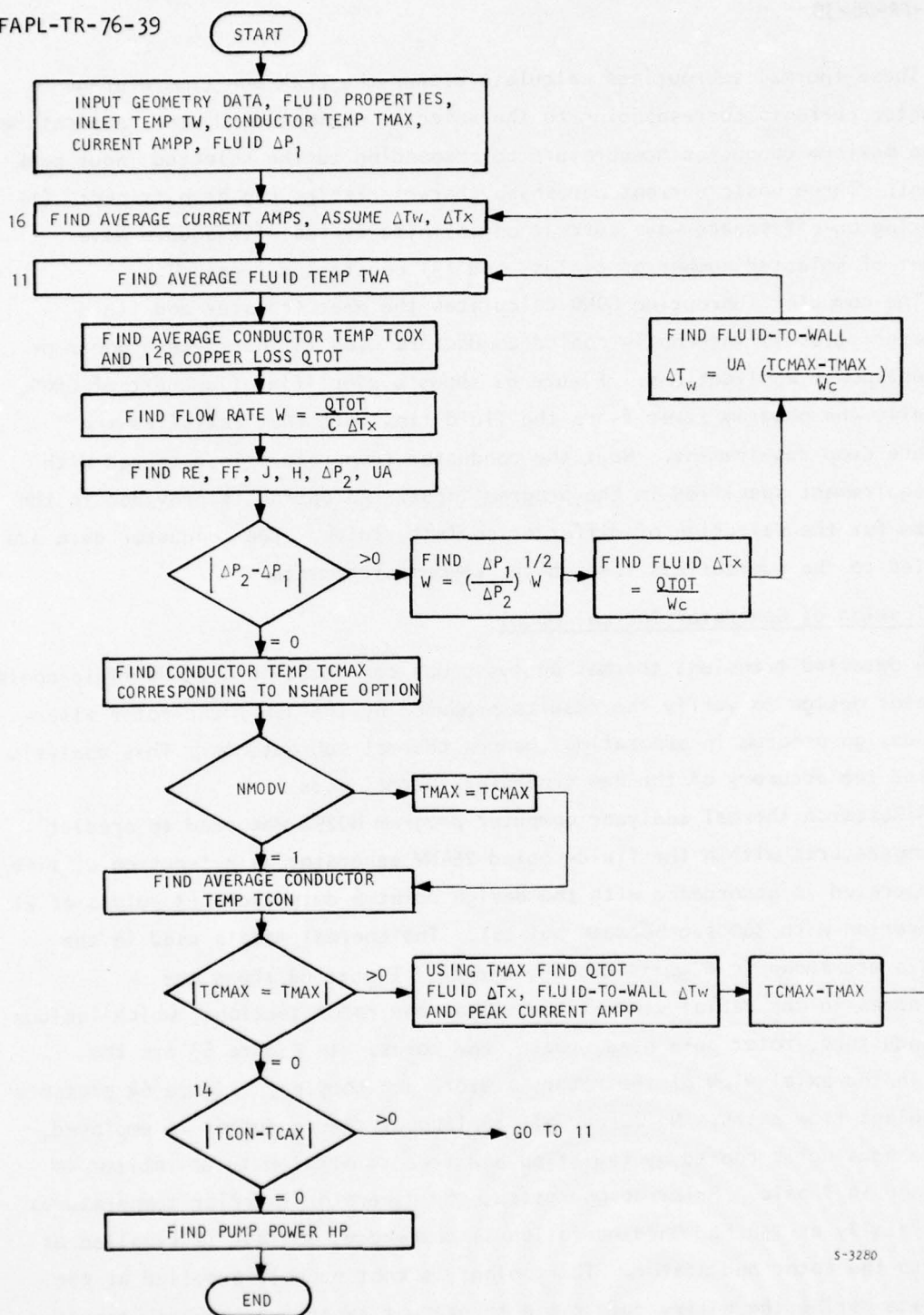


Figure 61. Simplified Flow Chart of Subroutine COND



169

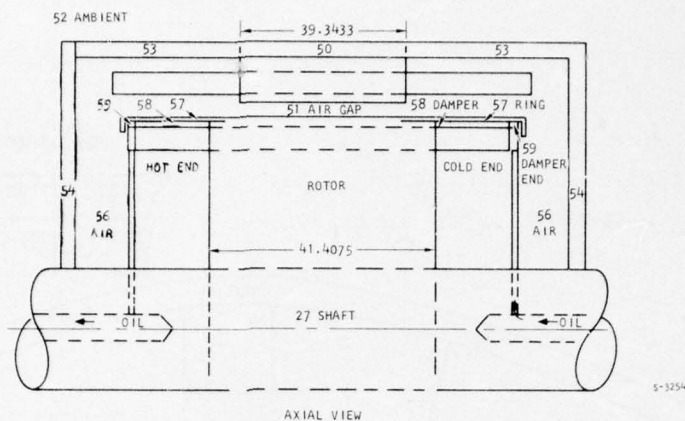


Figure 63. Axial View of 25-MW Generator Thermal Model

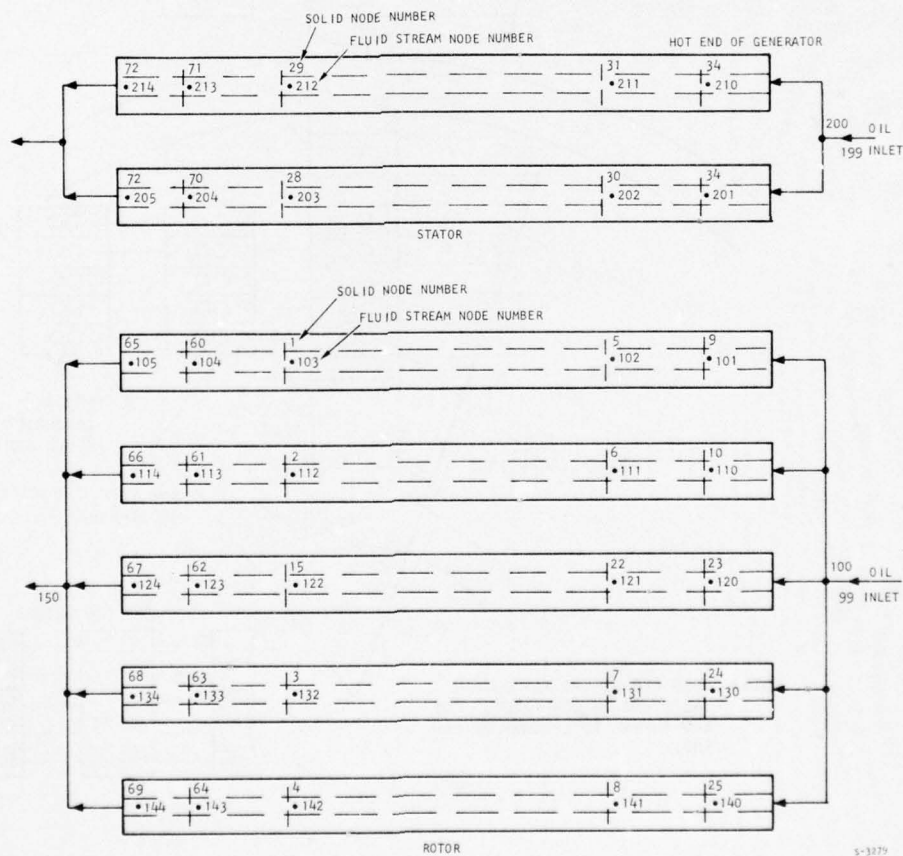


Figure 64. Coolant Oil Flow Paths

AD-A032 634

AIRESEARCH MFG CO OF CALIFORNIA TORRANCE
HIGH POWER STUDY--CONVENTIONAL GENERATORS, SUPERCONDUCTING GENE--ETC(U)
JUL 76 L SCHIPPER
76-12446

F/G 10/2

F33615-75-C-2071

UNCLASSIFIED

AFAPL-TR-76-39

NL

3 OF 5
AD
A032634



A summary of the results obtained from the independent thermal analysis is presented in Table 49.

The results indicate that after 3 cycles of operation consisting of 3-power-on periods and 2 power-off periods, the maximum winding temperature will be 398°F. This temperature will prevail at nodes 66, 67, and 68, which are the rotor end section conductors at the coolant outlet end of the generator (refer to Figures 62 and 63). Other temperatures within the rotor and stator are briefly summarized in Table 49 and in Figure 65. Due to centrifugal action, the oil entering the rotor conductors will reach a maximum pressure of 2052 psia and temperature of 242 F. The flow stream results also are summarized in Table 49. The independent thermal analysis and the thermal subroutine incorporated into the generator design program indicate that the temperatures and coolant data compare most favorably, thus verifying the accuracy of the thermal part of the generator design program.

Coolant Selection

An important consideration in the hollow-conductor, fluid-cooled, round-rotor generator design is the selection of a suitable coolant fluid. The important fluid dynamic and thermal properties for coolant selection are (1) high fluid thermal capacity rate as explained in the following paragraph, and (2) low viscosity to minimize flow frictional losses and minimize the pumping power required to recirculate the coolant. The high fluid thermal capacity rate indicates that the selected fluid should have both high density and high specific heat. For compatibility with the electric generator, the selected fluid also must have good dielectric strength.

In the round-rotor fluid-cooled design, the coolant flows at high velocity through the entire length of each conductor. At this high velocity, the temperature difference between the fluid and the conductor at any point becomes small, but the temperature rise of the coolant flowing through the conductors is large. Therefore, the temperature rise of the conductors is more affected by the fluid thermal capacity rate than the convection heat transfer between the conductor and the coolant. For this reason, the most desirable fluid passage configuration in the conductor is one that produces a minimum wetted perimeter for a given cross-sectional area, such as a single circular hole. This results in a minimum flow friction loss for high-velocity fluid flow in the conductor.

TABLE 49

SUMMARY OF RESULTS OBTAINED FROM
THERMAL ANALYZER PROGRAM H0298

Node	Temperature, °F	Node	Temperature, °F
12	340	44	161
15	359	46	267
16	293	49	175
21	179	50	159
22	334	51	299
23	332	52	130
27	158	56	189
28	328	58	187
30	318	62	395
32	281	67	398
34	317	70	343
35	376	72	344
37	198		
		<u>Rotor</u>	<u>Stator</u>
Generator supply oil temperature, °F		230	230
Conductor inlet oil temperature, °F		242	230
Conductor outlet oil temperature, °F		334	265
Generator supply oil pressure, psia		200	200
Conductor inlet oil pressure, psia		2052	193
Conductor outlet oil pressure, psia		1941	49
Note: Results are given for 63 sec of operation.			

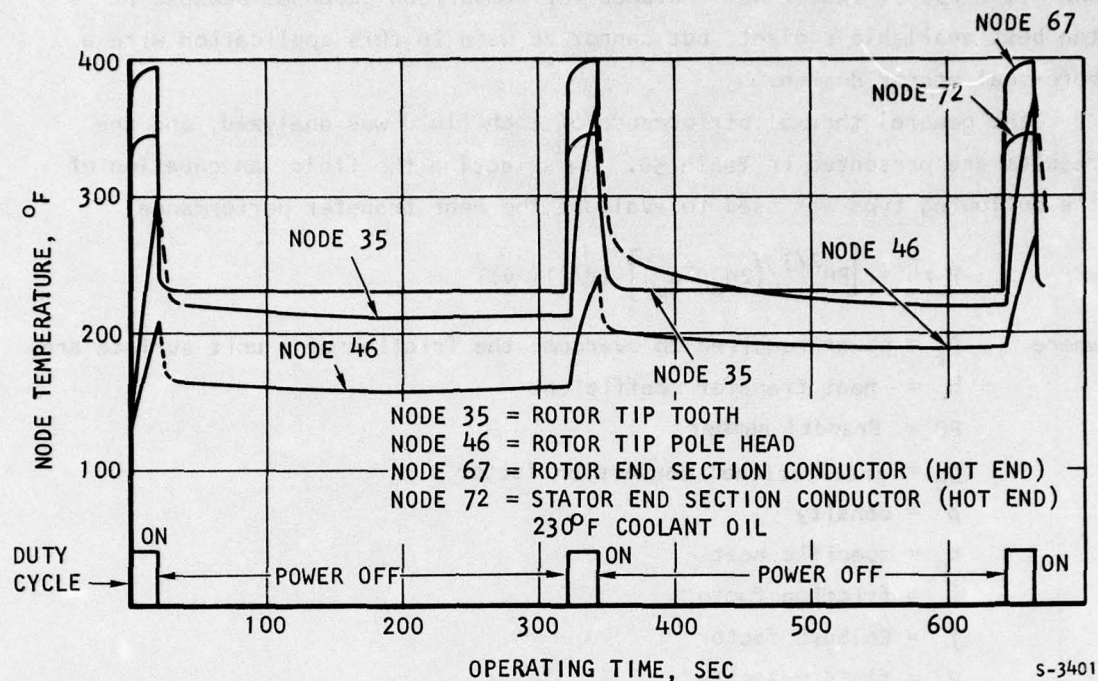


Figure 65. Generator Transient Temperatures

Most dielectric oils have a low specific heat and high viscosity, making them nonoptimum coolants for this type of design. Cryogenic fluids such as liquid nitrogen or argon might be considered, if it is desirable to have the conductors very cold to increase their electrical conductivity or thermal capacitance in a high-power-level pulsed operation. Water cooling is preferred for high-current-density continuous operation, because it provides the highest thermal capacity rate through the conductors with the least pressure drop. Unfortunately, the flow-cooled stator with a bore seal cannot use water as the coolant because moisture must be completely excluded from the dielectric fluid to prevent hydrolysis of the insulation.

A parametric thermal study was conducted to compare candidate coolants for the generator cooling fluid. The coolants evaluated were water, FC-75, Coolanol 45 (OS-139), DC 331, GESF 1148, DC200, Transil Oil 10-C, MIL-L-7808,

and MIL-L-23699. Water was included for comparison purposes because it is the best available coolant, but cannot be used in this application with a bore-seal stator design.

The general thermal performance of each fluid was analyzed, and the results are presented in Table 50. In selecting the fluid, an equation of the following type was used to evaluate the heat transfer performance:

$$P_f/h = \left[PR^{2/3} / (2g_c \rho^2 c_p) \right] (f/j) (\rho v)^2$$

where P_f = power required to overcome the friction of a unit surface area
 h = heat transfer coefficient
 PR = Prandtl number
 g_c = gravitational conversion factor
 ρ = density
 c_p = specific heat
 f = friction factor
 j = Colburn factor
 v = fluid velocity

The best heat transfer fluid will have the lowest (P_f/h) value. The (P_f/h) values of the fluids presented herein have been compared with water.

Based on characteristics shown in Table 50, several fluids were selected for further evaluation. These fluids were water, FC-75, Coolanol-45 (OS-139), DC-200, and MIL-L-23699. A comparison of these fluids in a 25-MW alternator design with various duty cycle operating conditions showed FC-75 requires about 7 times the pumping horsepower of water for equivalent cooling. Also DC 200 and OS-139 require about 11 to 12 times the pumping power of water for equivalent cooling. The MIL-L-23699 turbine lubricating oil requires about 40 to 50 times the pumping horsepower of water for equivalent cooling. These studies confirmed the simple coolant selection relationship presented above.

From consideration of the thermal stability, dielectric strength, vapor pressure, corrosion, and cooling capabilities, three fluids (DC-200, OS-139, and MIL-L-23699) were selected for coolants in the final generator design. Of these three coolants, DC-200 has the best properties and is like typical transformer oils. The other possible coolant (MIL-L-323699) has the advantage

TABLE 50

BASIC PROPERTIES OF CANDIDATE COOLANTS

Fluid	Density, lb/cu ft	Specific Heat, Btu/lb-°F	Thermal Conductivity, Btu/ft-hr-°F	Viscosity, lb/ft-sec	Dielectric Strength, volts/mil	ρ_f/h
Water	100 F-62.0		100 F-0.364	100 F-0.458 x 10 ⁻³		
	150 F-61.2	1.0	150 F-0.384	150 F-0.292 x 10 ⁻³		1.0
	200 F-60.1		200 F-0.394	200 F-0.205 x 10 ⁻³		
FC-75	100 F-108	100 F-0.251	100 F-0.078	100 F-0.74 x 10 ⁻³		
	150 F-104	150 F-0.264	150 F-0.074	150 F-0.56 x 10 ⁻³	77 F-550	7.4
	200 F-100	200 F-0.275	200 F-0.071	200 F-0.38 x 10 ⁻³		
Coolanol-45	200 F-50	200 F-0.513	200 F-0.0752	200 F-0.00205	185 F-180	17.5
Silicone oil DC 331	100 F-57.8	100 F-0.43	100 F-0.076	100 F-0.0050		
	150 F-56.2	150 F-0.438	150 F-0.075	150 F-0.0032	77 F-780	20.4
	200 F-54.7	200 F-0.447	200 F-0.071	200 F-0.00222		
Silicone oil GESF 1148	100 F-56.4	100 F-0.440	100 F-0.111	100 F-0.026		
	150 F-55.2	150 F-0.444	150 F-0.106	150 F-0.012	77 F-435	32.3
	200 F-54.1	200 F-0.457	200 F-0.101	200 F-0.0064		
Silicone oil DC 200 2 CS	100 F-54.4	100 F-0.434	100 F-0.062	100 F-0.00098		
	150 F-52.6	150 F-0.446	150 F-0.061	150 F-0.00073	77 F-350	11.2
	200 F-51.0	200 F-0.457	200 F-0.06	200 F-0.00056		
Transil oil 10-C	100 F-54.3	100 F-0.446	100 F-0.078	100 F-0.00555		
	150 F-53.2	150 F-0.474	150 F-0.0775	150 F-0.00264	70 F-300	11.9
	200 F-52.1	200 F-0.502	200 F-0.077	200 F-0.0012		
MIL-L-7808	100 F-57	100 F-0.471	100 F-0.0859	100 F-0.00564		
	150 F-55.75	150 F-0.491	150 F-0.0847	150 F-0.00405		17.6
	200 F-54.5	200 F-0.512	200 F-0.0823	200 F-0.00227		
MIL-L-23699	100 F-61.58	100 F-0.447	100 F-0.0858	100 F-0.01822		
	150 F-60.27	150 F-0.464	150 F-0.084	150 F-0.007203		24.4
	200 F-58.95	200 F-0.481	200 F-0.0823	200 F-0.00363		

of also being a good lubricant for the bearings, gearbox, and turbine so that its use would require only one fluid for cooling and lubricating the system.

Cooling System

To make a valid comparison of the thermal-lag and fluid-cooled generators, it is necessary to assess the penalties associated with the use of the cooling system required by the fluid-cooled machine. A schematic diagram of the cooling system selected for use by the fluid-cooled generator is shown in Figure 66.

1. Description

The cooling system is of the recirculation type using water as an evaporative heat sink. Coolant is recirculated in a closed loop by an electric-motor-driven pump. The heat absorbed by the coolant in the generator is transferred to the water in the boiler. This causes the water to evaporate; the latent heat of vaporization of the water is used to remove the heat absorbed. The steam generated in the boiler is dumped overboard through a control valve that regulates the boiling pressure and, hence, temperature. For calculation purposes in this study, a boiling pressure slightly above sea level ambient was assumed.

A water blow-down reservoir is used to maintain required water level in the boiler. By adjusting the tank size, sufficient water can be carried for any mission. Use of water as the generator heat sink provides appropriate aircraft-independent operation.

The coolant loop utilizes a reservoir/accumulator to accommodate differential thermal expansion of the coolant in the closed recirculation loop.

2. System Wet Weight

Figure 67 shows the weight of the cooling system as a function of the generator power level, efficiency of the generator, and the operating duration. This weight includes the water boiler, recirculation pump and motor, coolant reservoir/accumulator, water tank, control valve, plumbing, structure, coolant inventory, and water inventory.

3. Coolant Pump and Motor

Figure 68 presents the coolant flow rate, coolant pump and motor weight, and coolant pump motor input power required as a function of generator output

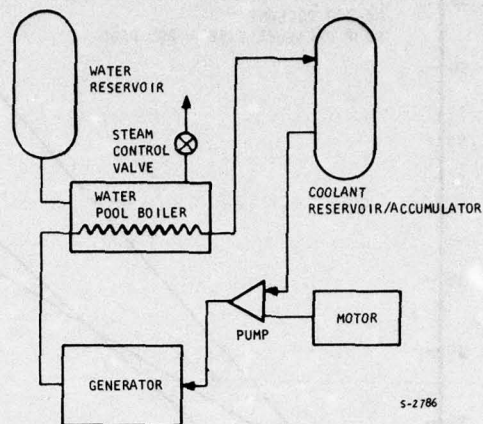


Figure 66. Cooling System Schematic Diagram

DC-200 COOLANT

P = GENERATOR OUTPUT POWER, MW

 η = GENERATOR EFFICIENCY, PERCENT

n = NUMBER OF POWER PULSES DURING MISSION

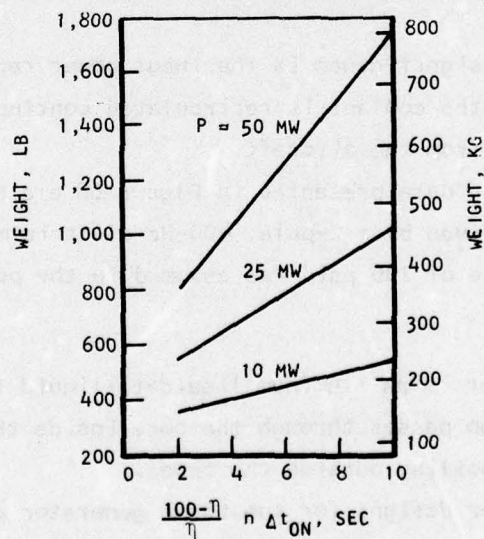
 Δt_{ON} = DURATION OF A SINGLE POWER PULSE, SEC

Figure 67. Cooling System Weight vs Generator Power Level, Efficiency, and Operating Duration

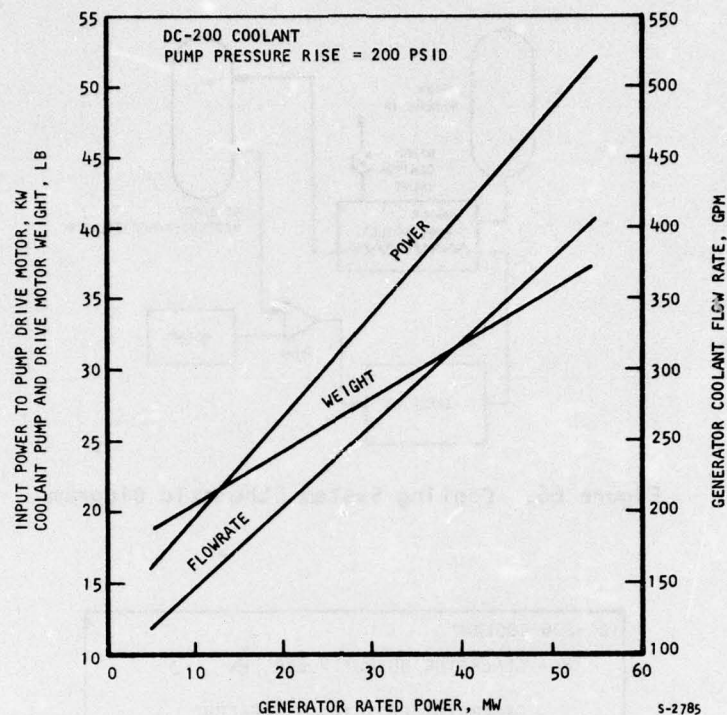


Figure 68. Power, Weight and Flow Rate of Coolant Pump and Motor as a Function of Generator Power Level

power. The item of significance is the input power required to the pump's electric motor. If the coolant is recirculated continuously, this power will have to be supplied from the aircraft.

The coolant pump data presented in Figure 68 are based on a centrifugal impeller directly driven by a 2-pole, 400-Hz electric motor at 23,400 rpm. A coolant pressure rise of 200 psid was assumed in the pump with DC-200 coolant.

4. Water Boiler

The water boiler is an aluminum liquid-to-liquid tubular heat exchanger. The coolant makes two passes through the core inside the tubes. The water is evaporated by pool boiling outside the tubes.

The water boiler designs for the three generator power levels corresponding to the design points 1 through 8 are summarized in Table 51. These designs are based on the performance of an existing water boiler used in the

TABLE 51

WATER BOILER DESIGN SUMMARY

Generator Power Level, MW	10	25	50
Coolant	DC-200	DC-200	DC-200
Coolant flow rate, gpm	147.7	228.3	378.6
Heat load, kW	870	1873	3262
Coolant pressure drop, psid	52	52	52
Dry boiler weight, lb	31.6	48.8	80.9
Coolant inventory, lb	10.5	16.2	26.8
Water inventory, lb	51.8	80.1	132.8
Water use rate, lb/min	60.1	129.2	225.0
Coolant flow length, in.	32.0	32.0	32.0
Water flow length, in.	7.8	7.8	7.8
No-flow length, in.	8.1	12.5	20.7

TLRV application. Basically, the heat exchanger sizing for the present application involved scaling the no-flow dimension to meet the heat load and flow rate requirements.

MECHANICAL AND STRUCTURAL DESIGN

The design of a successful high-power, lightweight electrical generator depends on good mechanical and structural design as well as good electro-magnetic design. A successful mechanical and structural design requires close attention to the interrelationships of many factors. The most important of these factors as well as the AiResearch design philosophy in attaining the high-power, lightweight generator objectives are discussed in the following paragraphs.

Stress Considerations

Critical stresses in the rotor and stator structures are usually combinations of the following loads:

- (a) Centrifugal stresses due to rotation (rotor)
- (b) Thermal stresses due to nonuniform temperature distribution (rotor and stator)
- (c) Stresses induced by cooling fluid pressure (rotor and stator)
- (d) Assembly stresses due to shrink or force fits and initial tightening, etc. (rotor and stator)
- (e) Stresses due to externally induced loads such as shock and vibration environments, etc. (rotor and stator)
- (f) Stresses due to electromagnetically induced loads (rotor and stator)

Thorough structural design analyses must include all of the preceding effects in determining and designing for adequate margins of safety on yield and fatigue life. In addition, in assessing the total deflections to be expected by the rotor, the static and dynamic parts of the structure must be evaluated to determine: (1) the structural spring rates of stator end bell, bearings, and bearing mounts to avoid resonant vibrations and rotor critical speeds; and (2) the structural spring rates to maintain rotor-stator air gaps, thus avoiding transient physical interference.

The two principal elements of the generator are the stator and rotor. Factors important in the design of each are discussed in the following paragraph.

1. Stator Design

The stator makes up a very substantial portion of the generator weight; consequently, great care should be exercised in the design phase to ensure a lightweight structure. Typically, for fluid-cooled stators, the support structure will be in the form of concentric cylindrical shells with end caps. Aluminum, titanium, or composite materials may be used for the outer shell and the end caps, with aluminum oxide being the primary choice for the inner cylinder. Loads that are important are those caused by coolant fluid pressure, and those due to thermal and environmental effects. The structure may be designed as a pressure vessel for initial sizing with modification to

accept the other loads. The end cap design is particularly important as the end caps also form the bearing housing. The interaction of unbalance in the rotor and the stiffness of the stator structure must be carefully assessed; otherwise, undesirable critical speed problems may arise.

2. Rotor Design

Rotor stresses are primarily induced by rotation. The centrifugal stress is proportional to the square of the speed, and there is obviously a limit at which mechanical failure occurs. High tip speeds are, therefore, realized for any rotor design only after very careful analysis of individual design. Fast startup requirements introduce additional stresses in the rotor, particularly in the teeth, copper coil end turns, and the end shaft. Secondary stresses that must be included in the analysis are those caused by thermal gradients and stress amplifications caused by discontinuities at the rotor slots and by localized conductor loads.

In rotors of the type investigated, there is an additional stress consideration associated with the end ring or hoop retainer shrunk over the rotor to carry the radial load of rotor end turns. It is the largest diameter component in the rotor and thus subject to the highest centrifugal stresses. Radial growth of these rings can cause reduction in air gap or possible rotor rub, slippage of the rings with respect to the rotor, and high bending stresses in the coil end turns, which may eventually induce coil failure. The end rings, therefore, are critical parts of the rotor and can impose limitations on design speed. High material strength-to-weight ratio is required to reduce centrifugal loading; high elastic modulus helps to reduce deflection under load. Candidate materials include titanium alloys, Inconel 718, or stainless steel and various filament bonding ring materials including Kevlar, graphite, and S-glass. Banding tape and ring designs with loads similar to those predicted for the reference alternator designs have been proven in the AiResearch state-of-the-art car (SOAC) program.

The other major consideration in the design of high-speed generator rotors is the general one of rotor dynamics and critical speeds. Such treatment is common to all rotating equipment built by AiResearch, and extensive and diverse experience has been accumulated in these areas confirming the analytical techniques developed. In general, it is desirable to operate the

rotor below the first critical speed, thereby avoiding potential problems. This is achieved by the combination of rotor mass and shaft geometry, primarily, with the bearing housing and support structure playing important secondary roles. Due to geometric and other design considerations, it is often not practical to operate below critical speeds. This is the case in the present study where the quest for lowest weight produces machines of high length-to-diameter ratio (minimum weight at maximum permissible motor peripheral rotational speeds).

Structural Analysis

It was beyond the scope of the study to prepare detail designs of the generators at all eight design points and for both the thermal-lag and fluid-cooled machines; however, to be confident that the machine designs obtained in this study could be built and were structurally sound, two representative designs were investigated in some detail. These two designs are:

- (a) 25-MW thermal-lag generator with duty cycle specified by design point 6 (see Drawing L2106296 in Section 3 for a cross-sectional view of this machine).
- (b) 25-MW DC-200 fluid-cooled generator fulfilling the duty cycle requirements of design points 3, 4, 5, and 6 (see Drawing L2016297 in Section 3 for a cross-sectional view of this machine).

Careful consideration was given to the selection of materials and fabrication and assembly techniques. Materials were selected to be compatible with the construction forms of the elements of the machine while simultaneously possessing those properties that produce a lightweight generator. Some of the representative materials investigated and their pertinent physical properties are presented in Table 52. Included are both magnetic and structural materials having high strength-to-weight ratio and high elastic modulus including several promising fibrous composites.

Table 53 presents the materials parts list for the two generators. This table lists the materials selected for use in the major machine elements. All the materials listed have been used in previous AiResearch designs and have been thoroughly characterized in such areas as optimum heat treatment, weldability, machinability, etc. This includes the advanced composite materials

TABLE 52

REPRESENTATIVE MATERIALS FOR HIGH-POWER ALTERNATOR STUDY

Material Designation	F_{tu} , ksi	F_{ty} , ksi	Elong, percent	ρ Density, lb/cu in.	Modulus of Elasticity, psi $\times 10^{-6}$	$\frac{F_{tu}}{\rho}$ in. $\times 10^{-3}$	Component
Inconel 718	180	150	12	0.297	29.6	605	Hoop ring non-magnetic structure
Alloy steel HP 9-4-20	190	175	12	0.28	28.8	678	Rotor, stator magnetic structure
Alloy steel HP 9-4-30	220	185	10	0.28	28.3	785	Rotor, static magnetic structure
Titanium alloy 6 Al-4V solution-treated and aged	160	145	8	0.16	16.0	1000	Hoop ring, non-magnetic structure
Fiberglass-epoxy S994 Glass, (V/o ~ 60)	200	-	1	0.07	7	2860	Hoop ring
Boron-epoxy (V/o ~ 60)	180	-	0.03	0.07	20	2570	Hoop ring
Graphite-epoxy (V/o ~ 55)	180	-	0.03	0.06	22	3000	Hoop ring
Kevlar/epoxy	210	-	1.7	0.051	12	4200	Hoop ring

used in the rotor end rings of the thermal-lag generator. For example, the fiberglass-epoxy has been used by AiResearch as a hoop ring to restrain the rotor coil end turns in a 600-hp, 4300-rpm dc traction motor for railroad use.

Table 54 summarizes the stresses calculated at critical locations in the generator. As can be seen, the stresses at these locations are below the allowable stresses by a considerable amount, providing a substantial margin of safety.

Bearings

Numerous bearing arrangements are possible for machinery of the size and weight of the present application. The choice depends upon desired life, environmental loading, desired lubrication system, and critical speed considerations. The solutions to bearing design usually include one of the following approaches:

TABLE 53

MATERIALS PARTS LIST
25-MW OUTPUT; 3 PULSES; 21 SEC ON; 300 SEC OFF

Machine Element	Material	
	Thermal Lag	Fluid Cooled
Stator lamination	2V-Permendur	2V-Permendur
Stator housing	6061 Al	6061 Al
End bells	A356 Al	A356 Al
Stator conductor	Cu, CDA 102	Cu, CDA 102
Stator conductor insulation	Class H, epoxy-mica	Class H, epoxy-mica
Rotor core	HP9-4-20 steel	HP9-4-20 steel
Rotor conductor	Cu, CDA 102	Cu, CDA 102
Rotor end rings	Fiber-epoxy	Inconel 718
Rotor insulation	Hard mica splitting	Hard mica splitting
Coil blocking/bracing	Epoxy	Epoxy
Stator stack retainer	6061 Al	6061 Al

TABLE 54

STRUCTURAL ANALYSIS SUMMARY
25-MW OUTPUT; 3 PULSES; 21 SEC ON; 300 SEC OFF

Part Name	Thermal Lag		Fluid Cooled	
	Characteristic	Allowable	Characteristic	Allowable
Coil retaining wedge	Compressive stress 93,849 psi	150,000 psi	Compressive stress 71,331 psi	150,000 psi
Slot	Cyclic stress 30,950 psi	94,000 psi	Cyclic stress 12,597 psi	94,000 psi
Field conductor	Contact stress 8,838 psi	10,000 psi	Contact stress 3,412 psi	10,000 psi
End rings	Hoop stress 114,210 psi	203,000 psi	Hoop stress 117,340 psi	150,000 psi

- (a) Roller bearing at one rotor end with a preloaded tandem set of angular contact bearings at the other rotor end to handle thrust loads
- (b) Roller bearings at both rotor ends with a double-acting hydrodynamic thrust bearing at one rotor end
- (c) Angular-contact bearings at each rotor end
- (d) Floating-sleeve journal bearings plus a double-acting hydrodynamic bearing at one rotor end

All four configurations of bearings have seen extensive use at AiResearch in many different rotating groups. Configuration (a) has been tentatively selected for use in the high-power generators; however, a more thorough analysis of the system dynamics may show that another configuration is superior. The selection of configuration (a) was based on engineering judgement and experience in the design of similar types of machines.

Configurations (a) through (c) are the usual solutions to alternator bearing requirements due to the relatively straightforward engineering required to develop satisfactory solutions. Extensive background experience is available both in alternator design and turbomachinery design to allow confident prediction of workable design configurations. Usually, such bearings setups are mounted in resilient mounts to allow the unit to pass more easily through critical speed regions.

Configuration (d) is the bearing solution used on AiResearch turbochargers for diesel engine supercharging. The typical turbocharger runs at speeds up to 100,000 rpm, well above the first solid-body mode and flexural resonances. The floating sleeve provides hydraulic damping to permit excursions through the critical speed and minimize hydraulic power losses in the bearings over straight journals. They are also very inexpensive in large-quantity production. Development programs to qualify the designs tend to be more expensive than for antifriction bearings.

Lubrication of bearings generally depends on the service required. For long life and reliable performance, some method of forcing oil through the bearings is required. Whether this is achieved by jet lubrication or wick lubrication is optional. Good design practice requires that both races be kept reasonably cool, either with the lubricant or by suitable mounting.

In certain applications, grease-pack bearings perform very satisfactorily provided rotational speeds, or more accurately, the product of rotational speed (in rpm) and the inner diameter (in mm) is kept to a reasonable value. By engineering judgement, a value of 300,000 to 400,000 is desirable, but values in excess of 1,000,000 have been used successfully in special applications.

Critical Speed Analysis

Critical speeds of the generator rotors are of concern due to the unusually high length-to-diameter ratio (L/D) possessed by many of the conventional generator point designs. Consequently, a critical speed analysis was conducted to ensure that a suitable design could be obtained for all point designs. The details of this analysis are reproduced in Appendix B. The result of this analysis is confirmation that the generators can be designed with high length-to-diameter ratios (high-speed rotors) with operating speeds at least 20 percent away from the nearest critical speed; however, for most point designs, two critical speeds must be traversed to reach the generator operating speed. This indicates that during the detailed design of the high-power generator, engineering analysis must be exercised to achieve a successful machine design free of critical speed problems.

The geometric configuration assumed for the rotor in the critical speed analysis was a hollow right-circular cylinder of outer diameter D , inner diameter $0.46D$, and length L with stub shafts at each end for bearing support. Bearings with spring rates ranging from 800,000 lb/in. (soft) to 1,500,000 lb/in. (stiff) were investigated with both rigid mounts* and resilient mounts. The resilient mount spring rates investigated ranged from 100,000 lb/in. (soft) to 400,000 lb/in. (stiff). By varying the combinations of bearing stiffness and mount resilience, the effective spring rate of the complete dynamic system (rotor, stub shaft, bearing and bearing mount) can be modulated over a wide range. This, in turn, results in the ability to shift the critical speeds of the rotor such that they do not occur near the operating speed by proper selection of the bearings and bearing mounts.

* Rigid implies stiff in comparison to the bearing, not necessarily infinitely stiff. A bearing mount of high stiffness can be attained by making the bearing housing an integral part of the generator support structure.

Table 55 shows the generator rotor critical speeds estimated for all conventional generator point designs with four combinations of bearing stiffness and bearing mounts. Comparing the operating speed to the critical speeds for each bearing and mount combination allows the proper combination to be selected. The critical speeds, operating speeds and selected combination of bearing and mount are presented in Table 55. Notice that the first free body mode does not depend upon the bearing or bearing mounts and, consequently, can only be shifted by changing the geometry of the rotor.

For example, the thermal-lag generator rotor for point design 6 has an outside diameter $D = 11.60$ in. and length $L = 83.07$ in. for an L/D of 7.16. The operating speed is 12,500 rpm. Referring to Table 6-10, the only bearing/mount combination that results in a critical speed near the operating speed is a medium stiffness bearing in a stiff resilient mount. For this combination the second flexural mode is 11,745 rpm, only 6 percent below the operating speed. This bearing/mount combination is to be avoided. The medium stiffness bearing in a soft resilient mount has the largest spread in the critical speeds about the operating speed; however, three critical speeds must be traversed to reach the operating speed. A stiff bearing in a rigid mount has a slightly smaller spread in the critical speeds about the operating speed, but requires only two critical speeds to be traversed. Therefore, the latter is the best choice.

Table 55 shows that all generator designs must accelerate the rotor through the first critical speed during startup and most must also traverse the second critical speed. Although traversing these critical speeds during startup is not anticipated as a problem due to the rapid starting capability of the turbogenerator, it must be kept in mind during future design activities. Detailed critical speed analyses must be part of the detail generator design to avoid unforeseen problems.

It must be realized that traversing several critical speeds is inherent in the design of a generator designed for minimum weight achieved by high rotational speed. As the quest for lower and lower weight is pursued by going to higher and higher rotational speeds, more sophisticated rotating systems must be designed. For example, provisions may have to be made for hydraulic damping around the bearings to limit shaft deflections and consequent bearing

TABLE 55

**CRITICAL SPEED SUMMARY
HIGH-POWER CONVENTIONAL GENERATORS**

Point Design	Cooling Method	Bearing Stiffness	Bearing Mount	Generator Rotor Critical Speeds, RPM				Operating Speed, rpm	Selected Bearing and Mount Combination
				First Rigid Body and First Flexural Modes	Second Rigid Body Mode	Second Flexural Mode	First Free Body Mode		
1 and 2	Fluid cooled	Medium Medium Soft Stiff	Soft resilient Stiff resilient Rigid Rigid	3,308 4,887 7,040 7,959	6,566 9,729 13,542 15,027	13,232 19,548 28,162 31,837	60,738 60,738 60,738 60,738	14,000	Medium stiffness bearing in a stiff resilient mount
3, 4, 5 and 6	Fluid cooled	Medium Medium Soft Stiff	Soft resilient Stiff resilient Rigid Rigid	2,118 3,344 4,333 4,953	3,855 5,896 7,792 8,860	8,470 13,377 17,332 19,812	17,216 17,216 17,216 17,216	12,500	Soft bearing in a rigid mount
7 and 8	Fluid cooled	Medium Medium Soft Stiff	Soft resilient Stiff resilient Rigid Rigid	1,430 2,280 3,150 3,691	2,518 4,030 5,445 6,501	5,720 9,121 12,599 14,765	11,404 11,404 11,404 11,404	9,500	Soft bearing in a rigid mount
1	Thermal lag	Medium Medium Soft Stiff	Soft resilient Stiff resilient Rigid Rigid	2,741 4,316 5,524 7,407	5,374 8,511 10,825 13,846	10,966 17,263 22,095 29,630	52,962 52,962 52,962 52,962	14,000	Medium stiffness bearing in a stiff resilient mount
2	Thermal lag	Medium Medium Soft Stiff	Soft resilient Stiff resilient Rigid Rigid	2,804 4,419 5,659 7,628	5,522 8,751 11,133 14,288	11,215 17,675 22,634 30,512	58,403 58,403 58,403 58,403	14,000	Medium stiffness bearing in a stiff resilient mount
3	Thermal lag	Medium Medium Soft Stiff	Soft resilient Stiff resilient Rigid Rigid	1,758 2,774 3,646 4,452	3,155 5,078 6,822 7,951	7,031 11,096 14,584 17,809	15,146 15,146 15,146 15,146	12,500	Stiff bearing in a rigid mount
4	Thermal lag	Medium Medium Soft Stiff	Soft resilient Stiff resilient Rigid Rigid	1,610 2,857 4,300 5,432	3,077 5,493 8,195 10,442	6,439 11,427 17,200 21,730	68,998 68,998 68,998 68,998	8,500	Stiff bearing in a rigid mount
5	Thermal lag	Medium Medium Soft Stiff	Soft resilient Stiff resilient Rigid Rigid	1,765 2,787 3,664 4,480	3,171 5,106 6,865 8,005	7,060 11,147 14,654 17,918	15,343 15,343 15,343 15,343	12,500	Stiff bearing in a rigid mount
6	Thermal lag	Medium Medium Soft Stiff	Soft resilient Stiff resilient Rigid Rigid	1,852 2,936 3,872 4,806	3,368 5,449 7,379 8,642	7,406 11,745 15,486 19,222	17,883 17,883 17,883 17,883	12,500	Stiff bearing in a rigid mount
7	Thermal lag	Medium Medium Soft Stiff	Soft resilient Stiff resilient Rigid Rigid	1,326 2,228 3,152 3,691	2,437 4,118 5,852 7,140	5,304 8,912 12,608 14,764	17,373 17,373 17,373 17,373	9,500	Soft bearing in a rigid mount
8	Thermal lag	Medium Medium Soft Stiff	Soft resilient Stiff resilient Rigid Rigid	1,224 2,031 2,843 3,350	2,210 3,698 5,199 6,303	4,895 8,122 11,371 13,321	13,191 13,191 13,191 13,191	9,500	Stiff bearing in a rigid mount

loads. The analyses of critical speed problems, mode shape, and response characteristics requires elaborate analytical techniques (which were beyond the scope of the present study) mixed with mature engineering judgement.

Shutdown may be a more serious problem than startup. Due to the traversing of several critical speeds, a slow coastdown of the generator is not advisable. Positive braking capability of the turbogenerator rotating group may be necessary to avoid problems. In addition, because most mission duty cycles are pulsed operation, it may be necessary to speed-regulate the rotating assembly so coastdown near a critical speed does not occur between pulses.

ALGORITHMS

Simple mathematical algorithms have been developed for the generator, exciter, and cooling system. These algorithms are based on the point designs presented previously, and depend only on the generator output power level, generator efficiency, and duty cycle.

Linear regression by the method of least squares was used to obtain the algorithms presented. In the vast majority of cases, the coefficient of determination for these expressions exceeds 0.99, showing excellent agreement between the calculated result from the algorithm and the corresponding point-design result.

It should be understood that these algorithms are merely curve fitting expressions, and extending their use beyond the limits of the data used to obtain them will produce erroneous results. Therefore, these expressions should be used carefully outside the range of parametric values specified in the SOW.

The following definitions apply to all the algorithms presented in the subsequent paragraphs.

P = generator output power, MW

n = number of pulses

Δt_{ON} = duration of each pulse, sec

Δt_{OFF} = time between pulses, sec

$$\tau \equiv \left\{ \frac{n \Delta t_{ON}}{1 + \left[\frac{(n-1) \Delta t_{OFF}}{n \Delta t_{ON} + (n-1) \Delta t_{OFF}} \right]} \right\} = \text{effective ON time, sec}$$

Thermal-Lag Conventional Generators

Table 56 presents the algorithms for the thermal-lag conventional generators. Included are expressions for the alternator weight, diameter, length, rotational speed, dc voltage, efficiency, and rotor polar moment of inertia. The exciter weight, diameter, and length also are presented.

Notice that the thermal-lag generator designed at point design 4 does not conform to this table of algorithms. The algorithms presented result in a valid design at point design 4, but the resulting rotor has an operating speed above the first free body mode. It was arbitrarily decided to reduce the operating speed by inserting a gearbox between the turbine and generator to eliminate this situation.

Fluid-Cooled Conventional Generators

Table 57 presents the algorithms for the fluid-cooled (DC-200 fluid) conventional generators. Included are expressions for the alternator weight, diameter, length, rotational speed, dc voltage, efficiency, and rotor polar moment of inertia. The exciter weight, diameter, and length also are presented.

TABLE 56
THERMAL-LAG CONVENTIONAL GENERATOR ALGORITHMS

Parameter	Algorithm
WA, Alternator weight, lb	$WA = (-33.43 + 63.90 \ln \tau) P^{0.961}$
DA, Alternator diameter, in.	$DA = 13.27 \exp (0.010 P)$
LA, Alternator length, in.	$LA = (-0.612 + 27.69 \ln \tau) (-0.218 + 0.355 \ln P)$
WX, Exciter weight, lb	$WX = 22.47 + 5.248 P$
DX, Exciter diameter, in.	$DX = 8.600 \exp (0.010 P)$
LX, Exciter length, in.	$LX = 2.454 + 3.884 \ln P$
N, Rotational speed, rpm	$N = 15,209 - 113.3 P$
Vdc, dc voltage, V	$Vdc = (1700 + 519 \ln \tau) (0.665 + 0.0184 P)$
η , Efficiency, percent	$\eta = 100 - (1.0794 + 1.0583 \ln P) \exp (0.0043 \tau)$
I_p , Rotor inertia, in.-lb-sec ²	$I_p = (-3.845 + 7.248 \ln \tau) \exp (0.0576 P)$

TABLE 57
FLUID-COOLED CONVENTIONAL GENERATOR ALGORITHMS

Parameter	Algorithm
WA, Alternator weight, lb	$WA = 78.20 P^{1.116}$
DA, Alternator diameter, in.	$DA = 11.27 \exp (0.010 P)$
LA, Alternator length, in.	$LA = -59.86 + 47.06 \ln P$
WX, Exciter weight, lb	$WX = 78.00 + 7.682 P$
DX, Exciter diameter, in.	$DX = 7.435 \exp (0.010 P)$
LX, Exciter length, in.	$LX = 5.05 + 5.01 \ln P$
N, Rotational speed, rpm	$N = 15,209 - 113.3 P$
Vdc, dc voltage, V	$Vdc = 1794 + 55.54 P$
η , Efficiency, percent	$\eta = 89.28 + 1.153 \ln P$
I_p , Rotor inertia, in.-lb-sec ²	$I_p = 8.594 \exp (0.065 P)$

Cooling System

The algorithm for the cooling system is:

$$W = 130.0 P^{0.375} + 2.36 \frac{(100-\eta)}{\eta} n \Delta t_{ON}$$

where:

W = cooling system weight, lb

This weight includes the evaporative coolant, pool boiler, evaporant reservoir, coolant, coolant reservoir, recirculation pump, and associated plumbing with structure.

SECTION 7

SUPERCONDUCTING GENERATOR DESIGN CONSIDERATIONS AND TRADE STUDY

INTRODUCTION

This section describes the various design considerations involved in determining the optimal design of a high-power, lightweight superconducting electric generator. Parametric study results are also presented. For convenience, this section is subdivided as follows:

- Design considerations
- Selection of machine configuration
- Superconducting generator description
- Computer program
- Parametric studies
- Cooling system

SUMMARY

The trade studies conducted and machine layout drawings prepared establish the following guidelines with respect to high-power superconducting generators.

- (a) The selected superconducting generator concept consists of a rotating dewar containing the superconducting field with a stationary external armature. This concept was selected due to the compatibility of the present state of development with the time frame of the present application.
- (b) The superconducting generator concept preferred from the technical standpoint consists of a stationary dewar containing the superconducting field with a rotating external armature. This concept, however, is not compatible with the time frame of the present application.
- (c) A superconducting alternator design computer program based on the rotating-dewar, stationary-armature concept was prepared and provided to the Air Force.
- (d) There is an optimum rotational speed to obtain minimum weight at a given voltage level and power output.

- (e) Low-risk, high-flexibility designs are obtained at low voltage generator output.
- (f) The operating characteristics of the superconducting generator exclude fast-start capability. Continuous idling at operating speed is required.
- (g) Substantial dc power is required from an aircraft source to provide rapid charging of the superconducting field.
- (h) Logistics associated with superconducting generator airborne applications are complex and costly.
- (i) Efficient idle operation-to-power drive startup sequence remains to be demonstrated at the power levels of interest.

DESIGN CONSIDERATIONS

The major problems associated with the successful achievement of a superconducting generator design concept encompass the following key design considerations.

- (a) Efficient thermal design to (1) minimize heat leak, (2) obtain desired low temperature levels at low refrigerant consumption, and (3) avoid superconductor quenching problem
- (b) Rotating seal selection for pressure and temperature of the application
- (c) Refrigerant adiabatic temperature rise when a rotating superconducting field is used
- (d) Coil containment with displacement due to (1) thermal expansion, (2) electromagnetic forces, and/or (3) centrifugal forces (if located on rotor)
- (e) Rotor critical speed
- (f) Armature cooling for high-power-density capability
- (g) Large effective air gap due to (1) thermal provisions required for cryogenic field and (2) ironless armature and field
- (h) Rotor peripheral speed (stress limitations)
- (i) High magnetic shielding weight

Various means of avoiding, eliminating or minimizing these problems are subsequently discussed.

Thermal Design

Since the superconducting generator has a cryogenically cooled field and an ambient-temperature armature, very large temperature gradients exist within

the machine. Cryogenic refrigeration at liquid helium temperatures, whether it is provided by a closed-cycle refrigeration system or by helium used as an expendable material, is expensive in terms of both weight and cost. Consequently, for the superconducting generator to be advantageous, the machine must be carefully designed with respect to both the thermal and electrical factors that determine the cryogenic cooling load. Three factors that predominate in these considerations are: (1) heat leak into cryogenically cooled sections, (2) heat load due to electrical design factors, and (3) refrigerant utilization. Heat leak can be reduced by the use of (1) vacuum dewars, (2) cryogenically cooled radiation shields, (3) appropriate materials selection and (4) design to minimize heat conduction through supports, electrical loads, etc. The main electrical heat load will be due to eddy currents resulting from negative-sequence magnetic fields and other effects due to load imbalance, ripple voltages from rectifiers, etc. (the losses in the superconductor will be very small). The electrical heat load can be reduced by load balancing, filters, and shielding (in air gap, around end turns, or on the armature back). Refrigerant utilization is a function of the temperature levels for the required cooling effects. For example, poor refrigerant utilization is obtained if all of the waste heat must be dissipated at the lowest temperature level. Refrigerant utilization is improved by use of thermal or electrothermal heat shields and by use of a stationary field to avoid the adiabatic temperature rise obtained in a centrifugal or rotating field.

Mechanical Design

Mechanical design, which includes materials selection and stress analysis, is an important aspect of any design problem. Consideration must be given to materials selection and stress analysis to accommodate the electromagnetic forces obtained in the windings and the additional centrifugal forces where the windings are in a rotating element. In addition, the critical speeds will be an important factor for the rotor. In small generators, it is customary to design for operation below the first critical speed, while very large generators operate above the second critical speed. Critical speed can be controlled over a range by varying bearing span and/or rotor, bearing, and bearing mount stiffnesses. Stress analysis and proper structural design are particularly important for a superconducting generator because the iron used to provide the structure

in conventional machines is not available for this purpose (except for the backiron). In addition, much of this structure must be provided by nonmagnetic and/or nonconducting materials for proper electrical performance.

Electromagnetic Design

Superconducting fields are capable of supplying high flux densities above saturation for iron. Therefore, not much iron is used in the magnetic circuit (primarily for back shielding). This factor, combined with the space required for thermally isolating the superconducting field coils from the room temperature armature, leads to relatively large air gaps. Thus, the magnetic flux distribution will approximate that obtained in a free field, and the free-field flux distribution should be corrected for the effect of back shielding.

The armature windings are sized by considerations involving coil thickness and active length. Coil thickness is a function of the design output current and the current density, which is limited by cooling considerations. By use of an ironless armature in the superconducting generator, improved heat transfer is obtained; this permits use of air cooling at relatively high current densities. The highest current densities are obtained by liquid cooling of the conductors, the most effective method being flowing the fluid through hollow conductors. For large machine ratings and high peripheral speeds, the diameter is established by structural limitations. Therefore, the active length of the generator is primarily a function of the desired output power that can be obtained with the specific pole and structural configuration.

The optimum magnetic flux density and current density of the superconducting field depend upon the number of poles, coupling coefficient, energy stored in the field, rotational speed, and superconductor temperature. The armature current density is primarily a function of thermal design. Design constraints limiting the useable current and flux densities are imposed:

- (a) Maximum superconductor current density is set by temperature and flux density.
- (b) Configuration considerations limit maximum usable flux density to less than optimum for maximum power density.
- (c) Superconducting fields provide a flux density above the saturation limit of iron, eliminating iron from most of the magnetic circuit.
- (d) Relatively large effective air gap is unavoidable because of (1)

elimination of iron and (2) thermal provisions required for cryogenic cooling of superconducting field.

(e) Stress considerations limit rotor peripheral speed.

The tradeoffs between the field energy (W_f) and the coupling coefficient (k) are important in optimizing generator geometry for maximum power density or minimum specific weight. The coupling coefficient, which represents how well the field and armature are coupled, is:

$$k = \sqrt{\frac{M^2}{L_a L_f}}$$

where M = mutual inductance
 L_a = self inductance of armature winding
 L_f = self inductance of field winding

In general, the coupling coefficient decreases with an increase in the air gap, or in the number of poles. Other factors influencing this parameter include back shielding, coil geometry, magnetic flux density, current density, etc.

The energy stored in the field is:

$$W_f = \frac{1}{2} L_f I_f^2$$

where I_f = field current

W_f is limited by the critical current and critical flux density of the superconductor. The product of current and magnetic flux represents a superconductor merit factor for a superconducting generator.

Superconductor Characteristics

From the superconductor standpoint, an optimum design is obtained when a maximum field energy product (field flux times field current) is achieved. For a typical superconductor, this characteristic occurs at a flux density on the order of 60 kilogauss; however, configuration limitations restrict the maximum usable flux densities to lower values, on the order of 40 kilogauss. The design current density selected will be somewhat below the critical value to allow for inefficiencies in cooling and to allow a margin for transient and overload conditions.

Figure 69 shows that the field energy product is strongly sensitive to temperature. Since generator weight is proportional to this product, the importance of attaining the desired low temperature levels is evident. As mentioned previously, if the superconductor is contained in a rotating field it experiences a temperature rise in the rotor centrifugal field. This is illustrated by Figure 70, which shows the cryogenic helium temperature as a function of peripheral speed attained at the outermost radial point of the rotor.

Figure 70 indicates that the cryogenic helium temperature increases from 4.2 K to 5.2 K at a rotor peripheral speed of 500 ft/sec. This increase in superconductor temperature results in a decreased allowable field energy product, which is reflected in a superconducting generator weight increase. This increase in temperature also results in a loss in cryogenic helium cooling capacity, requiring increased refrigeration capability (either more helium or a higher-capacity closed-cycle refrigerator). Therefore, it is concluded that, from the standpoints of optimum superconductor performance and optimum refrigerant usage, field rotation is undesirable.

For a given superconductor formulation, the critical field/current characteristics vary with its form (wire gage, ribbon, number of superconductor filaments per strand, etc.). In general, smaller-gage superconductor wires should show superior stability under pulse-load conditions.

Superconducting Field Windings

Several important criteria must be met by the field windings:

- (a) They must have the highest possible current density to ensure a lightweight system.
- (b) They must be capable of rapid field changes (due to the load demands) without permanent loss of superconductivity.
- (c) They must be insulated to withstand voltages associated with field forcing.
- (d) They must be capable of being cooled, because there will be significant losses associated with rapid field changes and ripple fields not completely interrupted by the shield.
- (e) They must be well supported to avoid any winding motion under static or dynamic loads.

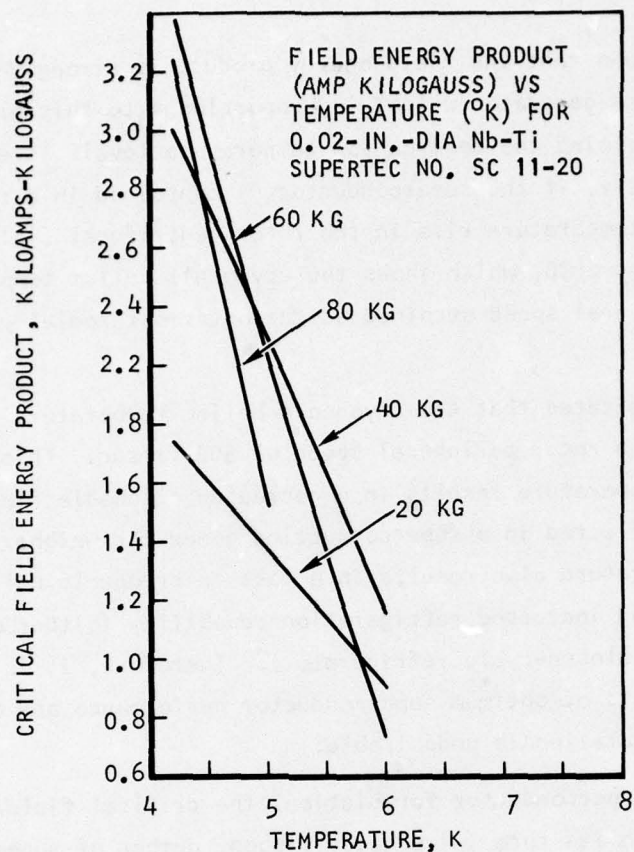
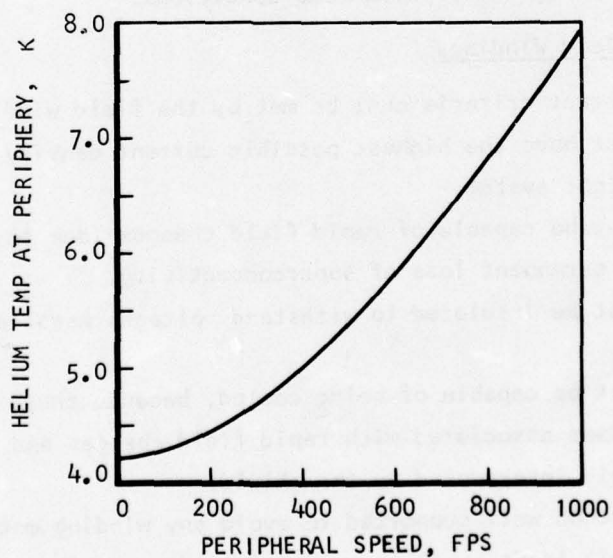


Figure 69. Typical Superconductor Wire Characteristics



S-3218

Figure 70. Helium Temperature Rise in Centrifugal Field

The field windings are heavily loaded magnetically, hence they are subject to vibrational force.

These conditions are identical in most respects to those required for the superconducting synchrotron magnets currently under development at many high-energy laboratories. It is possible to take advantage of that technology in considering the generator field winding.

Shielding

The negative sequence fields induced by armature load unbalance could induce eddy currents in the superconductor, greatly increasing the low-temperature cryogenic cooling load. A cryogenically cooled electrothermal shield will absorb these negative sequence fields at a somewhat higher temperature than the superconductor. If the shield is cooled to approximately 20 K, the eddy currents induced in the shield will provide a relatively small heat load because of the low resistivity of the shield (which will be either aluminum or copper). Other means of reducing the effect of negative sequence fields include use of back shields (either iron or copper), and the use of a metallic conducting (nonmagnetic) dewar wall. The latter will provide a portion of the shielding current. The magnet back shielding will have a significant effect on the voltage regulation characteristics of the generator. The shielding approach depends upon the type of generator design selected. For example, with a stationary generator field, the shielding (if it is also stationary) can be shaped in a cloverleaf pattern to provide the desired shielding at minimum weight. On the other hand, with a rotating field the shield must be of uniform thickness, and it must be thicker to accommodate the varying ac magnetic field produced by the rotating field. In addition, the shielding must use a stronger material with a lower permeability. Therefore, the shielding weight required for a rotating field will be considerably higher than that required with a stationary field.

Insulation

The space between the outer dewar shell and the electrothermal shield and the space between electrothermal shield and the superconducting coils must be evacuated for thermal isolation. These evacuated spaces may be filled with insulation or may remain void. The evacuated insulation schemes that can be

considered are:

Evacuated Fiberglass (Applicable for Nonrotating Dewars Only)--This insulation provides an effective thermal conductivity between normal ambient and liquid helium temperatures of approximately 0.000725 Btu/hr-ft-deg R. It can be employed to support the inner shell, is low-cost, and is simple to install.

Evacuated Multilayer Insulation (Applicable for Nonrotating Dewars Only)--Use of superinsulations such as aluminized Mylar or aluminum foil-fiberglass paper composites will provide an effective thermal conductivity of approximately 0.00014 Btu/hr-ft-deg R for this application. Installation requires great skill, resulting in relatively high cost; this cannot be used in load-bearing applications.

Vacuum Space with Discrete Radiation Shields (Applicable to Both Stationary and Rotating Dewars)--Using one or two shields, thermal performance intermediate to that of evacuated fiberglass and multilayer insulations can be obtained through this approach if effort is expended on achieving very low emissivity on all surfaces within the vacuum space; extreme care in surface preparation and handling procedures during fabrication is necessary.

Since these evacuated gaps must be of minimum thickness due to electrical considerations, the heat conducted across the gap by evacuated insulation may be greater than that radiated if low-emissivity coatings are applied.

Vacuum Seals

The use of a stationary vacuum vessel that is penetrated by rotating shafts has several serious disadvantages compared to designs in which the shafts penetrating the vacuum vessel are stationary relative to the vessel.

Perhaps the greatest drawback with a rotating vacuum seal is the consequence of its failure. Even in the presence of a leaky seal, the helium will maintain a high vacuum by cryopumping the air from the leak onto the coil and electrothermal shield. Thus, the only indication of a seal leak would be a slightly increased helium consumption rate. Frozen air will build up on the coil and shield until the rotor becomes badly unbalanced, forcing shutdown

of the generator, or until so much air accumulates on the rotor that liquid begins to form. This frozen air rapidly destroys the vacuum when it is thrown by the rotor to the outer shell. This causes the coil to go normal, and the accompanying heating will cause a rapid pressure rise in the vessel as the air vaporizes. Thus, the vessel must be equipped with a large relief valve.

Pumping the vessel will not alleviate this problem because the cryogenic rotor will pump more efficiently than any pump that could be attached to the vessel. Thus, leakage must be controlled by controlling the environment of the seals, rather than depending on the seals themselves.

This control is best attained by maintaining a guard vacuum outside the seals, and by placing a second set of seals between the guard vacuum and the air to reduce pumping requirements for the guard vacuum. To eliminate many vacuum system components and cold trap requirements when an active vacuum system is used, a permanently sealed guard vacuum is recommended. AiResearch has built many vacuum-insulated vessels designed for liquid helium service which use a permanently sealed vacuum. These vessels have been built to severe vibration, shock, and environment specifications, and have performed flawlessly for years after they were evacuated and sealed.

SELECTION OF MACHINE CONFIGURATION

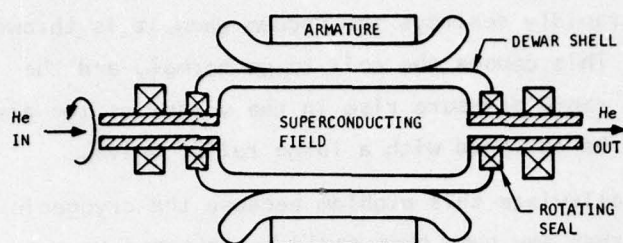
There are four basic superconducting generator configurations that can be employed. These variations all concern the method in which the liquid helium dewar is utilized and whether the field or armature rotates. These four design concepts are:

- (a) Stationary dewar, rotating superconducting field
- (b) Rotating dewar, rotating superconducting field
- (c) Stationary dewar and superconducting field, internal rotating armature
- (d) Stationary dewar and superconducting field, external rotating armature

These superconducting generator design concepts are illustrated in Figure 71.

Stationary-Dewar, Rotating-Field Concept

In the stationary-dewar rotating-field type of generator, a rotating superconducting field is contained in a dewar formed by a stationary outer wall and a rotating inner wall. This approach requires a rotating vacuum seal, which



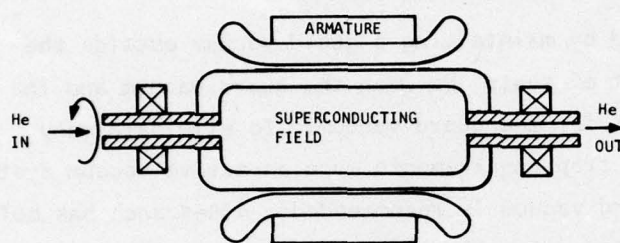
a. STATIONARY DEWAR, ROTATING FIELD

ADVANTAGES:

- STATIONARY DEWAR SHELL
- ZERO WINDAGE LOSSES

DISADVANTAGES:

- ROTATING VACUUM SEAL
- CONTINUOUS VACUUM PUMPING REQUIRED
- NONCONDUCTIVE DEWAR SHELL REQUIRED
- ADIABATIC TEMPERATURE RISE IN COOLING He



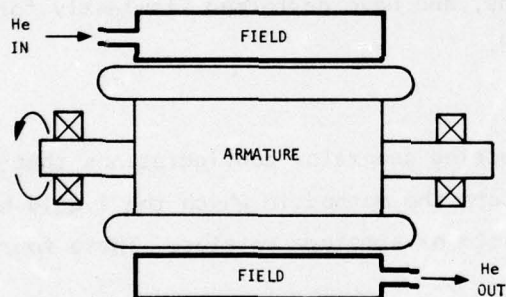
b. ROTATING DEWAR, ROTATING FIELD

ADVANTAGES:

- NO ROTATING VACUUM SEAL

DISADVANTAGES:

- DEWAR CENTRIFUGAL LOADS
- ADIABATIC TEMPERATURE RISE IN COOLING He



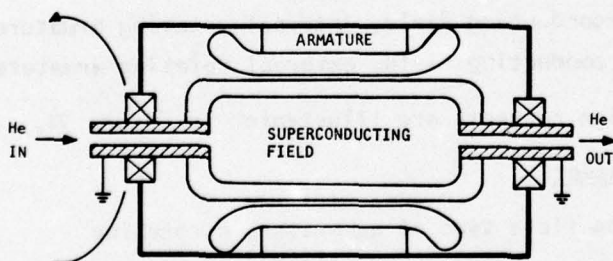
c. STATIONARY DEWAR AND FIELD, INTERNAL ROTATING ARMATURE

ADVANTAGES:

- STATIONARY DEWAR
- NO ROTATING He SEALS

DISADVANTAGES:

- ARMATURE COOLING DIFFICULT
- LARGE CRYOGENIC HEAT TRANSFER AREA



d. STATIONARY DEWAR AND FIELD, EXTERNAL ROTATING ARMATURE

ADVANTAGES:

- STATIONARY DEWAR
- NO ROTATING He SEALS

DISADVANTAGES:

- HIGH ROTOR PERIPHERAL VELOCITY

S-62390

Figure 71. Superconducting Generator Design Concepts

represents a major design problem. The system also requires a vacuum pump, which probably must operate continuously. Another problem area imposed by this design is the requirement for a nonconducting, nonmagnetic dewar shell. Numerous solutions to these problems are possible, but it is doubtful that the advantages would outweigh the disadvantages relative to the other approaches to be considered.

Rotating-Dewar, Rotating-Field Concept

The rotating-dewar, rotating-field generator incorporates inner and outer walls of the dewar that rotate with the superconducting field, thereby eliminating the need for rotating vacuum seals and nonconductive dewar walls. The primary disadvantage of this approach is the temperature rise experienced by the refrigerant (helium) in the rotor centrifugal force field. Although this temperature rise is not large (approximately 1.0 K for the rotational speeds of interest), it is sufficient to cause a significant reduction in attainable performance relative to a nonrotating superconductor. Another important disadvantage of rotating-field generators is the structure required to contain the superconductors. Further, a rotating cryogenic helium seal would have to be developed.

Stationary-Dewar-and-Field, Internal-Rotating-Armature Concept

In the stationary-dewar-and-field, internal-rotating-armature generator concept, the room-temperature armature rotates inside a stationary superconducting field. Maximum utilization is made of the superconductors by providing cooling to the minimum temperature obtainable with the cryogenic helium refrigerant. Although the cryogenic heat transfer area is larger, the cryogenic design is straightforward. It appears that this approach may permit higher energy fields (although this may be partially offset by reduced magnetic coupling, resulting in part from the structural requirement for supporting the armature coils). This arrangement has a low stiffness because of the small-diameter rotor; it may have critical speed problems.

Stationary-Dewar-and-Field, External-Rotating-Armature Concept

In this type of generator the superconducting field and the dewar are stationary, inside a rotating armature. Because the dewar and field are stationary, no rotating cryogenic helium seals are required and maximum refriger-

eration capacity is available from the helium. The stationary superconductor greatly reduces the generator field structural problems by eliminating the centrifugal loads. With this approach, the armature rotates at relatively high peripheral speeds, but the speeds required are within the state of the art and no problem is anticipated. The slip rings and brushes required to carry the armature current are also within the state of the art. It appears that in the final design the armature current will be lower than the field current. This configuration has the best magnetic coupling because the rotational loads of the windings are supported outside the armature winding. Also, the power winding is best suited to high-voltage designs because all the materials used are good insulators. A lighter weight magnetic shield also results with this approach. Because of the large diameter, the rotor will have high stiffness, hence minimum critical speed problems.

Selection of the Superconducting Generator Concept

The preferred superconducting generator concept is the rotating external armature with a stationary dewar and superconducting field. AiResearch believes this concept has the fewest potential problems in design and development and offers superior performance. Specifically, this concept offers the following potential advantages:

- (a) No rotating seals
- (b) Minimum refrigerant temperature (no adiabatic temperature rise)
- (c) No centrifugal loads on superconducting coils
- (d) High rotor stiffness (minimum critical speed problem)
- (e) Minimum air gap (rotor structural support outside magnetic field)
- (f) Minimum magnetic shielding weight

Although the preferred approach appears to be highly advantageous from the technical standpoint, it was rejected as being inapplicable to the high-power system program for the following reasons:

- (a) The stationary dewar and superconducting field and external rotating armature concept is unproven as yet.
- (b) The development work presently underway using this concept is for a naval propulsion application. The superconducting generator being developed is not directly applicable to the present program because

it is for a very low-speed motor operating at very low voltage.

- (c) Even if additional development work were initiated immediately on this preferred concept and directed specifically toward the high-power system application, the superconducting generator could not be developed within the time frame available for this application.

The selected superconducting generator concept is the rotating dewar with rotating superconducting field based on the work carried on in the past few years in the development of a prototype airborne unit. Westinghouse is presently developing a superconducting generator at the 10-MW power level. Therefore, with respect to superconducting design concepts, the use of rotating dewar and superconducting field is indicated. This selection, at this date, is primarily based on the short development time frame available for the present application.

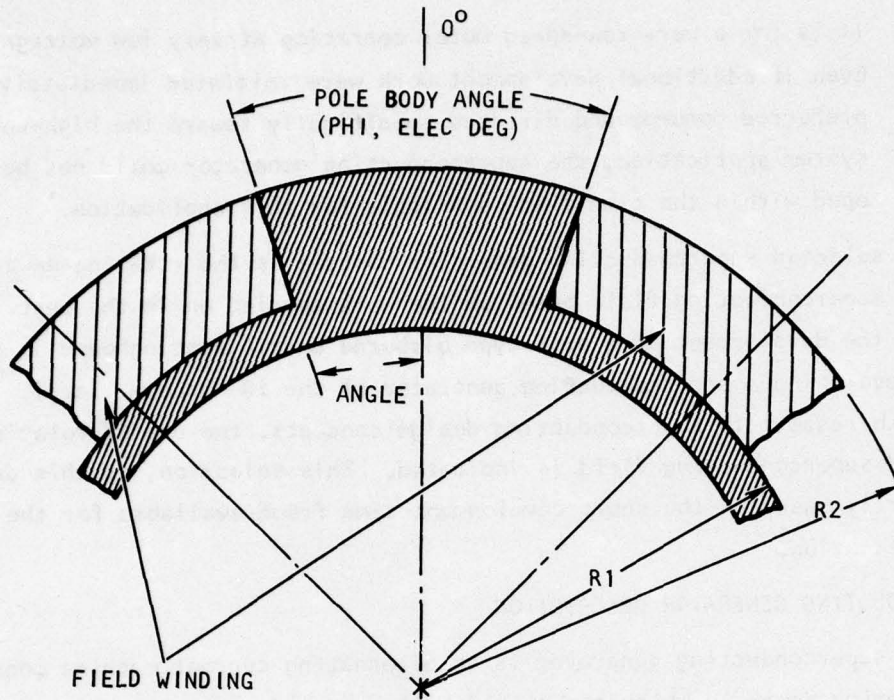
SUPERCONDUCTING GENERATOR DESCRIPTION

The superconducting generator is an alternating current machine consisting of a rotating dewar in which the liquid-helium-cooled superconducting coils are located, and a stationary stator that utilizes copper windings at normal temperatures. The geometric configuration of the superconducting generator is shown in Figures 72 through 74. Figure 72 shows a cross section of the rotor field winding (superconducting) and defines the field nomenclature. The stator winding (normal temperature) is shown, in cross section, in Figure 73 with the stator nomenclature. A cross section of the superconducting machine with the geometric nomenclature is presented in Figure 74.

The rotor is excited through slip rings, and 4.2 K liquid helium is provided to the superconducting field conductors in the rotor through a dynamic seal at the center axis of the rotor. The helium is circulated through the rotor windings, boiled off in an electrothermal damper shield, and exhausted back over the inlet feed. This machine utilizes an ironless stator design provided with a laminated iron core behind the stator windings to increase rotor-stator magnetic coupling and to provide magnetic shielding.

Stator

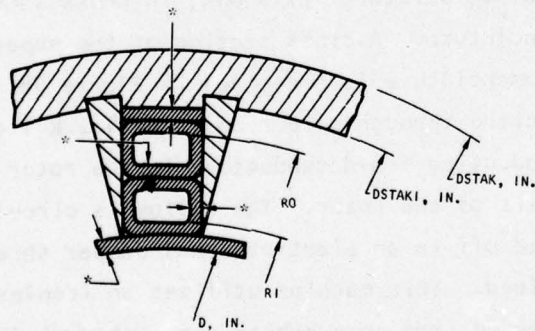
The ironless stator is electromagnetically similar to a conventional three-phase multipole stator winding with the following differences.



R_1 = SUPERCONDUCTOR INNER RADIUS
 R_2 = SUPERCONDUCTOR OUTER RADIUS

S-3287

Figure 72. Superconducting Field Rotor Configuration



* = TLINER
 DSTAK = STATOR LAMINATION OUTSIDE DIAMETER
 DSTAKI = STATOR LAMINATION INSIDE DIAMETER
 RO = STATOR COPPER OUTER RADIUS
 RI = STATOR COPPER INNER RADIUS
 D = STATOR BORE DIAMETER

S-3286

Figure 73. Stator Configuration

AL = STATOR STACK LENGTH
 EXT = STATOR WINDING EXTENSION
 G = AIR GAP
 ROTRLT = ROTOR ELECTROMAGNETIC LENGTH

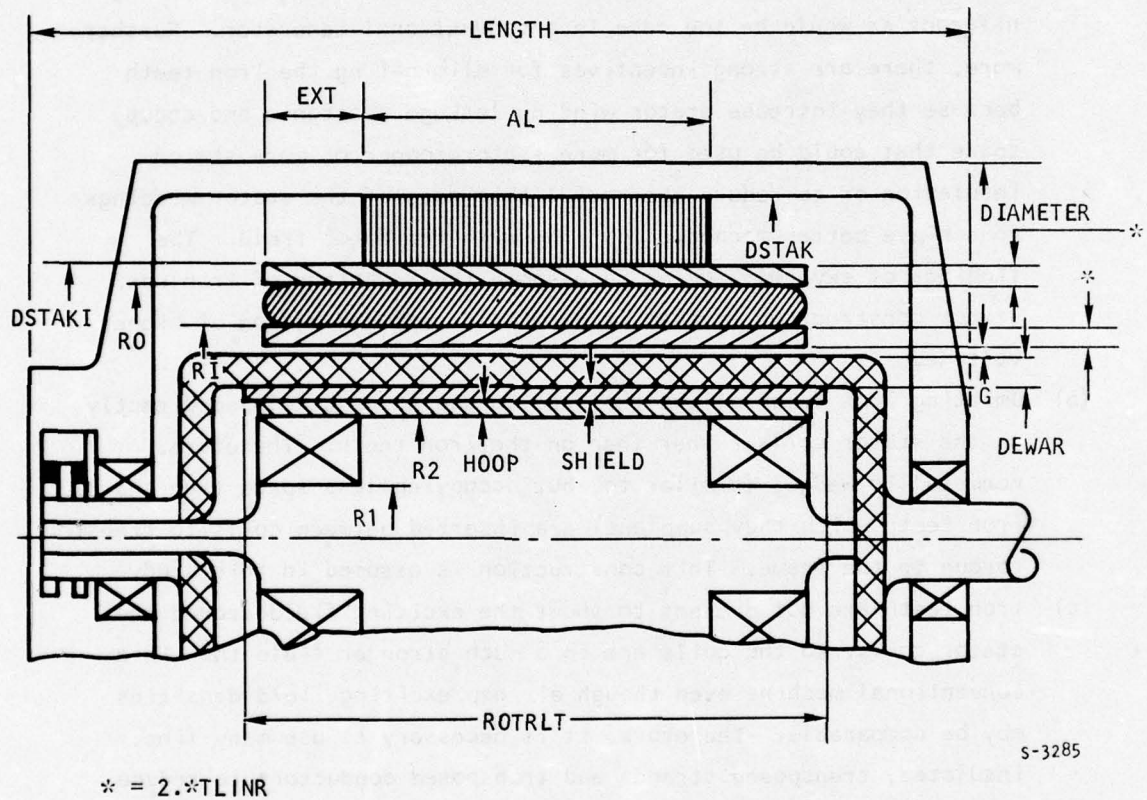


Figure 74. Superconducting Generator Cross Section and Geometric Nomenclature

- (a) Iron teeth between coils are omitted. The mmf provided by the superconducting field must be very high to drive the rotor flux through the reluctances of the air-core field coils and the large air gap separating the field coils from the stator coils (due to the space requirements of a field coil retaining hoop, damper, dewar wall, and mechanical clearances). Although omitting iron teeth in the stator further adds to the MMF required of the field, this increment relative to the basic exciting mmf is not nearly so significant as would be the case in a conventional generator. Furthermore, there are strong incentives for eliminating the iron teeth because they increase stator winding leakage reactance and occupy space that could be used for more stator copper or more stator insulation or to reduce the radial thickness of the stator windings to achieve better magnetic coupling with the rotor field. The findings of several studies have shown the advantage of ironless stator construction is that it permits direct generation of higher voltage.
- (b) Omitting iron teeth allows the load torque to be developed directly on the stator coils rather than on the iron teeth. Therefore, nonmetallic wedges (similar to, but occupying less space than the iron teeth which they supplant) are inserted between coils to transfer torque to the frame. This construction is assumed in this study.
- (c) Iron teeth are not present to shunt the exciting field around the stator coils, so the coils are in a much stronger field than in a conventional machine even though air gap exciting field densities may be comparable. Therefore, it is necessary to use many fine, insulated, transposed strands and transposed conductors to reduce the eddy currents that would otherwise be excited by the strong, high-gradient field. This reduces the space factor of the stator winding to perhaps 65 percent of what could be achieved with a solid conductor.
- (d) In lieu of a conventional diamond coil winding, the stator could be wound with a ring winding; however, while the ring winding offers simplified construction, it is not considered acceptable because it usually compromises electromagnetic performance of a machine except

possibly in the case of a machine with a low L/D. Compromise results because the return portion of the coil has high leakage reactance due to its proximity to the stator core iron; whereas in the diamond coil ends, proximity to iron is minimized. Further, the length (and therefore I^2R and the impedance drop) of the diamond coil end return is a constant value for a given stator diameter and pole configuration, so its significance diminishes as stator length increases. With the ring winding, the return coil length, losses, and impedance drop are directly proportional to stator length. A further consideration is that the diamond coil ends (in a superconducting machine, especially) are sufficiently active in producing useful emf, whereas the opposite is true with a ring coil return: any exciting field linkage produces a counter-emf.

Stator Core (Back-Iron)

The coupling of the rotor field into the stator is enhanced by providing a laminated iron core behind the stator coils. The stator core also provides a low-reluctance magnetic shield to prevent high magnetic induction in the space around the installation. Alternatively, shielding could be provided by a nonlaminated, nonmagnetic, low-resistivity electrical damper shield; however, shielding by an electrically reflecting damper is not considered appropriate for this application because it does not shield at zero speed, and also reduces, rather than enhances, the stator-rotor coupling.

Rotor

The rotor has superconducting field coils analagous to the coils of a salient-pole conventional machine; however, the coils are not supported in magnetic iron but are radially arranged about a nonmagnetic hub and constrained to this hub by a hoop of high-strength, nonmetallic fiber wrapping. Although magnetic materials could be used in the rotor, they usually operate far beyond saturation and, therefore, can introduce additional magnetic and thermal problems into the field. Where lightest weight is desired, as in this application, a given weight of iron is less effective than an equal weight of superconductor in achieving more power output.

Rotor Conductor

The rotor conductor is a niobium-titanium multi-twisted filament conductor in a copper matrix operated at 65 percent of 4.2 K short sample data. This allows some margin for losses under load and field changing and/or temperature rise due to heating of the liquid helium under vibration, shock, acceleration from the shaft center to the rotor coils due to centrifugal head, and changing rotational speed. Whether or not 65 percent gives adequate margin depends on many factors and must be experimentally verified under actual operating conditions. The required margin depends on the cooling effectiveness of the liquid helium permeating the coils, the matrix ratio, the adequacy and rigidity of the coil support structure, and the effectiveness of the electrothermal shield in preventing stator field variations from penetrating into the rotor field coils. It should be recognized that operating into a rectified and pulsed load, as required in this application, places a severe burden on the damper shield.

Rotor Coil Protection

The rotor coils and excitation circuit must be designed to permit non-destructive quenching of the superconducting coils. In large machines in which the stored field energy is high, quench protection may become more complex and may require voltage suppressors across each coil of the field. In the event that a multicircuit field coil connection or sectionalized coil protection is required to control voltage during a quench, the connection should be such that unbalanced magnetic forces sufficient to deflect the rotor and rub the stator cannot develop.

Electrothermal Shield

A very effective damper must be provided between the rotor fields and the stator to prevent excessive variation in the mutual field, which could quench the superconductor. The method of damping considered in these studies assumed that a cryogenic shield of pure copper or aluminum is incorporated inside the rotating dewar and cooled by boil-off of the liquid helium discharged from the field coils. A room-temperature damper also is possible (or a combination of room-temperature and cryogenic temperature damping is possible), but room-temperature damping is more practical in large machines in which the greater

damper thickness necessary due to higher resistivity (and deeper penetration depth) can be tolerated because the dewar wall thickness (constant regardless of size) is relatively less in relation to rotor diameter so that relatively more space is available for the shield.

The damper also is intended to intercept heat flow into the coil region, and it also has heat generated within itself due to damping currents. Therefore, some form of cooling is required for the damper.

Structural support of the damper is a critical design consideration. Even small magnetic and mechanical forces on a thin cylindrical shell near resonance can establish vibration and stresses that precipitate failure (or can cause excessive heating of a cryogenically cooled damper).

Dewar

The dewar excludes ambient heat from the field coils. How well it does this, determines, to a significant degree, the rate of helium consumption. Also, helium consumption is not greatly increased as machine size is increased because the dominant heat loads are not strong functions of machine size. Transporting helium from the storage dewar into the machine's dewar, and absorbing heat conducted from ambient along the field connection leads account for an important part of the refrigeration load.

Fault Protection

The superconducting field tends to be a constant flux source, and the stator winding has relatively low impedance due to ironless stator construction. Consequently, unusually high short-circuit and fault currents can be generated. Heating, torque, and magnetic forces on the stator conductors, field coils, and damper shield may present difficult problems under fault and abnormal load conditions. The use of external reactors or a transformer load would reduce this problem for external faults, but would not help in the case of internal faults in the machine. Because field current can not be turned off until after a fault condition exists and is detected, the mechanical and thermal design of the machine must be adequate to withstand this abuse; otherwise, a means for containment of a catastrophic failure of the superconducting generator must be provided.

COMPUTER PROGRAM

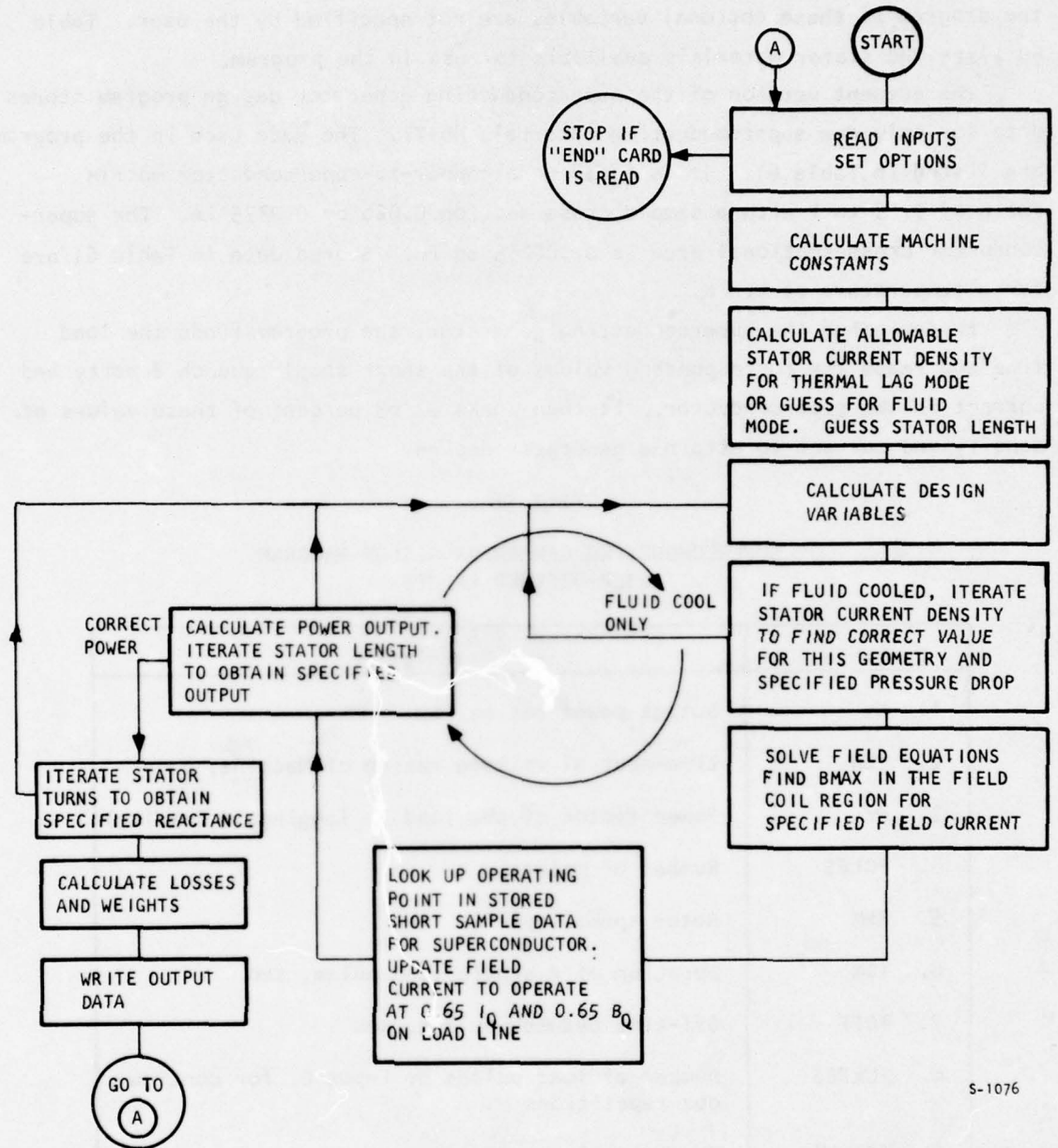
As part of the study program, AiResearch developed a superconducting alternator design computer program based on the superconducting-field-in-rotating-dewar, stationary-armature design concept. The generator geometry incorporated into the computer program is as has previously been discussed.

The superconducting generator design program is a digital computer program capable of computing superconducting three-phase salient-pole alternator machine designs over a wide range of ratings with a minimum of input data. The computer program provides a comprehensive tool for the study of high-power, superconducting, three-phase alternators. It can be used to produce specific generator designs or to conduct parametric studies of machines with either thermal-lag or fluid-cooled stator designs. In either case, the rotor is liquid-helium cooled.

This superconducting generator program allows optimization of weight, volume, efficiency, and other significant parameters as a function of such input variables as power level, voltage, rotational speed, duty cycle, and others. As few as 9 input data items suffice to produce a superconducting alternator design; however, up to 27 input data items may be used for specific design points or parametric studies.

A significant feature of this generator program is the incorporation of a thermal subroutine to minimize generator size and weight. This subroutine allows operation at the maximum current density permissible in the stator copper for a given duty cycle without exceeding the specified maximum copper temperature limit. Two operating modes can be used: (1) thermal lag wherein the heat generated in the stator is absorbed by the thermal capacitance of the stator materials, and (2) active cooling, which occurs when a fluid is circulated through the stator windings to absorb the heat generated for rejection to an external heat sink. In the fluid cooled mode, the machine design is relatively insensitive to duty cycle because steady-state operation is attained in a few seconds.

Figure 75 is a flow chart of the superconducting generator design program. This chart presents the fundamental logic employed in designing superconducting generators using this program.



S-1076

Figure 75. Superconducting Generator Design Program Flow Chart

Table 58 defines the nine variables that must be input by the user, and Table 59 lists the optional inputs together with the default values used by the program if these optional variables are not specified by the user. Table 60 lists the stator materials available for use in the program.

The present version of the superconducting generator design program stores data for only one superconducting material, Nb-Ti. The data used in the program are listed in Table 61. It is based on a copper-to-superconductor matrix ratio of 3.15 to 1 with a sample cross section 0.026 by 0.0375 in. The superconductor cross-sectional area is 0.000235 sq in. Stored data in Table 61 are for a temperature of 4.2 K.

In designing the superconducting generator, the program finds the load line and reads the corresponding values of the short sample quench density and current in the superconductor. It then works at 65 percent of these values of density and current to attain a generator design.

TABLE 58
SUPERCONDUCTING GENERATOR DESIGN PROGRAM
USER-DEFINED INPUTS

Variable	Description
1. KW	Output power rating, kW
2. VLN	Line-neutral voltage rating of machine, V
3. PF	Power factor of the load (- lagging, + leading)
4. POLES	Number of poles
5. RPM	Rotor speed, rpm
6. TON	Duration of a single load pulse, sec
7. TOFF	Off-time between pulses, sec
8. PULSES	Number of load pulses or input 0. for continuous repetitions
9. TSTART	The initial copper temperature, F

TABLE 59
SUPERCONDUCTING GENERATOR DESIGN PROGRAM

Variable	Description	If input = 0., Defaults to:
10. VPMIL	Dielectric strength of stator insulation, V/mil	80.
11. FTPSEC	Rotor tip speed at Dewar outer wall, ft/sec	500.
12. BETAC	Peak stator core flux density, kilolines/sq in.	100.
13. BHSI	Stator material code number	1.
14. TBI	Thickness of stator lamination, in.	0.01
15. CURDNS	Current density in the stator, A/sq in.	Program determined
16. TMAX	Maximum allowable stator temperature, F	400.
17. COOL	Type of stator cooling employed. Input 0. for thermal lag. Input fraction of conductor section which carries current; e.g., 0.65 to 0.85 for fluid cooling.	0.
18. TDEWAR	Thickness of rotating dewar (rotor) vacuum jacket, in.	0.55
19. RATIOA	(R1/R0) Ratio of stator copper inner radius to outer radius. This is program defined, so input 0.	0.
20. RATIOF	(R1/R2) Ratio of rotor superconductor inner radius to outer radius.	0.65
21. TSHELD	Thermal shield thickness, in.	0.3
22. XIPRT	Print switch to control amount of output detail (0. = mini- mum printout, 1. = maximum printout)	0.
23. SC0IL	Ratio of net stator conductor area to gross stator winding cross-sectional area.	0.65
24. THOOP	Field hoop thickness to contain field windings, in.	0.2
25. SC0ILF	Ratio of net field conductor area to gross field winding cross-sectional area	0.65
26. CUPRSC	Copper to superconductor matrix ratio	1.8:1
27. CODESC	Superconductor code (0. = Nb-Ti; this is the only supercon- ductor presently incorporated in the program)	0.
28. TEMPF	Field temperature, K (Note: 4.2 K must be used in this version of the program).	4.2
29. PHIDEG	Pole body angle, elec deg	60.
30. XLPU	Stator leakage reactance, per unit (Note: in the rectified mode, the power factor, PF, is a program-defined function of XLPU)	0.27
31. RECMOD	Type of load (0. = linear, 1. = rectified)	0.

TABLE 60
SUPERCONDUCTING GENERATOR DESIGN PROGRAM
STATOR MATERIALS

Code	Material	Thickness, in.
1.	M-15 HR	0.014
2.	M-19 HR	0.014
3.	Trancor "T"	0.007
4.	Trancor "T"	0.005
5.	2V Permendur	0.010
6.	HP-9-4-20 ingot	Solid
7.	4340 ingot	Solid
8.	Al 4750 at 1600 cps	0.006
9.	Monimax at 2000 cps	0.004
10.	1010 annealed	Solid
11.	HP9-4-20 at 500 F	Solid
12.	HIPERCO 27	0.008

TABLE 61
SUPERCONDUCTING GENERATOR DESIGN PROGRAM
Nb-Ti SUPERCONDUCTOR AT 4.2 K

Short Sample Quench Density, kilogauss	Current in Superconductor, A
48.0	200.0
55.0	175.0
58.0	165.0
58.8	162.0
60.0	159.0
61.0	155.0
62.5	150.0
64.0	145.0
66.0	140.0
67.0	137.0
69.0	130.0

There are two different types of output: a short format and a long format. The short format is generally sufficient for most purposes and is self-explanatory. A sample of the short format output is given in Figure 76. The long format includes additional internal details of the generator design plus a tabulation of the field components that allows a flux plot to be made, if desired.

PARAMETRIC STUDIES

The superconducting generator computer program was used to conduct a parametric study of the superconducting generator to determine the effect of major parameters on the machine design. Table 62 lists the baseline values used in the parametric study conducted.

Voltage Effects

The effect of voltage on generator weight at a constant 25-MW power level is shown in Figure 77. Generator weight is shown as a function of rotational speed for several levels of dc voltage. It is easily seen that the superconducting generator weight is highly sensitive to voltage level, the weight penalty becoming increasingly severe as the voltage output of the generator increases.

Rotational Speed Effects

The effect of variation of rotational speed on the weight of 25-MW superconducting generator designs at various voltage outputs can be seen by referring to Figure 77. The important conclusions to be drawn are:

- (a) There is an optimum rotational speed at each voltage level for which the generator weight is a minimum.
- (b) The optimum rotational speed shifts to lower values as the generator design output voltage increases.
- (c) The speed range at each voltage level at which the generator weight is near the optimum value is quite narrow. Weight increases very rapidly as the design rotational speed shifts away from optimum.

SAMPLE CASE 1, 25 MEGA-WATT LOW VOLTAGE DESIGN

TIME 13:57:01

USER DEFINED INPUTS

HW	25002.13	VOLTS, L-N	2000.00
PF	00.000	POLES	0.0
OPM	0000.	LOAD PULSE DURATION, SEC	120.0
TIME AFTERN PULSES, SEC	1.0	%%NO. OF LOAD PULSES	1.0
INITIAL COPPER TEMP, DEG F	230.0		

OPTIONAL INPUTS

DEFAULT= IF INPUT NO.0

TOLTS/MIL	100.0	80.0 V/MIL
TIP SPEED AT DENAR HALL	95.00	500.00 FT/BFC
STATOR C/PSE DENSITY (PEAK)162.		100.0 KL/30. IN.
STATOR MAT'L PV PERPENDICUR,01		SILICON STEEL
STATOR LAM THICKNESS	0.0100	.01 IN.
CURRENT DENSITY, STATOR	24397.	PROGRAM ITERATES TO OBTAIN SPECIFIED TEMP
MAX COPPER TEMPERATURE	398.78TATOR	400.0 DEG F
COOLING METHOD, FLUID	0.850	THERMAL LAG
DENAR THICKNESS, IN.	0.5500	.55 IN.
RATIOA	0.0110	PROG. DEFINES
RATIOB	0.0000	.00
SMELT THICKNESS, IN.	0.5000	.50 IN.
PRINT CONTROL	0.0	0.0 MINIMUM
STATOR WINDING FACTOR	0.6500	.65
FIELD WINDP THICK., IN.	0.2000	.20 IN.
WINDING FACTOR, FIELD	0.6500	.65
MATRIX RATIO, C/SC	1.800	1.8
SUPERCONDUCTOR CODE***	0.0	0.0000T
FIELD TEMP. DEG. C.***	0.200	.2 K.***
POLE BODY ANGLE, ELEC. DEG.	40.00	40. ELEC. DEG.
STATOR LEAKAGE REACT., PU	0.2617	.27 PER UNIT
RECTIFIER(1,10R LINEAR)0.1	1.000	0.0 LINEAR LOAD

OUTSIDE

TOTAL WEIGHT, LB, KG	1507.016	683.967	ALTERNATOR FRAME DIAMETER, IN, CM	26.165	66.469
SPECIFIC WEIGHT, LB/KN, KG/KN	0.086	0.027	STATOR STACK DIAMETER, IN, CM	20.964	52.963
IRON WEIGHT, LB, KG	601.000	273.020	ALTERNATOR OVERALL LENGTH, IN, CM	32.800	83.415
STATOR COPPER WEIGHT, LB, KG	160.000	71.211	ROTOR LENGTH, IN, CM	24.800	61.175
ARMATURE COPPER WEIGHT, LB, KG	307.000	139.688	ROTOR DIAMETER, IN, CM	14.375	36.478
ROTOR WEIGHT, LB, KG	400.330	181.590	ROTOR LENGTH/STATOR LENGTH RATIO	0.752	0.772
ROTOR INERTIA, IN-LB-SEC ² , N-Newton-M ²	26.366	0.294	SYNCHRONOUS REACTANCE, PU, PU	0.393	0.393
CORE LOSS, KW, KW	55.594	55.594	STATOR RES. REACTANCE, PU, PU	0.262	0.262
COPPER LOSS, KW, KW	65.636	65.636	STATOR RESISTANCE, PU, PU	0.00233	0.00233
TOTAL LOSS, KW, KW	121.230	121.230	ROTOR RES. REACTANCE, PU, PU	0.425	0.425
EFFICIENCY, PERCENT, PERCENT	0.000	0.000	FLUX PER POLE, KILOLINES, KILOLINES	15626.0	15626.0
DC CURRENT NEUTRAL, AMP/3Q IN, AMP/3Q CW	37071.8	57491.3	CORE FLUX, KILOLINES, KILOLINES	4985.1	4985.1
STATOR COOLANT TYPE	WATER JET IN		COOLANT DELTA-T, PSID, MEGAPASCAL	20.030	0.138
COOLANT FLOW RATE, GPM, LPM	198.122	749.051	COOLANT DELTA-T, DEG-F, DEG-C	25.107	13.946

* FOR FLUID COOLING, INPUT/NET(GROSS) FOR THE HEILLOW CONDUCTOR, FOR LAG COOLING, INPUT, IS CURRENT DENSITY IS INPUT, THE CORRESPONDING TEMPERATURE IS CALCULATED, OTHERWISE, DENSITY TO YIELD MAX TEMPERATURE IS CALCULATED.

***** CHARTING REPEATITIVE PULSES, INPUT NO. PULSES = 0, IN CONTINUOUS LAG MODE, THERMAL BRUNTERS ARE BYPASSED, CURRENT DENSITIES MUST BE SPECIFIED IN BYPASS MODE.

RESTRICTIONS... PF IS ALWAYS LAG, FIELD TEMP AND SUPERCONDUCTOR CODE MUST BE DEFAULT VALUES.

Figure 76. Sample Printout, Short Form

TABLE 62
BASELINE VALUES OF STUDY PARAMETERS

Parameter	Value
Number of poles	6
Type of load	Rectified
Apparent power factor	0.88 lagging
Stator leakage reactance, per unit	0.27
Insulation stress, V/mil	100
Tip speed at dewar wall, ft/sec	500
Stator material	2V PERMENDUR
Stator core density (peak), kilolines/sq in.	142
Superconductor	Nb-Ti
Matrix ratio, copper/superconductor	1.8:1
Superconductor temperature, K	4.2
Dewar thickness, in.	0.55
Shield thickness, in.	0.30
Field hoop thickness, in.	0.20
Pole body angle, electrical deg	60
Field winding factor	0.65
Stator winding factor	0.65
Ratio of rotor superconductor inner radius to outer radius	0.60
Stator coolant	MIL-L-23699
Stator copper initial temperature, F	230
Maximum stator copper temperature, F	400
Stator coolant pressure drop, psid	20
Stator coolant flow area, percent of conductor	15

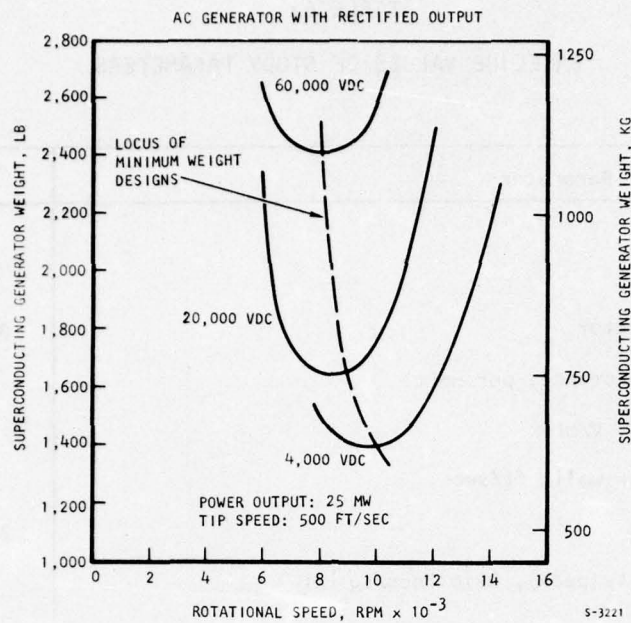


Figure 77. Superconducting Generator Weight as a Function of Rotational Speed and Dc Voltage

Figure 78 presents data similar to that of Figure 77, except that it is for low-voltage generator designs at various power levels, rather than several voltage levels at a constant power level. The significant features illustrated by Figure 78 are:

- (a) There is an optimum rotational speed at each power level for which the generator weight is a minimum.
- (b) The optimum rotational speed shifts to lower values as the generator design power output increases.
- (c) The speed range at each power level at which the generator weight is near the optimum value broadens as the power level is reduced; the speed range is rather narrow at 50 MW and quite broad at the 10-MW power level.

The diameters and length-to-diameter ratios of the superconducting generator designs are presented in Figure 79 as a function of design rotational speed. The significant machine geometry features affected by rotational speed as shown in Figure 79 are as follows.

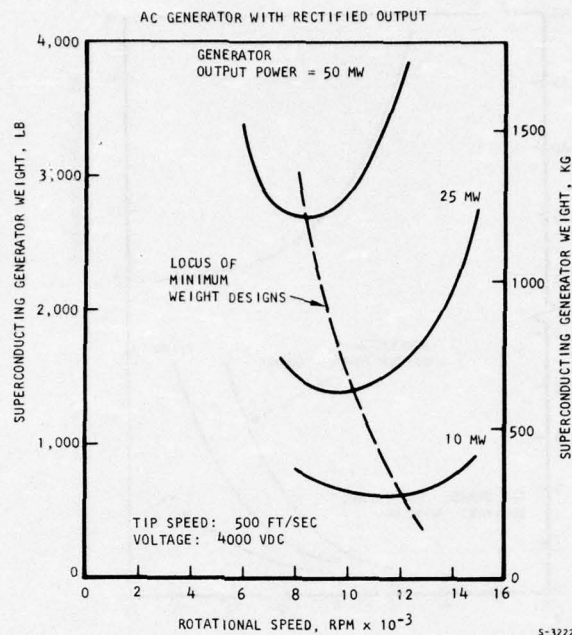


Figure 78. Superconducting Generator Weight as a Function of Rotational Speed and Power Level

- (a) The frame diameter of the generator varies inversely with rotational speed and is independent of output power level.
- (b) The machine length-to-diameter ratio increases rapidly with rotational speed at constant power output.
- (c) Constant machine length-to-diameter ratios can be maintained with increasing power levels by decreasing the generator rotor rotational speed.

Selection of the actual design value of rotational speed at any power level is not always determined by the generator alone. Optimum system weight may not occur at the optimum generator weight when the generator is driven directly by a turbine. In addition, other factors may influence the final rotational speed selection such as critical speeds or whether or not the use of a gearbox between the generator and drive turbine can be eliminated by compromising the design rotational speeds of the two individual units.

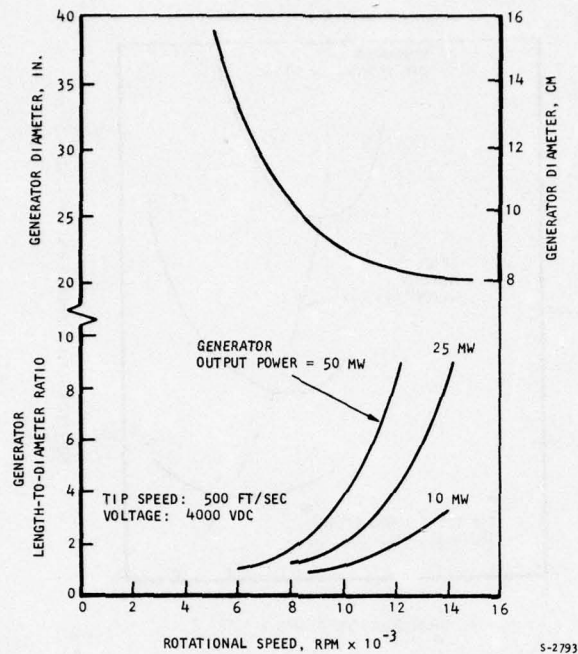


Figure 79. Superconducting Generator Diameter and Length-to-Diameter Ratio as a Function of Rotational Speed and Power Level

Although intuitively obvious, Figure 78 confirms that the superconducting generator weight increases with increasing power output capability. This figure also shows that the optimum design rotational speed to achieve minimum weight decreases with increasing power level.

COOLING SYSTEM

The stator cooling system for the superconducting generator will be essentially identical to that provided for fluid cooling the conventional generator as discussed previously.

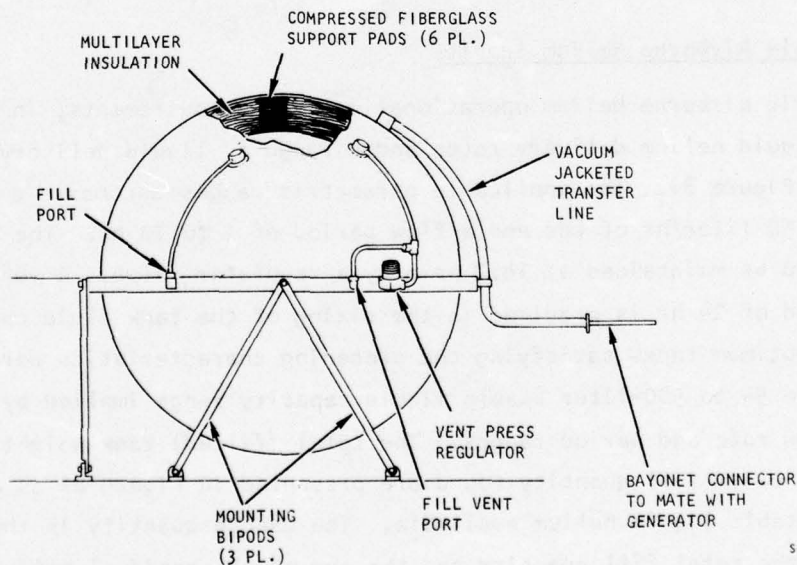
Cooling of the superconducting rotor (rotating dewar) requires the use of liquid helium. The helium required can be provided as an expendable stored in suitable tanks and used as needed, or by a closed-cycle helium liquefaction system.

Expendable Liquid Helium Storage

Figure 80 illustrates the type of storage vessel envisioned for storage of expendable liquid helium. Table 63 presents the pertinent data on this tankage for the 10-, 25-, and 50-MW superconducting generators. Notice that the tankage size and helium requirements do not depend on duty-cycle operating time; they are based on the total mission duration and standby requirements. This is because the helium cooling demand is primarily to compensate for the thermal heat leak into the rotating dewar.

In sizing the helium storage tank as shown in Table 63, a simple evacuated multilayer insulation approach is assumed, using materials that minimize structural weight. Use of vapor-cooled shields was not considered. In the absence of specific envelope constraints, it is assumed that a spherical tank configuration is satisfactory. The general tank characteristics are as follows:

- Insulation: evacuated crinkled single-aluminized Mylar
- Pressure vessel: Ti-5Al-2.5Sn alloy
- Vacuum jacket: 2219 aluminum alloy
- Pressure vessel support: compressed felted fiberglass pads



S-3255

Figure 80. Representation of the Liquid Helium Storage Vessel

TABLE 63
LIQUID HELIUM STORAGE SYSTEM SUMMARY*

Power, MW	10	25	50
Flow rate, liter/hr	18.3	20.3	23.3
Heat leak, Btu/hr	6.7	7.2	7.8
Girth ring dia., in.	44.07	45.04	46.40
Outer shell dia., in.	40.47	41.49	42.84
Tank assembly			
Dry weight, lb	129.1	139.3	152.4
Wet weight, lb	206.6	224.0	248.3
External lines, mounting pads, lb	10.0	10.0	10.0
Total system weight, lb	216.6	234.0	258.3

*Based on a 24-hr standby and a 10-hr mission.

1. Expendable Airborne Helium Supply

Parametric airborne helium operational delivery requirements, in terms of a range of liquid helium delivery rates and a range of liquid delivery periods are shown in Figure 81. The applicable parametric ranges encompass a flow rate of 5 to 50 liter/hr of LHe and a flow period of 1 to 10 hr. The tanks are assumed to be maintained at 14.7 psia by a regulator valve. A vented standby period of 24 hr is provided in the sizing of the tank fluid capacity.

Weight-optimum tanks satisfying the preceding characteristics were determined over the 5- to 500-liter usable liquid capacity range implied by the specified flow rate and period ranges. The total (filled) tank weight, volume penalty, and helium fill quantity found are presented in Figure 81 as a function of the usable liquid helium available. The usable quantity is the difference between the total fill quantity and the sum of the residual helium vapor and the vapor vented during the 24-hr standby period. The volume penalty is the cubical region having side dimensions equal to the tank outer diameter.

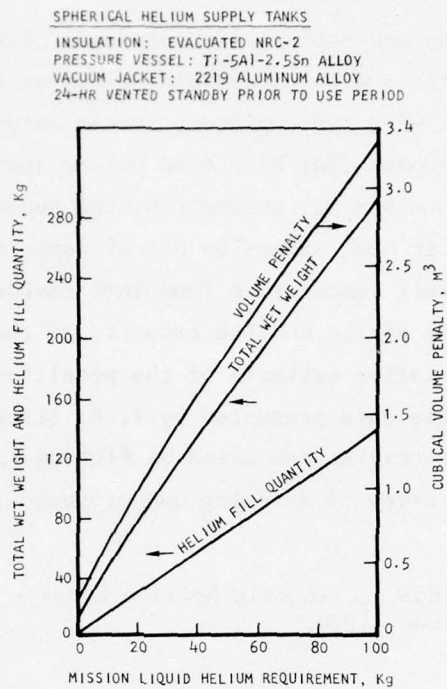


Figure 81. Weight and Volume of Expendable Liquid Helium Storage System

If the liquid demand rate is given in liter/hr, the mission liquid helium requirement on Figure 7-13 is:

$$W = 0.125 \dot{w} t, \text{ kg}$$

where \dot{w} = demand rate, liter/hr

t = flow period, hr

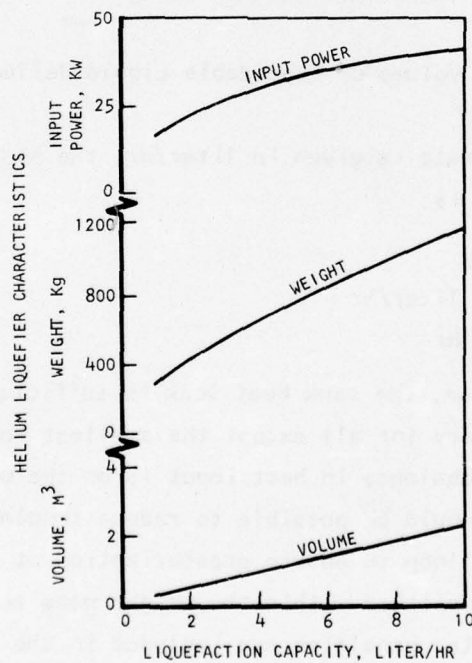
For the flow range specified, the tank heat leak is sufficient to maintain tank pressure during delivery for all except the smallest tanks used at the highest flow rates. The imbalance in heat input is on the order of $4W$, at most. In these cases, it would be possible to reduce insulation thickness slightly and add a buildup loop to ensure pressurization at high delivery rates. This could be accomplished within the weight penalties presented; therefore, no internal heater penalties are included in the weights presented.

2. Closed-Cycle Helium Liquefier Supply

For the duty periods and capacities indicated, closed-cycle helium supply systems are not competitive with expendable helium as shown in Figure 82. If high-risk development were contemplated, system weight penalties might be predicted that would approach that of stored helium systems, but power requirements would be high. To minimize consumption, the superconducting magnet dewar using the fluid must make extensive use of vapor cooling, resulting in a relatively high helium exit temperature from that device. This means that the liquefier cannot make use of the cooling capacity of the returning vapor.

To provide a conservative estimate of the penalties involved, Figure 82 has been prepared from the data presented by T. R. Strobridge of NBS-Boulder (Ref. 2*). Strobridge's results are based on fitting curves to characteristics obtained from a survey of existing and proposed refrigerator and liquefier systems.

* Ref. 2. T. R. Strobridge, "Cryogenic Refrigerators - an Updated Survey," NBS TN-655, June, 1974.



S-3247

Figure 82. Weight, Volume, and Power Requirements for Closed-Cycle Helium Liquefaction System

SECTION 8

TURBINE DESIGN CONSIDERATIONS AND TRADE STUDY

INTRODUCTION

This section describes the various design considerations involved in determining the performance characteristics of a high-power, low-fuel-consumption turbine that will provide a lightweight, auxiliary high-power system when integrated with the appropriate generator and propellant storage and feed system. For clarity, this section is subdivided into discussions of the following design areas:

- Aerodynamic turbine design considerations and characteristics
- Fast startup design considerations and characteristics
- Structural design considerations and characteristics

SUMMARY

The trade study described in this section established the following turbine design guidelines.

- (a) Supersonic operation should be selected in all stages of a multiple-stage turbine design. The prime consideration leading to this design approach is that the majority of the anticipated missions occur at altitude with a reduced, variable back pressure. The availability of latter-stage supersonic blade contour will reduce fuel consumption or increase mission duration for a fixed fuel quantity.
- (b) Fast startup on the order of 1.5 to 2.0 sec is possible for all power levels of interest without introducing unusual power system operational complexity. This fast startup operation is achievable with the use of either thermal-lag or fluid-cooled conventional generator design concepts.
- (c) Detailed thermal and structural analyses of turbine disc and blades verify the selected operational levels used in the design concepts.

- (d) The selection of rotational speed is governed by power level. At the low-power spectrum (10 MW), the use of a gear-driven concept is indicated because, at this power level, optimum component speed selection predominates. At the mid-power range of interest (25 MW), rotational speed compromises can be tolerated and the direct-driven multicomponent approach is indicated. At the high-power level of interest (50 MW), selection of assembly rotating speed is primarily dictated by turbine structural design considerations.

AERODYNAMIC TURBINE DESIGN CONSIDERATIONS AND CHARACTERISTICS

Design Considerations

The required combination of high power output, low specific propellant consumption, and possibly fast startup imposes the following restraints on the turbine design.

- (a) The turbine must have the ability to withstand high rotational speeds at relatively high inlet temperature to achieve high overall efficiency and the desired low specific fuel consumption (weight and cost reduction).
- (b) The turbine must have high performance capability over a wide operational range (design and off-design operation). These requirements result from fast startup and variable back pressure associated with variable altitude operation.
- (c) The turbine should be of minimum size and have a minimum number of stages to reduce the inertia of the rotating assembly and be capable of fast startup.
- (d) The turbine should have a minimum of design complexity to increase reliability and to reduce development risk and cost.

To achieve low fuel consumption, it is necessary to utilize the maximum available expansion head and to convert this head into power in an efficient turbine. Low fuel consumption generally dictates high-temperature, high-rotational-speed, high-pressure, multistage operation. In the intended application, the operational mode predominates due to fast startup requirements and variable-altitude back pressure. Turbine design parameters such as individual

stage nozzle expansion, therefore, must be selected to ensure a satisfactory fuel consumption throughout the entire operating range, rather than at a single or fixed operational mode. The design optimizing criteria are the combined effects of turbine efficiency and variable expansion head modified by structural considerations.

High power requirements, however, restrict the speed at which the turbine may operate. At the power levels of interest, high blade heights are required, which makes blade stress and blade vibration problems primary considerations in the selection of turbine speed. Although satisfactory turbine performance characteristics may be achieved at somewhat relaxed rotational speeds, turbine weight and, to some extent, startup requirements, dictate maximization of turbine speed. Additional limitations imposed on turbines include stress distribution, bearing wear, gear loading, and, to a minor degree, fuel pump suction specific speed considerations.

Design simplicity is required to ensure reliable operation, ease of fabrication, and reasonable development cost.

All of the preceding considerations must be included in the turbine design tradeoffs for this application.

Turbine Types

The power requirement and operating regimes are such that use of the axial-flow, impulse (or impulse-reaction) turbine design concept is recommended. Performance of tangential-flow, drag, Terry, radial-inflow, or radial-outflow designs is below, or at best equivalent to, the performance of a single-stage design, even with the natural flow staging tendency of some of these designs.

When considering multiple turbine stages, the pressure-compound design is preferred because turbine staging by the use of multiple-wheel, velocity-compound, or single-wheel reentry approaches results in lower performance. Furthermore, the lower performance is coupled with an increase in mechanical complexity caused by a further increase in critical blade height and a more complex housing. For axial-flow machines the turbine design flow concept can either be pure impulse or partial reactions. For an established operating condition, design techniques are sufficiently developed to allow the selection of the optimum design concept.

Techniques for Predicting Turbine Performance

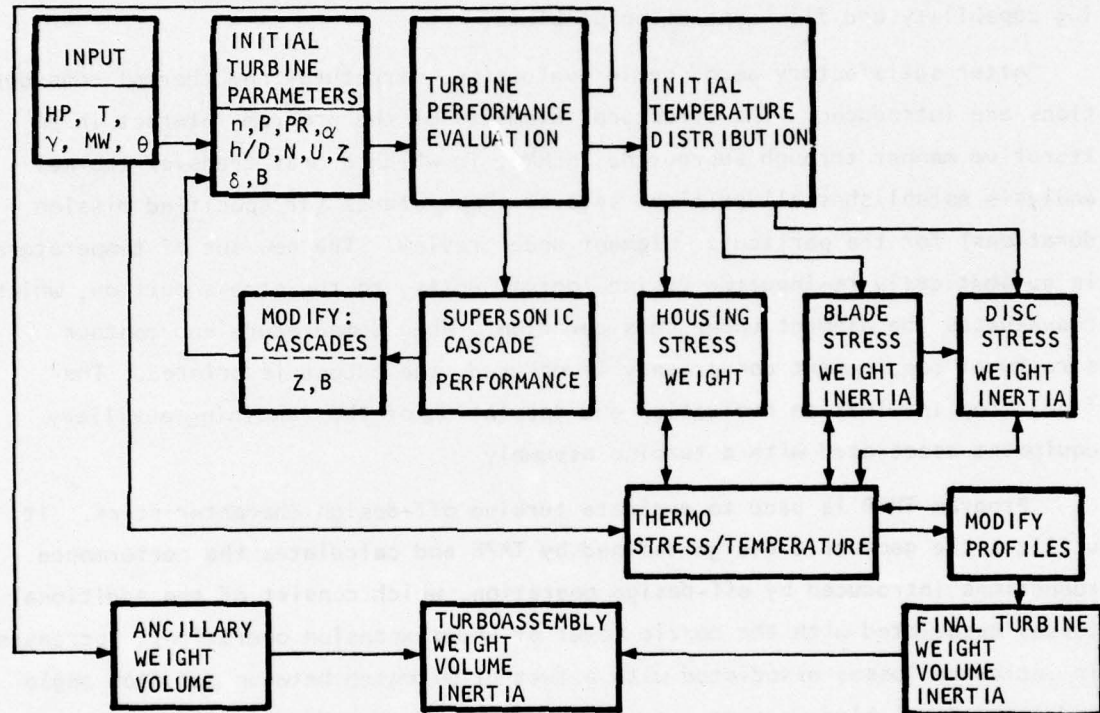
The adopted procedure for predicting the nominal design point performance and off-design performance of the turbine is illustrated in Figure 83. The technique combines the various aspects associated with turbine design and is based on AiResearch involvement and experience in high-head turbomachinery. The procedure is to integrate numerous stand-alone computer programs into a single computational procedure combining aerodynamics, structural, thermal, mission, inertia, size, and weight considerations. This allows an appropriate assessment of individual or complete assembly characteristics.

The basis of the nominal turbine design performance characterization is computer program TAPE. Subroutine A-2107 is used in the initial procedure to evaluate performance; dimensions; configuration (axial-impulse, multiple-stage, single-stage, and reentry); arc of admission; and losses for specified power requirements, rotational speed, propellant properties, pressure ratio, number of blades, blade height, aerodynamic and geometrical blockage factors, etc. This program is used to determine effects of design formulation on the performance of the turbine operating at specified fixed operating conditions (design points). Subsequently, since supersonic operation predominates, iteration on turbine blade number, chord, etc. is carried out to arrive at satisfactory supersonic blade sections based on the two-dimensional isentropic flow analysis given in References 3 and 4.* The method consists of converting the uniform parallel flow at the blade inlet into a vortex flow field, turning the vortex flow, and reconvertng to a uniform parallel flow at the blade exit. Additional flexibility has been incorporated into the program by adding an inlet and exit wedge angle calculation to the suction surface to allow for finite blade thickness.

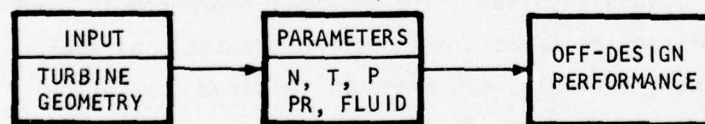
*Ref. 3: Boxer, Emanuel, Sterrett, James R., and John Wlodarski, Application of Supersonic Vortex-Flow Theory to the Design of Supersonic Impulse, NACA RM L52B06, 1952.

Ref. 4: Goldman, Louis J., and Vincent J. Scullin, Analytical Investigation of Supersonic Turbomachinery Blading, NASA TN D-4421, 1968.

● NOMINAL DESIGN PERFORMANCE (TAPE)



● OFF-DESIGN PERFORMANCE (TMAP)



- STARTUP
- DYNAMICS
- GROWTH POTENTIAL

S-3323

Figure 83. Turbine Performance Evaluation Procedure and Technique

The application of this design procedure involves the specification of inlet and outlet Mach numbers, the lower-surface Mach number, the upper-surface Mach number, the inlet and exit flow angle(s), and the specific heat and gas constant of the working fluid. An inlet wave pattern parameter is used to restrict the interaction of the expansion waves from the suction surface with those of the succeeding pressure surface. The final selection of the blade design is guided by considerations of blade shape, solidity, supersonic starting capability and flow separation problems.

After satisfactory aerodynamic evaluation, structural and thermal considerations are introduced. The structural elements of the program interact in an iterative manner through subroutine THERMO, in which a heat transfer thermal analysis establishes all critical sets of temperatures (at specified mission durations) for the particular element under review. The new set of temperatures is automatically re-inputted, using logical units, to the stress portion, which reevaluates the element under consideration. When temperature and contour structural requirement convergency is ensured, the output is printed. The final step involves an evaluation and tabulation of the remaining auxiliary equipment associated with a turbine assembly.

Program TMAP is used to evaluate turbine off-design characteristics. It utilizes the geometric design defined by TAPE and calculates the performance reductions introduced by off-design operation, which consist of the additional losses associated with the nozzle (over or underexpansion operation), increases in incidence losses associated with a further mismatch between gas flow angle and geometrical blade angles, variable speed, and the effects of density and viscosity on the parasitic losses involved. The off-design program is used to define operating characteristics associated with variable rotational speed (startup, shutdown, dynamics), variable back pressure (altitude operation), and growth potential of a design associated with variable operating conditions or propellants.

To substantiate the accuracy of turbine performance prediction, the TMAP program was used to assess the performance of a Zeus turbine wheel (originally developed at AiResearch for a solid-propellant-powered APU for the Nike-Zeus missile and subsequently used in the Spartan missile APU). Figure 84 shows the results of the performance evaluation correlating test and prediction at two off-design pressure ratios of this partial-admission, supersonic, axial-flow turbine.

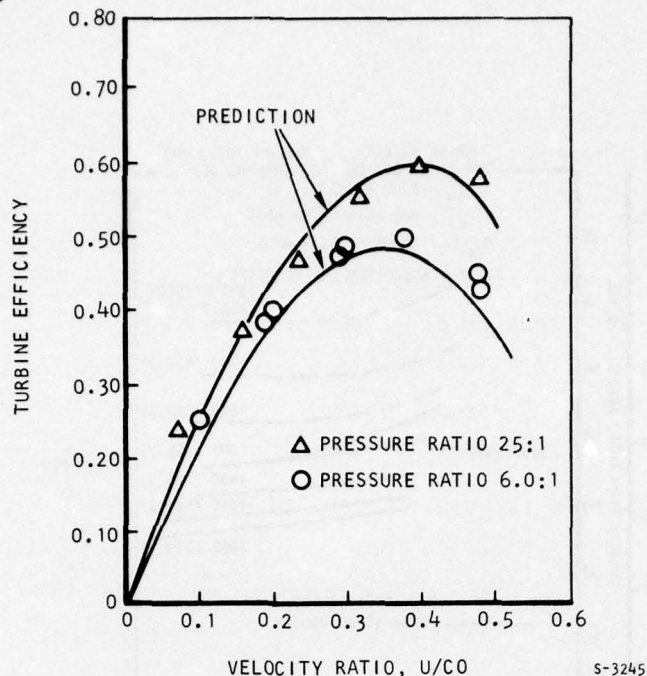


Figure 84. Zeus Turbine Off-Design Computer Program Performance Correlation

Turbine Performance Trade

The following paragraphs describe the turbine performance evaluation that was conducted. The procedure followed in assessing turbine performance design characteristics includes the selection of operating points, e.g., number of turbine stages, rotational speed, number of blades, and pitch velocity of individual stages, sea level and altitude operation, blade height or arc of admission optimization, and off-design power delivery capability. In addition, the use of variable propellants, the use of a multipropellant on a fixed turbine design, and fast startup operation also were evaluated.

In the trade and sensitivity study subsequently described, neat hydrazine monopropellant was primarily used. Hydrazine was selected as the baseline propellant based on achieving minimum weight; however, cost considerations and combustor development considerations may lead to the desirability of selecting alternative propellants as the turbine energy drive source.

1. Effects of Number of Stages, Rotational Speed, and Pitch Line Velocity

Typical effects of rotational speed and pitch line velocity on turbine performance for two- and three-stage turbine designs are shown in Figure 85.

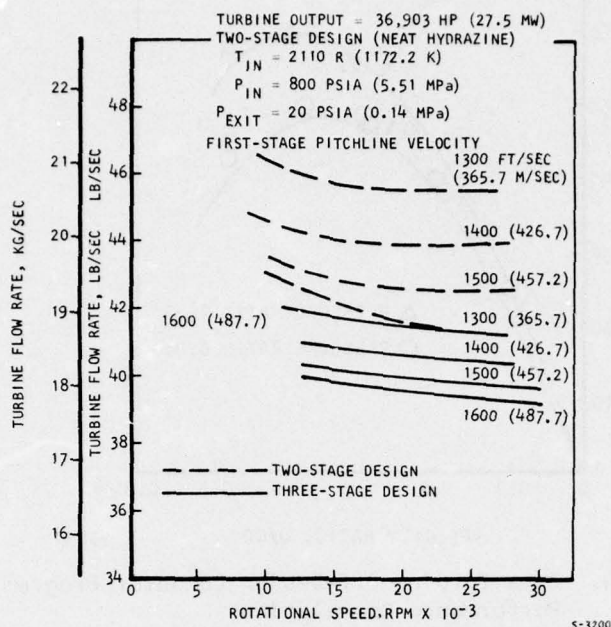


Figure 85. Effect of Turbine Stage, Rotational Speed, and Pitch Velocity

For the condition shown, increases in the number of stages and pitch line velocity help to reduce fuel consumption. Reduction in fuel consumption with increase in rotational speed is minimal provided a critical value is achieved. The power level selected for illustrating the effects of stage number is in the medium-power region of interest. The trend shown in Figure 85, however, is equally applicable at the higher or lower power regions of interest. Mechanical considerations lead to the selection of two stages rather than three because associated fuel consumption savings are rather minimal.

Figure 86 illustrates the procedure associated with the selection of rotational speed for the three power ranges of interest. Mechanical considerations of stress and blade vibration govern the selection of optimum rotational speed of the turbine as an individual component. It is desirable to operate at maximum permissible peripheral velocity and rotational speed. Increased peripheral speed reduces fuel consumption as shown in Figures 85 and 86. The prime attribute of high rotational speed, for a stated peripheral velocity, is decrease in turbine size, thus weight and inertia; however, decreasing the

TWO-STAGE DESIGN (NEAT HYDRAZINE)

$P_{IN} = 800 \text{ PSIA } (5.51 \text{ MPa})$; $T_{IN} = 2110 \text{ R } (1172.2 \text{ K})$

$P_{EXIT} = 20 \text{ PSIA } (0.14 \text{ MPa})$

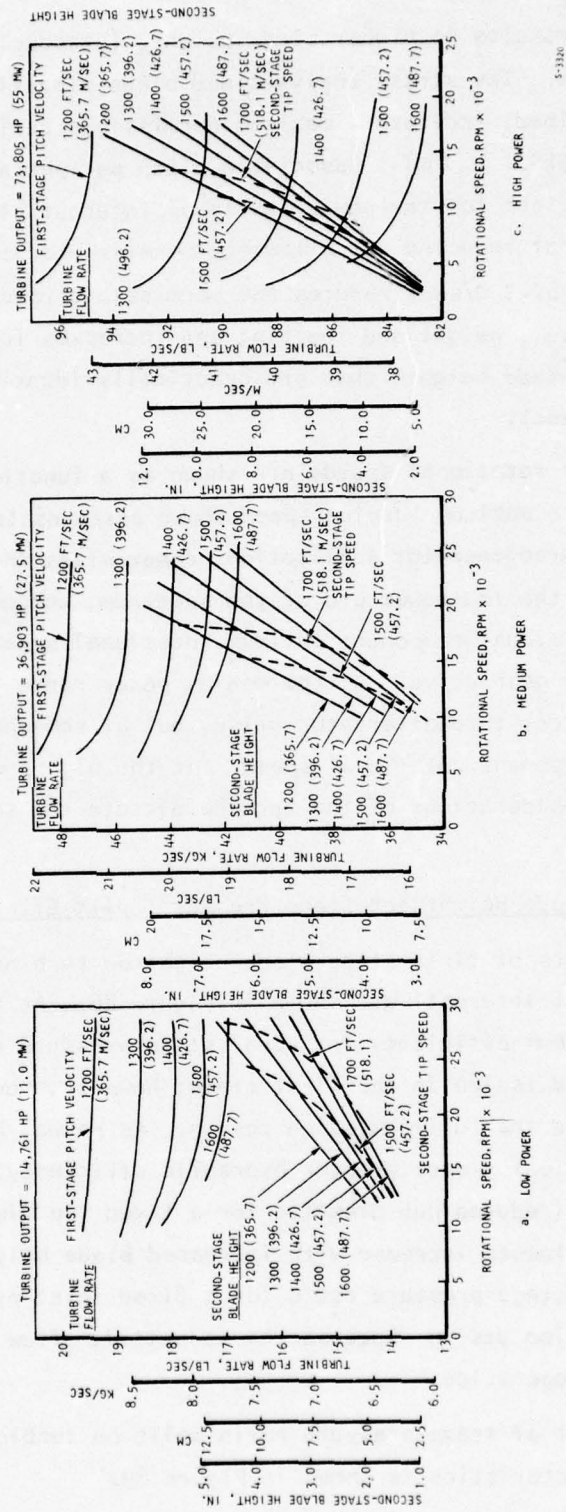


Figure 86. Rotational Speed Selection

turbine size results in higher blade height, introducing critical structural considerations. The stress analyses and blade vibration evaluation, subsequently described, indicate a maximum permissible peripheral tip speed of 1700 ft/sec (518.1 m/sec). Associated pitch peripheral speed and second-stage blade height for the power levels of interest also are shown in Figure 86. Notice that reducing the allowable permissible peripheral tip speed to 1500 ft/sec (457.2 m/sec) reduces the permissible rotational speed; increases turbine diameter, weight and inertia; and increases fuel consumption, while resulting in blade heights that are practically identical to those for 1700 ft/sec (518.1 m/sec).

Resultant rotational speeds are shown as a function of turbine power in Figure 87. The optimum turbine speed shown pertains to the turbine component only. In a turbogenerator application, compromises in rotational speeds are required. At the low-power end of the spectrum, component performances are such that individual component optimum rotational speed selection is indicated via the use of gear drive. At the medium power range, a reasonable compromise will allow direct turboalternator drive, but at somewhat different than optimum individual component rotational speed. At the high-power end of the spectrum, structural considerations of the turbine dictate the selection of turbogenerator speed.

First-Stage Blade Height and Stage Pressure Split Effects

The effects of first-stage blade height on turbine performance for the power levels of interest are shown in Figure 88. At the power levels of interest, optimum efficiency for equal stage pressure ratio split is achieved with partial admission in the first stage; however, mechanical considerations generally favor the full-admission design. As shown, high blade height (low partial admission) yields greater hydraulic efficiency and lower disc frictional losses (reduced hub diameter for a fixed tip diameter). Scavenging and blade pumping losses increase with increased blade height selection. Increasing the first-stage pressure ratio for a fixed inlet pressure also will lead to full admission design because the volumetric flow will increase at reduced back pressure operation.

The effect of stage pressure ratio split on turbine nominal design performance characteristics is shown in Figure 89.

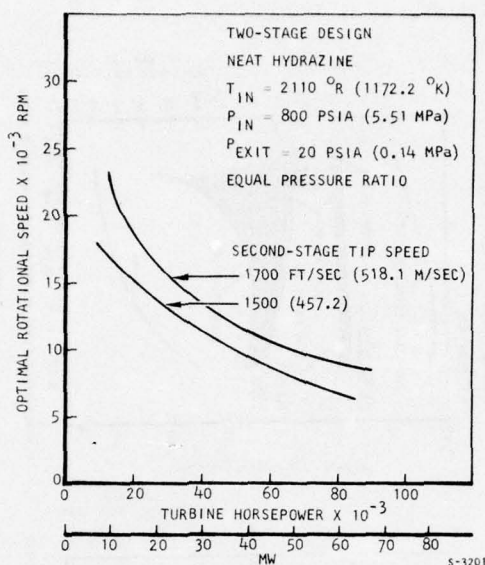


Figure 87. Optimal Turbine Rotational Speed

At nominal design operation, increasing first-stage pressure, for a stated overall pressure ratio, has only a minimal effect on turbine performance. In view of the relative insensitivity of stage pressure ratio split on overall turbine performance, substantial design latitude is introduced. For the overall pressure ratio of interest (40 to 50) the possible combinations encompass restriction of supersonic operation in the first stage with subsonic operation in the latter stage, or supersonic operation in both stages. With respect to multistage supersonic operation, the considerations include achievement of a reasonable stage work split with corresponding structurally and aerodynamically acceptable blade profiles.

In the present application, variable back pressure, due to variable altitude, will predominate. Accordingly, the selected stage pressure ratio split is based on achieving supersonic flow in both stages. This selection will further reduce fuel consumption, thus increasing mission duration capability associated with variable altitude operation. Multistage supersonic operation, at the overall pressure ratios of interest, has been successfully demonstrated in the recently developed AiResearch H_2-O_2 Space Shuttle APU turbine.

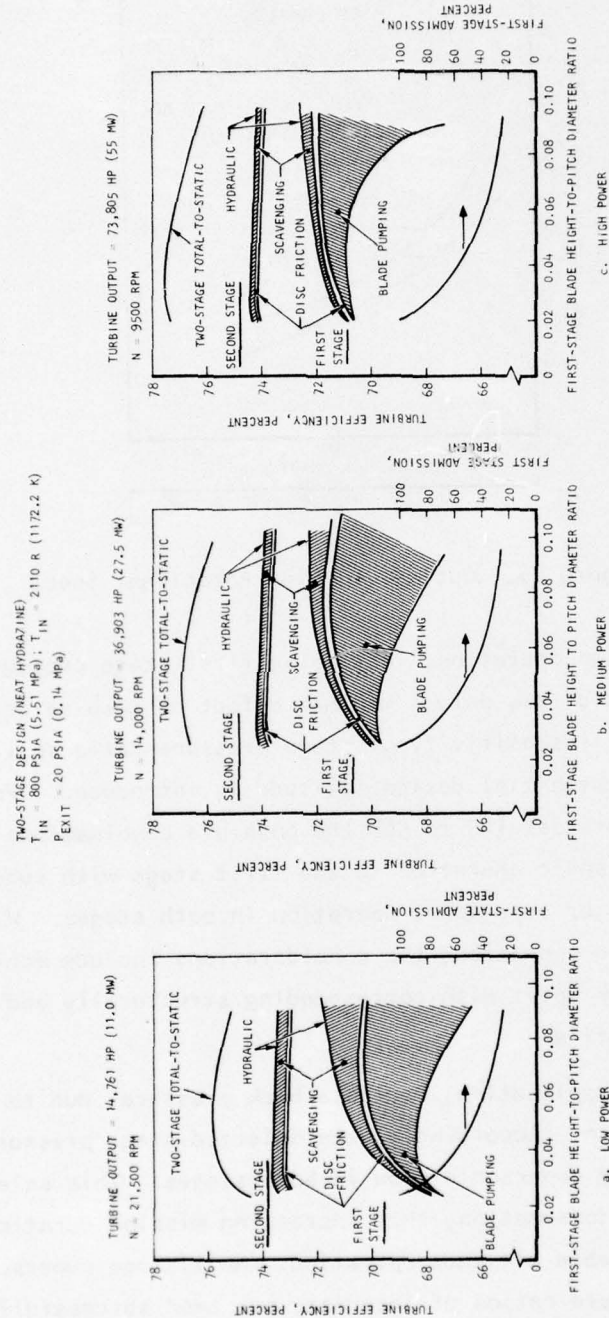


Figure 88. First-Stage Blade Height Optimization

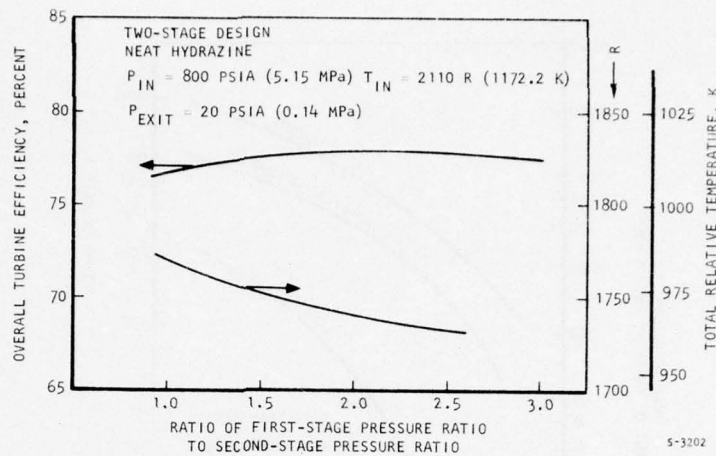


Figure 89. Stage Pressure Ratio Split

Turbine Weight and Inertia Versus Power

Optimized turbine weight and inertia as a function of turbine output is shown in Figure 90. The weight and inertia quoted pertain to a two-stage turbine optimized as an individual unit. In power system application, a compromise in component rotational speed may be dictated.

Altitude Operation

Because altitude operation predominates for this application, it is of interest to investigate the potential performance improvement associated with a turbine designed specifically for altitude operation. Results of such a trade study are illustrated in Figure 91. The first step in the trade is to optimize the nozzle expansion ratio. Altitude operation affects turbine performance in several ways. With respect to aerodynamic considerations, for a fixed nozzle inlet condition, increasing altitude (higher pressure ratio) increases the potential energy of the fuel and reduces the parasitic losses associated with turbine performance (windage and scavenging losses). The increased pressure ratio available with altitude, however, results in an overall decrease in turbine efficiency due to latter stage lower velocity ratio, high Mach number, and lower chord Reynolds number. Thus, optimization requires the evaluation of the available expansion head and associated efficiency. As shown in Figure 91, turbine flow rate is reduced with altitude operation, which means fuel consumption reduction or increased mission time is achieved (fixed propellant storage).

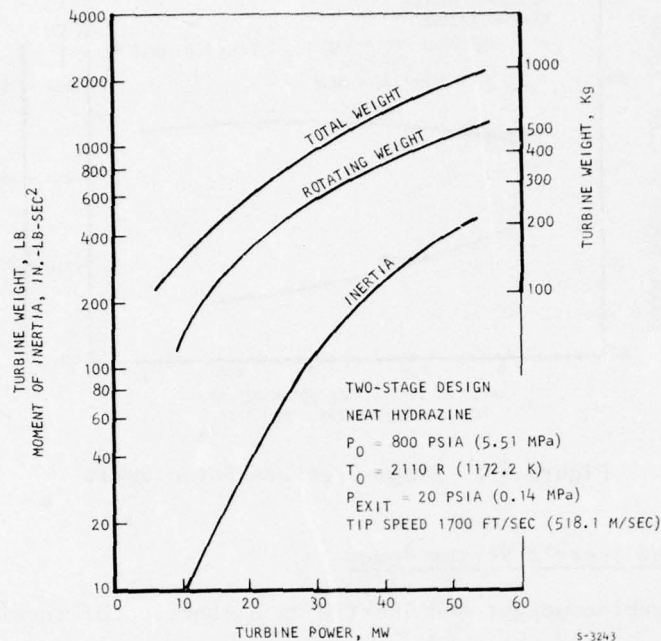


Figure 90. Optimized Turbine Weight and Inertia

Structural and weight considerations substantially negate the benefits associated with a turbine design optimized for altitude operation. The turbine flow rate achievement shown in Figure 91 pertains to maintaining a constant tip peripheral velocity at the latter stage (1700 ft/sec, 518.1 m/sec). The reduction in back pressure during altitude operation causes an increase in volumetric flow (due to reduced density), which imposes a speed reduction based on blade stress and vibrational considerations. The increased blade height and reduction in permissible rotational speed, with a constant peripheral speed, leads to increased tip diameter and turbine weight as shown in Figure 91.

A further consideration, which makes the selection of an altitude design concept questionable, is illustrated in Figure 92. Figure 92 illustrates typical off-design performance associated with sea level and altitude turbine design concepts. Both turbines are designed for identical output power (27.5 MW). The sea level design concept shows an increase in output with increase in pressure ratio at higher altitude operation. The increase in performance shown is predicated on the use of supersonic cascade contour in the

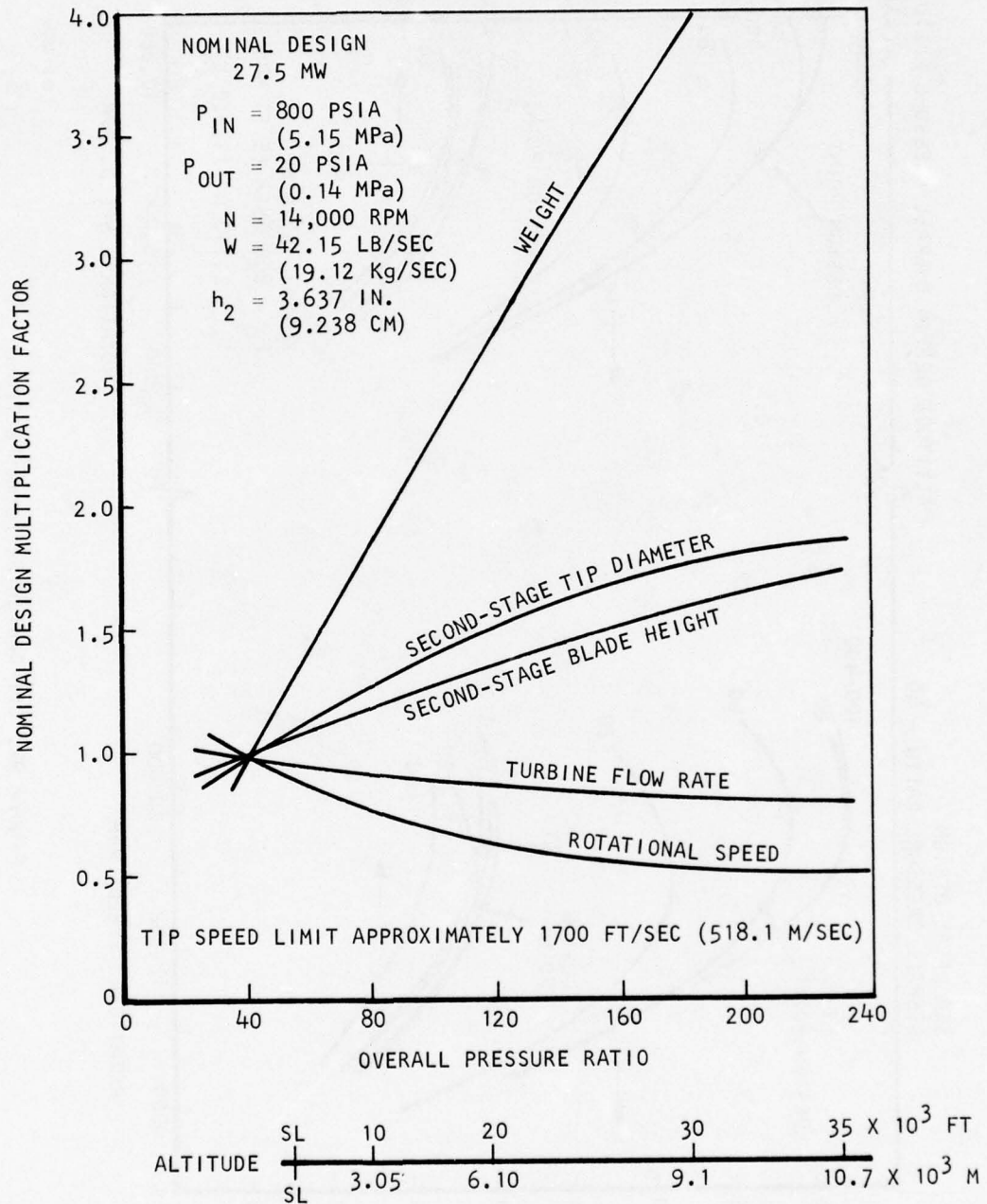
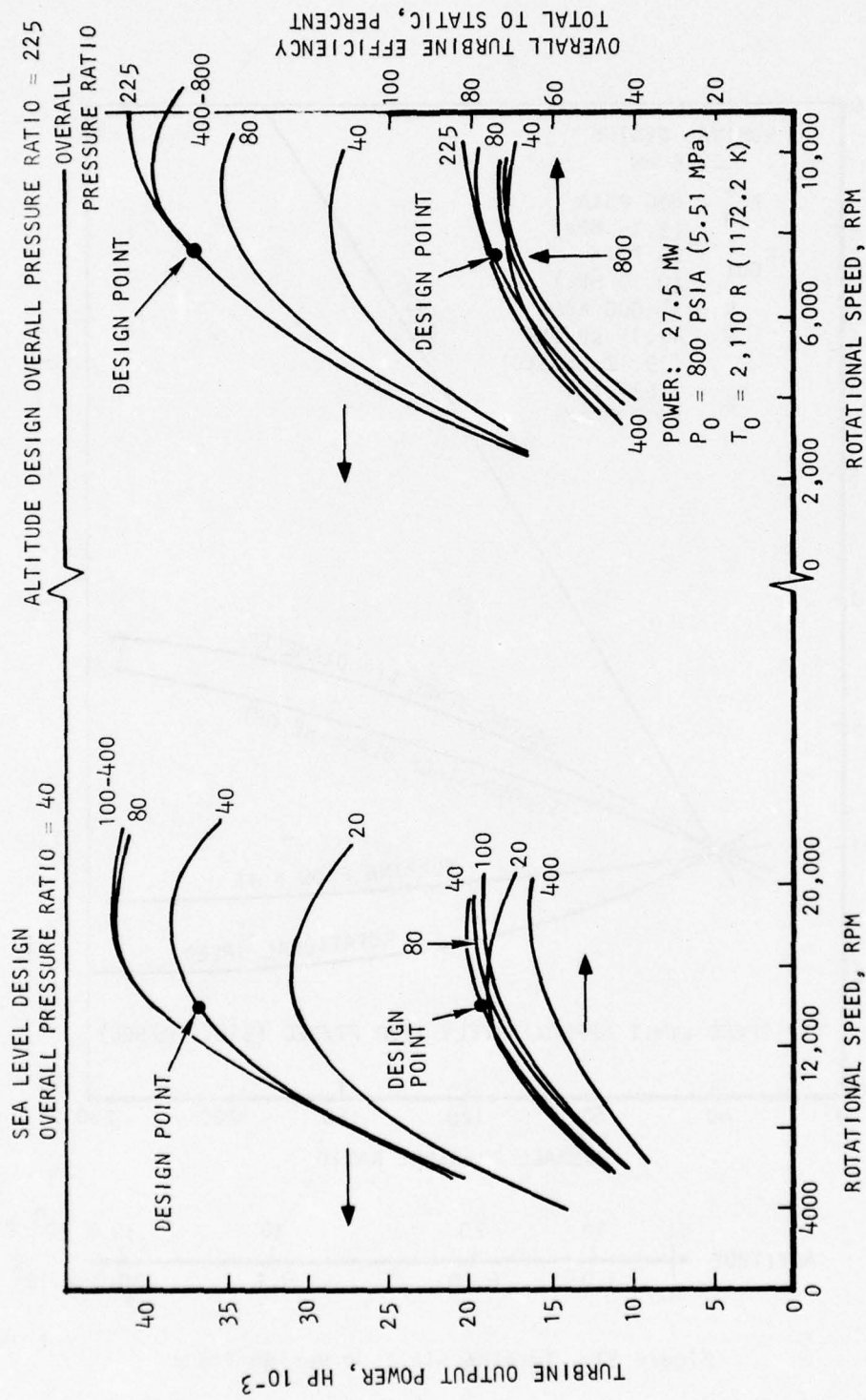


Figure 91. Turbine Altitude Design Trade

S-3242



S-3203

Figure 92. Off-Design Performance Trade

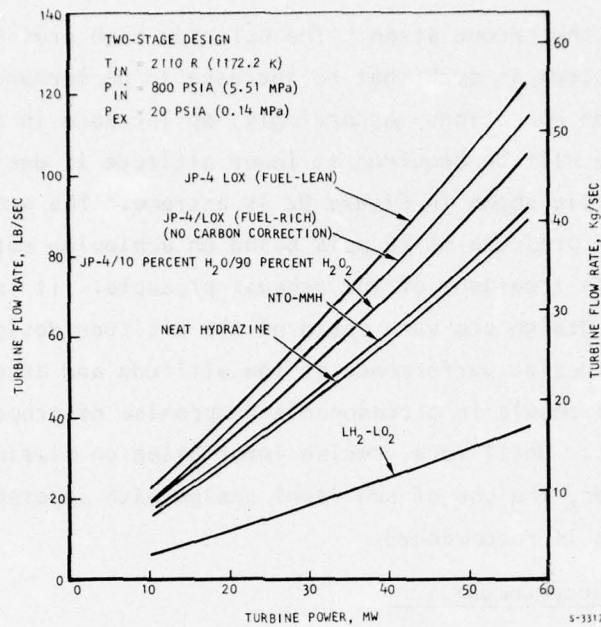
baseline design of the second stage. The selected high pressure ratio of the altitude design concept is such that no increase in performance results with increase in altitude operation. Accordingly, an increase in nozzle inlet pressure or temperature will be required at lower altitude if design power is required. The example shown in Figure 92 is extreme. The sea level design concept uses a back pressure of 20 psia based on achieving satisfactory blade height and expulsion treatment of the exhaust products. It is also possible to reduce the overall design pressure ratio of the altitude design to provide a combination of off-design performance at low altitude and acceptable altitude operation that will result in a reasonable compromise of propellant consumption and assembly weight. Until more precise information on mission requirement is established, however, the use of sea level design with supersonic blade contour in the second stage is recommended.

Propellant Performance Comparison

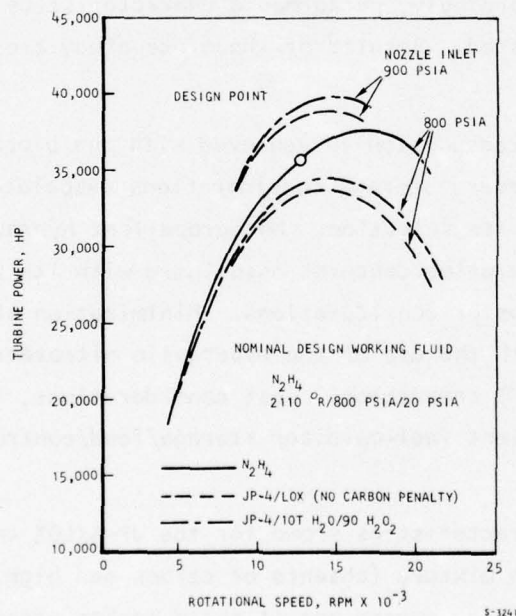
The bulk of the trade study was conducted for hydrazine as the base propellant; however, a substantial number of propellants, for various considerations, may be used. Accordingly, performance characteristics of the propellants of interest were established. Results of the trade study are shown in Figure 93a.

Minimum propellant consumption is achieved with the bipropellant combination of LH_2 and LO_2 ; however, storage considerations associated with cryogenic fuels seriously question its selection. Monopropellant hydrazine is the next best in performance. The prime concerns associated with its use encompass propellant cost and combustor considerations. Minimization of combustor complexity is associated with the use of the hypergolic nitrotetroxide (NTO) and monomethyl hydrazine (MMH) combustion. Cost considerations, in addition to the complexity of a bipropellant fuel-oxidizer storage/feed/control are of concern for this combination.

The performance characteristics shown for the JP-4/ LOX combination pertain to the use of a fuel-lean mixture (absence of carbon and high O/F sensitivity) and a fuel-rich mixture (high percentage of solid carbon present in the exhaust products). The fuel-rich combination shown encompasses no performance correction due to the potential presence of solid carbon in the exhaust products. The



a. PROPELLANT PERFORMANCE CHARACTERISTICS



b. FIXED TURBINE DESIGN, VARIABLE PROPELLANT

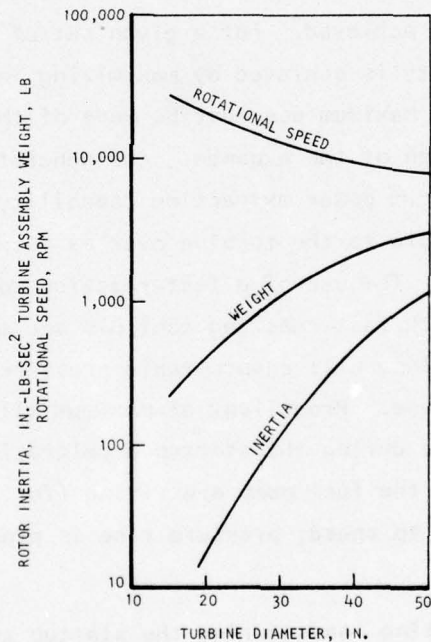
Figure 93. Propellant Performance Comparison

selection of the combination of JP-4/10% H_2O /90% H_2O_2 shows reasonable performance and low cost. The important considerations for this combination are the use of a bipropellant system and the high venting rate associated with the use of peroxide.

Figure 93b illustrates the effects of variable propellant use with a fixed turbine design. The nominal design uses neat hydrazine; substituting the use of either JP-4/LOX or JP-4/10% H_2O /90% H_2O_2 requires a slight increase in nozzle inlet pressure to achieve the desired power.

Turbine Algorithm

The turbine weight, inertia, and rotational speed algorithm developed under this study program is shown in Figure 94. The algorithm shown is based on the use of a two-stage turbine design using neat hydrazine in a turbogenerator system of interest in the Air Force application.



S-3244

Figure 94. Turbine Algorithm

The specific algorithm can be expressed, in terms of English units, as follows.

$$\begin{aligned} D_T &= (3.896 \times 10^5) N^{-1} \\ W &= 0.3455 D_T^{2.362} \\ I_p &= (1.967 \times 10^{-5}) D_T^{4.614} \end{aligned}$$

where:

$$\begin{aligned} N &= \text{rotational speed, rpm} \\ D_T &= \text{tip diameter, in.} \\ W &= \text{assembly weight, lb} \\ I_p &= \text{rotor inertia, in.-lb-sec}^2 \end{aligned}$$

FAST STARTUP DESIGN CONSIDERATIONS AND CHARACTERISTICS

One of the major operational requirements is that multiple-cycle, fast-startup capability must be achieved. For a given set of design requirements, fast acceleration capability is achieved by maximizing input power and minimizing the encountered load. Maximum use must be made of the available drive energy by appropriate design of the expander, gas generator, fuel supply, and associated controls. Maximum power extraction capability within these specified constraints must be available to the turbine over as much of the startup acceleration phase as possible. The use of a fast-reaction combustion chamber, close-coupled to the turbine, with fast-reacting controls and minimal supply line volume to minimize free volume will ensure rapid pressure and temperature rise in the initial ignition phase. Propellant at maximum allowed pressure and flow rate must be made available during the startup accelerating phase while flow and pressure delivery from the fuel pump are rising (for a throttle valve setting, flow is proportional to speed; pressure rise is proportional to the square of the speed).

Minimization of operating loads during the startup accelerating period requires: (1) proper operational sequencing of the loads, and (2) minimization of rotating assembly inertia. Secondary contributors to rotating assembly inertia, such as the gearbox, fuel pump, and lubrication pump, also must be considered.

In fast-startup turboalternator drive units, application of the full electrical load typically occurs somewhere near the end of the acceleration period; therefore, design power delivery must lag design speed delivery. With the additional requirement of maximum allowable speed excursion, power control must be employed in the startup phase in a time interval in which the acceleration rate is rapidly diminishing (lower turbine torque, high load torque). The gas generator could require preheating to initiate ignition; however, except for an increased heating power requirement, the effect on fast startup capability will be minimal if ignition is achieved.

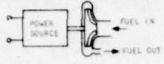
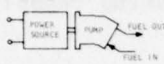
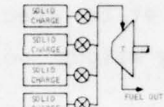
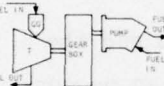
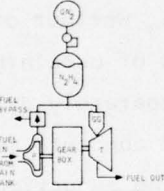
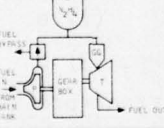
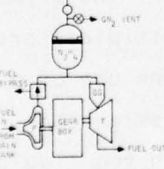
All of the preceding considerations must be fully assessed in arriving at a fast-startup design that is capable of providing power directly at the specified conditions, repeatable for the stated mission, and of satisfactory weight, volume, and operational sequence simplicity.

Fast-Start Fuel Assembly Concept Review

A review of fast-startup fuel assembly concepts was conducted and the results are summarized in Table 64. The fast-startup approaches can be conveniently subdivided into concepts that are either aircraft-dependent or integrated with the turbine assembly. The aircraft-dependent concepts, whether of centrifugal or variable-displacement pump approach, are techniques of obtaining high-pressure, high-flow delivery by the sudden acceleration of separately driven small pump units. Considerations that make the aircraft-dependent concepts less attractive than the APU-integrated concepts include the accompanying reduction in available startup time and the need for power source interfacing. The APU-integrated fast startup concepts encompass the potential use of: (1) a variable-displacement fuel pump, (2) separate high-pressure blowdown, (3) a rechargeable high-pressure accumulator, and (4) a rechargeable constant-pressure accumulator. The use of a solid propellant for startup provides upon demand the desired high pressure, high temperature, and high flow; however, the prime design considerations that negate its use are the complexity of multiple start cycles and possible solid propellant/catalyst carbon poisoning. The use of a variable-delivery fuel pump ensures high-pressure availability. Design considerations of concern include the compatibility of the device with the liquid propellant and the need for increased pressurization (200 to 300 psia) of the main fuel tank.

TABLE 64

FAST STARTUP CONCEPTS REVIEW

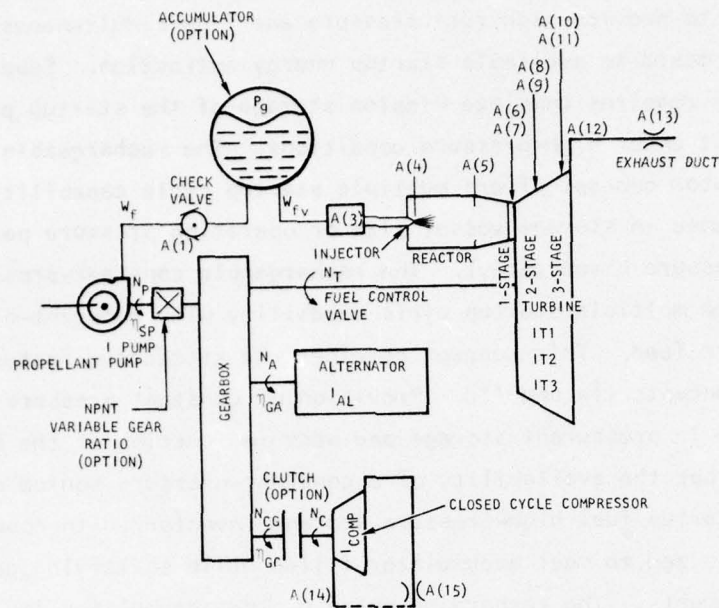
TYPES	POWER SOURCE	COMMENTS	
		ADVANTAGES	DISADVANTAGES
I AIRCRAFT DEPENDENT a. CENTRIFUGAL PUMP 	<ul style="list-style-type: none"> ELECTRICAL HYDRAULIC 	<ul style="list-style-type: none"> ESTABLISHED HYDRAZINE COMPATIBILITY LOW-INERTIA ASSEMBLY 	<ul style="list-style-type: none"> SYSTEM INTERFACE (POWER) HIGH ACCELERATION RATE TO MEET OVERALL SYSTEM STARTUP INCREASED PUMPING POWER TO ACHIEVE STARTUP POTENTIAL THERMAL RESTRICTIONS
b. VARIABLE DELIVERY DISPLACEMENT PUMP 	<ul style="list-style-type: none"> ELECTRICAL HYDRAULIC 	<ul style="list-style-type: none"> HIGH-PRESSURE AVAILABILITY LOW PUMPING POWER (HIGH EFFICIENCY) LOW INERTIA ASSEMBLY 	<ul style="list-style-type: none"> INTERFACE (POWER) HYDRAZINE COMPATIBILITY NEEDS TO BE FURTHER ESTABLISHED HIGH COMPONENTS WEIGHTS
II APU INTEGRATED a. SOLID PROPELLANT CHARGE 	<ul style="list-style-type: none"> APU SOLID PROPELLANT CHARGE 	<ul style="list-style-type: none"> HIGH-PRESSURE, HIGH-TEMPERATURE IMMEDIATELY AVAILABLE MISSILE APU APPLICATION 	<ul style="list-style-type: none"> MULTIPLE CHARGE, REQUIRED HIGH TEMPERATURE VALUING SEPARATE NOZZLE BLOCK (1ST STAGE) TO PREVENT CATALYST POISONING
b. VARIABLE DELIVERY DISPLACEMENT PUMP 	<ul style="list-style-type: none"> APU HYDRAZINE COMBUSTION PRODUCTS WITH MINIMAL PRESSURIZATION 	<ul style="list-style-type: none"> MINIMUM INTERFACE HIGH-PRESSURE AVAILABILITY LOW PUMPING POWER LOW-PRESSURE FUEL STORAGE HIGH NUMBER OF STARTUP CYCLES 	<ul style="list-style-type: none"> HYDRAZINE COMPATIBILITY NEED TO BE FURTHER ESTABLISHED HIGH COMPONENT WEIGHT MAIN FUEL TANK NEEDS TO BE SLIGHTLY PRESSURIZED (2-300 PSIA)
c. SEPARATE HIGH-PRESSURE BLOWDOWN 	<ul style="list-style-type: none"> APU HYDRAZINE COMBUSTION PRODUCTS WITH HIGH-PRESSURE PRESSURANT AND FUEL STORAGE 	<ul style="list-style-type: none"> MINIMUM INTERFACE CONSTANT HIGH-PRESSURE FUEL AVAILABLE 	<ul style="list-style-type: none"> RESTRICTED TO LOW NUMBER OF STARTUP CYCLES MUST CARRY FULL STARTUP FUEL AND GN₂ INVENTORY AT HIGH PRESSURE MAXIMUM HIGH-PRESSURE FUEL AND GN₂ STORAGE
d. RECHARGEABLE HIGH-PRESSURE ACCUMULATOR 	<ul style="list-style-type: none"> APU HYDRAZINE COMBUSTION PRODUCTS WITH HIGH-PRESSURE FUEL STORAGE AND NONCYCLE DEPENDENT MINIMAL PRESSURANT STORAGE 	<ul style="list-style-type: none"> MINIMUM INTERFACE NO STARTUP CYCLE LIMITATION FUEL SELF-PRESSURIZED AND AVAILABLE AT DESIRED CONDITIONS PER NEXT STARTUP CYCLE 	<ul style="list-style-type: none"> VARIABLE TURBINE INLET PRESSURE INCREASE IN ACCUMULATOR VOLUME PER START CYCLE OR HIGH OPERATIONAL PRESSURE TO MEET REQUIRED STARTUP
e. RECHARGEABLE CONSTANT PRESSURE ACCUMULATOR 	<ul style="list-style-type: none"> APU HYDRAZINE COMBUSTION PRODUCTS WITH HIGH-PRESSURE PRESSURANT AND FUEL STORAGE 	<ul style="list-style-type: none"> MINIMUM INTERFACE MINIMAL HIGH-PRESSURE FUEL STORAGE CONSTANT HIGH-PRESSURE FUEL AVAILABLE FUEL SELF-PRESSURIZED AND AVAILABLE AT DESIRED CONDITIONS FOR NEXT STARTUP CYCLE 	<ul style="list-style-type: none"> NUMBER OF STARTUP CYCLES AFFECTS REQUIRED GN₂ STORAGE SLIGHT GN₂ VENTING REQUIRED DURING ACCUMULATOR FUEL FILLING.

S-87964

The last three APU-integrated concepts of Table 64 (11c, 11d, and 11e) are all designed to provide high fuel pressure and flow simultaneously to the gas generator to maximize available startup energy extraction. Separate high-pressure blowdown requires complete mission storage of the startup pressurant gas and propellant under high-pressure conditions. The rechargeable high-pressure accumulator concept offers multiple startup cycle capabilities, but requires an increase in storage vessel size or operating pressure per startup cycle (due to pressure bleed decay). The rechargeable constant-pressure accumulator offers the multiple startup cycle capability with constant-blowdown-activated pressure feed. This concept combines the attractive features of the APU-integrated concepts 11a and 11d. Provision of constant pressure requires a slight increase in pressurant storage and vent (a function of the number of startup cycles), but the availability of a constant-pressure source allows a reduction in startup fuel high-pressure storage inventory. In concept 11e, the fuel pump is sized to meet accumulator fillup while satisfying gas generator requirements. The recharging phase of the accumulator imposes the use of a mechanical stop in the accumulator.

Startup System Model

An existing AiResearch computer program is available to evaluate fast startup turbine concepts and associated control requirements. The model allows investigation of the various techniques of achieving fast startup. It contains all elements that generally make up rotating assemblies. In the present turbo-drive subsystem loop, a fuel pump feeds through a check valve into a pressurized fuel accumulator. Downstream of the accumulator, a fuel control valve meters the fuel into the gas generator. The gas generator then provides hot gas to the turbine, which drives a choice of equipment through the gearbox. Driven components include an alternator, a fuel pump, and a recirculating compressor gas loop. The program offers the option of: (1) selection of components in the turbodrives loop, (2) the use of a print-plot of performance characteristics, and (3) incorporation of the effects of load step changes and steady-state operation on system performance. A system schematic of the fast startup program model is shown in Figure 95. Operating characteristics of the various components shown are incorporated in the basic program. These include line impedance, valve pressure drops, combustion temperature-pressure relationships, turbine



5-76668

Figure 95. Fast-Startup System Program Model System Schematic

performance prediction at design and off-design operating conditions (program TMAP), gearbox losses, compressor performance, fuel pump performance, alternator time constants, and component inertias. These operating characteristics are normalized so the following options are available through simple substitution of data cards.

- (a) Revised fuel design characteristics, physical dimensions, number of stages, new gas properties, etc.
- (b) Revised fuel design flow and operating speed. If variable ratio is desired, the maximum gear ratio and maximum pump overspeed can be stated.
- (c) Revised pressure drops across check valve, fuel control valve, and injectors.
- (d) Revised accumulator data such as initial pressure, total volume of accumulator, initial volume of propellant, and thermodynamic properties of pressurant gas.

- (e) Revised gas generator temperature-pressure relationship to correlate variable chamber and/or variable fuel.
- (f) Revised alternator dynamics and speed at the specified point of load application, varying from zero to 100 percent of design speed.
- (g) Revised control parameters for turbine speed control, such as time constants and rate feedback.

Fast Startup Performance

The availability of the computer program allows the effective evaluation of characteristics associated with fast startup turboalternator concepts. The assumed gas generator characteristics are shown in Figure 96.

The resultant startup times for the various conventional generator design points of interest are shown in Figure 97. For the conventional generator, whether of thermal-lag design or fluid-cooled design, anticipated startup times of 1.5 to 1.8 sec are possible. For a stated output, say 25 MW, the use of fluid cooling in lieu of thermal lag substantially reduces startup time or excess drive energy required. Fast startup of the superconducting generator concepts was not evaluated based upon considerations described in Section 7.

STRUCTURAL DESIGN CONSIDERATIONS AND CHARACTERISTICS

Key mechanical and structural elements associated with the successful design of a high-power turbine are reviewed here. The multiplicity of structural design efforts subsequently described must be conducted to establish the validity of the configuration(s) selected. In the final analyses, turbine design involves an appropriate balance between aerodynamic and structural considerations.

Thermal Performance Evaluation

AiResearch experience with high-speed turbomachinery has shown that thermal problems have a major effect on achieving desired reliability of a turbine assembly. Therefore, detailed thermal design studies must be performed and coordinated with other design activities to establish realistic designs that will minimize thermal problems. The available AiResearch transient and steady-state thermal analyzer computer program is used extensively for analysis and to

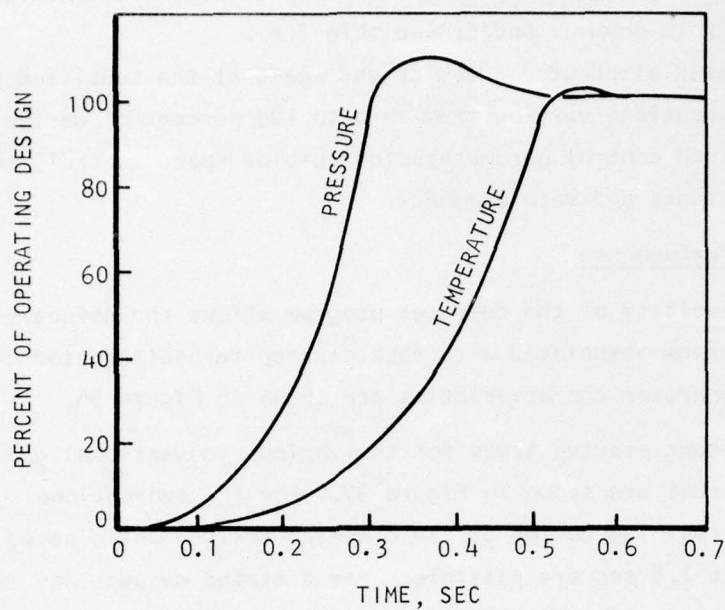
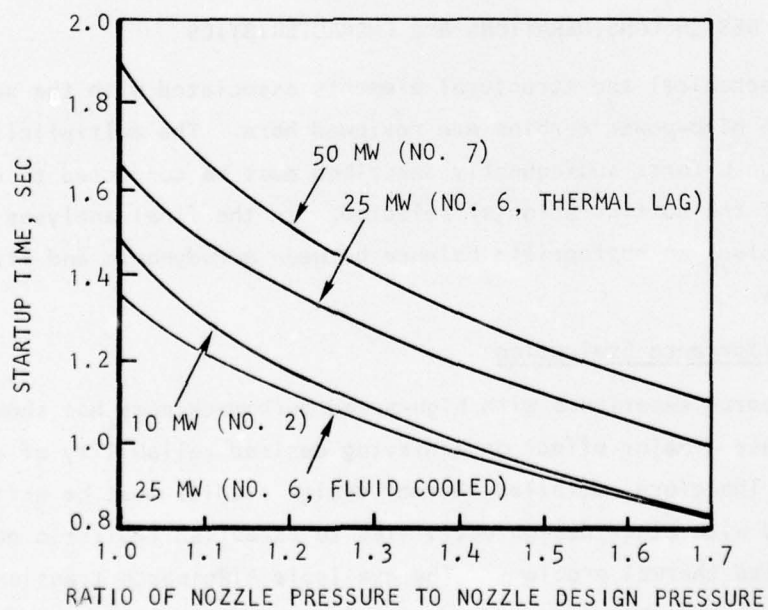


Figure 96. Pilot-Thermal Gas Generator Characteristics



S-3238

Figure 97. Startup Times

simulate real operating conditions. The transient and steady-state analyses are run to determine:

- (a) Thermal gradient in the assembly
- (b) The effect of differential thermal expansion on thermal stress and rotating part clearances
- (c) Bearing lubrication and cooling requirements
- (d) The effect of varying environmental conditions
- (e) Good designs with respect to thermal barriers, component arrangement, and leakage flow

Thermal Management Under Fast Startup, Normal Operation, and Shutdown

Several important thermal design considerations must be made in the design of a turbine unit with fast startup capability. In a turbine operating at design speed close to design turbine inlet temperature at zero output power, little temperature change occurs during the transition from zero to full load; however, large thermal gradients occur when a turbine starts from the cold condition. Large thermal gradients produce large thermal stresses that limit the low-cycle fatigue life of the turbine. The disc may be sized to limit these thermal stresses, but this sizing would increase the polar moment of inertia and make fast startup more difficult.

Cutting slots in the rim of the disc will relieve disc thermal stress and allow much greater low-cycle fatigue life for the turbine. Alternatively, a method in which sections of the blades are attached to the disc with "dovetail" or "fir tree" attachments also can be used. The thermal gradients in the attachment section also reduce thermal stresses into the hub of the disc.

Previous studies indicate that it is impractical to attempt to cool turbine blades of this size significantly below the hot gas recovery temperature. An extremely high heat transfer coefficient is produced by a hot gas mixture flowing at high velocity over the turbine blades. Therefore, any attempt to cool the turbine blades significantly will result in large thermal gradients and large thermal stresses in the blades. A high heat transfer coefficient also causes the turbine blades to heat rapidly when hot gas flow begins. In this condition, the blade leading edge heats more rapidly than the midchord region because the thermal capacitance of the leading edge is less, and the heat

transfer coefficient to the leading edge is greater. This produces high thermal stresses at the leading edge during turbine startup. The leading edge heat transfer coefficient is inversely proportional to the square root of the leading edge diameter, and the thermal capacitance is directly proportional to the square of the leading edge diameter. Therefore, an increase in the leading edge diameter significantly reduces the transient thermal gradient between the mid-chord region and the leading edge, and increases the low-cycle fatigue life of the turbine blade.

In this design, the largest practical leading edge diameter consistent with good aerodynamic performance must be used. A tapered cavity for the second stage is used in the midchord region of the blade to reduce stress at the root and decrease transient thermal gradients in the blade.

At shutdown operation, heat soakback from the turbine disc into the bearing carrier and thermal growth differential between the outer housing incorporating the nozzle box and the turbine rotor must be considered. The thermal expansion during both startup and shutdown will determine the running tip clearance, and thus turbine performance. The amount of heat leak into the bearing carrier will determine whether it is necessary to continue bearing cooling during the post-shutdown operation period.

Thermal Analyses

Substantial thermal analyses were conducted to evaluate the effects of various duty cycles on turbine design and to assist in the required stress evaluations and material selection.

To ascertain satisfactory temperature distribution of the turbine assembly during startup, normal operation, and shutdown at various anticipated duty cycles, a transient thermal evaluation was conducted. The potential application of four duty cycles were investigated. These cycles encompass:

Cycle A--A single burst of 120 sec with 3600 sec cooldown period

Cycle B--Three bursts of 21 sec on with 30 sec off and cooldown period of 1800 sec

Cycle C--Three bursts of 21 sec on with 150 sec off and cooldown period of 1800 sec

Cycle D--Three bursts of 21 sec on with 300 sec off and cooldown period of 300 sec

For the four cycles evaluated, the most stringent with respect to thermal distribution is associated with Cycle A, the single burst of 120 sec and cool-down period of 3600 sec. For this cycle, the maximum bearing temperature of 930 R (516.7 K) occurred 35 min after the shutdown. The thermal model used is shown in Figure 98. A typical temperature distribution (Cycle A) is shown in Figure 99.

As shown in Figures 98 and 99, node 9 (first-stage disc hub) and node 32 (turbine end bearing) reach their maximum operating temperature levels approximately midway through the cooldown period.

To ascertain the validity of the selection of turbine peripheral speed, rotational speed, blade height and chord, etc., required in the definition of turbine assembly weight, inertia, and performance, a detailed turbine temperature distribution as a function of position and time was evaluated. The turbine thermal history thus obtained is used to evaluate the various structural considerations required. Detailed temperature distributions of the first and second turbine stages are shown in Figures 100 and 101, respectively.

Structural Performance Evaluation

The objective of structural performance evaluation of the turbine power unit is to obtain a minimum-weight system consistent with required structural integrity, performance, life capability, and reliability. Some of the critical structural design considerations evaluated in the turbine study program are described below.

The turbine power unit may be required to accelerate from zero to full operational speed and power within 1 to 2 sec. During this fast startup, the turbine discs will experience large thermal gradients and possible overspeed conditions. In the stress analysis of the turbine discs there are three areas of prime concern: (1) overspeed capability, (2) disc growth, and (3) operational life.

The disc hub must be designed to withstand centrifugal loading without excessive growth or bursting. The turbine discs are designed so that the average tangential stress provides the required safety margin from minimum material ultimate strength at operating temperature during the maximum overspeed condition.

$$T_{\infty} = 64$$

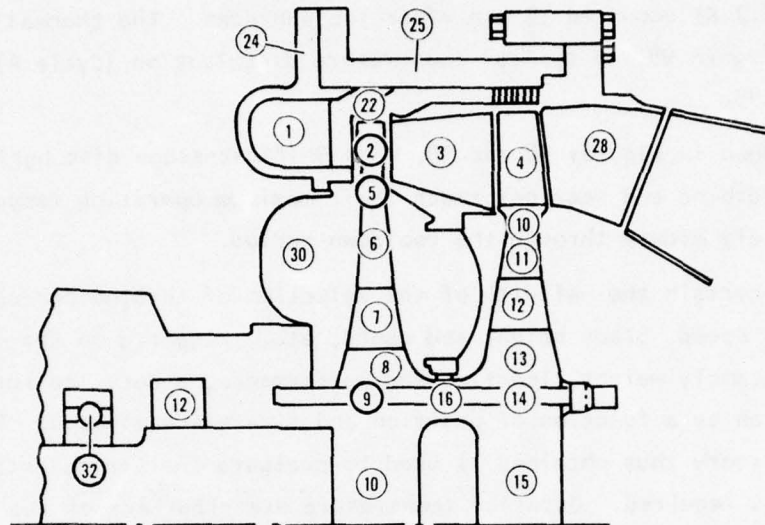


Figure 98. Turbine Assembly Nodal Model

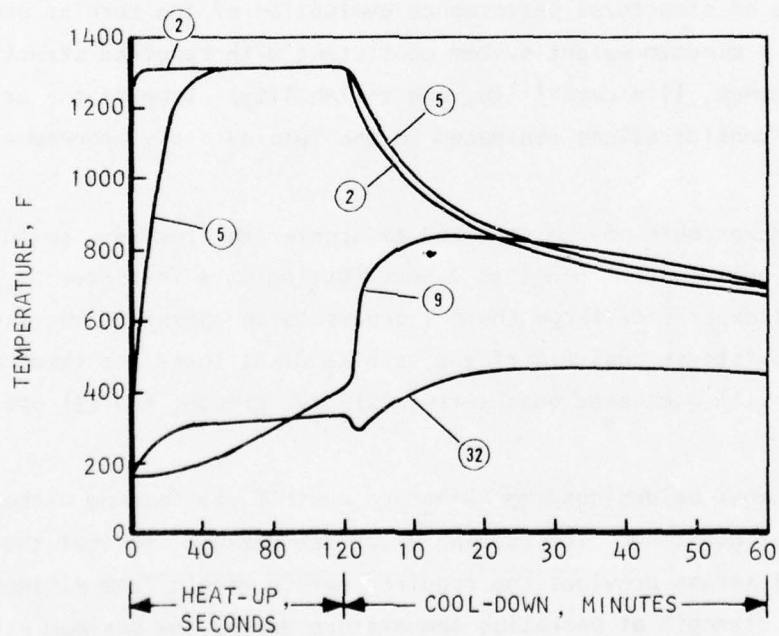


Figure 99. Cycle A Thermal Distribution

S-3288

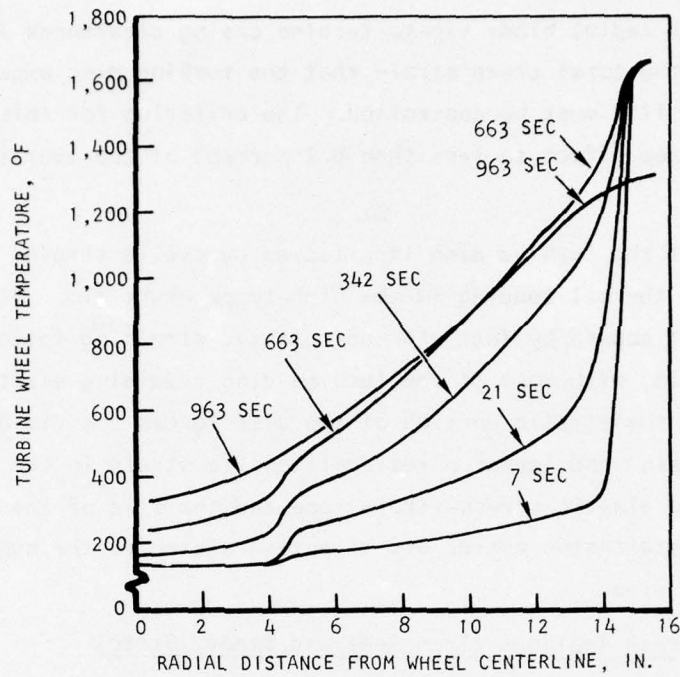
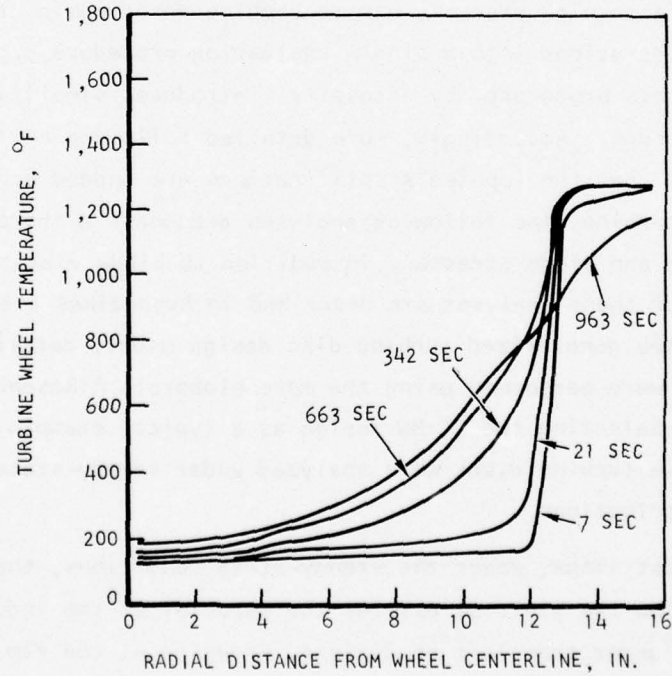


Figure 100. First-Stage Temperature Distribution



S-3240

Figure 101. Second-Stage Temperature Distribution

To maintain radial blade tip-to-turbine casing clearances and to prevent creep rupture, the total creep strain that the turbine disc experiences during its operational life must be controlled. The criterion for this design is to limit the creep effect to less than 0.2 percent of the overall allowable growth.

The life of the turbine disc is affected by cyclic strains caused by centrifugal and thermal loading in the high-temperature rim. Due to the large thermal gradient caused by fast startup, plastic straining followed by creep occurs in the rim, with most of the turbine disc remaining elastic. When loading is removed, the elastic portion of the disc forces the rim back to essentially zero strain, and leaves a residual tensile stress in the rim. The size of the resulting plastic stress-strain loop and the size of the hysteresis loops for subsequent start-stop cycles are directly related to the number of cycles the unit can survive.

Turbine Disc Stress Analyses (Transient and Steady State)

As previously stated, the design procedure followed in the performance evaluation of the turbine assembly was to combine aerodynamic, thermal, and structural considerations into a single evaluation procedure e.g., program TAPE; however, this procedure, by necessity, introduces simplifications in the evaluation procedure. Accordingly, more detailed follow-on analyses were conducted to ensure that the imposed simplifications are indeed acceptable. With respect to the turbine, the follow-on analyses encompass a thorough review of the turbine disc and blade stresses, in addition to blade vibration examination. Details of these analyses are described in Appendixes C and D.

To verify the generalized turbine disc design model, detailed turbine disc stress analyses were performed using the more elaborate AiResearch Computer Program X0815. Selecting the 25-MW design as a typical example, finite elements of the respective turbine discs were analyzed under steady-state and transient temperature distributions.

For the first stage, under the steady-state conditions, the resulting stresses are below the yield stress for the material at the indicated temperatures; however, under transient conditions, stresses at the rim exceeded allowable yield strength. Several disc profile modifications were attempted

without significant improvement. The adopted solution involves the use of a slotted disc to avoid the high negative tangential (hoop) stresses. A summary of the effective first-stage transient and steady-state stresses is shown in Figure 102. Remaining detail stress considerations are described in Appendix C.

The slotted disc is an acceptable approach to relieve the stresses encountered in the first-stage turbine. Alternative concepts involve the use of cast blades with fir trees. Table 65 summarizes the operational stresses of the first stage. This structural evaluation indicates satisfactory stress and burst margin under both steady-state and transient operation.

The resultant turbine disc profile of the second stage is very close to the one determined by the Program TAPE subroutine. The main difference is in the center thickness area required basically for transient operation. Because this information is an input to the program, subsequent structural evaluation,

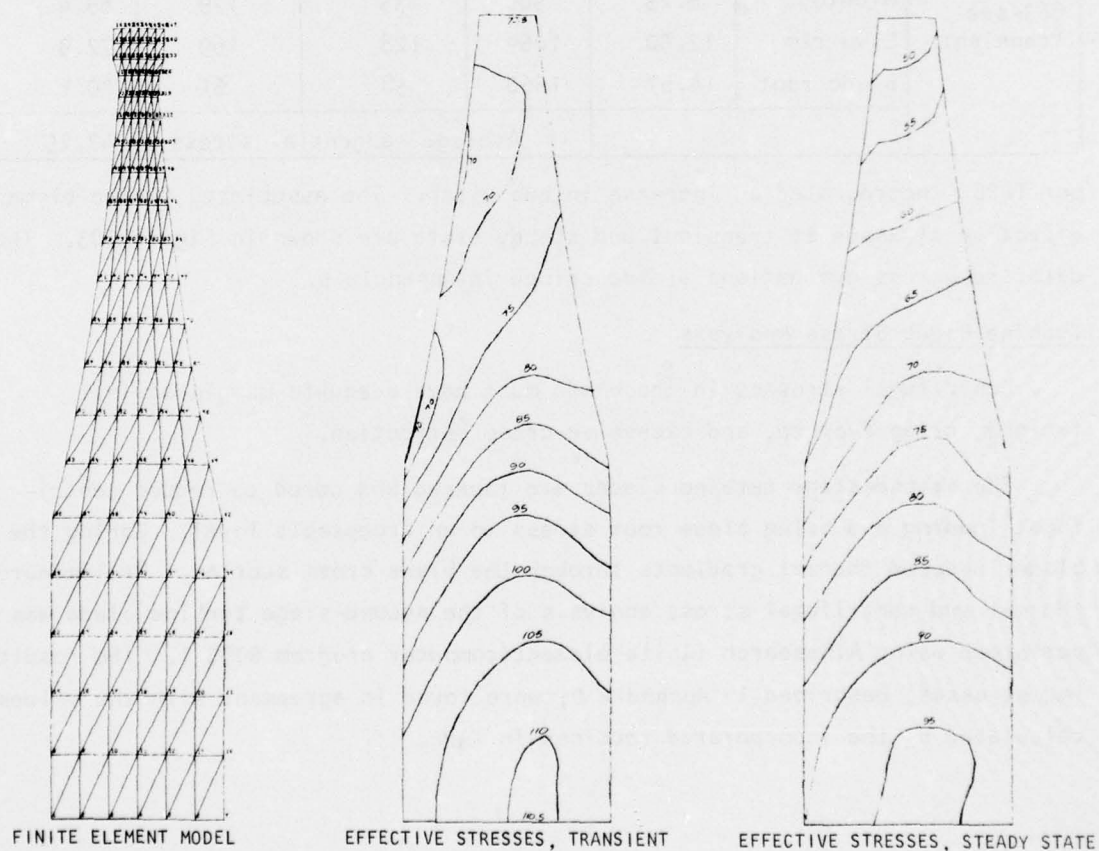


Figure 102. First-Stage Turbine Disc Stress Review

S-3369

TABLE 65
FIRST-STAGE TURBINE DISC STRESS SUMMARY

Condition @ 13125 rpm	Position	Radius, in.	Temp., °F	Material Properties		Maximum Effective Stress, ksi
				Yield Strength, ksi	Ultimate Strength, ksi	
Steady State	Center	0	1200	126	163	96.3
	Middle	6.25	1396	118	145	72.1
	Live rim	12.50	1592	80	83	48.7
	Blade root	14.67	1660	58	61	20.1
	Average tangential stress					57.65
663-sec Transient	Center	0	200	139	183	110.5
	Middle	6.25	500	135	179	85.4
	Live rim	12.50	1069	128	169	72.9
	Blade root	14.67	1660	58	61	20.1
	Average tangential stress					47.25

per TAPE, incorporated an increase in hub width. The associated finite element, effective stresses at transient and steady state are shown in Figure 103. The detailed stress evaluations are described in Appendix D.

Turbine Blade Stress Analysis

Centrifugal stresses in the blade must have adequate margin against fatigue, creep rupture, and excessive creep deflection.

The second-stage turbine blades are tapered and cored to reduce centrifugal loading and bring blade root stress to an acceptable level. Coring the blades reduced thermal gradients through the blade cross section. Preliminary thermal and centrifugal stress analysis of the second-stage turbine blade was performed using AiResearch finite element computer program BOSS 1. The resulting stresses, described in Appendix D, were found in agreement with the values calculated by the incorporated routines in TAPE.

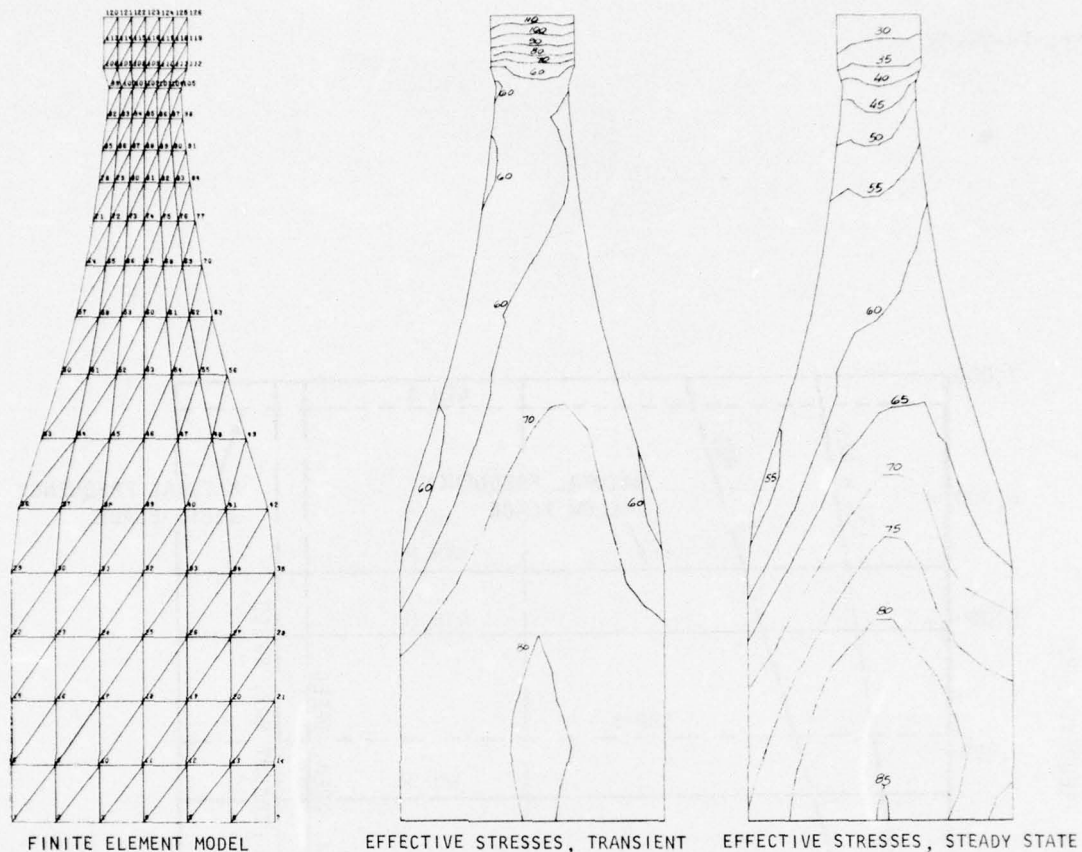


Figure 103. Second-Stage Turbine Disc Stress Review

S-3368

Turbine Blade Vibration Evaluation

A preliminary blade vibration analysis was conducted for the second-stage blade to investigate the possibility of blade structural resonance with aerodynamic excitation frequencies. The natural frequencies were determined using AiResearch computer program VIBE 1. The blade natural frequencies are plotted in the interference diagram, as shown in Figure 104. The first five vibration modes were investigated at zero rpm, 13,125 rpm (105 percent of maximum operating speed), and 8125 rpm (65 percent of maximum operating speed) for the use of either hollow or solid blades. The interference diagram shown in Figure 104 indicates that the 1 per revolution excitation is well below the maximum operating speed and that the 83 vanes possible excitation line intersects the first five modes below 6000 rpm. The use of hollow blades with an area taper ratio of 1.5 is quite acceptable (low stresses, non-critical natural frequencies, and lower weight).

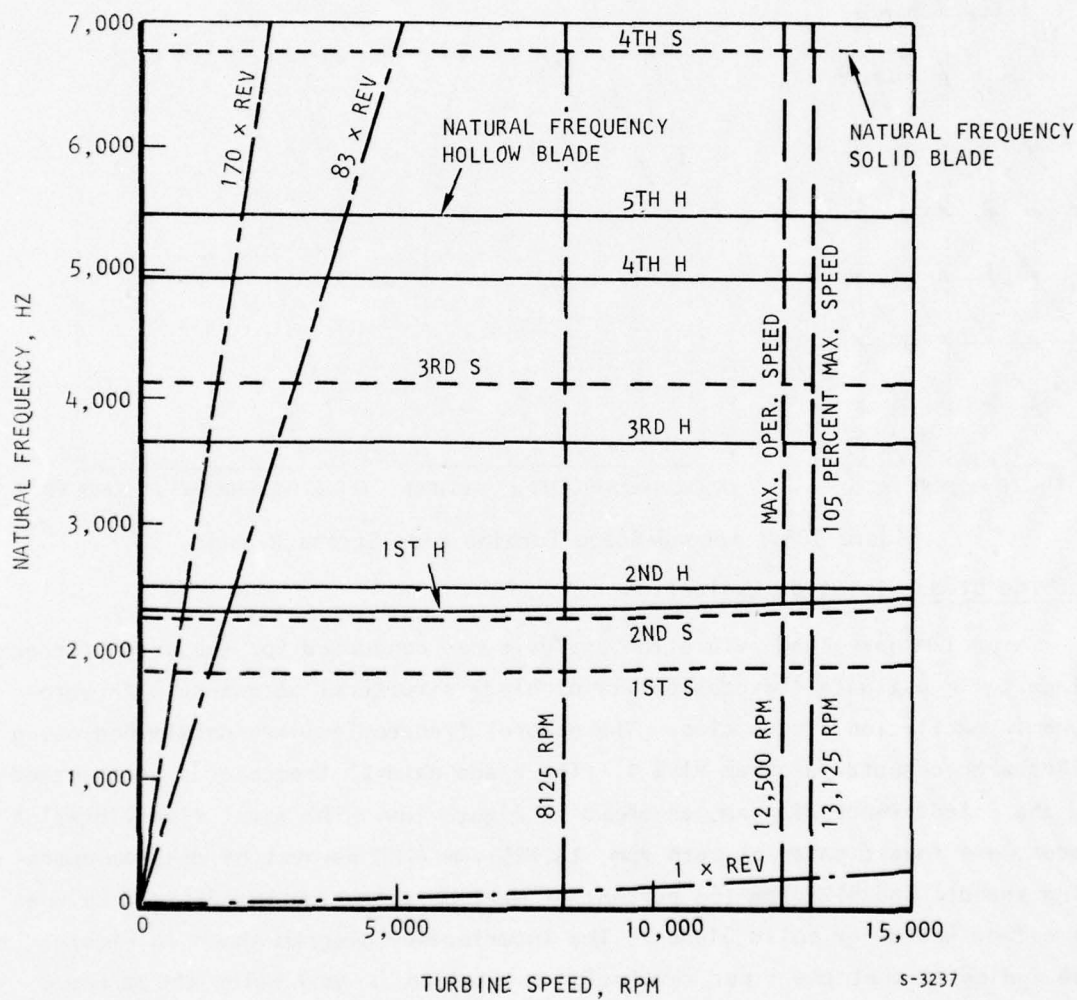


Figure 104. Second-Stage Turbine Blade Vibration--Interference Diagram

The stress and blade vibration analyses conducted primarily with highly sophisticated tools indicate that the resultant selected rotational speed, blade height, and peripheral speed are acceptable.

Bearings

Design for successful bearing operation at the anticipated rotational speed has the foremost single objective of ensuring that the bearing remains radially loose. Should the radial clearance be lost, the stress in the ball contact zone will increase very rapidly, causing temperature increases up to the melting point of the steel and thus leading to potential seizure of the bearing. There are five prime design considerations to retain radial looseness and to ensure stable bearing operation. These are: (1) ball separator design, (2) bearing lubrication, (3) external bearing loading, (4) bearing mounting fits and preloading, and (5) internal construction of the bearing.

Ball Separator Design

Outer ring band-controlled separators are used exclusively in high-speed bearings. Ball pocket clearance and outside diameter pilot clearance are established by computer analysis of the ball speed variation, and thus ball constraint is prevented except for severe misalignment or unbalance. Finally, the cage material must maintain strength at the operating temperature to prevent fracture or enlargement to the extent that the separator-land clearance is removed.

Lubrication

Bearing lubrication serves two functions in high-speed operation: (1) it provides a heat transfer medium, and (2) it lubricates the bearing. The presence of a lubricant, however, is no guarantee that lubrication will occur. The design requisite is to select a lubricant that will form a full uninterrupted film between the ball and raceway at the operating temperature. The design characteristics to be considered are viscosity, viscosity-temperature curve, and chemical base.

In addition, the ball spinning velocity must be computed and the viscous loss evaluated to complete the heat balance equation. In fairly lightly loaded turbine-driven machines, it is possible to reduce the ball spinning velocity by

opening the raceway curvatures and reducing the operating contact angle sufficiently to keep the lubrication in the full-film region. Some development is usually required to obtain the optimum value because the objective is very low contact angle (low operating clearance), and the calculated temperatures must be accurately determined. Loss of clearance is always possible and can even occur at minimal temperature errors (approximately 40 F).

External Loading

Minimizing external or applied loads is a design target. This includes the dynamic response of the rotating element over the entire speed range, acceleration loads, maneuver loads, vibration, and rotating assembly unbalance.

Generally, substantial thrust loads can be accepted, but radial loads must be kept at a minimum. The adverse effect of high radial loading is to force the balls to run in a plane out-of-normal to the shaft. When this occurs, ball (or separator) velocity, spin velocity, and operating contact angle vary widely during each shaft revolution. At high speed, the rate of heat generation exceeds the heat transfer capacity of the system, and bearing temperatures increase up to the softening point of the steel. If radial clearance is lost in the process, failure is immediate. If not, gross raceway deformation occurs and the bearings will subsequently seize.

Mounting Fits and Preloading

Preloading is accomplished by spring-loading the bearings in a conventional manner. The value of the preload is a compromise between the high-speed dynamics of the bearing, the losses consequent to high loads, fatigue life of the bearing, and the requirements for not exceeding the strength of the lubricant film.

With spring preloading, the outer ring fits must be cleared to permit axial shift. The shaft fits must be interference at all operating points for two reasons. First, interference provides a path for heat transfer from the inner race, and second, a loose shaft fit is equivalent to a gross unbalance condition.

Internal Bearing Geometry

High speed is defined for bearings as that regime of speed where the centrifugal force of the balls is significant relative to the forces on the balls reacting to the externally applied loads. Within this regime, the normal

contact angle-clearance-curvature relation ceases to apply. Centrifugal force is a body force and can be reacted only by the outer raceway, whereas the inner race reacts to the applied loads. As a result, the balls contact each race at a different angle. Since pure rolling motion can occur only on a diameter, the ball can roll only at the point of contact with one raceway, and must roll and spin relative to the outer raceway. The factor determining which race contact will be pure rolling motion is determined by the friction moment of the ball at that contact point.

With conventional angular contact bearings, inner race curvature is closer than the outer race curvature and the ball rolls relative to the inner race; however, as the speed increases, the loading increases at the outer race until the spin moment finally exceeds that at the inner race, at which time the ball will roll at the outer race. The ball spin control transaction can cause sudden failure. This type of failure can be prevented by tightening up the inner race curvature and/or increasing the preload.

Another potentially damaging condition at high speeds is the tendency of the balls to gyroscopically precess in an unstable motion, resulting in gross slippage and rapid failure. Normally, increasing the preload will prevent precession; however, at very high speeds it is also necessary to keep the contact angle low. This reduces the rate of change of angular momentum and, in combination with adequate preload, prevents precession.

Bearing Selection

Selection of a bearing for a particular application is based on a computer program available at AiResearch. This computer program has been extensively utilized to predict the behavior of rolling element bearings.

SECTION 9

TURBODRIVE SUBSYSTEM

The turbogenerator power unit requires a considerable amount of auxiliary equipment to produce useful power output, whether conventional or superconducting in concept. The auxiliary equipment includes: (1) propellant storage and delivery assembly, (2) gas generator assembly, (3) turbine assembly, (4) gear-box assembly, (5) electric generator assembly, (6) lubrication and cooling assembly, and (7) control assembly and associated valves. Figure 105 shows a typical turbogenerator subsystem. Following a discussion on potential propellants, the various auxiliary equipment that are not covered in other sections of this report are described in the order given above.

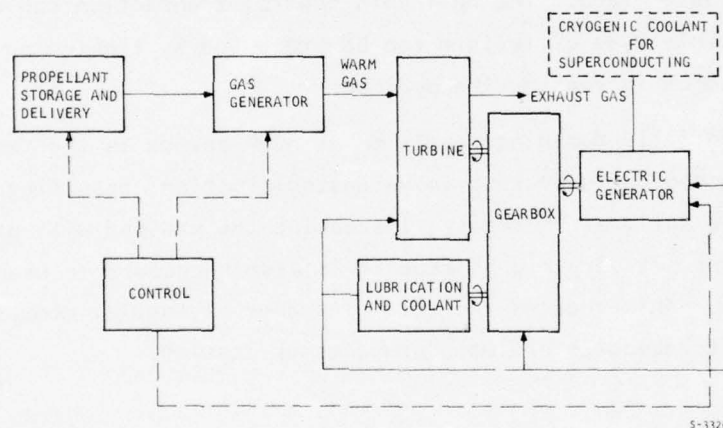


Figure 105. Block Diagram of Typical Turbogenerator Subsystem

PROPELLANTS

A wide variety of propellants is available for use in supplying hot gas. Generally, propellants are classified as either liquids or solids, although hybrid systems may be employed in which one of the reactants is a liquid and the other is a solid (or gel). For the present application, the multiple start mission requirement and associated design complexities are prime reasons for not considering the use of solid or gelled propellants as candidate energy sources. In practice, the selection of propellant is based on the following considerations (not necessarily in order of importance): (1) specific fuel consumption (weight and volume), (2) gas temperature at turbine inlet,

AD-A032 634

AIRESEARCH MFG CO OF CALIFORNIA TORRANCE
HIGH POWER STUDY--CONVENTIONAL GENERATORS, SUPERCONDUCTING GENE--ETC(U)
JUL 76 L SCHIPPER
76-12446

F/G 10/2

F33615-75-C-2071

UNCLASSIFIED

AFAPL-TR-76-39

NL

4 OF 5
AD
A032634



(3) combustion gas cleanliness, (4) ease of ignition, especially under fast startup, (5) long-term storability, and (6) shock and thermal stability.

In view of the high power requirement of the present application an additional key consideration, propellant cost, is introduced, which must be carefully assessed in both the development and operational phases of a high-power turbogenerator system. The propellant costs as quoted by Ref. 5 in dollars per lb are:

JP-4	-	0.0655	LOX	-	0.0285
MMH	-	6.40	H ₂ -O ₂	-	0.55
N ₂ H ₄	-	3.85	NTO	-	0.22
He	-	5.078			

Subsequent cost data, although not firmly established, indicate substantial further cost increases for some propellants.

Key candidate liquid propellants are summarized in Table 66. Many of these propellants can be used as either monopropellant or bipropellant combinations. Bipropellants, if hypergolic in makeup, provide an appropriate repeatable ignition. For the non-hypergolic combination, a substantial cost reduction is possible. Disadvantages of bipropellant concepts include a more complex fuel delivery system and more stringent control requirements. The simplified monopropellant delivery requires the use of catalyst or hypergol for decomposition. For example, hydrogen peroxide is decomposed by metallic silver, while hydrazine and most of its derivative mixtures are spontaneously ignited, at low temperatures, by a catalyst based on irridium.

Monopropellants

The storability of the monopropellants considered presents no problem, except for hydrogen peroxide. This compound is subjected to both homogeneous and heterogeneous decomposition. Special stabilized grades of 90 percent and 98 percent hydrogen peroxide that reduce the rate of decomposition are available (e.g., Becco MS Grade); however, even with the best materials (AI 99.7), decomposition amounts of about 0.1 percent per month (at 86 F) occur.

Ref. 5: High Power Study-Turbine Drive Systems, Final Report B76-3, 14 January 1976, AFWL - Open session, Rocketdyne Division, Rockwell International.

TABLE 66
KEY CHARACTERISTICS OF CANDIDATE PROPELLANTS

PROPELLANT	KEROSENE (UP 1, 3, 4, 6 AND RP 1)	NEAT HYDRAZINE	HYDRAZINE BLENDS	ETHYLENE OXIDE	HYDROGEN PEROXIDE	OTTO FUEL COMPOSITION II	HYDROGEN	OXYGEN	NITROGEN TETROXIDE
CHEMICAL FORMULA	$C_{12}H_{26}$ $C_{10}H_{22}$	N_2H_4	N_2H_4 PLUS N_2H_4 , N_2O , AND/OR H_2O , CO_2 , CH_4 , UHM	C_2H_4O	H_2O_2	C_8H_{18} , C_9H_{20} , $C_{10}H_{22}$, $C_{11}H_{24}$, $C_{12}H_{26}$, $C_{13}H_{28}$, $C_{14}H_{30}$, $C_{15}H_{32}$, $C_{16}H_{34}$, $C_{17}H_{36}$, $C_{18}H_{38}$, $C_{19}H_{40}$, $C_{20}H_{42}$, $C_{21}H_{44}$, $C_{22}H_{46}$, $C_{23}H_{48}$, $C_{24}H_{50}$, $C_{25}H_{52}$, $C_{26}H_{54}$, $C_{27}H_{56}$, $C_{28}H_{58}$, $C_{29}H_{60}$, $C_{30}H_{62}$, $C_{31}H_{64}$, $C_{32}H_{66}$, $C_{33}H_{68}$, $C_{34}H_{70}$, $C_{35}H_{72}$, $C_{36}H_{74}$, $C_{37}H_{76}$, $C_{38}H_{78}$, $C_{39}H_{80}$, $C_{40}H_{82}$, $C_{41}H_{84}$, $C_{42}H_{86}$, $C_{43}H_{88}$, $C_{44}H_{90}$, $C_{45}H_{92}$, $C_{46}H_{94}$, $C_{47}H_{96}$, $C_{48}H_{98}$, $C_{49}H_{100}$, $C_{50}H_{102}$, $C_{51}H_{104}$, $C_{52}H_{106}$, $C_{53}H_{108}$, $C_{54}H_{110}$, $C_{55}H_{112}$, $C_{56}H_{114}$, $C_{57}H_{116}$, $C_{58}H_{118}$, $C_{59}H_{120}$, $C_{60}H_{122}$, $C_{61}H_{124}$, $C_{62}H_{126}$, $C_{63}H_{128}$, $C_{64}H_{130}$, $C_{65}H_{132}$, $C_{66}H_{134}$, $C_{67}H_{136}$, $C_{68}H_{138}$, $C_{69}H_{140}$, $C_{70}H_{142}$, $C_{71}H_{144}$, $C_{72}H_{146}$, $C_{73}H_{148}$, $C_{74}H_{150}$, $C_{75}H_{152}$, $C_{76}H_{154}$, $C_{77}H_{156}$, $C_{78}H_{158}$, $C_{79}H_{160}$, $C_{80}H_{162}$, $C_{81}H_{164}$, $C_{82}H_{166}$, $C_{83}H_{168}$, $C_{84}H_{170}$, $C_{85}H_{172}$, $C_{86}H_{174}$, $C_{87}H_{176}$, $C_{88}H_{178}$, $C_{89}H_{180}$, $C_{90}H_{182}$, $C_{91}H_{184}$, $C_{92}H_{186}$, $C_{93}H_{188}$, $C_{94}H_{190}$, $C_{95}H_{192}$, $C_{96}H_{194}$, $C_{97}H_{196}$, $C_{98}H_{198}$, $C_{99}H_{200}$, $C_{100}H_{202}$, $C_{101}H_{204}$, $C_{102}H_{206}$, $C_{103}H_{208}$, $C_{104}H_{210}$, $C_{105}H_{212}$, $C_{106}H_{214}$, $C_{107}H_{216}$, $C_{108}H_{218}$, $C_{109}H_{220}$, $C_{110}H_{222}$, $C_{111}H_{224}$, $C_{112}H_{226}$, $C_{113}H_{228}$, $C_{114}H_{230}$, $C_{115}H_{232}$, $C_{116}H_{234}$, $C_{117}H_{236}$, $C_{118}H_{238}$, $C_{119}H_{240}$, $C_{120}H_{242}$, $C_{121}H_{244}$, $C_{122}H_{246}$, $C_{123}H_{248}$, $C_{124}H_{250}$, $C_{125}H_{252}$, $C_{126}H_{254}$, $C_{127}H_{256}$, $C_{128}H_{258}$, $C_{129}H_{260}$, $C_{130}H_{262}$, $C_{131}H_{264}$, $C_{132}H_{266}$, $C_{133}H_{268}$, $C_{134}H_{270}$, $C_{135}H_{272}$, $C_{136}H_{274}$, $C_{137}H_{276}$, $C_{138}H_{278}$, $C_{139}H_{280}$, $C_{140}H_{282}$, $C_{141}H_{284}$, $C_{142}H_{286}$, $C_{143}H_{288}$, $C_{144}H_{290}$, $C_{145}H_{292}$, $C_{146}H_{294}$, $C_{147}H_{296}$, $C_{148}H_{298}$, $C_{149}H_{300}$, $C_{150}H_{302}$, $C_{151}H_{304}$, $C_{152}H_{306}$, $C_{153}H_{308}$, $C_{154}H_{310}$, $C_{155}H_{312}$, $C_{156}H_{314}$, $C_{157}H_{316}$, $C_{158}H_{318}$, $C_{159}H_{320}$, $C_{160}H_{322}$, $C_{161}H_{324}$, $C_{162}H_{326}$, $C_{163}H_{328}$, $C_{164}H_{330}$, $C_{165}H_{332}$, $C_{166}H_{334}$, $C_{167}H_{336}$, $C_{168}H_{338}$, $C_{169}H_{340}$, $C_{170}H_{342}$, $C_{171}H_{344}$, $C_{172}H_{346}$, $C_{173}H_{348}$, $C_{174}H_{350}$, $C_{175}H_{352}$, $C_{176}H_{354}$, $C_{177}H_{356}$, $C_{178}H_{358}$, $C_{179}H_{360}$, $C_{180}H_{362}$, $C_{181}H_{364}$, $C_{182}H_{366}$, $C_{183}H_{368}$, $C_{184}H_{370}$, $C_{185}H_{372}$, $C_{186}H_{374}$, $C_{187}H_{376}$, $C_{188}H_{378}$, $C_{189}H_{380}$, $C_{190}H_{382}$, $C_{191}H_{384}$, $C_{192}H_{386}$, $C_{193}H_{388}$, $C_{194}H_{390}$, $C_{195}H_{392}$, $C_{196}H_{394}$, $C_{197}H_{396}$, $C_{198}H_{398}$, $C_{199}H_{400}$, $C_{200}H_{402}$, $C_{201}H_{404}$, $C_{202}H_{406}$, $C_{203}H_{408}$, $C_{204}H_{410}$, $C_{205}H_{412}$, $C_{206}H_{414}$, $C_{207}H_{416}$, $C_{208}H_{418}$, $C_{209}H_{420}$, $C_{210}H_{422}$, $C_{211}H_{424}$, $C_{212}H_{426}$, $C_{213}H_{428}$, $C_{214}H_{430}$, $C_{215}H_{432}$, $C_{216}H_{434}$, $C_{217}H_{436}$, $C_{218}H_{438}$, $C_{219}H_{440}$, $C_{220}H_{442}$, $C_{221}H_{444}$, $C_{222}H_{446}$, $C_{223}H_{448}$, $C_{224}H_{450}$, $C_{225}H_{452}$, $C_{226}H_{454}$, $C_{227}H_{456}$, $C_{228}H_{458}$, $C_{229}H_{460}$, $C_{230}H_{462}$, $C_{231}H_{464}$, $C_{232}H_{466}$, $C_{233}H_{468}$, $C_{234}H_{470}$, $C_{235}H_{472}$, $C_{236}H_{474}$, $C_{237}H_{476}$, $C_{238}H_{478}$, $C_{239}H_{480}$, $C_{240}H_{482}$, $C_{241}H_{484}$, $C_{242}H_{486}$, $C_{243}H_{488}$, $C_{244}H_{490}$, $C_{245}H_{492}$, $C_{246}H_{494}$, $C_{247}H_{496}$, $C_{248}H_{498}$, $C_{249}H_{500}$, $C_{250}H_{502}$, $C_{251}H_{504}$, $C_{252}H_{506}$, $C_{253}H_{508}$, $C_{254}H_{510}$, $C_{255}H_{512}$, $C_{256}H_{514}$, $C_{257}H_{516}$, $C_{258}H_{518}$, $C_{259}H_{520}$, $C_{260}H_{522}$, $C_{261}H_{524}$, $C_{262}H_{526}$, $C_{263}H_{528}$, $C_{264}H_{530}$, $C_{265}H_{532}$, $C_{266}H_{534}$, $C_{267}H_{536}$, $C_{268}H_{538}$, $C_{269}H_{540}$, $C_{270}H_{542}$, $C_{271}H_{544}$, $C_{272}H_{546}$, $C_{273}H_{548}$, $C_{274}H_{550}$, $C_{275}H_{552}$, $C_{276}H_{554}$, $C_{277}H_{556}$, $C_{278}H_{558}$, $C_{279}H_{560}$, $C_{280}H_{562}$, $C_{281}H_{564}$, $C_{282}H_{566}$, $C_{283}H_{568}$, $C_{284}H_{570}$, $C_{285}H_{572}$, $C_{286}H_{574}$, $C_{287}H_{576}$, $C_{288}H_{578}$, $C_{289}H_{580}$, $C_{290}H_{582}$, $C_{291}H_{584}$, $C_{292}H_{586}$, $C_{293}H_{588}$, $C_{294}H_{590}$, $C_{295}H_{592}$, $C_{296}H_{594}$, $C_{297}H_{596}$, $C_{298}H_{598}$, $C_{299}H_{600}$, $C_{300}H_{602}$, $C_{301}H_{604}$, $C_{302}H_{606}$, $C_{303}H_{608}$, $C_{304}H_{610}$, $C_{305}H_{612}$, $C_{306}H_{614}$, $C_{307}H_{616}$, $C_{308}H_{618}$, $C_{309}H_{620}$, $C_{310}H_{622}$, $C_{311}H_{624}$, $C_{312}H_{626}$, $C_{313}H_{628}$, $C_{314}H_{630}$, $C_{315}H_{632}$, $C_{316}H_{634}$, $C_{317}H_{636}$, $C_{318}H_{638}$, $C_{319}H_{640}$, $C_{320}H_{642}$, $C_{321}H_{644}$, $C_{322}H_{646}$, $C_{323}H_{648}$, $C_{324}H_{650}$, $C_{325}H_{652}$, $C_{326}H_{654}$, $C_{327}H_{656}$, $C_{328}H_{658}$, $C_{329}H_{660}$, $C_{330}H_{662}$, $C_{331}H_{664}$, $C_{332}H_{666}$, $C_{333}H_{668}$, $C_{334}H_{670}$, $C_{335}H_{672}$, $C_{336}H_{674}$, $C_{337}H_{676}$, $C_{338}H_{678}$, $C_{339}H_{680}$, $C_{340}H_{682}$, $C_{341}H_{684}$, $C_{342}H_{686}$, $C_{343}H_{688}$, $C_{344}H_{690}$, $C_{345}H_{692}$, $C_{346}H_{694}$, $C_{347}H_{696}$, $C_{348}H_{698}$, $C_{349}H_{700}$, $C_{350}H_{702}$, $C_{351}H_{704}$, $C_{352}H_{706}$, $C_{353}H_{708}$, $C_{354}H_{710}$, $C_{355}H_{712}$, $C_{356}H_{714}$, $C_{357}H_{716}$, $C_{358}H_{718}$, $C_{359}H_{720}$, $C_{360}H_{722}$, $C_{361}H_{724}$, $C_{362}H_{726}$, $C_{363}H_{728}$, $C_{364}H_{730}$, $C_{365}H_{732}$, $C_{366}H_{734}$, $C_{367}H_{736}$, $C_{368}H_{738}$, $C_{369}H_{740}$, $C_{370}H_{742}$, $C_{371}H_{744}$, $C_{372}H_{746}$, $C_{373}H_{748}$, $C_{374}H_{750}$, $C_{375}H_{752}$, $C_{376}H_{754}$, $C_{377}H_{756}$, $C_{378}H_{758}$, $C_{379}H_{760}$, $C_{380}H_{762}$, $C_{381}H_{764}$, $C_{382}H_{766}$, $C_{383}H_{768}$, $C_{384}H_{770}$, $C_{385}H_{772}$, $C_{386}H_{774}$, $C_{387}H_{776}$, $C_{388}H_{778}$, $C_{389}H_{780}$, $C_{390}H_{782}$, $C_{391}H_{784}$, $C_{392}H_{786}$, $C_{393}H_{788}$, $C_{394}H_{790}$, $C_{395}H_{792}$, $C_{396}H_{794}$, $C_{397}H_{796}$, $C_{398}H_{798}$, $C_{399}H_{800}$, $C_{400}H_{802}$, $C_{401}H_{804}$, $C_{402}H_{806}$, $C_{403}H_{808}$, $C_{404}H_{810}$, $C_{405}H_{812}$, $C_{406}H_{814}$, $C_{407}H_{816}$, $C_{408}H_{818}$, $C_{409}H_{820}$, $C_{410}H_{822}$, $C_{411}H_{824}$, $C_{412}H_{826}$, $C_{413}H_{828}$, $C_{414}H_{830}$, $C_{415}H_{832}$, $C_{416}H_{834}$, $C_{417}H_{836}$, $C_{418}H_{838}$, $C_{419}H_{840}$, $C_{420}H_{842}$, $C_{421}H_{844}$, $C_{422}H_{846}$, $C_{423}H_{848}$, $C_{424}H_{850}$, $C_{425}H_{852}$, $C_{426}H_{854}$, $C_{427}H_{856}$, $C_{428}H_{858}$, $C_{429}H_{860}$, $C_{430}H_{862}$, $C_{431}H_{864}$, $C_{432}H_{866}$, $C_{433}H_{868}$, $C_{434}H_{870}$, $C_{435}H_{872}$, $C_{436}H_{874}$, $C_{437}H_{876}$, $C_{438}H_{878}$, $C_{439}H_{880}$, $C_{440}H_{882}$, $C_{441}H_{884}$, $C_{442}H_{886}$, $C_{443}H_{888}$, $C_{444}H_{890}$, $C_{445}H_{892}$, $C_{446}H_{894}$, $C_{447}H_{896}$, $C_{448}H_{898}$, $C_{449}H_{900}$, $C_{450}H_{902}$, $C_{451}H_{904}$, $C_{452}H_{906}$, $C_{453}H_{908}$, $C_{454}H_{910}$, $C_{455}H_{912}$, $C_{456}H_{914}$, $C_{457}H_{916}$, $C_{458}H_{918}$, $C_{459}H_{920}$, $C_{460}H_{922}$, $C_{461}H_{924}$, $C_{462}H_{926}$, $C_{463}H_{928}$, $C_{464}H_{930}$, $C_{465}H_{932}$, $C_{466}H_{934}$, $C_{467}H_{936}$, $C_{468}H_{938}$, $C_{469}H_{940}$, $C_{470}H_{942}$, $C_{471}H_{944}$, $C_{472}H_{946}$, $C_{473}H_{948}$, $C_{474}H_{950}$, $C_{475}H_{952}$, $C_{476}H_{954}$, $C_{477}H_{956}$, $C_{478}H_{958}$, $C_{479}H_{960}$, $C_{480}H_{962}$, $C_{481}H_{964}$, $C_{482}H_{966}$, $C_{483}H_{968}$, $C_{484}H_{970}$, $C_{485}H_{972}$, $C_{486}H_{974}$, $C_{487}H_{976}$, $C_{488}H_{978}$, $C_{489}H_{980}$, $C_{490}H_{982}$, $C_{491}H_{984}$, $C_{492}H_{986}$, $C_{493}H_{988}$, $C_{494}H_{990}$, $C_{495}H_{992}$, $C_{496}H_{994}$, $C_{497}H_{996}$, $C_{498}H_{998}$, $C_{499}H_{1000}$, $C_{500}H_{1002}$, $C_{501}H_{1004}$, $C_{502}H_{1006}$, $C_{503}H_{1008}$, $C_{504}H_{1010}$, $C_{505}H_{1012}$, $C_{506}H_{1014}$, $C_{507}H_{1016}$, $C_{508}H_{1018}$, $C_{509}H_{1020}$, $C_{510}H_{1022}$, $C_{511}H_{1024}$, $C_{512}H_{1026}$, $C_{513}H_{1028}$, $C_{514}H_{1030}$, $C_{515}H_{1032}$, $C_{516}H_{1034}$, $C_{517}H_{1036}$, $C_{518}H_{1038}$, $C_{519}H_{1040}$, $C_{520}H_{1042}$, $C_{521}H_{1044}$, $C_{522}H_{1046}$, $C_{523}H_{1048}$, $C_{524}H_{1050}$, $C_{525}H_{1052}$, $C_{526}H_{1054}$, $C_{527}H_{1056}$, $C_{528}H_{1058}$, $C_{529}H_{1060}$, $C_{530}H_{1062}$, $C_{531}H_{1064}$, $C_{532}H_{1066}$, $C_{533}H_{1068}$, $C_{534}H_{1070}$, $C_{535}H_{1072}$, $C_{536}H_{1074}$, $C_{537}H_{1076}$, $C_{538}H_{1078}$, $C_{539}H_{1080}$, $C_{540}H_{1082}$, $C_{541}H_{1084}$, $C_{542}H_{1086}$, $C_{543}H_{1088}$, $C_{544}H_{1090}$, $C_{545}H_{1092}$, $C_{546}H_{1094}$, $C_{547}H_{1096}$, $C_{548}H_{1098}$, $C_{549}H_{1100}$, $C_{550}H_{1102}$, $C_{551}H_{1104}$, $C_{552}H_{1106}$, $C_{553}H_{1108}$, $C_{554}H_{1110}$, $C_{555}H_{1112}$, $C_{556}H_{1114}$, $C_{557}H_{1116}$, $C_{558}H_{1118}$, $C_{559}H_{1120}$, $C_{560}H_{1122}$, $C_{561}H_{1124}$, $C_{562}H_{1126}$, $C_{563}H_{1128}$, $C_{564}H_{1130}$, $C_{565}H_{1132}$, $C_{566}H_{1134}$, $C_{567}H_{1136}$, $C_{568}H_{1138}$, $C_{569}H_{1140}$, $C_{570}H_{1142}$, $C_{571}H_{1144}$, $C_{572}H_{1146}$, $C_{573}H_{1148}$, $C_{574}H_{1150}$, $C_{575}H_{1152}$, $C_{576}H_{1154}$, $C_{577}H_{1156}$, $C_{578}H_{1158}$, $C_{579}H_{1160}$, $C_{580}H_{1162}$, $C_{581}H_{1164}$, $C_{582}H_{1166}$, $C_{583}H_{1168}$, $C_{584}H_{1170}$, $C_{585}H_{1172}$, $C_{586}H_{1174}$, $C_{587}H_{1176}$, $C_{588}H_{1178}$, $C_{589}H_{1180}$, $C_{590}H_{1182}$, $C_{591}H_{1184}$, $C_{592}H_{1186}$, $C_{593}H_{1188}$, $C_{594}H_{1190}$, $C_{595}H_{1192}$, $C_{596}H_{1194}$, $C_{597}H_{1196}$, $C_{598}H_{1198}$, $C_{599}H_{1200}$, $C_{600}H_{1202}$, $C_{601}H_{1204}$, $C_{602}H_{1206}$, $C_{603}H_{1208}$, $C_{604}H_{1210}$, $C_{605}H_{1212}$, $C_{606}H_{1214}$, $C_{607}H_{1216}$, $C_{608}H_{1218}$, $C_{609}H_{1220}$, $C_{610}H_{1222}$, $C_{611}H_{1224}$, $C_{612}H_{1226}$, $C_{613}H_{1228}$, $C_{614}H_{1230}$, $C_{615}H_{1232}$, $C_{616}H_{1234}$, $C_{617}H_{1236}$, $C_{618}H_{1238}$, $C_{619}H_{1240}$, $C_{620}H_{1242}$, $C_{621}H_{1244}$, $C_{622}H_{1246}$, $C_{623}H_{1248}$, $C_{624}H_{1250}$, $C_{625}H_{1252}$, $C_{626}H_{1254}$, $C_{627}H_{1256}$, $C_{628}H_{1258}$, $C_{629}H_{1260}$, $C_{630}H_{1262}$, $C_{631}H_{1264}$, $C_{632}H_{1266}$, $C_{633}H_{1268}$, $C_{634}H_{1270}$, $C_{635}H_{1272}$, $C_{636}H_{1274}$, $C_{637}H_{1276}$, $C_{638}H_{1278}$, $C_{639}H_{1280}$, $C_{640}H_{1282}$, $C_{641}H_{1284}$, $C_{642}H_{1286}$, $C_{643}H_{1288}$, $C_{644}H_{1290}$, $C_{645}H_{1292}$, $C_{646}H_{1294}$, $C_{647}H_{1296}$, $C_{648}H_{1298}$, $C_{649}H_{1300}$, $C_{650}H_{1302}$, $C_{651}H_{1304}$, $C_{652}H_{1306}$, $C_{653}H_{1308}$, $C_{654}H_{1310}$, $C_{655}H_{1312}$, $C_{656}H_{1314}$, $C_{657}H_{1316}$, $C_{658}H_{1318}$, $C_{659}H_{1320}$, $C_{660}H_{1322}$, $C_{661}H_{1324}$, $C_{662}H_{1326}$, $C_{663}H_{1328}$, $C_{664}H_{1330}$, $C_{665}H_{1332}$, $C_{666}H_{1334}$, $C_{667}H_{1336}$, $C_{668}H_{1338}$, $C_{669}H_{1340}$, $C_{670}H_{1342}$, $C_{671}H_{1344}$, $C_{672}H_{1346}$, $C_{673}H_{1348}$, $C_{674}H_{1350}$, $C_{675}H_{1352}$, $C_{676}H_{1354}$, $C_{677}H_{1356}$, $C_{678}H_{1358}$, $C_{679}H_{1360}$, $C_{680}H_{1362}$, $C_{681}H_{1364}$, $C_{682}H_{1366}$, $C_{683}H_{1368}$, $C_{684}H_{1370}$, $C_{685}H_{1372}$, $C_{686}H_{1374}$, $C_{687}H_{1376}$, $C_{688}H_{1378}$, $C_{689}H_{1380}$, $C_{690}H_{1382}$, $C_{691}H_{1384}$, $C_{692}H_{1386}$, $C_{693}H_{1388}$, $C_{694}H_{1390}$, $C_{695}H_{1392}$, $C_{696}H_{1394}$, $C_{697}H_{1396}$, $C_{698}H_{1398}$, $C_{699}H_{1400}$, $C_{700}H_{1402}$, $C_{701}H_{1404}$, $C_{702}H_{1406}$, $C_{703}H_{1408}$, $C_{704}H_{1410}$, $C_{705}H_{1412}$, $C_{706}H_{1414}$, $C_{707}H_{$			

Ethylene oxide and Otto Fuel II require a considerably more complex ignition system than the hydrazine-base mixtures. Exhaust products of these fuels contain appreciable quantities of carbon, which is generally undesirable. Furthermore, the performance potential of both fuels is below that of many hydrazine mixtures.

Hydrazine (N_2H_4) is a liquid monopropellant fuel characterized by certain desirable properties. The absence of carbon leads to exceptional combustion gas cleanliness because only ammonia, nitrogen, and hydrogen are produced. Other advantages include its relatively low vapor pressure and high boiling point. The initial hydrazine decomposition reaction produces ammonia and nitrogen; further decomposition of ammonia produces quantities of hydrogen, which lowers the mean molecular weight of the combustion gases as well as the flame temperature. By controlling the fraction of ammonia decomposed in the gas generator, hydrazine can be used for a wide variety of applications. The addition of hydrazine nitrate is effective in increasing performance because of additional oxidation reaction, although care must be taken with this additive because of its tendency to increase shock sensitivity.

In an effort to depress the freezing point, increase the ease of ignition, and raise the fuel energy level, numerous hydrazine-based monopropellant mixtures have been developed. The mixtures considered usable in the present application include hydrazine-hydrazine nitrate-water mixtures and hydrazine-monomethylhydrazine-hydrazine nitrate-water mixtures.

Bipropellants

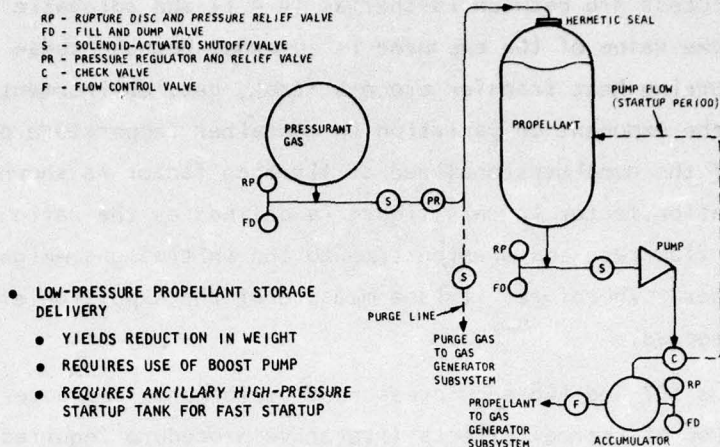
The few bipropellant mixtures of interest include the use of (1) hydrogen and oxygen (2) JP fuels with either peroxide or oxygen as oxidizer, and (3) hydrazine or monomethylhydrazine (MMH) with nitrogen tetroxide (NTO). The bipropellant combination of cryogenic hydrogen and oxygen is of interest because its use will result in a substantial reduction in fuel consumption. Furthermore, the high heat capacity of hydrogen makes it an ideal waste heat sink. Required storage volume and storage design concepts are the critical items. The use of kerosene base fuel is of interest because it provides potential integration with aircraft fuel requirements and low-cost utilization. The hypergolic combination of MMH and NTO eliminates the necessity of catalyst use.

PROPELLANT STORAGE AND DELIVERY ASSEMBLY

This assembly provides for storage of propellant and includes the means for supplying this propellant to the gas generator at the rates required. Basically, these functions can be accomplished using either a low-pressure storage tank with a boost pump or a blowdown system using stored high-pressure gas and propellant. Key design considerations for both concepts are given in Figure 106. Operating the unit with the low-pressure storage and delivery system using a pump is an attractive solution; however, it requires the availability of either a pressurized fuel accumulator start tank, bootstrap fuel pressurization reservoirs, and similar devices to ensure fast startup capability. With the high-pressure blowdown approach, the need for ancillary startup devices is negated because high-pressure propellant is readily available. The two key design variables encompass the determination of the propellant tank delivery pressure and pressurant storage supply pressure, both of which will result in substantial system weight increase when compared to the low-pressure storage and boost pump approach.

The pressurant gas assembly vessel must store the gas volume required to accommodate the expulsion of the propellant and provide flow for purging the propellant lines and gas generator between active firings. In design of systems incorporating blowdown processes, the common approach is to assume that the processes are adiabatic, and thus obtain expressions for the state of the gas in the tank throughout the process. In many cases, however, neglecting the effects of heat transfer lead to substantial error in predictions of system behavior.

Continuous expansion or blowdown of high-pressure gas from a storage vessel can be accomplished by three different processes. The initial consideration, therefore, is the establishment of the value for the polytropic exponent for the blowdown process. If the blowdown process occurs very rapidly such that little or no heat is transferred into the stored fluid, then the process in the tank is isentropic. If, however, the pressurant tank fluid can be held at constant temperature during fluid discharge, an isothermal process results. The third process may be termed the equilibrium process, implying that the gas remains in thermal equilibrium with the tank container by absorbing the heat stored in the metal and environment. The limits of the exponent of the



- HIGH-PRESSURE PROPELLANT STORAGE

- FEWER COMPONENTS REQUIRED
- FAST START POSSIBLE
- INCREASE IN ASSEMBLY WEIGHT

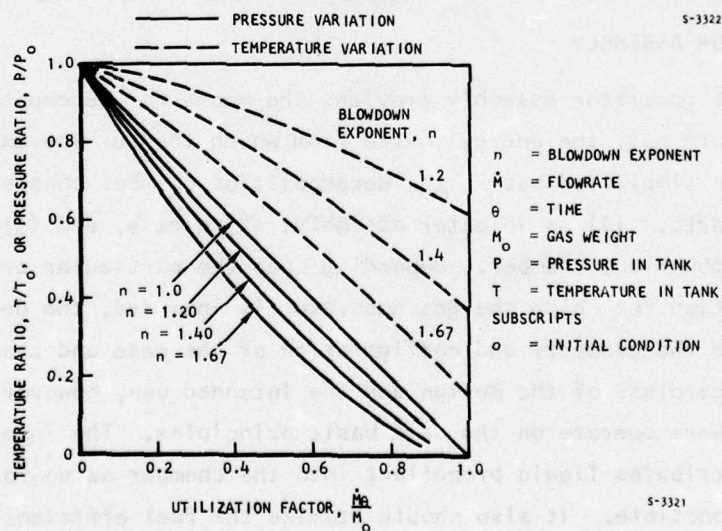
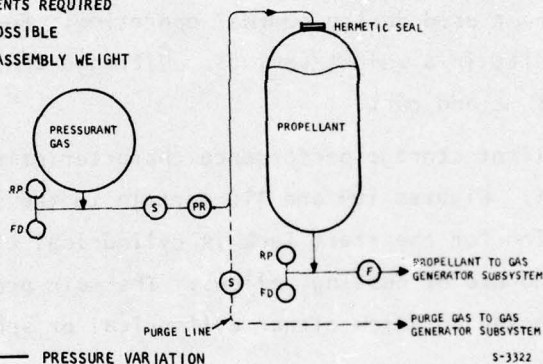


Figure 106. Propellant Storage and Delivery Design Considerations

blowdown process are between isothermal ($n = 1$) and adiabatic ($n = \gamma$). In practice, the value of the exponent is somewhat between these values depending on the occurring heat transfer process (tank, gas, environment, etc.). The effect of the exponent on variation in container temperature or pressure as a function of the nondimensionalized utilization factor is shown in Figure 106. The utilization factor in this figure is defined as the ratio of the product of the gas flow rate and mission time to the initial gas weight available in the container. Therefore, it is a measure of the expulsion efficiency of a blowdown process.

Figures 107 and 108 show pressurant performance characteristics, allowing the inclusion of thermal effects (iterative procedure required to establish operational exponent) using either nitrogen or helium. Figure 107 pertains to the pressurant used in the startup operational phase. Figure 108 pertains to the pressurant used during nominal operation. For both conditions, the use of helium results in a weight savings. Nitrogen use, however, results in a reduction in volume and cost.

Propellant storage performance characteristics are shown in Figures 109 through 111. Figures 109 and 110 pertain to the start tank. The geometrical configuration for the start tank is cylindrical with elliptical end caps incorporating the use of nesting bellows. The main propellant tank parameters (Figure 111) are chosen to allow either cylindrical or spherical shapes to be evaluated.

GAS GENERATOR ASSEMBLY

The gas generator assembly provides the means for decomposing the propellant into warm gas, the energy source from which the turbine extracts its power. On a simplified basis, the decomposition chamber consists of three principal parts: (1) an injector assembly, (2) a case, and (3) the decomposition (or combustion) chamber. Depending upon the particular propellant and the application for which the gas generator is intended, the design of the injector and the geometry and configuration of the case and chamber may vary widely. Regardless of the design and the intended use, however, all decomposition chambers operate on the same basic principles. The injector of the chamber distributes liquid propellant into the chamber as uniformly and efficiently as possible. It also should atomize the fuel efficiently for subsequent vaporization, offer minimum pressure loss, be self-cooling (to prevent heat soakback and possible detonation in the supply line), and be resistant to

NOTES:

1. PRESSURANT TANK CONFIGURATION IS SPHERICAL.
2. FULLY CHARGED TANK PRESSURE AT 40 F IS 4500 PSI.
3. FUEL IS HYDRAZINE (98.5%) AND WATER (1.5%).
4. NITROGEN TANK MATERIAL IS TITANIUM (SV-6AI-2Sn).
5. NITROGEN TANK DESIGNED FOR BURST AT 4 TIMES FULLY CHARGED PRESSURE AT 160 F.

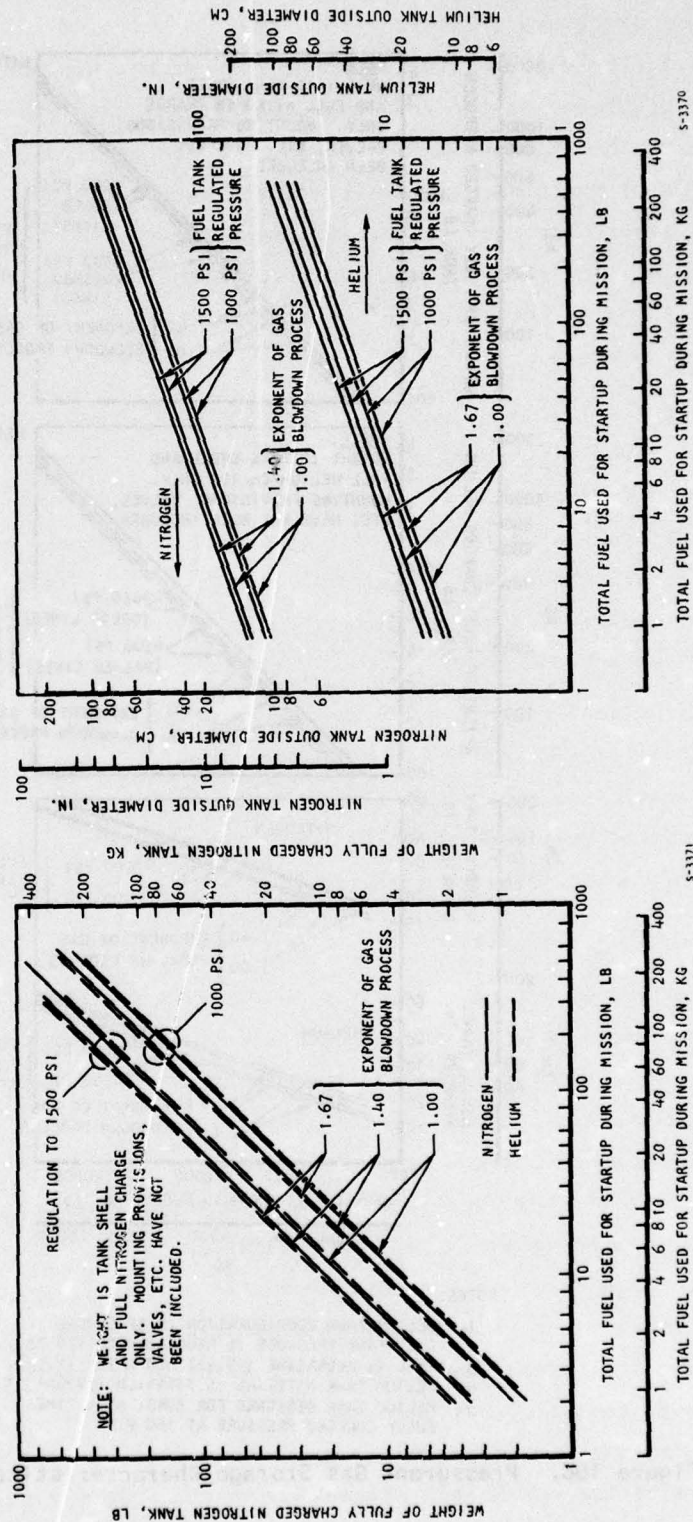
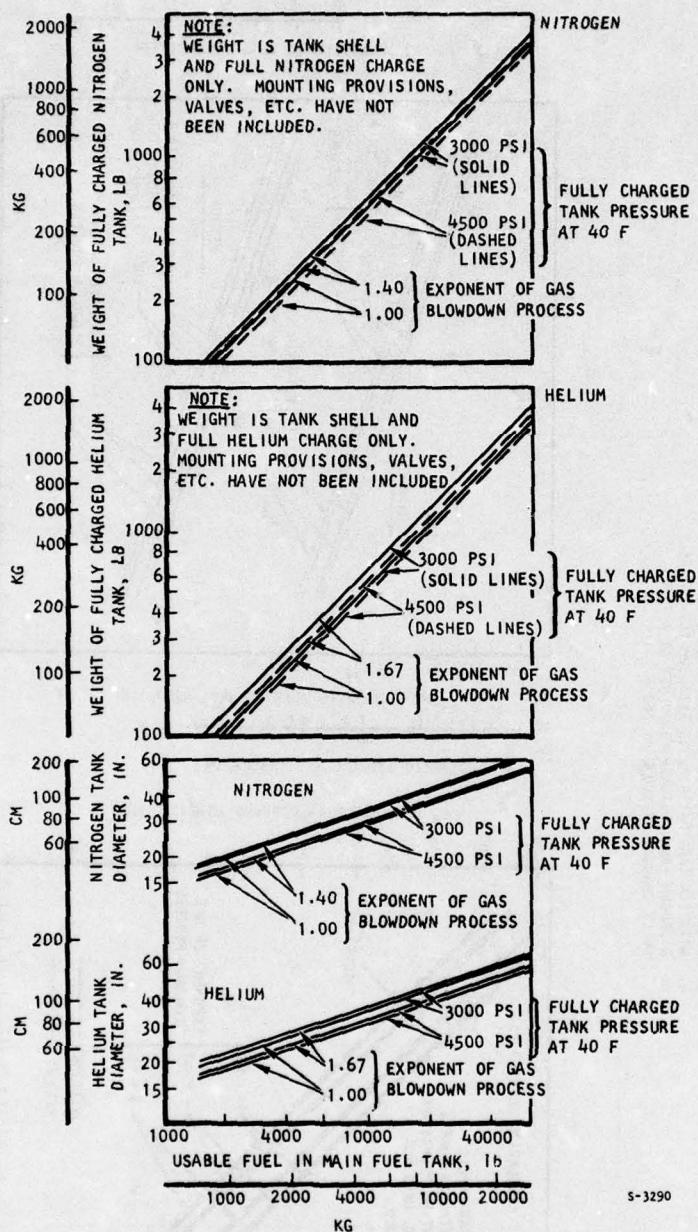


Figure 107. Pressurant Gas Storage Characteristics, Startup



NOTES:

1. HELIUM TANK CONFIGURATION IS SPHERICAL.
2. FUEL TANK PRESSURE IS REGULATED TO 100 PSI.
3. FUEL IS HYDRAZINE (98.5%) AND WATER (1.5%).
4. HELIUM TANK MATERIAL IS TITANIUM (6V-6A-2.5Sn).
5. HELIUM TANK DESIGNED FOR BURST AT 4 TIMES FULLY CHARGED PRESSURE AT 160 F.

Figure 108. Pressurant Gas Storage Characteristics Nominal Operation

NOTES:

1. TEMPERATURE IS 160 F
2. FUEL IS HYDRAZINE (98.5%) AND WATER (1.5%)
3. PRESSURE VESSEL IS TITANIUM-6V-6Al-2.5Sn
4. TANK IS DESIGNED FOR BURST AT 4 TIMES OPERATING PRESSURE
5. BELLWS IS STAINLESS STEEL

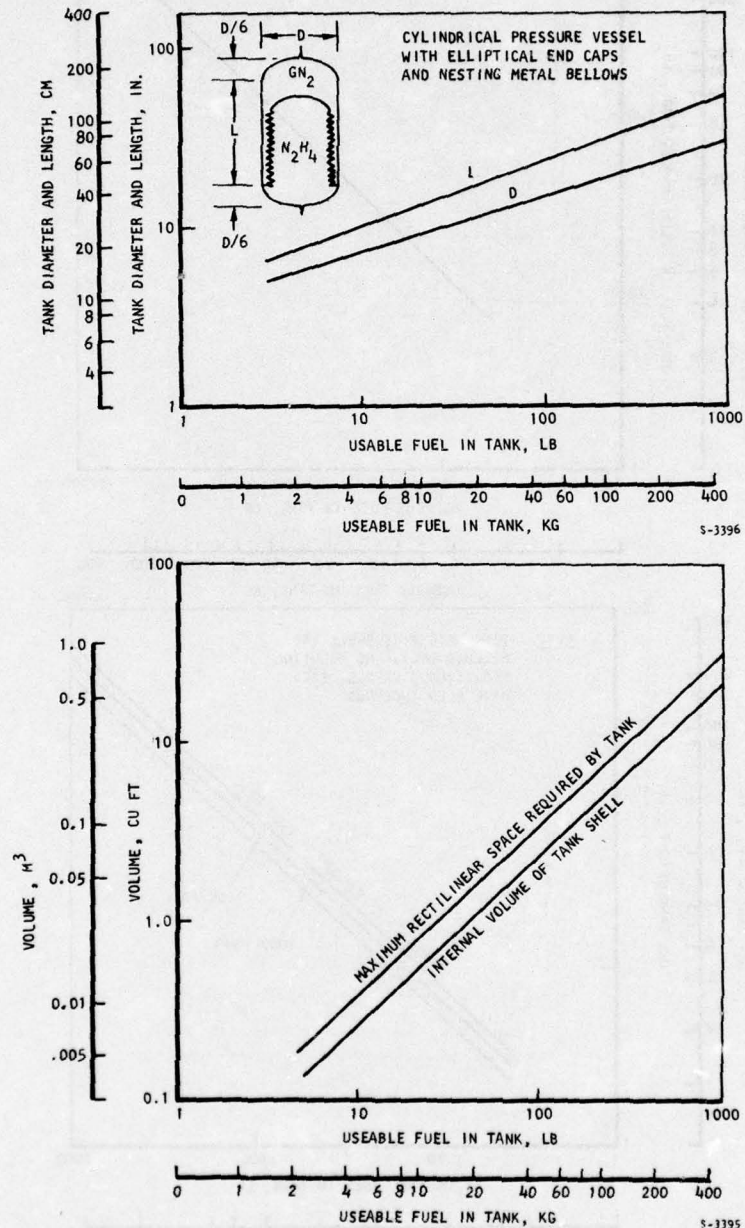


Figure 109. Propellant Start Tank Storage Characteristics

NOTES:

1. TEMPERATURE IS 160 F
2. FUEL IS HYDRAZINE (98.5%) AND WATER (1.5%)
3. PRESSURE VESSEL IS TITANIUM-6V-6Al-2.5Sn
4. TANK IS DESIGNED FOR BURST AT 4 TIMES OPERATING PRESSURE
5. BELLOW IS STAINLESS STEEL

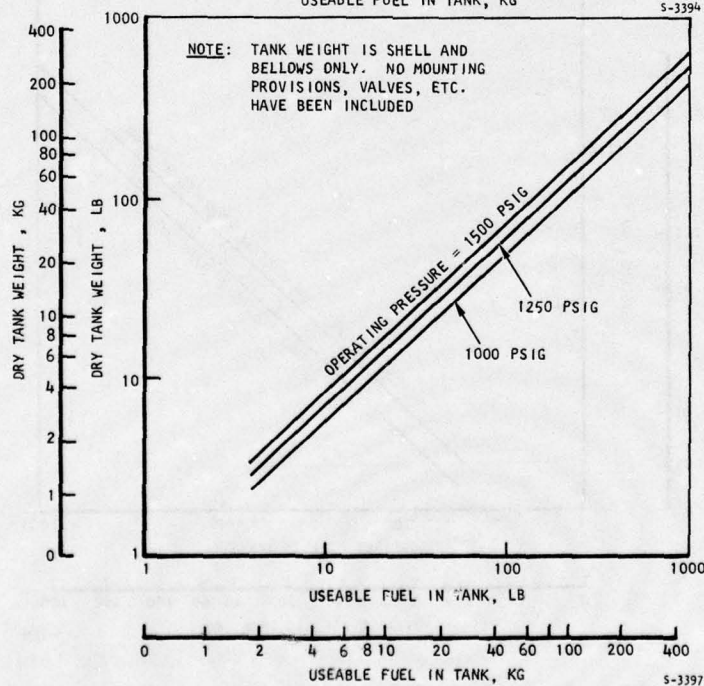
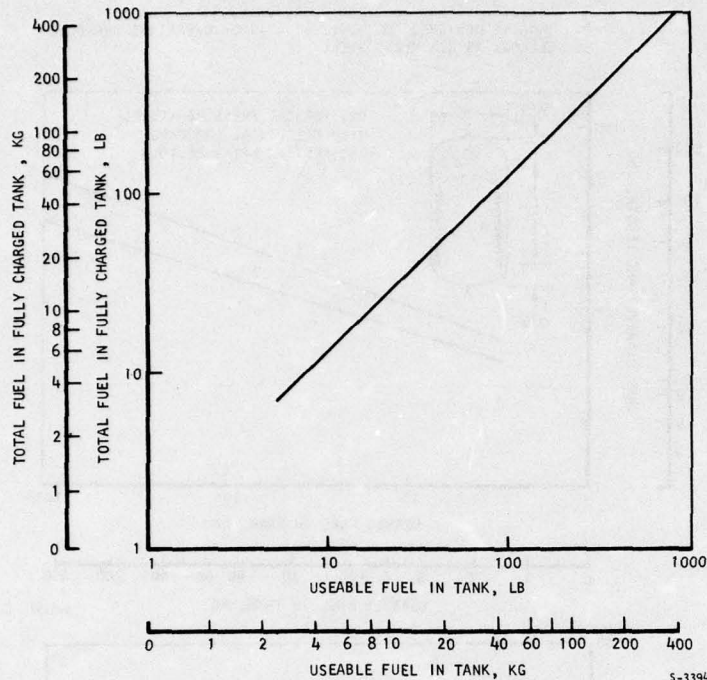


Figure 110. Propellant Start Tank Storage Characteristics

NOTES:

1. OPERATING PRESSURE IS 100 PSIG
2. ULLAGE IS 5 PERCENT.
3. TEMPERATURE IS 160 F.
4. FUEL IS HYDRAZINE (98.5%) AND WATER (1.5%)
5. TANK MATERIAL IS 6061 (T6) ALUMINUM OR TI-6V-2AL-2.5Sn
6. TANK IS DESIGNED FOR BURST AT 4 TIMES OPERATING PRESSURE
7. MINIMUM WALL THICKNESS IS 0.045 IN.

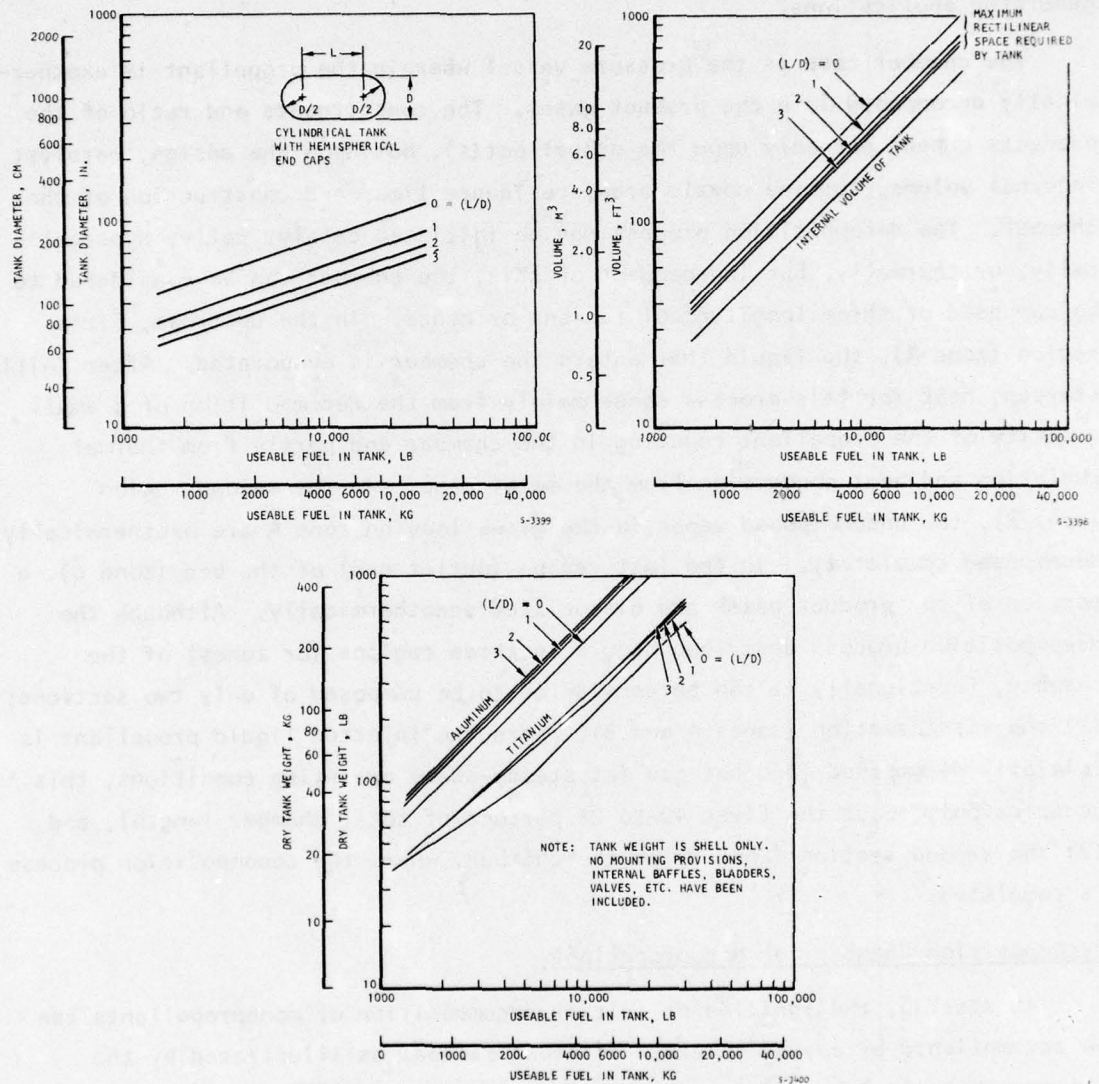


Figure 111. Propellant Main Storage Tank Characteristics

clogging or plugging. The manner in which it is injected has a marked effect on the response time, size, achievable life, and stability of operation. The three basic types of injectors used are (1) conical spray type, (2) showerhead type, and (3) the bed penetration (or "piccolo" tube) type. All three methods (with numerous variations) have been developed and used successfully in gas generator applications.

The chamber case is the pressure vessel wherein the propellant is exothermically decomposed into the product gases. The constituents and ratio of the products depend not only upon the propellant(s), but upon the design, catalyst, internal volume, turbine nozzle area, residence time, and construction of the chamber. The decomposition process may be initiated catalytically, hypergolically, or thermally, but independent of this, the chamber can be considered to be composed of three longitudinal regions or zones. In the upstream, first region (zone A), the liquid that enters the chamber is evaporated. After initial startup, heat for this process comes mainly from the decomposition of a small quantity of the propellant reacting in the chamber and partly from thermal radiation and heat conduction from the metal case. In the second region (zone B), the undecomposed vapor in the gases leaving zone A are exothermically decomposed completely. In the last region (outlet end) of the bed (zone C), a portion of the product gases are dissociated endothermically. Although the decomposition process described occurs in three regions (or zones) of the chamber, functionally it can be considered to be composed of only two sections: (1) the first section (zones A and B), where the injected liquid propellant is initially decomposed into hot gas (at steady-state operating conditions, this occupies only about the first 10 to 25 percent of total chamber length), and (2) the second section (zone C) of the chamber, where the decomposition process is completed.

Decomposition Chamber for Monopropellants

At startup, the ignition or initial decomposition of monopropellants can be accomplished by any of several different methods as illustrated by the chamber shown in Figure 112, as subsequently discussed.

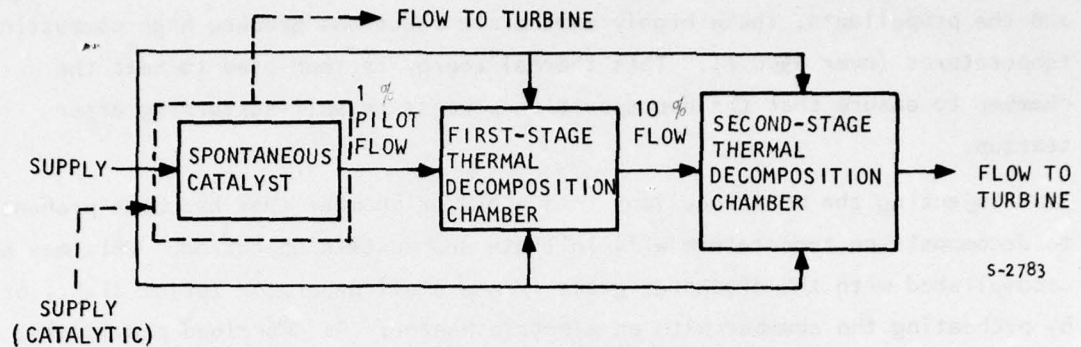


Figure 112. Decomposition Chamber Operation Options

1. Injecting a Monopropellant into a Spontaneous Catalyst

Injecting the monopropellant hydrazine-blend fuel into a bed of Shell 405 catalyst will cause it to decompose spontaneously; this is done in virtually all hydrazine thruster applications for spacecraft. The configuration of this chamber varies widely, depending upon the requirements. Similarly, injection of hydrogen peroxide into a bed of warm monel or silver wire screens will cause it to decompose. With these monopropellants, in addition to gas generator geometry, flow rate, catalyst surface area, and chamber pressure, factors that directly affect the amount of catalyst used for a given problem statement are: (1) the particular monopropellant blend used, (2) the propellant temperature, and (3) the catalyst material. Some monopropellants cannot be catalytically decomposed, and some catalysts are more active than others. For hydrazine-base propellants, however, adding nitrate ($N_2H_5NO_3$) results in a more active fuel, while adding water to either hydrazine or hydrogen peroxide will decrease the activity. Carbon in hydrazine-blend fuels (MMH, UDMH, etc.) poisons the catalyst. In addition, the amount of catalyst required to achieve rapid and reliable gas generator starts also depends upon the monopropellant, chamber geometry, and catalyst bed temperatures. A chamber that must start at -55 F with this temperature fuel requires approximately twice the amount of catalyst required at room temperature conditions. The Harshaw catalysts will only decompose hydrazine at temperatures over about 900 F.

2. Ignition by Mixing a Hypergol

For hydrazine blend monopropellants (and most hydrocarbon fuels), ignition may be achieved by mixing the fuel with a strong solid oxidizer such as iodine pentoxide (I_2O_5) or a liquid, such as inhibited red fuming nitric acid (IRFNA)

or nitrogen tetroxide (NTO, N_2O_4). Depending upon the oxidizer-to-fuel ratio and the propellants, these highly exothermic reactions produce high combustion temperatures (over 4500 F). This thermal energy is then used to heat the chamber to ensure that the decomposition process is self-sustaining after startup.

3. Injecting the Monopropellant into a bed or chamber that has been preheated to decomposition temperature will initiate and sustain operation. This may be accomplished with the discharge gases from a small generator (pilot light) or by preheating the chamber with an electric heater. As described previously, the decomposition of the monopropellant can be catalytic or thermal, and variations in these configurations include throughflow, regenerative, and staged designs where part of the design is catalytic, and the other thermal and staged as illustrated in Figure 112.

Performance characteristics of catalytic and pilot-thermal hydrazine monopropellant gas generators are illustrated in Figures 113 and 114. The chamber configurations for either the all catalytic or pilot-thermal designs are annular in shape and lead to the first-stage turbine nozzle ring at the outlet. The combustor concept is thus an integral part of the turbine assembly. This approach is deemed desirable to minimize system free pneumatic volume to enhance fast startup capability. In many respects, the arrangement of the annular combustor chamber, nozzles, and turbine are similar to that of well established gas turbine engine practice.

Decomposition Chambers (Combustors) for Bipropellants

The design, construction, methods of ignition, cooling, operation, and performance of decomposition chambers for rocket propulsion are well established. Design considerations of bipropellant chambers as they relate to an APU are presented. With the exception of the LH_2 - LO_2 and hydrazine candidates, all of the bipropellant systems will utilize a hydrocarbon fuel, and to achieve a gas temperature suitable for turbine long life, it will be necessary to burn either fuel-rich or oxidizer-rich. For the condition to burn fuel-rich, the success of this approach relies on the control of carbon formation at the extreme fuel-rich operating conditions; however, it is for this condition (fuel-rich) that the most desirable (low molecular weight) gases are generated.

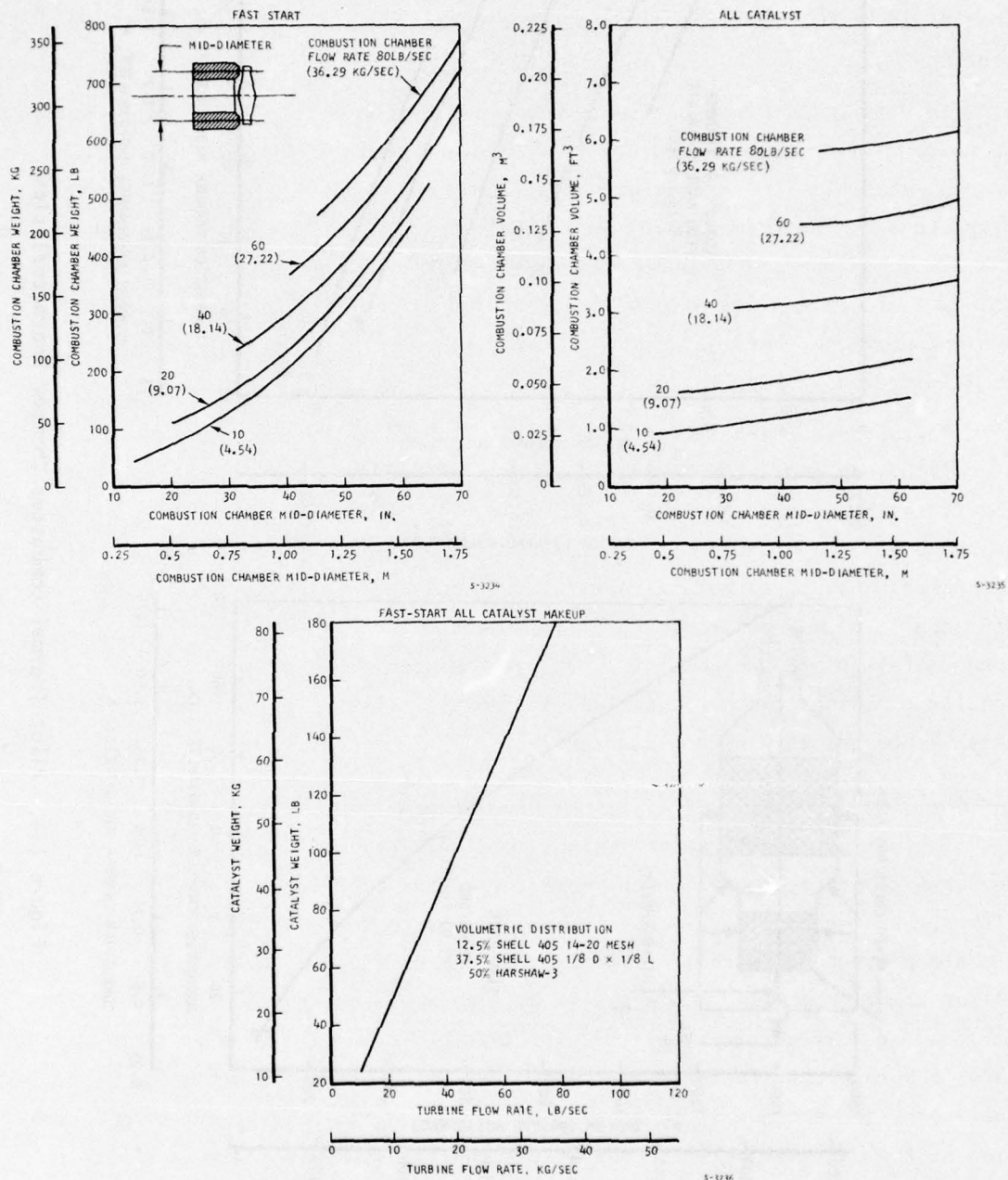


Figure 113. All Catalytic Combustor Chamber Characteristics

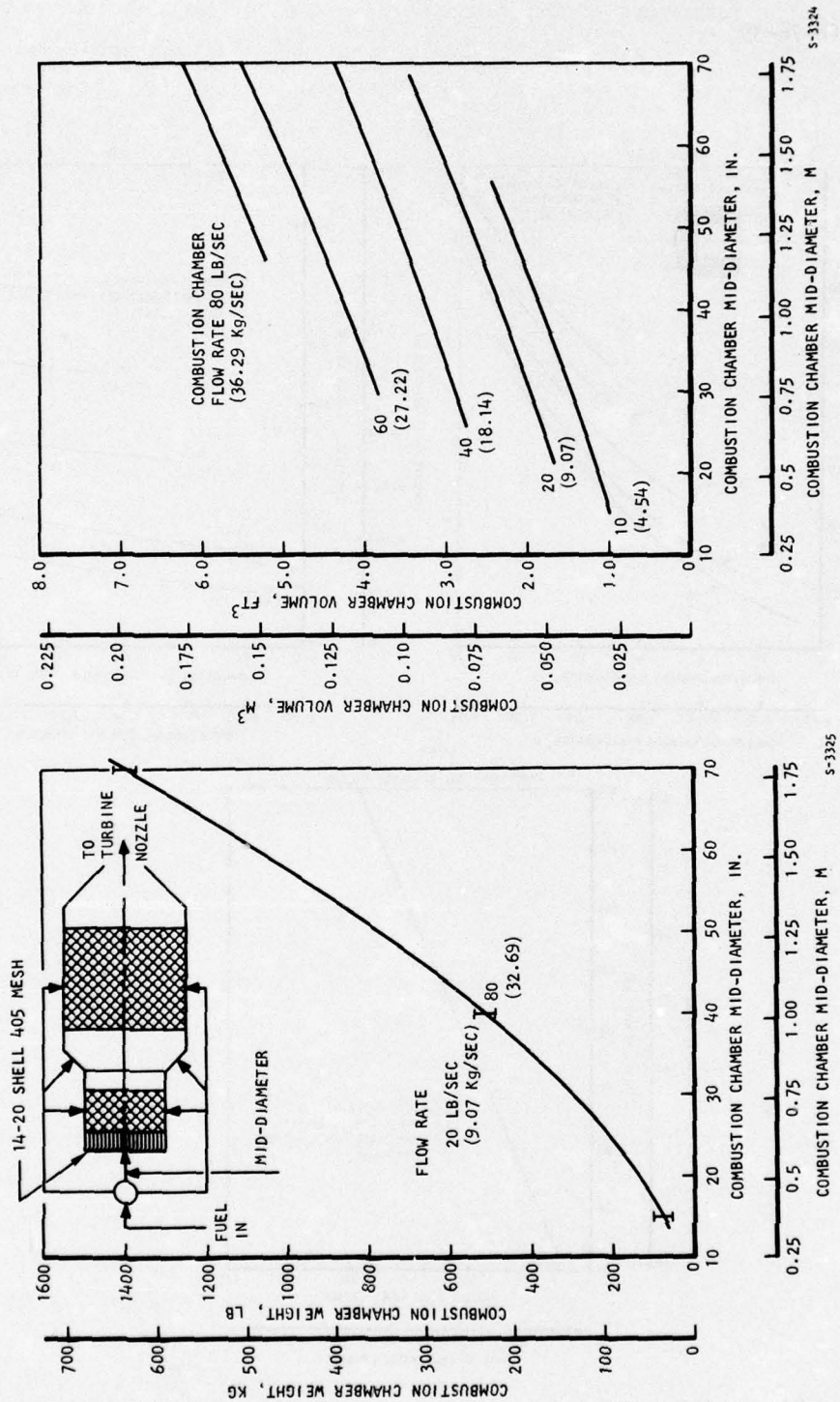


Figure 114. Pilot Thermal Combuster Chamber Characteristics

The carbon formation in the decomposition chamber or combustor may be classified into two types: (1) surface carbon, which is a graphite-like deposit formed at lower temperatures due to local enrichment of the combustible mixture, and (2) a soot or gas-phase, solid carbon formed in the flow at relatively high temperatures. Both types of carbon formation are undesirable. The surface deposits near the fuel injectors will cause a poor distribution of fuel, while the same deposits on the combustor walls will cause local heating or cracking due to uneven temperatures. The gas-phase carbon in the stream will reduce turbine efficiency because of random carbon-particle motion; clogging also may occur when the gas particles aggregate.

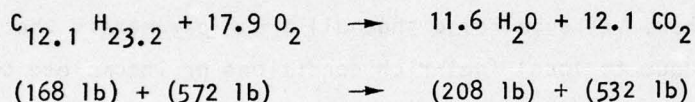
The extent of surface-carbon deposits in a combustor depends on a number of parameters such as propellant composition, (O/F ratio), atomization of fuel, flow pattern, and wall cooling. Although the exact process of carbon deposition is not established, it is believed that all these parameters that affect carbon formation are due to local fuel-rich conditions or incomplete combustion.

Poor atomization of the fuel will increase the carbon deposition, depending on droplet size. The combustor flow pattern will have a direct influence on local fuel mixing and combustion. An increase of flow turbulence will result in more intense and complete combustion with less carbon deposits. Cooled walls or cold fuel injectors have the effect of quenching combustion, leaving a layer of partially reacted or unreacted hydrocarbons on the surface. These surface-carbon deposits do not build up rapidly, but only occur after prolonged operation.

The mechanism of carbon formation in a gas stream involves a number of stages including aggregation and dehydrogenation. The gross effect is that in a fuel-rich mixture only part of the available fuel is burned in the primary combustion products. The remaining hydrocarbon molecules undergo a decomposition controlled by temperature, pressure, and residence time. It has been found that (1) the soot formation may be significantly reduced if pressure is lowered; (2) the soot formation increases with increasing equivalence ratio, but this trend is reversed when a certain equivalence is reached (this phenomenon is very important in selecting a proper O/F ratio; and (3) the molecular structure of hydrogen and carbon atoms has a significant effect on soot formation. Aromatic hydrocarbons (for example, benzene) are more prone to soot formation than naphthene (cyclohexene), olifins (hexane), and paraffins.

The carbon formation predicted by a chemical equilibrium computer program for a mixture of JP fuel and hydrogen peroxide is shown in Figure 115. This curve provides a useful starting point, but must be considered to be conservative in assessing this problem.

Since most JP fuels, RP-1, MMH, and UDMH consist of a rather wide mixture of hydrocarbons, neither qualitative nor quantitative knowledge of the reactions is clearly understood. An exact analysis of such fuels is difficult to obtain. For the gross effect of the combustion process, the calculation may be carried out by knowing the approximate hydrogen-carbon ratio. If it is assumed that a JP fuel has 1.9185 atoms of hydrogen for each atom of carbon, an average molecule of fuel may be represented as $C_{12.1} H_{23.2}$, with a molecular weight of 168. The following reaction is a simplified version of a JP fuel-oxygen reaction.



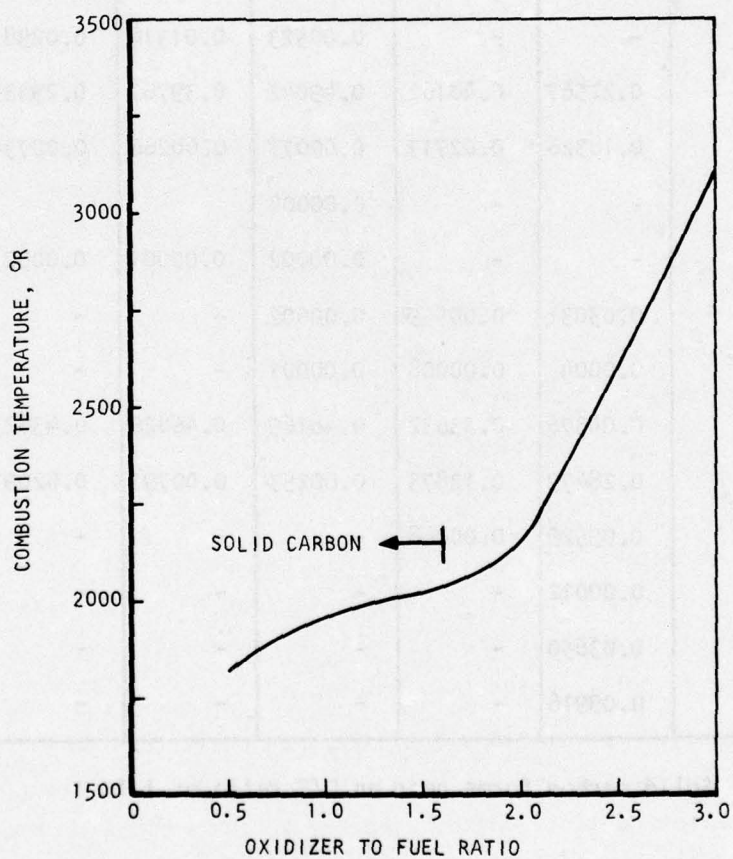
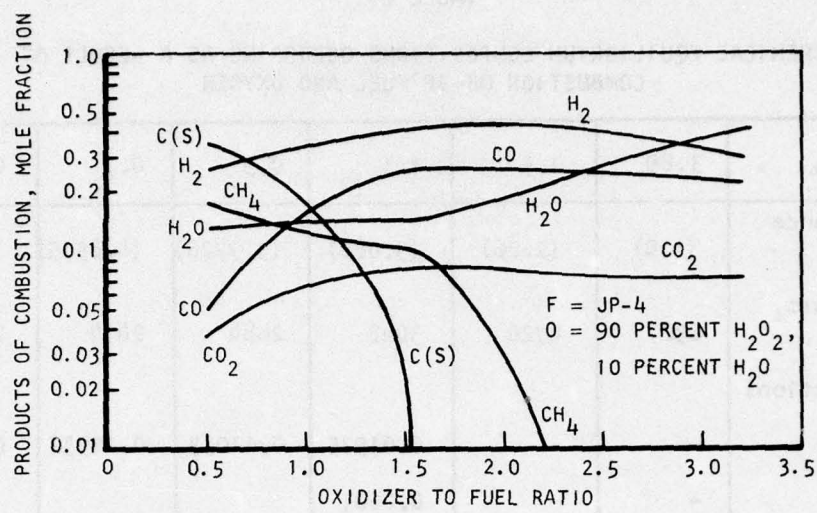
The stoichiometric ratio of oxygen-to-fuel therefore is 3.39.

In a fuel-rich combustion process, a large amount of water vapor and carbon monoxide would be expected, with very little carbon dioxide because the relative affinities of hydrogen, carbon, and carbon monoxide for oxygen are in that respective order. At higher temperatures, however, a large amount of hydrogen is observed at fuel-rich conditions. Hydrogen will be found by the following endothermic reaction



A typical example of this reaction is shown in Table 67, where at an O/F of 1.1, the combustion products would consist of 49 percent CO and 48 percent H_2 by volume. The hydrogen formation is advantageous to turbine operation because of its low molecular weight. The temperature, however, is too hot to be considered for use directly in the turbine.

The equilibrium calculations indicate that the carbon formation is strongly dependent on the O/F ratio and that improved turbine performance (very little solid carbon content) may be expected if the combustion products at high O/F ratios could be frozen. Two possible methods to achieve this are (1) to cool a relative lean combustion product through a fuel-cooled heat exchanger



S-3289

Figure 115. JP-4, 10 Percent H_2O , 90 Percent H_2O_2 Combustion

TABLE 67

CHEMICAL EQUILIBRIUM COMPOSITIONS OCCURRING AS A RESULT OF
COMBUSTION OF JP FUEL AND OXYGEN

O/F Ratio	3.89	1.5	1.1	0.9	0.7	0.5
(Equivalence Ratio)	(1.0)	(2.26)	(3.086)	(3.7726)	(4.8505)	(6.791)
Temperature, °F	6387	4726	3042	2684	2414	2210
Mole Fractions						
C(s)	-	-	0.01925	0.11033	0.20932	0.31695
CH ₃	-	-	0.0001			
CH ₄	-	-	0.00523	0.01314	0.02981	0.05822
CO	0.22567	0.48162	0.49042	0.39767	0.29435	0.18172
CO ₂	0.18326	0.02717	0.00077	0.00266	0.00734	0.01293
C ₂ H ₄	-	-	0.00004			
C ₂ H ₆	-	-	0.00002	0.00001	0.00001	0.00001
H	0.03031	0.00559	0.00002	-	-	-
HCO	0.0004	0.00008	0.00001	-	-	-
H ₂	0.04376	0.35632	0.48169	0.46826	0.43823	0.38943
H ₂ O	0.28479	0.12873	0.00253	0.00791	0.02093	0.04073
OH	0.09529	0.00048	-	-	-	-
HO ₂	0.00012	-	-	-	-	-
O	0.03850	-	-	-	-	-
O ₂	0.09916	-	-	-	-	-

NOTE: Solid carbon forms near an O/F ratio of 1.1

to the desired inlet turbine temperature so that the hydrocarbon in the system is inherently less than those fuel-rich conditions, and (2) to inject fuel into the combustion products to quench the species and reduce its temperature. The advantages of this system are to add more energy into the system through fuel injection and minimize the requirement of the heat exchanger.

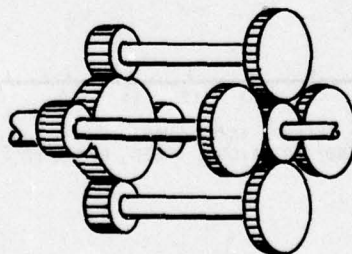
GEARBOX

Where the turbine and generator rotational speeds are incompatible or result in severe weight penalties, the use of a connecting gearbox has been assumed. This allows optimal turbine and generator designs to be used because matching of the rotational speeds of these components is no longer a restriction.

To minimize size and weight, flightweight construction was assumed and a high pitch-line velocity used. A value of 27,500 ft/min was felt to be representative of a present day practical upper limit and was therefore used in the gearbox analysis. This pitch-line velocity is presently achieved in the Garrett/AiResearch 731 turbofan engine fan drive gearbox.

Most gear ratios of interest in the high power system application investigated here fall in the 1.5 to 2.0 range (ratio of turbine speed to alternator speed). Although epicyclic gear trains result in minimum size and weight in many systems, they should not be used in the high-power system because the planetary gear system minimum ratio is 2.0 and, for the star gear system, the power level results in excessively wide gear face widths in comparison to diameter, which causes misalignment and load carrying problems.

The gear system configuration selected is the double-reduction, multiple branch type illustrated schematically in Figure 116 (for four branches). This results in a relatively lightweight gearbox for the power transmitted and provides a large degree of versatility.



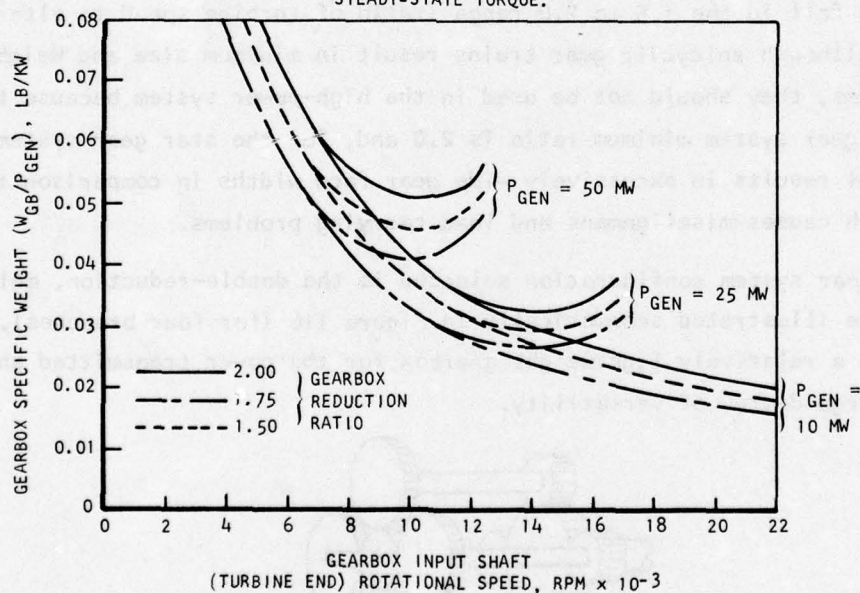
S-3375

Figure 116. Double-Reduction Four-Branch Assembly

Figure 117 shows the gearbox specific weight as a function of input shaft rotational speed, gearbox reduction ratio, and generator power level. Notice that the gearbox design is determined by the startup operation of the turbo-generator as well as the steady-state operation; the torque capability of the gearbox is dictated by the startup torque delivered by the turbine at zero speed with 100 percent of the steady-state gas flow rate. Because the steady-state turbine torque is approximately 60 percent of the startup torque, most of the gearbox operation is at considerably reduced stress levels. Should a faster startup be obtained by increasing the turbine inlet pressure above the steady-state value, the weight of the gearbox will increase in proportion to the total torque delivered to the input shaft.

DOUBLE REDUCTION--MULTIPLE BRANCH GEARBOX

- NOTES: 1. PITCH LINE VELOCITY = 27,500 FT/MIN
 2. SURFACE DURABILITY FACTOR = 1000 PSI
 3. GEARBOX INPUT POWER EQUALS 107 PERCENT OF GENERATOR OUTPUT POWER AT STEADY STATE.
 4. STARTUP TORQUE AT ZERO SPEED IS 67 PERCENT GREATER THAN STEADY-STATE TORQUE.



S-3271

Figure 117. Gearbox Specific Weight

The average density of the gearbox can be approximated by the following equation:

$$\rho_{GB} = 0.0522 P_{GEN}^{0.165}$$

where: ρ_{GB} = average gearbox density, lb/cu in.

P_{GEN} = generator output power level, MW

This equation was obtained from the point design gearboxes using linear regression by the method of least squares. The gearbox volume can thus be conveniently obtained by dividing the gearbox weight by its average density.

LUBRICATION ASSEMBLY

The lubrication assembly ensures positive lubrication of the gearbox bearings and gears and the turbine power unit. A schematic diagram depicting a positive feed lubrication system is shown in Figure 118. Types of applicable pumps include the conventional gear-on-gear, gear-in-gear designs, and because of the relatively high lubricant flow rate required, sliding vane and dynamic types (centrifugal). A major design consideration of the lubrication system is to adequately lubricate and cool all critical parts at the high-temperature condition while providing the least viscous friction loss associated with the airborne low-temperature soak condition.

The lubricating oil is circulated through the lubrication subsystem with a closed-loop system using a pump. Because of the large power levels involved in the turbine power unit, cooling of the lubricating oil is required. The coolant may be supplied from the aircraft or could be in the form of ram air, cryogenics, or liquid coolants. Further definition from the Air Force is required on heat sink availability.

Fuel and Lubricant Pumps

Two pumps will be required in the intended application, one pump to provide pressurized fuel to the gas generator for normal operation or to the startup tank if fast startup is required, and a second pump to provide positive feed of lubricant to the gearbox and bearings of the rotating assembly. In this application, initial fuel pressurization by gaseous blowdown provides sufficient suction head to prevent incipient cavitation of the fuel flow and

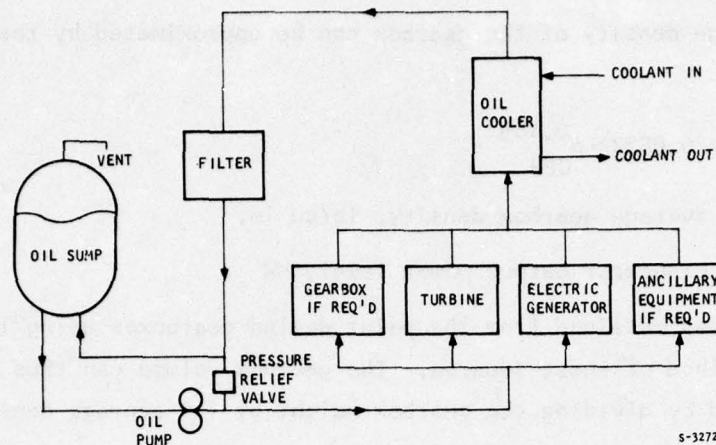


Figure 118. Lubrication Assembly Schematic Diagram

lubricant flow processes. Therefore, the suction specific speed relationship ceases to be a basic consideration. Considerations of the rotational speed, pressure rise, and flow required result in the selection of a centrifugal fuel pump and a Gerotor pump for forced circulation of the lubricant. Both types of pumps have been used previously in similar functions.

CONTROL ASSEMBLY

The control system includes all input-output sensing, conditioning, computation, monitoring, and associated components. The subsystem controls must provide all steady-state and transient functions required. These functions include:

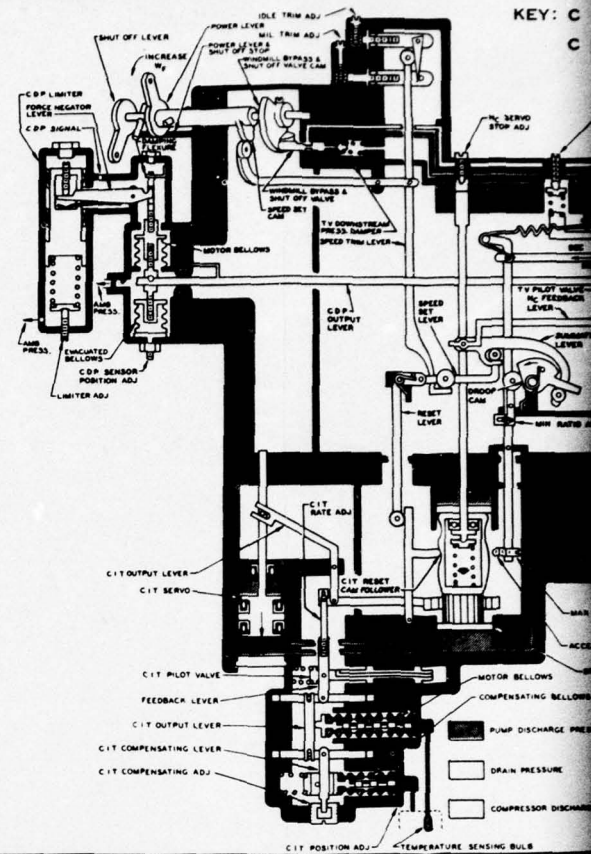
- Turn-on sequence
- Acceleration
- On speed and load changes
- Shutdown sequence
- Monitoring

The typical control system comprises: (1) sensing components, (2) input conditioning, (3) computation, (4) output conditioning, (5) output components, (6) monitoring, and (7) BITE. An integrated engine control system is responsible for obtaining the required performance under all operating conditions. It must compensate for ambient conditions, including temperatures and variations in system performance. Potential control concepts are summarized in Figure 119.

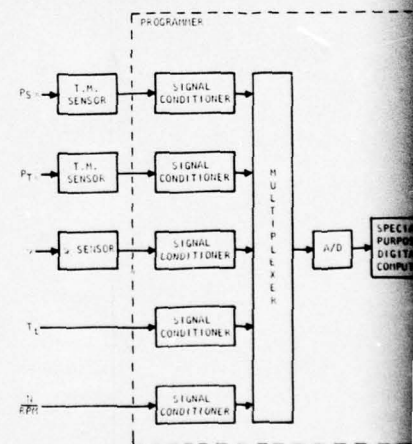
CONTROL OPERATING MODES

Operating Mode	Functional Purpose	Functional Description
Turn on	Establish conditions for starting	System readiness check Controller self-test Validation Hardness and component continuity Components Fuel conditions Pressure Temperature Quantity Lubrication conditions Temperature Pressure Fuel system preparation Condition fuel Activate fuel delivery assembly Energize pumps Open shutoff valves Ready to start signal
Start and acceleration	Accelerate TEGS from 0 to 100 percent speed	Energize fuel control components Fuel valves Torque motor Solenoid Protection circuits Overtemperature Excessive start time Low oil pressure Loss of speed sensor
On-speed	Operate TEGS at 100 percent speed	Control fuel system to maintain 100 percent speed Fuel valves Position LVDT, POT, Readout Protection circuits Overspeed Overtemperature Low oil pressure High oil temperature Loss of speed sensor Worst-case load change anticipation
Shutdown	Shut off TEGS subsystem	Normal protection Deenergize fuel control Close speed control valves Deactivate fuel delivery assembly Deenergize pumps Close shutoff valves
Monitoring	Provide indication of sub-system health and readiness	Bite Control self-test Turn-on validation Protection circuits Display Turbine speed Turbine TIT Fuel temperature, pressure, quantity Lube-oil temperature and pressure Fill fuel pressure

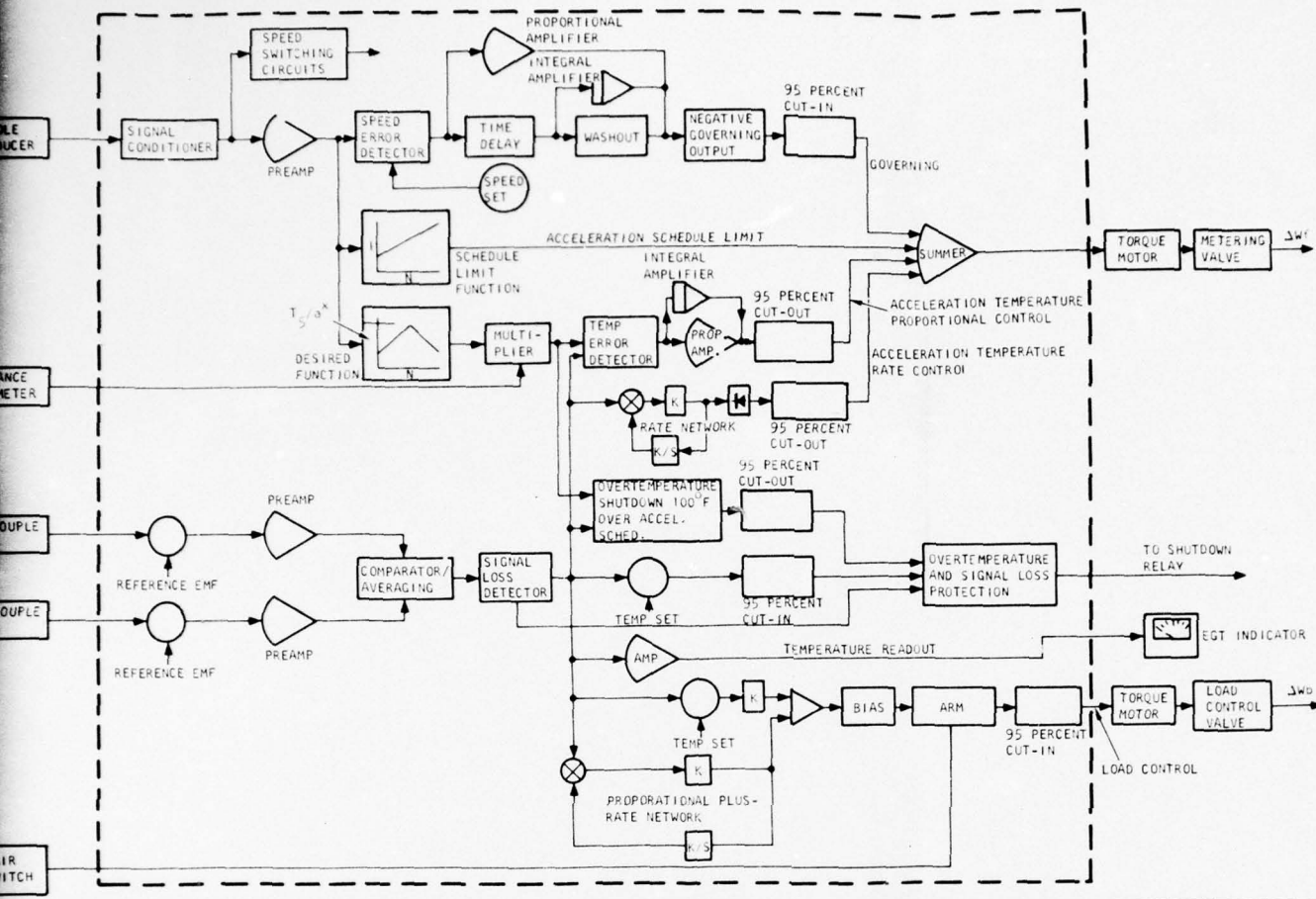
HYDROMECHANICAL CONTROL CONCEPTS



ELECTRONIC DIGITAL CONTROL CONCEPTS



LOGG CONTROL CONCEPTS



ADVANTAGES

- SAFETY
- WEIGHT
- COMPLEXITY
- PERFORMANCE
- RELIABILITY

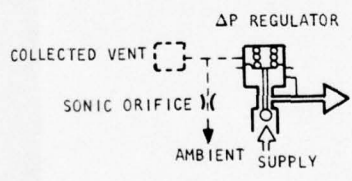
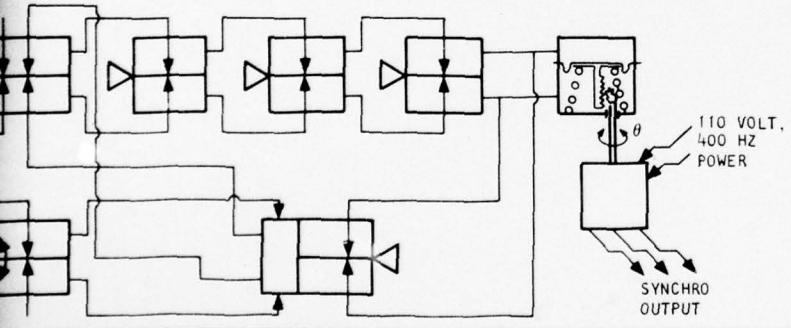
DISADVANTAGES

- COST
- MAINTAINABILITY

COMMENTS

- TYPICAL USAGE
- COMPLEX SYSTEMS
- EXOTIC RATE AND MONITORING REQUIREMENTS
- FAST RESPONSE SYSTEMS
- EXISTING APPLICATIONS
- F-14 INLET SYSTEM

CONCEPTS



ADVANTAGES

- WEIGHT
- SAFETY
- COST
- PERFORMANCE
- RELIABILITY
- MAINTAINABILITY
- COMPLEXITY

DISADVANTAGES

- COMPLEXITY

COMMENTS

- TYPICAL USAGE
- MODERATELY COMPLEX SYSTEM
- MINIMUM RATE AND MONITORING REQUIREMENTS
- MODERATE RESPONSE SYSTEMS
- EXISTING APPLICATIONS
- HARPOON FUEL MANAGEMENT SYSTEM

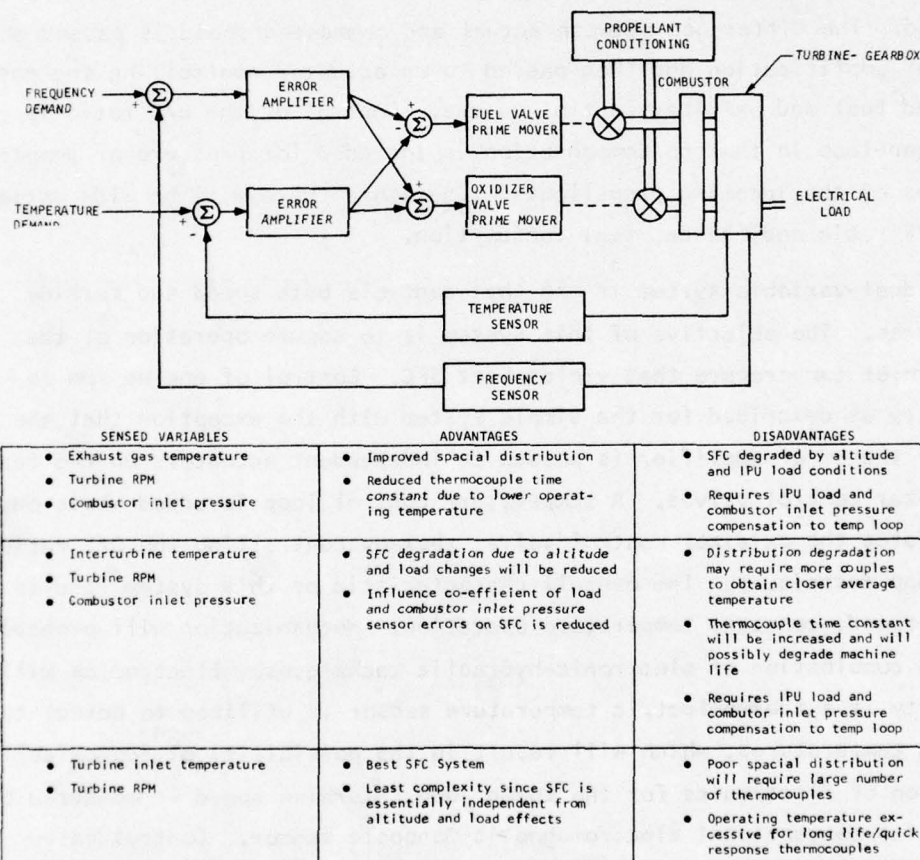
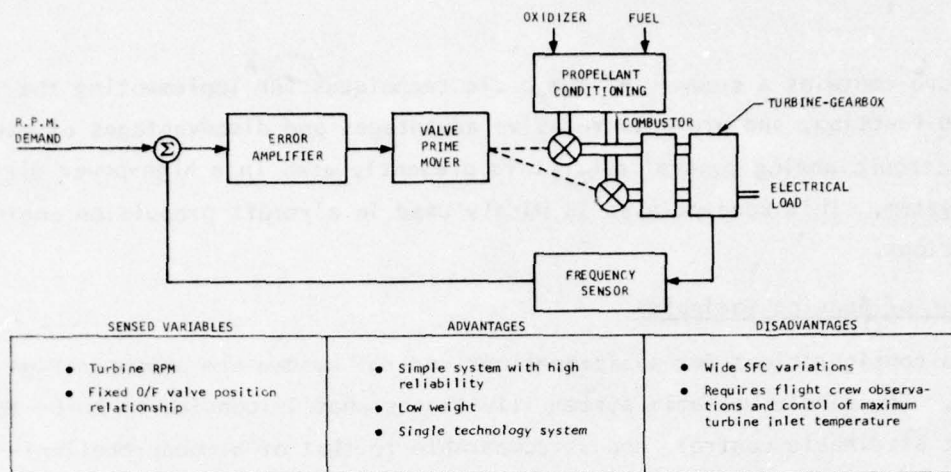
Figure 119. Control Operational Modes and Implementation Techniques

The figure contains a summary of the basic techniques for implementing the required function, and presents relative advantages and disadvantages of each. The electronic analog control concept is presently used in a high-power airborne system. This concept also is widely used in aircraft propulsion engine applications.

Selection of Sensing Variables

Two configurations for a bipropellant control system are shown in Figure 120. The single variable system illustrates what is considered to be the simplest attainable control, and is comparable to that of a monopropellant-fueled system. For this system, turbine speed is sensed by a transducer mounted at the rotating assembly, the output of which is compared to a reference speed. The difference between actual and commanded speed is passed through a stage of amplification and then passed to an actuator controlling the position of coupled fuel and oxidizer control valves. Control of the O/F ratio is essentially open-loop in that no compensation is included for pressure or temperature variations of the incoming propellants. Therefore there will be wide variations of the O/F ratio and, hence, fuel consumption.

The dual-variable system is one that controls both speed and turbine temperatures. The objective of this system is to ensure operation at the turbine inlet temperature that yields best SFC. Control of engine rpm is essentially as described for the simple system with the exception that the output of the error amplifier is passed to independent actuators on the fuel and oxidizer control valves. A temperature control loop is added whose output overmodulates the oxidizer control valve, thereby controlling the O/F ratio by closed-loop techniques. The overall characteristic of this system results in constant speed, constant temperature operation. Mechanization will probably involve a combination of electronic-hydraulic techniques. Electronics will be a necessity if a thermoelectric temperature sensor is utilized to detect turbine operating temperatures, which will result in the possibility of economical utilization of electronics for the speed loop. Turbine speed is measured by the use of a conventional electromagnetic monopole sensor. Control valve actuation with an electronic system can be achieved in many ways, the final choice being influenced mainly by the control valve characteristics.



S-59975-B

Figure 120. Bipropellant Control Systems

Valves

Valves are an integral part of the control assembly. The design of the valves interfaces in terms of response, weight, leakage, and activation approach. Various parameters that will affect valve design are listed in Table 68.

The characteristics, advantages, and disadvantages for the various types of valves are listed in Table 69. The valves include recirculation, shutoff, check, and relief, all of which will be required. The interface between the fluid valve and the electronic control output may be either electrical or pneumatic. From previous experience, the lightest weight and most reliable designs have quite often been electrically controlled and pneumatically actuated. For example, a shutoff valve would have a solenoid-operated pilot valve that controls the pneumatic actuator performing the shutoff functions. An electrical signal to the solenoid controls the shutoff valve, but the actuation is pneumatic.

TABLE 68
VALVE DESIGN PARAMETERS

Required Function	Desired Performance	Environmental Conditions	Design Features
Shutoff	Flow modulation	Ambient pressure range	Valve type
Check	Dynamic response	Ambient temperature range	Configuration
Pressure relief	Full closed leakage	Normal operating pressure range	Method of control
Flow control	Power required	Normal operating temperature range	Failure position
Fill	Minimum weight	Maximum operating pressure range with a system failure	Position indication
Vent		Maximum operating temperature range with a system failure	Structural Coupling and connectors

TABLE 69
VALVE SELECTION COMPARISON

Valve Function	Candidate Valve Type	Advantages	Disadvantages
Shutoff	Poppet	Extremely low leakage is obtainable in full closed position. Weight is lighter, in general, than the butterfly type in line sizes below approximately 1-1/2 in. Closure element is force balanced.	Pressure drop is high in full open position. Weight is heavier, in general, than the butterfly type in line sizes above approximately 1-1/2 in.
	Butterfly	Low pressure drop in the full open position. Weight is lighter, in general, than the poppet type in line sizes above approximately 2 in.	A moderate amount of leakage must be tolerated. Weight is heavier, in general, than the poppet type in line sizes below approximately 2 in. Closure element is force unbalanced. In a high pressure system this may result in a large actuator force requirement.
Pressure regulation and flow modulation and control	Poppet	A linear relationship between flow area and actuator stroke can be obtained by properly shaping the poppet. This may be a control system stability advantage. Closure element is force balanced.	Pressure drop usually is too high for use in a low-pressure system. Weight is heavier, in general, than the butterfly type in line sizes above approximately 1-1/2 in.
	Butterfly	Low pressure drop in the full open position. A moderate amount of leakage is usually tolerable. Weight is lighter, in general, than the poppet type in line sizes above approximately 2 in.	The nonlinear relationship between flow area and actuator stroke may cause system control problems due to instability when near the full open or full close positions. Weight is heavier, in general, than the poppet type in line sizes below approximately 2 in. Closure element is force unbalanced. In a high-pressure system this may result in a large actuator force requirement.
Pressure relief	Poppet	Extremely low leakage is obtainable in the full closed position. Size is generally small because the fluids being relieved usually have high densities.	
Check	Poppet	Extremely low leakage is obtainable when checking.	Pressure drop is high when flowing.
	Stiff flapper	Pressure drop is low when flowing.	A moderate amount of leakage must be tolerable in the check position.
	Flexible flapper	Pressure drop is low when flowing. Extremely low leakage is obtainable when checking.	The flapper flexibility is temperature sensitive and becomes stiff when cold.
Fill and vent	Bail check with cap	Check valve leakage is not critical because valve is sealed with a cap after filling.	

APPENDIX A

POTENTIAL APPLICATION OF AIR CUSHIONED RESEARCH VEHICLE GENERATOR

INTRODUCTION AND SUMMARY

Preliminary transient thermal analyses were conducted to predict the rotor winding temperatures of three basic ac generator sizes: 10-, 21-, and 25-MW. The analyses are focused on the potential application of a design based on the use of the Tracked Levitated Research Vehicle (TLRV) (formerly called Tracked Air Cushioned Research Vehicle (TACRV)) synchronous condenser with existing windings and with new windings. For the 21- and 25-MW generators, only oil-cooled conductors were analyzed while air-cooled conductors were considered for the 10-MW generator.

ANALYSES

The thermal analyses were performed on the following generator configurations:

- (a) 10-MW generator with no cooling of the windings.
- (b) 10-MW generator with forced air cooling of the windings.
- (c) 10-MW generator with MIL-L-23699 oil cooling of the windings.
- (d) 21-MW generator with liquid cooling. Liquids considered were deionized water, OS-139, FC-75, and DC-200.
- (e) 25-MW generator with liquid cooling. Same liquids as in (d) above.
- (f) 25-MW generator with twice the stack length as the TLRV synchronous condenser and MIL-L-23699 oil cooling. Full mean turn lengths are 107.103 in. for the stator and 90.4944 in. for the rotor versus 82.560 in. and 61.43 in., respectively, for the 25-MW generator of case (e) above.

Preliminary guidelines include a maximum winding temperature of 220°C (428°F) and a maximum pressure drop of 100 psi in oil cooled conductors for 10 mw generator and 500 psi for 21 mw and 25 mw generators. During the power off-time period the shaft rotation is assumed to be 10 rpm as compared with 5445 rpm during the on-time period.

Thermal models of the 10 mw TLRV generator are shown in Figures 1, 2, and 3. Figure 1 includes the solid nodes for the stator and rotor conductors, rotor pole head, stator teeth, and stator core. Additional nodes are shown in Figure 2 which applies to a generator with no cooling of the end windings. Figure 3 applies to the generator with air cooling of the windings. Cooling of the housing is accomplished by radiation and free convection to an ambient at 130°F and 14.7 psia. The baseline parameters of the 10 mw TLRV generator are listed in Table 1. Thermal models of the 21 mw and 25 mw are not currently available.

In accordance with the subsystem parameters requirements of Reference 1, the ac generators were analyzed using the following duty cycles:

Generator power, mw	10	10	21 and 25	21 and 25	21 and 25
Duty cycle					
On-time, sec	21	21	4	120	21
Off-time, sec	30	300	4	N/A	30
Number of cycles/mission	3	3	16	1	3

Additionally, the 10 mw generator was analyzed with on-time periods of 5 sec and 10 sec when it was determined that the 21 sec on-time period caused excessively high winding temperatures. This occurred when forced convection cooling of the windings was not considered.

RESULTS

Figure 4 presents the stator temperature for an uncooled 10 mw generator with new windings while Figure 5 presents the corresponding rotor temperatures. As noted the stator temperature approaches 1000°F when the on-time is 21 sec. In general the on-time should not exceed 9 sec if winding temperatures above 428°F are to be avoided with the uncooled generator.

The results for forced air cooling of the windings (new windings) are shown in Figures 6 and 7. The baseline cooling air flow rate is 9913 cfm (at 130°F and 14.7 psia). Other air flow rates such as 4957 cfm and 19,826 cfm were also considered to determine their effect on winding temperature. The results show that the alternate flow rates did not cause significant changes in the winding temperatures. In order to keep the generator winding temperatures below 428°F the off-time period should be longer than 180 sec.

By employing oil cooling of the windings considerable reduction in winding temperatures were achieved. In the case of the 10 mw TLRV generator with existing stator and rotor windings, Figure 8 shows that the stator winding temperature will slightly exceed 600°F. With new windings installed, and winding pressure drop limited to a minimum level of 40 psi, Figures 9 and 10 indicate all winding temperatures will be below 428°F. The pump power associated with Figures 9 and 10 are shown in Figures 11 and 12.

Numerous data were obtained on the 21 mw and 25 mw generators for the following fluids and conditions.

- | | | |
|----|----------------------------|---|
| 1. | Fluids | deionized water, OS-139, FC-75, and DC-200 |
| 2. | Duty cycles | 120 sec on only, 4 sec on - 4 sec off, and 21 sec on - 30 sec off |
| 3. | Coolant inlet temperatures | 130°F and 230°F |

For brevity only the data with MIL-L-23699 oil is summarized in this report in Tables 2, 3, and 4. The complete data were previously submitted for review. Table 2 indicates the 21 mw generator winding temperatures can be maintained below 428°F, however this is accomplished at the expense of high coolant power penalties approaching 100 hp for the rotor section and 110 hp for the stator section. Using oil cooling of the 25 mw generator with the shorter full mean turn conductor lengths, Table 3 reveals the required pump power will be about 50 percent higher than for the 21 mw generator. The required pump power drops considerably in the case of the 25 mw generator with the longer conductor lengths. Here a pump power of about 5 hp is needed for the rotor section and the stator section.

CONCLUSION

Based on the 10 mmw TLRV generator configuration with new windings, the results indicate liquid cooling will be required to achieve winding temperature below the guideline level of 428°F when the generator is subjected to the duty cycles of Reference 1. Air cooling will be adequate if the off-time period is longer than 180 sec with an on time of 21 sec.

The desired 25 mw generator configuration has not been firmly established at this time. However, the data obtained on a typical 21 and 25 mw generator covered in this analyses give approximations of the expected coolant flow and pump power ranges.

EXTRA NODES 32, 33, 35

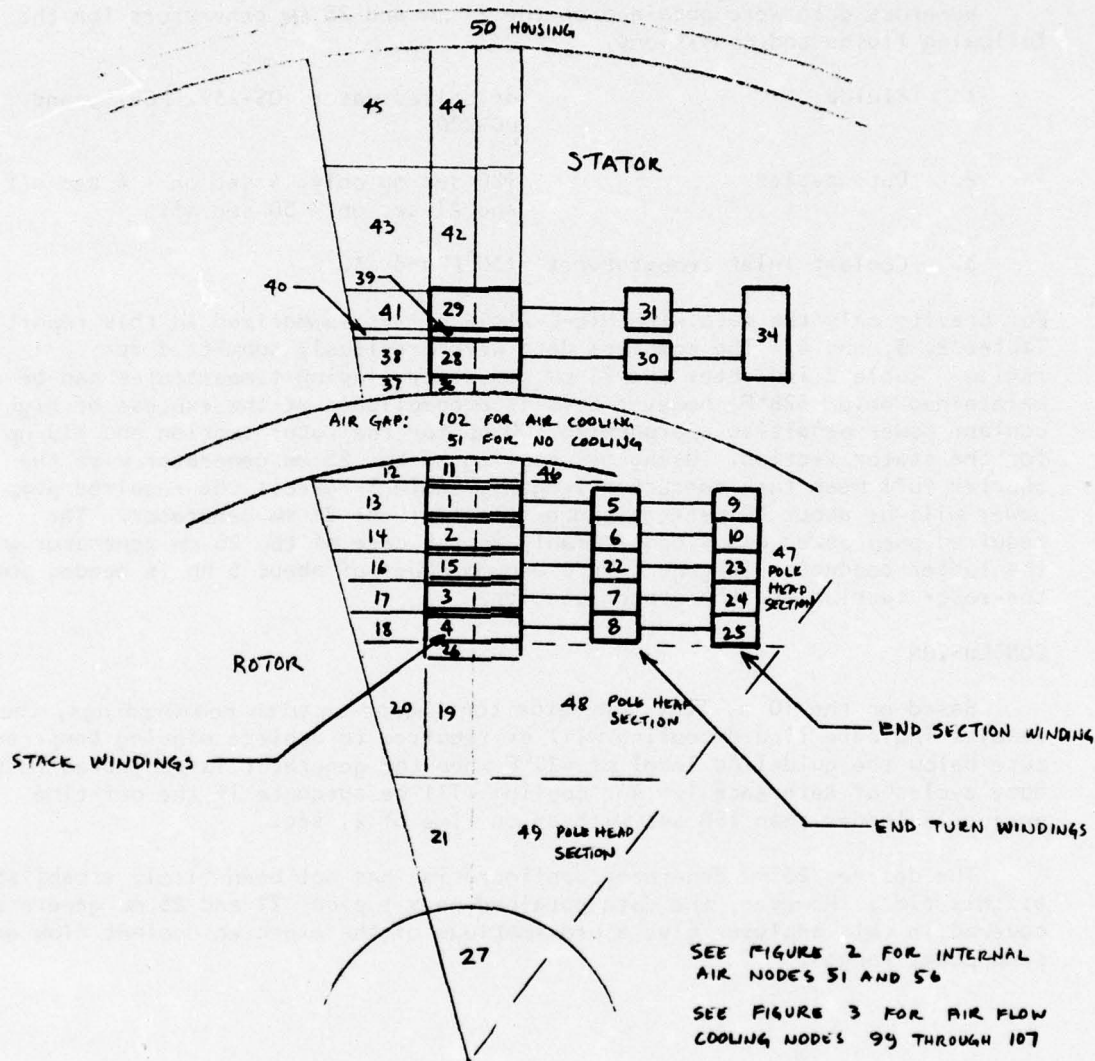


Figure 1. End View Thermal Model of 10 Megawatt Generator

• 52 AMBIENT AIR (133°F)

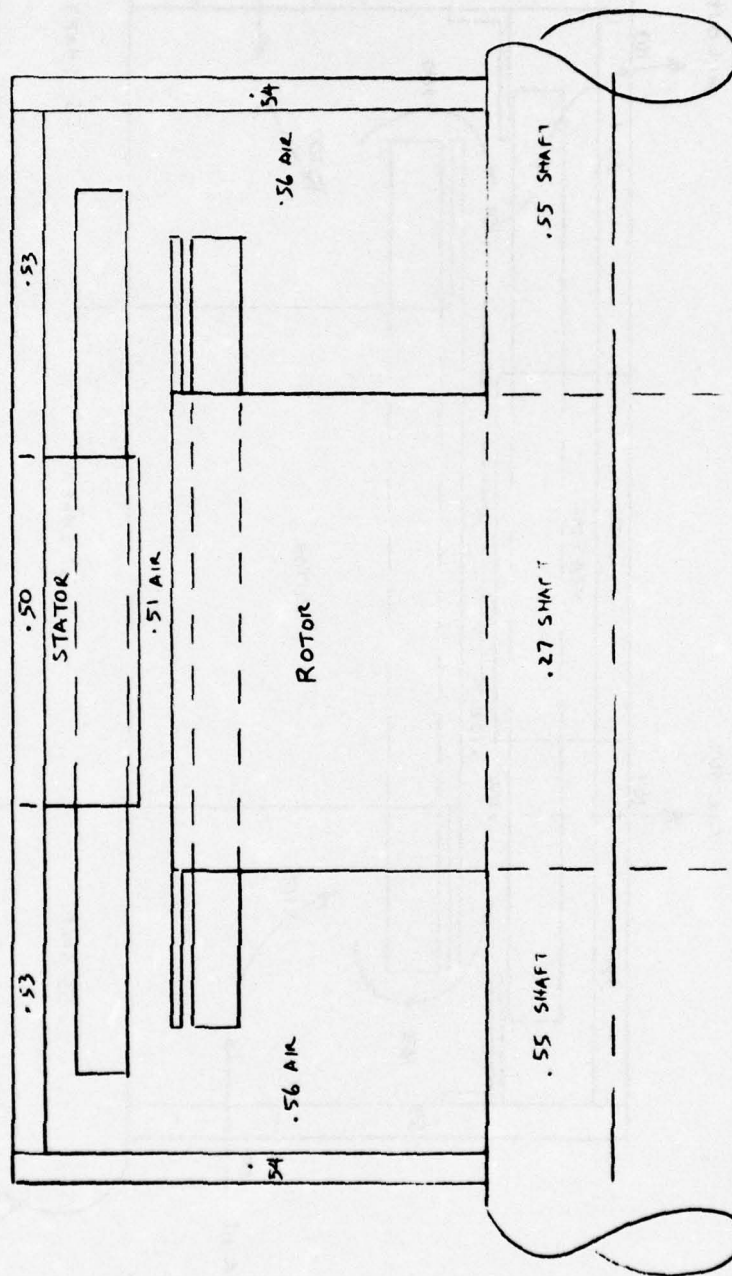


Figure 2. Partial Thermal Model of 10 Megawatt Generator Without Cooling

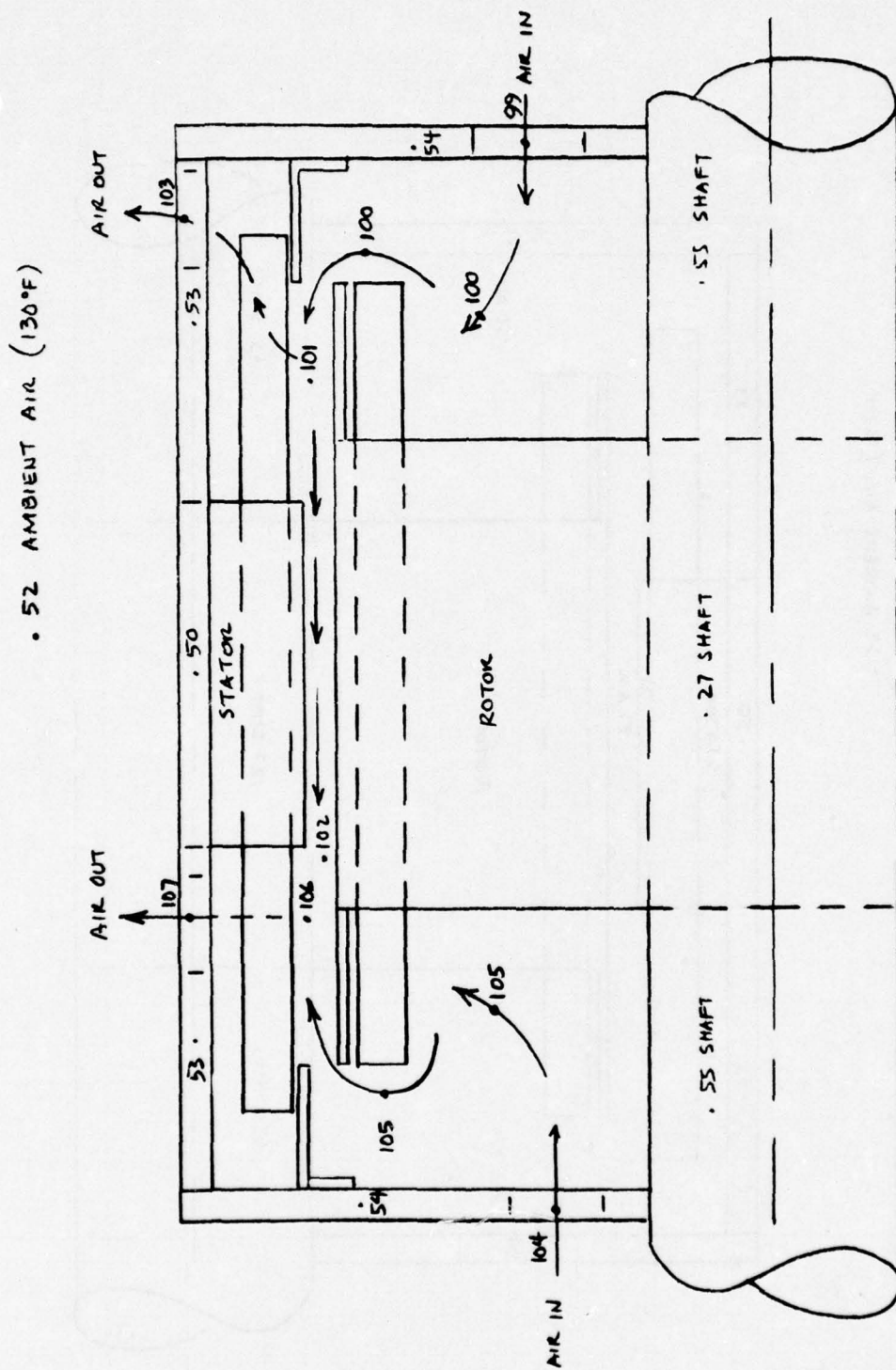


Figure 3. Partial Thermal Model of 10 Megawatt Generator with Air Cooling

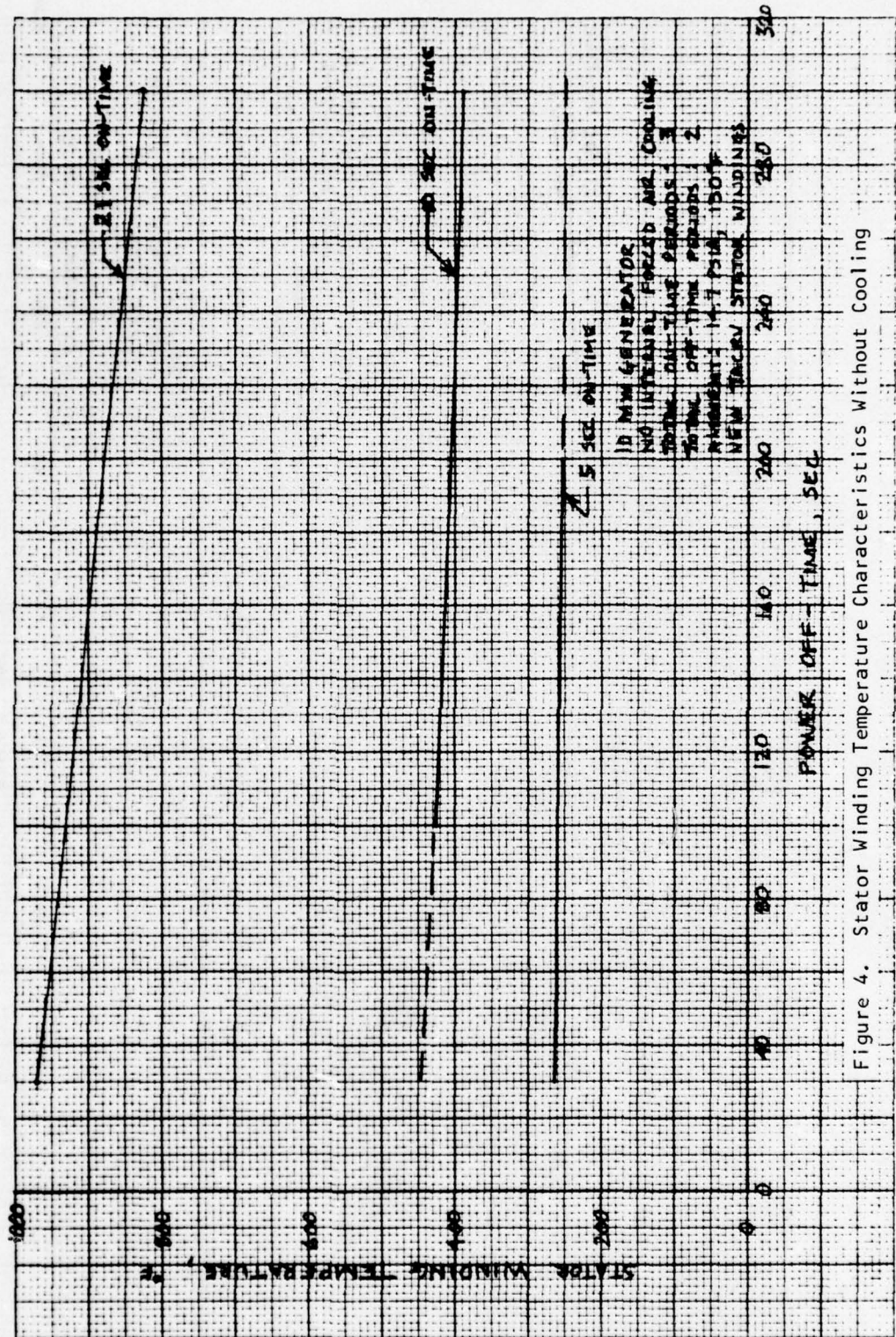


Figure 4. Stator Winding Temperature Characteristics Without Cooling

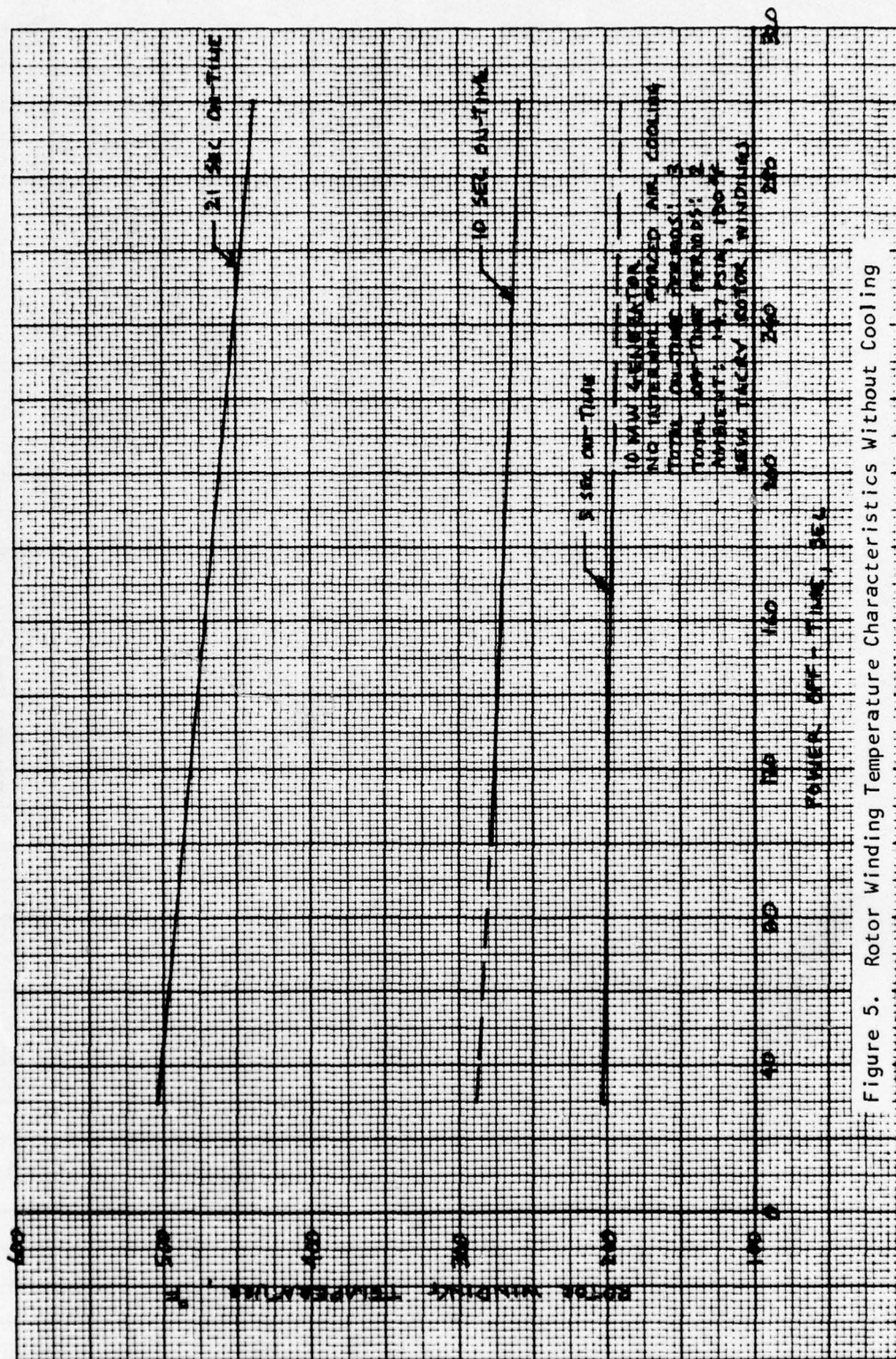


Figure 5. Rotor Winding Temperature Characteristics Without Cooling

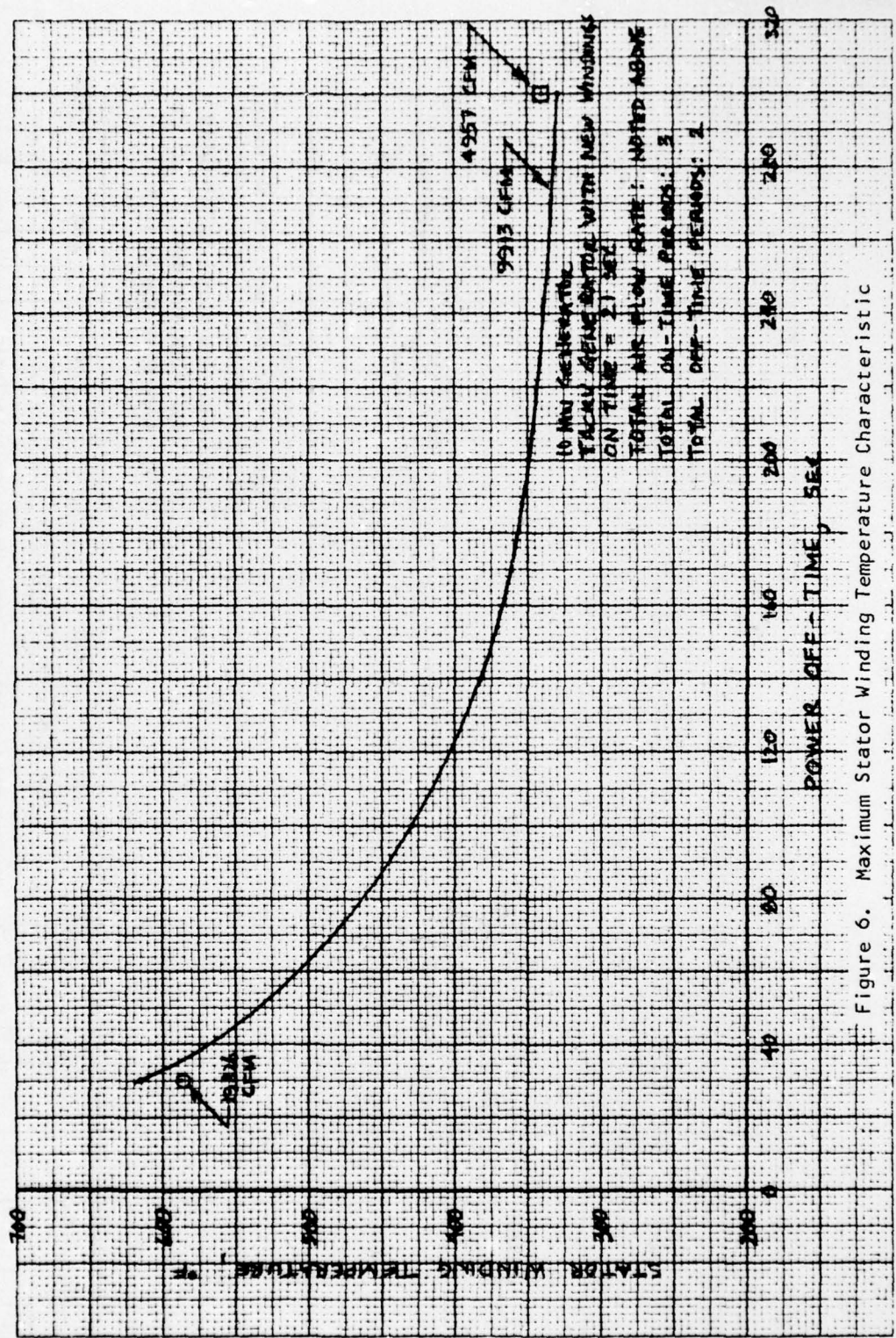


Figure 6. Maximum Stator Winding Temperature Characteristic

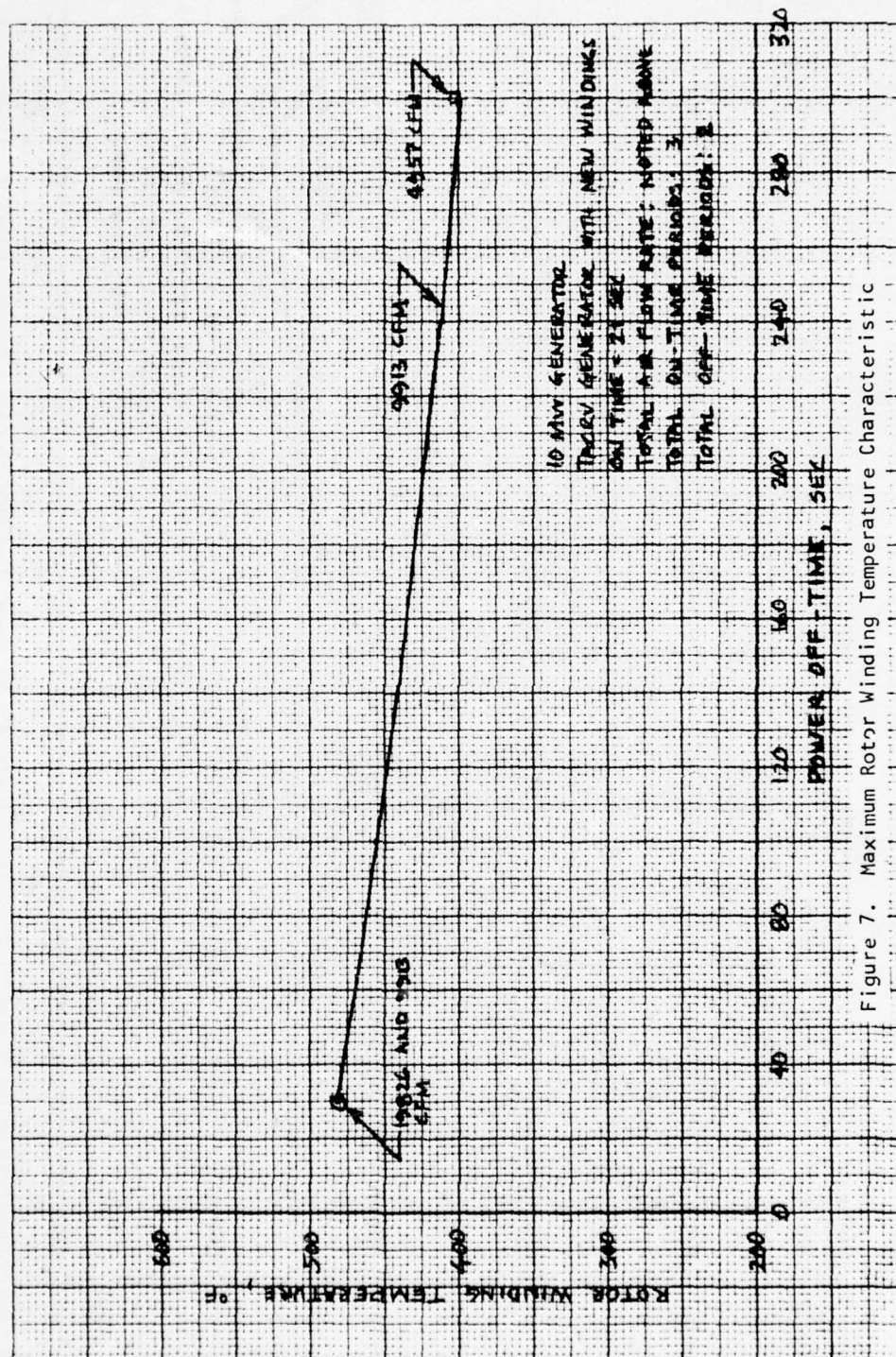


Figure 7. Maximum Rotor Winding Temperature Characteristic

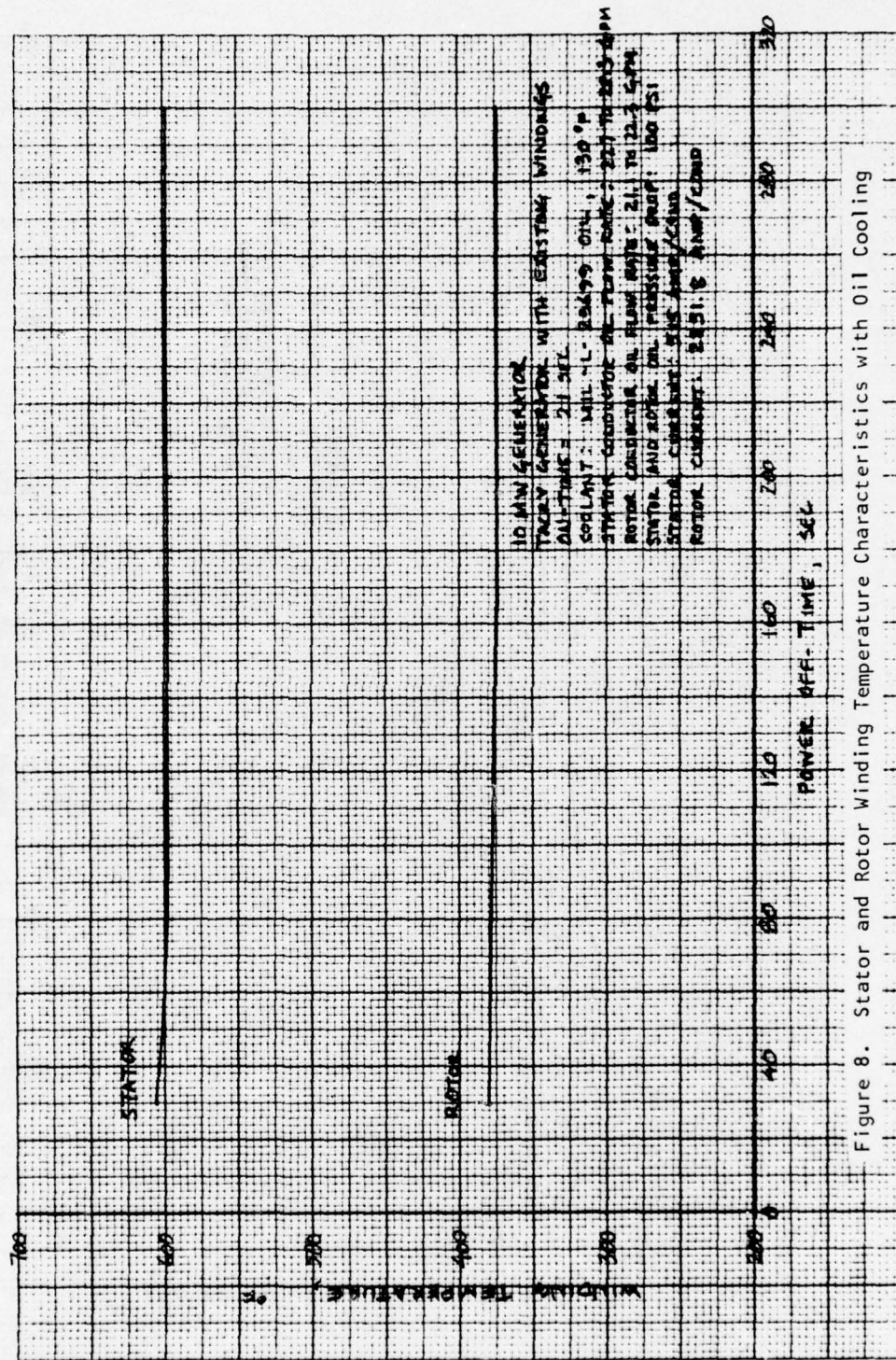


Figure 8. Stator and Rotor Winding Temperature Characteristics with Oil Cooling

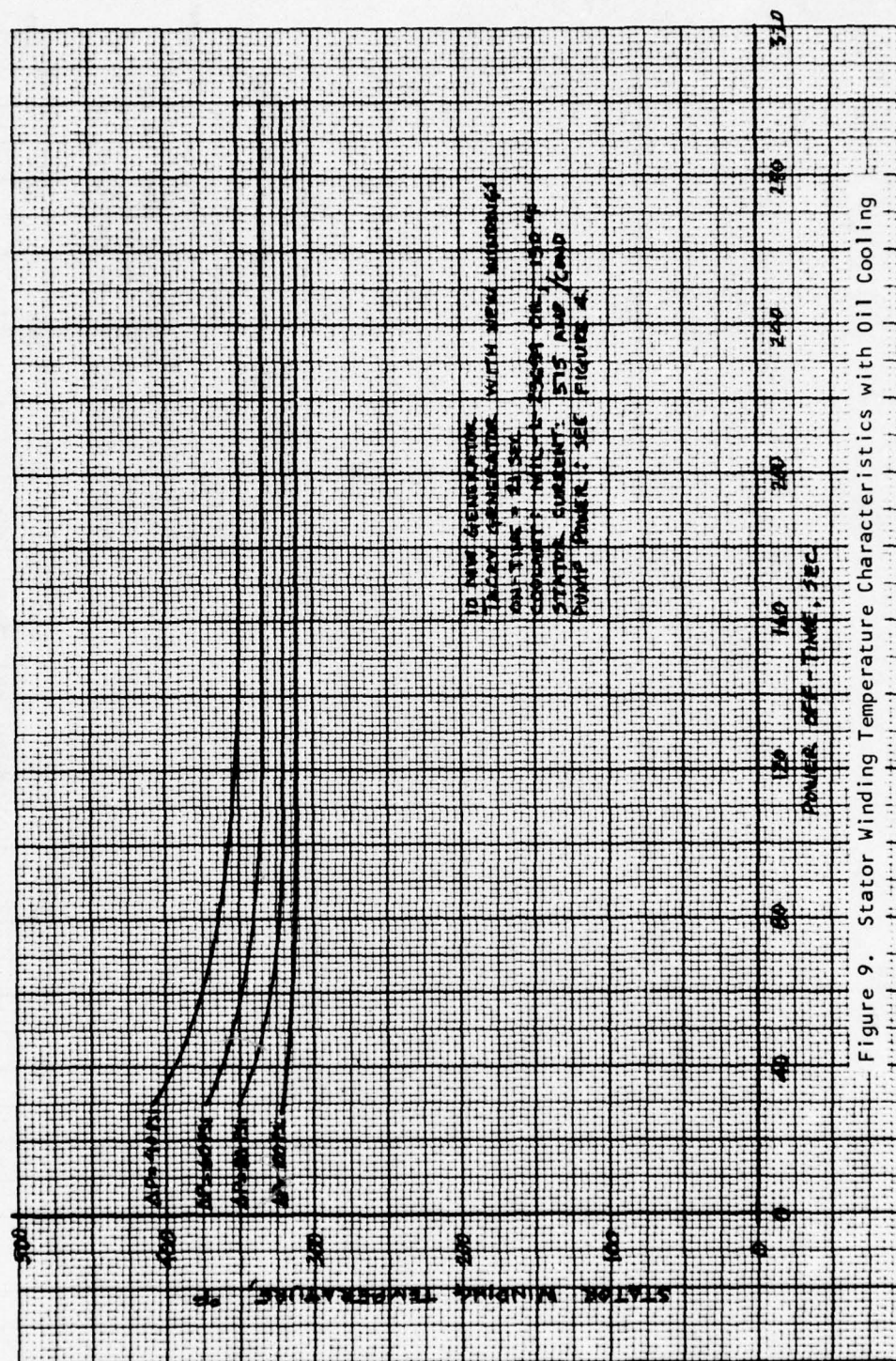


Figure 9. Stator Winding Temperature Characteristics with Oil Cooling

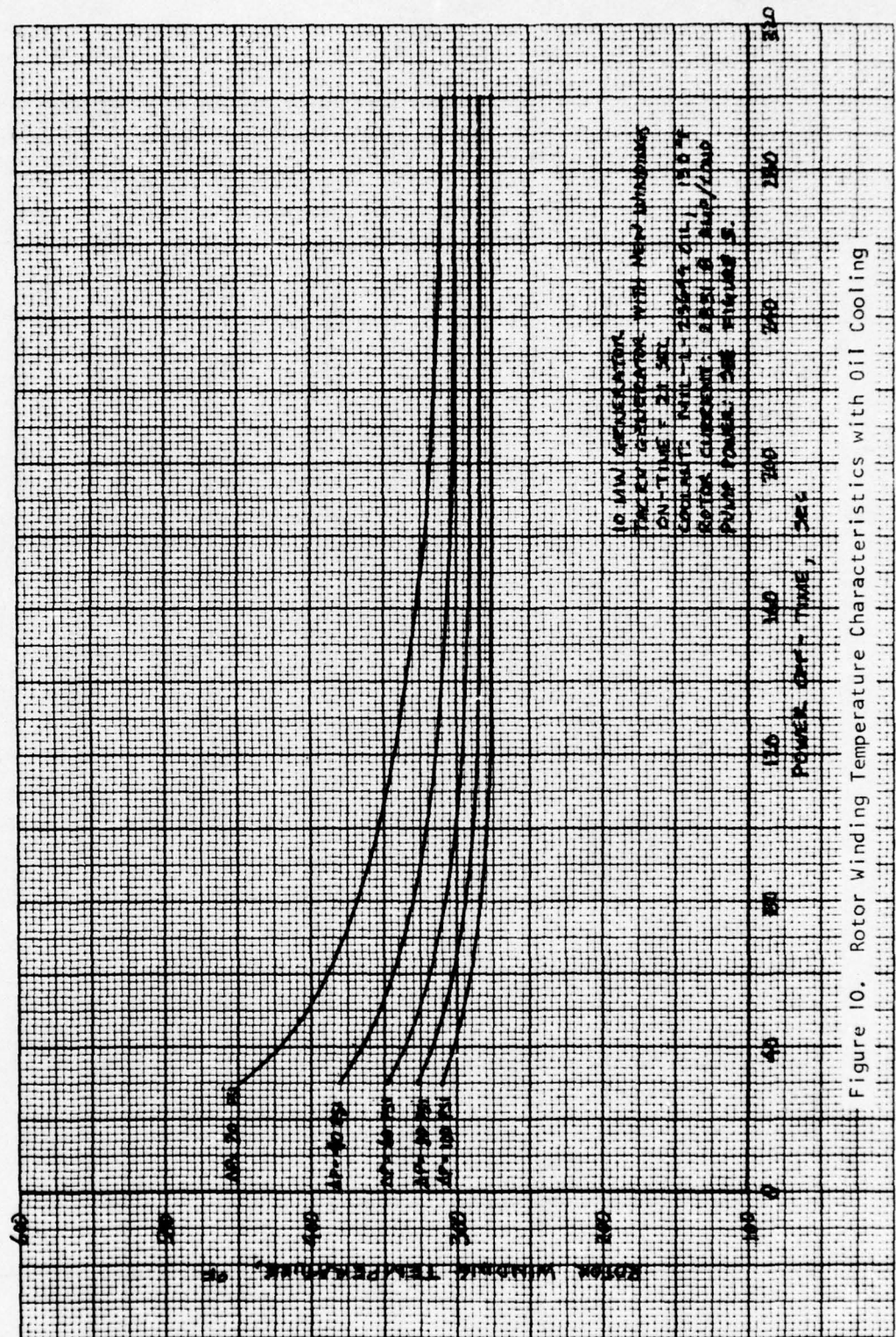


Figure 10. Rotor Winding Temperature Characteristics with Oil Cooling

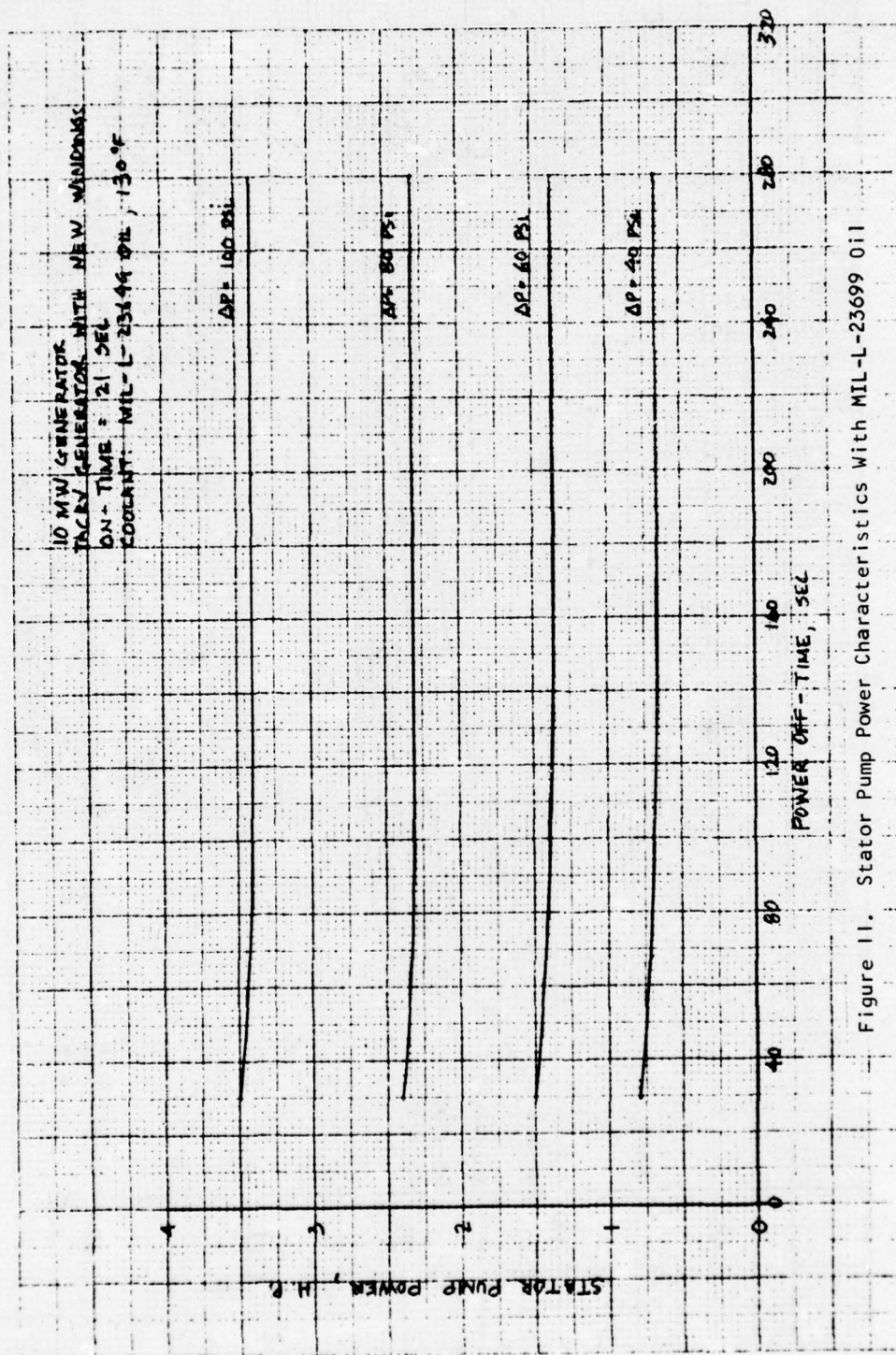


Figure 11. Stator Pump Power Characteristics with MIL-L-23699 Oil

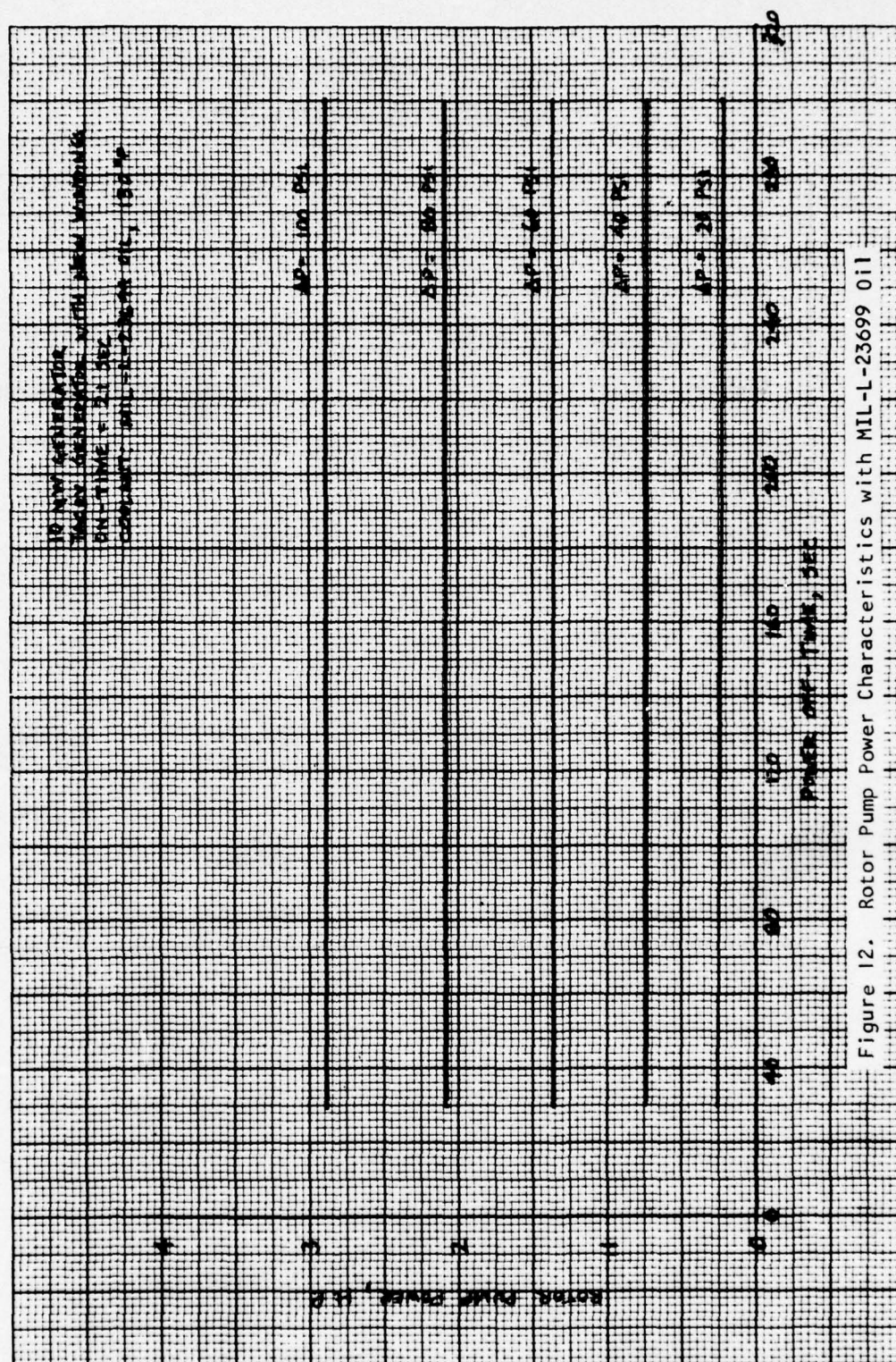


Figure 12. Rotor Pump Power Characteristics with MIL-L-23699 Oil

TABLE I
10 MEGAWATT TLRV GENERATOR DATA

	Stator	Rotor
Number of slots with coils	72	32
Number of slots without coils	0	16
Number of phases and poles	3 phases, 4 poles	
Apparent power	12.978 megavolt-amperes	
Rotational speed during on-time	---	1545
Stack length, inch	13.60	15.60
Stack OD, inch	32.08	21.46
Air gap, inch	0.4	0.4
Number of conductors per slot	2	5
Number of strands per conductor	6	1
Copper power loss, watts	324,179 (at 356°F)	222,294 (at 356°F)
Core power loss, watts	---	67,724.7
Stray load power loss, watts	129,780	---
Teeth power loss, watts	9664.13	---

TABLE 2
21 MW GENERATOR

Winding	Conductor Temperature, °F	On-Time, sec	Off-Time, sec	MIL-L-23699 Oil			
				Inlet Temp, °F	Flow Rate, gpm	Pressure Drop, psi	Pump Power, hp
Rotor	428	120	---	130	376.3	249	78.12
	402	120	---	130	415.6	301	104.2
	365	120	---	130	484.5	402	162.2
	390	4	4	130	224.9	100	18.82
	347	4	4	130	279.1	150	34.95
	321	4	4	130	326.1	200	54.43
	304	4	4	130	368.2	250	76.77
	438	21	30	130	333.7	200	55.6
	410	21	30	130	375.8	250	78.33
	388	21	30	130	413.8	300	103.4
	356	21	30	130	482.5	400	160.7
Stator	386	120	---	130	434.6	300	108.8
	406	4	4	130	359.6	200	60.06
	313	4	4	130	440.7	299	109.8
	380	21	30	130	435.7	301	109.1

Current Density = 28,915 amps/in.² for rotor,
25,774 amps/in.² for stator

TABLE 3
25 MW GENERATOR
(Short Mean Turn Conductor Length)

Winding	Conductor Temperature, °F	On-Time, sec	Off-Time, sec	MIL-L-23699 Oil			
				Inlet Temp, °F	Flow Rate, gpm	Pressure Drop, psi	Pump Power, hp
Rotor	No Available Data for rotor temp						
Stator	385	120	---	130	475.3	399	158.2
	349	120	---	130	524.2	500	218.6
	372	4	4	130	437.0	300	109.5
	326	4	4	130	495.0	401	165.2
	384	21	30	130	478.9	404	161.2
	349	21	30	130	524.0	500	218.7

Current Density = 36,801 amps/in.² for rotor
30,693 amps/in.² for stator

Full Mean Turn Conductor Length: 61.43 inch for rotor
82.56 inch for stator

TABLE 4

25 MW GENERATOR
(Long Mean Turn Conductor Length)

Winding	Conductor Temperature, °F	On-Time, sec	Off-Time, sec	MIL-L-23699 Oil			
				Inlet Temp, °F	Flow Rate, gpm	Pressure Drop, psi	Pump Power, hp
Rotor	392	120	---	230	144.0	39.8	4.78
	333	4	4	230	147.2	39.9	4.90
	378	21	30	230	145.5	40.0	4.85
	373	120	---	230	157.4	49.9	6.54
	322	4	4	230	159.9	49.6	6.61
	363	21	30	230	157.1	49.5	6.48
Stator	321	120	---	230	154.1	50.1	6.43
	284	4	4	230	151.3	50.3	6.34
	308	21	30	230	152.8	49.9	6.35
	332	120	---	230	136.6	40.0	4.56
	289	4	4	230	133.8	40.2	4.48
	314	21	30	230	135.1	39.9	4.49

Current Density: 13,709 amps/in.² for rotor
15,352 amps/in.² for stator

Full Mean Turn Conductor Length: 90.4944 inch for rotor
107.103 inch for stator

APPENDIX B

GENERATOR PARAMETRIC CRITICAL SPEED EVALUATION

INTRODUCTION AND SUMMARY

Critical speeds of a generator rotor with a hollow shaft are written in parametric form $f(D, L/D, K)$, where D is the rotor diameter, L is the length of the constant diameter, D , and K is the effective spring rate. The effective spring rate K is obtained by putting the bearings, the resilient mounts, the stub shafts, and the rotor center beam in series. The bore of the hollow rotor is assumed to be $0.4568 D$.

The corresponding curves may be used to estimate the trend of the critical speeds vs $f(D, L/D, K)$, but they should not be considered as the final answer, because they do not consider the effect of shear deflection and trunnion deflection or any variation in mass distribution. When the dimensions of the rotor are fixed available AiResearch Critical Speed Analysis Program V0250 may be used to accurately calculate all the critical speeds of the generator rotor.

DATE 8-26-75

PART NO. _____

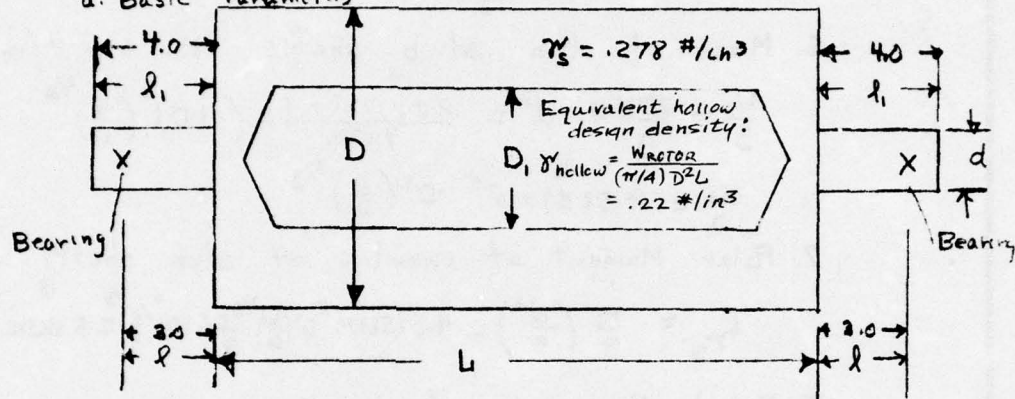
PREPARED BY Berry W. FosterCALC. NO. C-7489 SHEET NO. 1MODEL NO. AIRFORCE, H. P. Gen

CHECKED BY _____

Airforce, High Power Generator Study, Critical Speed.

I Dimensions of the generator rotor with hollow core

a. Basic Parameters



b. Assumptions

1. Stub shafts $l = 3.00$ in and $l_1 = 4.00$ in is constant for all generators
2. End trunnions are rigid with respect to stub shafts. Shear deflection is not considered.
3. Mass of rotor center

$$\frac{W_r}{g} = \frac{\pi h \pi L}{4g} D^2 = \frac{\pi_s \pi L}{4g} [D^2 - D_1^2]$$

$$D_1 = D \sqrt{\frac{\pi_s - \pi_h}{\pi_s}} = D \sqrt{\frac{.278 - .220}{.278}} = .4568 D \quad (1)$$

$$\frac{W_r}{g} = \frac{.278 \pi L}{4 \times 386} D^2 [1 - .4568^2] = 4.4764 \times 10^{-4} L D^2 \quad (2)$$

4. Polar moment of inertia of rotor center

$$I_{p_c} = \frac{\pi h \pi}{32g} D^4 [1 - .4568^4] = \frac{.278 \pi}{32 \times 386} L D^4 [1 - .4568^4]$$

$$I_{p_c} = 6.7628 \times 10^{-5} L D^4 \quad (3)$$

DATE 3-26-75

PART NO. _____

PREPARED BY Berry W FosterCALC. NO. C-7489 SHEET NO. 2MODEL NO. AIRFORCE - H.P. Gen

CHECKED BY _____

5. Diameter of the stub shaft

$$d = 2 \sqrt[3]{\frac{\pi D^2 L}{F_{ty}}} = .1 D \sqrt[3]{\frac{L}{D}}$$

6. Mass of the stub shafts $\gamma = .278 \text{ #/in}^3$

$$\frac{W_s}{g} = \frac{2\pi \gamma l}{4g} d^2 = \frac{2\pi \times .278 \times 4}{4 \times 386} \times (.1 D)^2 \left(\frac{L}{D}\right)^{2/3}$$

$$\frac{W_s}{g} = 4.5252 \times 10^{-5} D^2 \left(\frac{L}{D}\right)^{2/3}$$

7. Polar Moment of inertia of stub shafts

$$I_{Ps} = \frac{W_s}{g} \left(\frac{d^2}{8}\right) = 4.5252 \times 10^{-5} D^2 \left(\frac{L}{D}\right)^{2/3} \frac{1}{8} (.1 D)^2 \left(\frac{L}{D}\right)^{2/3} = 5.6565 \times 10^{-8} D^4 \left(\frac{L}{D}\right)^{4/3}$$

8. Total Mass of rotor

$$\frac{W}{g} = \frac{W_c}{g} + \frac{W_s}{g} = \left[4.764 \left(\frac{L}{D}\right) D + 4.5252 \left(\frac{L}{D}\right)^{2/3} D^2\right] 10^{-5}$$

9. Total Polar Moment of inertia of rotor

$$I_p = I_{pc} + I_{ps} = D^4 \cdot 10^{-5} \left[6.7628 \left(\frac{L}{D}\right) D + .005656 \left(\frac{L}{D}\right)^{4/3} D\right]$$

10. Moment of inertia of rotor about its diameter

$$I_D = I_p + \frac{W_c}{g} \frac{L^2}{12} + \frac{W_s}{g} (L + l)^2 + \frac{W_s}{g} \frac{l^3}{12}$$

$$I_D = \left[6.7628 \times 10^{-5} L D^4 + 5.6565 \times 10^{-8} D^4 \left(\frac{L}{D}\right)^{4/3} + 4.764 \times 10^{-4} L D^2 \frac{L^2}{12} + 4.5252 \times 10^{-5} D^2 \left(\frac{L}{D}\right)^{2/3} (L + 4)^2 + 4.5252 \times 10^{-5} D^2 \left(\frac{L}{D}\right)^{2/3} \frac{4^3}{12} \right]$$

$$I_D = \left(\frac{L}{D}\right) D^5 \cdot 10^{-5} \left[6.7628 + .0056565 \cdot \frac{1}{8} \left(\frac{L}{D}\right)^{1/3} + 3.7303 \left(\frac{L}{D}\right)^2 + 4.5252 \left(\frac{L}{D}\right)^{2/3} \left(\frac{L+4}{D}\right)^2 \left(\frac{1}{D}\right) + 24.1344 \left(\frac{L}{D}\right)^{2/3} \frac{1}{D^3} \right]$$

DATE 8-26-75

PART NO. _____

PREPARED BY Berry W. FosterCALC. NO. C-7489 SHEET NO. 3MODEL NO. AIRFORCE - H.P. Gen

CHECKED BY _____

11. Spring rate of one stub shaft $l = 3.0 \text{ in}$

$$\frac{1}{k_s} = \frac{l^3}{3E\pi r^4} + \frac{l^2 L}{2E\pi \frac{D^4}{16}} = \frac{4l^3}{\pi E} \left[\frac{1}{3(.050)^4 (\frac{L}{D})^4} + \frac{(\frac{L}{D})}{D^4} \right]$$

$$\frac{1}{k_s} = \frac{4 \times 27}{\pi \times 30 \times 10^6} \left[\frac{1}{3(.05)^4 D^4 (\frac{L}{D})^4} + \frac{(\frac{L}{D})}{D^4} \right] = \frac{.061115}{D^4 (\frac{L}{D})^4} + \frac{3.05577 \times 10^{-6}}{D^5}$$

See appendix in
"Mechanical Vibration"
by Den Hartog

12. Equivalent spring rate of rotor center at the bearings, solidity $s = .8$

$$2k_c = 2 \times 48 \left(\frac{EJ}{L^3} \right) = 96 \times \frac{\pi}{4} \times \frac{30 \times 10^6}{16} \left[1 - .432 \left(\frac{D}{L} \right)^3 \right]$$

$$2k_c = 1.08173 \times 10^8 \left(\frac{D}{L} \right)^3 \cdot D$$

13. Spring rate of one resilient Mount

 k_r

14. Spring rate of one bearing

 k_b 15. Effective spring rate at one bearing, k

$$\frac{1}{k} = \frac{1}{k_s} + \frac{1}{k_c} + \frac{1}{k_r} + \frac{1}{k_b}$$

$$\frac{1}{k} = \frac{.061115}{D^4 (\frac{L}{D})^4} + \frac{3.05577 \times 10^{-6}}{D^5} + \frac{\frac{1}{2} (\frac{L}{D})^3}{1.08173 \times 10^8 D^5} + \frac{1}{k_s} + \frac{1}{k_b}$$

16. C.G. is at midspan

17. $J = I_D - I_P$

$$J = 10^{-5} \left(\frac{L}{D} \right) D^5 \left[3.7303 \left(\frac{L}{D} \right)^2 + 4.5252 \left(\frac{D}{L} \right)^{\frac{1}{3}} \left(\frac{L}{D} \right)^2 \left(\frac{L}{D} \right) + 24.139 \left(\frac{D}{L} \right)^{\frac{1}{3}} \frac{1}{D^5} \right]$$

DATE 8-26-75

PART NO. _____

PREPARED BY Berry W FosterCALC. NO. C-7489 SHEET NO. 4MODEL NO. AIRFORCE - H.P. Sch

CHECKED BY _____

II Variable parameters D & L/D

A. Rotor Diameter Range $D = 8.0$ to 25 inB. Length to Diameter ratio $L/D = 2$ to 15 C. Solution of Equations on the HP-45 With $\square = \frac{L}{D}$
Variable

a. Total Mass of rotor

$$\frac{W}{g} = [\square \square D + \square] D^2$$

1. Definition of terms; $\square = \frac{L}{D}$; $\square = 4.5252 \times 10^{-5}$

$$\square = \square \square^{2/3}; \quad \square = 44.764 \times 10^{-5}$$

b. $J = I_d - I_p$; $\square = \frac{L}{D}$

$$J = \square \cdot D^4 \left[\square D + \square \left(\square + \frac{4}{D} \right) + \frac{\square}{D^2} \right]$$

1. Definition of terms $\square = 3.7303 \times 10^{-5}$; $\square = 4.5252 \times 10^{-5}$

$$\square = 24.1244 \times 10^{-5}; \quad \square = \square \cdot \square^2; \quad \square = \frac{\square}{\square^{1/3}}; \quad \square = \frac{\square}{\square^{1/3}}$$

c. Bearing Span and c.g. variable $\left(\frac{L}{D}\right)$, (D)

$$L_B = D \frac{L}{D} + 6.0$$

$$L_{c.g.} = L_B / 2$$

d. Sprung rate of one stub shafts

$$\frac{1}{k_s} = \frac{1}{D^2} \left[\frac{\square}{D^2} + \frac{\square}{D} \right]$$

1. Definition of terms

$$\square = \frac{L}{D}; \quad \square = .06115$$

$$\square = \frac{\square}{\square^{1/3}}; \quad \square = 3.05577 \times 10^{-6}; \quad \square = \square \cdot \square$$

e. Spring rate at rotor center $\square = \frac{L}{D}$; $\square = 1.68173 \times 10^{-8}$

$$2k_c = \square D^4; \quad \square = \frac{\square}{\square^3}$$

DATE 8-27-75

PART NO. _____

PREPARED BY Berry W FosterCALC. NO. C-7489 SHEET NO. 5MODEL NO. AIR FORCE - H.P. Geh

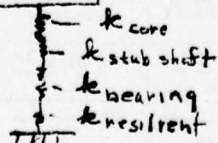
CHECKED BY _____

D. Solving For $\frac{W}{g}$; k_s ; k_c ; J ; k_B ; l_c

D	$\frac{Y}{D}$	$\frac{W}{g}$	k_s $\times 10^6$	k_c $\times 10^6$	$\frac{1}{k_s} + \frac{1}{k_c}$ $\times 10^{-6}$	J	k_B
8	2	.46298	.16845	.54.085	5.9550	11.637	22.00
	5	1.1460	.5631	3.462	2.0647	169.23	46.00
	10	2.3054	1.3287	.4327	3.0637	1,662.9	86.00
	15	3.4555	2.0280	.1282	8.2934	5,773.3	126.00
10	2	.90246	.41104	67.61	2.4476	34.041	26.00
	5	2.2514	1.3689	4.327	.9616	504.94	56.00
	10	4.4974	3.1808	.55408	2.1635	4785.3	106.00
	15	6.7421	4.7363	.1603	6.4494	16,561.	156.00
15	2	3.0377	2.0783	101.41	.4910	247.35	36.00
	5	7.5837	6.8585	6.490	.2999	3726.8	81.00
	10	15.155	15.356	.8113	1.2977	33,533.	156.00
	15	22.724	21.629	2439	4.1463	116,360.	231.00
20	2	7.1910	6.5662	135.215	.1598	11010.8	46.
	5	17.959	21.454	8.654	.1622	15,494.	106.
	10	35.895	46.384	1.0218	.9459	135,600.	206.
	15	53.827	62.263	.8205	3.1362	464,760.	306.
25	2	14.034	15.996	169.04	.0684	3045.6	56.0
	5	35.055	51.847	70.818	.1117	46913.	131.
	10	70.075	108.44	1.3522	.7498	403600.	256.
	15	105.09	139.56	.4164	2.4678	1,379,800.	381.

E. Approximation of First Flexural (No Gyro considered)

$$\frac{1}{2} \frac{W}{g}$$



$$\frac{1}{k} = \frac{1}{k_c} + \frac{1}{k_s} + \frac{1}{k_b} + \frac{1}{k_r}$$

$$f = \frac{1}{2\pi} \sqrt{\frac{k}{\frac{1}{2} \frac{W}{g}}} \quad \text{HZ.}$$

DATE

9-1-75

PART NO.

PREPARED BY Berry W. Foster

CALC. NO.

C-7489

SHEET NO.

6

MODEL NO.

AIRFORCE - H.P. Gen

CHECKED BY

E. First Flexural Critical Speed (No Gyr.)

$$f = \frac{1}{2\pi} \sqrt{\frac{k_b}{I_p}} = \frac{1}{2\pi} \sqrt{\frac{k_b}{\frac{\pi}{32} I_p}} = \frac{1}{\pi} \sqrt{\frac{k_b}{I_p}} \quad \text{Hz}$$

$$f = \frac{1}{\pi} \sqrt{\frac{k_b}{I_p}} \quad \text{Hz}$$

$k_b = 8 \times 10^6 \text{ lb/in / bearing}$	$k_b = 1.2 \times 10^6 \text{ lb/in / bearing}$			$k_b = 1.5 \times 10^6 \text{ lb/in / bearing}$		
	1×10^6	4×10^6	1.25×10^6	1×10^6	4×10^6	1.25×10^6
2	11.25	106.18	123.24	80.73	108.54	126.96
5	57.62	87.19	115.48	58.54	90.50	123.51
10	39.18	56.79	71.37	39.76	57.61	75.09
15	27.39	34.89	39.19	27.69	35.51	40.08
20	24.05	30.75	32.21	24.50	30.87	33.80
25	21.32	27.62	28.87	21.60	27.41	29.97
30	19.18	25.13	26.22	19.20	24.87	27.12
35	17.45	22.85	23.83	17.26	22.41	24.87
40	16.03	20.85	21.65	15.60	20.33	22.41
45	14.85	18.85	19.69	14.20	18.20	20.33
50	13.85	17.12	17.85	12.95	16.20	18.20
55	12.95	15.75	16.15	11.85	14.41	16.20
60	12.15	14.69	14.65	10.85	12.95	14.41
65	11.45	13.85	13.33	9.95	11.85	12.95
70	10.85	13.15	12.15	9.15	10.85	11.85
75	10.35	12.55	11.05	8.45	9.95	10.85
80	9.95	11.95	10.05	7.85	9.15	9.95
85	9.65	11.45	9.15	7.35	8.45	9.15
90	9.35	10.95	8.25	6.95	7.85	8.45
95	9.15	10.55	7.45	6.65	7.35	7.85
100	8.95	10.15	6.75	6.35	6.95	7.35
105	8.75	9.75	6.05	6.05	6.65	6.95
110	8.55	9.35	5.75	5.75	6.35	6.65
115	8.35	8.95	5.45	5.45	6.05	6.35
120	8.15	8.55	5.15	5.15	5.75	6.05
125	7.95	8.15	4.85	4.85	5.45	5.75
130	7.75	7.75	4.55	4.55	5.15	5.45
135	7.55	7.35	4.25	4.25	4.85	5.15
140	7.35	6.95	3.95	3.95	4.55	4.85
145	7.15	6.55	3.65	3.65	4.25	4.55
150	6.95	6.15	3.35	3.35	3.95	4.25
155	6.75	5.75	3.05	3.05	3.65	3.95
160	6.55	5.35	2.75	2.75	3.35	3.65
165	6.35	4.95	2.45	2.45	3.05	3.35
170	6.15	4.55	2.15	2.15	2.75	3.05
175	5.95	4.15	1.85	1.85	2.45	2.75
180	5.75	3.75	1.55	1.55	2.15	2.45
185	5.55	3.35	1.25	1.25	1.85	2.15
190	5.35	2.95	0.95	0.95	1.55	1.85
195	5.15	2.55	0.65	0.65	1.25	1.55
200	4.95	2.15	0.35	0.35	0.95	1.25

DATE 8-28-75

PART NO.

PREPARED BY Berry W. FosterCALC. NO. C-7482 SHEET NO. 7MODEL NO. AIRFORCE - 4 P. Gen

CHECKED BY

III Use the Wang Computer program Based on Pgs 180-181 of
Vibration Theory & Applications by W T Thomson, Prentice Hall, 1965
A Structural Model of High Power Generator

a. Basic Equation $f = \frac{1}{2\pi} \sqrt{\frac{1}{2}(a+c) \pm \sqrt{\frac{1}{4}(a-c)^2 + (b)^2}}$

where: $a = \frac{1}{m}(K_1 + K_2)$; $b = \frac{1}{m}(k_2 L_2 - k_1 L_1)$; $c = \frac{1}{J}(k_1 L_1^2 + k_2 L_2^2)$

① $m = \frac{W}{g}$ # sec²/in

② $J = I_D - I_P$ c.g.

$J = \# \text{ sec}^2 \text{ in}$

⑤ K_1

$K_2 = ⑥$

B. Rigid Mount

④ $L_T/2 = L_1$

$L_2 = L_T - L_1$

$L_T = ③$

$\frac{1}{K_1} + \frac{1}{K_2}$ $\times 10^6$	D	%	$K_1 = K_2 = 500,000 \#/\text{in}$				$K_1 = K_2 = 10^6 \#/\text{in}$				$K_1 = K_2 = 1.5 \times 10^6 \#/\text{in}$			
			$\frac{1}{K_1} + \frac{1}{K_2}$ $\times 10^{-6}$	f_1 Hz	f_2 Hz	$\frac{1}{K_1} + \frac{1}{K_2}$ $\times 10^{-6}$	f_1 Hz	f_2 Hz	$\frac{1}{K_1} + \frac{1}{K_2}$ $\times 10^{-6}$	f_1 Hz	f_2 Hz	$\frac{1}{K_1} + \frac{1}{K_2}$ $\times 10^{-6}$	f_1 Hz	f_2 Hz
5.955	8	2	*	234	513	*	331	725	*	405	788	*	483	788
2.085		5	*	149	282	*	210	389	*	258	483	*	270	483
3.064		10	*	104.88	167.91	*	148.31	237.4	*	181.68	270.23	*	228.7	270.23
8.293		15	*	85.7	132.0	*	121.1	186.7	*	148.4	228.7	*		
2.448	10	2	*			*			*			*		
1.962		5	1.048	106.1	198.4	.038	150.1	280.6	*	183.8	343.7	*		
2.169		10	*	75.09	122.00	*	106.19	172.58	*	130.6	211.32	*		
6.449		15	*	61.33	96.51	*	86.71	136.49	*	106.22	167.17	*		
.491	15	2	1.509			.509			1.176			*		
.300		5	1.700	57.82	105.14	.700	81.77	149.39	.367	100.15	182.97	*		
1.298		10	1.702	40.39	68.69	*	57.12	97.14	*	69.96	118.97	*		
4.146		15	*	33.41	54.15	*	47.24	76.58	*	57.86	93.79	*		
.1598	20	2	1.8402			1.8402			.5070			*		
.1622		5	1.8378	37.58	67.80	.8378	53.14	95.88	.5045	65.88	117.43	*		
.9439		10	1.0541	26.58	44.54	.0541	37.64	62.99	*	46.03	77.15	*		
3.1362		15	*	21.87	35.74	*	30.69	50.53	*	37.59	61.70	*		
.0684	25	2	1.9316			.9316			.5983			*		
.1117		5	1.8883	26.89	48.15	.8883	38.03	68.10	.555	46.58	83.41	*		
.7488		10	1.2512	19.02	32.08	.2512	26.09	45.73	*	39.95	55.57	*		
2.417		15	*	15.53	25.82	*	21.97	36.52	*	26.89	44.70	*		

* The stub shaft, k_s , and the rotor core, K_c , are too flexible to get given K_1 & K_2

DATE

7-1-75

PART NO.

PREPARED BY Berry W. Foster

CALC. NO.

C-7489

SHEET NO.

8

MODEL NO.

AIRFORCE - H.P. Gen

CHECKED BY

B. Rigid Body Frequencies With Hard Mounts and assumed Bearings (My = 0) springs which are the same at Both ends

Stub Shaft, k_s Core, k_c		$K_b = 800,000 \text{ #/in}$				$K_b = 1,000,000 \text{ #/in}$				$K_b = 1,200,000 \text{ #/in}$				$K_b = 1,500,000 \text{ #/in}$					
$\frac{1}{R_s} + \frac{1}{R_c}$ $\times 10^6$	D	$K = K_s \otimes \times 10^6$	f_1 Hz	f_2 Hz	$K = K_s \otimes \times 10^6$	f_1 Hz	f_2 Hz	$K = K_s \otimes \times 10^6$	f_1 Hz	f_2 Hz	$K = K_s \otimes \times 10^6$	f_1 Hz	f_2 Hz	$K = K_s \otimes \times 10^6$	f_1 Hz	f_2 Hz	$K = K_s \otimes \times 10^6$	f_1 Hz	f_2 Hz
5.955	8	.1388	123.3	270.3	.1438	127.0	272.5	.1473	127.0	272.5	.1510	128.4	281.7	.1510	128.4	281.7	.1510	128.4	281.7
2.465	5	.3017	115.5	218.7	.3263	123.6	233.9	.3450	123.6	233.9	.3661	127.3	240.9	.3661	127.3	240.9	.3661	127.3	240.9
3.064	10	.2318	71.4	114.3	.2461	75.1	120.3	.2566	75.1	120.3	.2680	76.9	122.9	.2680	76.9	122.9	.2680	76.9	122.9
8.293	15	.1048	39.2	60.4	.1076	40.1	61.8	.1096	40.1	61.8	.1116	40.5	62.4	.1116	40.5	62.4	.1116	40.5	62.4
2.448	10	.2704	123.3	260.9	.2900	130.9	277.8	.3043	130.9	277.8	.3211	134.3	284.3	.3211	134.3	284.3	.3211	134.3	284.3
.962	5	.4521	100.9	188.7	.5097	112.0	209.4	.5570	112.0	209.4	.6140	117.6	219.9	.6140	117.6	219.9	.6140	117.6	219.9
2.164	10	.2929	57.5	93.4	.3161	61.3	99.7	.3336	61.3	99.7	.3533	63.1	102.6	.3533	63.1	102.6	.3533	63.1	102.6
6.449	15	.1299	31.3	49.2	.1342	32.1	50.6	.1373	32.1	50.6	.1405	32.5	51.2	.1405	32.5	51.2	.1405	32.5	51.2
.491	15	.5744	97.9	195.3	.6707	112.3	264.0	.7551	112.3	264.0	.8638	121.1	239.5	.8638	121.1	239.5	.8638	121.1	239.5
.300	5	.6452	66.1	120.8	.7692	76.8	140.3	.8824	76.8	140.3	1.0345	83.2	152.0	1.0345	83.2	152.0	1.0345	83.2	152.0
1.298	10	.3925	36.2	60.1	.4352	37.6	65.7	.4692	37.6	65.7	.509	41.3	68.4	.509	41.3	68.4	.509	41.3	68.4
4.146	15	.1853	18.7	33.9	.1943	21.2	34.3	.2008	21.2	34.3	.2078	21.5	34.9	.2078	21.5	34.9	.2078	21.5	34.9
.1598	20	.7093	70.7	137.2	.8622	84.3	163.5	1.0069	84.3	163.5	1.2100	92.4	179.2	1.2100	92.4	179.2	1.2100	92.4	179.2
.1022	5	.7081	44.7	80.7	.8604	53.3	96.1	1.0045	53.3	96.1	1.2065	58.4	105.3	1.2065	58.4	105.3	1.2065	58.4	105.3
.9459	10	.4554	25.4	42.5	.5139	28.2	47.2	.5620	28.2	47.2	.6201	29.6	49.6	.6201	29.6	49.6	.6201	29.6	49.6
3.1362	15	.2228	14.5	23.9	.2418	15.4	25.4	.2579	15.4	25.4	.2630	15.7	25.9	.2630	15.7	25.9	.2630	15.7	25.9
.0884	25	.7525	52.4	99.5	.9360	63.3	120.3	1.1090	63.3	120.3	1.3604	70.1	133.3	1.3604	70.1	133.3	1.3604	70.1	133.3
.1117	5	.7344	32.6	58.4	.8795	39.1	70.1	1.0582	39.1	70.1	1.2847	43.1	77.2	1.2847	43.1	77.2	1.2847	43.1	77.2
.7488	10	.5003	19.0	51.6	.5718	21.4	36.1	.6321	21.4	36.1	.7065	22.6	38.1	.7065	22.6	38.1	.7065	22.6	38.1
2.4678	15	.2890	11.4	18.9	.2884	12.1	20.1	.3029	12.1	20.1	.3190	12.4	20.6	.3190	12.4	20.6	.3190	12.4	20.6

DATE 9-1-75

PART NO. _____

PREPARED BY Berry W. FosterCALC. NO. C-7489 SHEET NO. 9MODEL NO. AIR FORCE 11-1-50

CHECKED BY _____

C. Rigid Body Frequencies With Resilient Mount Spring
 Rate $K_r = 100,000$ lb/in at Both Ends with Assumed
 Bearings Spring Rates which are the same at
 Both Ends.

Stub Shaft, #s Core, #c		$K_b = 800,000 \text{ \#/in}$			$K_b = 1,200,000 \text{ \#/in}$			$K_b = 1,500,000 \text{ \#/in}$			
$\frac{1}{K_s} + \frac{1}{K_c}$ x10 ⁶	D	$\frac{L}{D}$	$K_1 = K_2$ ⑤ ⑥ #/in	f_1 Hz	f_2 Hz	$K_1 = K_2$ ⑤ ⑥ #/in	f_1 Hz	f_2 Hz	$K_1 = K_2$ ⑤ ⑥ #/in	f_1 Hz	f_2 Hz
5.955	8	2	58,123.	79.8	174.9	59,565.	80.8	177.1	60,162.	81.2	178.0
2.065		5	75,103.	57.6	109.1	77,529.	58.6	110.9	78,544.	59.0	111.6
3.064		10	69,862.	39.2	62.8	71,956.	39.8	63.7	72,830.	40.0	64.1
8.293		15	51,169.	27.4	42.3	52,284.	27.7	42.7	52,744.	27.8	42.9
2.448	10	2	73,003.	64.0	135.6	75,294.	65.0	137.7	76,251.	65.5	138.6
.962		5	81,887.	42.9	80.3	84,779.	43.7	81.7	85,994.	44.0	82.3
2.164		10	74,549.	29.0	47.1	76,939.	29.4	47.9	77,938.	29.6	48.2
6.449		15	56,500.	20.6	32.4	57,863.	20.9	32.8	58,426.	21.0	33.0
.491	15	2	83,172.	37.7	75.2	88,305.	38.4	76.6	89,624.	38.7	77.2
.300		5	86,580.	24.1	44.0	89,820.	24.5	44.8	91,185.	24.7	45.1
1.298		10	79,694.	16.3	27.1	82,431.	16.6	27.5	83,579.	16.7	27.7
4.146		15	64,952.	12.0	19.5	66,759.	12.2	19.8	67,510.	12.3	19.9
.1598	20	2	87,644.	24.9	48.2	90,966.	25.3	49.1	92,366.	25.5	49.5
.1672		5	87,626.	15.7	28.4	90,946.	16.0	28.9	92,346.	16.1	29.1
.9459		10	81,995.	10.8	18.0	84,895.	11.0	18.4	86,114.	11.0	18.5
3.1362		15	69,511.	8.1	13.3	71,584.	8.2	13.5	72,449.	8.3	13.6
.0684	25	2	88,352.	17.9	34.0	91,729.	18.2	34.6	93,153.	18.3	34.9
.1117		5	88,015.	11.3	20.2	91,366.	11.5	20.6	92,778.	11.6	20.7
.7488		10	83,342.	7.8	13.1	86,340.	7.9	13.3	87,600.	8.0	13.4
2.4678		15	72,878.	5.9	9.9	75,182.	6.0	10.0	76,136.	6.1	10.1

DATE 9-1-75

PART NO. _____

PREPARED BY Berry W. FosterCALC. NO. C-7487 SHEET NO. 10MODEL NO. AIRFORCE, H.P. GEN

CHECKED BY _____

D. Rigid Body Frequencies With Resilient Mount Spring
 Rate $K_r = 1400,000$ lb/in at Both ENDS with Assumed
 Bearing Spring Rates which are the same at
 Both Ends

Stub Shaft, K_s Core, K_c			$K_b = 800,000 \text{ \# / in}$				$K_b = 1,200,000 \text{ \# / in}$				$K_b = 1,500,000 \text{ \# / in}$			
$\frac{1}{K_s} + \frac{1}{K_c}$ $\times 10^6$	D	$\frac{L}{D}$	$K_1 = K_2$ ⑤ ⑥ # / in	f_1 Hz	f_2 Hz	$K_1 = K_2$ ⑤ ⑥ # / in	f_1 Hz	f_2 Hz	$K_1 = K_2$ ⑤ ⑥ # / in	f_1 Hz	f_2 Hz			
5.955	8	2	103,040.	106.2	232.9	107,460.	108.6	238.1	109,630.	109.6	240.2			
2.065		5	171,970.	87.2	165.1	185,240.	90.5	171.4	191,140.	92.0	174.1			
3.064		10	146,740.	56.8	91.0	156,320.	58.6	93.9	160,500.	59.4	95.1			
8.293		15	83,036.	34.9	53.8	86,012.	35.5	54.8	87,263.	35.8	55.2			
2.448	10	2	161,340.	95.2	201.5	172,970.	98.1	208.7	178,100.	100.0	211.8			
.962		5	212,220.	69.1	129.3	232,810.	72.4	135.4	242,210.	73.9	138.1			
2.164		10	169,090.	43.7	70.9	181,910.	45.3	73.6	187,590.	46.0	74.7			
6.449		15	98,049	27.2	42.7	102,230.	27.7	43.1	104,000.	28.0	44.0			
.491	15	2	235,790.	62.7	125.2	261,480.	66.1	131.8	273,400.	67.6	134.8			
.300		5	246,910.	40.6	74.2	275,230.	42.9	78.4	282,460.	43.9	80.2			
1.298		10	198,100.	25.7	42.7	215,920.	26.9	44.6	223,980.	27.4	45.4			
4.146		15	126,650	16.8	27.3	133,700.	17.3	28.0	136,750	17.5	28.3			
.1598	20	2	255,770.	42.5	82.4	266,280.	43.3	86.0	300,620	46.0	89.3			
.1622		5	255,610.	26.9	48.5	286,080.	28.4	51.3	300,400.	29.1	52.6			
.9457		10	212,350.	17.3	29.1	233,690.	18.2	30.4	243,160.	18.5	31.1			
3.1362		15	145,220	11.7	19.3	154,570.	12.1	19.9	158,460.	12.2	20.1			
.0634	25	2	261,890.	30.8	58.5	273,970.	32.6	61.9	309,110.	33.4	63.5			
.1017		5	258,950.	19.6	34.7	270,270.	20.5	36.7	305,090	21.0	37.6			
.7488		10	222,280.	12.7	21.4	244,970.	13.3	22.5	256,400.	13.1	23.0			
2.4678		15	160,830.	8.8	14.6	172,380.	9.1	15.2	177,480.	9.3	15.4			

DATE 9-4-75

PART NO. _____

PREPARED BY Berry W FosterCALC. NO. C-7489 SHEET NO. 11MODEL NO. AIR FORCE, H.P. Gen

CHECKED BY _____

E Free Body Frequency

a First free body of the Rotor Center D

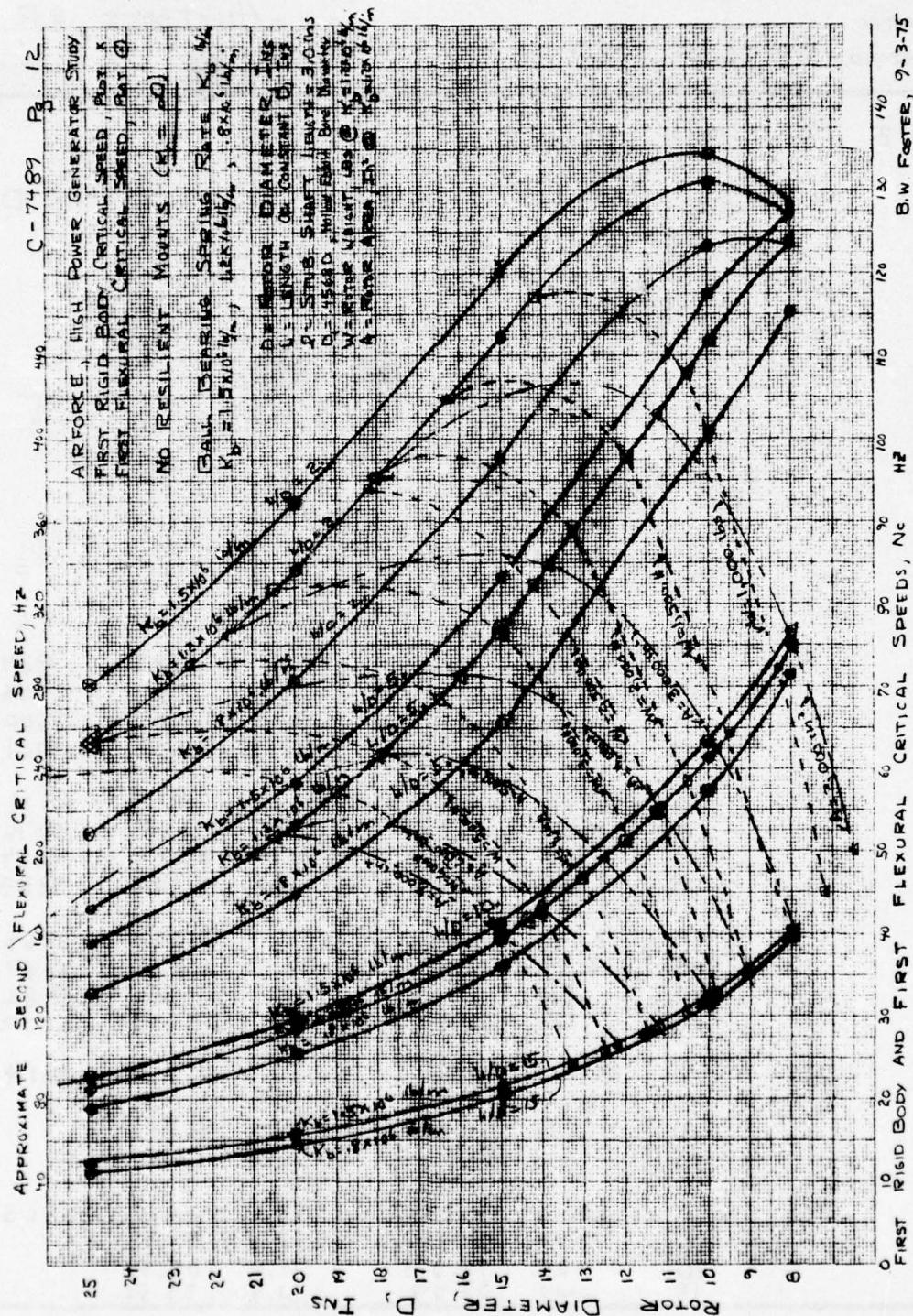
$$f_c = \frac{22.4}{\pi^2} \times \frac{1}{2\pi} \sqrt{\frac{k_c}{\frac{1}{2}(\frac{W}{g})}} = .5108 \sqrt{\frac{k_c}{(\frac{W}{g})}}$$

b. First free body of the stub shafts

$$f_s = \frac{1}{2\pi} \sqrt{\frac{k_s}{.23(\frac{W}{g})_s}} = \frac{1}{2\pi} \sqrt{\frac{k_s}{.23 \times 4.525 \times 10^{-5} D^2 (\frac{W}{g})^{2/3}}}$$

$$f_s = \frac{49.33}{D \cdot (\frac{W}{g})^{1/3}} \sqrt{k_s}$$

D	L/D	k_c #/in $\times 10^6$	$\frac{W}{g}$	f_c Hz	k_s #/in $\times 10^6$	f_s Hz
8	2	50.09	.463	5313.	.1685	8247.
	5	3.46	1.146	888.	.563	2706.
	10	.433	2.305	221.4	1.329	3300.
	15	.1282	3.456	98.4	2.028	3961.
10	2	67.61	.902	4422.	.411	2511.
	5	4.327	2.251	708.	1.369	3376.
	10	.541	4.497	177.2	3.181	4084.
	15	.1603	6.742	78.8	4.736	4353
15	2	101.41	3.038	2951.	2.078	3763.
	5	6.49	7.584	472.5	6.859	5037.
	10	.811	15.155	112.2	15.356	5982.
	15	.244	22.724	52.9	21.629	6202
20	2	135.22	7.191	2215.	6.560	5014.
	5	8.65	17.959	354.5	21.454	
	10	1.082	35.895	88.7	46.38	
	15	.321	53.827	39.45	62.21	
25	2	169.02	14.034	1773.	16.00	62651
	5	10.82	35.055	283.8	51.85	
	10	1.352	70.075	71.0	108.44	
	15	.406	105.09	31.8	139.56	



C-7489 Pg 13

AIRFORCE, HIGH POWER GENERATOR STUDY

FIRST RIGID BODY CRITICAL SPEED, PLOT A

FIRST FLEXURAL CRITICAL SPEED, PLOT Q

RESILIENT MOUNT SPRING RATE, $K_f = 44 \times 10^6 \text{ lb/in}$

BALL BEARING SPRING RATE, $K_b = 16 \text{ lb/in}$

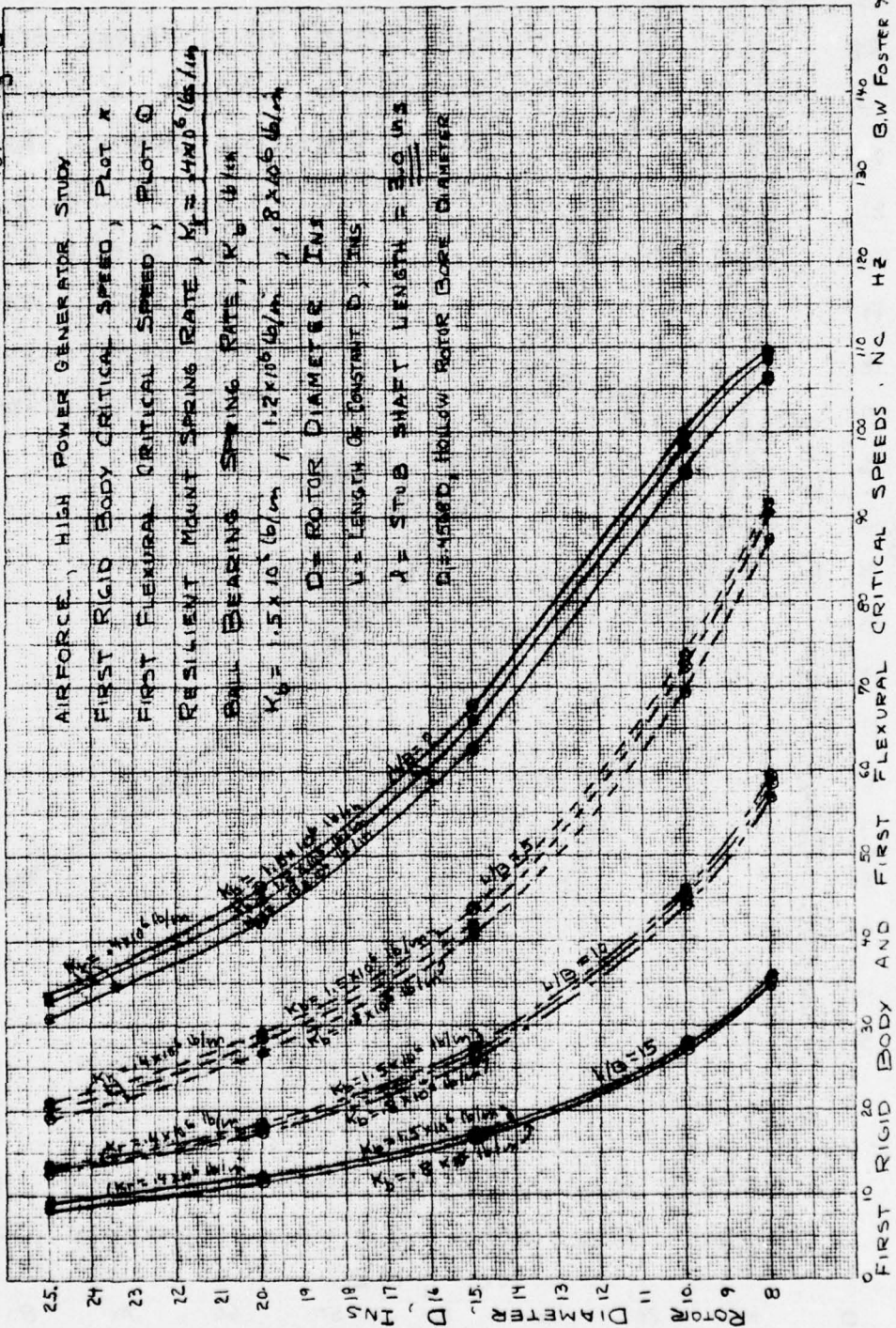
$K_b = 1.5 \times 10^6 \text{ lb/in}$, $1.2 \times 10^6 \text{ lb/in}$, $.8 \times 10^6 \text{ lb/in}$

D = ROTOR DIAMETER, IN

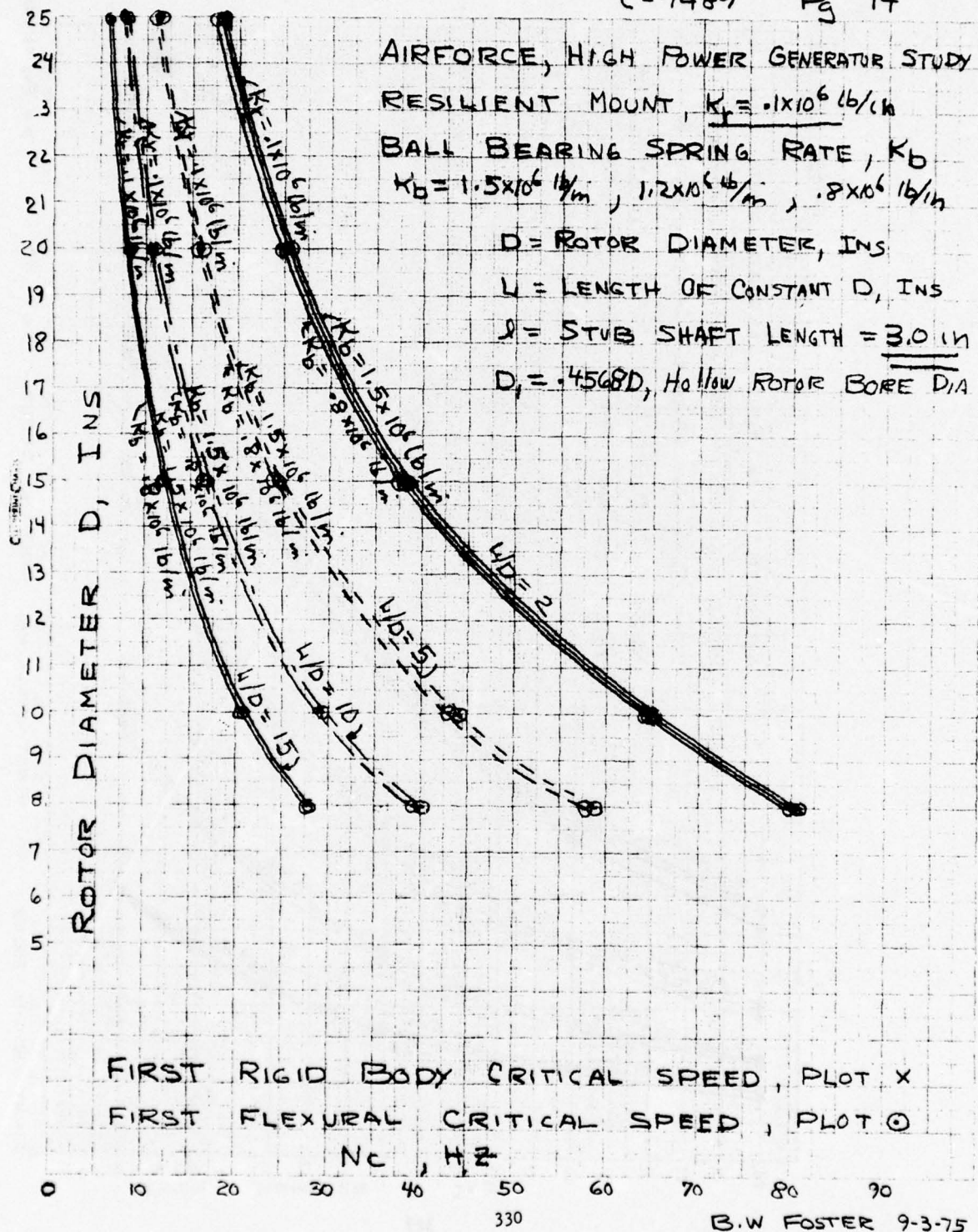
L = LENGTH OF CONSTANT D, IN

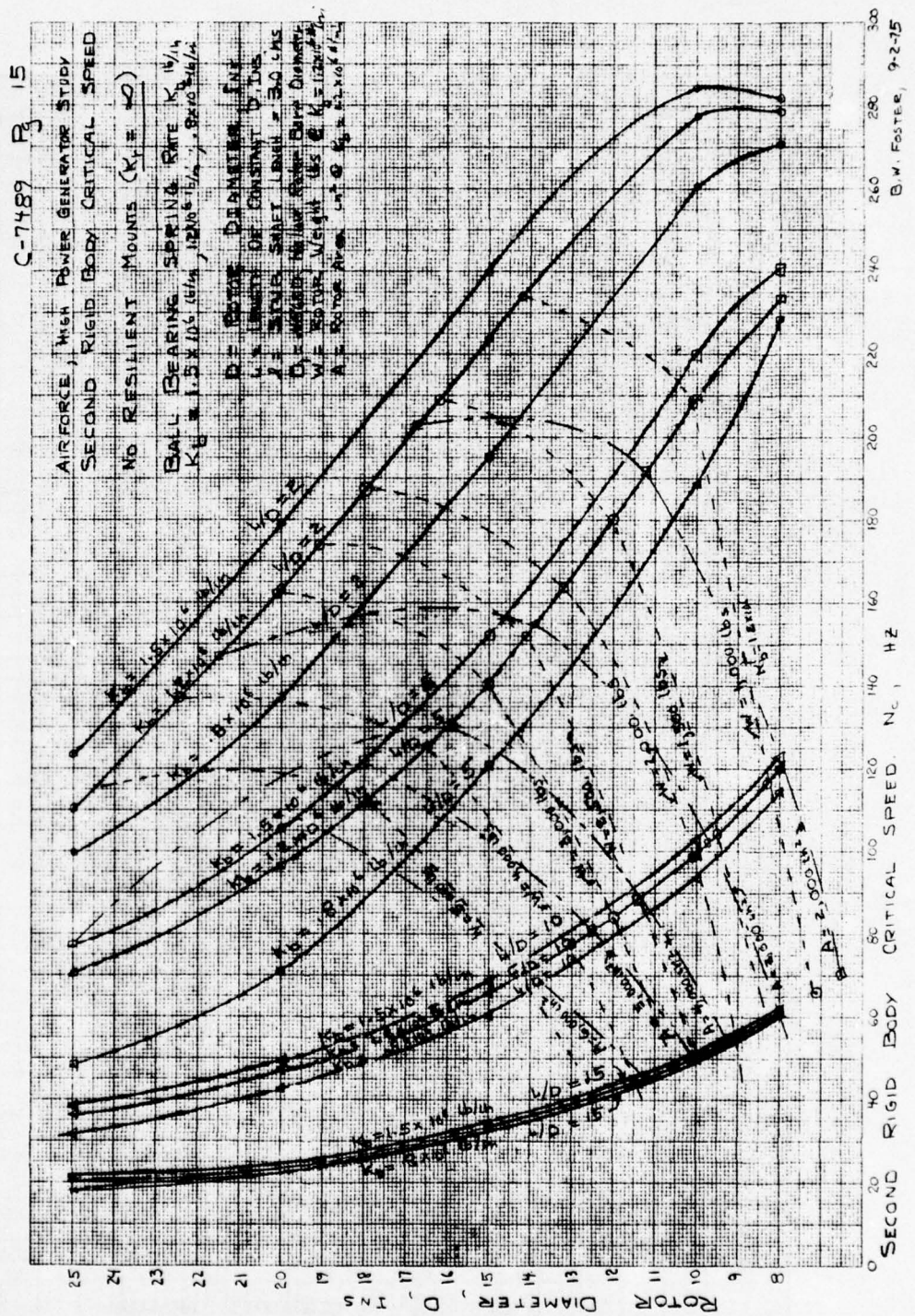
$\lambda = \text{STUB SHAFT LENGTH} = 3.0 \text{ IN}$

D = 45000, HOLLOW ROTOR BORE DIAMETER



B.W. FOSTER 9-3-75





C-7489 Pg 16

AIRFORCE, HIGH POWER GENERATOR STUDY

SECOND RIGID BODY CRITICAL SPEED

RESILIENT MOUNT SPRING RATE, $K_r = 400,000 \text{ lb/in}$

BALL BEARING SPRING RATE, $K_b, \text{ lb/in}$

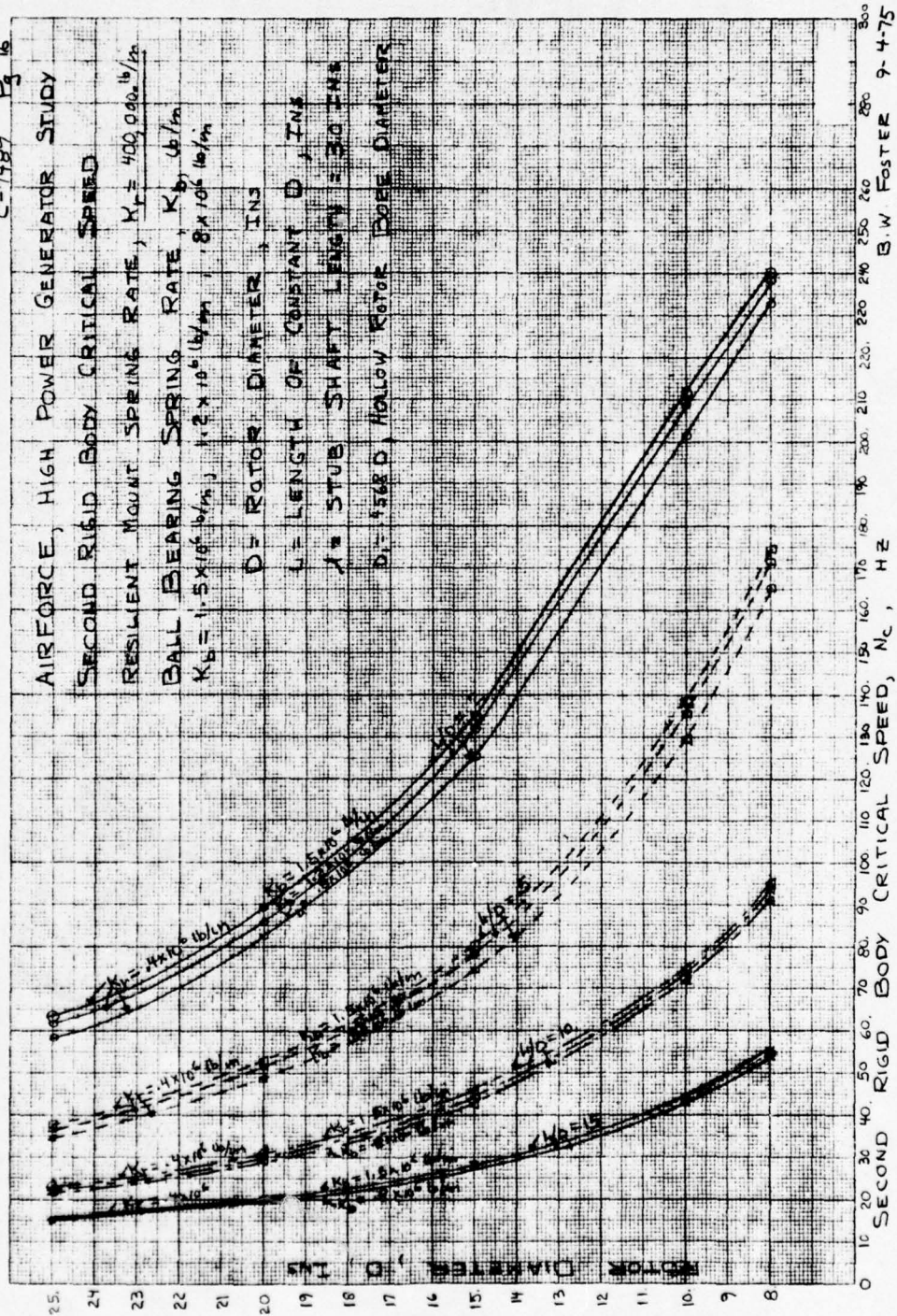
$K_b = 1.5 \times 10^6 \text{ lb/in}$, $1.2 \times 10^6 \text{ lb/in}$, $.8 \times 10^6 \text{ lb/in}$

$D = \text{ROTOR DIAMETER, IN}$

$L = \text{LENGTH OF CONSTANT D, IN}$

$L = \text{STUB SHAFT LENGTH} = 30 \text{ IN}$

$D = 156.8 \text{ D, HOLLOW ROTOR BORE DIAMETER}$



B.W. FOSTER 9-4-75

C-7489 P. 17

AIRFORCE HIGH POWER GENERATOR STUDY

SECOND RIGID BODY CRITICAL SPEED

RESILIENT MOUNT SPRING RATE, $K_v = 100,000 \text{ lb/in}$

BALL BEARING SPRING RATE, $K_b = 16 \text{ lb/in}$

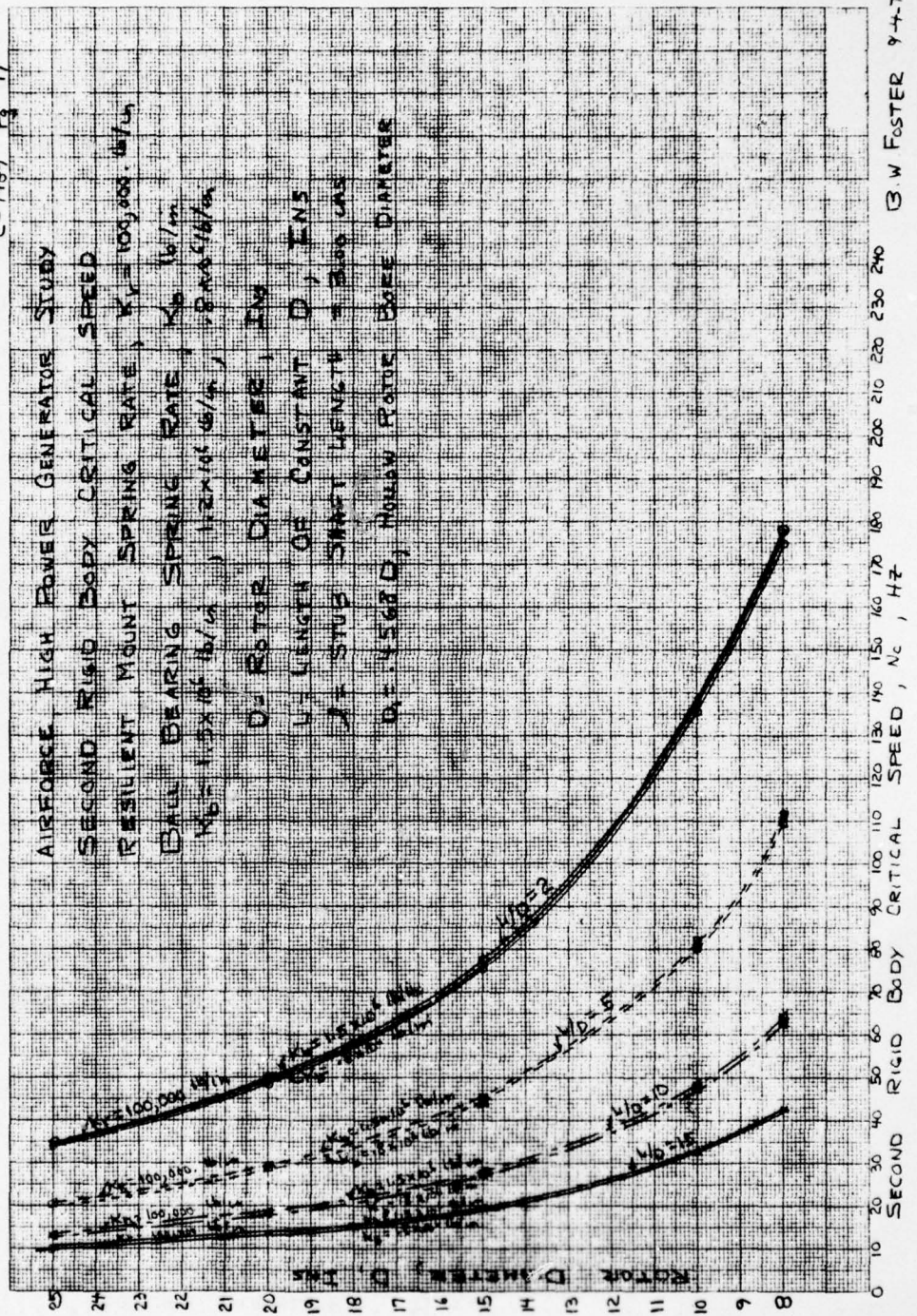
$M_b = 1.5 \times 10^6 \text{ lb/in}$, $1.2 \times 10^6 \text{ lb/in}$, $1.8 \times 10^6 \text{ lb/in}$

$D = \text{ROTOR DIAMETER, IN}$

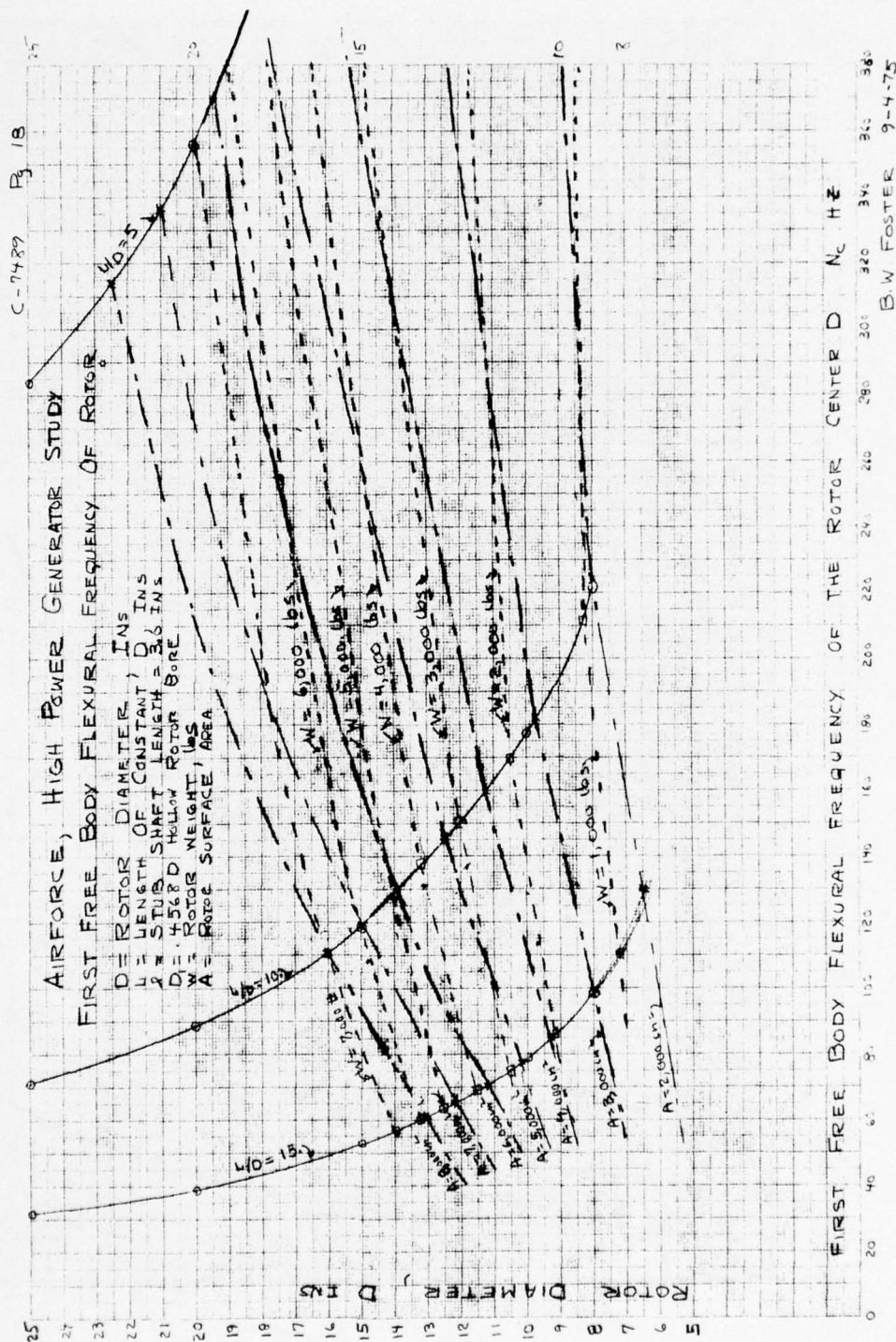
$L = \text{LENGTH OF CONSTANT } D, \text{ IN}$

$L = \text{STUB SHAFT LENGTH} = 3000 \text{ LBS}$

$D = 4.562 D$, HOLLOW ROTOR BORE DIAMETER



B W FASTER 9-4-75



DATE 8-28-75

PART NO. _____

PREPARED BY Berry W. FosterCALC. NO. 7489 SHEET NO. 19MODEL NO. AIRFORCE 14-P. Gel

CHECKED BY _____

G. Resilient Mount and Resilient Mount - Hard Mount Rigid Body Frequencies

$\frac{1}{k_s} + \frac{1}{k_c}$ $\times 10^{-6}$	D	W/D	$K_1 = K_2 = 250,000 \text{ #/in}$		$K_1 = 250,000 \text{ #/in}$ $K_2 = 500,000 \text{ #/in}$		$K_1 = 250,000 \text{ #/in}$ $K_2 = 1,000,000 \text{ #/in}$		$K_1 = 250,000 \text{ #/in}$ $K_2 = 2,500,000 \text{ #/in}$	
			$\frac{k_s + k_c}{k_s k_c}$ $\times 10^6$	f_1 Hz	f_2 Hz	f_1 Hz	f_2 Hz	f_1 Hz	f_2 Hz	f_1 Hz
5955	8	2	1.935	105.18	197.71	119.05	248.73	125.74	333.05	284.73
2165		5	1.936	74.16	118.73	83.00	150.02	86.42	203.77	87.35
3.064		10	*	60.57	93.36	67.56	118.38	73.07	161.54	70.74
6.893		15	*							
2448	10	2	1.552	75.04	140.30	84.28	115.41	89.57	235.10	91.00
.962		5	3.088	53.10	81.27	59.50	108.26	62.04	147.67	62.74
2.464		10	1.856	42.79	69.12	51.07	81.96	54.56	108.48	55.45
6.449		15	*							
.491	15	2	3.509	40.29	74.16	46.19	93.51	44.65	125.54	49.39
.300		5	3.700	28.42	47.36	32.47	60.42	33.92	81.81	34.52
.298		10	3.702	25.62	38.29	26.47	48.33	27.59	65.57	27.90
4.141		15	*							
.1598	20	2	3.8462	26.57	47.34	30.00	60.06	31.51	80.71	32.03
.1622		5	3.8378	18.79	31.49	18.79	31.49	17.97	43.15	28.19
.9459		10	3.0541	15.35	25.41	17.22	31.55			
3.1562		15	.8638							
.0614	25	2	3.9316	19.12	34.05	21.76	42.07	25.57	51.39	22.87
.1117		5	3.8883					13.10	30.63	13.04
.7488		10	3.2512							
2.4671		15	1.5328							

DATE 9-4-75

PART NO. _____

PREPARED BY Berry W. FosterCALC. NO. C-7489 SHEET NO. 20MODEL NO. AIRFORCE, H.P. Gen

CHECKED BY _____

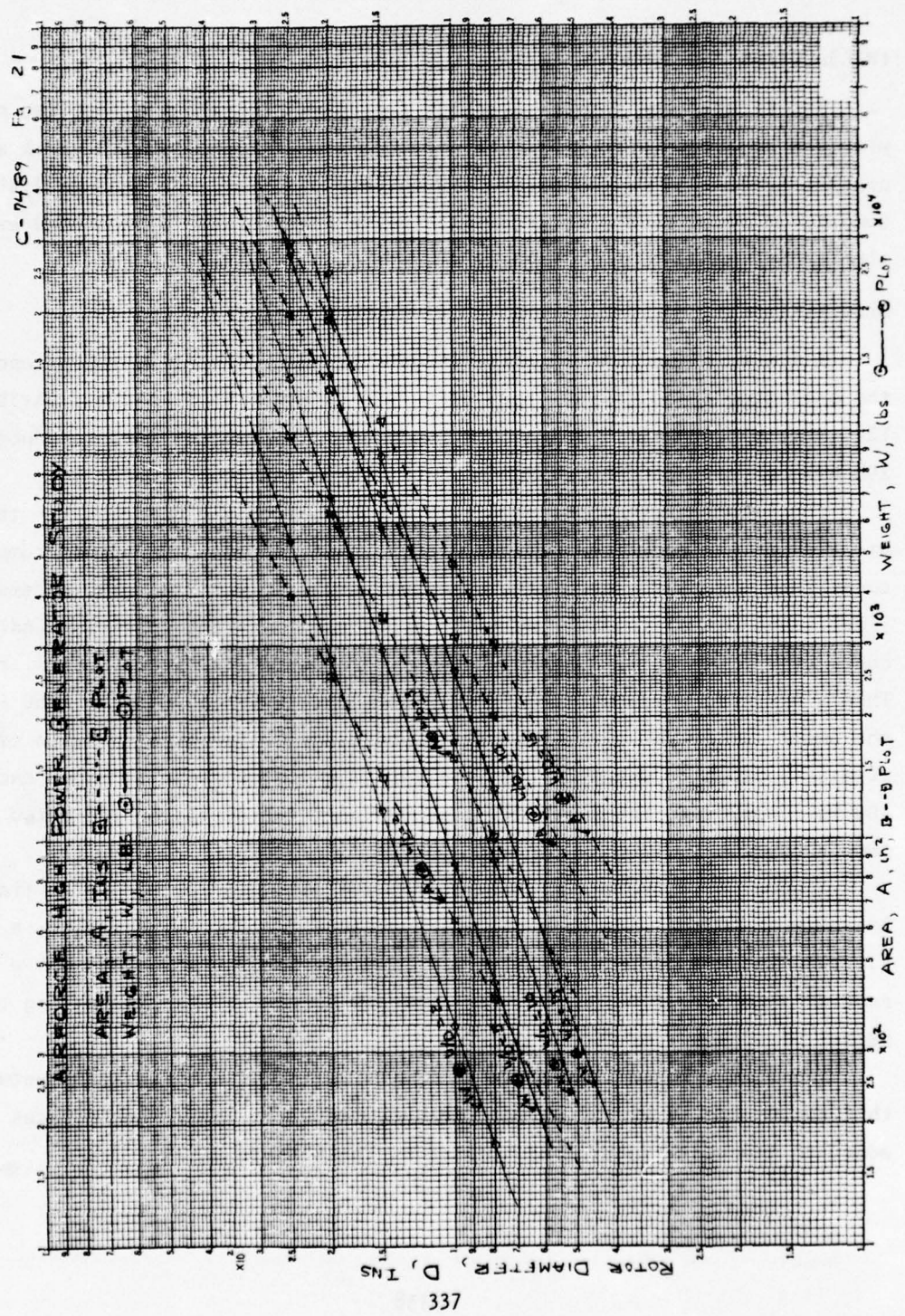
IV Weight and Surface Area of the Rotor**A Weight**

$$W = .1728 \left(\frac{L}{D}\right) D + .01747 \left(\frac{L}{D}\right)^3 D^2$$

B Surface Area

$$A = \pi D \cdot L = \pi D^2 \left(\frac{L}{D}\right)$$

D in	$\frac{L}{D}$	W lbs	A in ²
8	2	178.7	402.1
	5	442.4	1005.3
	10	889.9	2010.6
	15	1333.8	3016.
10.	2	348.3	628.3
	5	869.0	1571.0
	10	1736.0	3141.
	15	2602.	4712.
15	2	1172.5	1413.7
	5	2927.3	3534.
	10	5850.	7069.
	15	8771.	10,603.
20	2	2475.7	2513.
	5	6132.	6283.
	10	12,855.	12566.
	15	24,637.	18,850.
25	2	5,417.	3,927.
	5	13,531	9,817.
	10	27,048.	19,635.
	15	40,565.	29,452.



APPENDIX C

FIRST-STAGE TURBINE DISC STRESS ANALYSIS

INTRODUCTION AND SUMMARY

The first-stage turbine disc for the 25-MW high-power system was predesigned with the computer subroutine incorporated into TAPE program. A check and more precise evaluation was conducted via the use of detailed stress analysis Computer Program X-0815 to establish the validity of the predesigned evaluation technique.

DISC STRESSES

A finite element of the disc (Figure 1) was analyzed at 105 percent of the operating speed (13,125 rpm) using steady-state temperature distribution 1200 F at center and 1660 F at rim, and centrifugal blade loads produced by 208 blades integrated in the same disc forging (Astroloy, Cond. B).

The steady-state loads gave stresses below the yield stress for the material at the indicated temperature; however, once the transient temperature conditions were introduced, the stresses, especially at the rim, exceeded significantly the yield strength. The 663-sec transient condition indicates 200 F at the center with a progressive increase to 1200 F at 13.5 in. radius. Then a stronger gradient (390 F/in.) takes the temperature up to 1660 F at the outer rim (14.67 in.). The resulting tangential nominal elastic effective stresses, close to the disc rim, are very high compressive stresses exceeding 100 ksi, well into the plastic regime of the material at the indicated temperature.

Several disc profile modifications were attempted with no significant improvement. To avoid the high negative tangential (hoop) stresses, a slotted disc was considered (Figure 1a). This configuration assumes a slot root at a radius of 12.50 in. with 3 blades between slots, decreasing the number of blades from 208 to 207.

The live rim now is reduced to 12.50 in. radius with the zone between this radius and 14.67 in. as dead weight, producing centrifugal forces to be added to the centrifugal load created by the blades.

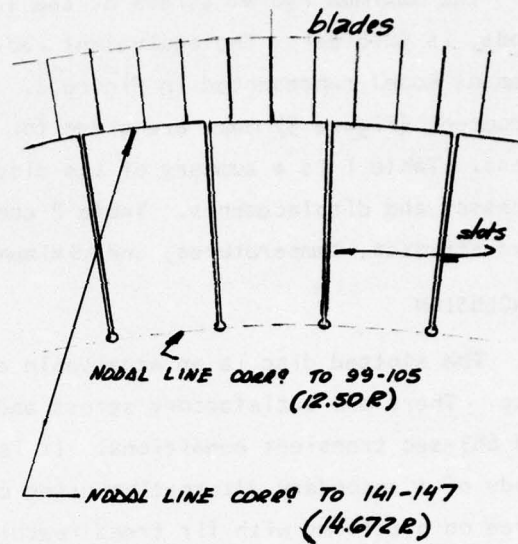
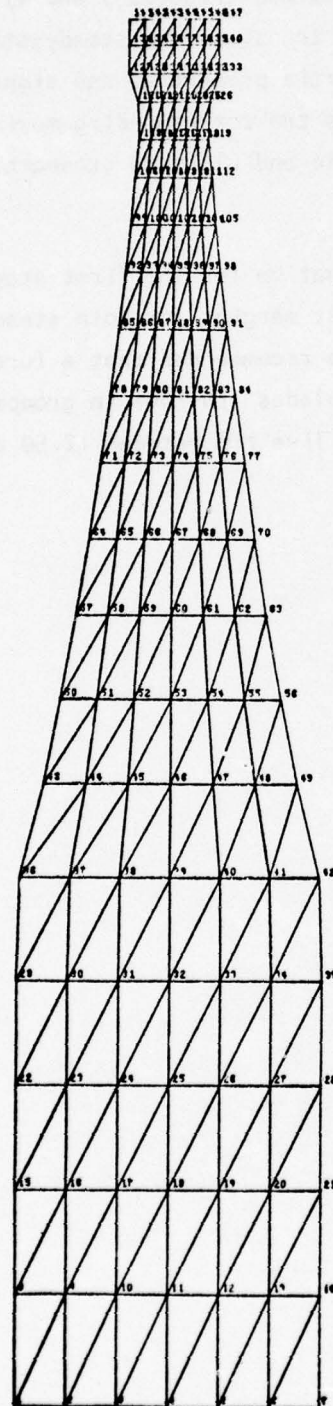


FIG. 1a - "Slotted" alternative

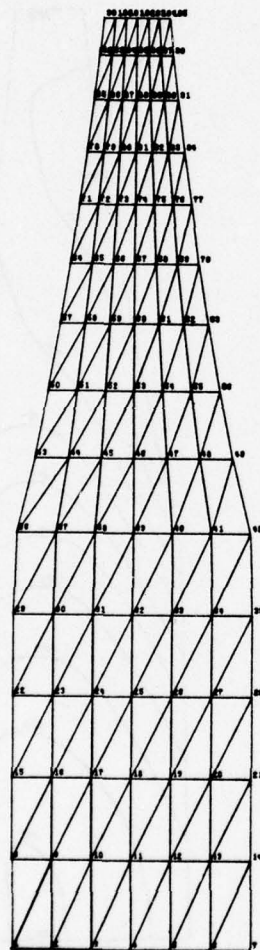
FIG. 1 - "FULL" DISK FINITE ELEMENT MODEL (1ST STAGE TURBINE DISK)

The maximum radial stress at the live rim, originated by those centrifugal loads, is 52.6 ksi. The equivalent radial loads were applied to the finite element model represented in Figure 2. The stress (Figures 3 and 4) and displacement (Figure 5) maps are given for both transient and steady-state conditions. Table 1 is a summary of the disc inertia properties and significant stresses and displacements. Table 2 compares the corresponding maximum effective stresses, temperatures, and minimum yield and ultimate strength.

CONCLUSION

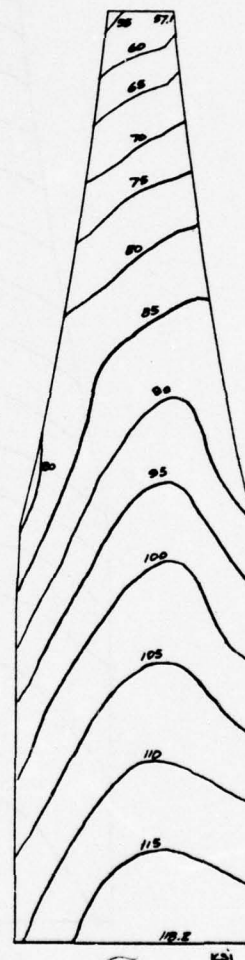
The slotted disc is an acceptable alternative for the first-stage turbine disc. There are satisfactory stress and burst margins for both steady-state and 663-sec transient conditions. It is also recommended that a further study of a secondary alternative using cast blades (IN-100) in groups of three on platforms with fir trees reaching a live rim between 12.50 and 13.00 in. radius be conducted.

HIGH POWER SYST-25 MW DP6- 1ST TURBINE DISK 663 SECS TRANSIENT



SLOTTED DISK
FIRST STAGE
FINITE ELEMENT MODEL

~ FIG. 2 ~

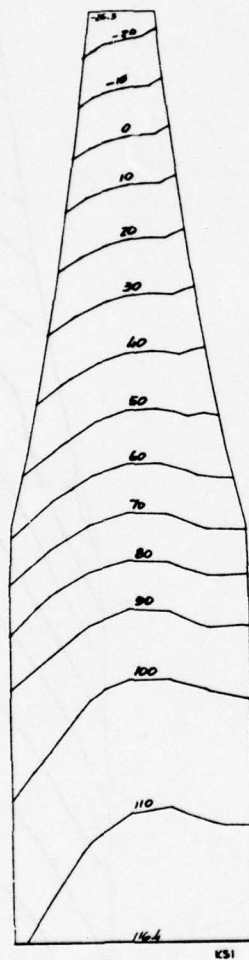


σ_r
(RADIAL CONSTANT STRESS)
663 SECS. TRANSIENT

~ FIG. 3a ~

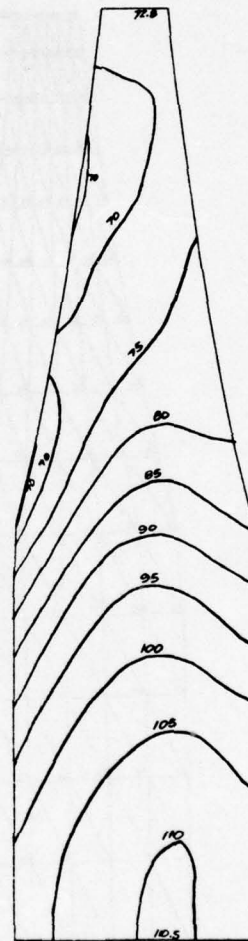
ST-12/75

663 SECS. TRANSIENT



(TANGENTIAL EFFECTIVE STRESS)
663 SECS. TRANSIENT

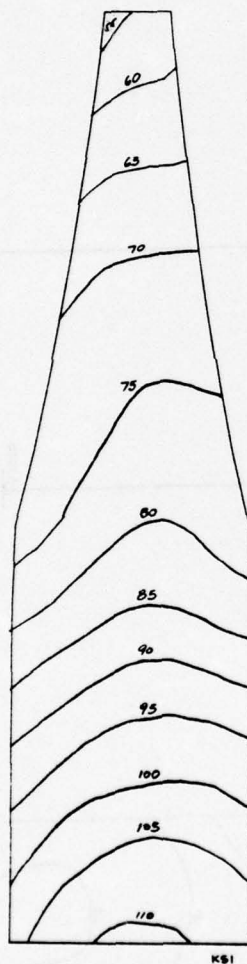
FIG. 3b ~



(EFFECTIVE CONSTANT STRESS)
663 SECS. TRANSIENT

~ 3c ~

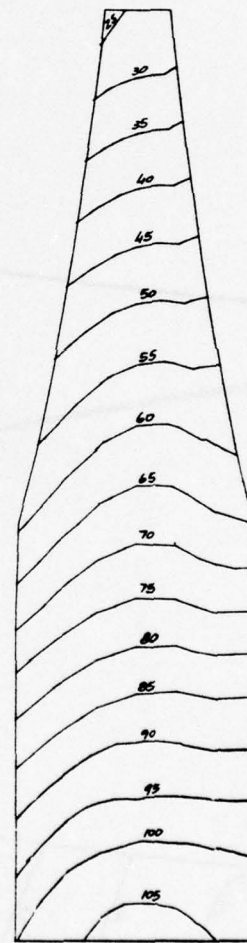
HIGH POWER SYST-25 MW DP6- 1ST
DISK
STEADY STATE



CS1

(RADIAL CONSTANT STRESS)
STEADY STATE

- FIG. 4 a -

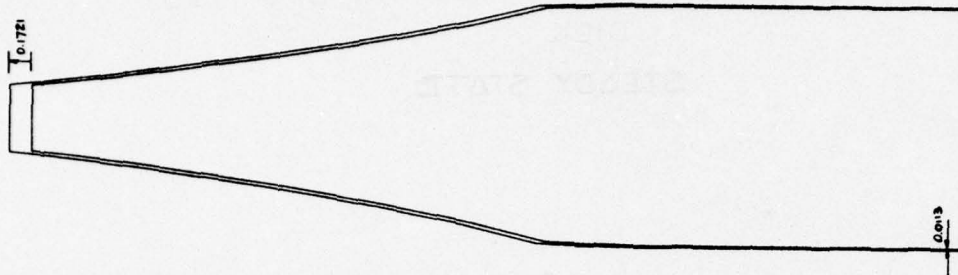


CS1

(TANGENTIAL EFFECTIVE STRESS)
STEADY STATE

- FIG. 4 b -

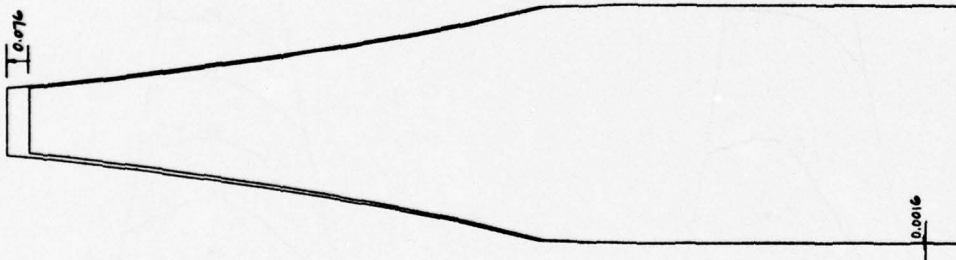
STEADY STATE



DISPLACEMENTS ~ IN.
STEADY STATE

~ FIG. 5b ~

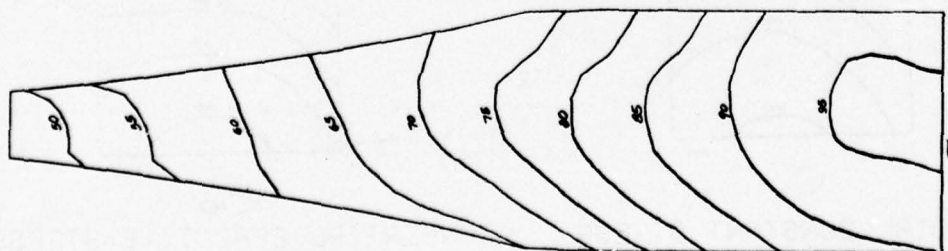
663 SECS TRANSIENT



DISPLACEMENTS ~ IN.
663 SECS. TRANSIENT

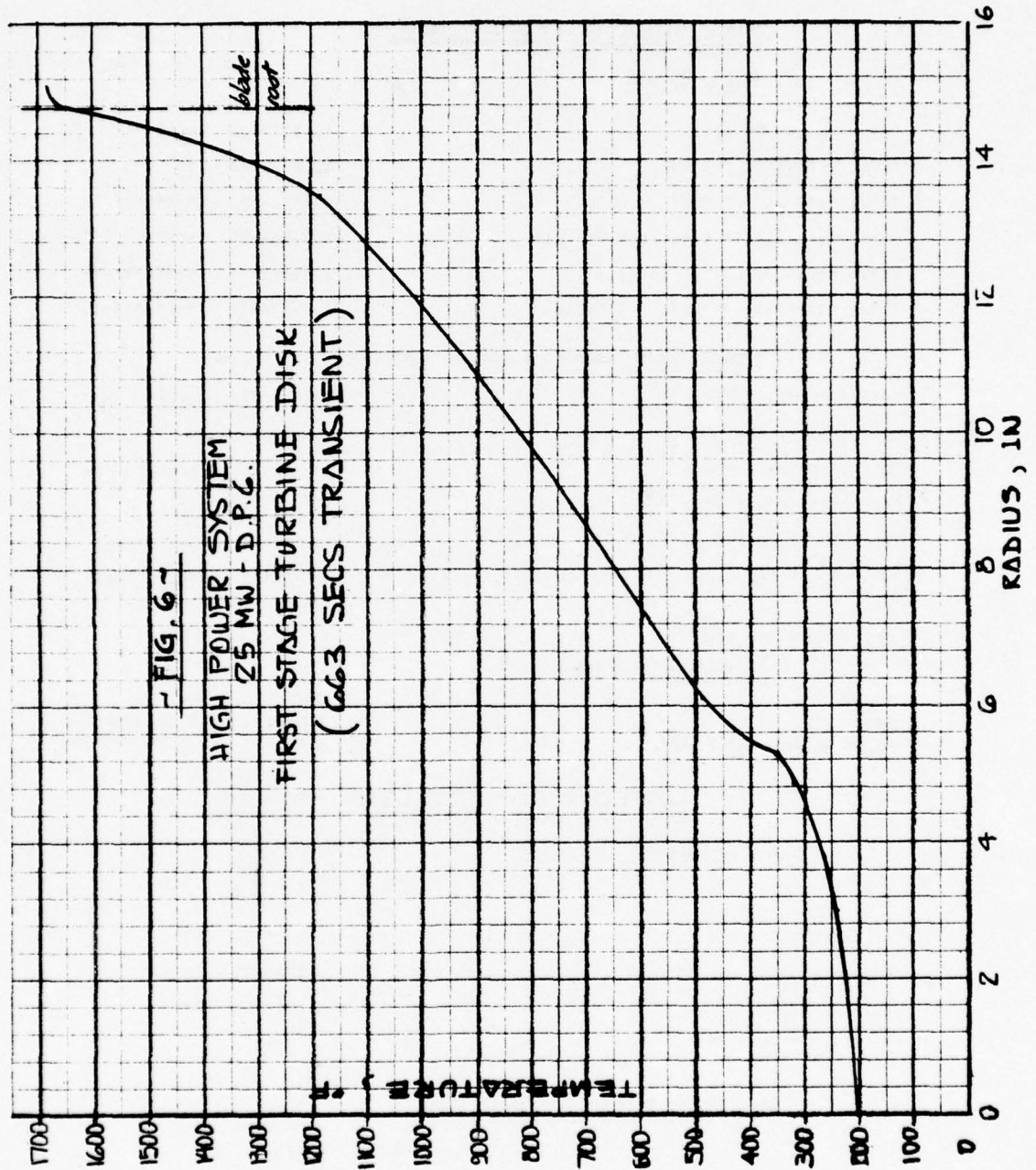
~ FIG. 5a ~

STEADY STATE



EFFECTIVE CONSTANT STRESS
STEADY STATE

~ FIG. 4c ~



COPY AVAILABLE TO DDC DOES NOT
PERMIT FULLY LEGIBLE PRODUCTION

TABLE 1
HIGH POWER SYSTEM - 25 MW - D.P.C.
1st. STAGE TURBINE DISK

DISK INERTIA PROPERTIES :

a) FULL DISK (1)

TOTAL VOLUME OF DISK	1.13777+03	IN**3
TOTAL WEIGHT OF THE BODY	3.25402+02	LB
TOTAL MASS OF THE BODY	8.02138+01	LB=SEC**2/IN
AXIAL DISTANCE TO C.G. FROM REF.LINE	-2.23414+03	INCHES
TOTAL POLAR MOMENT OF INERTIA	6.50842+01	LB=SEC**2*IN
TOTAL DIAMETRAL MOMENT OF INERTIA	3.29084+01	LB=SEC**2*IN

b) SLOTTED DISK : below slot root (1)

TOTAL VOLUME OF DISK	9.82973+02	IN**3
TOTAL WEIGHT OF THE BODY	2.81130+02	LB
TOTAL MASS OF THE BODY	7.27563+01	LB=SEC**2/IN
AXIAL DISTANCE TO C.G. FROM REF.LINE	-2.56931+03	INCHES
TOTAL POLAR MOMENT OF INERTIA	4.36974+01	LB=SEC**2*IN
TOTAL DIAMETRAL MOMENT OF INERTIA	2.22083+01	LB=SEC**2*IN

(1) : Blades not included

c) BLADES (208)

WEIGHT	8.6143	LB
MASS	2.2317+02	LB=SEC**2-IN
POLAR MOMENT OF INERTIA	5.12371	LB=SEC**2-IN

SLOTTED DISK STRESSES - DISPL.

1- STEADY STATE

	ELEM. OR NODE	VALUE	UNIT
MAX. EFFECTIVE STRESS	11- 12- 19	0.85099+04	PSI
MAX. RADIAL DISP.	109	1.72088+01	INCHES
MAX. AXIAL DISP.	36	-1.07917+02	INCHES
AVG. TANG. STRESS OF DISK		5.76501+04	PSI

2- 663 SECS. TRANSIENT

	ELEM. OR NODE	VALUE	UNIT
MAX. EFFECTIVE STRESS	11- 12- 19	1.11665+05	PSI
MAX. RADIAL DISP.	109	7.60838+02	INCHES
MAX. AXIAL DISP.	99	-8.07130+03	INCHES
AVG. TANG. STRESS OF DISK	346	4.72070+04	PSI

TABLE 2

First Stage Turbine Disk
Astroloy 'B' - 13125 rpm

Condition	Position	Radius in.	Temp. °F	Min. prop.		Max. effect. stress ksi
				Yield ksi	Ult. ksi	
Steady State	Center	0	1200	126	163	96.3
	Middle	6.25	1396	118	145	72.1
	Live Rim	12.50	1592	80	83	48.7
	Blade Root	14.67	1660	58	61	20.1
	Avg. tang. stress.....					57.65
663 secs. Transient	Center	0	200	139	183	110.5
	Middle	6.25	500	135	179	85.4
	Live Rim	12.50	1069	128	169	72.9
	Blade Root	14.67	1660	58	61	20.1
	Avg. tang. stress.....					47.25

APPENDIX D

SECOND-STAGE TURBINE VIBRATION AND STRESS EVALUATION

INTRODUCTION AND SUMMARY

A predesign via appropriate routines of TAPE was conducted for the second-stage turbine of a 25-MW high-power system study. The resulting design was further investigated in terms of potential blade vibration and confirmation of resulting blade and disc stress.

BLADE VIBRATIONS

The second-stage turbine blade is a hollow blade with approximately 3.25 in. span and 1.22 in. chord. The outside cross section is constant, while the inside is linearly tapered with an area taper ratio of 1.5 and machined from the same forging as the disc (Astroloy Condition B).

Since many area taper ratios are possible, including a solid blade, the examination reviewed the application of both extremes: the current minimum taper ratio of 1.5 with a root cross section area of 0.2643 sq in., and a full solid blade. It is assumed that if no natural frequencies exist within the turbine operating range speed for these extreme conditions, other taper ratios could be considered if the blade stress distribution requires it.

The first five vibration modes were investigated at 0 rpm, 13,125 rpm (105 percent of maximum operating), and 8125 rpm (65 percent of maximum operating) for both hollow and solid blades (Table 1).

The stresses also were computed. They were found in agreement with the values calculated by the TAPE program subroutines (Table 2). For 170 blades, the total weight is 36.49 lb for the hollow blades and 47.26 lb for the solid blades.

Figure 1 is the vibration interference diagram; the first five natural frequencies have been plotted versus the turbine operating speed. The 1-per-rev excitation is well below the maximum operating speed. The 83 vanes possible excitation line intersects the first five modes below 6000 rpm.

Though shaft vibration--both flexural and torsional--should be investigated, once the overall design is defined, the results of blade vibrations due to the disc operating speed do not indicate critical conditions.

Figures 2 and 3a through 3c depict the mode shapes for the first three natural frequencies of the solid and hollow blade. The stiffness/mass ratio is better for the hollow blade as the blade vibrates as a beamlike structure. When the structural sides (platelike) are drawn in frequencies closer to their own, the overall stiffness/mass characteristics are not any longer significant (Figure 3c).

The general conclusion is to agree with the preselection of the hollow blade with the area taper ratio of 1.5 because:

- (a) The maximum stresses (51 ksi) are acceptable at the maximum operating speed temperature (1300 F).
- (b) Its natural frequencies indicate noncritical conditions within the operating range. This must be rechecked for shaft vibrations.
- (c) It is lighter (23 percent) and less stressed (28 percent) than the solid blade configuration.

DISC STRESSES

The finite element model of Figure 4 was analyzed at 105 percent of maximum operating speed, 13,125 rpm, and a temperature map provided by Figure 7.

The disc profile is very close to the one preselected via TAPE subroutine. The main difference is the center area thickness, increased up to 4.1 in., basically due to the results obtained from the transient operation.

Figures 5a through 5c show the radial, tangential, and effective stresses (Hencky - Von Mises) corresponding to the 660-sec transient. Notice the effective stresses (116 ksi) at the blade interface. Those stresses can be tolerated because the minimum yield strength at 1260 F is 125 ksi (Astroloy Cond. B) and the origin of the stresses is the negative tangential stresses due to the thermal transient, not usually associated with crack propagation.

Figures 6a through 6d show the stress and displacement maps corresponding to the steady-state operation. Using a burst factor of 0.75, the burst margin is better than 60 percent for steady-state operation. The disc weight, excluding the blades, is 311.4 lb (Table 3).

AFAPL-TR-76-39
 DATE DEC. 10, 1975
 PART NO. _____
 PREPARED BY S. TEPPER

CALC. NO. _____ SHEET NO. 1
 MODEL NO. _____
 CHECKED BY _____

HIGH POWER STUDY
 25 MW SYSTEM (DES. PT. 6)
 ~ TURBINE ~
2ND STAGE

MODE	(1)	(2)	(3)
	AT RPM	HOLLOW BLADE CPS	SOLID BLADE CPS
FIRST	0	2356.7	1812.6
	8125	2372.4	1837.0
	13125	2395.2	1875.4
SECOND	0	2521.3	2268.6
	8125	2538.5	2289.2
	13125	2565.0	2321.3
THIRD	0	3653.2	4116.5
	8125	3658.6	4117.1
	13125	3665.5	4118.0
FOURTH	0	4975.4	6728.9
	8125	4978.1	6754.4
	13125	4981.5	6794.6
FIFTH	0	5411.7	7854.7
	8125	5421.6	7877.1
	13125	5436.1	7912.7

- NOTES : (1) Differential stiffening effect included
 Max. operating speed : 12500 RPM 105% OP. SPEED : 13125 rpm
 (2) Taper (area) ratio : 1.5 (Tip cross sect. area $\leq 0.1762 \text{ in}^2$)
 Estimated weight per blade $\leq 0.2147 \text{ lbs}$ (0.204 lbs)
 (3) Const. cross section, same outline as hollow blade.
 Estimated weight per blade $\leq 0.278 \text{ lbs}$
 Both blades 3.249 in. height, 1.22 in. chord.

— TABLE 1 —

AFAPL-TR-76-39
DATE DEC. 10, 1975
PART NO. _____
PREPARED BY S. TEPPER

CALC. NO. _____ SHEET NO. 2
MODEL NO. _____
CHECKED BY _____

HOLLOW BLADE

INPUT DATA

BLADE TIP RADIUS	15.8337	IN.
ROOT RADIUS	12.5850	IN.
HEIGHT	3.2487	IN.
ROOT CROSS-SECT. AREA ...	0.2643	IN ²
AREA TAPER RATIO	1.5000	--
TIP CROSS-SECTN. AREA ...	0.1762	IN ²
TIP VELOCITY	1727.19	FT/SEC
ANGULAR VELOCITY	1309.00	RAD/S.
	12500.00	RPM
WEIGHT DENSITY	0.3000	LB/IN ³

OUTPUT (DERIVED) DATA - ONE BLADE -

MASS DENSITY	0.000777	LBS ² /IN ⁴
BLADE INERTIA (*)	0.136886	LBS ² -IN
BLADE WEIGHT	0.2147	LBS
CENTRIFUGAL FORCE	13437.84	LBS
ROOT RADIAL STRESS	50838.35	PSI
(*) ABOUT ROTATIONAL AXIS		

OUTPUT DATA FOR...170...BLADES

TOTAL BLADE WEIGHT	36.4953	LBS
TOTAL BLADE INERTIA	23.27054	LBS ² -IN
TOTAL CENTR. FORCE	2284432.	LBS

FOR RIM WIDTH 1.2700 IN...	
RIM RADIAL STRESS	22747.96 PSI

FOR RIM DEPTH 0.3000 IN...	
LIVE RIM RADIAL STRESS	28332.07 PSI

SOLID BLADE

Centrifugal force	18756.2	LBS
Root radial stresses	71005.0	PSI
Rim radial stress	31771.6	PSI
Live rim radial stresses	39570.9	PSI

Total blade (170) weight	47.26	LBS
--------------------------------	-------	-----

~ TABLE 2 ~
TURBINE ~ 2 ND STAGE BLADE

DATE DEC. 10, 1975CALC. NO. _____ SHEET NO. 3

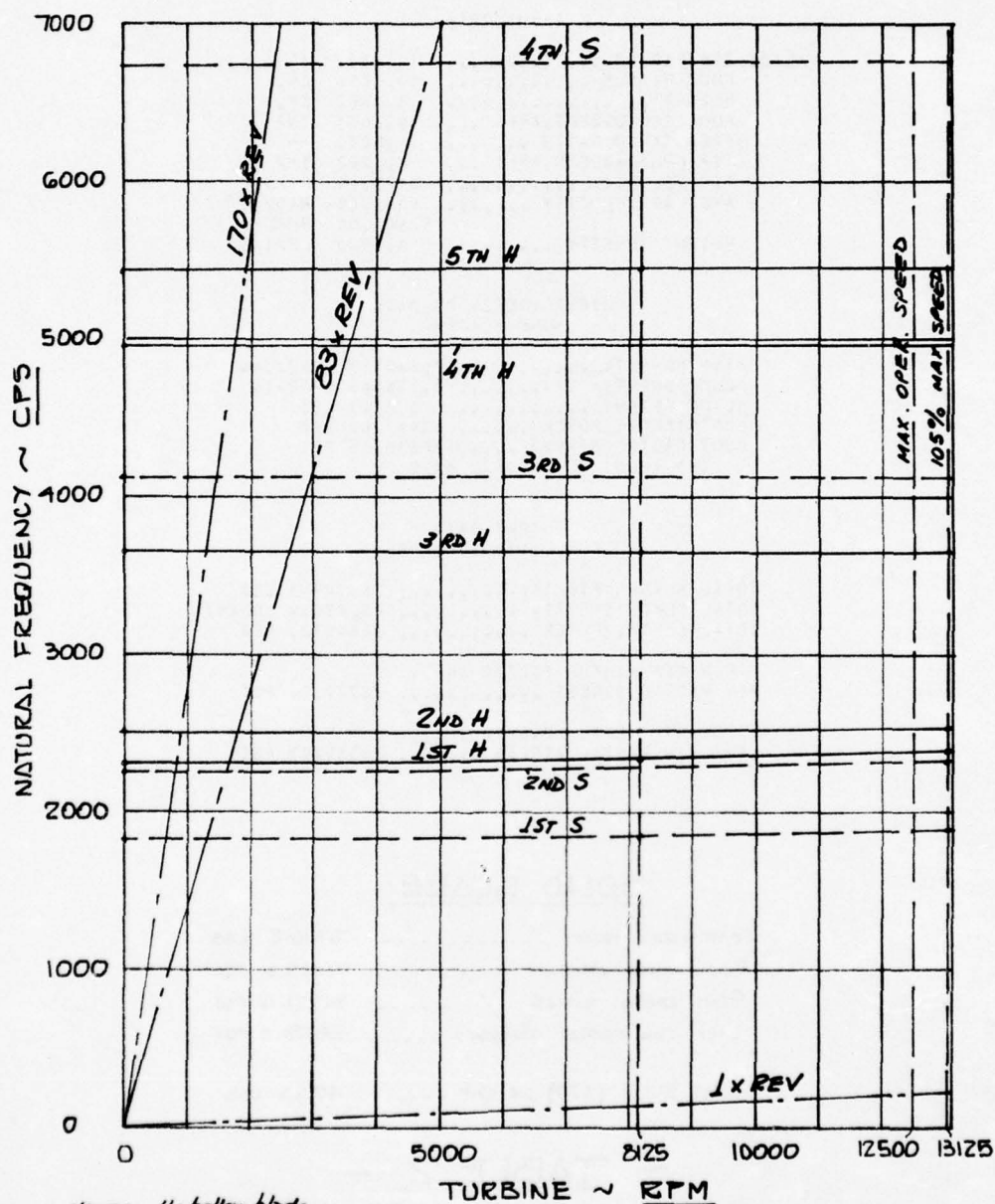
PART NO. _____

MODEL NO. _____

PREPARED BY S. TEPPEZ

CHECKED BY _____

HIGH POWER STUDY - 25 MW SYSTEM (DES. PT. 6)
 FIG. 1 - TURBINE ~ 2ND STAGE BLADE
 (NATURAL FREQUENCIES)



NOTES: H: hollow blade
 S: solid blade

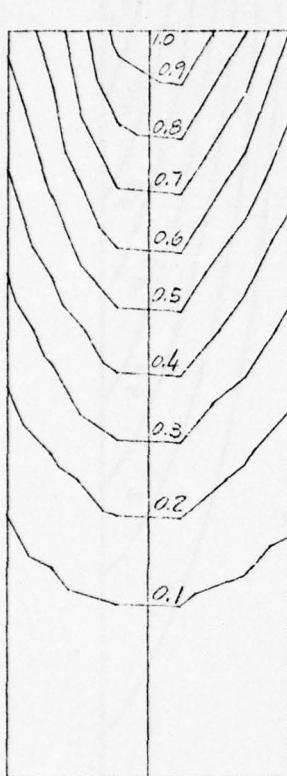
AFAPL-TR-76-39
DATE DEC 11, 1975

PART NO. _____
PREPARED BY S. TEPPER

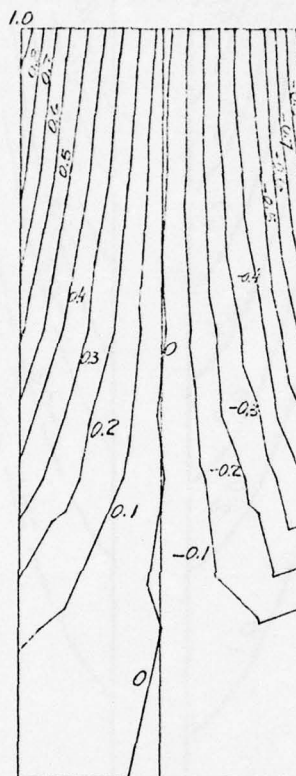
CALC. NO. _____ SHEET NO. _____

MODEL NO. _____

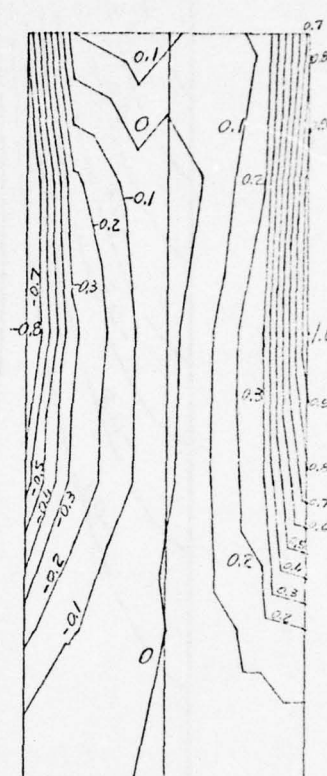
CHECKED BY _____



1st MODE



2nd MODE



3rd MODE

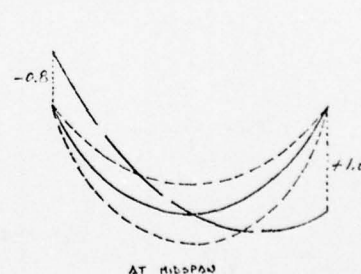
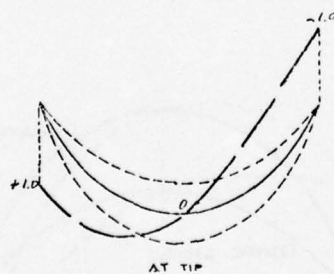
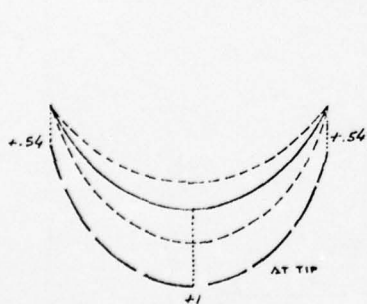


FIG. 2- SOLID BLADE ~ NATURAL FREQUENCIES
MODE SHAPES

S.T. 12-75

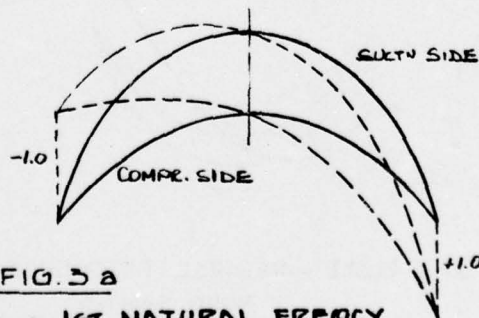
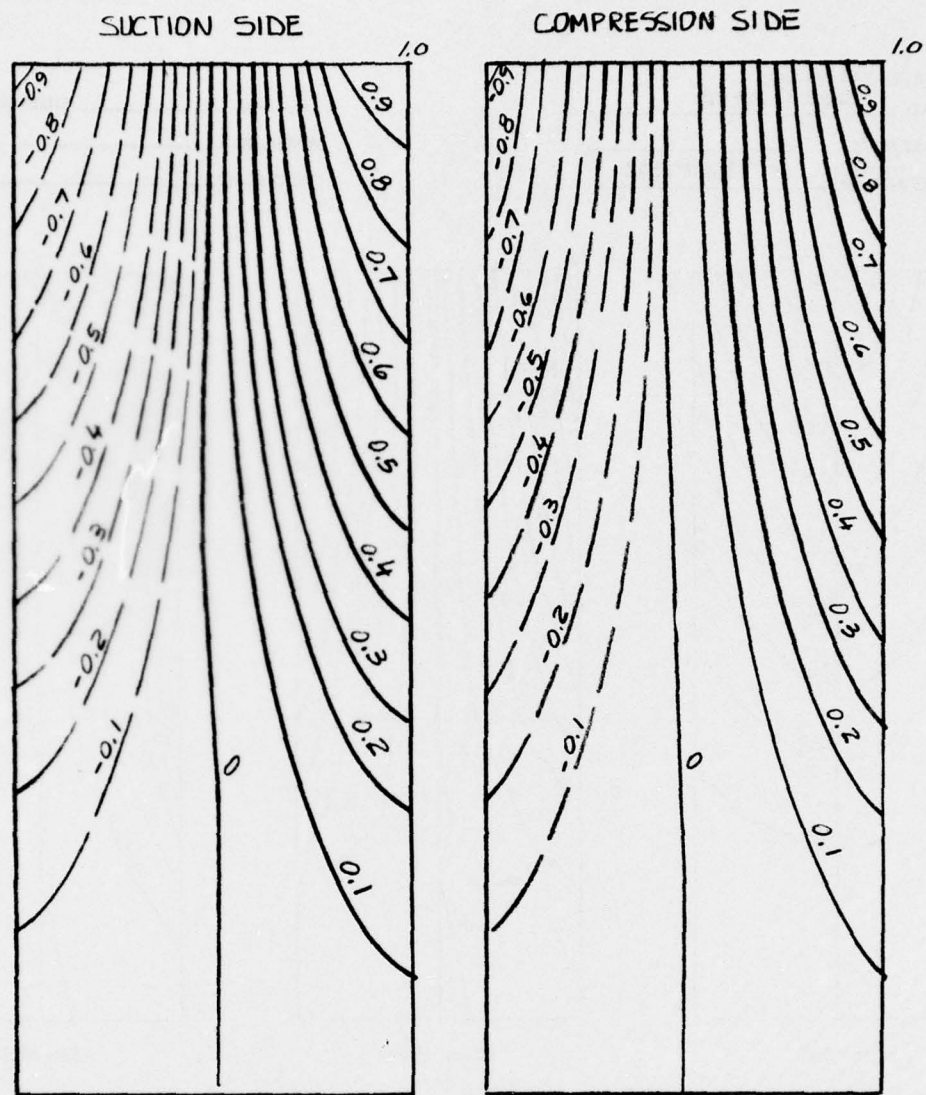


FIG. 5.2
HOLLOW BLADE - 1ST NATURAL FREQUENCY.
MODE SHAPE

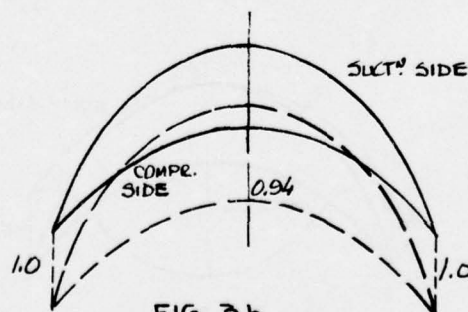
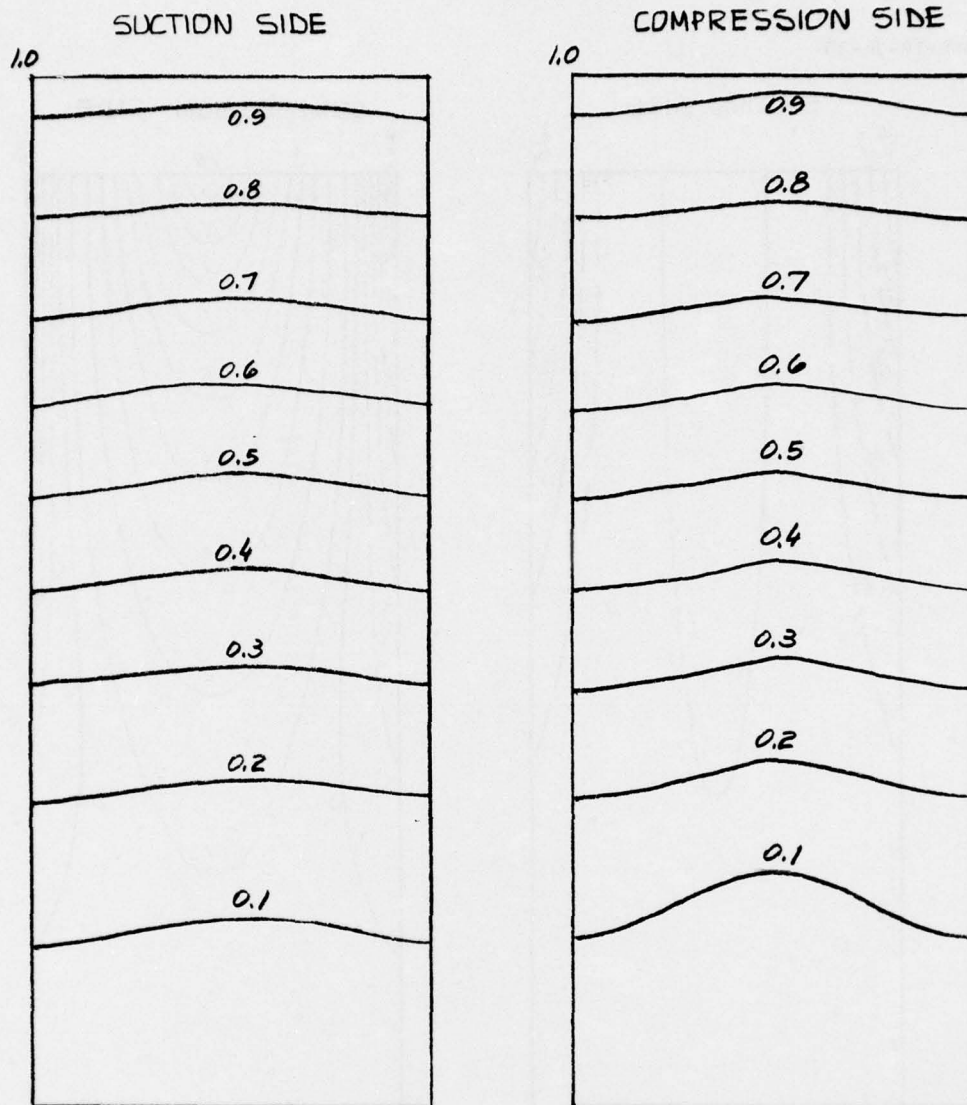


FIG. 3b
HOLLOW BLADE - 2ND NATURAL FREQ.
MODE SHAPE

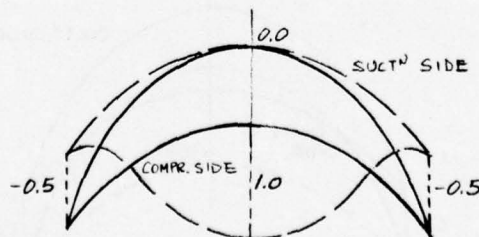
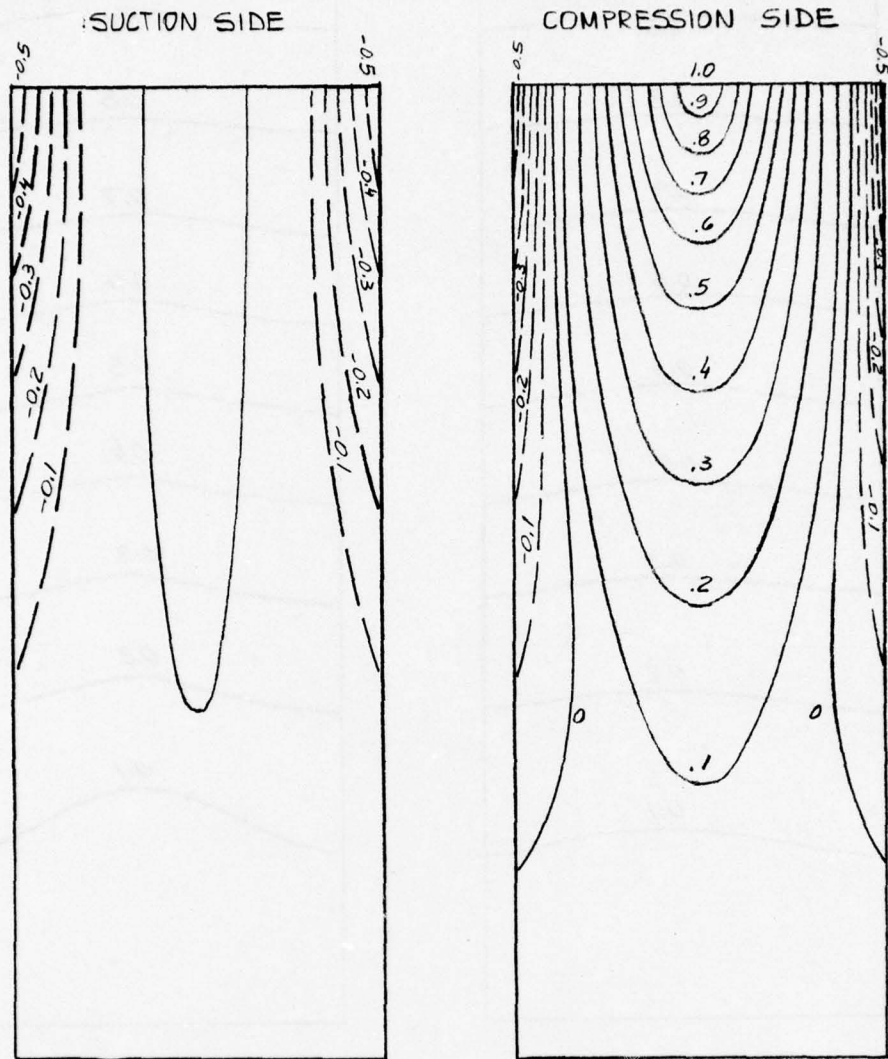
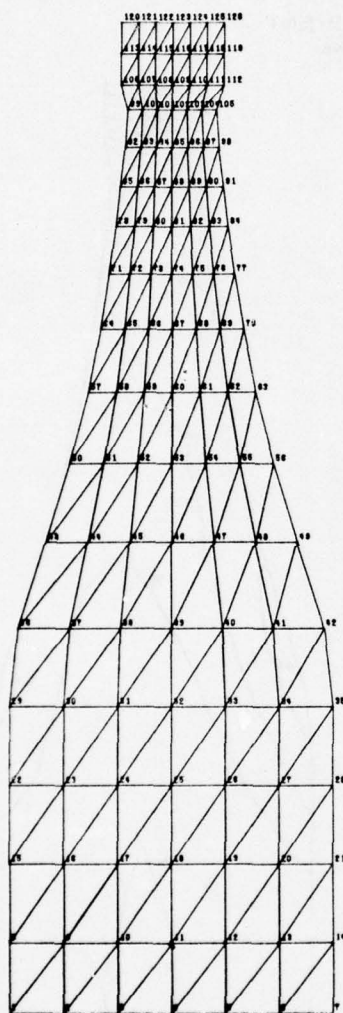


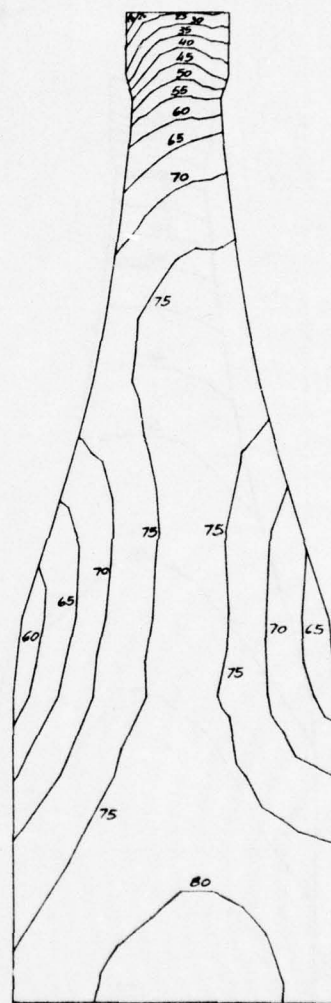
FIG. 3C
HOLLOW BLADE - 3 RD NATURAL FREQ
MODE SHAPE

HIGH POWER SYSTEM 25 MW DP6 S-TEPPER 2ND STAGE TURBINE DISK



FINITE ELEMENT MODEL

FIG. 4



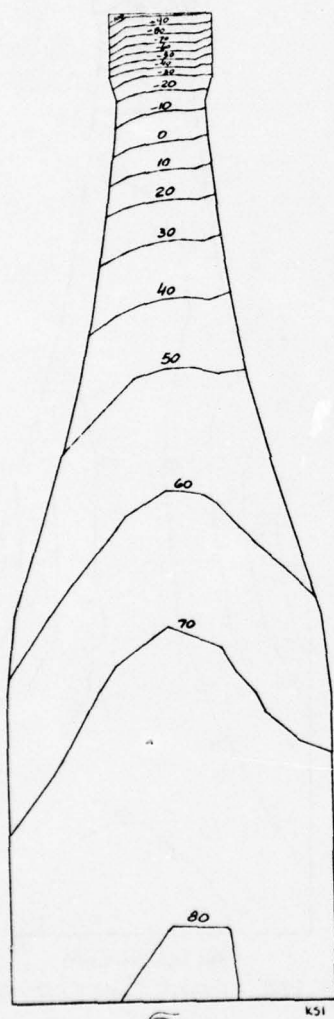
(880 SECS TRANSIENT)

KSI

RADIAL CONSTANT STRESS σ_r

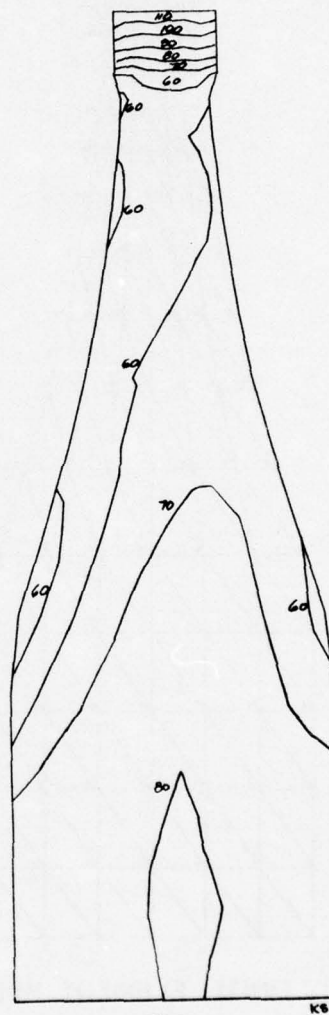
FIG. 5a

660 SECS TRANSIENT
2ND STAGE TURBINE
DISK



TANGENTIAL EFFECTIVE STRESS

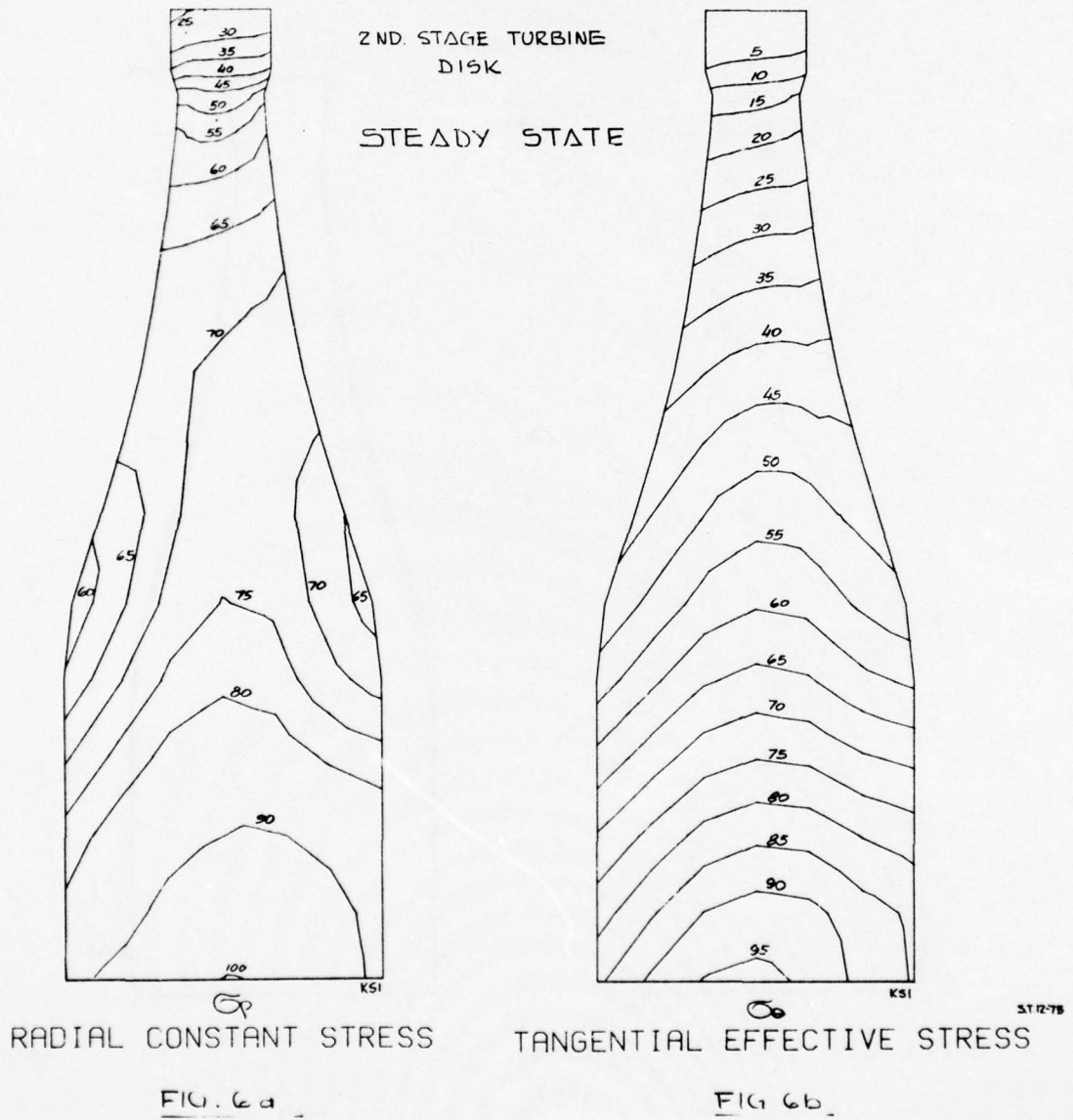
FIG. 5b



EFFECTIVE CONSTANT STRESS

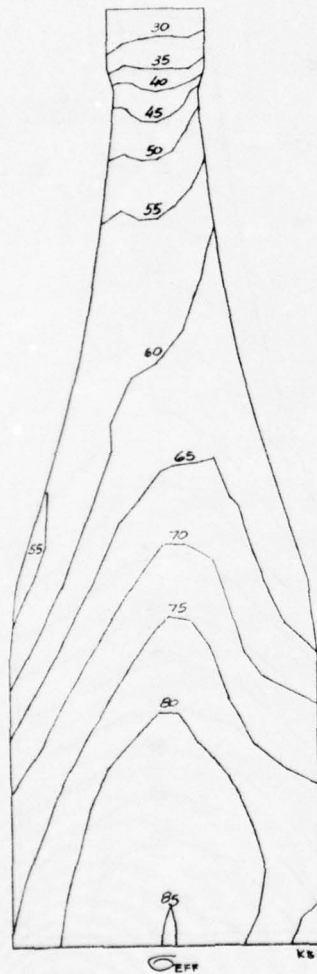
FIG. 5c

HIGH POWER SYSTEM 25 MW DP6 S-TEPPER



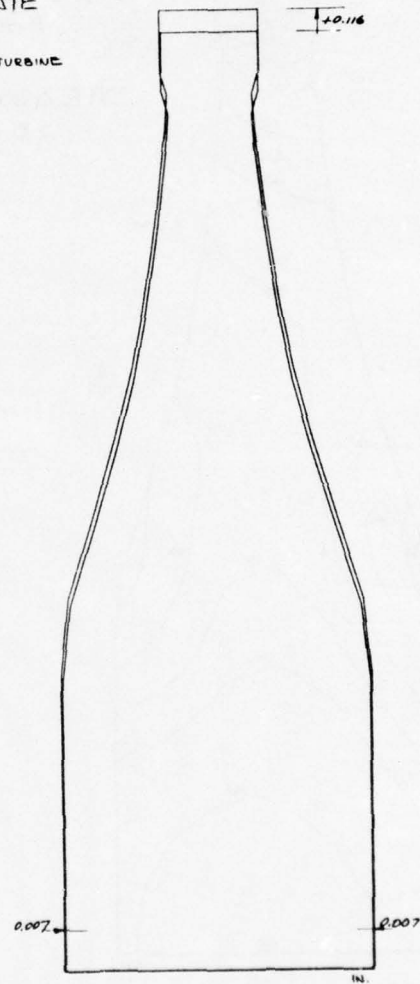
STEADY STATE

END STAGE TURBINE
DISC



EFFECTIVE CONSTANT STRESS

FIG. 6c



DISPLACEMENTS

FIG. 6d

ST. 12-79

	ELEM. OR NODE	VALUE	UNIT
<u>MAX. EFFECTIVE STRESS</u>	10- 11- 12	8.85976+04	PSI
<u>MAX. RADIAL DISP</u>	126	1.16307+01	INCHES
<u>MAX. AXIAL DISP.</u>	36	-1.01804+02	INCHES
<u>AVEG. TANG. STRESS OF DISK</u>		4.39155+04	PSI
<u>TOTAL VOLUME OF DISK</u>		1.08892+03	IN**3
<u>TOTAL WEIGHT OF THE BODY (*)</u>		3.11432+02	LB
<u>TOTAL MASS OF THE BODY (*)</u>		8.05983+01	LB=SEC**2/IN
<u>AXIAL DISTANCE TO C.G. FROM REF. LINE</u>		-3.03584+03	INCHES ≈ 0
<u>TOTAL POLAR MOMENT OF INERTIA (*)</u>		4.735556+01	LB=SEC**2=IN
<u>TOTAL DIAPYETRAL MOMENT OF INERTIA (*)</u>		2.42366+01	LB=SEC**2=IN

(*) Blades not included

TABLE 3

AD-A032 634

AIRESEARCH MFG CO OF CALIFORNIA TORRANCE
HIGH POWER STUDY--CONVENTIONAL GENERATORS, SUPERCONDUCTING GENE--ETC(U)
JUL 76 L SCHIPPER

F/G 10/2

F33615-75-C-2071

UNCLASSIFIED

76-12446

AFAPL-TR-76-39

NL

5 OF 5

AD
A032634



END

DATE

FILMED

1-77

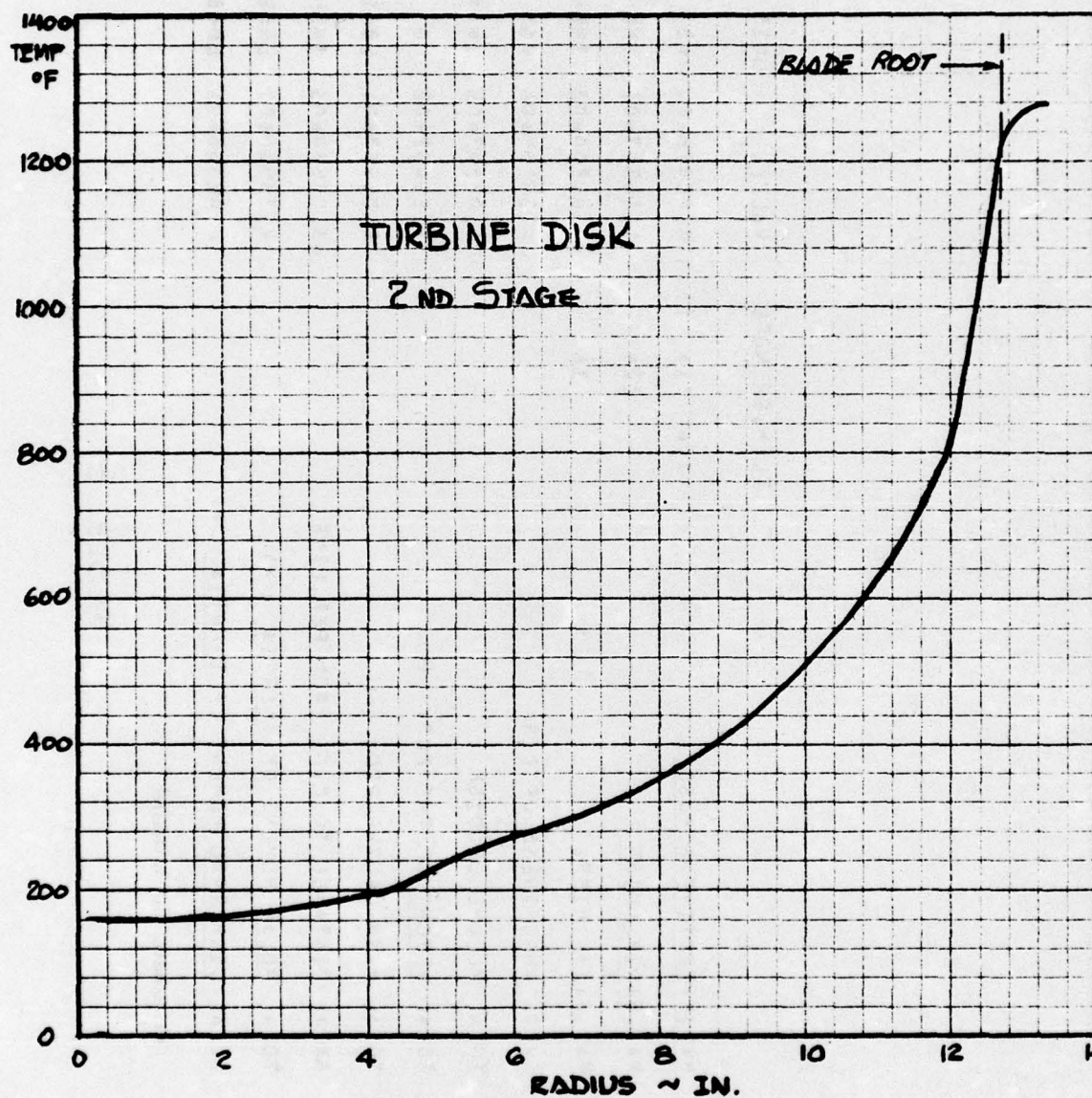


FIG. 7 ~ 663 SECS. TRANSIENT